



日中笹川医学奨学金制度  
第 43 期〈学位取得コース〉研究者

報 告 書

2021 年 4 月～2024 年 3 月

公益財団法人 日中医学協会

日中笹川医学奨学金制度＜学位取得コース＞：第43期研究者

研究者 No.	氏名	所属機関	受け入れ機関	指導責任者	掲載頁
		研究テーマ			
G 4301	範 彬	貴州医科大学附属医院・講師	北海道大学大学院医学研究院 腫瘍病理学	田中 伸哉 教授	p. 1
		基質荷電を用いたドパミン作動性神経細胞への新規分化法の確立			
G 4302	趙 雪	上海交通大学医学院附属同仁医院・主治医師	千葉大学大学院医学研究院泌尿器科学	市川 智彦 教授	p. 8
		アミノ酸トランスポーターを介した前立腺癌分子機構の解明（前列腺癌とアミノ酸トランスポーター）			
G 4303	姚 利	千葉大学大学院看護学研究科・博士課程学生	千葉大学大学院看護学研究科看護学専攻	正木 治恵 教授	p. 129
		在留中国人高齢者の若いへの準備教育プログラムの開発 ービデオカンファレンスを活用してー			
G 4304	張 茂芮	西南医科大学附属口腔医院・医師	東京医科歯科大学大学院医歯学総合研究科 生体補綴歯科学分野	若林 則幸 教授	p. 154
		骨誘導因子 Runx2 mRNA と VEGF mRNA 医薬を用いた顎骨再生			
G 4305	江 傑	東莞市人民医院・副主任医師	日本医科大学大学院医学研究科 解析人体病理学	清水 章 教授	p. 188
		腎疾患の進展機序の解明とその制御			
G 4306	王 晴	中国医科大学附属第四医院・主治医師	順天堂大学医学部 消化器外科講座上部消化管外科学	峯 真司 教授	p. 194
		食道癌に対する基礎的臨床的研究			
G 4307	張 瑛	寧波市医療センター李惠利医院・主治医師	横浜市立大学大学院医学研究科 消化器内科学	前田 慎 主任教授	p. 210
		肝胆膵疾患・炎症性腸疾患における超音波を主体とした画像診断と治療			
G 4308	葉 盛	南京紅十字血液センター・副主任医師	奈良県立医科大学大学院医学研究科 循環器システム医科学	中川 修 招聘教授	p. 226
		ADAMTS13 による VON WILLEBRAND 因子制御破綻がもたらす疾患の病態解析			
G 4309	王 喻	京都大学大学院医学研究科・博士課程学生	京都大学大学院医学研究科附属 がん免疫総合研究センター	本庶 佑 センター長 京都大学高等 研究院特別教 授	p. 232
		PD-1 阻害による免疫賦活化異常疾患の研究			
G 4310	孔 徳川	上海市疾病予防コントロールセンター・主治医師	熊本大学大学院医学教育部 ヒトレトロウイルス学共同研究センター 感染免疫学分野	上野 貴将 教授	p. 238
		新型コロナウイルスの複製を制御する宿主因子の同定と機能解析			
			国立感染症研究所感染病理部	徳永 研三 主任研究官	

日中笹川医学奨学金制度<学位取得コース>評価書

課程博士：指導教官用



第 43 期

研究者番号：G4301

作成日：2024年3月11日

氏名	範 彬	FAN BIN	性別	M	生年月日	1987/09/01
所属機関（役職）	貴州医科大学附属医院病理科（住院医师）					
研究先（指導教官）	北海道大学大学院医学研究院病理学分野腫瘍病理学教室（田中 伸哉 教授）					
研究テーマ	基質荷電を用いたドパミン作動性神経細胞への新規分化法の確立 Establishment of a novel method of differentiation into dopaminergic neurons using substrate charge					
専攻種別	<input type="checkbox"/> 論文博士			<input checked="" type="checkbox"/> 課程博士		

研究者評価（指導教官記入欄）

成績状況	優 <input checked="" type="checkbox"/> 良 可 不可 学業成績係数=	取得単位数
		取得単位数／取得すべき単位数総数 19/16
学生本人が行った研究の概要	<p>（研究概要）本研究では荷電ハイドロゲルを用いて human iPS 細胞の分化と基質荷電との関連について解析する。まず分化を試みる細胞はパーキンソン病の治療細胞としても注目されているドパミン作動性細胞である。ドパミン作動性細胞への分化誘導は多数報告があるが、いずれも高価な試薬を多くの試薬を組み合わせた複雑なプロトコルを有する。荷電との関連は報告がない。</p> <p>（方法）本研究では以下の点について解析する。①human iPS 細胞のドパミン作動性細胞分化と基質荷電との関連について解析する。②基質荷電を用いた新たな分化プロトコルを確立する。③トランスクリプトーム解析、モデル動物への移植を行い、従来法で作成したドパミン作動性細胞との比較を行う。</p> <p>（結果）2022年度では Human iPS 細胞を用いて、荷電ハイドロゲルにて分化誘導28日目は、ドパミン作動性細胞マーカー（TH、CORIN、DAT、AADC）は高発現している結果を得た。ドパミン作動性細胞誘導することが出来た。基質荷電を用いた新たな分化プロトコルを確立した。2023年度では Human iPS 細胞を用いて、ドパミン誘導する酵素である AADC Knock out 細胞の樹立を行った。AADC Knock out 細胞は上流因子 L-DOPA の増加が見られた。</p> <p>（今後の展望） 今年度はトランスクリプトーム解析を行い、さらにモデル動物への移植を行い、AADC Knock out 細胞により細胞療法を試み予定です。</p>	
総合評価	<p>【良かった点】 本人の取り込みが早く、現時点研究は順調に進んでおり、iPS 細胞の培養、iPS 細胞の荷電ハイドロゲルの誘導分化、RT-PCR の解析、ノックダウン細胞の樹立も完了致しました。 さらに今年度はトランスクリプトーム解析、モデル動物への移植を行い、細胞療法を試み予定です。大学院4年目で、論文の作成も取り込み中です。 本研究では世界初、荷電ハイドロゲルにより安価でドパミン作動性細胞の誘導が出来た。AADC Knock out 細胞により細胞療法は上手く行けば、今後臨床応用に大きく期待出来る。</p>	
	<p>【改善すべき点】 特になし。</p>	
	<p>【今後の展望】 まず、本人は大学院4年目で、論文のまとめ、学位の取得段階に入ります。 本研究においては、今年度はトランスクリプトーム解析を行い、さらにモデル動物への移植を行い、AADC Knock out 細胞により細胞療法を試み予定です。細胞療法について、様々な条件で検討しなければならないですが、上手く行けばパーキンソン病の臨床応用に大きく期待出来る。今年度は大学院4年目で、論文のまとめ、学位の取得段階に入ります。</p>	
学位取得見込	学位取得見込み	
		評価者（指導教官名） 谷川 聖（田中 伸哉）

# 日中笹川医学奨学金制度<学位取得コース>報告書 研究者用



第43期

研究者番号: G4301

作成日: 2024年3月 11 日

氏名	范 彬	FAN BIN	性別	M	生年月日 1987/09/01
所属機関(役職)	貴州医科大学附属医院病理科(住院医师)				
研究先(指導教官)	北海道大学大学院医学研究院病理学分野腫瘍病理学教室(田中 伸哉 教授)				
研究テーマ	基質荷電を用いたドーパミン作動性神経細胞への新規分化法の確立 Establishment of a novel method of differentiation into dopaminergic neurons using substrate charge				
専攻種別	論文博士	<input type="checkbox"/>	課程博士	<input checked="" type="checkbox"/>	

**1. 研究概要(1)**

1) 目的(Goal) To develop the protocol based on using an electrically charged hydrogel so that allowed to generate very consistent numbers of matured dopaminergic neurons from human iPSC lines which could generate L-DOPA.

2) 戦略(Approach)

1. Induction of dopaminergic neuron differentiation from iPSCs using charged hydrogels

2. Development of AADC KO Dopaminergic neuron

3. Evaluation of function to synthesize L-DOPA

4. Animal model of Parkinson's disease (therapeutic experiment)

3) 材料と方法 (Materials and methods)

Materials: Induced pluripotent stem cells, iPSCs; Charged hydrogels; 3-acrylamidopropyl-trimethyl-ammonium Chloride; 2-Acrylamido-2-methylpropanesulfonic acid; In my research, I used 2 kinds of gels, C1A9 and C2A8, the C means positive charge while the A means negative charge. C1A9 means the kind of gel has 10% positive charge, and 90% negative charge.

Methods: 1. Dopaminergic (DA) neurons differentiation culture on PS Dish or Charged hydrogels; 2. Morphological observation on PS Dish or Charged hydrogels; 3. Expression analysis of differentiation marker mRNA by real-time PCR; 4. Protein expression analysis by Western blotting; 5. Establishment of AADC knockout cell line using CRISPR/Cas9 system; 6. Evaluation of L-DOPA and Dopamine production using HPLC and ELISA methods; 7. Animal model of Parkinson's disease (therapeutic experiment)

4) 実験結果 (Results)

1. Using a protocol that induces dopaminergic neurons, induction with PS Dish was successful.

2. Moreover, using hydrogels, dopaminergic neurons were induced more efficiently than PS Dish.

3. AADC knockdown dopaminergic neurons were successfully induced on PS Dish.

4. Using hydrogel to simulate the neural microenvironment and efficiently induce dopaminergic neurons is expected to contribute to the development of translational medical technology for the treatment of refractory neurological diseases.

5) 考察 (Discussion)

Parkinson's disease is one of the most common neurological disorders. It is characterized by the loss of dopaminergic neurons. And the deficiency of L-DOPA is the main character of Parkinson's disease.

It is known that human pluripotent stem cells (PSCs) was successfully differentiated into DA neurons by Daisuke Doi[1] and the DA neurons had a good survival and lack of neural overgrowth indicate that it is promise for the development of cell-based therapies in Parkinson's disease.

However, it was reported [2] that the protocol has several problems: Low transfection efficiency, the DA neuron are not matured enough and the function of DA neurons largely depending on the source of hiPSCs.

It is known that the surface charge and wettability of artificial substrate are contributed to cell adhesion on scaffold, and surface charge of the substrates may directly affect adhesion of cellular membrane proteins.[3] [4]

Charged hydrogels electrically charged porous hydrogels can serve as scaffolds for brain parenchymal defects, and stepwise transplantation of NSCs into the hydrogel following gel implantation may induce the reconstruction of brain tissue along with the implanted hydrogels. Currently, various biomaterials have been used in human regenerative medicine, and biomedical engineering for specific tissues has become an important method to compensate for organ dysfunction.[5]

The available protocol of DA differentiation could be developed based on using an electrically charged hydrogel so that allowed to generate very consistent numbers of matured dopaminergic neurons from human iPSC lines.

And it was reported that Aromatic L-amino acid decarboxylase (AADC) could help L-DOPA change into dopamine, so if AADC is knocked out, the protocol may suspend in the step which L-DOPA change into dopamine, so the AADC-deficient dopaminergic cells may produce L-DOPA constantly.

Now, in the result of my research, it was proved the charged hydrogel could successfully induce dopaminergic neurons.

Moreover, using hydrogels, dopaminergic neurons were induced more efficiently than PS Dish.

In the morphology of cells, the DA neurons appeared in Day 14, which was earlier than PS dish group. But as the charge of the hydrogel, the amount of cell is less than the PS dish group.

On the other hand, in the result of qPCR, the target genes TH, FOXA2, DAT, NURR and Lmx1B of hydrogel group were much higher than the control group. And in Western blot, the related protein was also higher than the control group, that means the charged hydrogel could actually develop the efficiently than PS Dish. The function of DA neurons was better than PS Dish.

Especially the TH and DAT, was almost two folds to the PS Dish, meaning it could generate much more L-DOPA and Dopamine than in the PS dish.

Aromatic L-amino acid decarboxylase (AADC) could help L-DOPA change into dopamine. It could promote the combination of L-DOPA and TH to generate dopamine. AADC deficient attribute to the deficient synthesis of dopamine. So, the AADC-deficient dopaminergic cells may produce L-DOPA constantly.[6][7]

In this part, I am still working on it. First, it must be proven whether there is any difference between AADC knock out group and control group on PS dish. Then use the charged hydrogel to induce these two kinds of cells differentiating into DA neurons. Next, check whether there is any difference in L-DOPA and Dopamine between all the groups. Further research is required in the future..

#### 6)参考文献 (References)

- [1] Daisuke Doi et al, Isolation of human induced pluripotent stem cell-derived dopaminergic progenitors by cell sorting for successful transplantation. *Stem Cell Reports*. 2014 Mar 6;2(3):337-50.
- [2] Sameehan Mahajani et al, Homogenous generation of dopaminergic neurons from multiple hiPSC lines by transient expression of transcription factors. *Cell Death Dis*. 2019 Nov 27;10(12):898.
- [3] Yusuke Arima et al, Effect of wettability and surface functional groups on protein adsorption and cell adhesion using well-defined mixed self-assembled monolayers. *Biomaterials* 28, 3074-3082 (2007).
- [4] J H Lee et al, Cell behavior on polymer surfaces with different functional groups. *Biomaterials*. 1994 Jul;15(9):705-11.
- [5] Satoshi Tanikawa et al, Engineering of an electrically charged hydrogel implanted into a traumatic brain injury model for stepwise neuronal tissue reconstruction. *Scientific reports*. 13, 2233 (2023).
- [6] Toni S. Pearson et al, AADC deficiency from infancy to adulthood: Symptoms and developmental outcome in an international cohort of 63 patients. *J Inher Metab Dis*. 2020; 43:1121-1130.
- [7] Wassenberg et al. Consensus guideline for the diagnosis and treatment of aromatic L-amino acid decarboxylase (AADC) deficiency. *Orphanet Journal of Rare Diseases* (2017) 12:12.

## 1. 研究概要(1)

1) 目的(Goal) To develop the protocol based on using an electrically charged hydrogel so that allowed to generate very consistent numbers of matured dopaminergic neurons from human iPSC lines which could generate L-DOPA.

## 2) 戦略(Approach)

1. Induction of dopaminergic neuron differentiation from iPSCs using charged hydrogels

2. Development of AADC KO Dopaminergic neuron

3. Evaluation of function to synthesize L-DOPA

4. Animal model of Parkinson's disease (therapeutic experiment)

## 3) 材料と方法(Materials and methods)

Materials: Induced pluripotent stem cells, iPSCs; Charged hydrogels; 3-acrylamidopropyl-trimethyl-ammonium Chloride; 2-Acrylamido-2-methylpropanesulfonic acid; In my research, I used 2 kinds of gels, C1A9 and C2A8, the C means positive charge while the A means negative charge. C1A9 means the kind of gel has 10% positive charge, and 90% negative charge. Methods:

1. Dopaminergic (DA) neurons differentiation culture on PS Dish or Charged hydrogels; 2. Morphological observation on PS Dish or Charged hydrogels; 3. Expression analysis of differentiation marker mRNA by real-time PCR; 4. Protein expression analysis by Western blotting; 5. Establishment of AADC knockout cell line using CRISPR/Cas9 system; 6. Evaluation of L-DOPA and Dopamine production using HPLC and ELISA methods; 7. Animal model of Parkinson's disease (therapeutic experiment)

## 実験結果(Results).

1. Using a protocol that induces

dopaminergic neurons, induction with PS Dish was successful.

2. Moreover, using hydrogels, dopaminergic neurons were induced more efficiently than PS Dish.

3. AADC knockdown dopaminergic neurons were successfully induced on PS Dish.

4. Using hydrogel to simulate the neural microenvironment and efficiently induce dopaminergic neurons is expected to contribute to the development of translational medical technology for the treatment of refractory neurological diseases.

## 5) 考察(Discussion)

Parkinson's disease is one of the most common neurological disorders. It is characterized by the loss of dopaminergic neurons. And the deficiency of L-DOPA is the main character of Parkinson's disease.

It is known that human pluripotent stem cells (PSCs) was successfully differentiated into DA neurons by Daisuke Doi[1] and the DA neurons had a good survival and lack of neural overgrowth indicate that it is promise for the development of cell-based therapies in Parkinson's disease.

However, it was reported [2] that the protocol has several problems: Low transfection efficiency, the DA neuron are not matured enough and the function of DA neurons largely depending on the source of hiPSCs.

It is known that the surface charge and wettability of artificial substrate are contributed to cell adhesion on scaffold, and surface charge of the substrates may directly affect adhesion of cellular membrane proteins.[3] [4]

Charged hydrogels electrically charged porous hydrogels can serve as scaffolds for brain parenchymal defects, and stepwise transplantation of NSCs into the hydrogel following gel implantation may induce the reconstruction of brain tissue along with the implanted hydrogels. Currently, various biomaterials have been used in human regenerative medicine, and biomedical engineering for specific tissues has become an important method to compensate for organ dysfunction.[5]

The available protocol of DA differentiation could be developed based on using an electrically charged hydrogel so that allowed to generate very consistent numbers of matured dopaminergic neurons from human iPSC lines.

And it was reported that Aromatic L-amino acid decarboxylase (AADC) could help L-DOPA change into dopamine, so if AADC is knocked out, the protocol may suspend in the step which L-DOPA change into dopamine, so the AADC-deficient dopaminergic cells may produce L-DOPA constantly.

Now, in the result of my research, it was proved the charged hydrogel could successfully induce dopaminergic neurons.

Moreover, using hydrogels, dopaminergic neurons were induced more efficiently than PS Dish.

In the morphology of cells, the DA neurons appeared in Day 14, which was earlier than PS dish group. But as the charge of the hydrogel, the amount of cell is less than the PS dish group.

On the other hand, in the result of qPCR, the target genes TH, FOXA2, DAT, NURR and Lmx1B of hydrogel group were much higher than the control group. And in Western blot, the related protein was also higher than the control group, that means the charged hydrogel could actually develop the efficiently than PS Dish. The function of DA neurons was better than PS Dish. Especially the TH and DAT, was almost two folds to the PS Dish, meaning it could generate much more L-DOPA and Dopamine than in the PS dish.

Aromatic L-amino acid decarboxylase (AADC) could help L-DOPA change into dopamine. It could promote the combination of L-DOPA and TH to generate dopamine. AADC deficient attribute to the deficient synthesis of dopamine. So, the AADC-deficient dopaminergic cells may produce L-DOPA constantly.[6][7]

In this part, I am still working on it. First, it must be proven whether there is any difference between AADC knock out group and control group on PS dish. Then use the charged hydrogel to induce these two kinds of cells differentiating into DA neurons. Next, check whether there is any difference in L-DOPA and Dopamine between all the groups. Further research is required in the future..

## 6) 参考文献(References)

[1] Daisuke Doi et al, Isolation of human induced pluripotent stem cell-derived dopaminergic progenitors by cell sorting for successful transplantation. Stem Cell Reports. 2014 Mar 6;2(3):337-50.

[2] Sameehan Mahajani et al, Homogenous generation of dopaminergic neurons from multiple hiPSC lines by transient expression of transcription factors. Cell Death Dis. 2019 Nov 27;10(12):898.

[3] Yusuke Arima et al, Effect of wettability and surface functional groups on protein adsorption and cell adhesion using well-defined mixed self-assembled monolayers. Biomaterials 28, 3074-3082 (2007).

[4] J H Lee et al, Cell behavior on polymer surfaces with different functional groups. Biomaterials. 1994 Jul;15(9):705-11.

[5] Satoshi Tanikawa et al, Engineering of an electrically charged hydrogel implanted into a traumatic brain injury model for stepwise neuronal tissue reconstruction. Scientific reports. 13, 2233 (2023).

[6] Toni S. Pearson et al, AADC deficiency from infancy to adulthood: Symptoms and developmental outcome in an international cohort of 63 patients. J Inher Metab Dis. 2020; 43:1121-1130.

[7] Wassenberg et al. Consensus guideline for the diagnosis and treatment of aromatic L-amino acid decarboxylase (AADC) deficiency. Orphanet Journal of Rare Diseases (2017) 12:12.

## 2. 執筆論文 Publication of thesis ※記載した論文を添付してください。Attach all of the papers listed below.

論文名 1 Title						
掲載誌名 Published journal						
	年	月	巻(号)	頁 ~	頁	言語 Language
第1著者名 First author			第2著者名 Second author			第3著者名 Third author
その他著者名 Other authors						
論文名 2 Title						
掲載誌名 Published journal						
	年	月	巻(号)	頁 ~	頁	言語 Language
第1著者名 First author			第2著者名 Second author			第3著者名 Third author
その他著者名 Other authors						
論文名 3 Title						
掲載誌名 Published journal						
	年	月	巻(号)	頁 ~	頁	言語 Language
第1著者名 First author			第2著者名 Second author			第3著者名 Third author
その他著者名 Other authors						
論文名 4 Title						
掲載誌名 Published journal						
	年	月	巻(号)	頁 ~	頁	言語 Language
第1著者名 First author			第2著者名 Second author			第3著者名 Third author
その他著者名 Other authors						
論文名 5 Title						
掲載誌名 Published journal						
	年	月	巻(号)	頁 ~	頁	言語 Language
第1著者名 First author			第2著者名 Second author			第3著者名 Third author
その他著者名 Other authors						

3. 学会発表 Conference presentation ※筆頭演者として総会・国際学会を含む主な学会で発表したものを記載してくだ

※Describe your presentation as the principal presenter in major academic meetings including general meetings or international me

学会名 Conference					
演題 Topic					
開催日 date	年	月	日	開催地 venue	
形式 method	<input type="checkbox"/> 口頭発表 Oral	<input type="checkbox"/> ポスター発表 Poster	言語 Language	<input type="checkbox"/> 日本語	<input type="checkbox"/> 英語 <input type="checkbox"/> 中国語
共同演者名 Co-presenter					
学会名 Conference					
演題 Topic					
開催日 date	年	月	日	開催地 venue	
形式 method	<input type="checkbox"/> 口頭発表 Oral	<input type="checkbox"/> ポスター発表 Poster	言語 Language	<input type="checkbox"/> 日本語	<input type="checkbox"/> 英語 <input type="checkbox"/> 中国語
共同演者名 Co-presenter					
学会名 Conference					
演題 Topic					
開催日 date	年	月	日	開催地 venue	
形式 method	<input type="checkbox"/> 口頭発表 Oral	<input type="checkbox"/> ポスター発表 Poster	言語 Language	<input type="checkbox"/> 日本語	<input type="checkbox"/> 英語 <input type="checkbox"/> 中国語
共同演者名 Co-presenter					
学会名 Conference					
演題 Topic					
開催日 date	年	月	日	開催地 venue	
形式 method	<input type="checkbox"/> 口頭発表 Oral	<input type="checkbox"/> ポスター発表 Poster	言語 Language	<input type="checkbox"/> 日本語	<input type="checkbox"/> 英語 <input type="checkbox"/> 中国語
共同演者名 Co-presenter					

4. 受賞(研究業績) Award (Research achievement)

名称 Award name	国名 Country		受賞年 Year of	年	月
	国名 Country		受賞年 Year of	年	月

## 5. 本研究テーマに関わる他の研究助成金受給 Other research grants concerned with your research them

受給実績 Receipt record	<input type="checkbox"/> 有 <input type="checkbox"/> 無
助成機関名称 Funding agency	
助成金名称 Grant name	
受給期間 Supported period	年 月 ~ 年 月
受給額 Amount received	円
受給実績 Receipt record	<input type="checkbox"/> 有 <input type="checkbox"/> 無
助成機関名称 Funding agency	
助成金名称 Grant name	
受給期間 Supported period	年 月 ~ 年 月
受給額 Amount received	円

## 6. 他の奨学金受給 Another awarded scholarship

受給実績 Receipt record	<input type="checkbox"/> 有 <input type="checkbox"/> 無
助成機関名称 Funding agency	
奨学金名称 Scholarship name	
受給期間 Supported period	年 月 ~ 年 月
受給額 Amount received	円

## 7. 研究活動に関する報道発表 Press release concerned with your research activities

※記載した記事を添付してください。Attach a copy of the article described below

報道発表 Press release	<input type="checkbox"/> 有 <input type="checkbox"/> 無	発表年月日 Date of release	
発表機関 Released medium			
発表形式 Release method	・新聞 ・雑誌 ・Web site ・記者発表 ・その他( )		
発表タイトル Released title			

## 8. 本研究テーマに関する特許出願予定 Patent application concerned with your research theme

出願予定 Scheduled	<input type="checkbox"/> 有 <input type="checkbox"/> 無	出願国 Application	
出願内容(概要) Application contents			

## 9. その他 Others

--

指導責任者(記名) 田中 伸哉

日中笹川医学奨学金制度<学位取得コース>評価書

課程博士：指導教官用



第 43 期

研究者番号：G4302

作成日：2024年3月1日

氏名	趙雪	ZHAO XUE	性別	M	生年月日	1985/02/09
所属機関（役職）	上海交通大学医学院附属同仁医院泌尿器外科（主治医師）					
研究先（指導教官）	千葉大学大学院 医学研究院泌尿器科学（市川 智彦 教授）					
研究テーマ	アミノ酸トランスポーターを介した前立腺癌分子機構の解明（前立腺癌とアミノ酸トランスポーター） Elucidation of the molecular mechanism of prostate cancer via amino acid transporter (prostate cancer and amino acid transporter)					
専攻種別	<input type="checkbox"/> 論文博士			<input checked="" type="checkbox"/> 課程博士		

研究者評価（指導教官記入欄）

成績状況	(優) 良 可 不可 学業成績係数=4.0	取得単位数
		45/30
学生本人が行った研究の概要	中間報告後の一年の研究活動の中で、前立腺癌とアミノ酸トランスポーターに関する総括論文を第一著者として、他に5つの論文を共同著者として発表した。第33回日本尿路結石症学会で口頭発表を行った。国立がん研究センターの特任研究員として、人工知能技術を用いてロボット支援前立腺癌手術のスキルを評価システムの開発に携わり、すでに成果を上げている。順調に研究を進め、博士論文を執筆している。	
総合評価	<b>【良かった点】</b> 詳細な専門知識と優れた学修能力を有している。研究プロジェクトでは、深い理解力と鋭い分析能力を発揮しており、学術分野での成功に必要な基盤を築いた。継続して学修する能力や課題解決能力に優れている。新規に着手した人工知能の研究領域や手法を積極的に探求し、難題に挑戦するとともに、冷静で粘り強い姿勢をもってそれらを克服し解決している。これらの探求心と課題解決能力は、将来の研究活動や職務における多大なる成果につながるものと評価している。また、人格も優れており、コミュニケーション能力の高さや他人に対して常に心を開き、同僚との良好なチームワークを築きながら研究を推進している。他人の意見も謙虚に聞き入れ、それを自分自身の行動に反映することにより、自分自身だけでなく研究グループとしての共通の目標の達成にも貢献している。当教室において無くてはならない人材として期待するとともに、高く評価している。	
	<b>【改善すべき点】</b> 中間評価で提示された点はすべて改善されている。	
	<b>【今後の展望】</b> 将来の展望に関して大きなポテンシャルを持ち、学術分野で優れた業績を上げる能力を持っていると確信している。継続的な努力と学修、研究の深化、そして積極的な学術交流と協力により、当該領域に新しい思考や成果をもたらす、その分野を切り開く先駆者となることを期待している。	
学位取得見込	十分な学術的基盤と研究の潜在能力を持っている。専心して学び、努力し、自身の優位性を最大限に発揮すれば、博士号を取得するだけでなく、研究領域において多大なる成果を挙げることができると確信している。	
評価者（市川 智彦）		

# 日中笹川医学奨学金制度<学位取得コース>報告書 研究者用



第43期

研究者番号: G4302

作成日: 2024年3月1日

氏名	赵雪	ZHAO XUE	性別	M	生年月日	1985/02/09
所属機関(役職)	上海交通大学医学院附属同仁医院泌尿器外科(主治医師)					
研究先(指導教官)	千葉大学大学院 医学研究院泌尿器科学(市川 智彦 教授)					
研究テーマ	アミノ酸トランスポーターを介した前立腺癌分子機構の解明(前立腺癌とアミノ酸トランスポーター) Elucidation of the molecular mechanism of prostate cancer via amino acid transporter (prostate cancer and amino acid transporter)					
専攻種別	論文博士	<input type="checkbox"/>	課程博士	<input checked="" type="checkbox"/>		

## 1. 研究概要(1)

### 1) 目的(Goal)

目的: ①アミノ酸トランスポーター阻害剤の去勢抵抗性前立腺癌(CRPC)に対する作用効果の解明(In vivo)。②LAT1を含めたトランスポーターを介したCRPC治療モデルの構築と、実臨床への応用を目指す。③前立腺がんに関する人工知能技術を用いた臨床研究が行われている。

研究背景: 社会の高齢化が進むにつれて、前立腺癌の発病率は年々増加している。前立腺癌の治療において、無視できないのは、前立腺癌が最終的に去勢抵抗型前立腺癌(CRPC)に転換することである。我々は、前立腺癌がCRPCに移行するメカニズムとして、アンドロゲン受容体(AR)に制御されるトランスポーターとしてLAT1(LAT1-4F2hcヘテロダイマー型トランスポーター)を同定した[1]。LAT1複合体は前立腺癌において特異的な発現亢進が報告されている[2]。さらに、SCL3A2遺伝子(4F2hc)はCRPCに関与するアンドロゲン受容体のスプライスバリエーション(Ar-V7)の特異的標的遺伝子であることを発見した[1]。LAT1阻害剤(JPH 203)はすでに消化器腫瘍において第一相臨床試験を完了し、良好な結果を得た[3]。SGLT-2阻害剤は糖尿病で臨床応用されていることから、LAT1を含めたアミノ酸トランスポーターの阻害剤もCRPC患者において臨床応用の可能性が示唆される。本研究の目的はLAT1を含むアミノ酸トランスポーターの阻害剤を応用した、去勢抵抗性前立腺癌(CRPC)治療モデル(In vivo)の構築を提案する。最終的には、第二相臨床試験をCRPC患者において実現させる。近年、人工知能技術が飛躍的に進歩し、臨床分野での応用例や研究の方向性が出てきていることから、人工知能による泌尿器科の研究をテーマにしている。

### 2) 戦略(Approach)

千葉大学泌尿器科学研究室は、2016年からアミノ酸トランスポーターの第一人者である大阪大学 金井好克教授、千葉大学 安西尚彦教授、LAT1阻害剤を供給するジェイファーマ株式会社と共同研究を行っている。複数の先行研究成果[1,2,4-7]と豊富な共同研究経験があり、後続研究の実現が可能である。研究者本人はLAT1-4F2hc複合体と前立腺癌に関する総説論文2編が発表され、前立腺癌とLAT1複合体の分野に対して比較的十分な理解と認識を持っている。

LAT阻害剤(JPH203)の利用: 大阪大学 金井好克教授、ジェイファーマ株式会社とのMTAを締結済。共同研究として、LAT1の特異的阻害剤(JPH203)の臨床応用へ向けた解析を進める。すでに、膵臓癌と胆管癌にて第一層臨床試験UMIN00016840終了しており、軽度の副作用(12%のAST上昇)と25カ月の長期奏効例を胆管癌患者に認めている。

本研究では、上記の先行研究と共同プロジェクトに基づいて、3つのステップで結論を導き出すことが期待される。現在の展望は以下の通り記述する。①前立腺がんCRPC細胞株の確立、LAT1関係の検証です。②CRPCモデルマウスの作成、JPH203を用いた治療実験を行う。③上記の①②の調査で得られたデータをもとに比較分析して臨床利用の妥当性を判断する。3つのステップを3年計画として、1年目は計画通りに前立腺がんLAT1の関係を調べ、細胞の培養や実験を行う。調査をもとにまとめたレビュー論文2本が学術誌に掲載されました。2年目には細胞のスクリーニングに成功し、siRNAを使って4F2hc遺伝子をノックアウトしました。ノックダウン後の細胞の増殖、侵襲、転移の様子が観察されています。また国立がん研究センターの特任研究員として、ロボットで支援する前立腺がん手術(RARP)をAI分析評価システムの開発にも携わりました。3年目は主にマウスモデルの作成と博士論文の作成を行う。

### 3) 材料と方法(Materials and methods)

研究方法及び内容: 免疫不全マウスの皮下移植前立腺癌モデルを用いてLAT1阻害剤(JPH203)臨床応用へ向けたIn Vivo解析を行う。

① CRPC細胞系(LNCaP, DU145, PC-3)におけるLAT阻害剤の作用効果の解明。(細胞形態、成長、分化、代謝、アポトーシス、信号伝導経路など。)

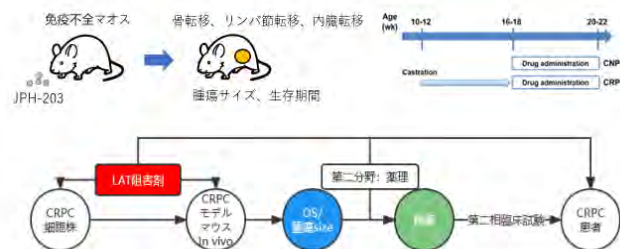
- CRPC細胞系(LNCaP, DU145, PC-3)のLAT1-4F2hcをrtPCRで検証、LAT1-4F2hcのタンパク質量をWestern-Blottingで検証。
- siRNAを作用させるCRPC細胞系のLAT1-4F2hc量と関連タンパク質量をrtPCRとWestern-Blottingで検証。
- 2種類の細胞株を選択し、JPH203を投入する。LAT1-4F2hc量と関連タンパク質量をrtPCRとWestern-Blottingで検証。
- JPH203投入後の細胞株で細胞増殖実験、migration/invasion assayなど、細胞の成長、侵襲、転移などの能力を比較する。

② 去勢、非去勢モデルにて16w-18wにて薬剤投与(経静脈的)を開始し、腫瘍増大抑制効果とマウスの生存期間延長効果を解析する。

前立腺腫瘍細胞を6~8週目の免疫不全のオスのヌードマウスをランダムに4つのグループ(去勢/非去勢治療群と対照群)に分けて皮下注射し、細胞を入れてから24時間後にバイオライトイメージングで腫瘍の成長を監視し、その後2週間ごとに4週間監視する。治療群は16~18週間にJPH203を使用し、バイオライトイメージングで腫瘍の変化を監視し、画像ソフトウェアで定量的な比較する。

グループ間の生存期間を比較する。

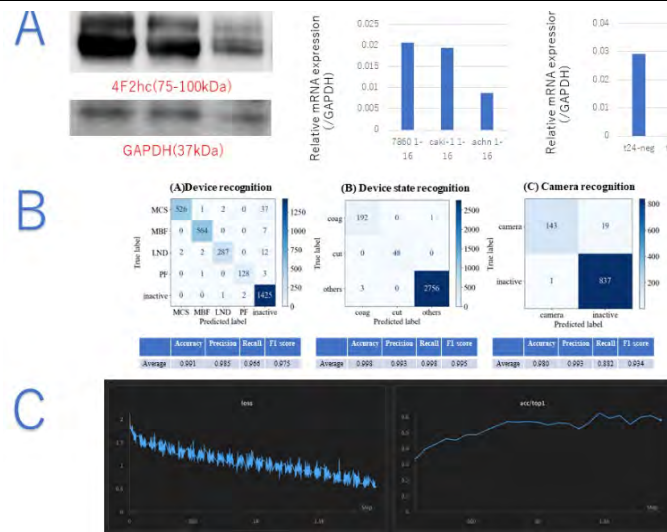
③ 得られた結果と抗腫瘍効果、副作用を含めて分析し、臨床応用の可能性を探索する。



1. 研究概要(2)

4) 実験結果(Results)

A. 4F2hc高発現の2種類の細胞を選別し、westernとrtPCRで検証し、siRNAを用いて4F2hcをノックダウンしました。ノックダウン後の細胞の増殖、侵襲、転移の様子が観察されています。



国立がん研究センターの特任研究員として、ロボットで支援する前立腺がん手術(RARP)をai分析評価システムの開発にも携わりました。

B.画像認識技術に基づいたRARP手術ユーザーインターフェース認識モデルを構築し、手術器具とCUT/COAGオン操作の認識精度を高めました(0.98~0.998)

C.現在、学習中の人工知能がRARP手術縫合の操作を認識するモデルを構築中で、精度は60%に達しています(学習中)。

5) 考察(Discussion)

5.1) 抗アンドロゲン治療(ADT)におけるLAT1の上昇が、前立腺がん細胞の進行を促すことがわかっている[2]。LAT1はCRPC細胞株で強く発現する。LAT1ノックアウトは細胞の増殖、移動、侵襲を著しく減少させる。慢性ADTの患者では、LAT1の高発現は生化学的無再発期の低下と相関している[2]。慢性ADTを伴う22Rv1 CRPC腫瘍において、LAT1のタンパク質およびmRNAレベルでの発現が増加していることが確認されている[8]。SugiuraはAR-v7とLAT1-4F2hc複合体の潜在的な関係を示しました。AR-v7はアンドロゲンの欠乏で下流の標的遺伝子を活性化する。4F2hcはAR-v7の下流のターゲットの1つです。CRPC組織における4F2hc発現レベルの有意な上昇は、予後不良を示唆している[9]。

トランスポーターの阻害剤には、輸送化合物と、非輸送化合物がある。現在の薬理学では、細胞内に蓄積せず、親和性が高い非輸送系化合物が輸送系化合物より優れていると考えられている[10]。JPH203 (KYT-0353)は、2009年にLAT1特異的阻害剤として開発されました[11]。そして、JPH203は最近、LAT1の効果的な阻害剤として広く研究されている。JPH203は、mTORC1とAktの組成活性化を妨害し、c-Mycの発現を低下させ、細胞死に関与するCHOP転写因子が介在するフラクタンパク反応を誘発する[12]。第I相臨床研究では、JPH203には良好な耐性があり、胆道癌治療の予後が良好であることが報告されており、胆道癌に対する疾患抑制率は約60%でした[3]。ですから、我々はCRPCでJPH203の第I相と第II相の研究を行う予定です。また、日本の研究チームはT3やJPH203に似たSKN系LAT1阻害剤[13,14]を開発しました。近年、大阪大学の金井教授らの研究チームは、新しいLAT1阻害剤「OKYシリーズ」を開発している。OKY化合物では、OKY-034はLAT1に対して高い阻害性と特異性を示しました。上記のアミノ酸LAT1阻害剤は競合阻害剤ですが、OKY-034はアミノ酸の骨格を持たないため、非競合阻害剤のスタイルを持っています。非競合阻害剤は、内因性アミノ酸基質と競合的に反応する必要があるため、少量(低濃度)で効果を示すことができます。また、OKY-034はT3やSKNといった大きな疎水点を必要としないため、比較的水溶性に優れ、経口投与が可能です。膵臓がん患者におけるOKY-034の安全性と有効性のI/IIa相試験は大阪大学病院で行われている(UMIN000036395)[15]。これらの薬はまもなく前立腺がんの治療に使われる。

前立腺がんにおけるアミノ酸トランスポーターLAT1-4F2hc複合体の臨床的意義は、他の腫瘍細胞と同様に、次第に解明されつつある。LAT1-4F2hcは前立腺がんの診断、治療、予後評価に重要な役割を果たしている。前立腺がんに関連するアミノ酸トランスポーター阻害剤であるJPH203は、近い将来泌尿器系腫瘍の診断と治療戦略を変える可能性がある。

5.2) 23年以上も臨床に応用されてきたロボット補助根治前立腺切除術(RARP)[16]は患者数は年々増加している。現在、米国の根治前立腺切除術の約70%がこの方法で行われています[17]。医者の技術と予後には有意な関係があり、患者の予後に影響を与える重要な要因の1つです[18-20]。しかし、現在の主流の外科技術評価システムは、専門家評価表モデル[21]に基づいています。例えば、腹腔鏡手術スキルの総合評価(GOALS)[22]、技術スキルの客観的構造化評価(OSATS)[23]、医療失敗パターンと効果分析(HFMEA)[24]などです。これらの評価ツールは、評価に時間がかかるだけでなく、専門家の労力と個人的な判断を必要とします。評価の専門家が介在することで、評価結果が主観的になることは避けられません。そのため、手術のスキル評価をいかに自動化、効率化し、客観的な評価結果にするかが重要な課題となっています。私たちの人工知能(AI)による画像認識技術モデルが、この問いに答える方向を示しているようです。

6) 参考文献(References)

[1] Sugiura, M. et al. Identification of AR-V7 downstream genes commonly targeted by AR/AR-V7 and specifically targeted by AR-V7 in castration resistant prostate cancer. *Transl Oncol* 14, 100915.

[2] Xu, M. et al. Up-Regulation of LAT1 during Antiandrogen Therapy Contributes to Progression in Prostate Cancer Cells. *J Urol* 195, 1588-1597.

[3] Okano, N. et al. First-in-human phase I study of JPH203, an L-type amino acid transporter 1 inhibitor, in patients with advanced solid tumors. *Invest New Drugs* 38, 1495-1506.

[4] Higuchi, K. et al. Characterization of the expression of LAT1 as a prognostic indicator and a therapeutic target in renal cell carcinoma. *Sci Rep* 9, 16776.

[5] Maimaiti, M. et al. Expression of L-type amino acid transporter 1 as a molecular target for prognostic and therapeutic indicators in bladder carcinoma. *Sci Rep* 10, 1292.

[6] Babu, E. et al. Identification of a novel system L amino acid transporter structurally distinct from heterodimeric amino acid transporters. *J Biol Chem* 278, 43838-43845.

[7] Okunushi, K. et al. JPH203, a newly developed anti-cancer drug, shows a preincubation inhibitory effect on L-type amino acid transporter 1 function. *J Pharmacol Sci* 144, 16-22.

[8] Malviya, G.; Patel, R.; Salji, M.; Martinez, R.S.; Repiscak, P.; Mui, E.; Champion, S.; Mrowinska, A.; Johnson, E.; AlRasheedi, M.; et al. 18F-Fluciclovine PET metabolic imaging reveals prostate cancer tumour heterogeneity associated with disease resistance to androgen deprivation therapy. *EJNMMI Research* 2020, 10, 143.

[9] Sugiura, M.; Sato, H.; Okabe, A.; Fukuyo, M.; Mano, Y.; Shinohara, K.-i.; Rahmutulla, B.; Higuchi, K.; Maimaiti, M.; Kanesaka, M. Identification of AR-V7 downstream genes commonly targeted by AR/AR-V7 and specifically targeted by AR-V7 in castration resistant prostate cancer. *Translational oncology* 2021, 14, 100915.

[10] Wiriyasermkul, P.; Moriyama, S.; Kongpracha, P.; Nagamori, S. [Drug Discovery Targeting an Amino Acid Transporter for Diagnosis and Therapy]. *Yakugaku Zasshi* 2021, 141, 501-510.

[11] Oda, K.; Hosoda, N.; Endo, H.; Saito, K.; Tsujihara, K.; Yamamura, M.; Sakata, T.; Anzai, N.; Wempe, M.F.; Kanai, Y.; et al. L-type amino acid transporter 1 inhibitors inhibit tumor cell growth. *Cancer Sci* 2010, 101, 173-179.

[12] Rosilio, C.; Nebout, M.; Imbert, V.; Griessinger, E.; Neffati, Z.; Benadiba, J.; Hagenbeek, T.; Spits, H.; Reverso, J.; Ambrosetti, D. L-type amino-acid transporter 1 (LAT1): a therapeutic target supporting growth and survival of T-cell lymphoblastic lymphoma/T-cell acute lymphoblastic leukemia. *Leukemia* 2015, 29, 1253-1266.

[13] Kongpracha, P.; Nagamori, S.; Wiriyasermkul, P.; Tanaka, Y.; Kaneda, K.; Okuda, S.; Ohgaki, R.; Kanai, Y. Structure-activity relationship of a novel series of inhibitors for cancer type transporter L-type amino acid transporter 1 (LAT1). *J Pharmacol Sci* 2017, 133, 96-102.

[14] Nagamori, S.; Wiriyasermkul, P.; Okuda, S.; Kojima, N.; Hari, Y.; Kiyonaka, S.; Mori, Y.; Tominaga, H.; Ohgaki, R.; Kanai, Y. Structure-activity relations of leucine derivatives reveal critical moieties for cellular uptake and activation of mTORC1-mediated signaling. *Amino Acids* 2016, 48, 1045-1058.

[15] Wiriyasermkul, P.; Moriyama, S.; Kongpracha, P.; Nagamori, S. [Drug Discovery Targeting an Amino Acid Transporter for Diagnosis and Therapy]. *Yakugaku Zasshi* 2021, 141, 501-510.

[16] Binder, J.; Kramer, W. Robotically-assisted laparoscopic radical prostatectomy. *BJU Int* 2001, 87, 408-410.

[17] Gandaglia, G.; Montorsi, F.; Karakiewicz, P.I.; Sun, M. Robot-assisted radical prostatectomy in prostate cancer. *Future Oncol* 2015, 11, 2767-2773.

[18] Stulberg, J.J.; Huang, R.; Kreutzer, L.; Ban, K.; Champagne, B.J.; Steele, S.R.; Johnson, J.K.; Holl, J.L.; Greenberg, C.C.; Bilimoria, K.Y. Association Between Surgeon Technical Skills and Patient Outcomes. *JAMA Surg* 2020, 155, 960-968.

[19] Goldenberg, M.G.; Goldenberg, L.; Grantcharov, T.P. Surgeon Performance Predicts Early Continence After Robot-Assisted Radical Prostatectomy. *J Endourol* 2017, 31, 858-863.

[20] Hashimoto, T.; Yoshioka, K.; Gondo, T.; Kamoda, N.; Satake, N.; Ozu, C.; Horiguchi, Y.; Namiki, K.; Nakashima, J.; Tachibana, M. Learning curve and perioperative outcomes of robot-assisted radical prostatectomy in 200 initial Japanese cases by a single surgeon. *J Endourol* 2013, 27, 1218-1223.

[21] Boal, M.W.E.; Anastasiou, D.; Tesfai, F.; Ghamrawi, W.; Mazomenos, E.; Curtis, N.; Collins, J.W.; Sridhar, A.; Kelly, J.; Stoyanov, D.; et al. Evaluation of objective tools and artificial intelligence in robotic surgery technical skills assessment: a systematic review. *Br J Surg* 2024, 111.

[22] Vassiliou, M.C.; Feldman, L.S.; Andrew, C.G.; Bergman, S.; Leffondré, K.; Stanbridge, D.; Fried, G.M. A global assessment tool for evaluation of intraoperative laparoscopic skills. *Am J Surg* 2005, 190, 107-113.

[23] Martin, J.A.; Regehr, G.; Reznick, R.; MacRae, H.; Murnaghan, J.; Hutchison, C.; Brown, M. Objective structured assessment of technical skill (OSATS) for surgical residents. *Br J Surg* 1997, 84, 273-278.

[24] Lovegrove, C.; Novara, G.; Motttrie, A.; Guru, K.A.; Brown, M.; Challacombe, B.; Popert, R.; Raza, J.; Van der Poel, H.; Peabody, J.; et al. Structured and Modular Training Pathway for Robot-assisted Radical Prostatectomy (RARP): Validation of the RARP Assessment Score and Learning Curve Assessment. *Eur Urol* 2016, 69, 526-535.

## 2. 執筆論文 Publication of thesis ※記載した論文を添付してください。Attach all of the papers listed below.

論文名 1 Title	Tumor Location and a Tumor Volume over 2.8 cc Predict the Prognosis for Japanese Localized Prostate Cancer.					
掲載誌名 Published journal	Cancers					
	2022 年 12 月	14 (23) 巻(号)	5823 頁 ~ 5836 頁	言語 Language	英語	
第1著者名 First author	<u>Xue Zhao</u>	第2著者名 Second author	Shinichi Sakamoto	第3著者名 Third author	Haruki Baba	
その他著者名 Other authors	Yasutaka Yamada, Junryo Rii, Ayumi Fujimoto, Manato Kanesaka, Nobuyoshi Takeuchi, Tomokazu Sazuka, Yusuke Imamura, Koichiro Akakura, Tomohiko Ichikawa.					
論文名 2 Title	Targeting L-type amino acid transporter 1 in urological malignancy: Current status and future perspective.					
掲載誌名 Published journal	J Pharmacol Sci					
	2022 年 12 月	150 (4) 巻(号)	251 頁 ~ 258 頁	言語 Language	英語	
第1著者名 First author	Sangion Pae	第2著者名 Second author	Shinichi Sakamoto	第3著者名 Third author	<u>Xue Zhao</u>	
その他著者名 Other authors	Shinpei Saito, Takaaki Tamura, Yusuke Imamura, Tomokazu Sazuka, Yoshie Reien, Yuri Hirayama, Hirofumi Hashimoto, Yoshikatsu Kanai, Tomohiko Ichikawa, Naohiko Anzai.					
論文名 3 Title	Contribution of LAT1-4F2hc in Urological Cancers via Toll-like Receptor and Other Vital Pathways.					
掲載誌名 Published journal	Cancers					
	2022 年 1 月	14 (1) 巻(号)	229 頁 ~ 248 頁	言語 Language	英語	
第1著者名 First author	<u>Xue Zhao</u>	第2著者名 Second author	Shinichi Sakamoto	第3著者名 Third author	Maihulan Maimaiti	
その他著者名 Other authors	Naohiko Anzai, Tomohiko Ichikawa.					
論文名 4 Title	Serum Testosterone Level Determines the Treatment Strategy of Advanced Prostate Cancer.					
掲載誌名 Published journal	Horizons in Cancer Research (Book)					
	2023 年 4 月	85 巻(号)	Chapter 3 頁 ~ Chapter 3 頁	言語 Language	英語	
第1著者名 First author	<u>Xue Zhao</u>	第2著者名 Second author	Shinichi Sakamoto	第3著者名 Third author	Shuhei Kamada	
その他著者名 Other authors	Akinori Takei, Yusuke Imamura, Tomohiko Ichikawa.					
論文名 5 Title	Contribution of the L-Type Amino Acid Transporter Family in the Diagnosis and Treatment of Prostate Cancer.					
掲載誌名 Published journal	International Journal of Molecular Sciences					
	2023 年 2 月	24 巻(号)	6178 頁 ~ 6195 頁	言語 Language	英語	
第1著者名 First author	<u>Xue Zhao</u>	第2著者名 Second author	Shinichi Sakamoto	第3著者名 Third author	Jiaxing Wei	
その他著者名 Other authors	Sangion Pae, Shinpei Saito, Tomokazu Sazuka, Yusuke Imamura, Naohiko Anzai, Tomohiko Ichikawa.					

## 2. 執筆論文 Publication of thesis ※記載した論文を添付してください。Attach all of the papers listed below.

論文名 6 Title	Machine- learning predicts time-series prognosis factors in metastatic prostate cancer patients treated with androgen deprivation therapy.				
掲載誌名 Published journal	Scientific Reports				
	2023 年 4 月	13(1) 巻(号)	6325 頁 ~ 6334 頁	言語 Language	英語
第1著者名 First author	Shinpei Saito	第2著者名 Second author	Shinichi Sakamoto	第3著者名 Third author	Kosuke Higuchi
その他著者名 Other authors	Kodai Sato, <u>Xue Zhao</u> , Ken Wakai, Manato Kanesaka, Shuhei Kamada, Nobuyoshi Takeuchi, Tomokazu Sazuka, Yusuke Imamura, Naohiko Anzai, Tomohiko Ichikawa, Eiryu Kawakami.				
論文名 7 Title	The Oncological and Functional Prognostic Value of Unconventional Histology of Prostate Cancer in Localized Disease Treated with Robotic Radical Prostatectomy: An International Multicenter 5-Year Cohort Study				
掲載誌名 Published journal	EUROPEAN UROLOGY ONCOLOGY				
	2024 年 1 月	23 巻(号)	印刷中 頁 ~ 頁	言語 Language	英語
第1著者名 First author	David Leung	第2著者名 Second author	Daniele Castellani	第3著者名 Third author	Rossella Nicoletti
その他著者名 Other authors	Roser Vives Dilme, Jesus Moreno Sierra, Sergio Serni, Carmine Franzese, Giuseppe Chiacchio, Andrea Benedetto Galosi, Roberta Mazzucchelli, Erika Palagonia, Paolo Dell'Oglio, Antonio Galfano, Aldo Massimo Bocciardi, <u>Xue Zhao</u> , Chi Fai Ng, Hsiang Ying Lee, Shinichi Sakamoto, Nikhil Vasdev, Juan Gomez Rivas, Riccardo Campi, Jeremy Yuen-Chun Teoh.				
論文名 8 Title	Tumor localization by Prostate Imaging and Reporting and Data System (PI-RADS) version 2.1 predicts prognosis of prostate cancer after radical prostatectomy.				
掲載誌名 Published journal	Scientific Reports				
	2023 年 6 月	13(1) 巻(号)	10079 頁 ~ 10088 頁	言語 Language	英語
第1著者名 First author	Ayumi Fujimoto	第2著者名 Second author	Shinichi Sakamoto	第3著者名 Third author	Takuro Horikoshi
その他著者名 Other authors	<u>Xue Zhao</u> , Yasutaka Yamada, Junryo Rii, Nobuyoshi Takeuchi, Yusuke Imamura, Tomokazu Sazuka, Keisuke Matsusaka, Jun-Ichiro Ikeda, Tomohiko Ichikawa.				
論文名 9 Title	Preoperative PI-RADS v2.1 Scoring System Improves Risk Classification in Patients Undergoing Radical Prostatectomy.				
掲載誌名 Published journal	Anticancer Research				
	2023 年 12 月	43(12) 巻(号)	5705 頁 ~ 5712 頁	言語 Language	英語
第1著者名 First author	Yudai Fukui	第2著者名 Second author	Yasutaka Yamada	第3著者名 Third author	Shinichi Sakamoto
その他著者名 Other authors	Takuro Horikoshi, <u>Xue Zhao</u> , Kodai Sato, Sakie Nanba, Yoshihiro Kubota, Manato Kanesaka, Ayumi Fujimoto, Hiroki Shibata, Yusuke Goto, Tomokazu Sazuka, Yusuke Imamura, Takashi Uno, Tomohiko Ichikawa.				
論文名 10 Title	Copy Number Gain in Androgen Receptors Predicts the Poor Prognosis in Japanese Castration-resistant Prostate Cancer.				
掲載誌名 Published journal	Anticancer Research				
	2024 年 2 月	44(2) 巻(号)	639 頁 ~ 647 頁	言語 Language	英語
第1著者名 First author	Shinichi Sakamoto	第2著者名 Second author	Keisuke Ando	第3著者名 Third author	Sangjon Pae
その他著者名 Other authors	<u>Xue Zhao</u> , Kazuko Sakai, Kodai Sato, Shinpei Saito, Yasutaka Yamada, Junryo Rii, Yusuke Goto, Tomokazu Sazuka, Yusuke Imamura, Naohiko Anzai, Koichiro Akakura, Kazuto Nishio, Tomohiko Ichikawa.				

3. 学会発表 Conference presentation ※筆頭演者として総会・国際学会を含む主な学会で発表したものを記載してください

※Describe your presentation as the principal presenter in major academic meetings including general meetings or international meetings

学会名 Conference	日本尿路結石症学会第33回学術集会			
演題 Topic	SWLハイボリュームセンターにおけるSkin to Stone Distance(SSD)と尿管結石破碎効率に関する検討			
開催日 date	2023 年 8 月 25 日	開催地 venue	久留米市	
形式 method	<input checked="" type="checkbox"/> 口頭発表 Oral <input type="checkbox"/> ポスター発表 Poster	言語 Language	<input checked="" type="checkbox"/> 日本語 <input type="checkbox"/> 英語 <input type="checkbox"/> 中国語	
共同演者名 Co-presenter	坂本 信一, 野積 和義, 柴田 裕貴, 山田 康隆, 五島 悠介, 今村 有佑, 市川 智彦			
学会名 Conference				
演題 Topic				
開催日 date	年 月 日	開催地 venue		
形式 method	<input type="checkbox"/> 口頭発表 Oral <input type="checkbox"/> ポスター発表 Poster	言語 Language	<input type="checkbox"/> 日本語 <input type="checkbox"/> 英語 <input type="checkbox"/> 中国語	
共同演者名 Co-presenter				
学会名 Conference				
演題 Topic				
開催日 date	年 月 日	開催地 venue		
形式 method	<input type="checkbox"/> 口頭発表 Oral <input type="checkbox"/> ポスター発表 Poster	言語 Language	<input type="checkbox"/> 日本語 <input type="checkbox"/> 英語 <input type="checkbox"/> 中国語	
共同演者名 Co-presenter				
学会名 Conference				
演題 Topic				
開催日 date	年 月 日	開催地 venue		
形式 method	<input type="checkbox"/> 口頭発表 Oral <input type="checkbox"/> ポスター発表 Poster	言語 Language	<input type="checkbox"/> 日本語 <input type="checkbox"/> 英語 <input type="checkbox"/> 中国語	
共同演者名 Co-presenter				

4. 受賞(研究業績) Award (Research achievement)

名称 Award name	国名 Country		受賞年 Year of award	年 月
	国名 Country		受賞年 Year of award	年 月

## 5. 本研究テーマに関わる他の研究助成金受給 Other research grants concerned with your research theme

受給実績 Receipt record	<input checked="" type="checkbox"/> 有 <input type="checkbox"/> 無
助成機関名称 Funding agency	国立研究開発法人 科学技術振興機構 (JST)
助成金名称 Grant name	全方位イノベーション創発博士人材養成プロジェクト
受給期間 Supported period	2023 年 4 月 ~ 2024 年 3 月
受給額 Amount received	770,000 円
受給実績 Receipt record	<input type="checkbox"/> 有 <input type="checkbox"/> 無
助成機関名称 Funding agency	
助成金名称 Grant name	
受給期間 Supported period	年 月 ~ 年 月
受給額 Amount received	円

## 6. 他の奨学金受給 Another awarded scholarship

受給実績 Receipt record	<input type="checkbox"/> 有 <input checked="" type="checkbox"/> 無
助成機関名称 Funding agency	
奨学金名称 Scholarship name	
受給期間 Supported period	年 月 ~ 年 月
受給額 Amount received	円

## 7. 研究活動に関する報道発表 Press release concerned with your research activities

※記載した記事を添付してください。Attach a copy of the article described below

報道発表 Press release	<input type="checkbox"/> 有 <input checked="" type="checkbox"/> 無	発表年月日 Date of release	
発表機関 Released medium			
発表形式 Release method	・新聞 ・雑誌 ・Web site ・記者発表 ・その他( )		
発表タイトル Released title			

## 8. 本研究テーマに関する特許出願予定 Patent application concerned with your research theme

出願予定 Scheduled	<input type="checkbox"/> 有 <input checked="" type="checkbox"/> 無	出願国 Application	
出願内容(概要) Application contents			

## 9. その他 Others

--

指導責任者(記名) 市川 智彦

## Article

# Tumor Location and a Tumor Volume over 2.8 cc Predict the Prognosis for Japanese Localized Prostate Cancer

Haruki Baba <sup>1,†</sup>, Shinichi Sakamoto <sup>1,\*,†</sup>, Xue Zhao <sup>1,†</sup> , Yasutaka Yamada <sup>1</sup>, Junryo Rii <sup>1</sup> , Ayumi Fujimoto <sup>1</sup>, Manato Kanesaka <sup>1</sup>, Nobuyoshi Takeuchi <sup>1</sup>, Tomokazu Sazuka <sup>1</sup>, Yusuke Imamura <sup>1</sup>, Koichiro Akakura <sup>2</sup> and Tomohiko Ichikawa <sup>1</sup>

<sup>1</sup> Department of Urology, Chiba University Graduate School of Medicine, Chiba 260-8670, Japan

<sup>2</sup> Department of Urology, Japan Community Health-Care Organization Tokyo Shinjuku Medical Center, Tokyo 162-8543, Japan

\* Correspondence: rbatbat1@chiba-u.jp; Tel.: +81-43-226-2134; Fax: +81-43-226-2136

† These authors contributed equally to this work.

**Simple Summary:** About 40% of men with localized prostate cancer experience biochemical recurrence after radical prostatectomy. The early detection of disease progression is important for optimal post-operative treatment and follow-up. Our study reviewed 557 patients with prostate cancer who underwent radical prostatectomy and found that a tumor volume over 2.8 cc was a novel independent predictive factor for biochemical recurrence. We further established a novel risk assessment model based on tumor volume and location (posterior and peripheral zone). We confirmed that the risk model could stratify patients' prognoses. In addition to the previously reported biomarkers, these novel factors obtained from the surgical specimen may provide better prognostic information in patients with prostate cancer.



**Citation:** Baba, H.; Sakamoto, S.; Zhao, X.; Yamada, Y.; Rii, J.; Fujimoto, A.; Kanesaka, M.; Takeuchi, N.; Sazuka, T.; Imamura, Y.; et al. Tumor Location and a Tumor Volume over 2.8 cc Predict the Prognosis for Japanese Localized Prostate Cancer. *Cancers* **2022**, *14*, 5823. <https://doi.org/10.3390/cancers14235823>

Academic Editor: Grace Lu-Yao

Received: 5 November 2022

Accepted: 24 November 2022

Published: 25 November 2022

**Publisher's Note:** MDPI stays neutral with regard to jurisdictional claims in published maps and institutional affiliations.



**Copyright:** © 2022 by the authors. Licensee MDPI, Basel, Switzerland. This article is an open access article distributed under the terms and conditions of the Creative Commons Attribution (CC BY) license (<https://creativecommons.org/licenses/by/4.0/>).

**Abstract:** (1) Objective: Our study investigated the prognostic value of tumor volume and location in prostate cancer patients who received radical prostatectomy (RP). (2) Methods: The prognostic significance of tumor volume and location, together with other clinical factors, was studied using 557 patients who received RP. (3) Results: The receiver operating characteristic (ROC) curve identified the optimal cutoff value of tumor volume as 2.8 cc for predicting biochemical recurrence (BCR). Cox regression analysis revealed that a tumor in the posterior area ( $p = 0.031$ ), peripheral zone ( $p = 0.0472$ ), and tumor volume  $\geq 2.8$  cc ( $p < 0.0001$ ) were predictive factors in univariate analysis. After multivariate analysis, tumor volume  $\geq 2.8$  cc ( $p = 0.0225$ ) was an independent predictive factor for BCR. Among them, a novel risk model was established using tumor volume and location in the posterior area and peripheral zone. The progression-free survival (PFS) of patients who met the three criteria (unfavorable group) was significantly worse than other groups ( $p \leq 0.001$ ). Furthermore, multivariate analysis showed that the unfavorable risk was an independent prognostic factor for BCR. The prognostic significance of our risk model was observed in low- to intermediate-risk patients, although it was not observed in high-risk patients. (4) Conclusion: Tumor volume ( $\geq 2.8$  cc) and localization (posterior/peripheral zone) may be a novel prognostic factor in patients undergoing RP.

**Keywords:** tumor volume; tumor location; prostate cancer; biochemical recurrence; prognostic factor

## 1. Introduction

Prostate cancer (Pca) is the most common malignant tumor in men. About 2.6 million cases are newly diagnosed and 34,500 deaths of Pca are estimated per year in the United States [1]. Radical prostatectomy (RP) for the treatment of prostate cancer has made remarkable progress since it widely emerged around 1900. At present, RP is still the standard treatment option for localized Pca [2]. However, the frequency of biochemical recurrence (BCR) has been reported to be about 40% within 10 years after RP [3]. Once BCR

occurs, about 3.5% of patients will inevitably develop resistance to androgen deprivation therapy, also known as castration-resistant prostate cancer (CRPC) [4]. CRPC has been reported to cause death within 2 to 4 years [5]. Therefore, BCR is the major clinical issue to be detected and addressed in patients who received RP.

A lot of clinical studies have evaluated predictive factors and/or risk models for BCR after RP. Serum prostate-specific antigen (PSA) is the mainstay to detect the BCR of patients after surgery [6], and it has been recommended to keep close monitoring until PSA reaches 0.2 ng/mL [7]. In addition to PSA kinetics, Gleason score, PSA density, pathological and clinical stages, surgical margin, and other clinical factors have been studied for their prognostic significance, however, these factors could not predict BCR independently [8]. To better distinguish the recurrence risk and evaluate the prognosis after RP, more innovative predictors or models are unmet clinical needs. The individualized management after treatment requires effective recurrence risk prediction to implement timely intervention and avoid overtreatment. Previous studies showed that the tumor volume was related to the clinical manifestations of prostate cancer [9]. A tumor with a volume of less than 0.5 cc is considered as insignificant prostate cancer, and aggressive treatment may not be needed [10,11]. Recently, several studies proposed the novel definition of insignificant prostate cancer as a tumor volume of less than 2.5 cc [11–17], or less than 2.0 cc [18]. However, it was found that the BCR risk increased with tumor volume over 2.49 cc, indicating that the tumor volume was deeply involved in the progression of Pca [19]. Furthermore, little is known about the relationship between different prostate areas and tumor volumes, and their impact on BCR. Herein, we examined the prognostic role of tumor volume and location in patients with localized Pca for a better treatment strategy and postoperative follow-up.

## 2. Methods

### 2.1. Study Design and Setting

Clinical data of 557 patients who received RP at Chiba University Hospital and affiliated hospitals between 2006 and 2020 were retrospectively reviewed. The study was approved by the clinical review committee of our institution (#1768) and the written informed consent of all patients participating in the study was obtained. All participants or designated agents accepted a standardized data collection protocol, including personal postoperative follow-up information and medical record. The study is in accordance with the Japanese ethical document.

### 2.2. Patients

The inclusion criteria were RP for biopsy-proven prostate cancer performed at Chiba University Hospital and affiliated hospitals; whole-mount step-section pathologic maps available for tumor volume-calculation and localization. The exclusion criteria were neoadjuvant hormone therapy; radiation therapy; poor pathologic map quality; short follow-up term (<12 months).

### 2.3. Variables

Baseline clinical data included age, BMI, serum PSA, PSA F/T ratio, serum testosterone, biopsy positive rate, Gleason score (GS), clinical TNM staging, surgical prostate specimen, tumor volume, tumor location, surgical resect margin, and pathological TNM staging. Each patient came to our institution every 3 months after RP and had blood samples taken for PSA measurement until the occurrence of BCR or death was confirmed.

After RP, an elevated serum PSA level (>0.2 ng/mL) was defined as BCR [6].

### 2.4. Tumor Volume and Location Estimation Method

#### 2.4.1. Measurement of Tumor Volume

The prostatectomy specimens were step-sectioned transversely at 5-mm intervals. All the specimens were mounted on slides. Tumor volume was calculated by scanning the

and had blood samples taken for PSA measurement until the occurrence of BCR or death was confirmed.

After RP, an elevated serum PSA level (>0.2 ng/mL) was defined as BCR [6].

2.4.1. Measurement of Tumor Volume

The prostatectomy specimens were step-sectioned transversely at 5-mm intervals. All the specimens were mounted on slides. Tumor volume was calculated by scanning the sliced specimen, and the area of the tumor was analyzed using ImageJ software. Total tumor volume = tumor area × thickness of specimen × 1.2 (correction for shrinkage).

2.4.2. Tumor Localization

All specimens were serially sectioned from the tip to the base at 5 mm intervals, and the bladder neck and vertex edges were submitted as vertical sections. According to the anatomical structure, the specimen was divided into the following regions: the peripheral zone (PZ), the transition zone (TZ), and the central zone (CZ). The region within 1.0 cm or 1.5 cm from the tip of the prostate was identified as the Apex region. The prostatic urethra is an anatomic marker for a tumor to be classified as anterior or posterior (Figure 1). If a tumor showed a slight extension to another site, >80% volume in the main area was the criterion for defining the origin of the tumor in this area. Each RP sample was reviewed by two pathologists.

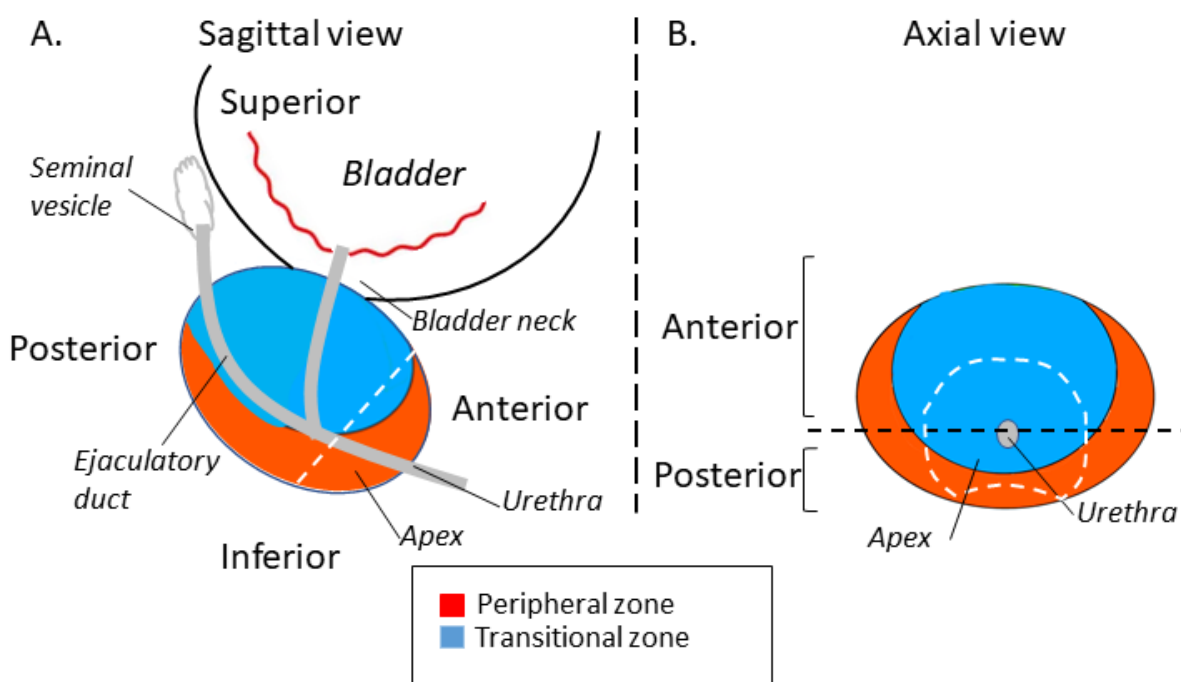


Figure 1. Schematic diagram of an anatomical division of the prostate. The location of the Anterior/Posterior and Peripheral/Transitional Zones are described. (A) Sagittal view. (B) Axial view.

2.5. Statistical Methods

JMP Pro (Version 16.0; SAS Institute Inc., Cary, NC, USA) was used for statistical analysis. Univariate cox proportional hazards model analysis was performed on the baseline data classified by the median value of the outcome measurement to determine predictive factors of the BCR. The significant variables ( $p < 0.05$ ) were further analyzed by multivariable cox proportional hazards model regression. The optimal cutoff value of tumor volume was obtained by calculating Area Under the Curve (AUC) from the Receiver Operating Characteristic (ROC) curve analysis. To evaluate the interaction between tumor volume and location, 3 risk factors related to volume and location obtained from univariate and multivariate cox regression analysis were combined into a risk classification model. This model was grouped according to the number of risk factors displayed: favorable; 0 risk factor, moderate; 1 or 2 risk factors, unfavorable; all 3 risk factors. Kaplan–Meier method was used to evaluate progression-free survival (PFS). Statistical significance was set at  $p < 0.05$ .

### 3. Results

#### 3.1. Participants

In total, 557 patients were enrolled in the study. Follow-up terms ranged from 12 to 161.5 months, with a median follow-up time of 45.3 months. As of the end of the study, 66 (11.8%) patients had BCR, and 9 (1.6%) patients died (not due to prostate cancer). The median age of all patients was 67 years old. The median preoperative PSA level was 7.71 ng/mL. The biopsy GS was 7 or less in 79.7%, 8 in 8.6%, and 9 or more in 11%. Overall, 64.8% of patients were pathological TNM stage 2c or above, and 1.4% were positive for lymph node metastasis. According to the risk grouping of Pca by the American Cancer Society (ACS), 77 (13.8%) patients were classified into the low-risk group, 279 (50.1%) were classified into the intermediate-risk group, and 201 (36.1%) were classified into the high-risk group. The median tumor volume was 2.12 cc. Seminal vesicle invasion was observed in 8.6%, the extracapsular invasion was seen in 24.8%, and 30.3% had positive margins. The tumor distributions were in the apex area (63.7%), middle area (63.4%), and bladder neck (21.4%). Regarding the anterior or posterior area of the prostate, 48.1% of the tumors were in the anterior, and 52.4% were in the posterior. Overall, 67.1% were located in the PZ and 37.3% were in the TZ (Table 1).

**Table 1.** Characteristics of patients.

Characteristics	
Number of patients	557
Median age at operation (range), years	67 (46–77)
Median follow-up time (range), months	45.3 (12–161.5)
Median initial PSA (range) (ng/mL)	7.71 (2.15–87.16)
Gleason score sum, n (%)	
≤7	444 (79.7)
8	48 (8.6)
≥9	61 (11.0)
T stage, n (%)	
≤2b	195 (35.0)
≥2c	361 (64.8)
Risk Group; Low/Intermediate/High, n (%)	77 (13.8)/279 (50.1)/201 (36.1)
Tumor Volume (range), cc	2.12 (0.02–57)
Tumor Location, n (%)	
apex	355 (63.7)
middle	353 (63.4)
bladder neck	119 (21.4)
Tumor Location, n (%)	
anterior	268 (48.1)
posterior	292 (52.4)
Tumor Location, n (%)	
PZ	374 (67.1)
TZ	208 (37.3)
N stage, n (%)	
positive	8 (1.4)
Seminal Vesicle Invasion, n, (%)	48 (8.6)
Extracapsular Extension, n, (%)	138 (24.8)
Resection Margins, n, (%)	169 (30.3)
PSA Recurrence, n, (%)	66 (11.8)

PSA = prostate-specific antigen; T stage = tumor stage; N stage = lymph node stage; PZ = peripheral zone; TZ = transition zone.

#### 3.2. Predictive Factors for Progression-Free Survival (PFS)

The ROC curve was used to calculate the relationship between BCR and tumor volume, and the optimal cutoff value was identified as 2.8 cc (AUC = 0.69) (Supplementary Figure S1A). We analyzed different tumor volume cutoff values (0.5 cc, 1.0 cc, 2.0 cc, 2.8 cc, 3.0 cc, 3.5 cc) and compared HR and *p*-values. The results confirmed that 2.8 cc is the optimal cut-off value as a

predictive factor for BCR (Table 2). (The cutoff values of two tumor volumes with  $p < 0.0001$  that were not selected (3.0 cc and 3.5 cc) were also verified by corresponding models, as shown in Supplementary Figures S2 and S3).

**Table 2.** Univariable and multivariable cox proportional hazard regression models in predictive factors for PFS in localized Pca (overall risk).

	Univariable				Multivariable		
	Cut Off	HR	95% CI	p Value	HR	95% CI	p Value
Age	$\geq 67$	0.96	0.59–1.57	0.8842			
initial PSA	$\geq 7.71$ ng/mL	1.65	1.00–2.73	0.0505			
PSAD	$\geq 0.26$	2.06	1.21–3.53	0.0082	1.51	0.73–3.09	0.2643
GS	$\geq 7$	1.15	0.46–2.88	0.7593			
T stage	$\geq T3$	4.66	2.81–7.73	<0.0001	1.69	0.77–3.71	0.1894
RM	positive	4.18	2.46–7.10	<0.0001	1.99	0.94–4.20	0.0712
Tumor location	Apex	1.45	0.70–3.02	0.3166			
	PZ	3.28	1.01–10.60	0.0472	2.21	0.49–10.05	0.3030
	posterior	2.24	1.07–4.65	0.0314	1.72	0.72–4.12	0.2193
TV	$\geq 0.5$ cc	1.61	0.73–3.53	0.2344			
	$\geq 1.0$ cc	2.18	1.11–4.27	0.0240			
	$\geq 2.0$ cc	2.74	1.55–4.82	0.0005			
	$\geq 2.8$ cc **	3.10	1.86–5.17	<0.0001	2.47	1.14–5.36	0.0225 *
	$\geq 3.0$ cc	2.96	1.80–4.88	<0.0001			
	$\geq 3.5$ cc	2.80	1.72–4.58	<0.0001			

PSA = prostate-specific antigen; PSAD = prostate-specific antigen density; GS = Gleason score; T stage = tumor stage; RM = resection margins; HR = hazard ratio; CI = confidence interval; \*  $p$ -value < 0.05, \*\* tumor volume cutoff value based on the ROC curve.

Univariate and multivariate predictors for BCR obtained from cox proportional hazard analysis are shown in Table 2. The predictors for BCR were pathological stage  $T \geq 3$  (HR = 4.66 [95% CI: 2.81–7.73],  $p < 0.0001$ ), positive surgical margin (HR = 4.18 [95% CI: 2.46–7.10],  $p < 0.0001$ ), tumor volume  $\geq 2.8$  cc (HR = 3.10 [95% CI: 1.86–5.17],  $p < 0.0001$ ), followed by PSA density  $\geq 0.26$  (HR = 2.06 [95% CI: 1.21–3.53],  $p = 0.0082$ ), tumor located in the Posterior region (HR = 2.24 [95% CI: 1.07–4.65],  $p = 0.0314$ ), tumor located in the PZ (HR = 3.28 [95% CI: 1.01–10.6],  $p = 0.0472$ ). The multivariate analysis showed that the independent predictor of BCR was only tumor volume  $\geq 2.8$  cc (HR = 2.47 [95% CI: 1.14–5.36],  $p = 0.0225$ ) (Table 2).

The Kaplan–Meier method was used to evaluate the PFS curve. The PFS of patients with tumors located in the PZ was inferior to those in the TZ (Figure 2A  $p = 0.0354$ ). Furthermore, patients harboring tumors located in the posterior had shorter PFS than those in the anterior area (Figure 2B  $p = 0.027$ ). Consistent with cox analysis, there was no significant difference between the PFS of the patients with tumors in the apex and not-apex area (Figure 2C  $p = 0.3135$ ). PFS in the patients with tumor volume  $\geq 2.8$  cc was significantly inferior to those with less than 2.8 cc (Figure 2D  $p < 0.0001$ ).

### 3.3. Model for Predicting PFS by Tumor Volume at Specific Location

Based on the analysis of clinical factors related to BCR in Table 2 and Figure 2, tumor volume and tumor location (PZ and Posterior location) were statistically significant predictive factors. Therefore, we established a risk classification model using tumor volume and location to stratify patients on the basis of risk of progression. The three risk factors that predict BCR in the model are tumor volume  $\geq 2.8$  cc, tumor located in PZ, and tumor located in the posterior area. The capability of the unfavorable risk to predict BCR was

independent predictor of BCR was only tumor volume  $\geq 2.8$  cc (HR = 2.47 [95% CI: 1.14–5.36]  $p = 0.0225$ ) (Table 2).

The Kaplan–Meier method was used to evaluate the PFS curve. The PFS of patients with tumors located in the PZ was inferior to those in the TZ (Figure 2A  $p = 0.0354$ ). Furthermore, patients harboring tumors located in the posterior had shorter PFS than those in the anterior area (Figure 2B  $p = 0.027$ ). Consistent with cox analysis, there was no significant difference between the PFS of the patients with tumors in the apex and not-apex area (Figure 2C)  $p = 0.3135$ . PFS in the patients with tumor volume  $\geq 2.8$  cc was significantly inferior to those with less than 2.8 cc (Figure 2D  $p < 0.0001$ ).

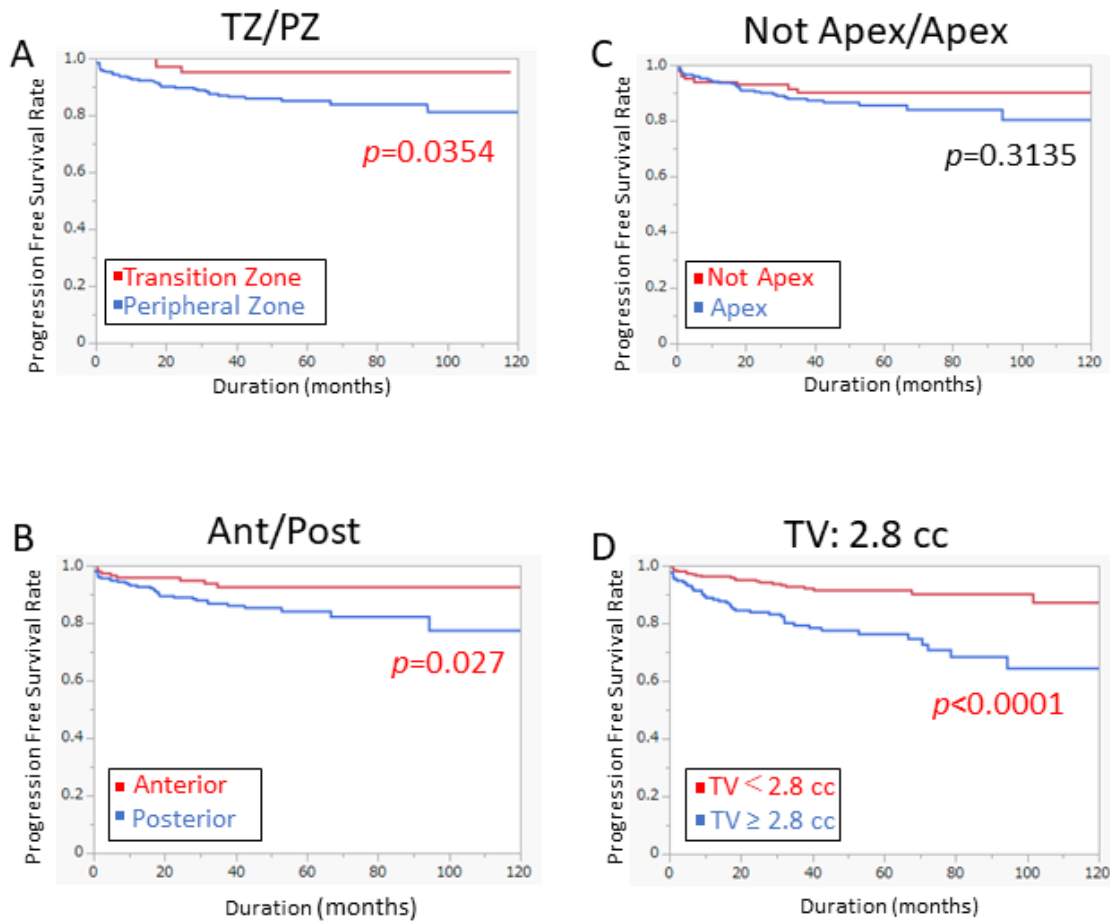


**Figure 2.** Prognostic significance of tumor location and tumor volume. (A) Patients with tumor in the PZ had significantly worse PFS than those in the TZ ( $p = 0.0354$ ). (B) Patients with tumor in the posterior region had significantly worse PFS than those in the anterior region ( $p = 0.027$ ). (C) There was no difference in PFS between apex and non-apex regions. (D) Patients with tumor volume  $\geq 2.8$  cc had significantly worse PFS than those  $< 2.8$  cc ( $p < 0.0001$ ).

3.3. Model for Predicting PFS by Tumor Volume at Specific Location

Based on the analysis of univariable and multivariable cox proportional hazards regression models in predictive factors for PFS in localized PCa (overall risk) and with unfavorable risk were statistically significant predictive factors. Therefore, we established a risk classification model using tumor volume and location to stratify patients on the basis of risk of progression. The three risk

Cut Off	Univariable			Multivariable		
	HR	95% CI	p-value	HR	95% CI	p-value
Age $\geq 67$	0.96	0.59–1.57	0.8842	-	-	-
initial PSA $\geq 7.71$ ng/mL	1.63	1.00–2.73	0.0505	-	-	-
PSAD $\geq 0.26$	1.03	0.51–2.33	0.9302	1.55	0.76–3.15	0.2307
GS $\geq 7$	1.15	0.46–2.88	0.7593	-	-	-
T stage $\geq T3$	4.66	2.81–7.73	<0.0001	1.64	0.74–3.65	0.2261
RM positive	4.18	2.46–7.10	<0.0001	2.09	0.99–4.42	0.0548
Unfavorable Risk PZ + Post + TV $\geq 2.8$ cc	4.74	2.60–8.65	<0.0001	3.16	1.52–6.56	0.0020 *

PSA = prostate-specific antigen; PSAD = prostate-specific antigen density; GS = Gleason score; T stage = tumor stage; RM = resection margins; PZ + Post + TV $\geq 2.8$  cc = tumor volume  $\geq 2.8$  cc in posterior location of peripheral zone; HR = hazard ratio; CI = confidence interval; \*  $p$ -value  $< 0.05$ .

To further explore the predictive ability of the novel risk model, we divided the patients into the low-risk group, intermediate-risk group, and high-risk group according to

the risk grouping of Pca by the American Cancer Society (ACS) [20] and validated the predictive value of the risk models among different ACS risk groups. In the analysis of the high-risk group, our unfavorable risk model could not predict disease progression independently (Table 4). However, the risk factors were the only independent predictor for PFS among patients with low to intermediate-risk groups (HR 4.43 [95% CI: 1.51–13.01],  $p = 0.0068$ ) (Table 5).

**Table 4.** Univariable and multivariable cox proportional hazard regression models in predictive factors for PFS in localized Pca (high risk).

	Cut Off	Univariable			Multivariable		
		HR	95% CI	<i>p</i> Value	HR	95% CI	<i>p</i> Value
Age	≥67	0.76	0.40–1.47	0.4167	-	-	-
initial PSA	≥7.71 ng/mL	1.04	0.52–2.08	0.9097	-	-	-
PSAD	≥0.26	1.9	0.82–4.40	0.1326	-	-	-
GS	≥7	1.29	0.18–9.46	0.7991	-	-	-
T stage	≥T3	4.38	2.11–9.10	<0.0001	1.98	0.75–5.25	0.1701
RM	positive	4.65	2.16–10.02	<0.0001	2.37	0.95–5.91	0.0649
Unfavorable Risk	PZ + Post + TV2.8 cc	3.5	1.64–7.47	0.0012	1.87	0.77–4.53	0.1653

PSA = Prostate Specific Antigen; PSAD = Prostate Specific Antigen Density; GS = Gleason Score; T stage = Tumor Stage; RM = Resection Margins; HR = Hazard Ratio; CI = Confidence Interval.

**Table 5.** Univariable and multivariable cox proportional hazard regression models in predictive factors for PFS in localized Pca (low to intermediate risk).

	Cut Off	Univariable			Multivariable		
		HR	95% CI	<i>p</i> Value	HR	95% CI	<i>p</i> Value
Age	≥67	1.07	0.51–2.25	0.8546	-	-	-
initial PSA	≥7.71 ng/mL	1.56	0.74–3.28	0.2458	-	-	-
PSAD	≥0.26	1.52	0.72–3.19	0.2716	-	-	-
GS	≥7	0.74	0.26–2.15	0.5855	-	-	-
T stage	≥T3	3.34	1.59–7.01	0.0015	0.97	0.28–3.38	0.961
RM	positive	3.03	1.42–6.47	0.0043	1.38	0.43–4.41	0.5904
Unfavorable Risk	PZ + Post + TV2.8 cc	4.71	1.75–12.69	0.0022	4.43	1.51–13.01	0.0068 *

PSA = prostate-specific antigen; PSAD = prostate-specific antigen density; GS = Gleason score; T stage = tumor stage; RM = resection margins; HR = hazard ratio; CI = confidence interval; PZ + Post + TV2.8 cc = tumor volume ≥ 2.8 cc in posterior location of the peripheral zone. \*  $p$ -value < 0.05.

### 3.4. Risk Model to Stratify Patient Prognosis

According to our established risk model, we divided the patients into three groups (favorable; displayed zero risk factors, moderate; displayed one or two risk factors, unfavorable; displayed all three risk factors). Overall, 61, 343, and 104 patients were classified as belonging to the favorable, moderate, and unfavorable group, respectively (Figure 3A).

The PFS curves of the three groups of patients (Figure 3B) showed that the PFS of the unfavorable group was significantly worse than that of the moderate group ( $p < 0.0001$ ) and the favorable group ( $p = 0.001$ ), while there was no significant difference between the moderate group and the favorable group ( $p = 0.1150$ ).

The median tumor volume of the three groups was 1.33 cc, 1.81 cc, and 4.92 cc, respectively and there were significant differences between the three groups (Figure 3C).

According to our established risk model, we divided the patients into three groups (favorable; displayed zero risk factors, moderate; displayed one or two risk factors, unfavorable; displayed all three risk factors). Overall, 61, 343, and 104 patients were classified as belonging to the favorable, moderate, and unfavorable group, respectively (Figure 3A).

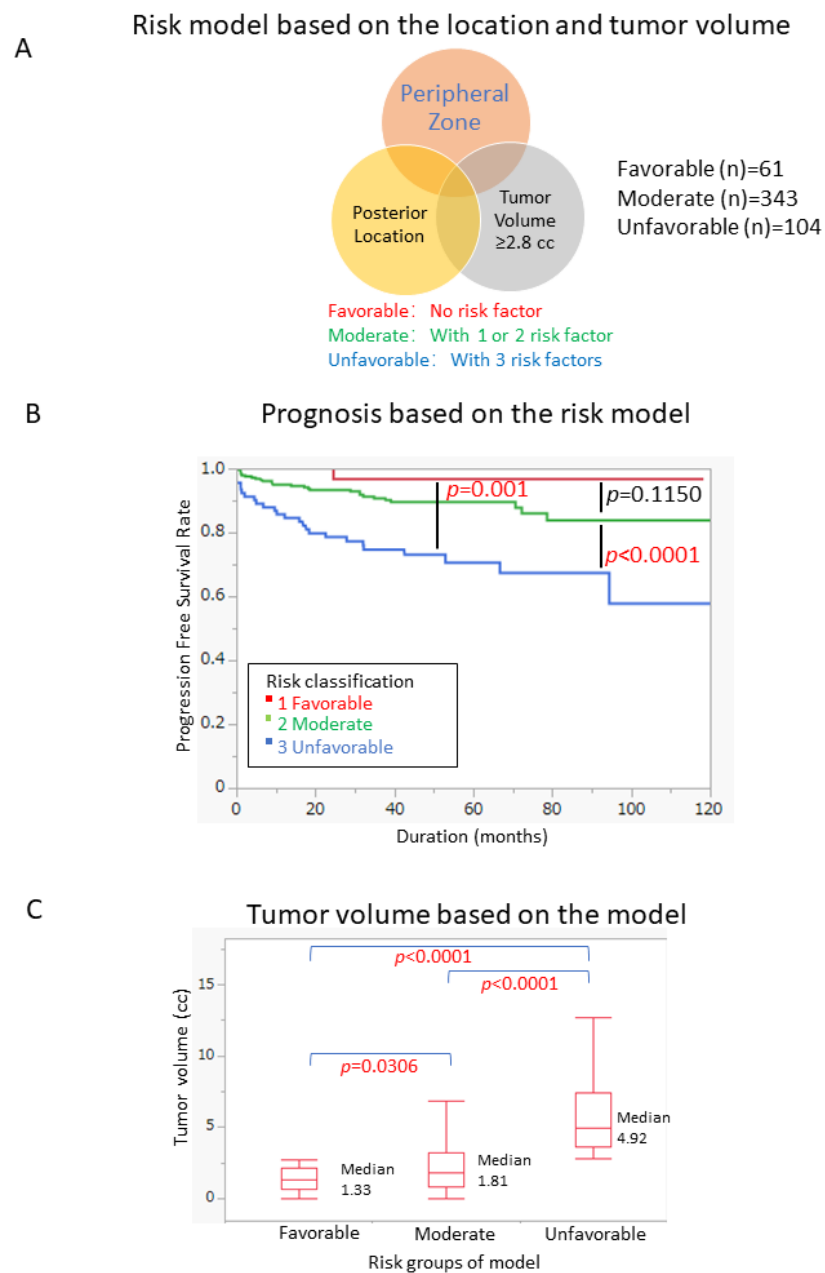


**Figure 3.** Prognostic model based on the location and tumor volume (A) Venn diagram of risk model based on the location and tumor volume. (B) Risk classification significantly differentiated the PFS between the Favorable and Unfavorable group ( $p=0.001$ ) and the Moderate and Unfavorable group ( $p<0.0001$ ). (C) The tumor volume showed significant differences among different risk groups.

In addition, we analyzed the impact of tumor volume on PFS in different prostate regions with the tumor volume of 2.8 cc as the threshold (Figure 4). The results suggested that the PFS of tumor  $\geq 2.8$  cc in the PZ is significantly worse than that of less than 2.8 cc (Figure 4A  $p < 0.0001$ ). Similar results were observed for tumors  $\geq 2.8$  cc in the posterior location (Figure 4C  $p < 0.0001$ ). Of note, the 2.8 cc cutoff value in TZ also showed a significant difference in PFS between the two groups (Figure 4B  $p = 0.0345$ ). On the other hand, the significant difference was not seen in the anterior area (Figure 4D  $p = 0.0873$ ).

In addition, we analyzed the impact of tumor volume on PFS in different prostate regions with the tumor volume of 2.8 cc as the threshold (Figure 4). The results suggested that the PFS of tumor  $\geq 2.8$  cc in the PZ is significantly worse than that of less than 2.8 cc (Figure 4A  $p < 0.0001$ ). Similar results were observed for tumors  $\geq 2.8$  cc in the posterior location (Figure 4C  $p < 0.0001$ ). Of note, the 2.8 cc cutoff value in TZ also showed a significant difference in PFS between the two groups (Figure 4B  $p = 0.0345$ ). On the other hand, the significant difference was not seen in the anterior area (Figure 4D  $p = 0.0873$ ).

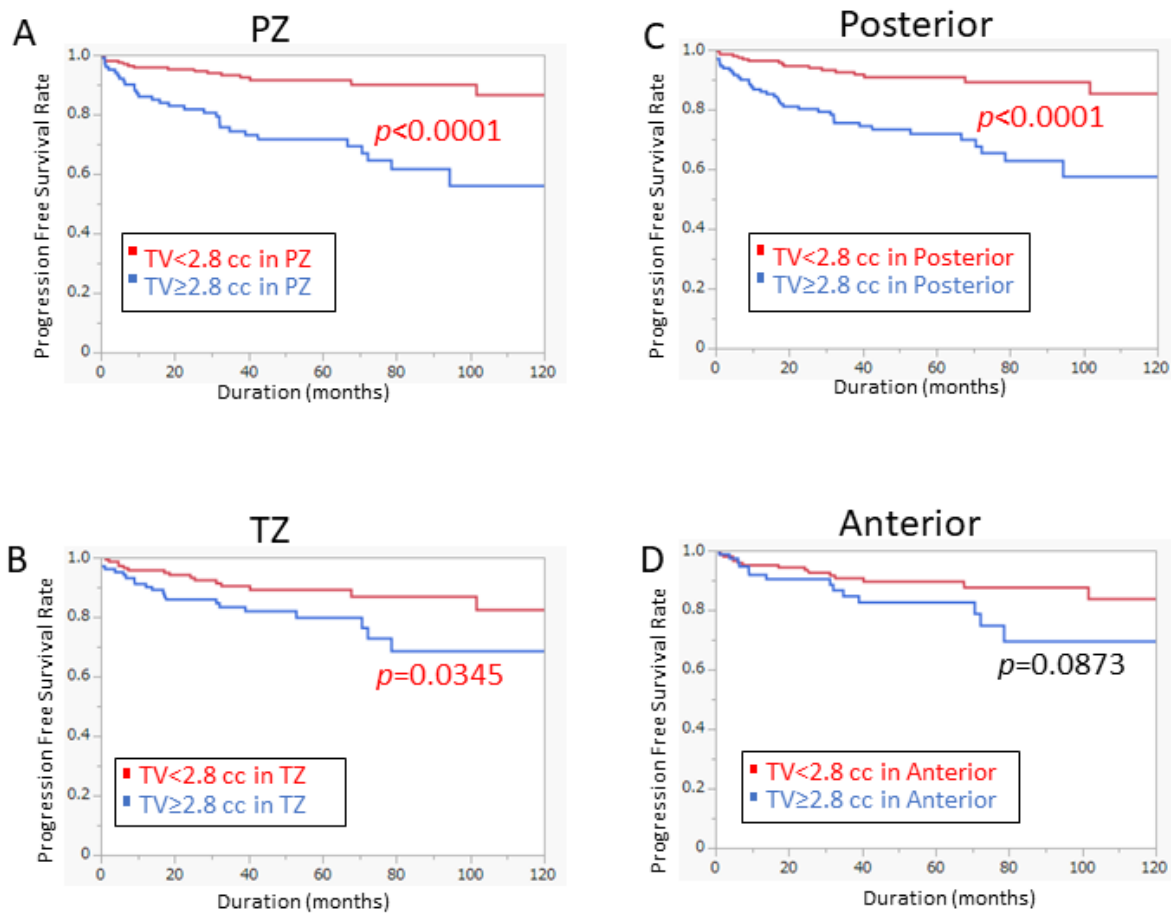


**Figure 4.** Prognostic significance of Tumor volume  $\geq 2.8$  cc based on the location. (A) Patients with tumor volume  $\geq 2.8$  cc had significantly worse PFS in the PZ ( $p < 0.0001$ ). (B) Patients with tumor volume  $\geq 2.8$  cc had significantly worse PFS in the TZ ( $p = 0.0345$ ). (C) Patients with tumor volume  $\geq 2.8$  cc had significantly worse PFS in the posterior region ( $p < 0.0001$ ). (D) In the anterior region, there was no difference in PFS by tumor volume cutoff of 2.8 cc.

**4. Discussion**

In our study, a tumor with a volume  $\geq 2.8$  cc was identified as an independent predictive factor for BCR ( $p = 0.0225$ ). Furthermore, we established novel risk classification together with PZ and posterior location, which distinguished PFS between different risk groups. We believe this risk model will provide novel prognostic significance in patients who received RP.

Previous studies showed the positive surgical margin after RP is a potential predictive factor for BCR [21–29]. It is difficult to completely avoid the incidence of positive surgical margins through objective methods. Several studies found that positive surgical margins with limited length [30,31], locations [32], or quantity [33] decreased the correlation with BCR. Another study showed that tumor volume was associated with BCR in patients who underwent RP with negative surgical margins [34]. In addition, tumor volume and GS were even more significant predictors for BCR than positive margins [35] and the location of the tumor could predict the incidence of positive surgical margins [36–39]. Multivariate analysis showed that the predictive value of our risk model was superior to the positive surgical margin. These findings suggested that focusing on tumor volume and location, not only resection margins will give us better prognostic information in the treatment of localized Pca.

Regarding the prognostic significance of tumor localization, tumors originating in the TZ have been reported to be associated with a better prognosis in comparison with those

in the PZ [39–41]. Augustin et al. found that the location of prostate cancer in the TZ was associated with better progression-free survival after RP ( $p = 0.0402$ ) [40]. However, the zonal location offers no advantage over the well-established prognostic factors in predicting recurrence. Some more detailed anatomical differentiation (anterior, posterior, the apex of prostate, bladder neck) also revealed the difference in tumor location on prognosis [42,43]. Magheli et al. found that tumors in the anterior prostate were associated with favorable pathological features and improved biochemical-free survival, although it was not an independent predictor of BCR [42]. There are also some studies that have concluded that tumor location is not related to prognosis [44,45].

Tumor volume has been reported to show a significant correlation with BCR after RP [46–50]. Generally, tumor volume  $< 0.5$  cc has been considered as an insignificant Pca, which has a low potential of recurrence [51]. The predictive factors for BCR in patients with low-volume prostate cancer ( $\leq 0.5$  cc) have not been well studied [52]. Several reports proposed to increase the thresholds of volume for insignificant cancer to avoid over-treatment [14], however, other studies showed that the modified criteria had a higher risk of BCR in Gleason 4/5 cancer [53]. The tumor volume was superior to the percentage of cancer (tumor volume/prostate volume ratio) for predicting the prognosis after RP [54]. Different tumor volume cut-off values were proposed to determine the prognosis of Pca. Friedersdorff et al. suggested that tumor volume  $\geq 5$  cc (AUC = 0.79) was a significant prognostic factor for BCR [55]. Another study set the cut-off values as: minimal ( $\leq 1.0$  cc), middle (1.1–5.0 cc), or extended ( $> 5.0$  cc) [47]. Shin et al. divided the tumor volume into three groups according to 2 cc and 5 cc, in multivariate analysis, recurrence-free survival could be independently predicted [56]. The tumor volume in the surgical specimen after neoadjuvant therapy was investigated and the study showed that patients with residual tumors  $\geq 1.0$  cc in the specimen had a higher risk of BCR [57]. Raison et al. studied 685 British patients who underwent laparoscopic and robot-assisted RP and revealed that 2.5 cc (AUC = 0.71) was the best cutoff value for predicting BCR [58]. Of note, some studies showed that the tumor volume alone may not be able to evaluate the prognosis of recurrence and prognosis after RP [13,59]. O’Neil et al. suggested that tumors in some locations are larger and more likely to invade the sites that are prone to recurrence [37]. However, there have been no studies that have analyzed the prognostic value of tumor volume combined with tumor localization.

In our study, we attempted to evaluate the potential interaction between tumor volume and location, the tumor volume cutoff value obtained by the ROC curve was 2.8 cc (AUC = 0.69). Therefore, we used the tumor volume threshold ( $\geq 2.8$  cc) of the specific location to improve the capability of our risk model. We hypothesized that the larger tumor volume in the PZ and/or posterior of the prostate may be associated with BCR. Our findings demonstrated that the prognostic significance of tumor volume over 2.8 cc varied by tumor localization (Figure 4). In our model, the interaction between prostate tumor location and volume was a promising predictor of prostate BCR. Interestingly, our risk model was an independent predictor in patients with low and intermediate risk while it was not in patients with high risk. Extended dissection during surgery and close follow-up after surgery may enhance clinical benefit in patients who met our criteria.

The limitations of this study are as follows. First, our study included a single Asian race. Compared with the western population, the Asian population has a lower incidence and mortality of prostate cancer [60]. The tumor volume of African American men with prostate cancer is larger than that of white men [61]. The risk of BCR in black Americans has been reported to be 1.6 times higher than that in white Americans [62]. These results suggested that there may be differences in clinical and pathological features between races. Further validation of our risk model will be warranted in other patients’ cohorts. Second, our study may need to be further investigated using genomic analysis. The previous study has revealed that prostate cancer risk alleles are associated with prostate cancer volume and prostate size [63]. Downregulation of PAH and AOC1 and upregulation of DDC, LIN01436, and ORM1 were associated with the development of prostate cancer [8,64].

Molecular and cellular biological studies are also closely related to the site of prostate tumorigenesis [41]. Studying the specific genes behind it could improve understanding of the region or cell-type characteristics of prostate cancer. These features account for differences in tumor progression and invasion between different regions of the prostate [41]. The unique biological characteristics of tumor types in different prostate regions can help guide individualized treatment and patient risk stratification. Finally, further validation of our clinical parameters using the latest imaging system PSMA/PET [65] or artificial intelligence system (deep learning) [66] may enhance the clinical importance of this study.

## 5. Conclusions

Tumor volume  $\geq 2.8$  cc was an independent predictive factor for BCR in patients who received RP. Furthermore, we established a novel risk model using tumor volume over 2.8 cc and tumor location (PZ and/or posterior). Our risk classification could predict patient prognosis and will help us to optimize peri-operative and post-operative treatment strategies.

**Supplementary Materials:** The following supporting information can be downloaded at: <https://www.mdpi.com/article/10.3390/cancers14235823/s1>, Figure S1: (A) Tumor volume cut off based on the ROC curve. (B) Tumor volume based on the location; Figure S2: (A) A supplemental model that included the 3.0 cc tumor volume as one of the factors in the risk model. (B) Risk classification significantly differentiated the PFS between the Favorable and Unfavorable group ( $p = 0.0008$ ) and the Moderate and Unfavorable group ( $p < 0.0001$ ); Figure S3: (A) A supplemental model that included the 3.5 cc tumor volume as one of the factors in the risk model. (B) Risk classification significantly differentiated the PFS between the Favorable and Unfavorable group ( $p = 0.0001$ ) and the Moderate and Unfavorable group ( $p < 0.0001$ ).

**Author Contributions:** H.B. contributed to collecting data, preparing figures, and writing; S.S. and X.Z. contributed to analyzing data, collecting bibliography, drawing tables, and writing; Y.Y. and J.R. contributed to analyzing data; A.F., M.K., N.T., T.S., Y.I. and K.A. contributed to collecting data; S.S. and T.I. contributed to the supervision of all the activities; The first draft of the manuscript was prepared by H.B. and X.Z. performed subsequent amendments. S.S. revised the manuscript. All authors have read and agreed to the published version of the manuscript.

**Funding:** The present study was supported by grants from Grant-in-Aid for Scientific Research (C) (20K09555 to S.S.), Grant-in-Aid for Scientific Research (B) (20H03813 to T.I.), and the Japan China Sasakawa Medical Fellowship (to X.Z.).

**Institutional Review Board Statement:** The study was conducted in accordance with the Declaration of Helsinki, and approved by the Institutional Review Board (or Ethics Committee) of Chiba University of Graduate School of Medicine and School of Medicine (protocol code 1768 and date of approval 1 March 2018).

**Informed Consent Statement:** Informed consent was obtained from all subjects involved in the study.

**Data Availability Statement:** The data presented in this study are available on request from the corresponding author.

**Conflicts of Interest:** The authors declare no conflict of interest. The funders had no role in the design of the study; in the collection, analyses, or interpretation of data; in the writing of the manuscript, or in the decision to publish the results.

## Abbreviations

Pca	prostate cancer
RP	radical prostatectomy
BCR	biochemical recurrence
CRPC	castration-resistant prostate cancer
PSA	prostate-specific antigen
PZ	peripheral zone

TZ	transition zone
CZ	central zone
TV	tumor volume
GS	Gleason score
ROC	Receiver Operating Characteristic
AUC	Area Under the Curve
PFS	Progression-Free Survival
ACS	American Cancer Society

## References

1. Siegel, R.L.; Miller, K.D.; Fuchs, H.E.; Jemal, A. Cancer statistics, 2022. *CA Cancer J. Clin.* **2022**, *72*, 7–33. [[CrossRef](#)]
2. Costello, A.J. Considering the role of radical prostatectomy in 21st century prostate cancer care. *Nat. Rev. Urol.* **2020**, *17*, 177–188. [[CrossRef](#)] [[PubMed](#)]
3. Han, M.; Partin, A.W.; Pound, C.R.; Epstein, J.I.; Walsh, P.C. Long-term biochemical disease-free and cancer-specific survival following anatomic radical retropubic prostatectomy. The 15-year Johns Hopkins experience. *Urol. Clin. N. Am.* **2001**, *28*, 555–565. [[CrossRef](#)]
4. Everist, M.M.; Howard, L.E.; Aronson, W.J.; Kane, C.J.; Amling, C.L.; Cooperberg, M.R.; Terris, M.K.; Freedland, S.J. Socioeconomic status, race, and long-term outcomes after radical prostatectomy in an equal access health system: Results from the SEARCH database. *Urol. Oncol.* **2019**, *37*, 289.e11–289.e17. [[CrossRef](#)] [[PubMed](#)]
5. Pagliarulo, V. Androgen Deprivation Therapy for Prostate Cancer. *Adv. Exp. Med. Biol.* **2018**, *1096*, 1–30. [[CrossRef](#)] [[PubMed](#)]
6. Cookson, M.S.; Aus, G.; Burnett, A.L.; Canby-Hagino, E.D.; D’Amico, A.V.; Dmochowski, R.R.; Eton, D.T.; Forman, J.D.; Goldenberg, S.L.; Hernandez, J. Variation in the definition of biochemical recurrence in patients treated for localized prostate cancer: The American Urological Association Prostate Guidelines for Localized Prostate Cancer Update Panel report and recommendations for a standard in the reporting of surgical outcomes. *J. Urol.* **2007**, *177*, 540–545. [[PubMed](#)]
7. Teeter, A.E.; Griffin, K.; Howard, L.E.; Aronson, W.J.; Terris, M.K.; Kane, C.J.; Amling, C.L.; Cooperberg, M.R.; Freedland, S.J. Does Early Prostate Specific Antigen Doubling Time after Radical Prostatectomy, Calculated Prior to Prostate Specific Antigen Recurrence, Correlate with Prostate Cancer Outcomes? A Report from the SEARCH Database Group. *J. Urol.* **2018**, *199*, 713–718. [[CrossRef](#)] [[PubMed](#)]
8. Wei, J.; Wu, X.; Li, Y.; Tao, X.; Wang, B.; Yin, G. Identification of Potential Predictor of Biochemical Recurrence in Prostate Cancer. *Int. J. Gen. Med.* **2022**, *15*, 4897–4905. [[CrossRef](#)]
9. Stamey, T.A.; Freiha, F.S.; McNeal, J.E.; Redwine, E.A.; Whittemore, A.S.; Schmid, H.P. Localized prostate cancer. Relationship of tumor volume to clinical significance for treatment of prostate cancer. *Cancer* **1993**, *71*, 933–938. [[CrossRef](#)] [[PubMed](#)]
10. Epstein, J.I.; Walsh, P.C.; Carmichael, M.; Brendler, C.B. Pathologic and clinical findings to predict tumor extent of nonpalpable (stage t1 c) prostate cancer. *JAMA* **1994**, *271*, 368–374. [[CrossRef](#)] [[PubMed](#)]
11. Wolters, T.; Roobol, M.J.; van Leeuwen, P.J.; van den Bergh, R.C.; Hoedemaeker, R.F.; van Leenders, G.J.; Schröder, F.H.; van der Kwast, T.H. A critical analysis of the tumor volume threshold for clinically insignificant prostate cancer using a data set of a randomized screening trial. *J. Urol.* **2011**, *185*, 121–125. [[CrossRef](#)]
12. Ploussard, G.; Epstein, J.I.; Montironi, R.; Carroll, P.R.; Wirth, M.; Grimm, M.-O.; Bjartell, A.S.; Montorsi, F.; Freedland, S.J.; Erbersdobler, A. The contemporary concept of significant versus insignificant prostate cancer. *Eur. Urol.* **2011**, *60*, 291–303. [[CrossRef](#)]
13. Ito, Y.; Udo, K.; Vertosick, E.A.; Sjoberg, D.D.; Vickers, A.J.; Al-Ahmadie, H.A.; Chen, Y.B.; Gopalan, A.; Sirintrapun, S.J.; Tickoo, S.K.; et al. Clinical Usefulness of Prostate and Tumor Volume Related Parameters following Radical Prostatectomy for Localized Prostate Cancer. *J. Urol.* **2019**, *201*, 535–540. [[CrossRef](#)] [[PubMed](#)]
14. Ting, F.; van Leeuwen, P.J.; Delprado, W.; Haynes, A.M.; Brenner, P.; Stricker, P.D. Tumor volume in insignificant prostate cancer: Increasing the threshold is a safe approach to reduce over-treatment. *Prostate* **2015**, *75*, 1768–1773. [[CrossRef](#)]
15. Fugini, A.V.; Antonelli, A.; Giovanessi, L.; Gardini, V.C.; Abuhilal, M.; Zambolin, T.; Tardanico, R.; Simeone, C.; Cunico, S.C. Insignificant Prostate Cancer: Characteristics and Predictive Factors. *Urol. J.* **2011**, *78*, 184–186. [[CrossRef](#)] [[PubMed](#)]
16. Antonelli, A.; Vismara Fugini, A.; Tardanico, R.; Giovanessi, L.; Zambolin, T.; Simeone, C. The percentage of core involved by cancer is the best predictor of insignificant prostate cancer, according to an updated definition (tumor volume up to 2.5 cm<sup>3</sup>): Analysis of a cohort of 210 consecutive patients with low-risk disease. *Urology* **2014**, *83*, 28–32. [[CrossRef](#)]
17. Yamada, Y.; Sakamoto, S.; Sazuka, T.; Goto, Y.; Kawamura, K.; Imamoto, T.; Nihei, N.; Suzuki, H.; Akakura, K.; Ichikawa, T. Validation of active surveillance criteria for pathologically insignificant prostate cancer in Asian men. *Int. J. Urol.* **2016**, *23*, 49–54. [[CrossRef](#)] [[PubMed](#)]
18. Frankcombe, D.E.; Li, J.; Cohen, R.J. Redefining the Concept of Clinically Insignificant Prostate Cancer. *Urology* **2020**, *136*, 176–179. [[CrossRef](#)]
19. Schiffmann, J.; Connan, J.; Salomon, G.; Boehm, K.; Beyer, B.; Schlomm, T.; Tennstedt, P.; Sauter, G.; Karakiewicz, P.I.; Graefen, M.; et al. Tumor volume in insignificant prostate cancer: Increasing threshold gains increasing risk. *Prostate* **2015**, *75*, 45–49. [[CrossRef](#)] [[PubMed](#)]

20. Wolf, A.M.; Wender, R.C.; Etzioni, R.B.; Thompson, I.M.; D'Amico, A.V.; Volk, R.J.; Brooks, D.D.; Dash, C.; Guessous, I.; Andrews, K.; et al. American Cancer Society guideline for the early detection of prostate cancer: Update 2010. *CA Cancer J. Clin.* **2010**, *60*, 70–98. [[CrossRef](#)]
21. Sooriakumaran, P.; Dev, H.S.; Skarecky, D.; Ahlering, T. The importance of surgical margins in prostate cancer. *J. Surg. Oncol.* **2016**, *113*, 310–315. [[CrossRef](#)] [[PubMed](#)]
22. Matti, B.; Reeves, F.; Prouse, M.; Zargar-Shoshtari, K. The impact of the extent and location of positive surgical margins on the risk of biochemical recurrence following radical prostatectomy in men with Gleason 7 prostate cancers. *Prostate* **2021**, *81*, 1428–1434. [[CrossRef](#)]
23. Ploussard, G.; Drouin, S.J.; Rode, J.; Allory, Y.; Vordos, D.; Hoznek, A.; Abbou, C.C.; de la Taille, A.; Salomon, L. Location, extent, and multifocality of positive surgical margins for biochemical recurrence prediction after radical prostatectomy. *World J. Urol.* **2014**, *32*, 1393–1400. [[CrossRef](#)] [[PubMed](#)]
24. Meeks, J.J.; Eastham, J.A. Radical prostatectomy: Positive surgical margins matter. *Urol. Oncol.* **2013**, *31*, 974–979. [[CrossRef](#)] [[PubMed](#)]
25. Li, K.; Li, H.; Yang, Y.; Ian, L.H.; Pun, W.H.; Ho, S.F. Risk factors of positive surgical margin and biochemical recurrence of patients treated with radical prostatectomy: A single-center 10-year report. *Chin. Med. J.* **2011**, *124*, 1001–1005. [[PubMed](#)]
26. Sammon, J.D.; Trinh, Q.D.; Sukumar, S.; Ravi, P.; Friedman, A.; Sun, M.; Schmitges, J.; Jeldres, C.; Jeong, W.; Mander, N.; et al. Risk factors for biochemical recurrence following radical perineal prostatectomy in a large contemporary series: A detailed assessment of margin extent and location. *Urol. Oncol.* **2013**, *31*, 1470–1476. [[CrossRef](#)]
27. Wu, S.; Lin, S.X.; Wirth, G.J.; Lu, M.; Lu, J.; Subtelny, A.O.; Wang, Z.; Dahl, D.M.; Olumi, A.F.; Wu, C.L. Impact of Multifocality and Multilocation of Positive Surgical Margin After Radical Prostatectomy on Predicting Oncological Outcome. *Clin. Genitourin. Cancer* **2019**, *17*, e44–e52. [[CrossRef](#)] [[PubMed](#)]
28. Eastham, J.A.; Kuroiwa, K.; Otori, M.; Serio, A.M.; Gorbonos, A.; Maru, N.; Vickers, A.J.; Slawin, K.M.; Wheeler, T.M.; Reuter, V.E.; et al. Prognostic significance of location of positive margins in radical prostatectomy specimens. *Urology* **2007**, *70*, 965–969. [[CrossRef](#)] [[PubMed](#)]
29. Aydin, H.; Tsuzuki, T.; Hernandez, D.; Walsh, P.C.; Partin, A.W.; Epstein, J.I. Positive proximal (bladder neck) margin at radical prostatectomy confers greater risk of biochemical progression. *Urology* **2004**, *64*, 551–555. [[CrossRef](#)] [[PubMed](#)]
30. Sooriakumaran, P.; Ploumidis, A.; Nyberg, T.; Olsson, M.; Akre, O.; Haendler, L.; Egevad, L.; Nilsson, A.; Carlsson, S.; Jonsson, M.; et al. The impact of length and location of positive margins in predicting biochemical recurrence after robot-assisted radical prostatectomy with a minimum follow-up of 5 years. *BJU Int.* **2015**, *115*, 106–113. [[CrossRef](#)] [[PubMed](#)]
31. Shikanov, S.; Song, J.; Royce, C.; Al-Ahmadie, H.; Zorn, K.; Steinberg, G.; Zagaja, G.; Shalhav, A.; Eggner, S. Length of positive surgical margin after radical prostatectomy as a predictor of biochemical recurrence. *J. Urol.* **2009**, *182*, 139–144. [[CrossRef](#)] [[PubMed](#)]
32. Kang, Y.J.; Abalajon, M.J.; Jang, W.S.; Kwon, J.K.; Yoon, C.Y.; Lee, J.Y.; Cho, K.S.; Ham, W.S.; Choi, Y.D. Association of Anterior and Lateral Extraprostatic Extensions with Base-Positive Resection Margins in Prostate Cancer. *PLoS ONE* **2016**, *11*, e0158922. [[CrossRef](#)] [[PubMed](#)]
33. Vrang, M.L.; Røder, M.A.; Vainer, B.; Christensen, I.J.; Gruschy, L.; Brasso, K.; Iversen, P. First Danish single-institution experience with radical prostatectomy: Impact of surgical margins on biochemical outcome. *Scand. J. Urol. Nephrol.* **2012**, *46*, 172–179. [[CrossRef](#)]
34. You, D.; Jeong, I.G.; Song, C.; Cho, Y.M.; Hong, J.H.; Kim, C.S.; Ahn, H. High percent tumor volume predicts biochemical recurrence after radical prostatectomy in pathological stage T3a prostate cancer with a negative surgical margin. *Int. J. Urol.* **2014**, *21*, 484–489. [[CrossRef](#)]
35. De La Roca, R.L.; Da Cunha, I.W.; Bezerra, S.M.; Da Fonseca, F.P. Radical prostatectomy and positive surgical margins: Relationship with prostate cancer outcome. *Int. Braz. J. Urol.* **2014**, *40*, 306–315. [[CrossRef](#)]
36. Hashine, K.; Ueno, Y.; Shinomori, K.; Ninomiya, I.; Teramoto, N.; Yamashita, N. Correlation between cancer location and oncological outcome after radical prostatectomy. *Int. J. Urol.* **2012**, *19*, 855–860. [[CrossRef](#)] [[PubMed](#)]
37. O'Neil, L.M.; Walsh, S.; Cohen, R.J.; Lee, S. Prostate carcinoma with positive margins at radical prostatectomy: Role of tumour zonal origin in biochemical recurrence. *BJU Int.* **2015**, *116* (Suppl. 3), 42–48. [[CrossRef](#)] [[PubMed](#)]
38. Song, C.; Kang, T.; Yoo, S.; Jeong, I.G.; Ro, J.Y.; Hong, J.H.; Kim, C.S.; Ahn, H. Tumor volume, surgical margin, and the risk of biochemical recurrence in men with organ-confined prostate cancer. *Urol. Oncol.* **2013**, *31*, 168–174. [[CrossRef](#)]
39. Shannon, B.A.; McNeal, J.E.; Cohen, R.J. Transition zone carcinoma of the prostate gland: A common indolent tumour type that occasionally manifests aggressive behaviour. *Pathology* **2003**, *35*, 467–471. [[CrossRef](#)]
40. Augustin, H.; Hammerer, P.G.; Blonski, J.; Graefen, M.; Palisaar, J.; Daghofer, F.; Huland, H.; Erbersdobler, A. Zonal location of prostate cancer: Significance for disease-free survival after radical prostatectomy? *Urology* **2003**, *62*, 79–85. [[CrossRef](#)]
41. Ali, A.; Du Feu, A.; Oliveira, P.; Choudhury, A.; Bristow, R.G.; Baena, E. Prostate zones and cancer: Lost in transition? *Nat. Rev. Urol.* **2022**, *19*, 101–115. [[CrossRef](#)] [[PubMed](#)]
42. Magheli, A.; Rais-Bahrami, S.; Peck, H.J.; Walsh, P.C.; Epstein, J.I.; Trock, B.J.; Gonzalgo, M.L. Importance of tumor location in patients with high preoperative prostate specific antigen levels (greater than 20 ng/ml) treated with radical prostatectomy. *J. Urol.* **2007**, *178*, 1311–1315. [[CrossRef](#)] [[PubMed](#)]

43. Hayee, A.; Lugo, I.; Iakymenko, O.A.; Kwon, D.; Briski, L.M.; Zhao, W.; Nemov, I.; Punnen, S.; Ritch, C.R.; Pollack, A.; et al. Anterior or Posterior Prostate Cancer Tumor Nodule Location Predicts Likelihood of Certain Adverse Outcomes at Radical Prostatectomy. *Arch. Pathol. Lab. Med.* **2022**, *146*, 833–839. [[CrossRef](#)]
44. Mygatt, J.G.; Cullen, J.; Streicher, S.A.; Kuo, H.C.; Chen, Y.; Young, D.; Gesztes, W.; Williams, G.; Conti, G.; Porter, C.; et al. Race, tumor location, and disease progression among low-risk prostate cancer patients. *Cancer Med.* **2020**, *9*, 2235–2242. [[CrossRef](#)]
45. Augustin, H.; Erbersdobler, A.; Graefen, M.; Fernandez, S.; Palisaar, J.; Huland, H.; Hammerer, P. Biochemical recurrence following radical prostatectomy: A comparison between prostate cancers located in different anatomical zones. *Prostate* **2003**, *55*, 48–54. [[CrossRef](#)]
46. Meng, Y.; Li, H.; Xu, P.; Wang, J. Do tumor volume, percent tumor volume predict biochemical recurrence after radical prostatectomy? A meta-analysis. *Int. J. Clin. Exp. Med.* **2015**, *8*, 22319–22327.
47. Kim, K.H.; Lim, S.K.; Shin, T.Y.; Kang, D.R.; Han, W.K.; Chung, B.H.; Rha, K.H.; Hong, S.J. Tumor volume adds prognostic value in patients with organ-confined prostate cancer. *Ann. Surg. Oncol.* **2013**, *20*, 3133–3139. [[CrossRef](#)] [[PubMed](#)]
48. Thompson, I.M., III; Salem, S.; Chang, S.S.; Clark, P.E.; Davis, R.; Herrell, S.D.; Kordan, Y.; Baumgartner, R.; Phillips, S.; Smith, J.A., Jr.; et al. Tumor volume as a predictor of adverse pathologic features and biochemical recurrence (BCR) in radical prostatectomy specimens: A tale of two methods. *World J. Urol.* **2011**, *29*, 15–20. [[CrossRef](#)]
49. Yuk, H.D.; Byun, S.S.; Hong, S.K.; Lee, H. The tumor volume after radical prostatectomy and its clinical impact on the prognosis of patients with localized prostate cancer. *Sci. Rep.* **2022**, *12*, 6003. [[CrossRef](#)]
50. Ates, M.; Teber, D.; Gözen, A.S.; Tefekli, A.; Sugiono, M.; Hruza, M.; Rassweiler, J. Do tumor volume, tumor volume ratio, type of nerve sparing and surgical experience affect prostate specific antigen recurrence after laparoscopic radical prostatectomy? A matched pair analysis. *J. Urol.* **2007**, *177*, 1771–1775; discussion 1775–1776. [[CrossRef](#)] [[PubMed](#)]
51. Hashimoto, Y.; Okamoto, A.; Imai, A.; Yoneyama, T.; Hatakeyama, S.; Yoneyama, T.; Koie, T.; Kaminura, N.; Ohyama, C. Biochemical outcome of small-volume or insignificant prostate cancer treated with radical prostatectomy in Japanese population. *Int. J. Clin. Oncol.* **2012**, *17*, 119–123. [[CrossRef](#)]
52. Furusato, B.; Rosner, I.L.; Osborn, D.; Ali, A.; Srivastava, S.; Davis, C.J.; Sesterhenn, I.A.; McLeod, D.G. Do patients with low volume prostate cancer have prostate specific antigen recurrence following radical prostatectomy? *J. Clin. Pathol.* **2008**, *61*, 1038–1040. [[CrossRef](#)]
53. Lee, D.H.; Koo, K.C.; Lee, S.H.; Rha, K.H.; Choi, Y.D.; Hong, S.J.; Chung, B.H. Analysis of different tumor volume thresholds of insignificant prostate cancer and their implications for active surveillance patient selection and monitoring. *Prostate Int.* **2014**, *2*, 76–81. [[CrossRef](#)] [[PubMed](#)]
54. Chung, B.I.; Tarin, T.V.; Ferrari, M.; Brooks, J.D. Comparison of prostate cancer tumor volume and percent cancer in prediction of biochemical recurrence and cancer specific survival. *Urol. Oncol.* **2011**, *29*, 314–318. [[CrossRef](#)]
55. Friedersdorff, F.; Groß, B.; Maxeiner, A.; Jung, K.; Miller, K.; Stephan, C.; Busch, J.; Kilic, E. Does the Prostate Health Index Depend on Tumor Volume?—A Study on 196 Patients after Radical Prostatectomy. *Int. J. Mol. Sci.* **2017**, *18*, 488. [[CrossRef](#)] [[PubMed](#)]
56. Shin, S.J.; Park, C.K.; Park, S.Y.; Jang, W.S.; Lee, J.Y.; Choi, Y.D.; Cho, N.H. Total intraglandular and index tumor volumes predict biochemical recurrence in prostate cancer. *Virchows Arch.* **2016**, *469*, 305–312. [[CrossRef](#)] [[PubMed](#)]
57. Miyake, H.; Sakai, I.; Harada, K.; Takechi, Y.; Hara, I.; Eto, H. Prognostic significance of the tumor volume in radical prostatectomy specimens after neoadjuvant hormonal therapy. *Urol. Int.* **2005**, *74*, 27–31. [[CrossRef](#)] [[PubMed](#)]
58. Raison, N.; Servian, P.; Patel, A.; Santhirasekaram, A.; Smith, A.; Yeung, M.; Lloyd, J.; Mannion, E.; Rockall, A.; Ahmed, H.; et al. Is tumour volume an independent predictor of outcome after radical prostatectomy for high-risk prostate cancer? *Prostate Cancer Prostatic Dis.* **2021**, 1–5. [[CrossRef](#)]
59. Salomon, L.; Levrel, O.; Anastasiadis, A.G.; Irani, J.; De La Taille, A.; Saint, F.; Vordos, D.; Cicco, A.; Hoznek, A.; Chopin, D.; et al. Prognostic significance of tumor volume after radical prostatectomy: A multivariate analysis of pathological prognostic factors. *Eur. Urol.* **2003**, *43*, 39–44. [[CrossRef](#)]
60. Akaza, H.; Onozawa, M.; Hinotsu, S. Prostate cancer trends in Asia. *World J. Urol.* **2017**, *35*, 859–865. [[CrossRef](#)] [[PubMed](#)]
61. Fuletra, J.G.; Kamenko, A.; Ramsey, F.; Eun, D.D.; Reese, A.C. African-American men with prostate cancer have larger tumor volume than Caucasian men despite no difference in serum prostate specific antigen. *Can. J. Urol.* **2018**, *25*, 9193–9198.
62. Gupta, K.; Mehrotra, V.; Fu, P.; Scarberry, K.; MacLennan, G.T.; Gupta, S. Racial disparities in biochemical recurrence of prostate cancer. *Am. J. Clin. Exp. Urol.* **2022**, *10*, 266–270. [[PubMed](#)]
63. Reinhardt, D.; Helfand, B.T.; Cooper, P.R.; Roehl, K.A.; Catalona, W.J.; Loeb, S. Prostate cancer risk alleles are associated with prostate cancer volume and prostate size. *J. Urol.* **2014**, *191*, 1733–1736. [[CrossRef](#)] [[PubMed](#)]
64. Helfand, B.T.; Paterakos, M.; Wang, C.H.; Talaty, P.; Abran, J.; Bennett, J.; Hall, D.W.; Lehman, A.; Aboushwareb, T. The 17-gene Genomic Prostate Score assay as a predictor of biochemical recurrence in men with intermediate and high-risk prostate cancer. *PLoS ONE* **2022**, *17*, e0273782. [[CrossRef](#)]
65. Santos, A.; Mattioli, A.; Carvalheira, J.B.; Ferreira, U.; Camacho, M.; Silva, C.; Costa, F.; Matheus, W.; Lima, M.; Etchebehere, E. PSMA whole-body tumor burden in primary staging and biochemical recurrence of prostate cancer. *Eur. J. Nucl. Med. Mol. Imaging* **2021**, *48*, 493–500. [[CrossRef](#)]
66. Pinckaers, H.; van Ipenburg, J.; Melamed, J.; De Marzo, A.; Platz, E.A.; van Ginneken, B.; van der Laak, J.; Litjens, G. Predicting biochemical recurrence of prostate cancer with artificial intelligence. *Commun. Med.* **2022**, *2*, 64. [[CrossRef](#)] [[PubMed](#)]



## Full paper

# Targeting L-type amino acid transporter 1 in urological malignancy: Current status and future perspective



Sangjon Pae <sup>a, b</sup>, Shinichi Sakamoto <sup>a, \*</sup>, Xue Zhao <sup>a</sup>, Shinpei Saito <sup>a, b</sup>, Takaaki Tamura <sup>a</sup>, Yusuke Imamura <sup>a</sup>, Tomokazu Sazuka <sup>a</sup>, Yoshie Reien <sup>b</sup>, Yuri Hirayama <sup>b</sup>, Hirofumi Hashimoto <sup>b</sup>, Yoshikatsu Kanai <sup>c</sup>, Tomohiko Ichikawa <sup>a</sup>, Naohiko Anzai <sup>b</sup>

<sup>a</sup> Department of Urology, Chiba University Graduate School of Medicine, Chiba, Japan

<sup>b</sup> Department of Pharmacology, Chiba University Graduate School of Medicine, Chiba, Japan

<sup>c</sup> Bio-system Pharmacology, Osaka University Graduate School of Medicine, Osaka, Japan

## ARTICLE INFO

## Article history:

Received 9 September 2021

Received in revised form

18 September 2022

Accepted 3 October 2022

Available online 7 October 2022

## Keywords:

LAT1

4F2hc

Prostate cancer

Renal cancer

Bladder cancer

## ABSTRACT

Amino acid transporters are responsible for the uptake of amino acids, critical for cell proliferation. L-type amino acid transporters play a major role in the uptake of essential amino acids. L-type amino acid transporter 1 (LAT1) exerts its functional properties by forming a dimer with 4F2hc. Utilizing this cancer-specificity, research on diagnostic imaging and therapeutic agents for malignant tumors targeting LAT1 progresses in various fields. In hormone-sensitive prostate cancer, the up-regulation of L-type amino acid transporter 3 (LAT3) through the androgen receptor (AR) has been identified. On the other hand, in castration-resistant prostate cancer, the negative regulation of LAT1 through AR has been determined. Furthermore, 4F2hc: a binding partner of LAT1, was identified as the specific downstream target of Androgen Receptor Splice Variant 7: AR-V7. LAT1 has been suggested to contribute to acquiring castration resistance in prostate cancer, making LAT1 a completely different therapeutic target from anti-androgens and taxanes. Increased expression of LAT1 has also been found in renal and bladder cancers, suggesting a contribution to acquiring malignancy and progression. In Japan, clinical trials of LAT1 inhibitors for solid tumors are in progress, and clinical applications are now underway. This article will summarize the relationship between LAT1 and urological malignancies.

© 2022 The Authors. Production and hosting by Elsevier B.V. on behalf of Japanese Pharmacological Society. This is an open access article under the CC BY-NC-ND license (<http://creativecommons.org/licenses/by-nc-nd/4.0/>).

## 1. Introduction

Living organisms require substances in order to function and, ultimately, to sustain life. In particular, the organism needs to take

*Abbreviations:* ABC, ATP binding cassette; AR, androgen receptor; AR-V7, androgen receptor splicing variant 7; BAT, b0 amino acid transporter; CCRC, clear cell renal cell carcinoma; CRPC, castration resistant prostate cancer; DHT, dihydrotestosterone; GC, gemcitabine/cisplatin combined chemotherapy; HAT, heterodimeric amino acid transporters; HSPC, hormone sensitive prostate cancer; LAT, L-type amino acid transporter; mTOR, mammalian target of rapamycin; mTORC, mammalian target of rapamycin complex; MVAC, methotrexate/vinblastine/doxorubicin/cisplatin combined chemotherapy; PSMA, prostate specific membrane antigen; SLC, solute carrier.

\* Corresponding author. Chiba University Graduate School of Medicine, 1-8-1 Inohana, Chuo-ku, Chiba City, Chiba 260-8670, Japan.

E-mail address: [rbbat1@gmail.com](mailto:rbbat1@gmail.com) (S. Sakamoto).

Peer review under responsibility of Japanese Pharmacological Society.

<https://doi.org/10.1016/j.jphs.2022.10.002>

1347-8613/© 2022 The Authors. Production and hosting by Elsevier B.V. on behalf of Japanese Pharmacological Society. This is an open access article under the CC BY-NC-ND license (<http://creativecommons.org/licenses/by-nc-nd/4.0/>).

in essential nutrients such as carbohydrates, fats, and proteins from the outside. Proteins are metabolized into amino acids via peptides by digestive enzymes, and amino acid molecules are absorbed through the epithelial mucosa of the small intestine and transferred to the bloodstream, where they undergo various metabolic processes. The mechanism responsible for this transport is the amino acid transporter, which contributes to maintaining biological functions. Amino acid transporters play a role in maintaining cell survival by transferring amino acids, which are essential for living organisms, into cells and maintaining tissue specificity by transporting them in a particular direction.<sup>1</sup> The amino acids taken up are used for protein biosynthesis, activation of the mTOR (mammalian target of rapamycin) pathway, an important signal for cell growth and proliferation, and maintenance of redox reactions and homeostasis in cells.<sup>2,3</sup>

Amino acid transporters can be broadly classified into the ABC (ATP binding cassette) family and SLC (solute carrier) family. The

ABC family transports ATP by co-benefiting and utilizing its energy and 7 subgroups have been identified in humans. The SLC (solute carrier) family transports without conjugating with ATP. L-type amino acid transporter 1: LAT1 (*SLC7A5*), which is the subject of this paper, can be classified as a solute carrier: SLC, and SLCs are further classified into families with different exchange substrates and localization and perform various functions.

Metabolism occurs in cancer cells as it does in normal tissues, but more nutrients may be required to compensate for changes in the surrounding environment and the frequency of cell growth. In Japan, a phase II clinical trial of JPH203, a selective inhibitor of LAT1, is underway in biliary tract cancer.

In this article, we report the physiological functions of amino acid transporters and their relevance to malignancies, especially urological cancers, focusing on LAT1, which is upregulated in malignant tumors.

## 2. Biological functions of LATs amino acid transporter and cancer

LAT1 is an ATP-independent, sodium-independent, 12-fold transmembrane amino acid transporter belonging to the SLC7 family. It has been reported to cause decreased leucine uptake and cell proliferation in LAT1 knockout cells.<sup>4</sup> Therefore, it is thought that the exchange substrate transports a wide range of essential amino acids, mainly leucine.<sup>5–9</sup>

The SLC7 family described above consists of L-type amino acid transporters: LAT (*SLC7A5-13*, *SLC7A15*) and cationic amino acid transporters: CAT (*SLC7A1-4*, *SLC7A14*). Among these, LAT forms a heterodimeric amino acid transporter complex: HATC and constitutes its light subunit.<sup>10–16</sup>

LAT1 (17), L-type amino acid transporter 3: LAT3 (*SLC43A1*),<sup>18</sup> and system ASC transporter 2: ASCT2 (*SLC1A5*)<sup>19</sup> have been reported to be upregulated in tumor cells.<sup>20–22</sup> Gastrointestinal malignancies, breast cancer, prostate cancer, renal cancer, bladder cancer, lung cancer, glioma, endometrial cancer, and pancreatic cancer, have been identified to express a high level of LAT1.<sup>4,6,7,23–30</sup> (Table 1).

Leucine, a major exchange substrate of LAT, is an essential amino acid and one of the signal regulators of mTORC1 (mammalian target of rapamycin complex 1). mTORC1 is known to regulate mRNA translation,<sup>31</sup> ribosome biogenesis by regulating rRNA transcription,<sup>32</sup> and autophagy, and thus plays a role in regulating protein synthesis and cell proliferation.

LAT3 and LAT4 have been found to have fewer exchange substrates than LAT1 and LAT2 (18, 33) (Table 1).

## 3. Heterodimeric amino acid transporters

Some members of the SLC7 family form heterodimeric amino acid transporters (HATs). These include a 14-transmembrane cationic amino acid transporter and a 12-transmembrane heterodimeric amino acid transporter.<sup>1,34</sup> LAT1 is disulfide-linked to the SLC3 family members 4F2hc (4F2 heavy chain: *SLC3A2*). BAT1 (*SLC7A9*) is disulfide-linked to rBAT (related to b0 amino acid transporter: *SLC3A1*)<sup>35</sup> (Fig. 1). Heterodimeric amino acid transporters have the structural feature of being composed of a light subunit and a heavy subunit, which form a dimer through disulfide bonds. This morphological feature is thought to enable the localization of LAT1 on the plasma membrane, which cannot be achieved by LAT1 alone. As an example, it has been reported that in the absence of 4F2hc, LAT1 exists inside the cell, but in the presence of 4F2hc, it moves to the cell surface by forming HATs.<sup>36</sup>

Although LAT1 and L-type amino acid transporter 2: LAT2 can transport leucine by themselves, their substrate affinity and specificity have also been found to be regulated by 4F2hc.<sup>37</sup> Because of

this property, HATs are also thought to be involved in the pathogenesis of aminoaciduria (cystinuria, lysinuria), tumor cell proliferation, and glial tumor invasion<sup>18,30,34,35,38,39</sup> (Table 2).

## 4. Relationship between LAT1 and LAT2

Both LAT1 and LAT2 are sodium-independent amino acid transporters that form HATs through disulfide bonds with 4F2hc. LAT1 and LAT2 have similar functions due to the commonality of their exchange substrates, but LAT2 is thought to have a broader range of exchange substrates. In addition, LAT2 is distributed in the proximal tubules of kidneys and small intestinal epithelium and is involved in the uptake and reabsorption of amino acids from the body.<sup>40,41</sup> On the other hand, the expression of LAT1 in normal tissues can be observed in the brain, testis, and placenta.<sup>17,42,43</sup> Although LAT2 is commonly expressed in the brain, testis, and placenta, it is also involved in the absorption and reabsorption of amino acids, suggesting that LAT2 is mainly responsible for the uptake of amino acids from outside the body and LAT1 is mainly responsible for the uptake of amino acids into specific cells.

In another aspect, LAT1 is known to be upregulated in various tumor cells and has been reported to be a poor prognostic factor, while LAT2 has been reported to be less distributed in malignant tumors and more distributed in normal tissues. Therefore, it is possible that LAT1 and LAT2 have a tumor type and a normal tissue type property, respectively<sup>17</sup> (Fig. 2).

## 5. LAT1 and 4F2hc characteristics

Tumor cells require increased uptake of glucose and amino acids for their biosynthesis, related to their rapid growth and changes in the surrounding environment.<sup>44</sup> In amino acids, increased expression of amino acid transporters in tumor cells has been observed in various cancer types.

The exchange substrate of LAT1 is an essential amino acid, and when a single molecule of amino acid is taken into the cell, glutamine is transported out of the cell instead.<sup>45</sup> However, since glutamine is required for ATP production in tumor cells, high expression of ASCT2 (*SLC1A5*), a sodium-dependent neutral amino acid transporter that can take glutamine into the cell, allows tumor cells maintenance of intracellular glutamine levels.<sup>20</sup> This glutamine is used for ATP production and prevents the depletion of the exchange substrate of LAT1 (Fig. 3).

4F2hc functions as a heavy subunit of the transporter complex and plays a role in the localization and stabilization of LAT1 on the plasma membrane and as an enhancer of integrin signaling.<sup>11,45–50</sup> 4F2hc deficiency results in the loss of intracellular amino acid pools, including leucine and arginine, which are active factors of mTOR kinase,<sup>48,51</sup> and increased oxidative stress, DNA damage, and radiosensitivity in head and neck squamous cell carcinoma cells.<sup>11</sup>

## 6. Application of LAT1 to diagnostic imaging

The increased expression of LAT1 in tumor cells has been studied for the detection of malignant tumors by imaging diagnosis. FDG-PET, which is currently used in clinical practice, is an imaging diagnosis in which the glucose that tumor cells consume in large amounts is radiolabeled (18F-FDG: 18-fluodeoxyglucose) the presence or absence of accumulation is confirmed. However, the accumulation of FDG is not specific to malignant tumors but also occurs in areas with high physiological accumulation, such as the brain, and inflammatory cells, making differential diagnosis often tricky. In evaluating malignant tumors of the urinary tract, FDG is excreted in the urine. Thus, hyperaccumulation around the urinary tract often masks

**Table 1**  
LAT expression and function.

protein	gene	substance selectivity	expression pattern	subtype
LAT1 <sup>4,6,7,23-30</sup>	SLC7A5	broad (Leu, Ile, Phe, Met, Tyr, His, Try, Val)	cancer testis brain ovary placenta spleen colon blood brain barrer fetal liver kidney	system L1
LAT2 <sup>17,29,36,39,40-42</sup>	SLC7A8	broad (Gly, Ala, Ser, Thr, Cys, Asn, Gln, Met, Leu, Ile, Val, Phe, Tyr, Trp, His)	testis prostate small intestine lung heart spleen liver brain placenta ovary fetal liver muscle	system L1
LAT3 <sup>18,23,58</sup>	SLC43A1	narrow (Leu, Ile, Val, Phe, Met)	prostate liver muscle kidney placenta	system L2
LAT4 <sup>33</sup>	SLC43A2	narrow (Leu, Ile, Val, Phe, Met)	kidney placenta peripheral blood leukocytes small intestine	system L2

renal, pelvis, ureteral, bladder, and prostate cancers. In addition, the detection rate of prostate cancer is estimated to be even lower because of the weak accumulation of FDG.

Imaging diagnosis targeting amino acids instead of glucose is being studied. In 2016, the U.S. FDA approved FACBC PET labeled with 18-F on ACBC (Aminocyclobutane carboxylic acid), taken

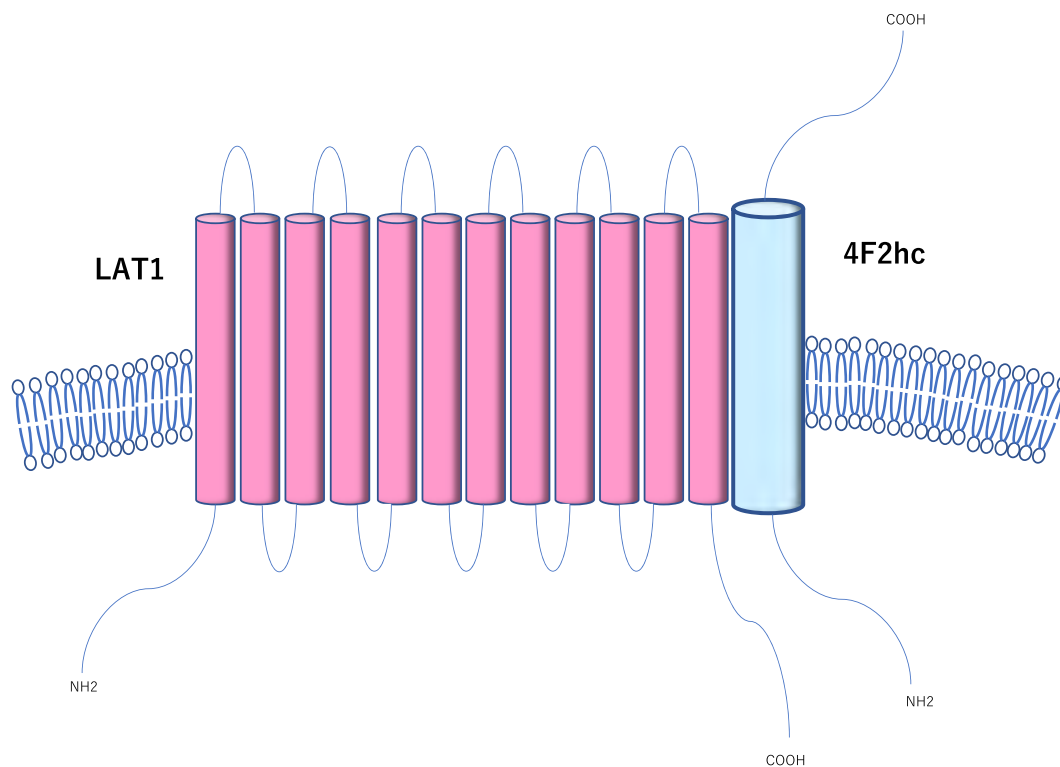


**Fig. 1.** Scheme shows the representation of LAT1/4F2hc complex. The structures of the LAT1 and 4F2hc heterodimers on the plasma membrane are shown in simplified form: LAT1 is a 12-fold transmembrane amino acid transporter that serves as the light chain of the dimer; 4F2hc is a single-fold transmembrane amino acid transporter that forms a dimer with LAT1 by disulfide bonds.

**Table 2**  
Examples of heterodimeric amino acid transporters.

heavy chain (gene)	light chain	disease	expression pattern
rBAT ( <i>SLC3A1</i> ) <sup>10,34</sup>	b (0,+)-AT1 ( <i>SLC7A9</i> )	cystinuria	kidney intestine liver pancreas
4F2hc ( <i>SLC3A2</i> ) <sup>12,46,59</sup>	LAT1 ( <i>SLC7A5</i> ) y + LAT2 ( <i>SLC7A6</i> ) y + LAT1 ( <i>SLC7A7</i> ) LAT2 ( <i>SLC7A8</i> ) ASC1 ( <i>SLC7A10</i> ) xCT ( <i>SLC7A11</i> )	cancer	ubiquitous (depend on the light chain)

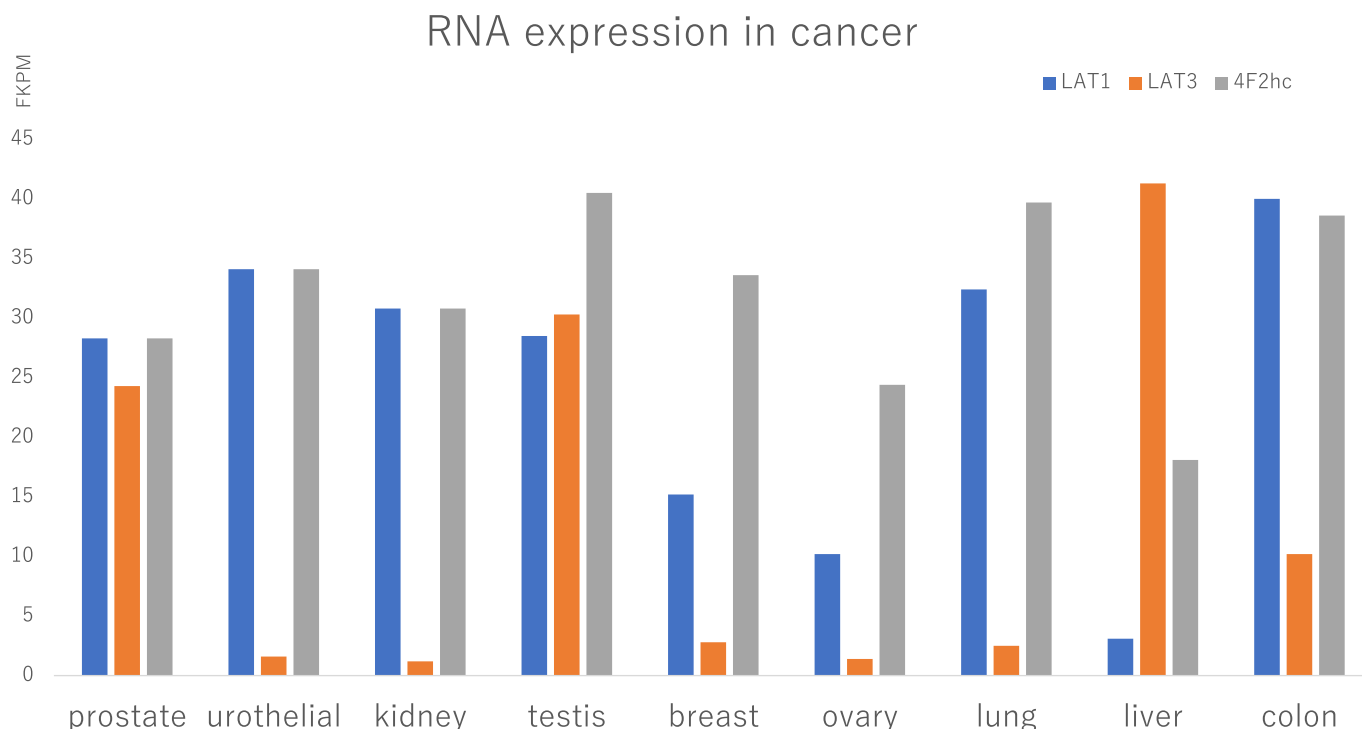


**Fig. 2.** The expression of LAT1, LAT3, and 4F2hc in tumor cells is shown, and LAT1 expression is more upregulated in many tumors than LAT3, which is the reason why LAT1 may be the tumor cell type amino acids transporter. However, in prostate and testicular cancers, LAT3 is expressed to the same extent. There may be differences in expression depending on hormone sensitivity in prostate cancer and histology in testicular cancer. Reference: the protein atlas (<https://www.proteinatlas.org/>).

into the body as an amino acid but is not metabolized intracellularly and does not degrade image quality, for the evaluation of recurrence of prostate cancer. Although FACBCs were expected to be taken up into cells by amino acid transporters, it was later found that their main bodies were actually LAT1 and ASCT2,<sup>52</sup> which is consistent with the increased expression of LAT1 in prostate cancer, as will be discussed later. It should also be noted that PSMA-PET, which uses ligands that bind to PSMA (prostate-specific membrane antigen), is applied in prostate cancer, but is entirely different from PET which targets amino acid transporters.

In addition, the construction of diagnostic imaging systems targeting LAT1, such as 18-FMT (18-F- $\alpha$ -methyltyrosine), which has higher malignancy specificity, has been proposed, and the usefulness of cancer-specific accumulation in patients with advanced lung cancer and esophageal cancer has been proposed.<sup>53,54</sup> Furthermore, 18F-FBPA (4-borono-2-18F-L-phenylalanine), which also targets LAT1, significantly reduced accumulation in inflammatory cells, which is often a problem with FDG, albeit in vitro.<sup>55</sup> In Japan, a phase I study of a nuclear medicine test targeting LAT1

using F-18 NKO-035, which is a PET probe with high selectivity for LAT1, has been completed. Its clinical application will be evaluated through further studies.

Thus, the high expression of LAT1 in tumor cells will enable new imaging modalities and may change the existing diagnostic protocols, such as FACBC PET in locally treated prostate cancer.

## 7. LAT1 targeting cancer therapy

As mentioned above, LAT1 is abundantly expressed in tumors and contributes significantly to the survival of tumor cells. Research on therapeutic drugs that target LAT1 for cancer control is also underway.

BCH (2-aminobicyclo-(2,2,1)-heptane-2-carboxylic acid) is a selective inhibitor of the L-type amino acid transporter and has been found to inhibit cell growth and proliferation by blocking leucine uptake into cells, as well as inducing apoptosis.<sup>4</sup> Triiodothyronine and thyroxine have also been reported to inhibit LAT1-mediated phenylalanine incorporation into cells.<sup>56</sup>

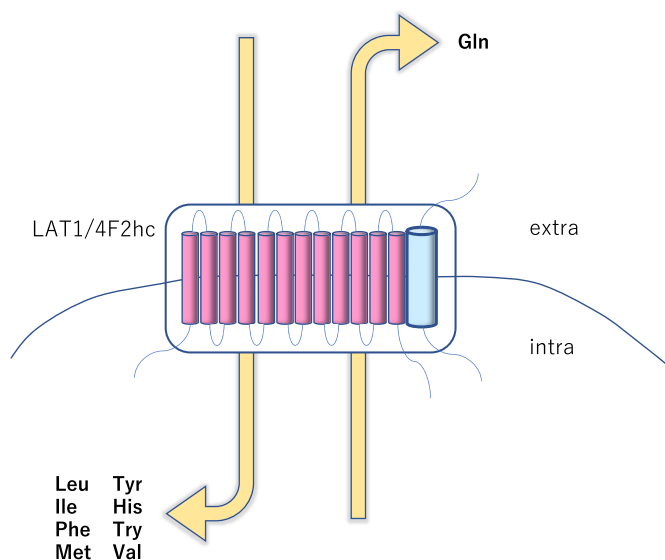


**Fig. 3.** Scheme shows the substances of LAT1/4F2hc. LAT1 is sodium-independent and transports a single molecule of glutamine out of the cell, and at the same time takes up large side-chain neutral amino acids such as leucine, histidine, methionine, isoleucine, valine, phenylalanine, tyrosine, and tryptophan into the cell.

Considering that LAT1 is more abundantly expressed in tumor cells, it can be expected that selective inhibition of LAT1 among L-type amino acid transporters will result in more minor damage to normal cells. JPH203 ((S)-2-amino-3-(4-((5-amino-2-phenylbenzo[d]oxazol-7-yl)methoxy)-3,5-dichlorophenyl)) is a selective inhibitor of LAT1 and has been reported to inhibit tumor cell growth in a concentration-dependent manner by inhibiting leucine uptake.<sup>57</sup> Phase I clinical trials of JPH203 for solid tumors have been completed in Japan, and its safety and tolerability have been confirmed. In addition, long-term responses in biliary tract cancer patients were confirmed in this study, and anti-tumor effects are expected.<sup>58</sup> A phase II study in biliary tract cancer is currently underway.

## 8. LAT1 and urological cancer

### 8.1. LAT1 in prostate cancer

There have been significant changes in the treatment of prostate cancer in recent years. In addition to primary hormone therapy, known as vintage hormone therapy, early administration of novel androgen receptor inhibitors for high-risk hormone-sensitive prostate cancer has been established. However, prostate cancer is known to progress to castration-resistant prostate cancer under androgen deprivation therapy, and the sequential therapy is still unclear.

LAT1 expression intensity is significantly correlated with the prognosis of prostate cancer patients and the Gleason score, and its potential as a biomarker for prostate cancer has been explored, and the relationship between prostate cancer and LAT1 has been clarified.<sup>27</sup> In addition, LAT1 expression is upregulated in castration-resistant prostate cancer cells compared to hormone-sensitive prostate cancer cells, and knockdown of LAT1 inhibits cancer cell proliferation, migration, and invasion.<sup>8</sup> In addition, in multivariate analysis, LAT1 expression has been reported to be an independent prognostic factor for castration-resistant prostate cancer.<sup>8</sup>

It has been reported that LAT3 expression is upregulated in hormone-sensitive prostate cancer cells before acquiring castration

resistance.<sup>59</sup> Thus, it has been reported that androgen receptor (AR) increases LAT3 expression, while LAT3 expression is decreased and LAT1 expression is increased in castration-resistant prostate cancer that has acquired resistance after AR inhibition (Fig. 4).

As there are various factors, expression of androgen receptor splicing variant-7: AR-V7 leads hormone-sensitive prostate cancer to progress to castration-resistant prostate cancer under androgen deprivation therapy. One of the specific target genes of AR-V7 is *SLC3A2*, which encodes 4F2hc.<sup>60</sup> It suggests a link between the acquisition of castration resistance and the expression of the LAT1 coactivator.

Although there are various treatments for castration-resistant prostate cancer, they all have limited efficacy. In addition, drugs that target androgen receptors may cause early resistance to these drugs due to the increased expression of AR-V7.<sup>61</sup> The introduction of drugs that do not target the androgen receptor, such as the PARP inhibitor (Olaparib) for *BRCA* mutation-positive unresectable prostate cancer, a new drug for prostate cancer currently approved in Japan, may change the treatment of prostate cancer.

### 8.2. LAT1 in bladder cancer

The 5-year survival rate of stage IV bladder cancer is 19% (2012–2013 data of Japan), and it is not a malignant tumor with a good prognosis, so a therapeutic agent with an unprecedented mechanism of action is desirable.

In the treatment of advanced bladder cancer, cisplatin-based chemotherapy (GC: gemcitabine/cisplatin, MVAC: methotrexate/vinblastine/doxorubicin/cisplatin), which was introduced in the 1980s, is still used as the primary treatment until pembrolizumab, an anti-PD-1 antibody, was validated as second-line therapy in 2017.<sup>62,63</sup> Furthermore, in 2020, avelumab is approved as maintenance therapy for first-line treatment, and bladder cancer treatment is undergoing significant changes.<sup>64</sup>

In human bladder cancer tissues, LAT1 and 4F2hc are highly expressed compared to normal cells,<sup>4,45</sup> and siLAT1 and JPH203, a selective LAT1 inhibitor, inhibit cell proliferation, migration, and invasion in bladder cancer cell lines.<sup>65</sup> In addition, multivariate analysis showed a significant reduction in overall survival in cases with high expression of LAT1, which correlated with a higher grade of pathological T classification and tumor grade.<sup>65</sup> Furthermore, insulin-like growth factor-binding protein-5 (IGFBP-5) was identified as a downstream target of JPH203.<sup>65</sup>

### 8.3. LAT1 in renal cancer

The kidney contains a variety of transporters that maintain physiological functions such as reabsorption and excretion. As for amino acid transporters, LAT2 is expressed in the proximal tubule and is responsible for the reabsorption of amino acids.<sup>66</sup>

Regarding the relationship between LAT1 and renal cancer, it has been found that the expression of mRNA in tumors of the clear cell renal cell carcinoma: CCRC is increased compared to normal tissues and that the expression of LAT2 and LAT3 is decreased compared to normal tissues.<sup>23</sup>

In a retrospective analysis, immunostaining of CCRC showed that the expression of LAT1 was increased compared to normal tissues,<sup>67</sup> and the overall survival rate and progression-free survival rate were significantly decreased in the group with high expression of LAT1 (23, 67). It was also reported that JPH203 decreased the leucine uptake rate of renal cancer cells and inhibited cell proliferation, migration, and invasion in renal cancer cell lines.<sup>67</sup>

An association between LAT1 mRNA expression and malignancy has also been suggested, with the highest expression in grade 3

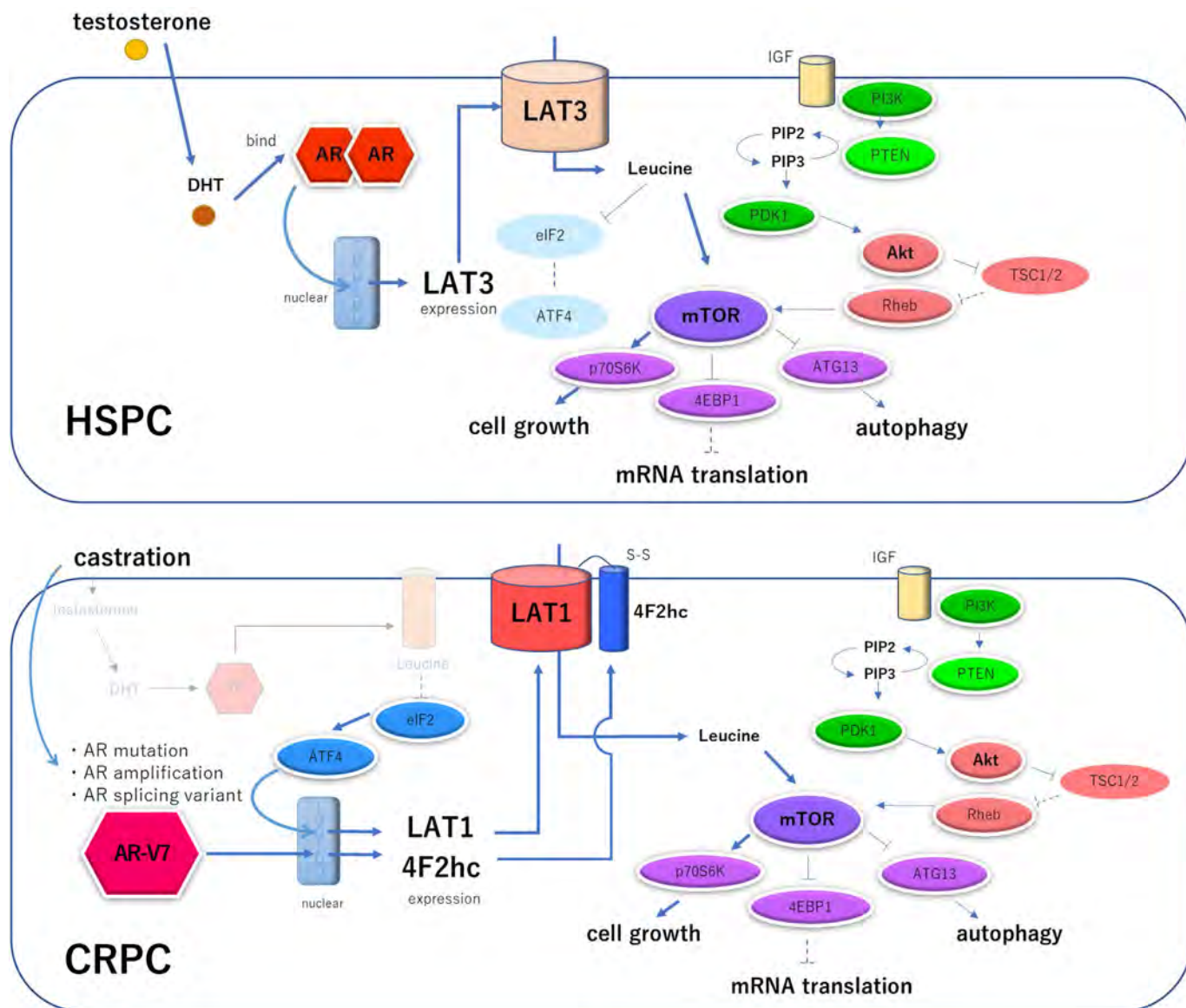


**Fig. 4.** Scheme shows the association of LATs and prostate cancer. The association of hormone-sensitive prostate cancer (HSPC) and castration-resistant prostate cancer (CRPC) with LAT is shown. In untreated HSPC, testosterone is metabolized by 5-alpha reductase to dihydrotestosterone (DHT), which binds to the androgen receptor (AR), forms a dimer, enters the nucleus, and drives LAT3 transcription, resulting in increased LAT3 expression, and contributes to the activation of the mTOR pathway. When hormone therapy is used as a treatment, testosterone disappears, i.e., castration occurs, and ARs that no longer bind DHT mutate, amplify, and form splicing variants. In particular, AR-V7 is able to enter the nucleus without testosterone stimulation, and 4F2hc is present in its downstream signaling. In addition, the depletion of leucine from the cells, which LAT3 took up, leads to the loss of eIF2 repression and the entry of ATF4 into the nucleus. It increases the expression of LAT1, and LAT1 and 4F2hc form a dimer, which allows leucine to enter the cell and promotes tumor cell growth. Reference:<sup>68</sup>

nephrectomy specimens and higher expression in the pT3–4 group compared to the pT1–2 group.<sup>23</sup>

Since the relationship between LAT1 and renal cancer remains unresolved, further analysis is warranted.

**9. Conclusion**

Although the relationship between malignancy and LAT1 has become clear in recent years, there are still many unanswered questions in urology. In addition, although there are a significant number of basic analyses, there are still few clinical reports.

The treatment of urological malignant tumors is in the midst of a transition from cell-killing anti-cancer drugs to the era of newer therapies represented by molecularly targeted drugs and immune checkpoint inhibitors. In prostate cancer, treatment options have expanded from classical hormone therapy and anti-cancer drugs to

novel hormone drugs and PARP inhibitors that target *BRCA1/2* mutations.

LAT1 is involved in the growth and proliferation of malignant tumors at a completely different mechanism than conventional diagnostic and therapeutic targets. In other words, LAT1 is a useful target molecule for diagnostic imaging and therapy. Thus, LAT1 may cause a paradigm shift in cancer diagnosis and therapy.

**Declaration of Competing Interest**

The author has no conflict of interest to declare in this work.

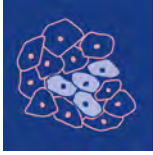
**Acknowledgements**

This work was supported by [JSPS KAKENHI] grant number [21H03065, 21K19348, 20H03813 and 20K09555].

## References

- Kanai Y, Endou H. Heterodimeric amino acid transporters: molecular biology and pathological and pharmacological relevance. *Curr Drug Metabol.* 2001;2(4):339–354.
- Chen O, Manig F, Lehmann L, et al. Dual role of ER stress in response to metabolic co-targeting and radiosensitivity in head and neck cancer cells. *Cell Mol Life Sci.* 2021;78(6):3021–3044.
- Woo Y, Lee HJ, Jung YM, Jung YJ. mTOR-mediated antioxidant activation in solid tumor radioresistance. *JAMA Oncol.* 2019;2019, 5956867.
- Kim DK, Kanai Y, Choi HW, et al. Characterization of the system L amino acid transporter in T24 human bladder carcinoma cells. *Biochim Biophys Acta.* 2002;1565(1):112–121.
- Kim CH, Park KJ, Park JR, et al. The RNA interference of amino acid transporter LAT1 inhibits the growth of KB human oral cancer cells. *Anticancer Res.* 2006;26(4b):2943–2948.
- Marshall AD, van Geldermalsen M, Otte NJ, et al. LAT1 is a putative therapeutic target in endometrioid endometrial carcinoma. *Int J Cancer.* 2016;139(11):2529–2539.
- Hayashi K, Jutabha P, Endou H, Anzai N. c-Myc is crucial for the expression of LAT1 in MIA Paca-2 human pancreatic cancer cells. *Oncol Rep.* 2012;28(3):862–866.
- Xu M, Sakamoto S, Matsushima J, et al. Up-regulation of LAT1 during anti-androgen therapy contributes to progression in prostate cancer cells. *J Urol.* 2016;195(5):1588–1597.
- Liang Z, Cho HT, Williams L, et al. Potential biomarker of L-type Amino acid transporter 1 in breast cancer progression. *Nucl Med Mol Imaging.* 2011;45(2):93–102.
- Jiang Y, Cao Y, Wang Y, et al. Cysteine transporter SLC3A1 promotes breast cancer tumorigenesis. *Theranostics.* 2017;7(4):1036–1046.
- Digomann D, Kurth I, Tyutyunnykova A, et al. The CD98 heavy chain is a marker and regulator of head and neck squamous cell carcinoma radiosensitivity. *Clin Cancer Res.* 2019;25(10):3152–3163.
- Chiduzha GN, Johnson RM, Wright GSA, Antonyuk SV, Muench SP, Hasnain SS. LAT1 (SLC7A5) and CD98hc (SLC3A2) complex dynamics revealed by single-particle cryo-EM. *Acta Crystallogr D.* 2019;75(7):660–669.
- Zhang L, Liu W, Liu F, et al. Corrigendum to "IMCA induces ferroptosis mediated by SLC7A11 through the AMPK/mTOR pathway in colorectal cancer". *Oxid Med Cell Longev.* 2020;2020, 6901472.
- Gu Y, Albuquerque CP, Braas D, et al. mTORC2 regulates amino acid metabolism in cancer by phosphorylation of the cystine-glutamate antiporter xCT. *Mol Cell.* 2017;67(1):128–138. e7.
- Meyer AR, Engevik AC, Willet SG, et al. Cystine/Glutamate antiporter (xCT) is required for chief cell plasticity after gastric injury. *Cell Mol Gastroenterol Hepatol.* 2019;8(3):379–405.
- Goji T, Takahara K, Negishi M, Katoh H. Cystine uptake through the cystine/glutamate antiporter xCT triggers glioblastoma cell death under glucose deprivation. *J Biol Chem.* 2017;292(48):19721–19732.
- Kanai Y, Segawa H, Miyamoto K, Uchino H, Takeda E, Endou H. Expression cloning and characterization of a transporter for large neutral amino acids activated by the heavy chain of 4F2 antigen (CD98). *J Biol Chem.* 1998;273(37):23629–23632.
- Babu E, Kanai Y, Chairoungdua A, et al. Identification of a novel system L amino acid transporter structurally distinct from heterodimeric amino acid transporters. *J Biol Chem.* 2003;278(44):43838–43845.
- Utsunomiya-Tate N, Endou H, Kanai Y. Cloning and functional characterization of a system ASC-like Na<sup>+</sup>-dependent neutral amino acid transporter. *J Biol Chem.* 1996;271(25):14883–14890.
- Fuchs BC, Bode BP. Amino acid transporters ASCT2 and LAT1 in cancer: partners in crime? *Semin Cancer Biol.* 2005;15(4):254–266.
- Kobayashi K, Ohnishi A, Promsuk J, et al. Enhanced tumor growth elicited by L-type amino acid transporter 1 in human malignant glioma cells. *Neurosurgery.* 2008;62(2):493–503. discussion -4.
- Kaira K, Oriuchi N, Imai H, et al. L-type amino acid transporter 1 and CD98 expression in primary and metastatic sites of human neoplasms. *Cancer Sci.* 2008;99(12):2380–2386.
- Betsunoh H, Fukuda T, Anzai N, et al. Increased expression of system large amino acid transporter (LAT)-1 mRNA is associated with invasive potential and unfavorable prognosis of human clear cell renal cell carcinoma. *BMC Cancer.* 2013;13:509.
- Ebara T, Kaira K, Saito J, et al. L-type amino-acid transporter 1 expression predicts the response to preoperative hyperthermo-chemoradiotherapy for advanced rectal cancer. *Anticancer Res.* 2010;30(10):4223–4227.
- Furuya M, Horiguchi J, Nakajima H, Kanai Y, Oyama T. Correlation of L-type amino acid transporter 1 and CD98 expression with triple negative breast cancer prognosis. *Cancer Sci.* 2012;103(2):382–389.
- Nawashiro H, Otani N, Shinomiya N, et al. L-type amino acid transporter 1 as a potential molecular target in human astrocytic tumors. *Int J Cancer.* 2006;119(3):484–492.
- Sakata T, Ferdous G, Tsuruta T, et al. L-type amino-acid transporter 1 as a novel biomarker for high-grade malignancy in prostate cancer. *Pathol Int.* 2009;59(1):7–18.
- Takeuchi K, Ogata S, Nakanishi K, et al. LAT1 expression in non-small-cell lung carcinomas: analyses by semiquantitative reverse transcription-PCR (237 cases) and immunohistochemistry (295 cases). *Lung Cancer.* 2010;68(1):58–65.
- del Amo EM, Urtti A, Yliperttula M. Pharmacokinetic role of L-type amino acid transporters LAT1 and LAT2. *Eur J Pharmaceut Sci.* 2008;35(3):161–174.
- Segawa H, Fukasawa Y, Miyamoto K, Takeda E, Endou H, Kanai Y. Identification and functional characterization of a Na<sup>+</sup>-independent neutral amino acid transporter with broad substrate selectivity. *J Biol Chem.* 1999;274(28):19745–19751.
- Thoreen CC, Chantranupong L, Keys HR, Wang T, Gray NS, Sabatini DM. A unifying model for mTORC1-mediated regulation of mRNA translation. *Nature.* 2012;485(7396):109–113.
- ladevaia V, Liu R, Proud CG. mTORC1 signaling controls multiple steps in ribosome biogenesis. *Semin Cell Dev Biol.* 2014;36:113–120.
- Bodoy S, Martín L, Zorzano A, Palacín M, Estévez R, Bertran J. Identification of LAT4, a novel amino acid transporter with system L activity. *J Biol Chem.* 2005;280(12):12002–12011.
- Fotiadis D, Kanai Y, Palacín M. The SLC3 and SLC7 families of amino acid transporters. *Mol Aspect Med.* 2013;34(2–3):139–158.
- Bröer S, Palacín M. The role of amino acid transporters in inherited and acquired diseases. *Biochem J.* 2011;436(2):193–211.
- Mastroberardino L, Spindler B, Pfeiffer R, et al. Amino-acid transport by heterodimers of 4F2hc/CD98 and members of a permease family. *Nature.* 1998;395(6699):288–291.
- Kantipudi S, Jeckelmann JM, Ucurum Z, Bosshart PD, Fotiadis D. The heavy chain LAT1 and LAT2. *Int J Mol Sci.* 2020;21(20).
- Verrey F, Closs El, Wagner CA, Palacín M, Endou H, Kanai Y. CATs and HATs: the SLC7 family of amino acid transporters. *Pflügers Arch.* 2004;447(5):532–542.
- Wang Q, Holst J. L-type amino acid transport and cancer: targeting the mTORC1 pathway to inhibit neoplasia. *Am J Cancer Res.* 2015;5(4):1281–1294.
- Pineda M, Fernández E, Torrents D, et al. Identification of a membrane protein, LAT-2, that Co-expresses with 4F2 heavy chain, an L-type amino acid transport activity with broad specificity for small and large zwitterionic amino acids. *J Biol Chem.* 1999;274(28):19738–19744.
- Rossier G, Meier C, Bauch C, et al. LAT2, a new basolateral 4F2hc/CD98-associated amino acid transporter of kidney and intestine. *J Biol Chem.* 1999;274(49):34948–34954.
- Nakamura E, Sato M, Yang H, et al. 4F2 (CD98) heavy chain is associated covalently with an amino acid transporter and controls intracellular trafficking and membrane topology of 4F2 heterodimer. *J Biol Chem.* 1999;274(5):3009–3016.
- Prasad PD, Wang H, Huang W, et al. Human LAT1, a subunit of system L amino acid transporter: molecular cloning and transport function. *Biochem Biophys Res Commun.* 1999;255(2):283–288.
- DeBerardinis RJ, Chandel NS. We need to talk about the Warburg effect. *Nat Metab.* 2020;2(2):127–129.
- Yanagida O, Kanai Y, Chairoungdua A, et al. Human L-type amino acid transporter 1 (LAT1): characterization of function and expression in tumor cell lines. *Biochim Biophys Acta.* 2001;1514(2):291–302.
- de la Ballina LR, Cano-Crespo S, González-Muñoz E, et al. Amino acid transport associated to cluster of differentiation 98 heavy chain (CD98hc) is at the cross-road of oxidative stress and amino acid availability. *J Biol Chem.* 2016;291(18):9700–9711.
- Digomann D, Linge A, Dubrovská A. SLC3A2/CD98hc, autophagy and tumor radioresistance: a link confirmed. *Autophagy.* 2019;15(10):1850–1851.
- Cormerais Y, Giuliano S, LeFloch R, et al. Genetic disruption of the multifunctional CD98/LAT1 complex demonstrates the key role of essential amino acid transport in the control of mTORC1 and tumor growth. *Cancer Res.* 2016;76(15):4481–4492.
- Bröer S, Bröer A, Hamprecht B. Expression of the surface antigen 4F2hc affects system-L-like neutral-amino-acid-transport activity in mammalian cells. *Biochem J.* 1997;324(Pt 2):535–541 (Pt 2).
- Yan R, Zhao X, Lei J, Zhou Q. Structure of the human LAT1-4F2hc heteromeric amino acid transporter complex. *Nature.* 2019;568(7750):127–130.
- Torrents D, Estévez R, Pineda M, et al. Identification and characterization of a membrane protein (y+L amino acid transporter-1) that associates with 4F2hc to encode the amino acid transport activity y+L: a candidate gene for LYSI-NURIC protein intolerance. *J Biol Chem.* 1998;273(49):32437–32445.
- Ono M, Oka S, Okudaira H, et al. [14C]Fluciclovine (alias anti-[14C]FACBC) uptake and ASCT2 expression in castration-resistant prostate cancer cells. *Nucl Med Biol.* 2015;42(11):887–892.
- Sohda M, Miyazaki T, Honjyo H, et al. 18F-FAMT PET is useful to distinguish between specific uptake and nonspecific uptake compared to 18F-fluorodeoxyglucose position emission tomography in esophageal cancer patients. *Dig Surg.* 2018;35(5):383–388.
- Kaira K, Higuchi T, Sunaga N, et al. Usefulness of 18F- $\alpha$ -Methyltyrosine PET for therapeutic monitoring of patients with advanced lung cancer. *Anticancer Res.* 2016;36(12):6481–6490.
- Watabe T, Hatazawa J. (18F)-FBPA as a tumor specific tracer of L-type amino acid transporter 1 (LAT1): PET evaluation in tumor and inflammation compared to (18F)-FDG and (11C)-methionine. *Hellenic J Nucl Med.* 2015;18(Suppl 1):149.

56. Uchino H, Kanai Y, Kim DK, et al. Transport of amino acid-related compounds mediated by L-type amino acid transporter 1 (LAT1): insights into the mechanisms of substrate recognition. *Mol Pharmacol*. 2002;61(4):729–737.
57. Oda K, Hosoda N, Endo H, et al. L-type amino acid transporter 1 inhibitors inhibit tumor cell growth. *Cancer Sci*. 2010;101(1):173–179.
58. Okano N, Naruge D, Kawai K, et al. First-in-human phase I study of JPH203, an L-type amino acid transporter 1 inhibitor, in patients with advanced solid tumors. *Invest N Drugs*. 2020;38(5):1495–1506.
59. Rii J, Sakamoto S, Sugiura M, et al. Functional analysis of LAT3 in prostate cancer: its downstream target and relationship with androgen receptor. *Cancer Sci*. 2021;112(9):3871–3883. <https://doi.org/10.1111/cas.14991>.
60. Sugiura M, Sato H, Okabe A, et al. Identification of AR-V7 downstream genes commonly targeted by AR/AR-V7 and specifically targeted by AR-V7 in castration resistant prostate cancer. *Transl Oncol*. 2021;14(1), 100915.
61. Antonarakis ES, Lu C, Wang H, et al. AR-V7 and resistance to enzalutamide and abiraterone in prostate cancer. *N Engl J Med*. 2014;371(11):1028–1038.
62. von der Maase H, Hansen SW, Roberts JT, et al. Gemcitabine and cisplatin versus methotrexate, vinblastine, doxorubicin, and cisplatin in advanced or metastatic bladder cancer: results of a large, randomized, multinational, multicenter, phase III study. *J Clin Oncol*. 2000;18(17):3068–3077.
63. Bellmunt J, de Wit R, Vaughn DJ, et al. Pembrolizumab as second-line therapy for advanced urothelial carcinoma. *N Engl J Med*. 2017;376(11):1015–1026.
64. Powles T, Park SH, Voog E, et al. Avelumab maintenance therapy for advanced or metastatic urothelial carcinoma. *N Engl J Med*. 2020;383(13):1218–1230.
65. Maimaiti M, Sakamoto S, Yamada Y, et al. Expression of L-type amino acid transporter 1 as a molecular target for prognostic and therapeutic indicators in bladder carcinoma. *Sci Rep*. 2020;10(1):1292.
66. Kandasamy P, Gyimesi G, Kanai Y, Hediger MA. Amino acid transporters revisited: new views in health and disease. *Trends Biochem Sci*. 2018;43(10):752–789.
67. Higuchi K, Sakamoto S, Ando K, et al. Characterization of the expression of LAT1 as a prognostic indicator and a therapeutic target in renal cell carcinoma. *Sci Rep*. 2019;9(1), 16776.
68. Kokal M, Mirzakhani K, Pungsrinont T, Baniahmad A. Mechanisms of androgen receptor agonist- and antagonist-mediated cellular senescence in prostate cancer. *Cancers*. 2020;12(7).



Review

---

# Contribution of LAT1-4F2hc in Urological Cancers via Toll-like Receptor and Other Vital Pathways

---

Xue Zhao, Shinichi Sakamoto, Maihulan Maimaiti, Naohiko Anzai and Tomohiko Ichikawa



Review

# Contribution of LAT1-4F2hc in Urological Cancers via Toll-like Receptor and Other Vital Pathways

Xue Zhao <sup>1,2</sup>, Shinichi Sakamoto <sup>1,\*</sup> , Maimulan Maimaiti <sup>3</sup> , Naohiko Anzai <sup>4</sup>  and Tomohiko Ichikawa <sup>1</sup>

<sup>1</sup> Department of Urology, Chiba University Graduate School of Medicine, Chiba 260-8670, Japan; abesusuki@126.com (X.Z.); ichikawa@vmail.plala.or.jp (T.I.)

<sup>2</sup> Department of Urology, Tongren Hospital, Shanghai Jiao Tong University School of Medicine, Shanghai 200336, China

<sup>3</sup> Department of Tumor Pathology, Chiba University Graduate School of Medicine, Chiba 260-8670, Japan; marghulanmaimaiti@gmail.com

<sup>4</sup> Department of Pharmacology, Chiba University Graduate School of Medicine, Chiba 260-8670, Japan; anzai@chiba-u.jp

\* Correspondence: rbatbat1@gmail.com; Tel.: +81-43-226-2134; Fax: +81-43-226-2136

**Simple Summary:** LAT1-4F2hc complex is an important amino acid transporter. It mainly transports specific amino acids through the cell membrane, provides nutrition for cells, and participates in a variety of metabolic pathways. LAT1 plays a role in transporting essential amino acids including leucine, which regulates the mTOR signaling pathway. However, the importance of SLCs is still not well known in the field of urological cancer. Therefore, the purpose of this review is to report the role of the LAT1-4F2hc complex in urological cancers, as well as their clinical significance and application. Moreover, the inhibitor of LAT1-4F2hc complex is a promising direction as a targeted therapy to improve the treatment and prognosis of urological cancers.

**Abstract:** Tumor cells are known for their ability to proliferate. Nutrients are essential for rapidly growing tumor cells. In particular, essential amino acids are essential for tumor cell growth. Tumor cell growth nutrition requires the regulation of membrane transport proteins. Nutritional processes require amino acid uptake across the cell membrane. Leucine, one of the essential amino acids, has recently been found to be closely associated with cancer, which activate mTOR signaling pathway. The transport of leucine into cells requires an L-type amino acid transporter protein 1, LAT1 (SLC7A5), which requires the 4F2 cell surface antigen heavy chain (4F2hc, SLC3A2) to form a heterodimeric amino acid transporter protein complex. Recent evidence identified 4F2hc as a specific downstream target of the androgen receptor splice variant 7 (AR-V7). We stressed the importance of the LAT1-4F2hc complex as a diagnostic and therapeutic target in urological cancers in this review, which covered the recent achievements in research on the involvement of the LAT1-4F2hc complex in urinary system tumors. In addition, JPH203, which is a selective LAT1 inhibitor, has shown excellent inhibitory effects on the proliferation in a variety of tumor cells. The current phase I clinical trials of JPH203 in patients with biliary tract cancer have also achieved good results, which is the future research direction for LAT1 targeted therapy drugs.

**Keywords:** L-type amino acid transporter 1 (LAT1, SLC7A); 4F2 cell-surface antigen heavy chain (4F2hc, SLC3A2); urinary system tumors; diagnosis; targeted therapy



**Citation:** Zhao, X.; Sakamoto, S.; Maimaiti, M.; Anzai, N.; Ichikawa, T. Contribution of LAT1-4F2hc in Urological Cancers via Toll-like Receptor and Other Vital Pathways. *Cancers* **2022**, *14*, 229. <https://doi.org/10.3390/cancers14010229>

Academic Editor: David Wong

Received: 13 November 2021

Accepted: 2 January 2022

Published: 4 January 2022

**Publisher's Note:** MDPI stays neutral with regard to jurisdictional claims in published maps and institutional affiliations.



**Copyright:** © 2022 by the authors. Licensee MDPI, Basel, Switzerland. This article is an open access article distributed under the terms and conditions of the Creative Commons Attribution (CC BY) license (<https://creativecommons.org/licenses/by/4.0/>).

## 1. Introduction

Continuous proliferative signaling is the main feature of malignant tumors [1]. These signals trigger tumor cells to divide, causing tumor cells to grow rapidly in an uncontrollable way. Among all of these nutrients, Eagle discovered in 1955 that essential amino acids (EAA) were required for cell growth in vitro [2]. Later, studies found that the uptake of EAA in malignant tumor cells was higher than in normal tissues [3–5]. After being delivered into

the cells, these amino acids were utilized to make proteins, nucleic acids, lipids, and ATP. Cancer cells have higher up-regulated transporters that facilitate the entrance of exogenous amino acids into cells, compared to normal cells, and the steady acquisition of amino acids by cancer cells is important for cancer growth [6]. HATs (heteromeric amino acid transporters) are a special type of solute transporter. They are made up of two subunits, one heavy and one light, that are linked by a conserved disulfide bond [7]. The heavy subunit is a member of the SLC3 family, whereas the light subunit belongs to the SLC7 family.

The SLC3 family now includes two glycoproteins (rBAT (SLC3A1)) and 4F2hc (SLC3A2, also known as CD98) [7]. Heavy subunits of the SLC3 family, such as 4F2hc, were discovered in 1998 and are necessary for the proper trafficking of the heterodimer to the plasma membrane [8].

Regarding the SLC7 family, Kanai first isolated a cDNA from rat C6 glioma cells through expression cloning in 1998. The cDNA encodes a new Na<sup>+</sup>-independent neutral amino acid transporter called LAT1 [9]. In 1999, Kanai's team further isolated a cDNA from the rat small intestine, which encodes another transporter called LAT2 [10]. The former two proteins belong to the solute carrier family 7 (SLC7). After that, LAT3 [11] and LAT4 [12] were gradually discovered. These two belong to the SLC43 family. The L-type amino acid transporter, which consists of all former four subunits (LAT1-4), is an important pathway for EAA to enter the cell. Subsequently, Wang found that (18)F-labeled fluoroalkyl phenylalanine derivatives as PET tracers were more likely to bind to LAT1 in tumors, and the specific accumulation of this tracer in tumor cells suggested that LAT1 was expressed in a large number of malignant tumors, thus preliminarily revealing the close relationship between LAT1 and malignant tumors [13]. In 2016, U.S. Food and Drug Administration approved trans-1-amino-3-18F-fluorocyclobutanecarboxylic-acid (anti-[18F]-FACBC) PET for the detection of prostate cancer in patients with elevated prostate-specific-antigen following curative treatment [14]. LAT1 is known to be the primary target of FACBC [15]. The usefulness of LAT1 in PET imaging has already been validated in clinical practice.

In a previous extensive review, Wang reported that among the four LAT transporters, LAT1 (SLC7A5) is overexpressed in various cancers, which is more widespread than the other three LAT transporters [3]. Subsequent research intensified and found that the complex composed of 4F2hc and LAT1 played a key role in the occurrence and development of multiple human tumors. How to block the transport of nutrients by HATs to malignant tumor cells to achieve the purpose of inhibiting the occurrence and development of malignant tumor cells is an attractive research topic.

However, the importance of SLCs is still not well known in the field of urological cancer. In particular, LAT1 is a target of FACBC PET [15], which has important imaging implications in prostate cancer, following PSMA PET. Recently, 4F2hc, which binds to LAT1, has been identified as a specific downstream signal of AR-V7, a cause of castration resistance [16]. JPH203, a specific inhibitor of LAT1, has already completed Phase I clinical trials in Japan and may be applied to prostate cancer in the future [17].

Therefore, in this review, we summarized the latest advances in research on the role of the LAT1-4F2hc complex in urinary system tumors and emphasized the importance of the LAT1-4F2hc complex as a diagnostic and therapeutic target in urinary system tumors.

## 2. LAT1-4F2hc Complex and Structural Characteristics

LAT1 is made up of two layers of 12 putative transmembrane segments (TMs). TM1, TM3, TM6, TM8, and TM10 make up the inner layer, which is encircled by the outer layer. The outer layer is made up of TM2, TM4, TM5, TM7, TM9, TM11, and TM12. LAT1's N- and C-terminal ends are intracellularly localized, whereas 4F2hc's N- and C-terminal ends are intracellularly and extracellularly localized. The contact between 4F2hc and LAT1 is limited to one side of LAT1, while TM1 and TM6 of LAT1 are construction switches, which are essential for the alternate entry transport mechanism of the LeuT-fold transporters, and their positions are far away from the coordination of 4F2hc. Therefore, 4F2hc seems to stabilize the scaffold domain of LAT1 in the membrane, which may contribute to the

local conformational shift of gating elements (such as TM1, TM2, TM6, and TM10) during alternate entry cycles [18–20] (Figure 1A–C).

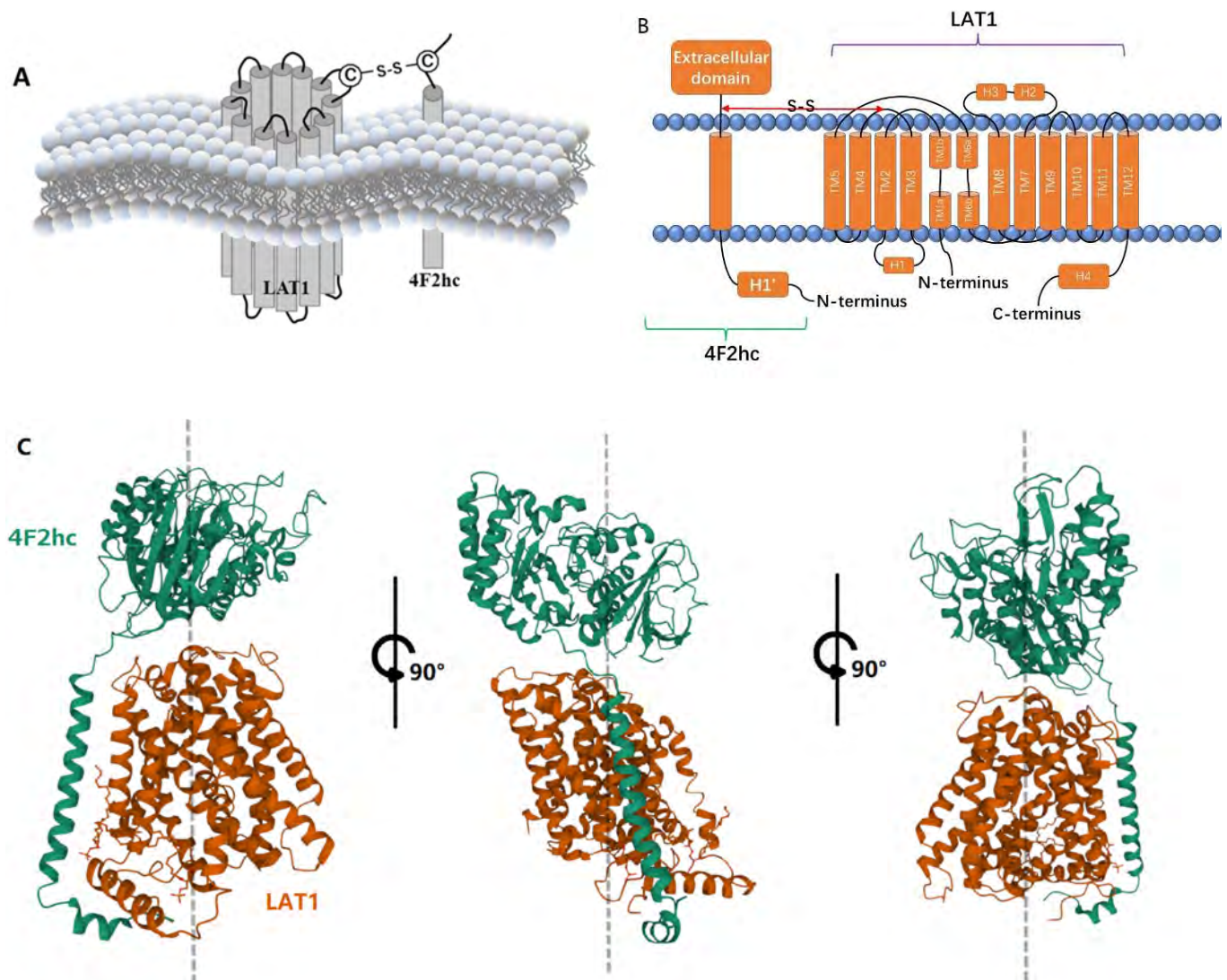


**Figure 1.** Structure of LAT1-4F2hc Complex: (A) Hypothetical model of the complex of LAT1 and 4F2hc; (B) LAT1 has 12 transmembrane units, while 4F2hc has only one. The two are covalently connected by disulfide bonds; (C) FIG1 (C) Images created using Mol\*, the PDB ID: 6IRS, Structure of the human LAT1-4F2hc heteromeric amino acid transporter complex. [19], Mol\* (D. Sehnal, S. Bittrich, M. Deshpande, R. Svobodová, K. Berka, V. Bazgier, S. Velankar, S.K. Burley, J. Koča, A.S. Rose (2021) Mol\* Viewer: modern web app for 3D visualization and analysis of large biomolecular structures. Nucleic Acids Research. doi: 10.1093/nar/gkab314 [21]), and RCSB PDB.

According to the structure of LAT1-4F2hc heterodimeric amino acid transporter protein complex, 4F2hc had only one transmembrane helix that seemed to be unable to form a transmembrane transporter pore. It shows that 4F2hc has a lack of amino acid transport activity. In contrast, LAT1 shows a typical membrane transport protein helical bundle structure. That is the reason why past studies have reported that LAT1 is the only sole transport-competent unit, and 4F2hc does not play any significant role in the internal transport function [22]. Now, there are different views about it. Glycoprotein 4F2hc acts as a molecular chaperone to make LAT1 the final location on the cell membrane [23]. In the absence of 4F2hc, LAT1 is present in the intracellular compartment, while 4F2hc can independently reach the plasma membrane [8,23]. In the presence of LAT1, the surface

expression pattern of 4F2hc changes, restricting it to cell-cell adhesion sites [23]. 4F2hc is necessary for the transport of LAT1 to the plasma membrane, and LAT1 is believed to determine the transport properties of heterodimers. It is obvious that LAT1 and 4F2hc cannot work alone without each other. Meanwhile, in many forms of cancer, increased 4F2hc expression levels have been linked to a worse prognosis in several studies [24–27]. The most critical structure involved in the interaction of the complex is the disulfide bond between the two proteins [8,23]. The functional role of the disulfide bond is still unclear. It does not seem to be involved in the ectopic of the two proteins to the membrane, nor in the transport of amino acids. However, recent studies have shown that disulfide bonds are important for regulating 4F2hc-related cation channels [28].

LAT1-4F2hc heterodimeric amino acid transporter protein complex is a transmembrane transporter that independent of Na<sup>+</sup> and pH. It imports large neutral amino acids (such as leucine and phenylalanine) for intracellular amino acid exchange (e.g., glutamine) [7,29], which are abundant in cells that require a constant supply of amino acids, such as nerve cells, activated T cells, placental cells, glial cells, and blood-brain barrier (BBB) endothelial cells [9,30,31]. In BBB, LAT1-4F2hc complex is stereospecific (L > D) [32]. Compared with LAT1 in peripheral tissues [33], it has a higher affinity for amino acids. Studies have shown that the affinity of LAT1 to intracellular amino acids is higher than that of extracellular amino acids, demonstrating that the quantity of intracellular substrate regulates LAT1 transport rate [34]. Due to its own transport characteristics, the LAT1-4F2hc complex often plays a key role in drug absorption, distribution and toxicity by mediating drug transmembrane transport, and often represents unexpected off-target of drugs [35].

### 3. LAT1/4F2hc and Human Diseases (Pain & Inflammation)

Existing studies have found that LAT1-4F2hc complex is widely associated with human diseases, such as inflammation, pain, hypoxia, and tumors [36–38].

Inhibition of LAT1 eliminated mTORC1 activation, plasmablast differentiation, and CpG (toll-like receptor TLR9 ligand)-stimulated B cell production of IgG and inflammatory cytokines. The influx of L-leucine through LAT1 regulates the activity of mTORC1 and the immune response of human B cells [37,38]. Among the most common nociceptive pathways, LAT1 may be a feasible new target for pain. LAT1 expression and regulation link it to key cell types and pathways related to pain. LAT1 regulates the Wnt/frizzled/ $\beta$ -catenin signal transduction pathway. The LAT1-4F2hc complex may also be involved in pain pathways related to T cells and B cells. The expression of LAT1 induces the activation of the mammalian target of rapamycin (mTOR) signal axis, which is related to inflammation and neuropathic pain. Similarly, hypoxia and tumors can induce the activation of hypoxia-inducible factor 2 $\alpha$ , which not only promotes the expression of LAT1 but also promotes the activation of mTORC1 [36]. As the common node of the T cell, B cell, and mTOR pathway, LAT1-4F2hc plays a vital role in human diseases. It has also received increasing attention as an important target for autoimmune diseases, chronic pain diseases, and tumors.

### 4. LAT1/4F2hc and Tumors

Many tumor cells lines [39–41] and human malignancies, such as breast, prostate, lung, colorectal, and gliomas [42–47], have high levels of LAT1 expression. In these tumors, LAT1 plays an important role in growth and survival. RNA interference (RNAi) [44,48–51] and genetic disruption by zinc fingers nucleases-mediated [52] LAT1-knockout in cancer cells caused that leucine absorption and cell proliferation were both inhibited. As a result, LAT1 is being evaluated as a potential therapeutic target for reducing cancer cell growth and proliferation [53,54].

Similarly, in human neoplasms such as prostate cancer, gastric cancer, lung pleomorphic carcinoma, and neuroendocrine carcinoma, 4F2hc expression is upregulated [24,27,41,55]. Increased 4F2hc expression is linked to a worse chance of survival, cell proliferation, and metastasis [56]. Since 4F2hc binds with LAT1 on the membranous surface of cancer cells, these results are not difficult to understand.

The LAT1-4F2hc complex is also closely related to tumor glutamine metabolism. The amount of glutamine required by cancer cells exceeds the supply produced by endogenous synthesis, resulting in the up-regulation of glutamine metabolism in many carcinogenic changes. LAT1-4F2hc complex controls the flux of glutamine and other amino acids involved in glutaminolysis and glutamine-regulated homeostasis [35]. LAT1-4F2hc complex exchanges Gln for leucine and other amino acids, which can lead to mTOR activation.

By influencing the mammalian target protein of rapamycin complex 1 (mTORC1), the amino acid leucine has been demonstrated to increase protein synthesis and accelerate cell development, whereas LAT1 has been linked to mTORC1 signaling and, as a result, cancer progression [6,57].

In cancer cells, however, LAT1 not only boosts mTORC1 activity but also enhances MYC and EZH2 signaling. Through the AKT, MAPK, and cell-cycle related P21 and P27 signal pathways, 4F2hc has been demonstrated to affect cancer cell proliferation. The expression of 4F2hc and LAT1 is reportedly codependent, and the downregulation of either subunit destabilizes the partner [8]. (Figure 2, Table 1).

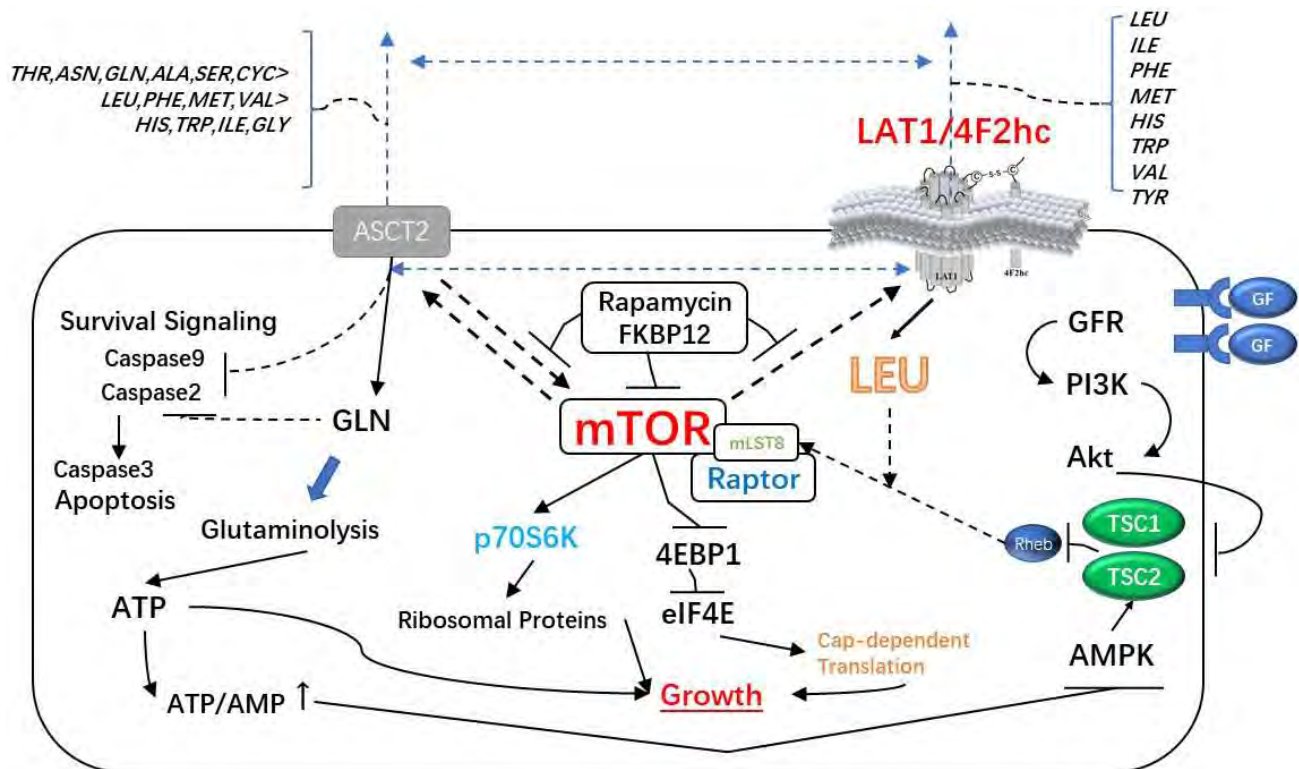


**Figure 2.** The Major Signaling Pathways Affected by LAT1-4F2hc Complex: The LAT1-4F2HC complex not only enhances mTORC1 activity but also enhances MYC and EZH2 signaling pathways. Moreover, it can affect the proliferation of cancer cells through AKT, MAPK and cell cycle-related P21 and P27 signaling pathways.

**Table 1.** LAT1-4F2hc and Common Tumors.

Cancer Types	Cell Lines	Downstream Effects of LAT1/4F2hc	Other Related Factors	References
NSCLC	A549, H1299	Mice with smaller tumors, lower leucine absorption, lower mTORC1 activity, amino acid stress, lower proliferation, and lower EZH2 expression and activity	Ki-67, VEGF, CD31, CD34, HIF-1a, mTOR, ASCT2	[27,52,58–63]
Gastric cancer	SGC-7901, MKN-45, MGC-803, CRL-5974	Decreases in proliferation, migration and invasion	Ki-67	[25,64–69]
Pancreatic cancer	MIA, Paca-2	Reductions in mTORC1 activity, decreases in proliferation and angiogenesis	Ki-67, VEGF, c-Myc, CD147	[50,70–74]
Biliary tract cancer	KKU-M055, KKU-M213	JPH203 first in human phase I clinical trial. Well-tolerated.	Ki-67	[75–81]
Ovarian cancer	SKOV3, IGROV1, A2780, OVCAR-3	Decreases in proliferation	ASCT2, SN2, p70S6K, LAT2	[82–85]
Breast cancer & TNBC	MCF-7, ZR-75, MDA-MB-232	Decreases in proliferation	ADS, HER2, TN, Ki-67, ER, PgR	[45,86–90]

LAT1-4F2hc Complex

## 5. LAT1/4F2hc and Urological Tumors

### 5.1. LAT1/4F2hc and Prostate Cancer

LAT1-4F2hc complex plays an important role in growth and survival in PCa cells. Sakata used LAT1 as a biomarker for highly malignant prostate cancer in 2009 [47]. The increased expression of LAT1 in prostate cancer is a new independent biomarker of high malignancy that can be used to estimate prognosis in conjunction with the Gleason score [47].

Trans-1-amino-3-18F-fluorocyclobutanecarboxylic-acid (anti-[18F]-FACBC) is an amino acid PET tracer, which shows good prospects in visualizing PCa [91]. The tracer is used for the evaluation of l-amino acid transport, LAT1 is known to be the primary target of FACBC [15]. In 2016, 18F-FACBC has been approved by the US Food and Drug Administration (FDA) and the European Commission (EC) to detect PCa in patients with elevated PSA after previous treatments [14]. Approval is based on encouraging diagnostic performance and histologically confirmed data from patients with biochemical relapse [92]. Recently, it was included in the National Comprehensive Cancer National (NCCN) guidelines for the treatment of patients with recurrent PCa. The usefulness of LAT1 in PET imaging has already been validated in clinical practice.

Wang reported [57] that when LAT activity was inhibited, activating transcription factor 4-mediated overexpression of amino acid transporters such as ASCT1, ASCT2, and 4F2hc occurred, all of which were regulated by the androgen receptor. LAT suppression inhibited M-phase cell cycle genes regulated by E2F family transcription factors, including UBE2C, CDC20, and CDK1, which are important castration-resistant prostate cancer regulators. In silico analysis of BCH-downregulated genes revealed that in metastatic castration-resistant prostate cancer, 90.9 percent are statistically significantly upregulated. Finally, in vivo, LAT1 knockdown decreased tumor development, cell cycle progression, and spontaneous metastasis in xenografts [57].

Patel studied the functional characterization and molecular expression of large neutral amino acids of LAT1 in prostate cancer PC-3 cells [93]. It proves that LAT1 is mainly responsible for the uptake of large neutral amino acids and has functional activity in PC-3

cells. The fact that Ile-quinidine generates a considerable increase in absorption compared to quinidine suggests that LAT1 could be used to improve the cellular permeability of poorly cell-permeable anticancer medicines. This cell line can also be utilized as an *in vitro* model to investigate the interaction of large-scale neutral amino acid conjugated pharmaceuticals with the LAT1 transporter [94].

In PCa cell lines, DU145 cells had the highest levels of 4F2hc protein expression, followed by PC-3 and C4-2 cells. In C4-2 and DU145 cells, 4F2hc expression was found to be substantially greater than LAT1 expression. Cell growth, migration, and invasion are all inhibited by Si4F2hc. 4F2hc and LAT1 expression in PCa tissue and association with clinical variables. The expression levels (4F2hc and LAT1/high and low) are associated with various tumor prognoses [24]. The data from the same study [24] revealed that SKP-2 is a downstream and particular target gene of 4F2hc. SKP-2 is associated with cell cycle, DNA replication, and cell division.

#### 5.1.1. AR and LAT1-4F2hc Complex in CRPC (AR/AR-V7 and 4F2hc Promotes the Development of CRPC)

Xu reported that the up-regulation of LAT1 during anti-androgen therapy promotes the progression of PCa cells [44]. In hormone-resistant prostate cancer cell lines, LAT1 was shown to be substantially expressed. Knocking down LAT1 in LNCaP and C4-2 cells can drastically reduce cell proliferation, migration, and invasion. In patients receiving androgen deprivation therapy, high LAT1 expression was linked to a significantly shorter prostate-specific antigen recurrence-free survival [44].

Another study demonstrated a potential relationship between AR-V7 and 4F2hc [16]. AR-V7 activates downstream target genes in the absence of androgens. 4F2hc (SLC3A2) is one of the downstream target genes of AR-V7. AR-V7 gene knockdown leads to a decrease in the level of H3K27ac at the 4F2hc locus. The decrease in the expression of 4F2hc indicates that AR-V7 has a certain effect on the activation of 4F2hc expression. In clinical samples, the expression level of 4F2hc in benign lesions and primary PCa tissues was low, while the expression level of 4F2hc in CRPC tissues was significantly increased. The expression of 4F2hc in PCa patients with high AR-V7 expression is higher than that in PCa patients with low AR-V7 expression.

When LNCaP and LNCaP95 cell lines were treated with siRNA against 4F2hc, cellular growth was significantly suppressed [16]. Down-regulation of 4F2hc inhibited cell proliferation through apoptosis and cell senescence [16].

#### 5.1.2. LAT1/4F2hc Expression Is Coordinately Regulated during Prostate Cancer Progression (HSPC to CRPC)

Not all prostate tumor cell lines are closely related to LAT1. Otsuki found that LNCaP cells mainly express LAT3, and LAT1 was primarily expressed in DU145 and PC-3 cells [95]. Xu's research also gave similar results [44]. LAT3 was abundantly expressed in AR-expressing LNCaP and C4-2 cells, whereas it was barely expressed in AR-negative PC3 and DU145 cells, according to Rii's study [96].

Wang [97] reported the fact that LAT1 is highly expressed in androgen-insensitive PC-3 cells but LAT3 is highly expressed in androgen-sensitive LNCaP cells could be explained by transcriptional regulation of LAT1 and LAT3 expression. Changes in the microenvironment, such as starvation or hormone deprivation, can promote cancer formation and alter LAT1 and LAT3 expression. Reduced androgen receptor signaling may result in decreased LAT3 expression and, as another result, higher LAT1 expression. The results were confirmed by both nude mice samples and human samples [97]. LAT3 expression was higher in amplified AR patients. In a dose-dependent way, DHT stimulation enhanced LAT3 expression. Bicalutamide inhibited the effect of DHT on LAT3 expression. DHT treatment significantly boosted AR expression, which was reduced by bicalutamide [96] (Figure 3).

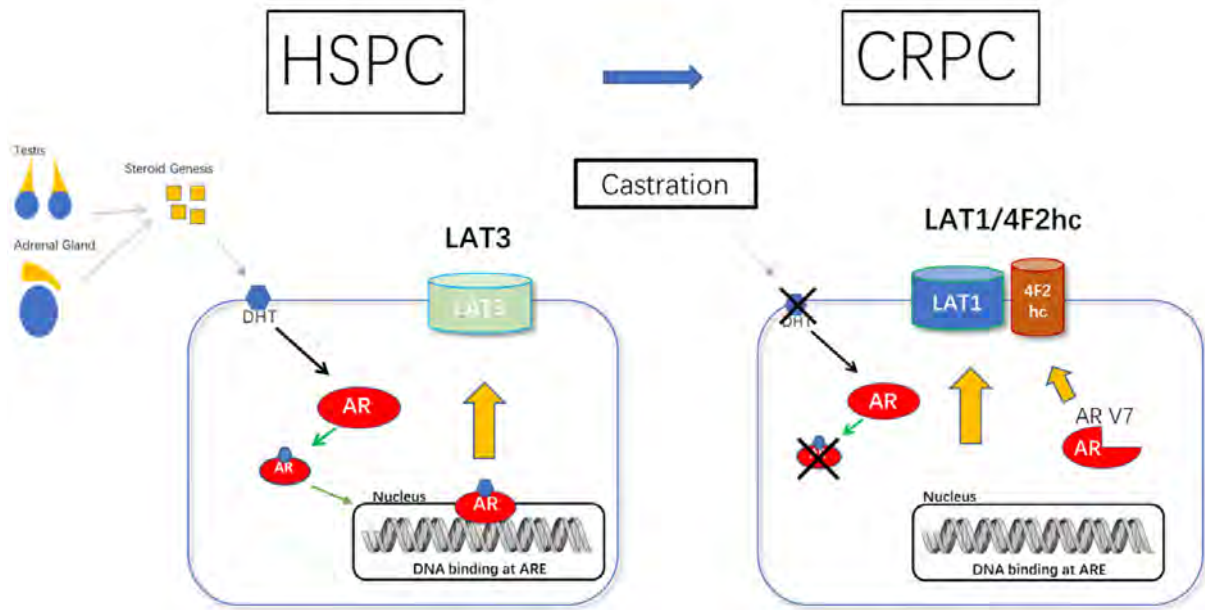


**Figure 3.** LAT Expression is Coordinately Regulated During Prostate Cancer Progression: Proposed model of LAT1-4F2hc/LAT3 in HSPC to CRPC. As HSPC progresses to CRPC, AR acts in reverse to cause low expression of LAT3 and high expression of LAT1.

Since high AR-V7 expression is one of the most common features of CRPC, AR-V7 expression following LH-RH therapy up-regulates the 4F2hc expression [16].

Based on the above evidence, LAT1/4F2hc can be independent PCa biomarkers and therapeutic targets, respectively. They can also collectively influence the transformation of PCa to CRPC and promote both progressions through the mentioned pathways below (Figure 4).

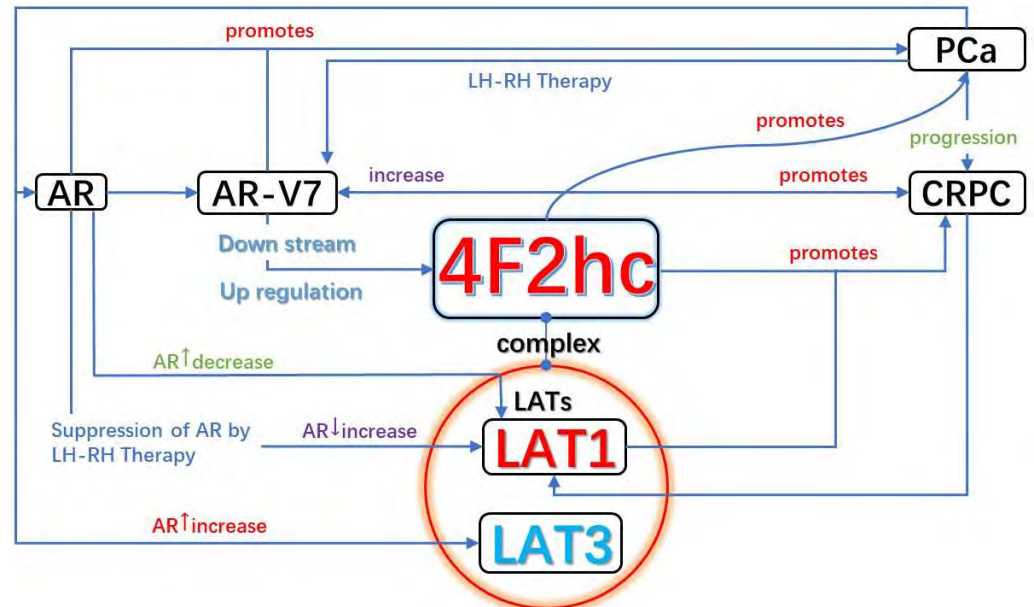


**Figure 4.** Relationship of LAT1-4F2hc and PCa & CRPC: The relationship between LATx-4F2hc and AR(AR-V7) and different stages of prostate cancer. Reduced androgen receptor signaling and variation of androgen receptors may result in decreased LAT3 expression and higher LAT1 expression.

## 5.2. LAT1/4F2hc and Renal Cancer

There are few studies on LAT1 and renal clear cell carcinoma. In 2013, Hironori [42] studied the expression of LAT1, LAT2, LAT3, LAT4, and 4F2hc mRNA in clear cell renal cell carcinoma tissues. It was found that the expression of LAT1 mRNA in tumor tissue was considerably higher than in non-tumor tissue, but the expression of LAT2 and LAT3 mRNA was lower. There was no difference in LAT4 and 4F2hc mRNA expression between tumor and non-tumor tissues. Poorly differentiated tumors, local invasion, microvascular invasion, and metastasis are all linked to increased LAT1 mRNA expression. Higher LAT1 mRNA levels in the blood are linked to a shorter total survival period. Phosphorylated S6 ribosomal protein levels are related to metastatic potential. The level of phosphorylated S6 ribosomal protein is positively linked with the expression of LAT1 mRNA in primary cancers [42].

Higuchi investigated the LAT1 expression profile in RCC tissues as well as its relationships with clinical variables retrospectively [98]. Most of the tissues (92 percent) had cancer-associated LAT1 expression. Patients with high LAT1 expression levels had lower overall survival and progression-free survival than those with low LAT1 expression levels, and these correlations were confirmed by univariate and multivariate analyses [98].

Tumors grow and evolve through continuous crosstalk with the surrounding microenvironment. New evidence shows that angiogenesis and immunosuppression often occur simultaneously to deal with this crosstalk [99]. At present, one strategy to achieve a higher clinical response in the study of renal cell carcinoma is to produce a more effective anti-tumor contraction by combining multiple immune checkpoints. However, the toxicity profile is higher [100]. T cells can shape tumor blood vessels and tumor endothelial cells, prevent the recruitment and infiltration of effector immune cells while remodeling ECM, and further inhibit the migration and infiltration of functional immune cells. The tumor vascular system actively participates in immunosuppression. The abnormal pathophysiological mechanism of tumor vessels can lead to the production of immunosuppressive molecules and inhibit the function of effective T cytotoxic cells. At the same time, the production of chemokines and cytokines promotes the differentiation and activation of immunosuppressive cells. These cells can also inhibit the activity of cytotoxic T cells. On the contrary, in the blood vessels, these mechanisms also down-regulate a variety of adhesion molecules, which are very important for the rolling, adhesion, and transport of T cells into the cancer environment. The normal tumor vascular system can improve T cell infiltration, enhance immune response, stop the immunosuppressive environment, make it a more immunoactivated phenotype, and work together with cancer immunotherapy. Anti-vascular endothelial growth factor receptor (anti-VEGFR) is the first to realize the normalization and functional recovery of tumor vascular system by tissue perfusion and reducing intratumoral hypoxia [99]. In the current studies of cancers [71,101,102], angiogenesis in vitro/in vivo experiments was inhibited by eliminating the function or expression of LAT1. It regulates proliferation, translation, and angiogenesis VEGF-A signal [102]. LAT1 is a central transporter of essential amino acids in human umbilical vein endothelial cells [103]. LAT1 also mediated miR-126 on primary human lung microvascular endothelial cells' angiogenesis via regulation of mTOR signaling [104]. LAT1 expression correlated significantly with CD98, VEGF, CD34 expression, and microvessel density in the primary and metastatic sites of tumors [41,81,105–108]. VEGF and CD34 are also related to angiogenesis. These studies further revealed the dual role of LAT1-4F2hc in tumor cells and stromal endothelial cells. The therapeutic inhibition of LAT1-4F2hc may provide an ideal choice for strengthening anti-angiogenesis therapy. Lat1-4f2hc is a potential therapeutic target for anti-tumor angiogenesis and maintenance of the normal vascular system. Therefore, the combination of antiangiogenic therapy and immunotherapy seems to have the potential to break the balance of the tumor microenvironment and improve the treatment response of renal cell carcinoma. It can be a novel paradigm to envision tailored approaches in renal cell-carcinoma and other urological tumors.

### 5.3. LAT1/4F2hc and Bladder Cancer

In 2002, Kyung reported the characterization of the system L amino acid transporter in T24 cells [93]. T24 human bladder cancer cells express LAT1 and its associated protein 4F2hc in the plasma membrane, however, T24 cells do not express the other system L isoform LAT2. The majority of [<sup>14</sup>C]L-leucine uptake is mediated by LAT1 in T24 cells [93].

Baniasadi [109] reported the gene expression profile of inhibiting LAT1 in T24 human bladder cancer cells. BCH influences the expression of a vast number of genes involved in cell survival and physiological function, according to researchers. These findings contribute to a better understanding of the intracellular signaling pathways involved in cell growth suppression produced by LAT1 inhibitors, which could be utilized as a target for anticancer drug development [44,109].

Maimaiti studied the expression profile and functional role of LAT1 in bladder cancer [110]. This is the first study to show that LAT1 plays a role in bladder cancer, and it also found IGFBP-5 to be a new downstream target for inhibiting LAT1. High LAT1 expression was found to be an independent predictive factor for overall survival in multivariate analysis. Patients with high LAT1 and IGFBP-5 expression had a significantly lower overall survival than those with low expression. LAT1 levels are linked to pathological staging, LDH, and NLR. In vitro, inhibiting LAT1 prevents cell proliferation, migration, and invasion. In aggressive BC patients, IGFBP-5 expression is also linked to a better prognosis [110] (Table 2).

Table 2. LAT1-4F2hc and Urological Tumors.

Cancer Types	Cell Lines	LAT1-4F2hc and Urological Tumors				Other Related Factors	Meanings	References
		Expression		Be Inhibited Downstream Effects				
		LAT1	4F2hc	LAT1	4F2hc			
Prostate cancer	LNCAP	↑(Not express [95])	↑					
	LNCAP95	↑	↑					
	C4-2	↑	↑	BCH, JPH203, R1881, ESK242	Lower leucine absorption, Lower mTORC1 activity, Amino acid stress, Down regulation of ATF4-mediated genes, Reduced tumor metastasis ability in PC3-CRC metastatic tumor mouse model.	Lower proliferation, higher apoptosis, and several gene expression changes.		
	PC3	↑	↑	BCH, R1881, AR-V7 knockdown				[16,24,44,57,94,95,97,111]
	DU145	↑	N/A					
	VCAP	↑	↑					
Renal cancer	Caki-1	↑	N/A					
	ACHN	↑	N/A					
	ccRCC tissue	↑	→(by mRNA detection)	JPH203	Lower mTORC1 activity, Reduced p70S6K and 4E-BP1.	N/A	S6 ribosomal protein (Ser-235/236)	[42,98]
Bladder cancer	T24	↑	↑	BCH, JPH203, SHAT1	Cell growth inhibition, inhibit phosphorylation of MAPK/Erk, AKT, p70S6K, and 4EBP-1. Decreases in migration and invasion activities.	Reduced Leucine intake and tumor cell growth.		
	5637	↑	N/A					[93,109,110,112]

## 6. Inhibitors of LAT1/4F2hc and Targeted Therapy

Due to its own transport characteristics of the SLC family, the LAT1-4F2hc complex often plays a key role in drug absorption, distribution and toxicity by mediating drug transmembrane transport [35]. However, only a small number of SLCs have been locked by drugs or chemical probes till now. Three main factors hinder the development of new chemical entities that can regulate SLC activity. First, most studies on this super population are relatively insufficient, and the biological functions or substrates of many SLCs are still unclear. Second, there is a lack of high-quality biological tools, specific, and reliable reagents and special databases. Finally, the number of functional analyses required to study such diverse objectives is still limited [113]. It is reported radioligand uptake assays have been widely employed to study LAT1 [114], but the radioligand uptake assays cannot distinguish inhibitors from substrates. The LAT1-4F2hc complex is overexpressed in many cancer cells and is thought to be a viable anticancer therapeutic target since inhibiting it reduces cancer cell viability dramatically.

BCH and JPH203 are LAT1-4F2hc complex inhibitors that have been studied extensively. BCH is a non-metabolic leucine analogue. In 2006, Baniyadi [109] found that BCH has an impact on the expression of many genes involved in cell survival and physiological activity. These data help to understand the intracellular signal transduction of cell growth inhibition induced by LAT1 inhibitors and can be used as a candidate for anticancer drug therapy [109]. Later studies proposed the use of N-butyl-N-(4-hydroxybutyl) nitrosamine (BBN) treatment to induce high expression of LAT1/4F2hc in rat bladder cancer cells [101] and proposed some directions for anti-LAT1/4F2hc drugs. JPH203 was discovered by Oda in 2010 and was originally known as KYT-0353 [115]. JPH203 is a highly selective LAT1 inhibitor produced by synthetic chemistry and in vitro screening based on triiodothyronine (T3). JPH203 showed excellent selective inhibition of LAT1 and showed potential as a novel antitumor agent. JPH203 interferes with constitutive activation of mTORC1 and Akt, reduces c-MyC expression, and triggers a folding protein response mediated by CHOP transcription factors associated with cell death [116]. Since then, several studies have confirmed that JPH203 has an impressive inhibitory effect on the growth of common tumor cells, such as colon cancer [115,117], gastric carcinoma [64], medulloblastoma [118], osteosarcoma [119], thyroid cancer [120,121], endocrine-resistant breast cancer [122], pituitary tumor [123], head and neck cancer cells [124], and T-cell Acute lymphoblastic leukemia (T-ALL)/lymphoma (T-LL) cells [116], etc.

In terms of urinary tumors, Maimaiti [110] found that in bladder cancer cells JPH203 inhibits the absorption of leucine by >90%. JPH203 inhibits the phosphorylation of MAPK/Erk, AKT, p70S6K, and 4EBP-1. JPH203 inhibits IGF-mediated igfb5 expression and AKT phosphorylation [110].

In the area of RCC, Higuchi [98] has tested the effects of JPH203 on RCC-derived Caki-1 and ACHN cells. JPH203 suppressed the proliferation of various cell types in a dose-dependent manner. According to the findings, the migration and invasion operations were stifled by JPH203 [98].

In the area of PCa, Otsuki [95] found that LAT1 was primarily expressed in DU145 and PC-3 cells. BCH or JPH203 inhibited leucine uptake and cell proliferation in a dose-dependent manner [95]. A Phase I clinical study found that JPH203 was well-tolerated and provided promising activity against biliary tract cancer [17]. The authors are currently planning Phase I and II study of JPH203 in CRPC [17].

These studies also show the potential of JPH203 for the treatment of urological cancers.

In 2021, Yan [125] synthesized three LAT1 inhibitors, JX-075, JX-078, and JX-119, and used cryo-EM to solve the inhibitors' complex structures with the LAT1-4F2hc complex. They also solved the LAT1-4F2hc complex coupled with Diiodo-Tyr's cryo-EM structure. LAT1 is found in an outward-occluded conformation in all the combinations of these complexes. These structures might reflect two distinct inhibitory processes, giving significant information for medication development in the future [125].

Of particular interest is the first Phase I clinical trial of JPH203 [17]. Although several studies have demonstrated that JPH203 can inhibit leucine uptake by tumor cells and show concentration-dependent cytotoxicity in vitro or good results in transplanted tumor models, Phase I clinical trial in humans is a milestone. Okano assessed dose-limiting toxicity in the first cycle using the 3 + 3 design. Seventeen Japanese patients with advanced solid tumors were enrolled and treated daily with JPH203 intravenously for 7 days. The maximum safe tolerated dose of JPH203 was defined as 60 mg/m<sup>2</sup>. The suitable RP2D is 25 mg/m<sup>2</sup>. Partial response was observed in one biliary tract cancer (BTC) patient at 12 mg/m<sup>2</sup>, and disease control was achieved in three of the six BTC patients at both the 12 mg/m<sup>2</sup> and 25 mg/m<sup>2</sup> levels. The disease control rate of BTC was 60%. The JPH203 molecule is predominantly metabolized into Nac-JPH203 by N-acetyltransferase 2 in liver cells [126]. Patients' N-acetyltransferase 2 phenotype (rapid/non-rapid) was found to predict the safety and efficacy of JPH203. A lower Nac-JPH203/JPH203 ratio is critical for maximizing the anti-tumor effect of JPH203 [17].

Of course, there are still some deficiencies and limitations in the study of urinary tumors and LAT1-4F2hc complexes mentioned above.

In BBN-induced bladder cancer, LAT1-4F2hc was not expressed by porous endothelial cells. Whether LAT1-4F2hc expression depends on endothelial cell structure is unclear. Fenestration of microvascular endothelial cells is not a stable event, because endothelial cells with fenestration in BBN-induced rat bladder cancer were transformed into endothelial cells without fenestration 5 min after injection of VEGF inhibitor, and fenestration recovered 30 min later [101]. The molecular mechanisms of amino acid transport in normal and tumor microvascular endothelial cells need further study. However, the LAT1-4F2hc complex is closely related to angiogenesis [41,71,81,101,102,105–108]. This makes it possible for the LAT1-4F2hc complex to improve the effectiveness of cancer immunotherapy by improving immune vascular crosstalk [99].

In prostate cancer-related experiments, although downregulation of LAT1 and LAT3 in tumor cells inhibits the growth of prostate cancer cells, it remains to be determined what other mechanisms of prostate cancer resistance can be triggered by targeting LAT1 (such as activation of ATF4).

Most of the studies were conducted in vitro, not in vivo. Although the phase I clinical trial of JPH203 against biliary tract cancer has achieved good results, the clinical trial has not yet involved any urinary tumors. In addition, the number of patients included in some studies is relatively small, or the follow-up time is not long, and the prognostic impact of LAT1 inhibition on tumor patients with different stages has not been thoroughly solved. Most of the specimens studied are in vitro tumor specimens after surgery, and the expression of LAT1-4F2hc in early tumors and its influence on tumors are also a key link that needs to be studied.

Finally, targeted therapy of LAT1-4F2hc does not directly kill cancer cells, but blocks amino acid transport, resulting in loss of nutritional basis and self-apoptosis of cancer cells. This has led some investigators to suggest that targeting LAT1-4F2hc is more suitable for slow-progressing tumors. Therefore, further studies are needed to obtain more evidence that LAT1-4F2HC therapy is also suitable for highly aggressive and rapidly progressing tumors.

## 7. Conclusions

### *Significant Contribution of the LAT1-4F2hc in Urological Cancers*

These studies and experiments above are helping us to understand how cancer cells metabolize differently from normal cells, as well as the therapeutic targets that could be interfered with in these different metabolisms of proliferation. The abnormal proliferation of tumor cells usually depends on the nutrient microenvironment generated by these abnormal metabolic patterns. Recognizing and blocking the nutrient absorption pathways of malignant tumors are usually the key points in the diagnosis and treatment

of malignant tumors. The LAT1-4F2hc complex is such a target with both diagnostic and therapeutic significance.

The LAT1-4F2hc complex mediates a variety of pathways, such as T cells, B cells, and mTOR pathways, and is also closely related to Toll-like receptors and vascular endothelial growth factors. This has caused the LAT1-4F2hc complex to become a common factor in many diseases, such as autoimmune diseases, pain, tumors.

The clinical significance of the LAT1-4F2hc complex in urinary cancer has gradually begun to be explored and confirmed, just like in other tumor cells. LAT1-4F2hc upregulation seems to be a common phenomenon in cancers. It is a reliable tumor biomarker and the target of imaging tracer, which can be used for the diagnosis and prognosis of urinary malignant tumors. It is also a meaningful therapeutic target. In fact, great efforts have been made to decipher the biology of LAT1-4F2hc. While a complete scenario has not yet been painted, a combination of bioinformatics, in vitro, and animal experiments has revealed some previously unknown aspects of LAT1-4F2hc transport mechanisms, substrate specificity, and regulation. These results provide a strong basis for pharmacological studies in which inhibitors of LAT1-4F2hc, such as JPH203. JPH203 can act well on a variety of tumor cells. Its phase I clinical trial in humans is a great milestone for researchers and patients.

However, the study of LAT1-4F2hc is still rare and not thorough in the field of urinary tumors. The results obtained so far are not fully in line with the fact that LAT1-4F2hc should play a prominent role in the field of urinary cancers. Its transport, regulation of expression/function, effects of posttranslational modifications on its stability/activity, interactions with other amino acid transporters and upstream and downstream genes, reaction with chemotherapy sensitivity/resistance, relationship with immunotherapy of sensitivity/resistance, is worthy for further research. In addition, Whether the phase I or II clinical trials of JPH203 in patients with urinary tumors can improve the prognosis of urinary tumors and whether there are corresponding biomarkers that can be used to predict the sensitivity and prognosis of inhibitors are also worthy of study.

As a future direction, we are currently pursuing the utility of LAT1 as a biomarker in urological tumors. In recent years, the usefulness of liquid biopsy has been suggested in clinical practice. The expression of LAT1 in blood, including CTCs, ctDNA, and Exosome, is currently being examined through collaborative research.

We hope to prove its usefulness not only as an inhibitor but also as a companion di-agnostic agent in the near future.

In conclusion, LAT1-4F2hc plays an important role in the diagnosis, treatment, and prognosis assessment of urinary system tumors. Cancer-related amino acid transporters may change the diagnostic and treatment strategy of urological tumors in near future.

**Author Contributions:** X.Z. contributed to collecting bibliography, preparing figures, and writing; S.S. and M.M. contributed to drawing structure figures and writing; S.S., N.A. and T.I. contributed to supervision of all the activities. The first draft of the manuscript was prepared by X.Z., M.M. performed subsequent amendments. S.S. revised the manuscript. All authors have read and agreed to the published version of the manuscript.

**Funding:** This research received no external funding.

**Acknowledgments:** The present study was supported by grants from the Japan Society for the Promotion of Science (20H03813 to T.I., 20K09555 to S.S., and 21H03065 to N.A.) and Japan China Sasakawa Medical Fellowship (to X.Z.).

**Conflicts of Interest:** The authors declare no conflict of interest. The funders had no role in the design of the study; in the collection, analyses, or interpretation of data; in the writing of the manuscript, or in the decision to publish the results.

## References

1. Hanahan, D.; Weinberg, R.A. Hallmarks of cancer: The next generation. *Cell* **2011**, *144*, 646–674. [[CrossRef](#)]
2. Eagle, H. Nutrition needs of mammalian cells in tissue culture. *Science* **1955**, *122*, 501–514. [[CrossRef](#)]

3. Qi, W.; Guan, Q.; Sun, T.; Cao, Y.; Zhang, L.; Guo, Y. Improving detection sensitivity of amino acids in thyroid tissues by using phthalic acid as a mobile phase additive in hydrophilic interaction chromatography-electrospray ionization-tandem mass spectrometry. *Anal. Chim. Acta* **2015**, *870*, 75–82. [[CrossRef](#)]
4. Kirikae, M.; Diksic, M.; Yamamoto, Y.L. Quantitative measurements of regional glucose utilization and rate of valine incorporation into proteins by double-tracer autoradiography in the rat brain tumor model. *J. Cereb. Blood Flow Metab. Off. J. Int. Soc. Cereb. Blood Flow Metab.* **1989**, *9*, 87–95. [[CrossRef](#)]
5. Wang, L.B.; Shen, J.G.; Zhang, S.Z.; Ding, K.F.; Zheng, S. Amino acid uptake in arterio-venous serum of normal and cancerous colon tissues. *World J. Gastroenterol.* **2004**, *10*, 1297–1300. [[CrossRef](#)]
6. Wang, Q.; Holst, J. L-type amino acid transport and cancer: Targeting the mTORC1 pathway to inhibit neoplasia. *Am. J. Cancer Res.* **2015**, *5*, 1281–1294.
7. Fotiadis, D.; Kanai, Y.; Palacin, M. The SLC3 and SLC7 families of amino acid transporters. *Mol. Asp. Med.* **2013**, *34*, 139–158. [[CrossRef](#)] [[PubMed](#)]
8. Mastroberardino, L.; Spindler, B.; Pfeiffer, R.; Skelly, P.J.; Loffing, J.; Shoemaker, C.B.; Verrey, F. Amino-acid transport by heterodimers of 4F2hc/CD98 and members of a permease family. *Nature* **1998**, *395*, 288–291. [[CrossRef](#)]
9. Kanai, Y.; Segawa, H.; Miyamoto, K.; Uchino, H.; Takeda, E.; Endou, H. Expression cloning and characterization of a transporter for large neutral amino acids activated by the heavy chain of 4F2 antigen (CD98). *J. Biol. Chem.* **1998**, *273*, 23629–23632. [[CrossRef](#)]
10. Segawa, H.; Fukasawa, Y.; Miyamoto, K.; Takeda, E.; Endou, H.; Kanai, Y. Identification and functional characterization of a Na<sup>+</sup>-independent neutral amino acid transporter with broad substrate selectivity. *J. Biol. Chem.* **1999**, *274*, 19745–19751. [[CrossRef](#)]
11. Babu, E.; Kanai, Y.; Chairoungdua, A.; Kim, D.K.; Iribe, Y.; Tangtrongsup, S.; Jutabha, P.; Li, Y.; Ahmed, N.; Sakamoto, S.; et al. Identification of a novel system L amino acid transporter structurally distinct from heterodimeric amino acid transporters. *J. Biol. Chem.* **2003**, *278*, 43838–43845. [[CrossRef](#)]
12. Bodoy, S.; Martin, L.; Zorzano, A.; Palacin, M.; Estevez, R.; Bertran, J. Identification of LAT4, a novel amino acid transporter with system L activity. *J. Biol. Chem.* **2005**, *280*, 12002–12011. [[CrossRef](#)] [[PubMed](#)]
13. Wang, L.; Qu, W.; Lieberman, B.P.; Plossl, K.; Kung, H.F. Synthesis, uptake mechanism characterization and biological evaluation of (18)F labeled fluoroalkyl phenylalanine analogs as potential PET imaging agents. *Nucl. Med. Biol.* **2011**, *38*, 53–62. [[CrossRef](#)]
14. Laudicella, R.; Albano, D.; Alongi, P.; Argiroffi, G.; Bauckneht, M.; Baldari, S.; Bertagna, F.; Boero, M.; Vincentis, G.; Sole, A.D.; et al. (18)F-Facbc in Prostate Cancer: A Systematic Review and Meta-Analysis. *Cancers* **2019**, *11*, 1348. [[CrossRef](#)]
15. Tulipan, A.J.; Salberg, U.B.; Hole, K.H.; Vlatkovic, L.; Aarnes, E.K.; Revheim, M.E.; Lyng, H.; Seierstad, T. Amino acid transporter expression and 18F-FACBC uptake at PET in primary prostate cancer. *Am. J. Nucl. Med. Mol. Imaging* **2021**, *11*, 250–259. [[PubMed](#)]
16. Sugiura, M.; Sato, H.; Okabe, A.; Fukuyo, M.; Mano, Y.; Shinohara, K.I.; Rahmutulla, B.; Higuchi, K.; Maimaiti, M.; Kanesaka, M.; et al. Identification of AR-V7 downstream genes commonly targeted by AR/AR-V7 and specifically targeted by AR-V7 in castration resistant prostate cancer. *Transl. Oncol.* **2021**, *14*, 100915. [[CrossRef](#)]
17. Okano, N.; Naruge, D.; Kawai, K.; Kobayashi, T.; Nagashima, F.; Endou, H.; Furuse, J. First-in-human phase I study of JPH203, an L-type amino acid transporter 1 inhibitor, in patients with advanced solid tumors. *Investig. New Drugs* **2020**, *38*, 1495–1506. [[CrossRef](#)]
18. Singh, N.; Ecker, G.F. Insights into the Structure, Function, and Ligand Discovery of the Large Neutral Amino Acid Transporter 1, LAT1. *Int. J. Mol. Sci.* **2018**, *19*, 1278. [[CrossRef](#)] [[PubMed](#)]
19. Yan, R.; Zhao, X.; Lei, J.; Zhou, Q. Structure of the human LAT1-4F2hc heteromeric amino acid transporter complex. *Nature* **2019**, *568*, 127–130. [[CrossRef](#)]
20. Fairweather, S.J.; Shah, N.; Brer, S. Heteromeric Solute Carriers: Function, Structure, Pathology and Pharmacology. *Adv. Exp. Med. Biol.* **2021**, *21*, 13–127. [[CrossRef](#)] [[PubMed](#)]
21. Sehna, D.; Bittrich, S.; Deshpande, M.; Svobodová, R.; Berka, K.; Bazgier, V.; Velankar, S.; Burley, S.K.; Koča, J.; Rose, A.S. Mol\* Viewer: Modern web app for 3D visualization and analysis of large biomolecular structures. *Nucleic Acids Res.* **2021**, *49*, W431–W437. [[CrossRef](#)]
22. Napolitano, L.; Scalise, M.; Galluccio, M.; Pochini, L.; Albanese, L.M.; Indiveri, C. LAT1 is the transport competent unit of the LAT1/CD98 heterodimeric amino acid transporter. *Int. J. Biochem. Cell Biol.* **2015**, *67*, 25–33. [[CrossRef](#)]
23. Nakamura, E.; Sato, M.; Yang, H.; Miyagawa, F.; Harasaki, M.; Tomita, K.; Matsuoka, S.; Noma, A.; Iwai, K.; Minato, N. 4F2 (CD98) heavy chain is associated covalently with an amino acid transporter and controls intracellular trafficking and membrane topology of 4F2 heterodimer. *J. Biol. Chem.* **1999**, *274*, 3009–3016. [[CrossRef](#)]
24. Maimaiti, M.; Sakamoto, S.; Sugiura, M.; Kanesaka, M.; Fujimoto, A.; Matsusaka, K.; Xu, M.; Ando, K.; Saito, S.; Wakai, K.; et al. The heavy chain of 4F2 antigen promote prostate cancer progression via SKP-2. *Sci. Rep.* **2021**, *11*, 11478. [[CrossRef](#)]
25. Horita, Y.; Kaira, K.; Kawasaki, T.; Mihara, Y.; Sakuramoto, S.; Yamaguchi, S.; Okamoto, K.; Ryozaawa, S.; Kanai, Y.; Yasuda, M.; et al. Expression of LAT1 and 4F2hc in Gastroenteropancreatic Neuroendocrine Neoplasms. *In Vivo* **2021**, *35*, 2425–2432. [[CrossRef](#)]
26. Chatsirisupachai, K.; Kitdumrongthum, S.; Panvongsa, W.; Janpipatkul, K.; Worakitchanon, W.; Lertjintanakit, S.; Wongtrakoon-gate, P.; Chairoungdua, A. Expression and roles of system L amino acid transporters in human embryonal carcinoma cells. *Andrology* **2020**, *8*, 1844–1858. [[CrossRef](#)]

27. Kaira, K.; Kawashima, O.; Endoh, H.; Imaizumi, K.; Goto, Y.; Kamiyoshihara, M.; Sugano, M.; Yamamoto, R.; Osaki, T.; Tanaka, S.; et al. Expression of amino acid transporter (LAT1 and 4F2hc) in pulmonary pleomorphic carcinoma. *Hum. Pathol.* **2019**, *84*, 142–149. [[CrossRef](#)]
28. Wagner, C.A.; Broer, A.; Albers, A.; Gamper, N.; Lang, F.; Broer, S. The heterodimeric amino acid transporter 4F2hc/LAT1 is associated in *Xenopus* oocytes with a non-selective cation channel that is regulated by the serine/threonine kinase sgk-1. *J. Physiol.* **2000**, *526*, 35–46. [[CrossRef](#)]
29. Verrey, F.; Closs, E.L.; Wagner, C.A.; Palacin, M.; Endou, H.; Kanai, Y. CATs and HATs: The SLC7 family of amino acid transporters. *Pflug. Arch.* **2004**, *447*, 532–542. [[CrossRef](#)]
30. Braun, D.; Kinne, A.; Bräuer, A.U.; Sapin, R.; Klein, M.O.; Köhrle, J.; Wirth, E.K.; Schweizer, U. Developmental and cell type-specific expression of thyroid hormone transporters in the mouse brain and in primary brain cells. *Glia* **2011**, *59*, 463–471. [[CrossRef](#)]
31. Sinclair, L.V.; Rolf, J.; Emslie, E.; Shi, Y.B.; Taylor, P.M.; Cantrell, D.A. Control of amino-acid transport by antigen receptors coordinates the metabolic reprogramming essential for T cell differentiation. *Nat. Immunol.* **2013**, *14*, 500–508. [[CrossRef](#)] [[PubMed](#)]
32. Smith, Q.R. Carrier-mediated transport to enhance drug delivery to brain. *Int. Congr. Ser.* **2005**, *1277*, 63–74. [[CrossRef](#)]
33. Pardridge, W.M. Brain metabolism: A perspective from the blood-brain barrier. *Physiol. Rev.* **1983**, *63*, 1481–1535. [[CrossRef](#)] [[PubMed](#)]
34. Meier, C.; Ristic, Z.; Klauser, S.; Verrey, F. Activation of system L heterodimeric amino acid exchangers by intracellular substrates. *EMBO J.* **2002**, *21*, 580–589. [[CrossRef](#)]
35. Wang, W.W.; Gallo, L.; Jadhav, A.; Hawkins, R.; Parker, C.G. The Druggability of Solute Carriers. *J. Med. Chem.* **2020**, *63*, 3834–3867. [[CrossRef](#)] [[PubMed](#)]
36. Alles, S.R.A.; Gomez, K.; Moutal, A.; Khanna, R. Putative roles of SLC7A5 (LAT1) transporter in pain. *Neurobiol. Pain* **2020**, *8*, 100050. [[CrossRef](#)] [[PubMed](#)]
37. Torigoe, M.; Maeshima, K.; Ozaki, T.; Omura, Y.; Gotoh, K.; Tanaka, Y.; Ishii, K.; Shibata, H. l-Leucine influx through Slc7a5 regulates inflammatory responses of human B cells via mammalian target of rapamycin complex 1 signaling. *Mod. Rheumatol.* **2019**, *29*, 885–891. [[CrossRef](#)]
38. Behzadi, P.; Garcia-Perdomo, H.A.; Karpinski, T.M. Toll-Like Receptors: General Molecular and Structural Biology. *J. Immunol. Res.* **2021**, *2021*, 9914854. [[CrossRef](#)] [[PubMed](#)]
39. Fuchs, B.C.; Bode, B.P. Amino acid transporters ASCT2 and LAT1 in cancer: Partners in crime? *Semin. Cancer Biol.* **2005**, *15*, 254–266. [[CrossRef](#)] [[PubMed](#)]
40. Kobayashi, K.; Ohnishi, A.; Promsuk, J.; Shimizu, S.; Kanai, Y.; Shiokawa, Y.; Nagane, M. Enhanced tumor growth elicited by L-type amino acid transporter 1 in human malignant glioma cells. *Neurosurgery* **2008**, *62*, 493–503, discussion 494–503. [[CrossRef](#)]
41. Kaira, K.; Oriuchi, N.; Imai, H.; Shimizu, K.; Yanagitani, N.; Sunaga, N.; Hisada, T.; Tanaka, S.; Ishizuka, T.; Kanai, Y.; et al. l-type amino acid transporter 1 and CD98 expression in primary and metastatic sites of human neoplasms. *Cancer Sci.* **2008**, *99*, 2380–2386. [[CrossRef](#)]
42. Betsunoh, H.; Fukuda, T.; Anzai, N.; Nishihara, D.; Mizuno, T.; Yuki, H.; Masuda, A.; Yamaguchi, Y.; Abe, H.; Yashi, M.; et al. Increased expression of system large amino acid transporter (LAT)-1 mRNA is associated with invasive potential and unfavorable prognosis of human clear cell renal cell carcinoma. *BMC Cancer* **2013**, *13*, 509. [[CrossRef](#)]
43. Ebara, T.; Kaira, K.; Saito, J.; Shioya, M.; Asao, T.; Takahashi, T.; Sakurai, H.; Kanai, Y.; Kuwano, H.; Nakano, T. L-type amino-acid transporter 1 expression predicts the response to preoperative hyperthermo-chemoradiotherapy for advanced rectal cancer. *Anticancer Res.* **2010**, *30*, 4223–4227. [[CrossRef](#)]
44. Xu, M.; Sakamoto, S.; Matsushima, J.; Kimura, T.; Ueda, T.; Mizokami, A.; Kanai, Y.; Ichikawa, T. Up-Regulation of LAT1 during Antiandrogen Therapy Contributes to Progression in Prostate Cancer Cells. *J. Urol.* **2016**, *195*, 1588–1597. [[CrossRef](#)]
45. Furuya, M.; Horiguchi, J.; Nakajima, H.; Kanai, Y.; Oyama, T. Correlation of L-type amino acid transporter 1 and CD98 expression with triple negative breast cancer prognosis. *Cancer Sci.* **2012**, *103*, 382–389. [[CrossRef](#)]
46. Nawashiro, H.; Otani, N.; Shinomiya, N.; Fukui, S.; Ooigawa, H.; Shima, K.; Matsuo, H.; Kanai, Y.; Endou, H. L-type amino acid transporter 1 as a potential molecular target in human astrocytic tumors. *Int. J. Cancer* **2006**, *119*, 484–492. [[CrossRef](#)]
47. Sakata, T.; Ferdous, G.; Tsuruta, T.; Satoh, T.; Baba, S.; Muto, T.; Ueno, A.; Kanai, Y.; Endou, H.; Okayasu, I. L-type amino-acid transporter 1 as a novel biomarker for high-grade malignancy in prostate cancer. *Pathol. Int.* **2009**, *59*, 7–18. [[CrossRef](#)]
48. Kim, C.H.; Park, K.J.; Park, J.R.; Kanai, Y.; Endou, H.; Park, J.C.; Kim, D.K. The RNA interference of amino acid transporter LAT1 inhibits the growth of KB human oral cancer cells. *Anticancer Res.* **2006**, *26*, 2943–2948.
49. Marshall, A.D.; van Geldermalsen, M.; Otte, N.J.; Anderson, L.A.; Lum, T.; Vellozzi, M.A.; Zhang, B.K.; Thoeng, A.; Wang, Q.; Rasko, J.E.; et al. LAT1 is a putative therapeutic target in endometrioid endometrial carcinoma. *Int. J. Cancer* **2016**, *139*, 2529–2539. [[CrossRef](#)]
50. Hayashi, K.; Jutabha, P.; Endou, H.; Anzai, N. c-Myc is crucial for the expression of LAT1 in MIA Paca-2 human pancreatic cancer cells. *Oncol. Rep.* **2012**, *28*, 862–866. [[CrossRef](#)]
51. Liang, Z.; Cho, H.T.; Williams, L.; Zhu, A.; Liang, K.; Huang, K.; Wu, H.; Jiang, C.; Hong, S.; Crowe, R.; et al. Potential Biomarker of L-type Amino Acid Transporter 1 in Breast Cancer Progression. *Nucl. Med. Mol. Imaging* **2011**, *45*, 93–102. [[CrossRef](#)]

52. Takeuchi, K.; Ogata, S.; Nakanishi, K.; Ozeki, Y.; Hiroi, S.; Tominaga, S.; Aida, S.; Matsuo, H.; Sakata, T.; Kawai, T. LAT1 expression in non-small-cell lung carcinomas: Analyses by semiquantitative reverse transcription-PCR (237 cases) and immunohistochemistry (295 cases). *Lung Cancer* **2010**, *68*, 58–65. [[CrossRef](#)]
53. Cormerais, Y.; Giuliano, S.; LeFloch, R.; Front, B.; Durivault, J.; Tambutté, E.; Massard, P.A.; de la Ballina, L.R.; Endou, H.; Wempe, M.F.; et al. Genetic Disruption of the Multifunctional CD98/LAT1 Complex Demonstrates the Key Role of Essential Amino Acid Transport in the Control of mTORC1 and Tumor Growth. *Cancer Res.* **2016**, *76*, 4481–4492. [[CrossRef](#)]
54. Nakanishi, T.; Tamai, I. Solute carrier transporters as targets for drug delivery and pharmacological intervention for chemotherapy. *J. Pharm. Sci.* **2011**, *100*, 3731–3750. [[CrossRef](#)]
55. Satoh, T.; Kaira, K.; Takahashi, K.; Takahashi, N.; Kanai, Y.; Asao, T.; Horiguchi, J.; Oyama, T. Prognostic Significance of the Expression of CD98 (4F2hc) in Gastric Cancer. *Anticancer Res.* **2017**, *37*, 631–636. [[CrossRef](#)]
56. Toyoda, M.; Kaira, K.; Shino, M.; Sakakura, K.; Takahashi, K.; Takayasu, Y.; Tominaga, H.; Oriuchi, N.; Nikkuni, O.; Suzuki, M.; et al. CD98 as a novel prognostic indicator for patients with stage III/IV hypopharyngeal squamous cell carcinoma. *Head Neck* **2015**, *37*, 1569–1574. [[CrossRef](#)]
57. Wang, Q.; Tiffen, J.; Bailey, C.G.; Lehman, M.L.; Ritchie, W.; Fazli, L.; Metierre, C.; Feng, Y.J.; Li, E.; Gleave, M.; et al. Targeting amino acid transport in metastatic castration-resistant prostate cancer: Effects on cell cycle, cell growth, and tumor development. *J. Natl. Cancer Inst.* **2013**, *105*, 1463–1473. [[CrossRef](#)]
58. Rajasinghe, L.D.; Hutchings, M.; Gupta, S.V. Delta-Tocotrienol Modulates Glutamine Dependence by Inhibiting ASCT2 and LAT1 Transporters in Non-Small Cell Lung Cancer (NSCLC) Cells: A Metabolomic Approach. *Metabolites* **2019**, *9*, 50. [[CrossRef](#)]
59. Kaira, K.; Takahashi, T.; Murakami, H.; Shukuya, T.; Kenmotsu, H.; Naito, T.; Oriuchi, N.; Kanai, Y.; Endo, M.; Kondo, H.; et al. Relationship between LAT1 expression and response to platinum-based chemotherapy in non-small cell lung cancer patients with postoperative recurrence. *Anticancer Res.* **2011**, *31*, 3775–3782.
60. Kaira, K.; Oriuchi, N.; Takahashi, T.; Nakagawa, K.; Ohde, Y.; Okumura, T.; Murakami, H.; Shukuya, T.; Kenmotsu, H.; Naito, T.; et al. LAT1 expression is closely associated with hypoxic markers and mTOR in resected non-small cell lung cancer. *Am. J. Transl. Res.* **2011**, *3*, 468–478.
61. Kaira, K.; Oriuchi, N.; Imai, H.; Shimizu, K.; Yanagitani, N.; Sunaga, N.; Hisada, T.; Kawashima, O.; Kamide, Y.; Ishizuka, T.; et al. Prognostic significance of L-type amino acid transporter 1 (LAT1) and 4F2 heavy chain (CD98) expression in surgically resectable stage III non-small cell lung cancer. *Exp. Ther. Med.* **2010**, *1*, 799–808. [[CrossRef](#)]
62. Kaira, K.; Oriuchi, N.; Imai, H.; Shimizu, K.; Yanagitani, N.; Sunaga, N.; Hisada, T.; Kawashima, O.; Kamide, Y.; Ishizuka, T.; et al. CD98 expression is associated with poor prognosis in resected non-small-cell lung cancer with lymph node metastases. *Ann. Surg. Oncol.* **2009**, *16*, 3473–3481. [[CrossRef](#)]
63. Dann, S.G.; Ryskin, M.; Barsotti, A.M.; Golas, J.; Shi, C.; Miranda, M.; Hosselet, C.; Lemon, L.; Lucas, J.; Karnoub, M.; et al. Reciprocal regulation of amino acid import and epigenetic state through Lat1 and EZH2. *EMBO J.* **2015**, *34*, 1773–1785. [[CrossRef](#)]
64. Muto, Y.; Furihata, T.; Kaneko, M.; Higuchi, K.; Okunushi, K.; Morio, H.; Reien, Y.; Uesato, M.; Matsubara, H.; Anzai, N. Different Response Profiles of Gastrointestinal Cancer Cells to an L-Type Amino Acid Transporter Inhibitor, JPH203. *Anticancer Res.* **2019**, *39*, 159–165. [[CrossRef](#)]
65. Ding, K.; Tan, S.; Huang, X.; Wang, X.; Li, X.; Fan, R.; Zhu, Y.; Lobie, P.E.; Wang, W.; Wu, Z. GSE1 predicts poor survival outcome in gastric cancer patients by SLC7A5 enhancement of tumor growth and metastasis. *J. Biol. Chem.* **2018**, *293*, 3949–3964. [[CrossRef](#)]
66. Wang, J.; Fei, X.; Wu, W.; Chen, X.; Su, L.; Zhu, Z.; Zhou, Y. SLC7A5 Functions as a Downstream Target Modulated by CRKL in Metastasis Process of Gastric Cancer SGC-7901 Cells. *PLoS ONE* **2016**, *11*, e0166147. [[CrossRef](#)]
67. Ichinoe, M.; Yanagisawa, N.; Mikami, T.; Hana, K.; Nakada, N.; Endou, H.; Okayasu, I.; Murakumo, Y. L-Type amino acid transporter 1 (LAT1) expression in lymph node metastasis of gastric carcinoma: Its correlation with size of metastatic lesion and Ki-67 labeling. *Pathol. Res. Pract.* **2015**, *211*, 533–538. [[CrossRef](#)]
68. Shi, L.; Luo, W.; Huang, W.; Huang, S.; Huang, G. Downregulation of L-type amino acid transporter 1 expression inhibits the growth, migration and invasion of gastric cancer cells. *Oncol. Lett.* **2013**, *6*, 106–112. [[CrossRef](#)]
69. Wang, J.; Chen, X.; Su, L.; Li, P.; Liu, B.; Zhu, Z. LAT-1 functions as a promotor in gastric cancer associated with clinicopathologic features. *Biomed. Pharmacother.* **2013**, *67*, 693–699. [[CrossRef](#)]
70. Sampedro-Núñez, M.; Bouthelie, A.; Serrano-Somavilla, A.; Martínez-Hernández, R.; Adrados, M.; Martín-Pérez, E.; Muñoz de Nova, J.L.; Cameselle-Teijeiro, J.M.; Blanco-Carrera, C.; Cabezas-Agricola, J.M.; et al. LAT-1 and GLUT-1 Carrier Expression and Its Prognostic Value in Gastroenteropancreatic Neuroendocrine Tumors. *Cancers* **2020**, *12*, 2968. [[CrossRef](#)]
71. Altan, B.; Kaira, K.; Watanabe, A.; Kubo, N.; Bao, P.; Dolgormaa, G.; Bilguun, E.O.; Araki, K.; Kanai, Y.; Yokobori, T.; et al. Relationship between LAT1 expression and resistance to chemotherapy in pancreatic ductal adenocarcinoma. *Cancer Chemother. Pharm.* **2018**, *81*, 141–153. [[CrossRef](#)] [[PubMed](#)]
72. Kaira, K.; Arakawa, K.; Shimizu, K.; Oriuchi, N.; Nagamori, S.; Kanai, Y.; Oyama, T.; Takeyoshi, I. Relationship between CD147 and expression of amino acid transporters (LAT1 and ASCT2) in patients with pancreatic cancer. *Am. J. Transl. Res.* **2015**, *7*, 356–363. [[PubMed](#)]
73. Yanagisawa, N.; Ichinoe, M.; Mikami, T.; Nakada, N.; Hana, K.; Koizumi, W.; Endou, H.; Okayasu, I. High expression of L-type amino acid transporter 1 (LAT1) predicts poor prognosis in pancreatic ductal adenocarcinomas. *J. Clin. Pathol.* **2012**, *65*, 1019–1023. [[CrossRef](#)] [[PubMed](#)]

74. Kaira, K.; Sunose, Y.; Arakawa, K.; Ogawa, T.; Sunaga, N.; Shimizu, K.; Tominaga, H.; Oriuchi, N.; Itoh, H.; Nagamori, S.; et al. Prognostic significance of L-type amino-acid transporter 1 expression in surgically resected pancreatic cancer. *Br. J. Cancer* **2012**, *107*, 632–638. [[CrossRef](#)]
75. Okanishi, H.; Ohgaki, R.; Okuda, S.; Endou, H.; Kanai, Y. Proteomics and phosphoproteomics reveal key regulators associated with cytostatic effect of amino acid transporter LAT1 inhibitor. *Cancer Sci.* **2021**, *112*, 871–883. [[CrossRef](#)]
76. Okano, N.; Hana, K.; Naruge, D.; Kawai, K.; Kobayashi, T.; Nagashima, F.; Endou, H.; Furuse, J. Biomarker Analyses in Patients with Advanced Solid Tumors Treated with the LAT1 Inhibitor JPH203. *In Vivo* **2020**, *34*, 2595–2606. [[CrossRef](#)]
77. Yothaisong, S.; Namwat, N.; Yongvanit, P.; Khuntikeo, N.; Puapairoj, A.; Jutabha, P.; Anzai, N.; Tassaneeyakul, W.; Tangsucharit, P.; Loilome, W. Increase in L-type amino acid transporter 1 expression during cholangiocarcinogenesis caused by liver fluke infection and its prognostic significance. *Parasitol. Int.* **2017**, *66*, 471–478. [[CrossRef](#)]
78. Kaira, K.; Sunose, Y.; Oriuchi, N.; Kanai, Y.; Takeyoshi, I. CD98 is a promising prognostic biomarker in biliary tract cancer. *Hepatobiliary Pancreat. Dis. Int.* **2014**, *13*, 654–657. [[CrossRef](#)]
79. Yanagisawa, N.; Hana, K.; Nakada, N.; Ichinoe, M.; Koizumi, W.; Endou, H.; Okayasu, I.; Murakumo, Y. High expression of L-type amino acid transporter 1 as a prognostic marker in bile duct adenocarcinomas. *Cancer Med.* **2014**, *3*, 1246–1255. [[CrossRef](#)]
80. Janpipatkul, K.; Suksen, K.; Borwornpinyo, S.; Jearawiriyapaisarn, N.; Hongeng, S.; Piyachaturawat, P.; Chairoungdua, A. Downregulation of LAT1 expression suppresses cholangiocarcinoma cell invasion and migration. *Cell. Signal.* **2014**, *26*, 1668–1679. [[CrossRef](#)]
81. Kaira, K.; Sunose, Y.; Ohshima, Y.; Ishioka, N.S.; Arakawa, K.; Ogawa, T.; Sunaga, N.; Shimizu, K.; Tominaga, H.; Oriuchi, N.; et al. Clinical significance of L-type amino acid transporter 1 expression as a prognostic marker and potential of new targeting therapy in biliary tract cancer. *BMC Cancer* **2013**, *13*, 482. [[CrossRef](#)]
82. Sato, K.; Miyamoto, M.; Takano, M.; Furuya, K.; Tsuda, H. Significant relationship between the LAT1 expression pattern and chemoresistance in ovarian clear cell carcinoma. *Virchows Arch. Int. J. Pathol.* **2019**, *474*, 701–710. [[CrossRef](#)]
83. Kaira, K.; Nakamura, K.; Hirakawa, T.; Imai, H.; Tominaga, H.; Oriuchi, N.; Nagamori, S.; Kanai, Y.; Tsukamoto, N.; Oyama, T.; et al. Prognostic significance of L-type amino acid transporter 1 (LAT1) expression in patients with ovarian tumors. *Am. J. Transl. Res.* **2015**, *7*, 1161–1171.
84. Fan, X.; Ross, D.D.; Arakawa, H.; Ganapathy, V.; Tamai, I.; Nakanishi, T. Impact of system L amino acid transporter 1 (LAT1) on proliferation of human ovarian cancer cells: A possible target for combination therapy with anti-proliferative aminopeptidase inhibitors. *Biochem. Pharmacol.* **2010**, *80*, 811–818. [[CrossRef](#)]
85. Kaji, M.; Kabir-Salmani, M.; Anzai, N.; Jin, C.J.; Akimoto, Y.; Horita, A.; Sakamoto, A.; Kanai, Y.; Sakurai, H.; Iwashita, M. Properties of L-type amino acid transporter 1 in epidermal ovarian cancer. *Int. J. Gynecol. Cancer Off. J. Int. Gynecol. Cancer Soc.* **2010**, *20*, 329–336. [[CrossRef](#)]
86. Thompson, C.; Rahman, M.M.; Singh, S.; Arthur, S.; Sierra-Bakhshi, C.; Russell, R.; Denning, K.; Sundaram, U.; Salisbury, T. The Adipose Tissue-Derived Secretome (ADS) in Obesity Uniquely Induces L-Type Amino Acid Transporter 1 (LAT1) and mTOR Signaling in Estrogen-Receptor-Positive Breast Cancer Cells. *Int. J. Mol. Sci.* **2021**, *22*, 6706. [[CrossRef](#)]
87. Ichinoe, M.; Mikami, T.; Yanagisawa, N.; Yoshida, T.; Hana, K.; Endou, H.; Okayasu, I.; Sengoku, N.; Ogata, H.; Saegusa, M.; et al. Prognostic values of L-type amino acid transporter 1 and CD98hc expression in breast cancer. *J. Clin. Pathol.* **2020**, *74*, 589–595. [[CrossRef](#)] [[PubMed](#)]
88. Bodoor, K.; Almomani, R.; Alqudah, M.; Haddad, Y.; Samouri, W. LAT1 (SLC7A5) Overexpression in Negative Her2 Group of Breast Cancer: A Potential Therapy Target. *Asian Pac. J. Cancer Prev. APJCP* **2020**, *21*, 1453–1458. [[CrossRef](#)] [[PubMed](#)]
89. Pocasap, P.; Weerapreeyakul, N.; Timonen, J.; Järvinen, J.; Leppänen, J.; Kärkkäinen, J.; Rautio, J. Tyrosine-Chlorambucil Conjugates Facilitate Cellular Uptake through L-Type Amino Acid Transporter 1 (LAT1) in Human Breast Cancer Cell Line MCF-7. *Int. J. Mol. Sci.* **2020**, *21*, 2132. [[CrossRef](#)]
90. Shennan, D.B.; Thomson, J. Inhibition of system L (LAT1/CD98hc) reduces the growth of cultured human breast cancer cells. *Oncol. Rep.* **2008**, *20*, 885–889. [[CrossRef](#)] [[PubMed](#)]
91. Nye, J.A.; Schuster, D.M.; Yu, W.; Camp, V.M.; Goodman, M.M.; Votaw, J.R. Biodistribution and radiation dosimetry of the synthetic nonmetabolized amino acid analogue anti-18F-FACBC in humans. *J. Nucl. Med.* **2007**, *48*, 1017–1020. [[CrossRef](#)] [[PubMed](#)]
92. Bach-Gansmo, T.; Nanni, C.; Nieh, P.T.; Zannoni, L.; Bogsrud, T.V.; Sletten, H.; Korsan, K.A.; Kieboom, J.; Tade, F.L.; Odewole, O.; et al. Multisite Experience of the Safety, Detection Rate and Diagnostic Performance of Fluciclovine ((18)F) Positron Emission Tomography/Computerized Tomography Imaging in the Staging of Biochemically Recurrent Prostate Cancer. *J. Urol.* **2017**, *197*, 676–683. [[CrossRef](#)] [[PubMed](#)]
93. Kim, D.K.; Kanai, Y.; Choi, H.W.; Tangtrongsup, S.; Chairoungdua, A.; Babu, E.; Tachampa, K.; Anzai, N.; Iribe, Y.; Endou, H. Characterization of the system L amino acid transporter in T24 human bladder carcinoma cells. *Biochim. Biophys. Acta* **2002**, *1565*, 112–121. [[CrossRef](#)]
94. Patel, M.; Dalvi, P.; Gokulgandhi, M.; Kesh, S.; Kohli, T.; Pal, D.; Mitra, A.K. Functional characterization and molecular expression of large neutral amino acid transporter (LAT1) in human prostate cancer cells. *Int. J. Pharm.* **2013**, *443*, 245–253. [[CrossRef](#)] [[PubMed](#)]
95. Otsuki, H.; Kimura, T.; Yamaga, T.; Kosaka, T.; Suehiro, J.I.; Sakurai, H. Prostate Cancer Cells in Different Androgen Receptor Status Employ Different Leucine Transporters. *Prostate* **2017**, *77*, 222–233. [[CrossRef](#)]

96. Rii, J.; Sakamoto, S.; Sugiura, M.; Kanesaka, M.; Fujimoto, A.; Yamada, Y.; Maimaiti, M.; Ando, K.; Wakai, K.; Xu, M.; et al. Functional analysis of LAT3 in prostate cancer: Its downstream target and relationship with androgen receptor. *Cancer Sci.* **2021**, *112*, 3871. [[CrossRef](#)]
97. Wang, Q.; Bailey, C.G.; Ng, C.; Tiffen, J.; Thoeng, A.; Minhas, V.; Lehman, M.L.; Hendy, S.C.; Buchanan, G.; Nelson, C.C.; et al. Androgen receptor and nutrient signaling pathways coordinate the demand for increased amino acid transport during prostate cancer progression. *Cancer Res.* **2011**, *71*, 7525–7536. [[CrossRef](#)]
98. Higuchi, K.; Sakamoto, S.; Ando, K.; Maimaiti, M.; Takeshita, N.; Okunushi, K.; Reien, Y.; Imamura, Y.; Sazuka, T.; Nakamura, K.; et al. Characterization of the expression of LAT1 as a prognostic indicator and a therapeutic target in renal cell carcinoma. *Sci. Rep.* **2019**, *9*, 16776. [[CrossRef](#)]
99. Solimando, A.G.; Summa, S.; Vacca, A.; Ribatti, D. Cancer-Associated Angiogenesis: The Endothelial Cell as a Checkpoint for Immunological Patrolling. *Cancers* **2020**, *12*, 3380. [[CrossRef](#)]
100. Motzer, R.J.; Tannir, N.M.; McDermott, D.F.; Aren Frontera, O.; Melichar, B.; Choueiri, T.K.; Plimack, E.R.; Barthelemy, P.; Porta, C.; George, S.; et al. Nivolumab plus Ipilimumab versus Sunitinib in Advanced Renal-Cell Carcinoma. *N. Engl. J. Med.* **2018**, *378*, 1277–1290. [[CrossRef](#)]
101. Kume, E.; Mutou, T.; Kansaku, N.; Takahashi, H.; Wempe, M.F.; Ikegami, M.; Kanai, Y.; Endou, H.; Wakui, S. Ultrastructural immunohistochemical study of L-type amino acid transporter 1-4F2 heavy chain in tumor microvasculatures of N-butyl-N-(4-hydroxybutyl) nitrosamine (BBN) induced rat bladder carcinoma. *Microscopy* **2017**, *66*, 198–203. [[CrossRef](#)]
102. Quan, L.; Ohgaki, R.; Hara, S.; Okuda, S.; Wei, L.; Okanishi, H.; Nagamori, S.; Endou, H.; Kanai, Y. Amino acid transporter LAT1 in tumor-associated vascular endothelium promotes angiogenesis by regulating cell proliferation and VEGF-A-dependent mTORC1 activation. *J. Exp. Clin. Cancer Res.* **2020**, *39*, 266. [[CrossRef](#)]
103. Hayashi, K.; Jutabha, P.; Kamai, T.; Endou, H.; Anzai, N. LAT1 is a central transporter of essential amino acids in human umbilical vein endothelial cells. *J. Pharm. Sci.* **2014**, *124*, 511–513. [[CrossRef](#)]
104. Cao, D.; Mikosz, A.M.; Ringsby, A.J.; Anderson, K.C.; Beatman, E.L.; Koike, K.; Petrache, I. MicroRNA-126-3p Inhibits Angiogenic Function of Human Lung Microvascular Endothelial Cells via LAT1 (L-Type Amino Acid Transporter 1)-Mediated mTOR (Mammalian Target of Rapamycin) Signaling. *Arter. Thromb. Vasc. Biol.* **2020**, *40*, 1195–1206. [[CrossRef](#)]
105. Kaira, K.; Oriuchi, N.; Imai, H.; Shimizu, K.; Yanagitani, N.; Sunaga, N.; Hisada, T.; Ishizuka, T.; Kanai, Y.; Endou, H.; et al. Prognostic significance of L-type amino acid transporter 1 (LAT1) and 4F2 heavy chain (CD98) expression in early stage squamous cell carcinoma of the lung. *Cancer Sci.* **2009**, *100*, 248–254. [[CrossRef](#)]
106. Kaira, K.; Oriuchi, N.; Shimizu, K.; Ishikita, T.; Higuchi, T.; Imai, H.; Yanagitani, N.; Sunaga, N.; Hisada, T.; Ishizuka, T.; et al. Correlation of angiogenesis with 18F-FMT and 18F-FDG uptake in non-small cell lung cancer. *Cancer Sci.* **2009**, *100*, 753–758. [[CrossRef](#)]
107. Okubo, S.; Zhen, H.N.; Kawai, N.; Nishiyama, Y.; Haba, R.; Tamiya, T. Correlation of L-methyl-11C-methionine (MET) uptake with L-type amino acid transporter 1 in human gliomas. *J. Neurooncol.* **2010**, *99*, 217–225. [[CrossRef](#)] [[PubMed](#)]
108. Haining, Z.; Kawai, N.; Miyake, K.; Okada, M.; Okubo, S.; Zhang, X.; Fei, Z.; Tamiya, T. Relation of LAT1/4F2hc expression with pathological grade, proliferation and angiogenesis in human gliomas. *BMC Clin. Pathol.* **2012**, *12*, 4. [[CrossRef](#)]
109. Baniasadi, S.; Chairoungdua, A.; Iribe, Y.; Kanai, Y.; Endou, H.; Aisaki, K.; Igarashi, K.; Kanno, J. Gene expression profiles in T24 human bladder carcinoma cells by inhibiting an L-type amino acid transporter, LAT1. *Arch. Pharmacol. Res.* **2007**, *30*, 444–452. [[CrossRef](#)] [[PubMed](#)]
110. Maimaiti, M.; Sakamoto, S.; Yamada, Y.; Sugiura, M.; Rii, J.; Takeuchi, N.; Imamura, Y.; Furihata, T.; Ando, K.; Higuchi, K.; et al. Expression of L-type amino acid transporter 1 as a molecular target for prognostic and therapeutic indicators in bladder carcinoma. *Sci. Rep.* **2020**, *10*, 1292. [[CrossRef](#)] [[PubMed](#)]
111. Martinez, R.S.; Salji, M.J.; Rushworth, L.; Ntala, C.; Rodriguez Blanco, G.; Hedley, A.; Clark, W.; Peixoto, P.; Hervouet, E.; Renaude, E.; et al. SLFN5 Regulates LAT1-Mediated mTOR Activation in Castration-Resistant Prostate Cancer. *Cancer Res.* **2021**, *81*, 3664–3678. [[CrossRef](#)]
112. Eltz, S.; Comperat, E.; Cussenot, O.; Roupret, M. Molecular and histological markers in urothelial carcinomas of the upper urinary tract. *BJU Int.* **2008**, *102*, 532–535. [[CrossRef](#)]
113. Dvorak, V.; Wiedmer, T.; Ingles-Prieto, A.; Altermatt, P.; Batoulis, H.; Barenz, F.; Bender, E.; Digles, D.; Durrenberger, F.; Heitman, L.H.; et al. An Overview of Cell-Based Assay Platforms for the Solute Carrier Family of Transporters. *Front. Pharm.* **2021**, *12*, 722889. [[CrossRef](#)]
114. Chien, H.C.; Colas, C.; Finke, K.; Springer, S.; Stoner, L.; Zur, A.A.; Venteicher, B.; Campbell, J.; Hall, C.; Flint, A.; et al. Reevaluating the Substrate Specificity of the L-Type Amino Acid Transporter (LAT1). *J. Med. Chem.* **2018**, *61*, 7358–7373. [[CrossRef](#)] [[PubMed](#)]
115. Oda, K.; Hosoda, N.; Endo, H.; Saito, K.; Tsujihara, K.; Yamamura, M.; Sakata, T.; Anzai, N.; Wempe, M.F.; Kanai, Y.; et al. L-type amino acid transporter 1 inhibitors inhibit tumor cell growth. *Cancer Sci.* **2010**, *101*, 173–179. [[CrossRef](#)] [[PubMed](#)]
116. Rosilio, C.; Nebout, M.; Imbert, V.; Griessinger, E.; Neffati, Z.; Benadiba, J.; Hagenbeek, T.; Spits, H.; Reverso, J.; Ambrosetti, D.; et al. L-type amino-acid transporter 1 (LAT1): A therapeutic target supporting growth and survival of T-cell lymphoblastic lymphoma/T-cell acute lymphoblastic leukemia. *Leukemia* **2015**, *29*, 1253–1266. [[CrossRef](#)] [[PubMed](#)]
117. Okunushi, K.; Furihata, T.; Morio, H.; Muto, Y.; Higuchi, K.; Kaneko, M.; Otsuka, Y.; Ohno, Y.; Watanabe, Y.; Reien, Y.; et al. JPH203, a newly developed anti-cancer drug, shows a preincubation inhibitory effect on L-type amino acid transporter 1 function. *J. Pharm. Sci.* **2020**, *144*, 16–22. [[CrossRef](#)]

118. Cormerais, Y.; Pagnuzzi-Boncompagni, M.; Schrotter, S.; Giuliano, S.; Tambutte, E.; Endou, H.; Wempe, M.F.; Pages, G.; Pouyssegur, J.; Picco, V. Inhibition of the amino-acid transporter LAT1 demonstrates anti-neoplastic activity in medulloblastoma. *J. Cell Mol. Med.* **2019**, *23*, 2711–2718. [[CrossRef](#)]
119. Choi, D.W.; Kim, D.K.; Kanai, Y.; Wempe, M.F.; Endou, H.; Kim, J.K. JPH203, a selective L-type amino acid transporter 1 inhibitor, induces mitochondria-dependent apoptosis in Saos2 human osteosarcoma cells. *Korean J. Physiol. Pharm.* **2017**, *21*, 599–607. [[CrossRef](#)]
120. Hafliger, P.; Graff, J.; Rubin, M.; Stooss, A.; Dettmer, M.S.; Altmann, K.H.; Gertsch, J.; Charles, R.P. The LAT1 inhibitor JPH203 reduces growth of thyroid carcinoma in a fully immunocompetent mouse model. *J. Exp. Clin. Cancer Res.* **2018**, *37*, 234. [[CrossRef](#)]
121. Enomoto, K.; Sato, F.; Tamagawa, S.; Gunduz, M.; Onoda, N.; Uchino, S.; Muragaki, Y.; Hotomi, M. A novel therapeutic approach for anaplastic thyroid cancer through inhibition of LAT1. *Sci. Rep.* **2019**, *9*, 14616. [[CrossRef](#)]
122. Shindo, H.; Harada-Shoji, N.; Ebata, A.; Sato, M.; Soga, T.; Miyashita, M.; Tada, H.; Kawai, M.; Kosaka, S.; Onuki, K.; et al. Targeting Amino Acid Metabolic Reprogramming via L-Type Amino Acid Transporter 1 (LAT1) for Endocrine-Resistant Breast Cancer. *Cancers* **2021**, *13*, 4375. [[CrossRef](#)]
123. Satou, M.; Wang, J.; Nakano-Tateno, T.; Teramachi, M.; Suzuki, T.; Hayashi, K.; Lamothe, S.; Hao, Y.; Kurata, H.; Sugimoto, H.; et al. L-type amino acid transporter 1, LAT1, in growth hormone-producing pituitary tumor cells. *Mol. Cell Endocrinol.* **2020**, *515*, 110868. [[CrossRef](#)] [[PubMed](#)]
124. Ueno, S.; Kimura, T.; Yamaga, T.; Kawada, A.; Ochiai, T.; Endou, H.; Sakurai, H. Metformin enhances anti-tumor effect of L-type amino acid transporter 1 (LAT1) inhibitor. *J. Pharm. Sci.* **2016**, *131*, 110–117. [[CrossRef](#)] [[PubMed](#)]
125. Yan, R.; Li, Y.; Muller, J.; Zhang, Y.; Singer, S.; Xia, L.; Zhong, X.; Gertsch, J.; Altmann, K.H.; Zhou, Q. Mechanism of substrate transport and inhibition of the human LAT1-4F2hc amino acid transporter. *Cell Discov.* **2021**, *7*, 16. [[CrossRef](#)] [[PubMed](#)]
126. Wempe, M.F.; Rice, P.J.; Lightner, J.W.; Jutabha, P.; Hayashi, M.; Anzai, N.; Wakui, S.; Kusuhara, H.; Sugiyama, Y.; Endou, H. Metabolism and pharmacokinetic studies of JPH203, an L-amino acid transporter 1 (LAT1) selective compound. *Drug Metab. Pharm.* **2012**, *27*, 155–161. [[CrossRef](#)]

## Chapter 3

# How Serum Testosterone Levels Determine the Treatment Strategy of Advanced Prostate Cancer

Xue Zhao<sup>1</sup>

Shinichi Sakamoto<sup>1,\*</sup>

Shuheï Kamada<sup>1</sup>

Akinori Takei<sup>2</sup>

Yusuke Imamura<sup>1</sup>

and Tomohiko Ichikawa<sup>1</sup>

<sup>1</sup>Department of Urology,

Chiba University Graduate School of Medicine, Chiba, Japan

<sup>2</sup>Department of Urology,

Funabashi Municipal Medical Center, Chiba, Japan

## Abstract

Most men with metastatic prostate cancer who receive androgen deprivation therapy (ADT) eventually became castration-resistant prostate cancer (CRPC) patients. In this review, we describe the role of serum testosterone (TST) levels in the progression and prognosis of prostate cancer based on several clinical studies of prostate cancer, and how to use testosterone levels to achieve the best treatment effect in different stages of the course.

Our data suggested both nadir testosterone < 20 ng/dL and testosterone reduction  $\geq$  480 ng/dL to be key prognostic factors for

---

\* Corresponding Author's Email: rbatbat1@gmail.com

In: Horizons in Cancer Research. Volume 85

Editor: Hiroto S. Watanabe

ISBN: 979-8-88697-698-4

© 2023 Nova Science Publishers, Inc.

primary androgen deprivation therapy (ADT) in advanced prostate cancer. Serum TST 13 ng/dL is the dividing point that determines the response and efficacy of CRPC to drug therapy. Patients with serum TST > 13 ng/dL had better curative effects on novel androgen receptor (AR) antagonist medicines. However, those serum TST < 13 ng/dL showed poor response to novel AR antagonists, but better response and efficacy to the treatments of Docetaxel and Cabazitaxel. Bipolar androgen therapy (BAT) can make CRPC sensitive to subsequent ADT. The sequential treatment of BAT and enzalutamide showed the potential to significantly improve the survival and prognosis of men with CRPC.

Based on the evidence, the dynamic of serum TST level provide a significant role in advanced prostate cancer patients who received ADT.

**Keywords:** testosterone, prostate cancer, prognosis, treatment effect, bipolar androgen therapy

## Introduction

One of the most prevalent cancers affecting the male genitourinary system is prostate cancer (PC) [1]. With 31,620 predicted fatalities in 2019, it continues to be the second most typical reason for cancer deaths among men in the United States [2]. An important turning point in the history of prostate cancer treatment occurred in 1941, when Dr. Charles Huggins discovered that androgen deprivation therapy (ADT) offered considerable palliative benefits for men with advanced prostate cancer [3].

Throughout the rest of history, ADT has remained the preferred prostate cancer therapy. Nevertheless, a number of studies have demonstrated that men who get ADT will inevitably develop castration-resistant prostate cancer (CRPC) [4, 5]. This is attributed, according to several theories [6-10], to persistent androgen receptor (AR) signaling. Newer oral medications that target the androgen axis of prostate cancer, such as the androgen receptor antagonist enzalutamide and the cytochrome P450 17A (CYP17A) inhibitor abiraterone, have been introduced into the clinic, improving overall survival in men with CRPC [11-15].

## Gradual Progress of Androgen Therapy for Prostate Cancer

At present, it appears that practically all methods of treating prostate cancer involve lowering serum testosterone and reducing androgen receptor signaling

(ARS). But, not to be overlooked, Huggins also proposed that treating prostate cancer with excessive androgens, a method he coined "hormone interference," would be effective in treating prostate cancer [16]. This shows that there may be a positive association between androgens and prostate cancer. Supraphysiologic levels of androgens have been shown to impede the proliferation of AR-positive human CRPC cell lines [17, 18]. In certain investigations, a number of potential explanations underlying this paradoxical impact have been clarified. Isaac demonstrated that AR is a licensing factor for DNA replication, plays a key role in DNA replication, and must be degraded as cells go through the cell cycle [18-21]. The enhanced ligand-bound AR in the nucleus is permanently present without degrading in the presence of supraphysiologic testosterone. DNA replication and relicensing are prevented by insufficient AR degradation, which causes cell death in succeeding cycles [20]. Bipolar androgen therapy (BAT), a treatment for CRPC, was developed as a result of the identification of these mechanisms [22].

Additionally, a significant number of findings were unexpected given the androgen hypothesis. For instance, there is no connection between prostate volume, PSA, endogenous testosterone levels, or prostate cancer [23-26], and analyses of population studies have discovered that not all naturally occurring testosterone levels are related to prostate cancer [24]. In addition, several lines of evidence have shown that reduced serum total testosterone levels and reduced free testosterone levels are associated with more aggressive PC and worse prognosis [27-30]. The findings also appear to suggest that the relationship between testosterone and PC is not a simple linear relationship and that there is a certain threshold associated with the onset and progression of cancer at various stages, in addition to the previously mentioned conflicting antitumor effects of various serum androgen levels.

Therefore, we searched the recent relevant literature and combined it with our clinical findings. The relationship between serum testosterone levels and different stages of prostate cancer was reviewed.

### **Serum Testosterone and Prostate Cancer**

The association between testosterone and prostate cancer in the past was primarily based on the idea that testosterone provides "fuel" and "energy" for prostate cancer cells. Following ADT therapy, the testosterone levels of PC patients dropped, leading to a significant number of patients with testosterone deficiency (TD). TD can cause a series of worrying health problems [31], and

testosterone replacement therapy (TRT) is the preferred treatment at present. TRT has been shown to improve or even reverse these symptoms [32, 33].

In the eyes of researchers, it opens the door to the use of testosterone replacement therapy (TRT) for patients with prostate cancer, but it also raises serious ethical and medical concerns.

1. *Androgen saturation model explains the paradoxical relationship between testosterone and prostate cancer.*

According to some studies, the highest (saturation) level of testosterone binding to AR takes place at relatively low concentrations [34, 35]. Low testosterone levels can affect PC negatively. The range of testosterone levels that can affect the PC in this setting is extremely constrained because once the ARs are fully occupied, excess testosterone cannot enter the cell to stimulate cell growth. Prostate tissue is sensitive to changes in testosterone levels at low concentrations but not at high concentrations [36, 37]. Young, healthy men with elevated serum total and free testosterone did not show elevated serum or semen PSA levels or increased prostate volume [38, 39]. Similar results were also seen in elder men [40].

2. *Testosterone replacement therapy (TRT) is safe and beneficial for TD patients with prostate cancer.*

Firstly, TRT does not increase the risk of prostate cancer in healthy individuals [41, 42]. Second, TRT does not encourage the progression or recurrence of early-stage prostate cancer. Following radical prostatectomy (RP), PC patients treated with various TRTs have not demonstrated any biochemical or clinical recurrence [43, 44]. Similarly, TRT caused no signs of PC recurrence or progression in prostate cancer patients receiving radiotherapy [45, 46].

There is proof that men with prostate cancer who are receiving TRT have a lower overall biochemical recurrence rate than those in the control group [47-49]. The increased androgen levels with TRT may have a protective effect on the recurrence of PC. These connections could point to a biological mechanism by which testosterone influences the differentiation and operation of healthy prostate epithelial cells. High or normal levels of testosterone may keep prostate and early PC cells in a well-differentiated state. Conversely, prostate cancer cells may become less differentiated and more malignant as a result of a gradual drop in testosterone brought on by advanced age or disease [50].

Men with PC and TD have a higher risk of disease aggressiveness [51]. Finally, low serum testosterone levels did not independently predict prostate cancer bone metastasis [52].

These offer a fresh approach to treating PC patients and point us in the right direction for research on the connection between serum testosterone and prostate cancer. High physiological testosterone levels are preventative for prostate cancer. Prostate cancer does not progress or recur after testosterone supplementation in PC patients [43-45, 48, 53-55].

### **Serum Testosterone and Androgen Deprivation Therapy (ADT)**

Previously, lower TST levels in patients who received ADT have been associated with a longer response of durations [56, 57]. The target TST level during ADT for prostate cancer is defined as less than 50ng/dl by current recommendations [58]. The target of 50 ng/dl has been contested, though, as more precise assays have been developed.

The clinical importance of a reduced TST in ADT has been reported in a number of studies. For the first time, Morote described the clinical significance of lower castration levels. They noted that the clinical significance of breakthrough TST increased at 20 and 50 ng/ dL and suggested that no breakthrough is a good predictor of survival in androgen-independent progression [57]. According to Perachino, TST at 6 months (40 ng/dl) was directly related to the risk of death during ADT [59]. After discussing OS and TST levels following six months of ADT, Bertaglia concluded that a TST level of less than 30 ng/dl was a positive prognostic factor for survival [56]. However, because patients with TST levels under 20 ng/dl rarely experienced fatal outcomes during the study, they were unable to fully evaluate lower TST levels. The median nadir TST was also 39 ng/dL, which is significantly higher than the data from our team (median minimum TST for the past six months was 13 ng/dl). This might be caused by variations in ADT protocols and patient traits like ethnicity, the prevalence of advanced cancer, and first-line local regional treatment.

Data from Japanese patients who received ADT as their initial prostate cancer treatment were retrospectively examined by our team [60, 61]. Significant prognostic factors included a nadir serum testosterone level of less than 20 ng/dL and a testosterone reduction of more than 480 ng/dL [60]. Additionally, based on the intervals before and after 6 months in which nadir

testosterone was less than 20 ng/dl, patients were divided into two groups: fast and slow. Between the two groups, there was no discernible difference in overall survival. The prognosis of ADT patients may depend less on the rate of testosterone decline and more on whether the lowest testosterone level is below 20 ng/dL [61].

### **Testosterone and Bipolar Androgen Therapy**

The term "bipolar" is used to emphasize that, with this strategy, there is a rapid cycle of testosterone between two extremes: from supraphysiologic serum testosterone levels back to levels near castration, repeated over multiple cycles. Due to their inability to completely degrade high levels of androgen-stabilized nuclear AR, CRPC cells that express high levels of AR are vulnerable to cell death when exposed to supraphysiologic testosterone. Supraphysiologic androgens can also cause deadly double-stranded DNA breaks in prostate cancer cells that have been chronically deficient in androgens. CRPC cells that have survived high testosterone levels due to low baseline AR levels or through adaptive downregulation of AR become susceptible to death when suddenly re-exposed to low testosterone during the treatment cycle because of the bipolar nature of the treatment [62].

A study [63] has shown that androgens can express the 'hit and run' mechanism in prostate cancer cells through androgen receptors. In a cell-autonomous manner, androgens can cause prostate cancer cells to maintain a quiescent and dormant state. Therefore, by inducing and/or strengthening self-sustaining quiescent cancer cells in disseminated solitary tumor foci, androgen deprivation and supplementation of the repeated cycle [i.e., bipolar androgen therapy (BAT)] can effectively inhibit tumor cells in the early stage of metastatic progression.

One of the factors that allows for DNA replication in prostate cancer is the androgen receptor (AR). During androgen ablation therapy and the development of prostate cancer into mCRPC, the expression of the AR protein was dramatically increased (50–100 folds). Nuclear AR in mCRPC cells binds to DNA at the origin of replication sites (ORS) during the G1 phase of the cell cycle as a component of the replication origin complex (ORC), which is necessary to allow DNA replication during the S phase.

From early mitosis until late mitosis, AR and ORC are linked. It must be degraded as a DNA licensing factor in order for re-licensing to take place in the following cell cycle. The increased ligand makes the AR bound by ORC excessively stable and prevents its complete degradation when there are medications present to supplement serum testosterone. Lack of sufficient mitotic AR degradation prevents DNA replication from restarting due to the ligand-dependent over stability, which causes cell death in the subsequent circulation [18-20] (Figure 1).

In the first BAT pilot study conducted by Schweizer in 2015, 16 asymptomatic mCRPC patients completed BAT for at least 3 months. The study showed that 50% of patients had a decrease in PSA, of which 28.6% had a decrease of more than 50%. Some soft tissue metastases were controlled in 10 patients according to imaging evaluation [64].

BAT was linked to appreciable gains in lipid parameters, quality of life, and body composition. For men with mCRPC, this has positive implications for their long-term health [65]. Systemic pain and calf swelling were the most frequent BAT side effects in the RESTORE study, which involved 90 patients. Hot flashes, breast tissue enlargement, and breast pain are typical sexual side effects [66] (Table 1).

It is worth mentioning in particular that a large (n = 180) randomized trial of BAT (TRANSFORMER) [71] compared the clinical or imaging progression free survival (PFS), safety, and quality of life (QoL) of asymptomatic anti-castration metastatic prostate cancer patients treated with bipolar androgen and enzalutamide.

Compared with enzalutamide, BAT maintains or improves the quality of life, especially in the areas of fatigue, physical and sexual function. The experiment also made a comparison of cross-treatment. Patients who were cross treated with enzalutamide after BAT showed a significantly enhanced response compared to patients who received enzalutamide immediately after the progression of abiraterone. The PSA-PFS of enzalutamide increased nearly threefold from 3.8 months after Abiraterone to 10.9 months after BAT. PSA50 response improved to 78% versus 25%, and OR improved to 29% versus 4%. This suggests that BAT may partially reverse the lineage plasticity of PC cells that lose AR addiction. In other words, BAT can reverse anti-androgen resistance through adaptive down-regulation of AR expression [71].

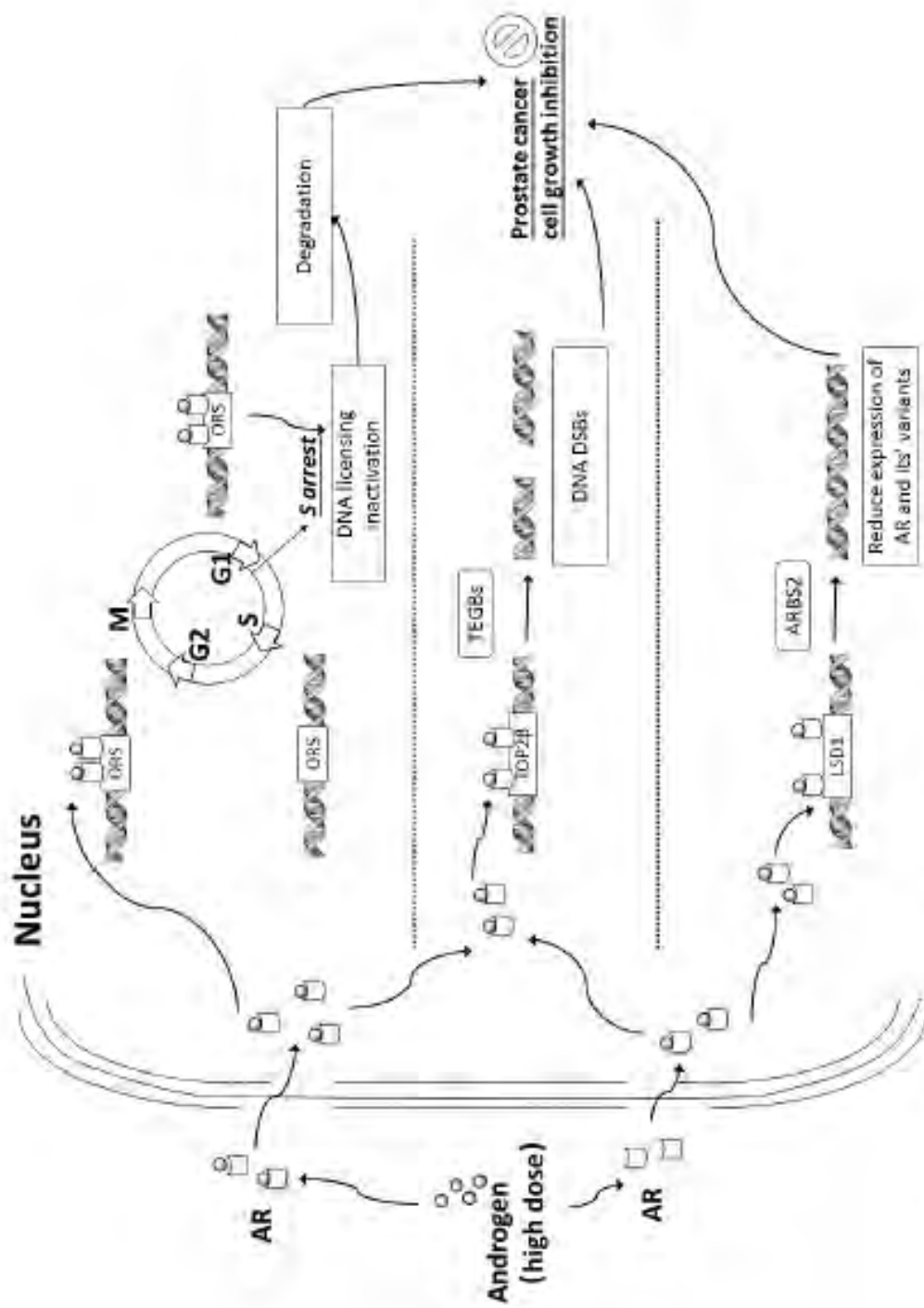


Figure 1. Mechanism of high dose androgen inhibiting the growth of prostate cancer cells.

**Table 1. Summary of current BAT research**

Patient status	Number	Treatment plan	Result	Reference
CRPC	12	Testosterone 5 mg transdermal patch or 1% gel for 1 week or 1 month.	30% of patients showed decreased PSA.	[67]
Early CRPC with micrometastasis	15	25, 50, or 75 mg/day transdermal testosterone.	Symptom progression in one patient, PSA decrease in three patients	[68]
Asymptomatic CRPC with low to moderate metastasis	16	Testosterone (400 mg intramuscular injection on the first day of the 28-day cycle) and etoposide (100 mg orally per day; days 1 to 14 of the 28-day cycle)	PSA decreased in half of the patients, and imaging regression occurred in half of the 10 patients with assessable soft tissue metastasis.	[64]
HSPC with low metastasis	29	Testosterone 400 mg intramuscularly on days 1, 29, and 57	PSA level < 4 ng/mL in 17 patients at 18 months	[69]
mCRPC developed after enzalutamide	30	Alternatively use BAT cycle for 3 months (400 mg intramuscular injection on the 1 <sup>st</sup> , 29 <sup>th</sup> or 57 <sup>th</sup> day), and then use ADT alone for 3 months	30% of patients achieved PSA decrease; 52% of patients recovered sensitivity to enzalutamide treatment (PSA decreased)	[70]
mCRPC (duration of abiraterone < or ≥ 6 months)	180	Testosterone 400 mg, intramuscularly once every 28 days or enzalutamide 160 mg per day, until clinical or imaging progress. Asymptomatic patients enter the cross-treatment link after the 28-day clearance period.	The PSA-PFS of enzalutamide increased nearly threefold, from 3.8 months after abiraterone to 10.9 months after BAT.	[71]

Another phase II BATMAN study evaluated the efficacy of alternating BAT and ADT in men with recurrent or advanced hormone-sensitive prostate cancer. Twenty-two (76%) patients in the study remained sensitive to castration after two rounds of BAT-ADT. Five of the seven nonresponders who progressed to CRPC at the end of the study responded to subsequent antiandrogenic therapy (using bicalutamide or enzalutamide) [72]. Other studies have also shown that BAT treatment can induce clinical responses and restore the sensitivity of previously treated CRPC patients to androgen receptor ablation [66, 71, 73, 74].

In addition, it is reported that the combination of BAT and enzalutamide may improve the clinical response rate of mCRPC patients to blocking PD-1 at the immune checkpoint [75].

### Serum Testosterone Determines CRPC Drug Therapy

It should be noted that there is also a close relationship between serum TST levels and responses to novel AR-targeted drugs [76]. The level of serum TST is expected to determine the best treatment strategy for patients with CRPC.

**Table 2.** Serum testosterone determines CRPC drug therapy

Serum Testosterone	Influence of Drug Therapy
TST $\geq$ 13 ng/dL	Better outcomes in Enzalutamide and/or Abiraterone. Good response to new AR-targeted drugs
TST < 13ng/dL	Poor response to novel AR antagonists, Better response and efficacy to Docetaxel

Our team studied the relationship between serum testosterone and treatment response and prognosis in patients treated with enzalutamide and Abiraterone. Studies have shown that higher TST levels ( $\geq$ 13 ng/dL) are associated with better outcomes in Enzalutamide and/or Abiraterone treated patients. The TST level of 13 ng/dL can predict the good response of CRPC patients to new AR-targeted drugs. Higher TST ( $\geq$ 13 ng/dL) at the beginning of an administration is related to a good response to new AR-targeted drugs, especially Enzalutamide [76]. Serum TST 13 ng/dL is the dividing point that determines the response and efficacy of CRPC to drug therapy [77]. Patients with serum TST  $\geq$ 13ng/dL had better curative effects on novel androgen receptor (AR) antagonist medicines. However, those serum TST < 13ng/dL

showed poor response to novel AR antagonists, but better response and efficacy to the treatments of Docetaxel and Cabazitaxel [76, 77] (Table 2).

## Conclusion

The relationship between prostate cancer and androgen has changed from the original single understanding in recent years due to the advancement and development of pertinent research. Of course, there are still a lot of unanswered questions regarding androgen and prostate cancer despite the abundance of basic analyses and clinical reports. For instance, the dosage of testosterone treatment and the proper BAT cycle.

Traditional hormone therapy and anti-cancer medications have been replaced by new hormone drugs that target the BRCA1/2 mutation and PARP inhibitors in the treatment of prostate cancer. Serum testosterone, however, continues to be a crucial biochemical factor that affects the effectiveness of new prostate cancer drug therapies as well as the prognosis of patients with the disease. It also plays a small but significant role in the proliferation and apoptosis of prostate cancer cells.

Simply put, the serum testosterone level is a helpful biochemical indicator for determining the treatment course and prostate cancer prognosis. Serum testosterone has a significant impact on the treatment, prognosis, and quality of life of patients with advanced prostate cancer in clinical practice.

## Reference

- [1] Rebecca, L., Siegel, R., Miller, K. D. & Jemal, A. Cancer statistics, 2017. *CA Cancer J Clin* 67, 7-30, doi:10.3322/caac.21387 (2017).
- [2] Siegel, R. L., Miller, K. D. & Jemal, A. Cancer statistics, 2019. *CA Cancer J Clin* 69, 7-34, doi:10.3322/caac.21551 (2019).
- [3] Huggins, C., Stevens, R. & Hodges, C. V. Studies on prostatic cancer: II. The effects of castration on advanced carcinoma of the prostate gland. *Archives of Surgery* 43, 209-223 (1941).
- [4] Knudsen, K. E. & Penning, T. M. Partners in crime: deregulation of AR activity and androgen synthesis in prostate cancer. *Trends Endocrinol Metab* 21, 315-324, doi:10.1016/j.tem.2010.01.002 (2010).
- [5] Vander Griend, D. J., Litvinov, I. V. & Isaacs, J. T. Conversion of androgen receptor signaling from a growth suppressor in normal prostate epithelial cells to an oncogene

- in prostate cancer cells involves a gain of function in c-Myc regulation. *International Journal of Biological Sciences* 10, 627 (2014).
- [6] Montgomery, R. B., Mostaghel, E. A., Vessella, R., Hess, D. L., Kalhorn, T. F., Higano, C. S., True, L. D., & Nelson, P. S. Maintenance of intratumoral androgens in metastatic prostate cancer: a mechanism for castration-resistant tumor growth. *Cancer Res* 68, 4447-4454, doi:10.1158/0008-5472.Can-08-0249 (2008).
- [7] Weber, M. J. & Gioeli, D. Ras signaling in prostate cancer progression. *Journal of Cellular Biochemistry* 91, 13-25 (2004).
- [8] Stanbrough, M., Bubley, G. J., Ross, K., Golub, T. R., Rubin, M. A., Penning, T. M., Febbo, P. G., & Balk, S. P. Increased expression of genes converting adrenal androgens to testosterone in androgen-independent prostate cancer. *Cancer Research* 66, 2815-2825 (2006).
- [9] Nacusi, L. P. & Tindall, D. J. Androgen receptor abnormalities in castration-recurrent prostate cancer. *Expert Review of Endocrinology & Metabolism* 4, 417-422 (2009).
- [10] Mohler, J. L. Castration-recurrent prostate cancer is not androgen-independent. *Hormonal Carcinogenesis V*, 223-234 (2008).
- [11] Ryan, C. J., M. R. Smith, K. Fizazi, F. Saad, P. F. A. Mulders, C. N. Sternberg, K. t Miller, C. J. Logothetis, N. D. Shore, E. J. Small, J. Carles, T. W. Flaig, M. E. Taplin, C. S. Higano, P. de Souza, J. S. de Bono, T. W. Griffin, P. De Porre, M. K. Yu, Y. C. Park, J. Li, T. Kheoh, V. Naini, A. Molina, D. E. Rathkopf, COU-AA-302 Investigators. Abiraterone acetate plus prednisone versus placebo plus prednisone in chemotherapy-naive men with metastatic castration-resistant prostate cancer (COU-AA-302): final overall survival analysis of a randomised, double-blind, placebo-controlled phase 3 study. *The Lancet Oncology* 16, 152-160 (2015).
- [12] Beer, T. M., Armstrong, A. J., Rathkopf, D., Loriot, Y., Sternberg, C. N., Higano, C. S., Iversen, P., Evans, C. P., Kim, C.-S., Kimura, G., Miller, K., Saad, F., Bjartell, A. S., Borre, M., Mulders, P., Tammela, T. L., Parli, T., Sari, S., van Os, S., Tombal, B. Enzalutamide in men with chemotherapy-naive metastatic castration-resistant prostate cancer: extended analysis of the phase 3 PREVAIL study. *European Urology* 71, 151-154 (2017).
- [13] de Bono, J. S., Logothetis, C. J., Molina, A., Fizazi, K., North, S., Chu, L., Chi, K. N., Jones, R. J., Goodman, O. B., Saad, F., Staffurth, J. N., Mainwaring, P., Harland, S., Flaig, T. W., Hutson, T. E., Cheng, T., Patterson, H., Hainsworth, J. D., Ryan, C. J., Scher, H. I. Abiraterone and increased survival in metastatic prostate cancer. *N Engl J Med* 364, 1995-2005, doi:10.1056/NEJMoa1014618 (2011).
- [14] Scher, H. I., Fizazi, K., Saad, F., Taplin, M.-E., Sternberg, C. N., Miller, K., de Wit, R., Mulders, P., Chi, K. N., Shore, N. D., Armstrong, A. J., Flaig, T. W., Fléchon, A., Mainwaring, P., Fleming, M., Hainsworth, J. D., Hirmand, M., Selby, B., Seely, L., & de Bono, J. S. Increased survival with enzalutamide in prostate cancer after chemotherapy. *New England Journal of Medicine* 367, 1187-1197 (2012).
- [15] Ryan, C. J., Smith, M. R., de Bono, J. S., Molina, A., Logothetis, C. J., de Souza, P., Fizazi, K., Mainwaring, P., Piulats, J. M., Ng, S., Carles, J., Mulders, P. F. A., Basch, E., Small, E. J., Saad, F., Schrijvers, D., Van Poppel, H., Mukherjee, S. D.,

- Suttman, H., Rathkopf, D. E. Abiraterone in metastatic prostate cancer without previous chemotherapy. *New England Journal of Medicine* 368, 138-148 (2013).
- [16] Huggins, C. Two principles in endocrine therapy of cancers: hormone deprivation and hormone interference. *Cancer Research* 25, 1163-1167 (1965).
- [17] Umekita, Y., Hiipakka, R. A., Kokontis, J. M. & Liao, S. Human prostate tumor growth in athymic mice: inhibition by androgens and stimulation by finasteride. *Proc Natl Acad Sci U S A* 93, 11802-11807, doi:10.1073/pnas.93.21.11802 (1996).
- [18] Isaacs, J. T., D'Antonio, J. M., Chen, S., Antony, L., Dalrymple, S. P., Ndikuyeze, G. H., Luo, J., & Denmeade, S. R. Adaptive auto-regulation of androgen receptor provides a paradigm shifting rationale for bipolar androgen therapy (BAT) for castrate resistant human prostate cancer. *Prostate* 72, 1491-1505, doi:10.1002/pros.22504 (2012).
- [19] Litvinov, I. V., Vander Griend, D. J., Antony, L., Dalrymple, S., De Marzo, A. M., Drake, C. G., & Isaacs, J. T. Androgen receptor as a licensing factor for DNA replication in androgen-sensitive prostate cancer cells. *Proc Natl Acad Sci U S A* 103, 15085-15090, doi:10.1073/pnas.0603057103 (2006).
- [20] Vander Griend, D. J., Litvinov, I. V. & Isaacs, J. T. Stabilizing androgen receptor in mitosis inhibits prostate cancer proliferation. *Cell Cycle* 6, 647-651 (2007).
- [21] D'Antonio, J. M., Vander Griend, D. J. & Isaacs, J. T. DNA licensing as a novel androgen receptor mediated therapeutic target for prostate cancer. *Endocr Relat Cancer* 16, 325-332, doi:10.1677/erc-08-0205 (2009).
- [22] Denmeade, S. R. & Isaacs, J. T. Bipolar androgen therapy: the rationale for rapid cycling of supraphysiologic androgen/ablation in men with castration resistant prostate cancer. *Prostate* 70, 1600-1607, doi:10.1002/pros.21196 (2010).
- [23] Platz, E. A., M. F. Leitzmann, N. Rifai, P. W. Kantoff, Yen-Ching Chen, M. J. Stampfer, W. C. Willett, E. Giovannucci. Sex steroid hormones and the androgen receptor gene CAG repeat and subsequent risk of prostate cancer in the prostate-specific antigen era. *Cancer Epidemiology Biomarkers & Prevention* 14, 1262-1269 (2005).
- [24] Roddam, A., Allen, N., Appleby, P. & Key, T. Endogenous Hormones and Prostate Cancer Collaborative Group. Endogenous sex hormones and prostate cancer: a collaborative analysis of 18 prospective studies. *J Natl Cancer Inst* 100, 170-183 (2008).
- [25] Muller, R. L., L. Gerber, D. M. Moreira, G. Andriole, R. Castro-Santamaria, S. J. Freedland. Serum testosterone and dihydrotestosterone and prostate cancer risk in the placebo arm of the Reduction by Dutasteride of Prostate Cancer Events trial. *European Urology* 62, 757-764 (2012).
- [26] Boyle, P., Koechlin, A., Bota, M., d'Onofrio, A., Zaridze, D. G., Perrin, P., Fitzpatrick, J., Burnett, A. L., & Boniol, M. Endogenous and exogenous testosterone and the risk of prostate cancer and increased prostate-specific antigen (PSA) level: a meta-analysis. *BJU International* 118, 731-741 (2016).
- [27] Shin, B. S., Eu Chang Hwang, Chang Min Im, Sun-ouck Kim, Seung Il Jung, Taek Won Kang, Dong Deuk Kwon, Kwangsung Park, and Soo Bang Ryu. Is a decreased serum testosterone level a risk factor for prostate cancer? A cohort study of Korean men. *Korean Journal of Urology* 51, 819-823 (2010).

- [28] Li, T., Sun, X. & Chen, L. Free testosterone value before radical prostatectomy is related to oncologic outcomes and post-operative erectile function. *BMC Cancer* 19, 1-10 (2019).
- [29] García-Cruz, E., Piqueras, M., Huguet, J., Peri, L., Izquierdo, L., Musquera, M., Franco, A., Alvarez-Vijande, R., Ribal, M. J., & Alcaraz, A. Low testosterone levels are related to poor prognosis factors in men with prostate cancer prior to treatment. *BJU International* 110, E541-E546 (2012).
- [30] Mearini, L., Zucchi, A., Nunzi, E., Villirillo, T., Bini, V., & Porena, M. Low serum testosterone levels are predictive of prostate cancer. *World Journal of Urology* 31, 247-252 (2013).
- [31] Morgentaler, A., M. Zitzmann, A. M. Traish, A. W. Fox, T. H. Jones, M. Maggi, S. Arver, A. Aversa, J. C. N. Chan, A. S. Dobs, G. I. Hackett, W. J. Hellstrom, P. Lim, B. Lumenfeld, G. Mskhalaya, C. C. Schulman, L. O. Torres. Fundamental Concepts Regarding Testosterone Deficiency and Treatment: International Expert Consensus Resolutions. *Mayo Clinic Proceedings*. 881-896 (Elsevier).
- [32] Rizk, P. J., Kohn, T. P., Pastuszak, A. W. & Khera, M. Testosterone therapy improves erectile function and libido in hypogonadal men. *Current Opinion in Urology* 27, 511 (2017).
- [33] Yassin, A., A. Haider, K. S. Haider, M. Caliber, G. Doros, F. Saad, W. Timothy Garvey. Testosterone therapy in men with hypogonadism prevents progression from prediabetes to type 2 diabetes: eight-year data from a registry study. *Diabetes Care* 42, 1104-1111 (2019).
- [34] Traish, A. M., Muller, R. E. & Wotiz, H. H. A new procedure for the quantitation of nuclear and cytoplasmic androgen receptors. *Journal of Biological Chemistry* 256, 12028-12033 (1981).
- [35] Traish, A., Williams, D., Hoffman, N. & Wotiz, H. Validation of the exchange assay for the measurement of androgen receptors in human and dog prostates. *Progress in Clinical and Biological Research* 262, 145-160 (1988).
- [36] Morgentaler, A. Testosterone and prostate cancer: an historical perspective on a modern myth. *European Urology* 50, 935-939 (2006).
- [37] Morgentaler, A. & Traish, A. M. Shifting the paradigm of testosterone and prostate cancer: the saturation model and the limits of androgen-dependent growth. *European Urology* 55, 310-321 (2009).
- [38] Cooper, C. S., Perry, P. J., Sparks, A. E. T., MacIndoe, J. H., Yates, W. R., & Williams, R. D. Effect of exogenous testosterone on prostate volume, serum and semen prostate specific antigen levels in healthy young men. *The Journal of Urology* 159, 441-443 (1998).
- [39] Bhasin, S., Woodhouse, L., Casaburi, R., Singh, A. B., Bhasin, D., Berman, N., Chen, X., Yarasheski, K. E., Magliano, L., Dzekov, C., Dzekov, J., Bross, R., Phillips, J., Sinha-Hikim, I., Shen, R., & Storer, T. W. Testosterone dose-response relationships in healthy young men. *American Journal of Physiology-Endocrinology And Metabolism* (2001).
- [40] Nair, K. S., Rizza, R. A., O'Brien, P., Dhatariya, K., Short, K. R., Nehra, A., Vittone, J. L., Klee, G. G., Basu, A., Basu, R., Cobelli, C., Toffolo, G., Man, C. D., Tindall, D. J., Melton, L. J., Smith, G. E., Khosla, S., & Jensen, M. D. DHEA in elderly

- women and DHEA or testosterone in elderly men. *New England Journal of Medicine* 355, 1647-1659 (2006).
- [41] Santella, C., Renoux, C., Yin, H., Yu, O. H. & Azoulay, L. Testosterone replacement therapy and the risk of prostate cancer in men with late-onset hypogonadism. *American Journal of Epidemiology* 188, 1666-1673 (2019).
- [42] Loeb, S., Folkvaljon, Y., Damber, J.-E., Ahlkal, J., Lambe, M., & Stattin, P. Testosterone replacement therapy and risk of favorable and aggressive prostate cancer. *Journal of Clinical Oncology* 35, 1430 (2017).
- [43] Kaufman, J. M. & Graydon, R. J. Androgen replacement after curative radical prostatectomy for prostate cancer in hypogonadal men. *The Journal of Urology* 172, 920-922 (2004).
- [44] Khera, M., & Lipshultz, L. I. Testosterone replacement therapy following radical prostatectomy. *The Journal of Sexual Medicine* 6, 1165-1170 (2009).
- [45] Balbontin, F. G., Moreno, S. A., Bley, E., Chacon, R., Silva, A., & Morgentaler, A. Long-acting testosterone injections for treatment of testosterone deficiency after brachytherapy for prostate cancer. *BJU International* 114, 125-130 (2014).
- [46] Pastuszak, A. W., Pearlman, A. M., Godoy, G., Miles, B. J., Lipshultz, L. I., & Khera, M. Testosterone replacement therapy in the setting of prostate cancer treated with radiation. *International Journal of Impotence Research* 25, 24-28 (2013).
- [47] Kaplan, A. L., Lenis, A. T., Shah, A., Rajfer, J. & Hu, J. C. Testosterone replacement therapy in men with prostate cancer: a time-varying analysis. *The journal of sexual medicine* 12, 374-380 (2015).
- [48] Ahlering, T. E., My Huynh, L., Towe, M., See, K., Tran, J., Osann, K., el Khatib, F. M., & Yafi, F. A. Testosterone replacement therapy reduces biochemical recurrence after radical prostatectomy. *BJU International* 126, 91-96 (2020).
- [49] Pastuszak, A. W., Pearlman, A. M., Lai, W. S., Godoy, G., Sathyamoorthy, K., Liu, J. S., Miles, B. J., Lipshultz, L. I., & Khera, M. Testosterone replacement therapy in patients with prostate cancer after radical prostatectomy. *The Journal of Urology* 190, 639-644 (2013).
- [50] Harman, S. M., Metter, E. J., Tobin, J. D., Pearson, J. & Blackman, M. R. Longitudinal effects of aging on serum total and free testosterone levels in healthy men. *The Journal of Clinical Endocrinology & Metabolism* 86, 724-731 (2001).
- [51] Park, J., Cho, S. Y., Jeong, S., Lee, S. B., Son, H., & Jeong, H. Low testosterone level is an independent risk factor for high-grade prostate cancer detection at biopsy. *BJU International* 118, 230-235 (2016).
- [52] Li, X. B., L. Zhang, Tai-Wen Rao, J. Chen, Yuan-Jing Leng, P. Huang. Low serum testosterone level does not predict bone metastasis of prostate cancer. *Zhonghua Nan Ke Xue* 23, 212-216 (2017).
- [53] Morales, A., Black, A. M. & Emerson, L. E. Testosterone administration to men with testosterone deficiency syndrome after external beam radiotherapy for localized prostate cancer: preliminary observations. *BJU International* 103, 62-64 (2009).
- [54] Kacker, R., Hult, M., San Francisco, I., Connors, W., Rojas, P., Dewolf, W., & Morgentaler, A. Can testosterone therapy be offered to men on active surveillance for prostate cancer? Preliminary results. *Asian Journal of Andrology* 18, 16 (2016).

- [55] Hashimoto, T. et al. *Urologic Oncology: Seminars and Original Investigations*. 530. e539-530. e514 (Elsevier).
- [56] Bertaglia, V. et al. Effects of serum testosterone levels after 6 months of androgen deprivation therapy on the outcome of patients with prostate cancer. *Clin Genitourin Cancer* 11, 325-330.e321, doi:10.1016/j.clgc.2013.01.002 (2013).
- [57] Morote, J., A. Orsola, J. Planas, E. Trilla, C. X. Raventós, L. Cecchini, and R. Catalán. Redefining clinically significant castration levels in patients with prostate cancer receiving continuous androgen deprivation therapy. *J Urol* 178, 1290-1295, doi:10.1016/j.juro.2007.05.129 (2007).
- [58] Tombal, B. The Importance of Testosterone Control in Prostate Cancer. *European Urology Supplements - EUR UROL SUPPL* 6, 834-839, doi:10.1016/j.eursup.2007.06.002 (2007).
- [59] Perachino, M., Cavalli, V. & Bravi, F. Testosterone levels in patients with metastatic prostate cancer treated with luteinizing hormone-releasing hormone therapy: prognostic significance? *BJU Int* 105, 648-651, doi:10.1111/j.1464-410X.2009.08814.x (2010).
- [60] Yamamoto, S., S. Sakamoto, X. Minhui, T. Tamura, K. Otsuka, K. Sato, M. Maimaiti, S. Kamada, A. Takei, M. Fuse, K. Kawamura, T. Imamoto, A. Komiya, K. Akakura, T. Ichikawa. Testosterone Reduction of  $\geq 480$  ng/dL Predicts Favorable Prognosis of Japanese Men With Advanced Prostate Cancer Treated With Androgen-Deprivation Therapy. *Clinical Genitourinary Cancer* 15, e1107–e1115 (2017).
- [61] Kamada, S., Sakamoto, S., Ando, K., Muroi, A., Fuse, M., Kawamura, K., Imamoto, T., Suzuki, H., Nagata, M., Nihei, N., Akakura, K., & Ichikawa, T. Nadir Testosterone after Long-Term Followup Predicts Prognosis in Patients with Prostate Cancer Treated with Combined Androgen Blockade. *J Urol* 194, 1264-1270, doi:10.1016/j.juro.2015.03.120 (2015).
- [62] Schweizer, M. T., Antonarakis, E. S., Wang, H., Ajiboye, A. S., Spitz, A., Cao, H., Luo, J., Haffner, M. C., Yegnasubramanian, S., Carducci, M. A., Eisenberger, M. A., Isaacs, J. T., & Denmeade, S. R. Effect of bipolar androgen therapy for asymptomatic men with castration-resistant prostate cancer: results from a pilot clinical study. *Sci Transl Med* 7, 269ra262, doi:10.1126/scitranslmed.3010563 (2015).
- [63] Bui, A. T., Huang, M.-E., Havard, M., Laurent-Tchenio, F., Dautry, F., & Tchenio, T. Transient exposure to androgens induces a remarkable self-sustained quiescent state in dispersed prostate cancer cells. *Cell Cycle* 16, 879-893, doi:10.1080/15384101.2017.1310345 (2017).
- [64] Schweizer, M. T., Antonarakis, E. S., Wang, H., Ajiboye, A. S., Spitz, A., Cao, H., Luo, J., Haffner, M. C., Yegnasubramanian, S., Carducci, M. A., Eisenberger, M. A., Isaacs, J. T., & Denmeade, S. R. Effect of bipolar androgen therapy for asymptomatic men with castration-resistant prostate cancer: results from a pilot clinical study. *Science Translational Medicine* 7, 269ra262-269ra262 (2015).
- [65] Marshall, C. H., J. Tunacao, V. Danda, Hua-Ling Tsai, J. Barber, R. Gawande, C. R. Weiss, S. R. Denmeade, C. Joshu. Reversing the effects of androgen-deprivation

- therapy in men with metastatic castration-resistant prostate cancer. *BJU Int* 128, 366-373, doi:10.1111/bju.15408 (2021).
- [66] Markowski, M. C., H. Wang, R. Sullivan, I. Rifkind, V. Sinibaldi, M. T. Schweizer, B. A. Teply, N. Ngomba, W. Fu, M. A. Carducci, C. J. Paller, C. H. Marshall, M. A. Eisenberger, J. Luo, E. S. Antonarakis, S. R. Denmeade. A Multicohort Open-label Phase II Trial of Bipolar Androgen Therapy in Men with Metastatic Castration-resistant Prostate Cancer (RESTORE): A Comparison of Post-abiraterone Versus Post-enzalutamide Cohorts. *Eur Urol* 79, 692-699, doi:10.1016/j.eururo.2020.06.042 (2021).
- [67] Morris, M. J., Huang, D., Kelly, W. K., Slovin, S. F., Stephenson, R. D., Eicher, C., Delacruz, A., Curley, T., Schwartz, L. H., & Scher, H. I. Phase 1 trial of high-dose exogenous testosterone in patients with castration-resistant metastatic prostate cancer. *European Urology* 56, 237-244 (2009).
- [68] Szmulewitz, R., Mohile, S., Posadas, E., Kunnavakkam, R., Karrison, T., Manchén, E., & Stadler, W. M. A randomized phase 1 study of testosterone replacement for patients with low-risk castration-resistant prostate cancer. *European Urology* 56, 97-104 (2009).
- [69] Schweizer, M. T., Wang, H., Lubner, B., Nadal, R., Spitz, A., Rosen, D. M., Cao, H., Antonarakis, E. S., Eisenberger, M. A., Carducci, M. A., Paller, C., & Denmeade, S. R. Bipolar androgen therapy for men with androgen ablation naïve prostate cancer: results from the phase II BATMAN study. *The Prostate* 76, 1218-1226 (2016).
- [70] Teply, B. A., H. Wang, B. Lubner, R. Sullivan, I. Rifkind, A. Bruns, A. Spitz, M. DeCarli, V. Sinibaldi, C. F. Pratz, C. Lu, J. L. Silberstein, J. Luo, M. T. Schweizer, C. G. Drake, M. A. Carducci, C. J. Paller, E. S. Antonarakis, M. A. Eisenberger, S. R. Denmeade. Bipolar androgen therapy in men with metastatic castration-resistant prostate cancer after progression on enzalutamide: an open-label, phase 2, multicohort study. *The Lancet Oncology* 19, 76-86 (2018).
- [71] Denmeade, S. R., H. Wang, N. Agarwal, D. C. Smith, M. T. Schweizer, M. N. Stein, V. Assikis, P. W. Twardowski, T. W. Flaig, R. Z. Szmulewitz, J. M. Holzbeierlein, R. J. Hauke, G. Sonpavde, J. A. Garcia, A. Hussain, O. Sartor, S. Mao, H. Cao, W. Fu, T. Wang, R. Abdallah, S. Jin Lim, V. Bolejack, C. J. Paller, M. A. Carducci, M. C. Markowski, M. A. Eisenberger, E. S. Antonarakis. TRANSFORMER: A Randomized Phase II Study Comparing Bipolar Androgen Therapy Versus Enzalutamide in Asymptomatic Men With Castration-Resistant Metastatic Prostate Cancer. *J Clin Oncol* 39, 1371-1382, doi:10.1200/jco.20.02759 (2021).
- [72] Schweizer, M. T., Wang, H., Lubner, B., Nadal, R., Spitz, A., Rosen, D. M., Cao, H., Antonarakis, E. S., Eisenberger, M. A., Carducci, M. A., Paller, C., & Denmeade, S. R. Bipolar Androgen Therapy for Men With Androgen Ablation Naïve Prostate Cancer: Results From the Phase II BATMAN Study. *Prostate* 76, 1218-1226, doi:10.1002/pros.23209 (2016).
- [73] Sena, L. A., Wang, H., Lim ScM, S. J., Rifkind, I., Ngomba, N., Isaacs, J. T., Luo, J., Pratz, C., Sinibaldi, V., Carducci, M. A., Paller, C. J., Eisenberger, M. A., Markowski, M. C., Antonarakis, E. S., & Denmeade, S. R. Bipolar androgen therapy sensitizes castration-resistant prostate cancer to subsequent androgen receptor

- ablative therapy. *Eur J Cancer* 144, 302-309, doi:10.1016/j.ejca.2020.11.043 (2021).
- [74] Teply, B. A., H. Wang, B. Lubber, R. Sullivan, I. Rifkind, A. Bruns, A. Spitz, M. DeCarli, V. Sinibaldi, C. F. Pratz, C. Lu, J. L. Silberstein, J. Luo, M. T. Schweizer, C. G. Drake, M. A. Carducci, C. J. Paller, E. S. Antonarakis, M. A. Eisenberger, S. R. Denmeade. Bipolar androgen therapy in men with metastatic castration-resistant prostate cancer after progression on enzalutamide: an open-label, phase 2, multicohort study. *Lancet Oncol* 19, 76-86, doi:10.1016/s1470-2045(17)30906-3 (2018).
- [75] Markowski, M. C., M. C. Markowski, E. Shenderov, M. A. Eisenberger, S. Kachhap, D. M. Pardoll, S. R. Denmeade, and E. S. Antonarakis. Extreme responses to immune checkpoint blockade following bipolar androgen therapy and enzalutamide in patients with metastatic castration resistant prostate cancer. *Prostate* 80, 407-411, doi:10.1002/pros.23955 (2020).
- [76] Sakamoto, S., Maimaiti, M., Xu, M., Kamada, S., Yamada, Y., Kitoh, H., Matsumoto, H., Takeuchi, N., Higuchi, K., Uchida, H. A., Komiya, A., Nagata, M., Nakatsu, H., Matsuyama, H., Akakura, K., & Ichikawa, T. Higher Serum Testosterone Levels Associated with Favorable Prognosis in Enzalutamide- and Abiraterone-Treated Castration-Resistant Prostate Cancer. *J Clin Med* 8, doi:10.3390/jcm8040489 (2019).
- [77] Ando, K., Sakamoto, S., Takeshita, N., Fujimoto, A., Maimaiti, M., Saito, S., Sanjyon, P., Imamura, Y., Sato, N., Komiya, A., Akakura, K., & Ichikawa, T. Higher serum testosterone levels predict poor prognosis in castration-resistant prostate cancer patients treated with docetaxel. *Prostate* 80, 247-255, doi:10.1002/pros.23938 (2020).



Review

# Contribution of the L-Type Amino Acid Transporter Family in the Diagnosis and Treatment of Prostate Cancer

Xue Zhao <sup>1</sup>, Shinichi Sakamoto <sup>1,\*</sup>, Jiaying Wei <sup>1</sup>, Sangjon Pae <sup>1,2</sup>, Shinpei Saito <sup>1,2</sup>, Tomokazu Sazuka <sup>1</sup>, Yusuke Imamura <sup>1</sup>, Naohiko Anzai <sup>2</sup> and Tomohiko Ichikawa <sup>1</sup>

<sup>1</sup> Department of Urology, Chiba University Graduate School of Medicine, Chiba 260-8670, Japan

<sup>2</sup> Department of Pharmacology, Chiba University Graduate School of Medicine, Chiba 260-8670, Japan

\* Correspondence: rbatbat1@gmail.com; Tel.: +81-43-226-2134; Fax: +81-43-226-2136

**Abstract:** The L-type amino acid transporter (LAT) family contains four members, LAT1~4, which are important amino acid transporters. They mainly transport specific amino acids through cell membranes, provide nutrients to cells, and are involved in a variety of metabolic pathways. They regulate the mTOR signaling pathway which has been found to be strongly linked to cancer in recent years. However, in the field of prostate cancer (PCa), the LAT family is still in the nascent stage of research, and the importance of LATs in the diagnosis and treatment of prostate cancer is still unknown. Therefore, this article aims to report the role of LATs in prostate cancer and their clinical significance and application. LATs promote the progression of prostate cancer by increasing amino acid uptake, activating the mammalian target of rapamycin (mTOR) pathway and downstream signals, mediating castration-resistance, promoting tumor angiogenesis, and enhancing chemotherapy resistance. The importance of LATs as diagnostic and therapeutic targets for prostate cancer was emphasized and the latest research results were introduced. In addition, we introduced selective LAT1 inhibitors, including JPH203 and OKY034, which showed excellent inhibitory effects on the proliferation of various tumor cells. This is the future direction of amino acid transporter targeting therapy drugs.

**Keywords:** prostate cancer; LAT1; LAT3; diagnosis; treatment



**Citation:** Zhao, X.; Sakamoto, S.; Wei, J.; Pae, S.; Saito, S.; Sazuka, T.; Imamura, Y.; Anzai, N.; Ichikawa, T. Contribution of the L-Type Amino Acid Transporter Family in the Diagnosis and Treatment of Prostate Cancer. *Int. J. Mol. Sci.* **2023**, *24*, 6178. <https://doi.org/10.3390/ijms24076178>

Academic Editors: Domingo González-Lamuño and Raquel Yahyaoui

Received: 27 February 2023  
Revised: 20 March 2023  
Accepted: 22 March 2023  
Published: 24 March 2023



**Copyright:** © 2023 by the authors. Licensee MDPI, Basel, Switzerland. This article is an open access article distributed under the terms and conditions of the Creative Commons Attribution (CC BY) license (<https://creativecommons.org/licenses/by/4.0/>).

## 1. Introduction

Tumor growth requires continuous nutritional support, of which essential amino acids (EAAs) are an important source [1]. The amino acid uptake was found to be higher in tumor tissue than in normal tissue [2]. The L-type amino acid transporter (LAT) family is a group of transmembrane transporter proteins composed of four members, LAT1, 2, 3, 4. The first two proteins belong to the solute vector family 7 (SLC7) and the latter two belong to SLC43. They are important pathways for essential amino acids to enter cells and are closely related to intracellular pathways [3–6].

The LAT family was upregulated in many tumors [7]. Prostate cancer (PCa) is the most frequent malignant tumor in men globally. In the United States, approximately 2.6 million new cases of PCa were identified each year, with an estimated 34,500 fatalities [8]. We primarily reviewed the relationship between the LAT family and PCa and analyzed the role of LATs in the diagnosis and treatment of PCa.

## 2. The Structure and Function of LATs

### 2.1. LAT1

LAT1 (SLC7A5) was discovered in 1998 [3,9]. It combines with 4F2hc (SLC3A2) heavy chain protein to form a transmembrane complex to play its biological role [10]. LAT1 is mainly responsible for the transport of large neutral amino acids. Generally, LAT1 is expressed in the normal human body mainly in the gastrointestinal mucosa,

testicular support cells, ovarian follicular cells, pancreatic islet cells, and endothelial cells that act as inter-tissue barriers (blood-brain, blood-retina, and blood-follicular barriers) [11]. Many neurotransmitters and neuroactive compounds cannot cross the blood-brain barrier, and most of them are synthesized in the brain. Therefore, LAT1, as the precursor of neurotransmitters and neuroactive compounds, plays an important role in amino acid uptake through the blood-brain barrier [12]. As previously stated, LAT1 expression in normal organisms is limited to specific cells and tissues. Studies have also shown that LAT1 exists in cells with high proliferation and differentiation ability, such as embryos and T-lymphocytes. During embryonic development, the LAT1 of syncytial trophoblast cells plays an indispensable role in the development of the placenta, contributing to the exchange of amino acids between mother and fetus. Systemic LAT1 knockout results in defects in the placenta, which can be fatal to the embryo in the second trimester [13]. There is no clear research result on the role of LAT1 in T cell differentiation, but previous studies have shown that LAT1 is related to the metabolic process of T lymphocyte differentiation. LAT1 expression is low in intrinsic T cells, whereas T cells at the differentiation stage specifically increase LAT1 expression by T cell receptors (TCR), ensuring sufficient nutrients to react with the antigen [10,14].

LAT1 provides branched-chain amino acid (BCAA), especially leucine, to the mammalian target of rapamycin complex1 (mTORC1), a major control factor of cell proliferation. mTORC1 senses amino acid signals and promotes cell proliferation through multiple downstream effectors related to gene expression and metabolism [15]. Upstream of mTORC1 is a complex of GTPase-activating protein (GAP), activity toward Rags 1 (GATOR1) and GATOR2. GATOR1 functions as a mTORC1 antagonist and GATOR2 functions as a mTORC1 agonist. GAP inhibits mTORC1 in the absence of amino acids. Leucine transports into the cell by LAT1 binds to the leucine sensor sestrin2. The interaction between leucine and sestrin2 can activate GATOR2 and inhibit GATOR1, thus promoting the function of mTORC1 to achieve the purpose of cell proliferation [16,17]. LAT1 expression is upregulated in many cancers, such as breast [18], lung [19], colorectal [20], renal [21], bladder [22], prostate [23], and gliomas [24].

One of the purposes of large quantities of amino acid transport in LAT1 in cancer cells is to use BCAAs as biosynthetic materials for the metabolic reprogramming of cancer cells. Branched-chain amino acid transferase (BCAT) deaminates free BCAAs to generate the appropriate branched-chain keto acid (BCKA). BCAT2 transforms BCAA into BCKA within the mitochondria, which is subsequently catalyzed by metabolic intermediates and acetyl-CoA into the TCA cycle, which is used for energy production and fatty acid metabolism [25] (Figure 1).

Another function of LAT1 that promotes tumor formation is to inhibit cell-damaging T-cell control in the tumor microenvironment. In the serine pathway, tryptophan is converted into kynurenine (Kyn) by 2, 3-Deoxygenase (TDO) and indoleamine 2, 3-Dioxygenase (IDO). In the physiological state, TDO and IDO levels are negligible, but in the cancer state, both enzymes rise dramatically. Through the continuous function of TDO and IDO, large amounts of Kyn can be synthesized. Kyn is transported from cancer cells to T cells by LAT1. In T cells, Kyn binds to the aryl hydrocarbon receptor (AHR), which inhibits the anti-tumor immune response of T cells and promotes the proliferation of cancer cells [26].

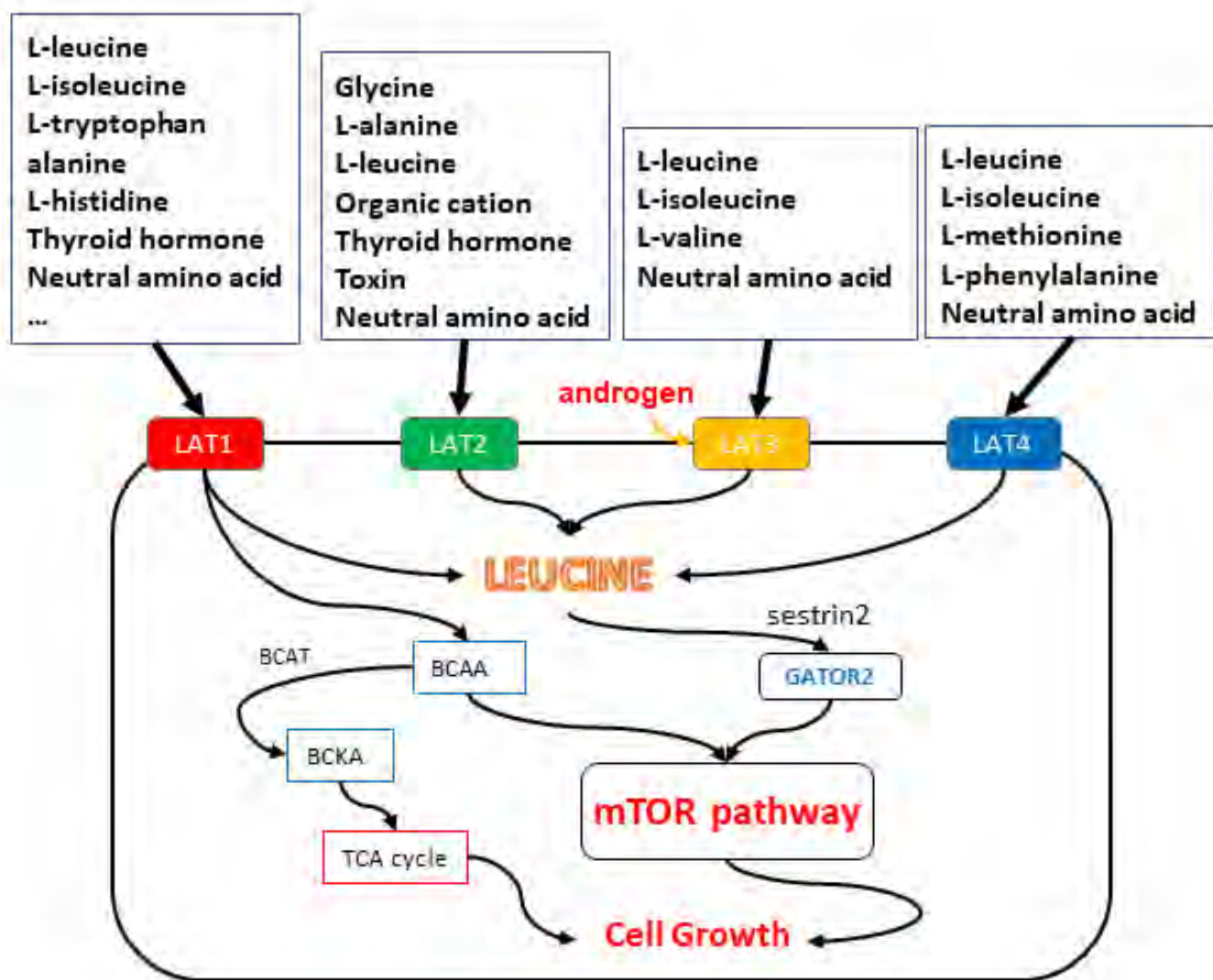


**Figure 1.** The substances that each LAT is mainly responsible for transporting are shown in the figure. LATs provide branched-chain amino acids (BCAAs), especially leucine, to mammalian target cells of rapamycin complex 1 (mTORC1), and the mTOR pathway is a major control factor in proliferation and cell growth. GATOR2 is a major negative regulator of mTORC1. Thus, BCAAs promote the function of the mTOR pathway and achieve the purpose of cell proliferation. In addition, LAT1 uses BCAAs as biosynthetic materials for the metabolic reprogramming of cancer cells. BCAT deaminates free BCAAs to form BCKA. It enters the TCA cycle and is used for energy production and fatty acid metabolism to promote cell proliferation.

LAT2 (SLC7A8) was discovered in 1999 [4,27,28]. The structure of LAT2 is similar to another function of LATs that promotes tumor formation is to inhibit cell-damaged T-cell control in the tumor microenvironment. In this pathway, the polycharged amino acids and small neutral amino acids [4]. LAT3 commonly expresses in normal humans [11] and is associated with the development of amino-aciduria [30]. Both LAT1 and LAT2 consist of 12 transmembrane domains that form pathways for their substrates [29]. They bind to the heavy glycoprotein sugar chain in the transmembrane and IDO, large amounts of kyn can be synthesized. Kyn is transported from the cancer cells to T cells by LAT1, in T cells, kyn binds to the aryl hydrocarbon receptor (AHR), which have suggested that 4F2hc lacks amino acid transport activity. Instead, the combined LAT1 and LAT2 units are the only ones with transport capacity [31]. But now, there are different cancer cells [26].

## 2.2. LAT2

bonds. Although 4F2hc does not appear to have a direct substrate transfer function [31], it enables more stable localization of LAT1 and LAT2 on the plasma membrane [32]. Previous studies have suggested that 4F2hc lacks amino acid transport activity. Instead, the combined LAT1 and LAT2 units are the only ones with transport capacity [31]. But now there are different views on it. 4F2hc acts as a molecular chaperone to enable LAT1 and LAT2 to become its final site on the membrane [32]. 4F2hc is required for the transport of LAT1 and LAT2 to the plasma membrane [9], where LAT1 and LAT2 are thought to determine the transport properties of heterodimers. At the same time, increased 4F2hc expression levels in many forms of cancer are associated with poorer prognosis in several studies [33–36] (Figure 2).

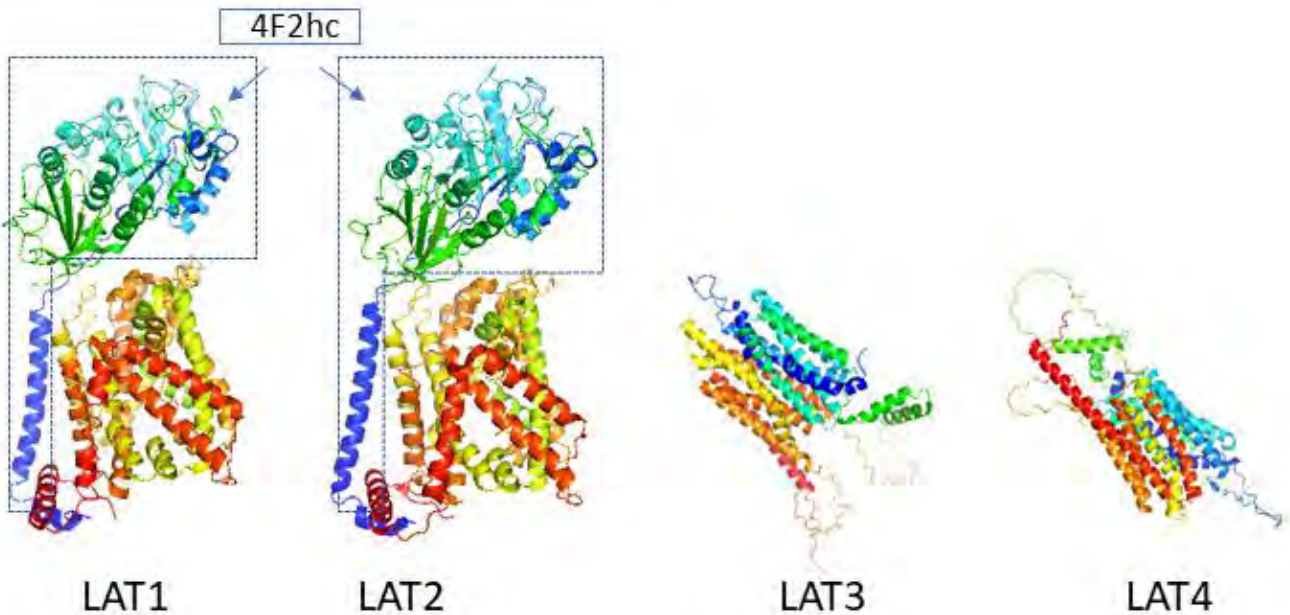


**Figure 2.** The three-dimensional conformation of LATs. Both LAT1 and LAT2 consist of 12 trans-

membrane domains that form pathways for their substrates. They bind to the heavy glycoprotein subunit 4F2hc via disulfide bonds. Unlike LAT1 and LAT2, the biological functions of LAT3 and LAT4 do not require binding to heavy chains and can exist independently. (Images created using PyMol\*, colored by chainbows, the PDB ID: 6IRS, 7CMI, the Uniprot ID: O75387, Q8N370, PyMol\* (version 2.5 Schrodinger, Warren L. DeLano), and RCSB PDB, and UniProt).

LAT3 (SLC43A1) was first named POV1, “Prostate cancer Overexpressed gene 1”, and it was upregulated in prostate cancer as a gene of unknown function [37]. It was really discovered definitively in 2003 [5]. LAT3 is usually expressed in the liver, skeletal muscle, and pancreas [38]. Overall LAT3 expression is low in the kidney, but LAT3 expression is

stronger in the apical plasma membrane of the podocyte foot processes. It shows that LAT3 is important for the development and maintenance of podocyte function and structure [39]. Another study has also shown that LAT3 expression is required for erythrocyte development to produce hemoglobin [40]. LAT3 can be upregulated in response to androgen, which is closely related to leucine uptake and cell proliferation in human prostate cancer cell lines [41].

LAT4 (SLC43A2) was discovered in 2005 and identified by homology with LAT3 [6]. LAT4 is usually expressed in epithelial cells of the small intestine, proximal renal tubules, and thick ascending limbs [6]. However, in mouse models, LAT4 is expressed in the intestine, kidney, brain, white adipose tissue, testis, and heart, but not detected in the liver, showing differences from human expression [6]. The physiological function of LAT4 in these organs is still not fully understood. In LAT4 knockout mice, newborn mice are smaller than wild-type mice, suggesting that LAT4 is important for growth and development [42].

LAT4 (SLC43A2) was discovered in 2005 and identified by homology with LAT3 [6]. LAT4 is usually expressed in epithelial cells of the small intestine, proximal renal tubules, and thick ascending limbs [6]. However, in mouse models, LAT4 is expressed in the intestine, kidney, brain, white adipose tissue, testis, and heart, but not detected in the liver, showing differences from human expression [6]. The physiological function of LAT4 in these organs is still not fully understood. In LAT4 knockout mice, newborn mice are smaller than wild-type mice, suggesting that LAT4 is important for growth and development [42].

LAT4 is not well understood, but it is thought to involve a symport mechanism, in which the transport of amino acids is coupled to the uphill movement of sodium ions against their concentration gradient. The movement of ions and amino acids is driven by the energy generated from the electrochemical gradient established by the sodium/potassium ATPase. The difference between LAT3 and LAT4 lies in their substrate specificity and tissue distribution. LAT3 has a higher affinity for large neutral amino acids, such as leucine and isoleucine [5], while LAT4 has a higher affinity for small neutral amino acids, such as alanine and serine [6] (Figures 1 and 2).

### 3. LATs and PCa

LATs promote PCa progression in several ways:

1. **Amino acid uptake:** LATs increase the uptake of essential amino acids into cancer cells, which supports their growth and survival. After being delivered into cells, these amino acids are used to make proteins, nucleic acids, lipids, and ATP. Compared with normal cells, cancer cells have higher upregulation transporters (LATs), which can promote the entry of foreign amino acids into cells, and the stable acquisition of amino acids by cancer cells is important for cancer growth. By increasing the availability of amino acids, LATs can promote PCa cell proliferation and invasion.
2. **Activation of signaling pathways:** LATs have been shown to activate various signaling pathways, including the mTOR pathway, which is involved in the regulation of cell growth, proliferation, metabolism, and survival. LAT1 [23] and LAT3 [41] are highly expressed in prostate cancer, providing branched-chain amino acids (BCAA) to the mammalian target protein of rapamycin complex (mTORC1), which senses amino acid signaling and promotes cell proliferation through multiple downstream effectors related to gene expression and metabolism [15]. Leucine, which enters the cell via LAT1, binds to the leucine sensor sestrin2. The interaction between leucine and sestrin2 can activate GATOR2 and inhibit GATOR1, thus promoting the function of mTORC1 and achieving the purpose of cell proliferation [16,17]. LATs can regulate mTOR activity by influencing the availability of essential amino acids, such as leucine, that activate the pathway.
3. **Drug resistance:** In PCa cells resistant to antiandrogen therapy (ADT), the expression of some LATs is up-regulated, which may promote the progression of PCa to castration-resistant prostate cancer (CRPC) through androgen receptor variants [43]. Changes in the microenvironment induced by hormone deprivation therapy can alter the expression of LAT1 and LAT3. Reduced androgen receptor signaling may lead to decreased LAT3 expression and, as another consequence, increased LAT1 expression. Changes in the microenvironment induced by hormone deprivation therapy can alter the expression of LAT1 and LAT3. Decreased androgen receptor signaling may lead to decreased LAT3 expression and, as another consequence, the production of the AR-V7 variant, resulting in increased 4F2hc expression, and decreased leucine, resulting in increased LAT1 expression. The two form a dimer that eventually causes leucine to be re-transported into the cell to promote cancer cell proliferation. PCa is transformed into CRPC, which is resistant to ADT treatment.
4. **Promotion of angiogenesis:** LATs have been implicated in the regulation of blood vessel formation (angiogenesis), which is essential for the growth and spread of PCa cells. Tumors grow and evolve through constant crosstalk with the surrounding microenvironment. New evidence suggests that angiogenesis and immunosuppression often occur together in response to this crosstalk [44]. For example, the expression of LAT1 was significantly correlated with the expression of VEGF, CD34, and microvascular density at the primary and metastatic sites [45–48]. VEGF and CD34 are factors related to angiogenesis. LAT1 can also mediate the angiogenesis of miR-126 on primary human pulmonary microvascular endothelial cells by regulating mTOR signaling [49].

5. Others: Increase the uptake of amino acids by inducing hemoglobin maturation [40]. LAT3 expression is required for the development of red blood cells to produce hemoglobin. LAT3 can be upregulated under the action of androgens [41], which leads to the increase of hemoglobin development and increases the way for tumor cells to obtain nutrients from another side, thus promoting their proliferation.

Current studies on prostate cancer and LATs usually focus on LAT1 and LAT3. There are few studies on LAT2 and LAT4. Studies show the main leucine transporters are different in different stages of prostate cancer, especially in the castration-resistant stage of androgen receptor (AR) expression [23,50]. Studies have found that LNCaP cells mainly express LAT3, while LAT1 is mainly expressed in DU145 and PC-3 cells [23,50]. According to Rii's study, LAT3 is highly expressed in LNCaP and C4-2 cells expressing AR, but hardly expressed in AR-negative PC3 and DU145 cells [51]. Changes in the microenvironment, such as starvation or hormone deprivation, can promote cancer formation and alter LAT1 and LAT3 expression. Reduced androgen receptor signaling may lead to decreased LAT3 expression and, as another consequence, increased LAT1 expression [41].

In addition to the common relationships mentioned above, we will describe the relationship between LAT1, 2, 3, 4, and prostate cancer respectively.

### 3.1. LAT1

It has been found that the up-regulation of LAT1 during antiandrogen therapy (ADT) promotes the progression of PCa cells. LAT1 is highly expressed in CRPC cell lines. LAT1 knockdown significantly reduces cell proliferation, migration, and invasion. High LAT1 expression is associated with poor biochemical recurrence-free periods in patients treated with chronic ADT [23]. Another study also confirmed that LAT1 expression is up-regulated at the protein and mRNA levels in 22Rv1 CRPC tumors with chronic ADT [52]. Sugiura demonstrated a potential relationship between AR-V7 and the LAT1-4F2hc complex. AR-V7 activates downstream target genes in the absence of androgens. 4F2hc is one of the downstream target genes of AR-V7. The expression level of 4F2hc in CRPC tissues is significantly increased, which correspondingly suggests poor prognosis of related patients [43]. Furthermore, a study shows ATF4 gene expression is upregulated during metastasis, suggesting that ATF4-mediated amino acid response element-containing gene regulation may be important for the development of metastatic CRPC [53]. ATF4-regulated genes, such as LAT1 and 4F2hc, show low expression in normal prostate tissue and primary prostate cancer, but they are significantly increased in metastatic prostate cancer, suggesting that these transporters are involved in the nutrient supply required for metastatic prostate cancer [53] (Figure 3).

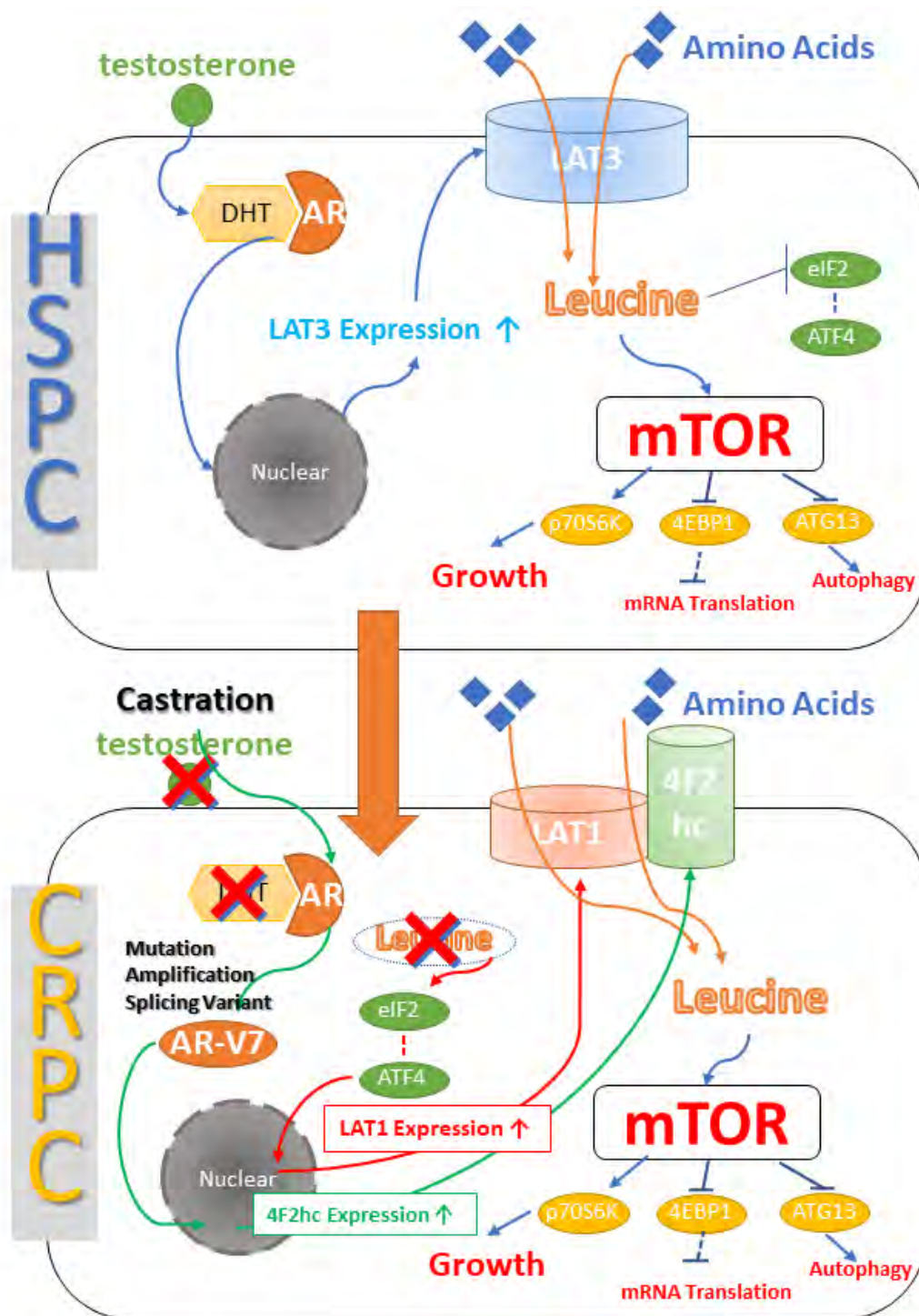


**Figure 3.** LAT is linked to both hormone-sensitive prostate cancer (HSPC) and castration-resistant prostate cancer (CRPC). In untreated HSPC, 5-alpha reductase converts testosterone to dihydrotestosterone (DHT), which binds to the androgen receptor (AR), enters the nucleus, and stimulates LAT3 transcription, resulting in increased LAT3 expression and contributing to the mTOR pathway activation. When hormone therapy is used to treat PCa, testosterone levels fall, resulting in castration, and ARs that no longer bind DHT change, increase, and generate splicing variants. AR-V7, in particular, can enter the nucleus in the absence of testosterone activation, and 4F2hc is present in its downstream signaling. Furthermore, the removal of leucine from the cells results in the lack of eIF2 repression and the admission of ATF4 into the nucleus. It enhances LAT1 expression, and LAT1 and 4F2hc form a dimer, allowing leucine into the cell and promoting tumor cell proliferation [54].

### 3.2. LAT2

LAT2 is reported to be less distributed in malignant tumors except for neuroendocrine tumors [55] and more distributed in normal tissues [3]. Therefore, LAT2 may be used as a reference marker for normal benign tissue or as an indication of a good prognostic outcome. One study [56] examined LAT1-4 expression and its association with clinical outcomes in a combined cohort of more than 18,000 radical prostatectomy specimens. The expression of LAT1-3 in prostate cancer is higher than that in benign tissues except for LAT4. The expressions of LAT2, LAT3, and ASCT2 are negatively correlated with  $GS \geq 8$ , lymph node invasion, and high Decipher score. The lowest decile of LAT3 and ASCT2 expression correlates with the worst MFS. LAT2 and LAT3 expression is associated with better clinical outcomes [56].  $y + LAT2$  (SLC7A6) is an alternative light subunit that constitutes the cationic and neutral amino acid heterodimer transport system  $y + L$ . A study [50] established the castration-resistant prostate cancer (CRPC) model LN-cr with androgen AR expression. Compared with LNCaP,  $y + LAT2$  expression is increased in LN-cr. These results suggest that androgen removal induces the down-regulation of LAT3 and up-regulation of  $y + LAT2$  in LNCaP cells.

### 3.3. LAT3

It is highly expressed in primary PCa [5]. Previous studies have shown that LAT3 expression is reduced in metastatic and/or castration-resistant cancers; therefore, LAT3 expression may be associated with androgen dependence in PCa [53]. In another word, LAT3 is highly expressed in prostate cancer cells that expressed the androgen receptor (AR). LAT3 is highly expressed in LNCaP and C4-2 cells that expressed AR but hardly expressed in PC3 and DU145 cells without AR. LAT3 mediates leucine uptake in LNCaP and PC3 cells [41]. Its expression is increased under the treatment of dihydrotestosterone and reduced under bicalutamide treatment [51]. Growth factors such as EGF activate the PI3K/Akt/mTORC1 signaling pathway, which regulates different protein synthesis programs leading to cell growth. This pathway relies on mTORC1 to detect adequate levels of intracellular amino acids, which inversely regulates LAT3 expression to enhance amino acid access [57]. LAT3 knockdown inhibits phosphorylation of mTOR, eukaryotic translation initiation factor 4EBP1, and ribosomal protein S6K1, but does not inhibit phosphorylation of Akt. And AR knockdown results are similar (Figure 3). Furthermore, as above mentioned, erythropoiesis involves increased uptake of neutral essential amino acids through LAT3 [40]. As red blood cells mature, their transcription profile changes, reflecting altered metabolic states, including induction of genes for iron and heme metabolism, as well as those involved in the amino acid cycle. The mRNA expression of LAT1 and LAT3 is significantly increased in mature red blood cells, but no 4F2hc expression is detected, suggesting that LAT1 may have no transport function [40]. The high expression of LAT3 in prostate cancer will undoubtedly promote the uptake of more amino acids by red blood cells on the other hand.

### 3.4. LAT4

There is currently little research on LAT4 and prostate cancer. A study [52] has shown that LAT4 expression is up-regulated in CRPC cell lines. Another study has found that 18F-labeled amino acids, such as 3-O-methyl-6-18F-fluoro-L-dopa (18F-OMFD) and 18F-fluorodihydroxyphenylalanine (18F-FDOPA), are important imaging agents for PET in vivo tumor display [58,59]. 18F-OMFD appears to be a suitable diagnostic imaging tracer for amino acid transport in poorly differentiated squamous cell head and neck carcinoma with increased LAT1 and LAT4 expression [59]. Similarly, 18F-OMFD and 18F-FDOPA should also have diagnostic values in CRPC with high LAT4 expression [52]. A study found that the expression of LAT4 increases after amino acid ingestion in mouse models treated with N-butyl- (4-hydroxybutyl) nitrosamine (BBN) [60]. However, further studies and evidence on the value of LAT4 in the diagnosis and treatment of prostate cancer are lacking.

Table 1 summarizes the specific relationship between LATs and prostate cancer, as well as the corresponding inhibitors (Table 1).

**Table 1.** The current relationship between LATs and prostate cancer. (Symbol ‘—’ represents that this cell line does not express the corresponding LATs according to the citation paper).

LATs	PCa Cell Lines	Up-Regulation of Expression	Inhibitors	Be Inhibited Effects	Diagnosis/Treatment
LAT1 [23,33,41,43,50,53,61]	LNCAP	↑/—	T3, BCH, JPH 203, ESK242, SKN, OKY-034	Lower proliferation, Higher apoptosis, Lower leucine absorption, Lower mTORC1 activity, Amino acid stress, Reduced tumor metastasis ability.	Used as a PET tracer transporter in the diagnosis of malignant tumors. As a target for targeted therapy.
	C4-2	↑			
	PC3	↑			
	DU145	↑			
	VCAP	↑			
	22Rv1	↑			
LAT2 [55,56]	prostate specimen	↑	BCH	N/A	Associated with a better prognosis.
LAT3 [5,41,51,53,54,62,63]	LNCAP	↑	ESK242, ESK246	Lower proliferation, higher apoptosis, Reduced tumor metastasis ability.	As a tumor marker for HSPC to CRPC transformation, As a targeted therapeutic target.
	C4-2	↑			
	PC3	—			
	DU145	—			
LAT4 [42,52,58,59]	22Rv1 (Simulate the CRPC situation)	↑	N/A	Growth retardation in mouse models.	Possible as a PET tracer target for 18F-labeled amino acids in CRPC.

#### 4. Prostate Cancer Diagnosis by LATs

##### 4.1. LAT1

Among amino acid transporters, LAT1 is selectively hyperactive in a variety of cancer cells [10]. The pathway for enhancing LAT1-mRNA expression is not yet clear but includes carcinogenic Myc and hypoxia-induced factors (HIFs) that can enhance its expression. That suggests the feedforward mechanism of tumor formation [64,65]. LAT1 can be used as a tumor marker for prostate cancer, and LAT1 expression is highly correlated with high proliferation index, stage, and poor prognosis [23,66].

In addition to being a tumor marker, LAT1 will play an important role in the diagnosis as a transporter. In other words, LAT1 selectively delivered drugs can be used for the diagnosis of PCa. LAT1 special use matrix of cancer diagnosis of positron emission computed tomography (PET) is a powerful technology for clinical prostate cancer detection. PET works by detecting the radioactive isotopes labeled on the tracer to find out where the tracer accumulates. Cancer cells accumulate PET tracers, which mimic the nutrients they need to proliferate. (18) F-labeled fluoroalkyl phenylalanine derivatives, as PET tracers, are more likely to bind to LAT1 in tumors, which demonstrates the effectiveness of 18f-labeled aromatic side chain pet tracer in the diagnosis of prostate malignancies [67]. The U.S. Food and Drug Administration approved trans-1-amino-3-18f-flucyclobutane carboxylic acid (anti-[18F]-FACBC) PET to detect prostate cancer in patients with elevated prostate-specific antigen after treatment in 2016 [68]. The utility of LAT1 in PET imaging has been demonstrated in clinical practice.

At present, Japan is further developing a new PET tracer based on LAT1 delivery, the NKO series. The goal is to adopt a simpler and more efficient 18f markup structure. At present, the clinical study in the normal human body has been completed [69].

##### 4.2. LAT3

As mentioned above, the expression level of LAT3 is different in different stages of prostate cancer. Studies have shown that LAT3 is regulated by androgen receptors. LAT3 is significantly reduced in CRPC, and LAT3 is also reduced after androgen deprivation therapy. LAT3 is expected to be a tumor marker to judge the progression of prostate cancer from HSPC to CRPC [41,43,51,53].

#### 4.3. LAT4

As mentioned above, 18F-OMFD has diagnostic value as a PET tracer in CRPCS with high LAT4 expression [59].

#### 5. Inhibitors of LATs and Targeted Therapy of PCa

Inhibitors that target transporters include compounds that transport as a substrate and non-transport compounds that act as blockers or exert an inhibitory effect on isosteroids. As transport inhibitors, the current mainstream view of pharmacology believes that non-transport compounds are superior to transport compounds because non-transport compounds do not accumulate in cells and have high affinity [69]. 2-aminobicyclo-(2,2,2,1)-heptane-2-carboxylic acid (BCH) (Figure 4(Aa)) is a nonmetabolic leucine analogue. BCH is a specific inhibitor of the sodium-independent L system (LAT1, LAT2, LAT3, and LAT4). In the study of LATs, BCH is widely used [53,70]. However, because BCH is delivered as a substrate and has a low specificity and affinity for LAT1, it has not been used at the clinical level. Clinical studies on anti-cancer drugs (inhibitors) targeting LATs mainly focus on LAT1 and LAT3.

Int. J. Mol. Sci. 2023, 24, x FOR PEER REVIEW

11 of 17

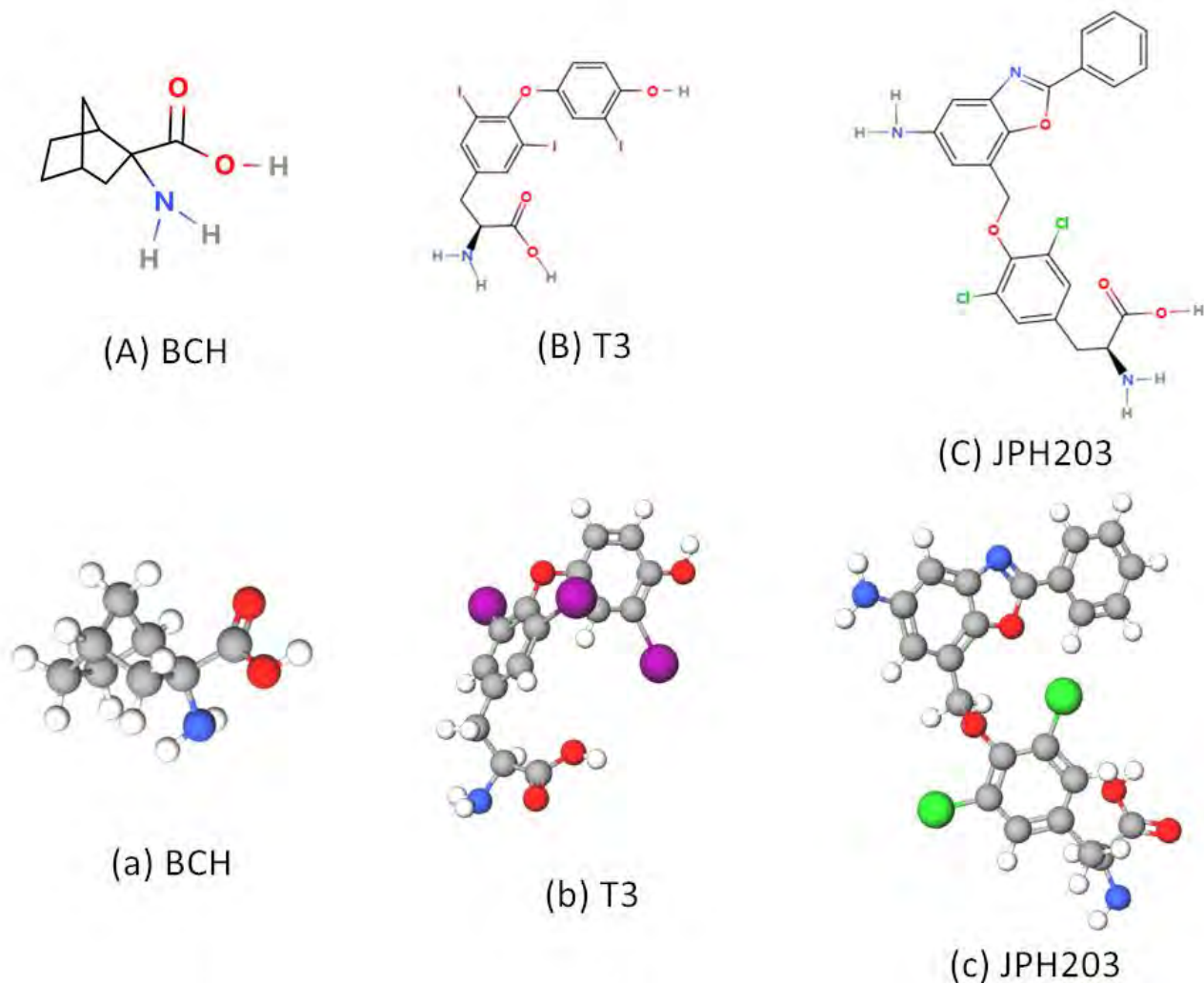


**Figure 4.** The 2D (A–C) and 3D (a–c) structures of LATs inhibitors. (A) BCH is a non-transportable system inhibitor. (B, C) (Bb, Cc) The core of T3 and JPH203 both contain an amino acid backbone and a bulky side chain.

In LAT1, the earliest reported specific LAT1 inhibitor was the thyroid hormone triiodothyronine (T3) (Figure 4(Bb)), which showed a high inhibitory effect (low  $K_i$  value) and was almost non-transportable molecule [71], thus providing an idea for the research and development of LAT1 inhibitors. Therefore, JPH203 (KYT-0353) (Figure 4(Cc)) was successfully developed in 2009 as a non-delivery LAT1-specific inhibitor (LAT1 blocker) [72]. The core structures of T3 and JPH203 both contain an amino acid backbone and a bulky

and was almost non-transportable molecule [71], thus providing an idea for the research and development of LAT1 inhibitors. Therefore, JPH203 (KYT-0353) (Figure 4(Cc)) was successfully developed in 2009 as a non-delivery LAT1-specific inhibitor (LAT1 blocker) [72]. The core structures of T3 and JPH203 both contain an amino acid backbone and a bulky side chain (Figure 4(Bb,Cc)). Then, JPH203 has recently been widely studied as a potent inhibitor of LAT1. JPH203, like T3, has a high affinity and is specific to LAT1, but does not affect LAT2. JPH203 interferes with the constitutive activation of mTORC1 and Akt, reduces c-MyC expression, and triggers a folding protein response mediated by CHOP transcription factors associated with cell death [73]. Since then, several studies have confirmed that JPH203 has a significant inhibitory effect on the growth of common tumor cells. A Phase I clinical study found that JPH203 is well tolerated and provided positive prognostic outcomes in the treatment of biliary tract cancer, with a disease control rate of approximately 60% against biliary tract cancer [74]. The authors are currently planning Phase I and II studies of JPH203 in CRPC. Although JPH203 has been shown in multiple studies to inhibit leucine uptake by tumor cells and has shown concentration-dependent cytotoxicity in vitro or performed well in transplanted tumor models, the human phase I clinical trial is a milestone. In addition, a Japanese research team has developed an SKN series of LAT1 inhibitors similar to T3 and JPH203 (Figure 5(Aa)) [75,76]. In recent years, a research team led by Professor Kanai at Osaka University is developing the OKY series of novel LAT1 inhibitors. Among OKY compounds, OKY-034 shows a high inhibitory effect and specificity against LAT1. The above amino acid LAT1 inhibitors are competitive inhibitors, but OKY-034 has a non-competitive inhibitor style because the structure of OKY-034 does not include the amino acid skeleton. The advantage of non-competitive inhibitors is that only small amounts (low concentrations) are required to show effect, due to the need to react competitively with the endogenous amino acid matrix. In addition, OKY-034 does not require large hydrophobic sites such as T3 and SKN, so it is relatively soluble and can be taken orally. Phase I/IIa trial of OKY-034 safety and efficacy in patients with pancreatic cancer is being conducted at Osaka University Hospital (UMIN000036395) [69]. It is believed that these drugs will soon be used to treat prostate cancer.

However, compared with LAT1, there is less evidence to support the general role of LAT2 in cancer, and it is more likely to be used as a benign biomarker. Since there is no known drug substrate or inhibitor targeting LAT2 except for BCH, unfortunately, no studies have been conducted on LAT2 as a tumor-targeted therapy. However, LAT2's innate ability to transport amino acids makes it a potential target for the diagnosis or treatment of prostate cancer based on amino acids.

In terms of LAT3, LAT3 knockdown inhibits cell proliferation, migration, invasion, and phosphorylation of p70S6K and 4EBP-1 [51]. Studies have shown that ESK242 and ESK246 are effective inhibitors of LAT3 (Figure 5(Bb)). ESK246 preferentially inhibits leucine transport through LAT3, while ESK242 can inhibit both LAT1 and LAT3. Its use in prostate cancer cells further suggests that ESK246 is a potent leucine uptake inhibitor that leads to decreased mTORC1 signaling, cyclin expression, and cell proliferation [63]. New anti-prostate cancer therapies targeting LAT3 may build on this.

not include the amino acid skeleton. The endogenous amino acid matrix. In addition, OKY-034 does not require large hydrophobic sites such as T3 and SKN, so it is relatively soluble and can be taken orally. Phase I/IIa trial of OKY-034 safety and efficacy in patients with pancreatic cancer is being conducted at Osaka University Hospital (UMIN000036395) [69]. It is believed that these drugs will soon be used to treat prostate cancer.

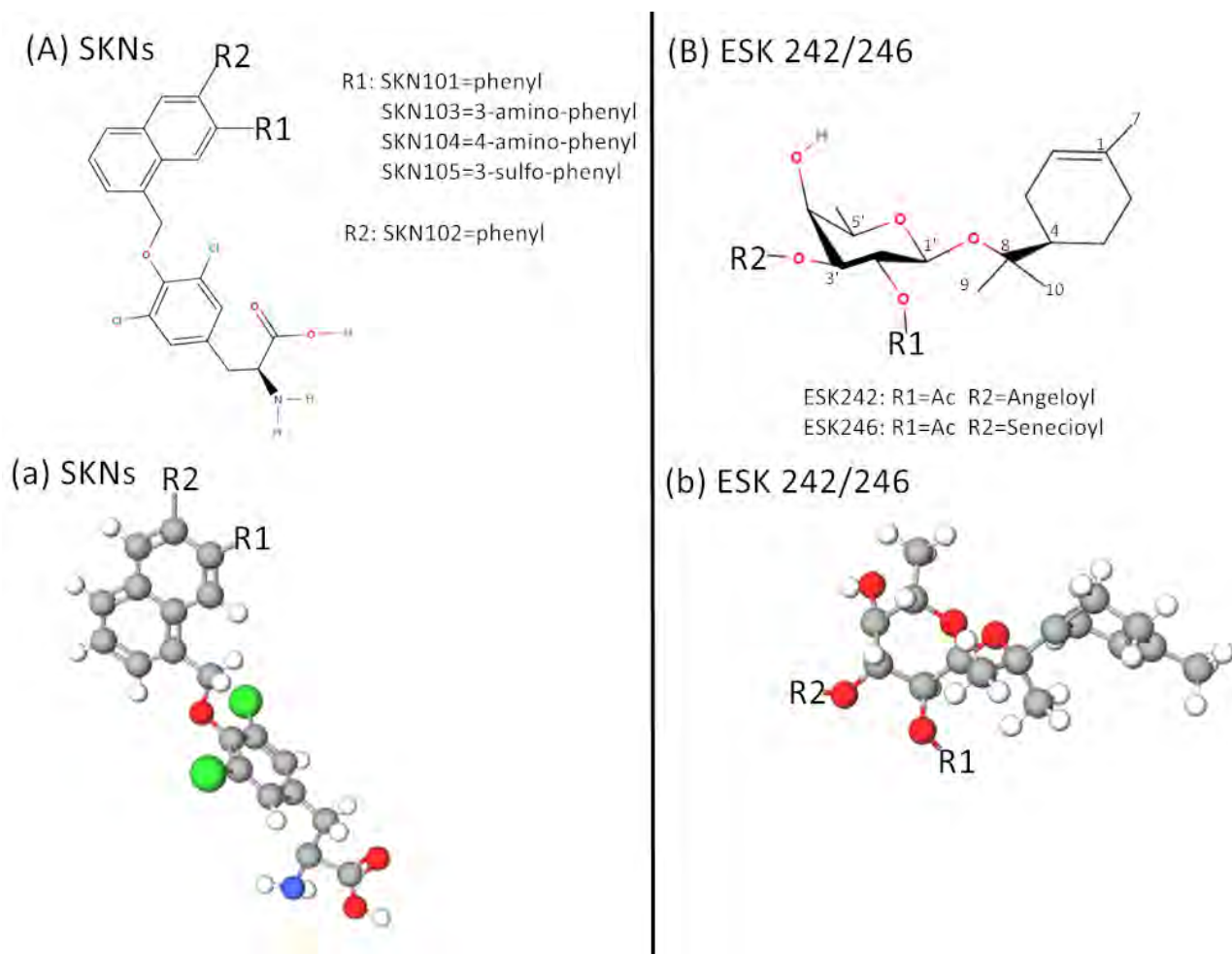


**Figure 5.** The 2D (A,B) and 3D (a,b) structures of LAT1 inhibitor SKN series and LAT3 inhibitor ESK series. (Aa) SKN series and JPH203 have similar molecular structures. (Bb) The ESK series shows a different molecular structure from LAT1 inhibitors such as T3, JPH203, and SKNs. ESK242 can inhibit both LAT1 and LAT3.

**6. Conclusions**

However, compared with LAT1, there is less evidence to support the general role of LAT2 in cancer, and it is more likely to be used as a benign biomarker. Since there is no known drug substrate or inhibitor targeting LAT2 except for BCL1, unfortunately, no studies have been conducted on LAT2 as a tumor-targeted therapy. However, LAT2's innate ability to transport amino acids makes it a potential target for the diagnosis or treatment of prostate cancer. Moreover, the specific expression levels of LAT1 and LAT3 have the value of judging the development of prostate cancer to castration-resistant prostate cancer, which can effectively guide the anti-androgen therapy of prostate cancer and predict the possibility of biochemical recurrence. In addition, LAT1 and LAT3 are also significant therapeutic targets for prostate cancer. Several inhibitors targeting the corresponding LATs are in clinical trials and are expected to be widely used in the targeted therapy of prostate cancer in the near future.

**Author Contributions:** X.Z. contributed to collecting bibliography, preparing figures, and writing; S.S. (Shinichi Sakamoto) contributed to drawing structure figures and writing; J.W., S.P., S.S. (Shinpei Saito), T.S. and Y.I. contributed to collecting bibliography; S.S. (Shinichi Sakamoto), N.A. and T.I. contributed to supervision of all the activities. The first draft of the manuscript was prepared by X.Z. and S.S. (Shinichi Sakamoto) revised the manuscript. All authors have read and agreed to the published version of the manuscript.

**Funding:** The present study was supported by grants from Grant-in-Aid for Scientific Research (C) (20K09555 to S.S.), Grant-in-Aid for Scientific Research (B) (20H03813 to T.I.), and the Japan China Sasakawa Medical Fellowship (to X.Z.).

**Institutional Review Board Statement:** Not applicable.

**Informed Consent Statement:** Not applicable.

**Data Availability Statement:** Not applicable.

**Conflicts of Interest:** The authors declare no conflict of interest. The funders had no role in the design of the study; in the collection, analyses, or interpretation of data; in the writing of the manuscript, or in the decision to publish the results.

## Abbreviation

PCa	prostate cancer
LAT	L-type amino acid transporter
mTOR	mammalian target of rapamycin
EAA	essential amino acid
SLC	solute vector family
TCR	T cell receptors
BCAA	branched-chain amino acid
mTORC	mammalian target of rapamycin complex
GAP	GTPase-activating protein
GATOR	GAP activity toward Rags
BCAT	branched-chain amino acid transferase
BCKA	branched-chain keto acid
Kyn	kynurenine
TDO	2, 3-Deoxygenase
IDO	indoleamine 2, 3-Dioxygenase
AHR	aryl hydrocarbon receptor
ADT	antiandrogen therapy
CRPC	castration-resistant prostate cancer
AR	androgen receptor
HSPC	hormone-sensitive prostate cancer
18F-OMFD	3-O-methyl-6-18F-fluoro-L-dopa
18F-FDOPA	18F-fluorodihydroxyphenylalanine
BBN	N-butyl- (4-hydroxybutyl) nitrosamine
HIFs	hyposia-induced factors
PET	positron emission computed tomography
BCH	2-aminobicyclo-(2,2,2,1)-heptane-2-carboxylic acid

## References

1. Eagle, H. Nutrition Needs of Mammalian Cells in Tissue Culture. *Science* **1955**, *122*, 501–504. [[CrossRef](#)]
2. Qi, W.; Guan, Q.; Sun, T.; Cao, Y.; Zhang, L.; Guo, Y. Improving detection sensitivity of amino acids in thyroid tissues by using phthalic acid as a mobile phase additive in hydrophilic interaction chromatography-electrospray ionization-tandem mass spectrometry. *Anal. Chim. Acta* **2015**, *870*, 75–82. [[CrossRef](#)] [[PubMed](#)]
3. Kanai, Y.; Segawa, H.; Miyamoto, K.-I.; Uchino, H.; Takeda, E.; Endou, H. Expression Cloning and Characterization of a Transporter for Large Neutral Amino Acids Activated by the Heavy Chain of 4F2 Antigen (CD98). *J. Biol. Chem.* **1998**, *273*, 23629–23632. [[CrossRef](#)] [[PubMed](#)]
4. Segawa, H.; Fukasawa, Y.; Miyamoto, K.-I.; Takeda, E.; Endou, H.; Kanai, Y. Identification and Functional Characterization of a Na<sup>+</sup>-independent Neutral Amino Acid Transporter with Broad Substrate Selectivity. *J. Biol. Chem.* **1999**, *274*, 19745–19751. [[CrossRef](#)]
5. Babu, E.; Kanai, Y.; Chairoungdua, A.; Kim, D.K.; Iribe, Y.; Tangtrongsup, S.; Jutabha, P.; Li, Y.; Ahmed, N.; Sakamoto, S.; et al. Identification of a Novel System L Amino Acid Transporter Structurally Distinct from Heterodimeric Amino Acid Transporters. *J. Biol. Chem.* **2003**, *278*, 43838–43845. [[CrossRef](#)] [[PubMed](#)]
6. Bodoy, S.; Martín, L.; Zorzano, A.; Palacín, M.; Estévez, R.; Bertran, J. Identification of LAT4, a Novel Amino Acid Transporter with System L Activity. *J. Biol. Chem.* **2005**, *280*, 12002–12011. [[CrossRef](#)] [[PubMed](#)]

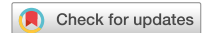
7. Wang, Q.; Holst, J. L-type amino acid transport and cancer: Targeting the mTORC1 pathway to inhibit neoplasia. *Am. J. Cancer Res.* **2015**, *5*, 1281–1294.
8. Siegel, R.L.; Miller, K.D.; Fuchs, H.E.; Jemal, A. Cancer statistics, 2022. *CA Cancer J. Clin.* **2022**, *72*, 7–33. [[CrossRef](#)]
9. Mastroberardino, L.; Spindler, B.; Pfeiffer, R.; Skelly, P.J.; Loffing, J.; Shoemaker, C.B.; Verrey, F. Amino-acid transport by heterodimers of 4F2hc/CD98 and members of a permease family. *Nature* **1998**, *395*, 288–291. [[CrossRef](#)]
10. Zhao, X.; Sakamoto, S.; Maimaiti, M.; Anzai, N.; Ichikawa, T. Contribution of LAT1-4F2hc in Urological Cancers via Toll-like Receptor and Other Vital Pathways. *Cancers* **2022**, *14*, 229. [[CrossRef](#)]
11. Nakada, N.; Mikami, T.; Hana, K.; Ichinoe, M.; Yanagisawa, N.; Yoshida, T.; Endou, H.; Okayasu, I. Unique and selective expression of L-amino acid transporter 1 in human tissue as well as being an aspect of oncofetal protein. *Histol. Histopathol.* **2014**, *29*, 217–227. [[CrossRef](#)]
12. Puris, E.; Gynther, M.; Auriola, S.; Huttunen, K.M. L-Type amino acid transporter 1 as a target for drug delivery. *Pharm. Res.* **2020**, *37*, 88. [[CrossRef](#)]
13. Ohgaki, R.; Ohmori, T.; Hara, S.; Nakagomi, S.; Kanai-Azuma, M.; Kaneda-Nakashima, K.; Okuda, S.; Nagamori, S.; Kanai, Y. Essential Roles of L-Type Amino Acid Transporter 1 in Syncytiotrophoblast Development by Presenting Fusogenic 4F2hc. *Mol. Cell. Biol.* **2017**, *37*, e00427-16. [[CrossRef](#)] [[PubMed](#)]
14. Sinclair, L.V.; Rolf, J.; Emslie, E.; Shi, Y.-B.; Taylor, P.M.; Cantrell, D.A. Control of amino-acid transport by antigen receptors coordinates the metabolic reprogramming essential for T cell differentiation. *Nat. Immunol.* **2013**, *14*, 500–508. [[CrossRef](#)] [[PubMed](#)]
15. Fuchs, B.C.; Bode, B.P. Amino acid transporters ASCT2 and LAT1 in cancer: Partners in crime? *Semin. Cancer Biol.* **2005**, *15*, 254–266. [[CrossRef](#)] [[PubMed](#)]
16. Wolfson, R.L.; Chantranupong, L.; Saxton, R.A.; Shen, K.; Scaria, S.M.; Cantor, J.R.; Sabatini, D.M. Sestrin2 is a leucine sensor for the mTORC1 pathway. *Science* **2016**, *351*, 43–48. [[CrossRef](#)]
17. Wolfson, R.L.; Sabatini, D.M. The Dawn of the Age of Amino Acid Sensors for the mTORC1 Pathway. *Cell Metab.* **2017**, *26*, 301–309. [[CrossRef](#)] [[PubMed](#)]
18. Furuya, M.; Horiguchi, J.; Nakajima, H.; Kanai, Y.; Oyama, T. Correlation of L-type amino acid transporter 1 and CD98 expression with triple negative breast cancer prognosis. *Cancer Sci.* **2012**, *103*, 382–389. [[PubMed](#)]
19. Kaira, K.; Oriuchi, N.; Imai, H.; Shimizu, K.; Yanagitani, N.; Sunaga, N.; Hisada, T.; Kawashima, O.; Iijima, H.; Ishizuka, T.; et al. Expression of L-type amino acid transporter 1 (LAT1) in neuroendocrine tumors of the lung. *Pathol. Res. Pract.* **2008**, *204*, 553–561. [[CrossRef](#)]
20. Ebara, T.; Kaira, K.; Shioya, M.; Asao, T.; Takahashi, T.; Sakurai, H.; Kanai, Y.; Kuwano, H.; Nakano, T. L-type Amino-acid Transporter 1 Expression Predicts the Response to Preoperative Hyperthermo-chemoradiotherapy for Locally Advanced Rectal Cancer. *Int. J. Radiat. Oncol.* **2010**, *78*, S330–S331. [[CrossRef](#)]
21. Betsunoh, H.; Fukuda, T.; Anzai, N.; Nishihara, D.; Mizuno, T.; Yuki, H.; Masuda, A.; Yamaguchi, Y.; Abe, H.; Yashi, M.; et al. Increased expression of system large amino acid transporter (LAT)-1 mRNA is associated with invasive potential and unfavorable prognosis of human clear cell renal cell carcinoma. *BMC Cancer* **2013**, *13*, 509. [[CrossRef](#)]
22. Maimaiti, M.; Sakamoto, S.; Yamada, Y.; Sugiura, M.; Rii, J.; Takeuchi, N.; Imamura, Y.; Furihata, T.; Ando, K.; Higuchi, K.; et al. Expression of L-type amino acid transporter 1 as a molecular target for prognostic and therapeutic indicators in bladder carcinoma. *Sci. Rep.* **2020**, *10*, 1292. [[CrossRef](#)]
23. Xu, M.; Sakamoto, S.; Matsushima, J.; Kimura, T.; Ueda, T.; Mizokami, A.; Kanai, Y.; Ichikawa, T. Up-Regulation of LAT1 during Antiandrogen Therapy Contributes to Progression in Prostate Cancer Cells. *J. Urol.* **2015**, *195*, 1588–1597. [[CrossRef](#)] [[PubMed](#)]
24. Nawashiro, H.; Otani, N.; Shinomiya, N.; Fukui, S.; Ooigawa, H.; Shima, K.; Matsuo, H.; Kanai, Y.; Endou, H. L-type amino acid transporter 1 as a potential molecular target in human astrocytic tumors. *Int. J. Cancer* **2006**, *119*, 484–492. [[CrossRef](#)] [[PubMed](#)]
25. Neinast, M.; Murashige, D.; Arany, Z. Branched Chain Amino Acids. *Annu. Rev. Physiol.* **2019**, *81*, 139–164. [[CrossRef](#)] [[PubMed](#)]
26. Opitz, C.A.; Litztenburger, U.M.; Sahm, F.; Ott, M.; Tritschler, I.; Trump, S.; Schumacher, T.; Jestaedt, L.; Schrenk, D.; Weller, M.; et al. An endogenous tumour-promoting ligand of the human aryl hydrocarbon receptor. *Nature* **2011**, *478*, 197–203. [[CrossRef](#)] [[PubMed](#)]
27. Pineda, M.; Fernández, E.; Torrents, D.; Estévez, R.; López, C.; Camps, M.; Lloberas, J.; Zorzano, A.; Palacín, M. Identification of a Membrane Protein, LAT-2, That Co-expresses with 4F2 Heavy Chain, an L-type Amino Acid Transport Activity with Broad Specificity for Small and Large Zwitterionic Amino Acids. *J. Biol. Chem.* **1999**, *274*, 19738–19744. [[CrossRef](#)] [[PubMed](#)]
28. Rossier, G.; Meier, C.; Bauch, C.; Summa, V.; Sordat, B.; Verrey, F.; Kühn, L.C. LAT2, a New Basolateral 4F2hc/CD98-associated Amino Acid Transporter of Kidney and Intestine. *J. Biol. Chem.* **1999**, *274*, 34948–34954. [[CrossRef](#)]
29. Verrey, F.; Closs, E.L.; Wagner, C.A.; Palacín, M.; Endou, H.; Kanai, Y. CATs and HATs: The SLC7 family of amino acid transporters. *Pflug. Arch.* **2004**, *447*, 532–542. [[CrossRef](#)]
30. Braun, D.; Wirth, E.K.; Wohlgemuth, F.; Reix, N.; Klein, M.O.; Grüters, A.; Köhrle, J.; Schweizer, U. Aminoaciduria, but normal thyroid hormone levels and signalling, in mice lacking the amino acid and thyroid hormone transporter Slc7a8. *Biochem. J.* **2011**, *439*, 249–255. [[CrossRef](#)] [[PubMed](#)]
31. Napolitano, L.; Scalise, M.; Galluccio, M.; Pochini, L.; Albanese, L.M.; Indiveri, C. LAT1 is the transport competent unit of the LAT1/CD98 heterodimeric amino acid transporter. *Int. J. Biochem. Cell Biol.* **2015**, *67*, 25–33. [[CrossRef](#)]

32. Nakamura, E.; Sato, M.; Yang, H.; Miyagawa, F.; Harasaki, M.; Tomita, K.; Matsuoka, S.; Noma, A.; Iwai, K.; Minato, N. 4F2 (CD98) Heavy Chain Is Associated Covalently with an Amino Acid Transporter and Controls Intracellular Trafficking and Membrane Topology of 4F2 Heterodimer. *J. Biol. Chem.* **1999**, *274*, 3009–3016. [[CrossRef](#)]
33. Maimaiti, M.; Sakamoto, S.; Sugiura, M.; Kanesaka, M.; Fujimoto, A.; Matsusaka, K.; Xu, M.; Ando, K.; Saito, S.; Wakai, K.; et al. The heavy chain of 4F2 antigen promote prostate cancer progression via SKP-2. *Sci. Rep.* **2021**, *11*, 1–14. [[CrossRef](#)] [[PubMed](#)]
34. Horita, Y.; Kaira, K.; Kawasaki, T.; Mihara, Y.; Sakuramoto, S.; Yamaguchi, S.; Okamoto, K.; Ryozaawa, S.; Kanai, Y.; Yasuda, M.; et al. Expression of LAT1 and 4F2hc in Gastroenteropancreatic Neuroendocrine Neoplasms. *In Vivo* **2021**, *35*, 2425–2432. [[CrossRef](#)]
35. Chatsirisupachai, K.; Kitdumrongthum, S.; Panvongsa, W.; Janpipatkul, K.; Worakitchanon, W.; Lertjintanakit, S.; Wongtrakoon-gate, P.; Chairoungdua, A. Expression and roles of system L amino acid transporters in human embryonal car-cinoma cells. *Andrology* **2020**, *8*, 1844–1858. [[CrossRef](#)] [[PubMed](#)]
36. Kaira, K.; Kawashima, O.; Endoh, H.; Imaizumi, K.; Goto, Y.; Kamiyoshihara, M.; Sugano, M.; Yamamoto, R.; Osaki, T.; Tanaka, S.; et al. Expression of amino acid transporter (LAT1 and 4F2hc) in pulmonary pleomorphic carcinoma. *Hum. Pathol.* **2018**, *84*, 142–149. [[CrossRef](#)]
37. Cole, K.A.; Chuaqui, R.F.; Katz, K.; Pack, S.; Zhuang, Z.; Cole, C.E.; Lyne, J.C.; Linehan, W.M.; Liotta, L.A.; Emmert-Buck, M.R. cDNA Sequencing and Analysis of POV1 (PB39): A Novel Gene Up-regulated in Prostate Cancer. *Genomics* **1998**, *51*, 282–287. [[CrossRef](#)] [[PubMed](#)]
38. Fukuhara, D.; Kanai, Y.; Chairoungdua, A.; Babu, E.; Bessho, F.; Kawano, T.; Akimoto, Y.; Endou, H.; Yan, K. Protein characterization of NA<sup>+</sup>-independent system L amino acid transporter 3 in mice: A potential role in supply of branched-chain amino acids under nutrient starvation. *Am. J. Pathol.* **2007**, *170*, 888–898. [[CrossRef](#)]
39. Sekine, Y.; Nishibori, Y.; Akimoto, Y.; Kudo, A.; Ito, N.; Fukuhara, D.; Kurayama, R.; Higashihara, E.; Babu, E.; Kanai, Y.; et al. Amino Acid Transporter LAT3 Is Required for Podocyte Development and Function. *J. Am. Soc. Nephrol.* **2009**, *20*, 1586–1596. [[CrossRef](#)]
40. Chung, J.; Bauer, D.E.; Ghamari, A.; Nizzi, C.P.; Deck, K.M.; Kingsley, P.D.; Yien, Y.Y.; Huston, N.C.; Chen, C.; Schultz, I.J. The mTORC1/4E-BP pathway coordinates hemoglobin production with L-leucine availability. *Sci. Signal.* **2015**, *8*, ra34. [[CrossRef](#)]
41. Wang, Q.; Bailey, C.G.; Ng, C.; Tiffen, J.; Thoeng, A.; Minhas, V.; Lehman, M.L.; Hendy, S.C.; Buchanan, G.; Nelson, C.C.; et al. Androgen Receptor and Nutrient Signaling Pathways Coordinate the Demand for Increased Amino Acid Transport during Prostate Cancer Progression. *Cancer Res.* **2011**, *71*, 7525–7536. [[CrossRef](#)] [[PubMed](#)]
42. Guetg, A.; Mariotta, L.; Bock, L.; Herzog, B.; Fingerhut, R.; Camargo, S.M.R.; Verrey, F. Essential amino acid transporter Lat4 (Slc43a2) is required for mouse development. *J. Physiol.* **2015**, *593*, 1273–1289. [[CrossRef](#)] [[PubMed](#)]
43. Sugiura, M.; Sato, H.; Okabe, A.; Fukuyo, M.; Mano, Y.; Shinohara, K.-I.; Rahmutulla, B.; Higuchi, K.; Maimaiti, M.; Kanesaka, M. Identification of AR-V7 downstream genes commonly targeted by AR/AR-V7 and specifically targeted by AR-V7 in castration resistant prostate cancer. *Transl. Oncol.* **2021**, *14*, 100915. [[CrossRef](#)]
44. Solimando, A.G.; De Summa, S.; Vacca, A.; Ribatti, D. Cancer-Associated Angiogenesis: The Endothelial Cell as a Checkpoint for Immunological Patrolling. *Cancers* **2020**, *12*, 3380. [[CrossRef](#)]
45. Kaira, K.; Sunose, Y.; Ohshima, Y.; Ishioka, N.S.; Arakawa, K.; Ogawa, T.; Sunaga, N.; Shimizu, K.; Tominaga, H.; Oriuchi, N.; et al. Clinical significance of L-type amino acid transporter 1 expression as a prognostic marker and potential of new targeting therapy in biliary tract cancer. *BMC Cancer* **2013**, *13*, 482. [[CrossRef](#)]
46. Kaira, K.; Oriuchi, N.; Shimizu, K.; Ishikita, T.; Higuchi, T.; Imai, H.; Yanagitani, N.; Sunaga, N.; Hisada, T.; Ishizuka, T. Correlation of angiogenesis with 18F-FMT and 18F-FDG uptake in non-small cell lung cancer. *Cancer Sci.* **2009**, *100*, 753–758. [[CrossRef](#)]
47. Okubo, S.; Zhen, H.-N.; Kawai, N.; Nishiyama, Y.; Haba, R.; Tamiya, T. Correlation of l-methyl-11C-methionine (MET) uptake with l-type amino acid transporter 1 in human gliomas. *J. Neuro-Oncol.* **2010**, *99*, 217–225. [[CrossRef](#)]
48. Haining, Z.; Kawai, N.; Miyake, K.; Okada, M.; Okubo, S.; Zhang, X.; Fei, Z.; Tamiya, T. Relation of LAT1/4F2hc expression with pathological grade, proliferation and angiogenesis in human gliomas. *BMC Clin. Pathol.* **2012**, *12*, 4. [[CrossRef](#)]
49. Cao, D.; Mikosz, A.M.; Ringsby, A.J.; Anderson, K.C.; Beatman, E.L.; Koike, K.; Petrache, I. MicroRNA-126-3p Inhibits Angiogenic Function of Human Lung Microvascular Endothelial Cells via LAT1 (L-Type Amino Acid Transporter 1)-Mediated mTOR (Mammalian Target of Rapamycin) Signaling. *Arter. Thromb. Vasc. Biol.* **2020**, *40*, 1195–1206. [[CrossRef](#)]
50. Otsuki, H.; Kimura, T.; Yamaga, T.; Kosaka, T.; Suehiro, J.-I.; Sakurai, H. Prostate Cancer Cells in Different Androgen Receptor Status Employ Different Leucine Transporters. *Prostate* **2016**, *77*, 222–233. [[CrossRef](#)]
51. Rii, J.; Sakamoto, S.; Sugiura, M.; Kanesaka, M.; Fujimoto, A.; Yamada, Y.; Maimaiti, M.; Ando, K.; Wakai, K.; Xu, M.; et al. Functional analysis of LAT3 in prostate cancer: Its downstream target and relationship with androgen receptor. *Cancer Sci.* **2021**, *112*, 3871–3883. [[CrossRef](#)]
52. Malviya, G.; Patel, R.; Salji, M.; Martinez, R.S.; Repiscak, P.; Mui, E.; Champion, S.; Mrowinska, A.; Johnson, E.; AlRasheedi, M.; et al. 18F-Fluciclovine PET metabolic imaging reveals prostate cancer tumour heterogeneity associated with disease resistance to androgen deprivation therapy. *EJNMMI Res.* **2020**, *10*, 143. [[CrossRef](#)]
53. Wang, Q.; Tiffen, J.; Bailey, C.G.; Lehman, M.L.; Ritchie, W.; Fazli, L.; Metierre, C.; Feng, Y.; Li, E.; Gleave, M.; et al. Targeting Amino Acid Transport in Metastatic Castration-Resistant Prostate Cancer: Effects on Cell Cycle, Cell Growth, and Tumor Development. *J. Natl. Cancer Inst.* **2013**, *105*, 1463–1473. [[CrossRef](#)]

54. Kokal, M.; Mirzakhani, K.; Pungsrinont, T.; Baniahmad, A. Mechanisms of Androgen Receptor Agonist- and Antagonist-Mediated Cellular Senescence in Prostate Cancer. *Cancers* **2020**, *12*, 1833. [\[CrossRef\]](#)
55. Barollo, S.; Bertazza, L.; Fernando, S.W.; Censi, S.; Cavedon, E.; Galuppini, F.; Pennelli, G.; Fassina, A.; Citton, M.; Rubin, B.; et al. Overexpression of L-Type Amino Acid Transporter 1 (LAT1) and 2 (LAT2): Novel Markers of Neuroendocrine Tumors. *PLoS ONE* **2016**, *11*, e0156044. [\[CrossRef\]](#)
56. Chu, C.E.; Alshalalfa, M.; Sjöström, M.; Zhao, S.G.; Liu, Y.; Chou, J.; Herlemann, A.; Mahal, B.; Kishan, A.U.; Spratt, D.E.; et al. Prostate-specific Membrane Antigen and Fluciclovine Transporter Genes are Associated with Variable Clinical Features and Molecular Subtypes of Primary Prostate Cancer. *Eur. Urol.* **2021**, *79*, 717–721. [\[CrossRef\]](#)
57. Zhang, B.K.; Moran, A.M.; Bailey, C.G.; Rasko, J.E.J.; Holst, J.; Wang, Q. EGF-activated PI3K/Akt signalling coordinates leucine uptake by regulating LAT3 expression in prostate cancer. *Cell Commun. Signal.* **2019**, *17*, 83. [\[CrossRef\]](#)
58. Feral, C.; Tissot, F.; Tosello, L.; Fakhry, N.; Sebag, F.; Pacak, K.; Taïeb, D. 18F-fluorodihydroxyphenylalanine PET/CT in pheochromocytoma and paraganglioma: Relation to genotype and amino acid transport system L. *Eur. J. Nucl. Med.* **2016**, *44*, 812–821. [\[CrossRef\]](#)
59. Haase, C.; Bergmann, R.; Fuechtner, F.; Hoepfing, A.; Pietzsch, J. L-Type Amino Acid Transporters LAT1 and LAT4 in Cancer: Uptake of 3-O-Methyl-6- 18F-Fluoro-L-Dopa in Human Adenocarcinoma and Squamous Cell Carcinoma In Vitro and In Vivo. *J. Nucl. Med.* **2007**, *48*, 2063–2071. [\[CrossRef\]](#)
60. Xie, X.-L.; Kakehashi, A.; Wei, M.; Yamano, S.; Takeshita, M.; Yunoki, T.; Wanibuchi, H. L-Leucine and L-isoleucine enhance growth of BBN-induced urothelial tumors in the rat bladder by modulating expression of amino acid transporters and tumorigenesis-associated genes. *Food Chem. Toxicol.* **2013**, *59*, 137–144. [\[CrossRef\]](#)
61. Patel, M.; Dalvi, P.; Gokulgandhi, M.; Kesh, S.; Kohli, T.; Pal, D.; Mitra, A.K. Functional characterization and molecular expression of large neutral amino acid transporter (LAT1) in human prostate cancer cells. *Int. J. Pharm.* **2013**, *443*, 245–253. [\[CrossRef\]](#)
62. Martinez, R.S.; Salji, M.J.; Rushworth, L.; Ntala, C.; Rodriguez Blanco, G.; Hedley, A.; Clark, W.; Peixoto, P.; Hervouet, E.; Renaude, E. SLFN5 Regulates LAT1-Mediated mTOR Activation in Castration-Resistant Prostate Cancer. *Cancer Res.* **2021**, *81*, 3664–3678. [\[CrossRef\]](#)
63. Wang, Q.; Grkovic, T.; Font, J.; Bonham, S.; Pouwer, R.H.; Bailey, C.G.; Moran, A.M.; Ryan, R.M.; Rasko, J.E.; Jormakka, M.; et al. Monoterpene Glycoside ESK246 from *Pittosporum* Targets LAT3 Amino Acid Transport and Prostate Cancer Cell Growth. *ACS Chem. Biol.* **2014**, *9*, 1369–1376. [\[CrossRef\]](#)
64. Yue, M.; Jiang, J.; Gao, P.; Liu, H.; Qing, G. Oncogenic MYC Activates a Feedforward Regulatory Loop Promoting Essential Amino Acid Metabolism and Tumorigenesis. *Cell Rep.* **2017**, *21*, 3819–3832. [\[CrossRef\]](#)
65. Zhang, B.; Chen, Y.; Shi, X.; Zhou, M.; Bao, L.; Hatanpaa, K.J.; Patel, T.; DeBerardinis, R.J.; Wang, Y.; Luo, W. Regulation of branched-chain amino acid metabolism by hypoxia-inducible factor in glioblastoma. *Cell. Mol. Life Sci.* **2020**, *78*, 195–206. [\[CrossRef\]](#)
66. Sakata, T.; Ferdous, G.; Tsuruta, T.; Satoh, T.; Baba, S.; Muto, T.; Ueno, A.; Kanai, Y.; Endou, H.; Okayasu, I. L-type amino-acid transporter 1 as a novel biomarker for high-grade malignancy in prostate cancer. *Pathol. Int.* **2009**, *59*, 7–18. [\[CrossRef\]](#)
67. Wang, L.; Qu, W.; Lieberman, B.P.; Plössl, K.; Kung, H.F. Synthesis, uptake mechanism characterization and biological evaluation of 18F labeled fluoroalkyl phenylalanine analogs as potential PET imaging agents. *Nucl. Med. Biol.* **2011**, *38*, 53–62. [\[CrossRef\]](#)
68. Laudicella, R.; Albano, D.; Alongi, P.; Argiroffi, G.; Bauckneht, M.; Baldari, S.; Bertagna, F.; Boero, M.; De Vincentis, G.; Del Sole, A.; et al. 18F-Facbc in Prostate Cancer: A Systematic Review and Meta-Analysis. *Cancers* **2019**, *11*, 1348. [\[CrossRef\]](#)
69. Wiriyaermlkul, P.; Moriyama, S.; Kongpracha, P.; Nagamori, S. Drug Discovery Targeting an Amino Acid Transporter for Diagnosis and Therapy. *Yakugaku Zasshi* **2021**, *141*, 501–510. [\[CrossRef\]](#)
70. Baniyadi, S.; Chairoungdua, A.; Iribe, Y.; Kanai, Y.; Endou, H.; Aisaki, K.-I.; Igarashi, K.; Kanno, J. Gene expression profiles in t24 human bladder carcinoma cells by inhibiting an l-type amino acid transporter, lat1. *Arch. Pharmacol. Res.* **2007**, *30*, 444–452. [\[CrossRef\]](#)
71. Morimoto, E.; Kanai, Y.; Kim, D.K.; Chairoungdua, A.; Choi, H.W.; Wempe, M.F.; Anzai, N.; Endou, H. Establishment and Characterization of Mammalian Cell Lines Stably Expressing Human L-Type Amino Acid Transporters. *J. Pharmacol. Sci.* **2008**, *108*, 505–516. [\[CrossRef\]](#)
72. Oda, K.; Hosoda, N.; Endo, H.; Saito, K.; Tsujihara, K.; Yamamura, M.; Sakata, T.; Anzai, N.; Wempe, M.F.; Kanai, Y.; et al. L-Type amino acid transporter 1 inhibitors inhibit tumor cell growth. *Cancer Sci.* **2009**, *101*, 173–179. [\[CrossRef\]](#)
73. Rosilio, C.; Nebout, M.; Imbert, V.; Griessinger, E.; Neffati, Z.; Benadiba, J.; Hagenbeek, T.; Spits, H.; Reverso, J.; Ambrosetti, D. L-type amino-acid transporter 1 (LAT1): A therapeutic target supporting growth and survival of T-cell lymphoblastic lymphoma/T-cell acute lymphoblastic leukemia. *Leukemia* **2015**, *29*, 1253–1266. [\[CrossRef\]](#)
74. Okano, N.; Naruge, D.; Kawai, K.; Kobayashi, T.; Nagashima, F.; Endou, H.; Furuse, J. First-in-human phase I study of JPH203, an L-type amino acid transporter 1 inhibitor, in patients with advanced solid tumors. *Investig. New Drugs* **2020**, *38*, 1495–1506. [\[CrossRef\]](#)

75. Kongpracha, P.; Nagamori, S.; Wiriyasermkul, P.; Tanaka, Y.; Kaneda, K.; Okuda, S.; Ohgaki, R.; Kanai, Y. Structure-activity relationship of a novel series of inhibitors for cancer type transporter L-type amino acid transporter 1 (LAT1). *J. Pharmacol. Sci.* **2017**, *133*, 96–102. [[CrossRef](#)]
76. Nagamori, S.; Wiriyasermkul, P.; Okuda, S.; Kojima, N.; Hari, Y.; Kiyonaka, S.; Mori, Y.; Tominaga, H.; Ohgaki, R.; Kanai, Y. Structure–activity relations of leucine derivatives reveal critical moieties for cellular uptake and activation of mTORC1-mediated signaling. *Amino Acids* **2016**, *48*, 1045–1058. [[CrossRef](#)]

**Disclaimer/Publisher’s Note:** The statements, opinions and data contained in all publications are solely those of the individual author(s) and contributor(s) and not of MDPI and/or the editor(s). MDPI and/or the editor(s) disclaim responsibility for any injury to people or property resulting from any ideas, methods, instructions or products referred to in the content.



OPEN

## Machine-learning predicts time-series prognosis factors in metastatic prostate cancer patients treated with androgen deprivation therapy

Shinpei Saito<sup>1,5</sup>, Shinichi Sakamoto<sup>1✉</sup>, Kosuke Higuchi<sup>2</sup>, Kodai Sato<sup>1,5</sup>, Xue Zhao<sup>1</sup>, Ken Wakai<sup>3</sup>, Manato Kanesaka<sup>1</sup>, Shuhei Kamada<sup>1</sup>, Nobuyoshi Takeuchi<sup>1</sup>, Tomokazu Sazuka<sup>1</sup>, Yusuke Imamura<sup>1</sup>, Naohiko Anzai<sup>4</sup>, Tomohiko Ichikawa<sup>1</sup> & Eiryō Kawakami<sup>5,6,7</sup>

Machine learning technology is expected to support diagnosis and prognosis prediction in medicine. We used machine learning to construct a new prognostic prediction model for prostate cancer patients based on longitudinal data obtained from age at diagnosis, peripheral blood and urine tests of 340 prostate cancer patients. Random survival forest (RSF) and survival tree were used for machine learning. In the time-series prognostic prediction model for metastatic prostate cancer patients, the RSF model showed better prediction accuracy than the conventional Cox proportional hazards model for almost all time periods of progression-free survival (PFS), overall survival (OS) and cancer-specific survival (CSS). Based on the RSF model, we created a clinically applicable prognostic prediction model using survival trees for OS and CSS by combining the values of lactate dehydrogenase (LDH) before starting treatment and alkaline phosphatase (ALP) at 120 days after treatment. Machine learning provides useful information for predicting the prognosis of metastatic prostate cancer prior to treatment intervention by considering the nonlinear and combined impacts of multiple features. The addition of data after the start of treatment would allow for more precise prognostic risk assessment of patients and would be beneficial for subsequent treatment selection.

Prostate cancer is one of the most common carcinomas, with an increasing incidence worldwide<sup>1</sup>. In Japan, prostate cancer was the leading cause of cancer and sixth leading cause of cancer-related deaths in 2016<sup>2</sup>. Deeper understanding of prostate cancer and the intrinsic function of androgens has led to the development of androgen deprivation therapy (ADT). ADT is the mainstay treatment for locally advanced and metastatic prostate cancer. ADT is also a treatment option for elderly patients with non-metastatic prostate cancer or those in poor general condition who are not candidates for surgery or radiation therapy. Prostate-specific antigen (PSA) is used as a prostate cancer-specific tumor marker that acts as a first guide and plays a key role in determining treatment efficacy of ADT. Recent reports have demonstrated that the modified Glasgow Prognostic Score (mGPS), lactate dehydrogenase (LDH) and alkaline phosphatase (ALP) levels, Eastern Cooperative Oncology Group (ECOG) performance status, and Gleason score are associated with different prognoses<sup>3,4</sup>.

The prognosis of prostate cancer varies considerably depending on whether the disease is non-metastatic or metastatic<sup>5</sup>. Many prognostic studies on metastatic castration-resistant prostate cancer (mCRPC) have been reported, while less information is available on non-castrated metastatic prostate cancer (NCMPC). Among the few reports available, a prognostic prediction model was published by Glass et al. in 2003<sup>6</sup> that classified patients

<sup>1</sup>Department of Urology, Graduate School of Medicine, Chiba University, 1-8-1 Inohana, Chuo-Ku, Chiba, Chiba 260-8670, Japan. <sup>2</sup>Kimitsu Chuo Hospital, Kisarazu, Chiba, Japan. <sup>3</sup>Teikyo University Chiba Medical Center, Ichihara, Chiba, Japan. <sup>4</sup>Department of Pharmacology, Graduate School of Medicine, Chiba University, Chiba, Chiba, Japan. <sup>5</sup>Department of Artificial Intelligence Medicine, Graduate School of Medicine, Chiba University, Chiba, Chiba, Japan. <sup>6</sup>Advanced Data Science Project (ADSP), RIKEN Information R&D and Strategy Headquarters, RIKEN, Kanagawa, Japan. <sup>7</sup>Institute for Advanced Academic Research (IAAR), Chiba University, Chiba, Chiba, Japan. ✉email: rbatbat1@gmail.com

into three prognostic groups according to four risk factors: bone lesion localization, performance status, PSA, and Gleason score. Based on the model proposed by Glass et al., Gravis et al. proposed a prediction model<sup>7</sup> that is excellent in that it only uses a single feature, ALP, which is obtained in routine clinical practice. However, the performance of the prognostic prediction model is insufficient, with a concordance index (C-index) of 0.64. To further improve prediction accuracy, it would be necessary to consider the time variation and interaction of the factors used for the prediction<sup>8</sup>.

Developments in computer technology have improved analytical methods for handling large-scale data, and machine learning has attracted attention also in the medical field. Machine-learning techniques are commonly used for data-driven diagnostic and prognostic predictions<sup>9,10</sup>. The greatest advantage of using machine learning is that it can be used to account for the combined, nonlinear effects of numerous variables and can make precise individualized predictions for heterogeneous patient populations. In recent years, machine learning-based survival analysis has been used in various carcinomas, handling many variables and enabling prognostic prediction with high accuracy<sup>11–13</sup>. In addition to cancer prognostic prediction, there are many other areas where machine learning can contribute to biomedical research, such as drug interaction analysis<sup>14,15</sup>.

Therefore, the purpose of this study was to develop a clinically applicable prognostic prediction model for prostate cancer treated with androgen deprivation therapy based on multiple features using machine learning. We then additionally examined the impact on prediction accuracy of incorporating features after the start of treatment. To ensure applicability in clinical practice, this study used features obtained routinely in medical practice, such as peripheral blood sampling and urinalysis.

## Result

**Patient background.** This study included 340 patients with prostate cancer. Of these, 30 patients who had started treatment at other hospitals were excluded (Fig. S1). A final total of 310 patients were included in the study, comprising 207 and 103 patients in the training and test cohorts, respectively. The median age was 74 years, and the median initial PSA level was 40.365. The rates of Gleason score  $\geq 8$  was 54.2%. The rate of metastasis was 41.6% (Table 1). No significant differences were observed between the training and test cohorts in patient backgrounds. Among the 36 features used as explanatory variables, only uric acid (UA) was significantly different between the training and test cohorts (Table 2).

**Prognostic prediction at the start of treatment.** To evaluate the usefulness of multiple variables for predicting prostate cancer prognosis, 36 features including age, peripheral blood tests, and urinalysis were used in the analysis. To maintain impartiality among models and avoid multicollinearity among features, the variables were first selected using RSF based on permutation importance calculated in the training cohort. Selected top important variables with positive permutation importance were used in subsequent RSF and Cox proportional hazards analyses. In addition, we created a prediction model for PSA (a tumor marker for prostate cancer) alone and compared its accuracy using the C-index (Fig. 1A). The C-indices for prediction in test cohort using the Cox proportional hazards model were 0.573, 0.488, and 0.582 for PFS, OS, and CSS, respectively. The corresponding C-indices for prediction using PSA alone were 0.684, 0.656, and 0.774, respectively. Finally, the corresponding mean C-indices (standard deviation) with RSF were 0.681 (0.002), 0.603 (0.005), and 0.832 (0.004), respectively. In terms of prediction at the start of treatment, the conventional prediction using PSA was almost as accurate as the RSF in predicting PFS, OS, and CSS, respectively. Next, we calculated the prognostic accuracy of the RSF model created above when applied separately to metastatic and non-metastatic prostate cancer patients. The results revealed improved OS prediction accuracy in metastatic prostate cancer, while, for non-metastatic tumors, predictive performance was poor for all predictions (Fig. 1B). We identified PSA as an important predictor in RSF for predicting PFS and LDH as an important predictor of OS and CSS (Fig. 1C–E).

**Prognostic predictions considering temporal changes after the start of treatment.** We further aimed to improve the prediction of metastatic prostate cancer by considering post-treatment changes. Patients with metastatic prostate cancer were assigned to the same training and test cohort as in the pretreatment analysis. In this analysis, the C-indices of the Cox proportional hazards model and prediction model using only PSA were calculated for comparison with the RSF model (Fig. 2). For predicting OS and CSS, the RSF model was more accurate than the other models: for the RSF model, it had the highest C-index (standard deviation) for predicting PFS at 150 days post-treatment at 0.766 (0.011), and at 120 days post-treatment the C-index for

Background	All patients (N = 310)	Training cohort (N = 207)	Test cohort (N = 103)	P value
Age, years (range)	74 (46–93)	74 (46–90)	74 (48–93)	0.2617
Initial PSA, ng/dL (range)	40.365 (0.19–13,050)	39.31 (2.05–13,050)	42.55 (0.19–6421.08)	0.6853
Gleason score $\geq 8$ , n (%)	168 (54.2)	116 (56)	52 (50.5)	0.3748
T $\geq 3$ , n (%)	193 (62.3)	128 (61.8)	65 (63.1)	0.8995
N+, n (%)	81 (26.1)	52 (25.1)	29 (28.2)	0.5848
M+, n (%)	129 (41.6)	87 (42)	42 (40.8)	0.9028

**Table 1.** Clinical backgrounds of 310 patients with prostate cancer. T  $\geq 3$  means tumor stage 3 or greater, N+ means lymph node metastasis, M+ means metastasis.

Factor	All patients (N = 310)	Training cohort (N = 207)	Test cohort (N = 103)	P value
Age (years)	74 (46–93)	74 (46–90)	74 (48–93)	0.2617
Initial PSA (ng/dL)	40.365 (0.19–13,050)	39.31 (2.05–13,050)	42.55 (0.19–6421.08)	0.6853
AST (U/L)	22 (11–129)	22 (12–95)	23 (11–129)	0.9234
ALT (U/L)	17 (5–102)	17 (5–102)	17 (5–80)	0.9014
LDH (U/L)	193.5 (82–4621)	197 (119–833)	192 (82–4621)	0.2807
GTP (U/L)	32 (9–358)	32.323 (10–215)	31.703 (9–358)	0.2882
TP (g/dL)	7 (5.1–8.6)	7 (5.1–8.4)	6.9 (5.1–8.6)	0.5483
Alb (g/dL)	4.1 (2.5–4.9)	4.1 (2.5–4.9)	4.1 (2.6–4.8)	0.9776
UA (mg/dL)	5.8 (2.2–12)	5.727 (2.2–9.2)	6 (3.4–12)	0.0414
UN (mg/dL)	16 (5–58)	16 (5–58)	16 (8–33)	0.4691
CRE (mg/dL)	0.84 (0.52–8.02)	0.84 (0.52–8.02)	0.84 (0.59–2.01)	0.417
Tbil (mg/dL)	0.7 (0.2–2.8)	0.7 (0.2–2.8)	0.7 (0.3–2.3)	0.4782
Dbil (mg/dL)	0.1 (0–0.3)	0.1 (0–0.3)	0.1 (0–0.3)	0.7917
TCHO (mg/dL)	186.2185 (101–303)	185 (101–275)	187.591 (119–303)	0.056
TG (mg/dL)	125.2795 (45–912)	121 (47–912)	136.711 (45–285)	0.8275
Ca (mg/dL)	9 (6.7–11.6)	9 (7.7–10.7)	8.9 (6.7–11.6)	0.6029
Na (mmol/L)	140 (130–146)	140 (130–146)	140 (132–144)	0.9252
K (mmol/L)	4.21845 (3.1–6.6)	4.2 (3.1–6.6)	4.3 (3.1–5.4)	0.2421
Cl (mmol/L)	106 (95–116)	106 (96–116)	105.693 (95–111)	0.8685
WBC ( $\times 10^3/\mu\text{L}$ )	6.2 (2.4–19.7)	6.2 (2.4–12.8)	6.3 (2.5–19.7)	0.4734
RBC ( $\times 10^6/\mu\text{L}$ )	4.33 (1.93–6.49)	4.35 (1.93–6.1)	4.29 (2.82–6.49)	0.9218
Hb (g/dL)	13.5 (5.5–18.3)	13.5 (5.5–17.6)	13.5 (8.1–18.3)	0.8833
HCT (%)	40 (16.5–53.8)	39.8 (16.5–51.9)	40.2 (24.3–53.8)	0.7497
MCV (fL)	92.4 (72.3–114)	92.3 (75.9–114)	92.9 (72.2–110)	0.6529
MCH (pg)	31.1 (22.5–38.1)	31.1 (24.6–37.5)	31.1 (22.5–38.1)	0.9092
MCHC (%)	33.6 (30.8–36.3)	33.6 (30.8–36.3)	33.6 (30.8–36.2)	0.4757
PLT ( $\times 10^3/\mu\text{L}$ )	206 (18–466)	205 (18–466)	211 (84–433)	0.5377
ALP (U/L)	247.5 (110–9481)	248 (110–9481)	246 (123–2469)	0.6496
PT (s)	11.4541 (9.9–20.4)	11.4022 (9.9–19.6)	11.66675 (10–20.4)	0.3152
PTINR	1.00371 (0.9–1.88)	1.00321 (0.9–1.76)	1.006855 (0.9–1.88)	0.6916
BS (mg/dL)	113.178 (74–282)	115.544 (74–282)	107.5 (86–213)	0.0984
CHE (U/L)	287 (112–539)	287 (115–539)	286.5 (112–468)	0.5798
CRP (mg/dL)	0.2 (0–24.9)	0.2 (0–24.9)	0.16444 (0–8.8)	0.1746
UpH	6 (5–8)	6 (5–8)	6 (5–8)	0.7532
URBC (/HPF)	1 (0–50)	1 (0–50)	1 (0–50)	0.7784
UWBC (/HPF)	1 (0–50)	1 (0–30)	1 (0–50)	0.2623

**Table 2.** Characteristics of analysis factor. The data in the brackets indicate a range of values.

predicting OS and CSS were 0.89 (0.006) and 0.883 (0.006), respectively. The Cox proportional hazards model and RSF had similar predictive performance in predicting PFS at 150 days after treatment initiation. On the other hand, the prediction performance of RSF was appreciably better than the other two models in predicting OS and CSS. Compared to the other prognostic prediction models, the RSF forecasting model tended to have less variation in forecast accuracy depending on the time of year. While RSF was able to predict prognosis for metastatic prostate cancer with relatively high accuracy, it was difficult to predict prognosis for non-metastatic prostate cancer with high accuracy (Fig. S2). In this prognostic analysis of metastatic prostate cancer patients, the addition of the Gleason score, an important pathologic factor in prostate cancer, as a predictor did not result in a notable improvement in prognostic accuracy (Fig. S3). The distribution of Gleason scores in patients with metastatic prostate cancer is shown in Table S1.

**Permutation importance in RSF analysis.** Feature importance can be used to explain the contribution of explanatory variables in machine learning predictions<sup>16</sup>. We used permutation importance, a type of feature importance, to evaluate the contribution of explanatory variables in the RSF. Permutation importance at the time of prediction when the C-index was maximum in each of the RSF analyses described above is presented in Fig. 2D–F. For PFS prediction at 150 days after the start of treatment, the most important variable was PSA after treatment. For the prediction of OS and CSS at 120 days after the start of treatment, the most important factors were LDH before treatment and ALP after treatment. For both OS and CSS prediction, PSA levels before and after treatment were not included as an important predictor.

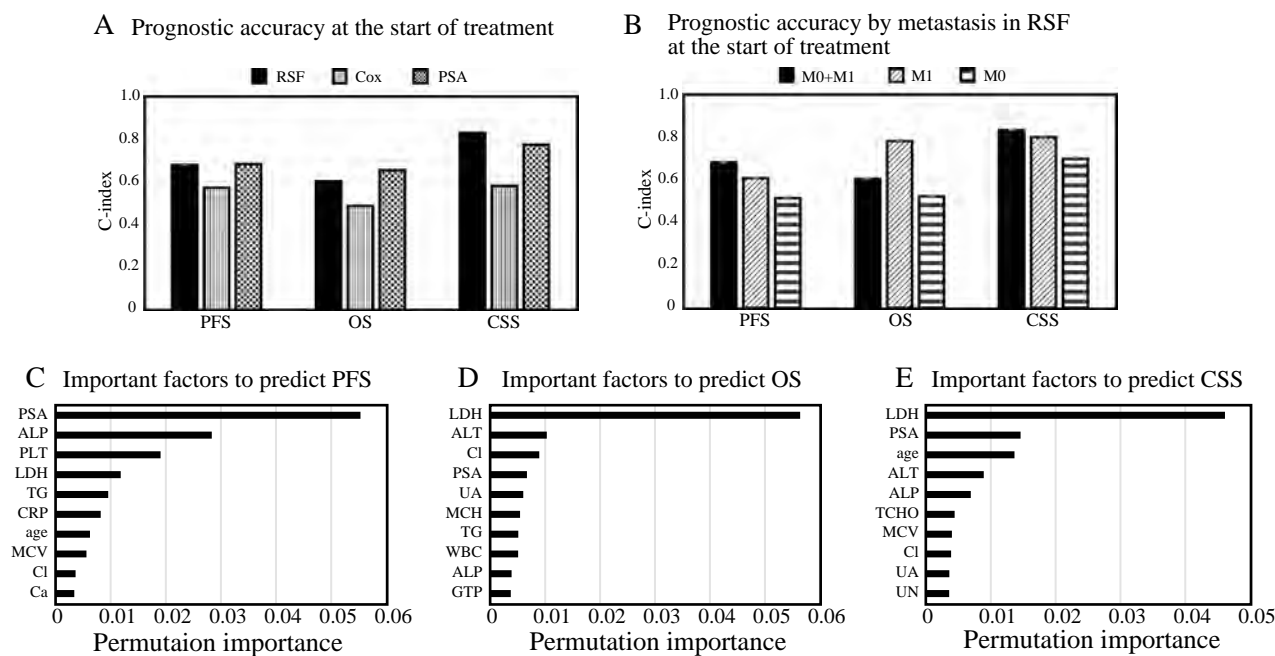


**Figure 1.** Comparison of accuracy of prognostic prediction models. (A) Comparison of C-index for each prognostic prediction model. Black, shaded, and horizontal bars indicate RSF, Cox proportional hazards, and PSA models, respectively. (B) Comparison of C-index for application of RSF model to patients with metastatic and non-metastatic prostate cancer. Black, striped, and dotted bars indicate all patients with prostate cancer, patients with metastatic prostate cancer, and patients with non-metastatic prostate cancer, respectively. (C to E) Permutation importance in prediction of progression (C), overall survival (D), and cancer specific survival (E) based on the RSF model.

**Construction of survival trees based on RSF.** As described in the previous section, prognosis prediction using RSF exhibited excellent accuracy. However, since RSF is an ensemble learning method with multiple survival trees and requires many explanatory variables, it is not easy to use it for prognostic prediction in real clinical practice. Therefore, we constructed a simplified survival tree model with a few most important variables in the RSF model. Since the contribution of post-treatment PSA was predominantly large in predicting PFS prognosis, and the benefit of combining multiple variables by survival tree was limited, we focused only on OS and CSS and constructed a survival tree model based on the top five important variables in the RSF models at 120 days after the start of treatment. The obtained survival trees predicting OS and CSS both consisted of LDH before treatment initiation and ALP 120 days after the start of treatment (Fig. 3A,C). The cut-off values of pre-treatment LDH and post-treatment ALP in the prediction models of OS and CSS were 248.5 IU/L and 342.5/326.5 U/L, respectively. The C-index for prediction accuracy was 0.85 for both OS and CSS. Based on these survival trees, three patient populations were identified that were associated with OS and CSS prognosis: the first was a very poor prognosis population with high preoperative LDH (> 248.5 IU/L), in which about 70% of patients would die within 5 years; the population with LDH < 248.5 IU/L was further divided into two groups based on post-treatment ALP. The group with high ALP is at intermediate risk and has a 5-year survival rate of about 70%. The population with low LDH before treatment and low ALP after treatment had a very good prognosis, with a 5-year survival rate exceeding 90% (Fig. 3B,D).

## Discussion

Compared to conventional statistical analysis, machine learning can handle a large number and variety types of variables, and the machine can automatically learn and discover rules and patterns underlying the data. Various analyses using machine learning have been reported to improve the diagnostic rates of imaging and biopsy tests for prostate cancer<sup>17,18</sup>. However, prognostic analyses using machine learning for ADT remain scarce. In this study, we developed an approach to predict the prognosis of metastatic prostate cancer treatment over time: at the start of treatment and after the start of treatment. Pre-treatment and post-treatment features were combined to achieve a more accurate prediction.

We attempted to predict prognosis for both non-metastatic and metastatic prostate cancer, but it was difficult to predict prognosis in patients with non-metastatic prostate cancer (Fig. S2). The RSF model at the start of treatment showed improved predictive accuracy in metastatic prostate cancer patients, while it showed decreased accuracy in non-metastatic prostate cancer patients. This may be due to the fact that non-metastatic prostate cancer patients in this study had a smaller proportion of cancer deaths than metastatic prostate cancer patients, and included more senility and death from other causes, which are difficult to predict from clinical laboratory data. Moreover, prognostic factors for non-metastatic prostate cancer are limited, with only a few factors, such

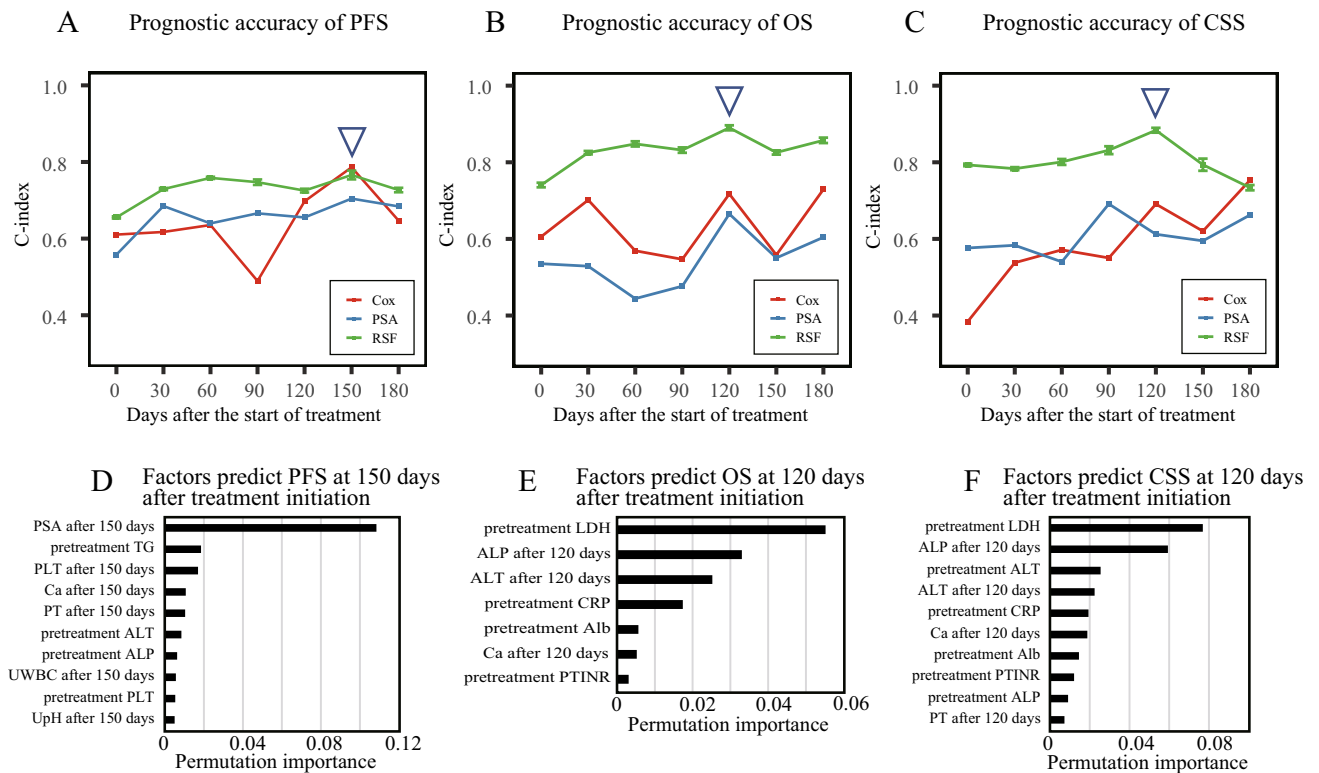


**Figure 2.** Time-series of prognostic accuracy for patients with metastatic prostate cancer. (A to C) Accuracy of prediction of progression (A), overall survival (B), and cancer specific survival (C). The green, red, and blue lines indicate the RSF, Cox proportional hazards, and prognostic PSA-based models, respectively. The triangle mark indicates the time point at which prediction accuracy was the highest for RSF prediction. Error bars represent standard deviations of 10 independent RSF. Permutation importance in prediction of progression at 150 days after treatment initiation (D), overall survival at 120 days after treatment initiation (E), and cancer-specific survival at 120 days after treatment initiation (F). The number of factors was defined as the top 10 factors or those with positive importance.

as PSA doubling time, reported in the literature<sup>19–21</sup>. Therefore, we focused on predicting the prognosis of metastatic prostate cancer. In this study, the RSF model was more accurate than other models in predicting OS and CSS in time-series metastatic prostate cancer. On the other hand, there was no significant difference in PFS prediction. First, the reason for the lack of significant difference in PFS prediction accuracy may be that factors other than PSA were less important in predicting PFS, since the definition of relapse in this study was biological relapse, which was defined as an increase in PSA. Second, the reason for the superior accuracy of the RSF model in predicting OS and CSS could be that parameters other than PSA are important as predictors in predicting OS and CSS, as shown by the results of Permutation Importance. Furthermore, regarding the difference between the RSF model and the Cox proportional hazards model, the RSF model may have been able to make more accurate predictions for many parameters in terms of its ability to make nonlinear predictions. However, since over-fitting should also be considered in this respect, we believe that validation using external data will be necessary in the future. Regarding the tumor marker PSA, our previous study reported no difference in OS according to initial PSA levels in patients with metastatic prostate cancer<sup>22</sup>. For prognostic factors other than PSA, the modified Glasgow Prognostic Score (mGPS), Eastern Cooperative Oncology Group (ECOG) performance status, LDH, ALP, and Gleason Score have been reported as prognostic factors for metastatic prostate cancer<sup>3,4</sup>. Among Japanese patients with de novo metastatic prostate cancer, LDH and C-reactive protein (CRP) have been reported as independent risk factors for OS in analyses identifying true high-risk groups that meet the CHAARTED or LATITUDE criteria<sup>23</sup>. Several studies support the results of this study. However, these were all prognostic analysis based on data at the start of treatment and did not include post-treatment changes. While prognostic predictions based on data at the start of treatment are important, the course of treatment affects the prognosis, and in some cases the actual prognosis differs from the initial risk assessment. To identify such cases and enable a more accurate prognosis, it is necessary to add post-treatment data as predictors and to update the prediction. In this study, we could first identify the poor prognosis group based on LDH at the start of treatment for both OS and CSS, and further classified the remaining patients into two groups with different prognoses using ALP after the start of treatment. This suggests that additional risk assessment during the course of treatment, in addition to risk classification at the start of treatment, can provide a more accurate prognosis. From a pathological perspective, we used the Gleason score in the RSF analysis, which has been used in existing risk classifications, but this did not clearly improve the C-index. Patients with metastatic prostate cancer tend to have high Gleason scores, and in fact, Gleason score  $\geq 8$  accounted for more than 70% of the patients in this case group.

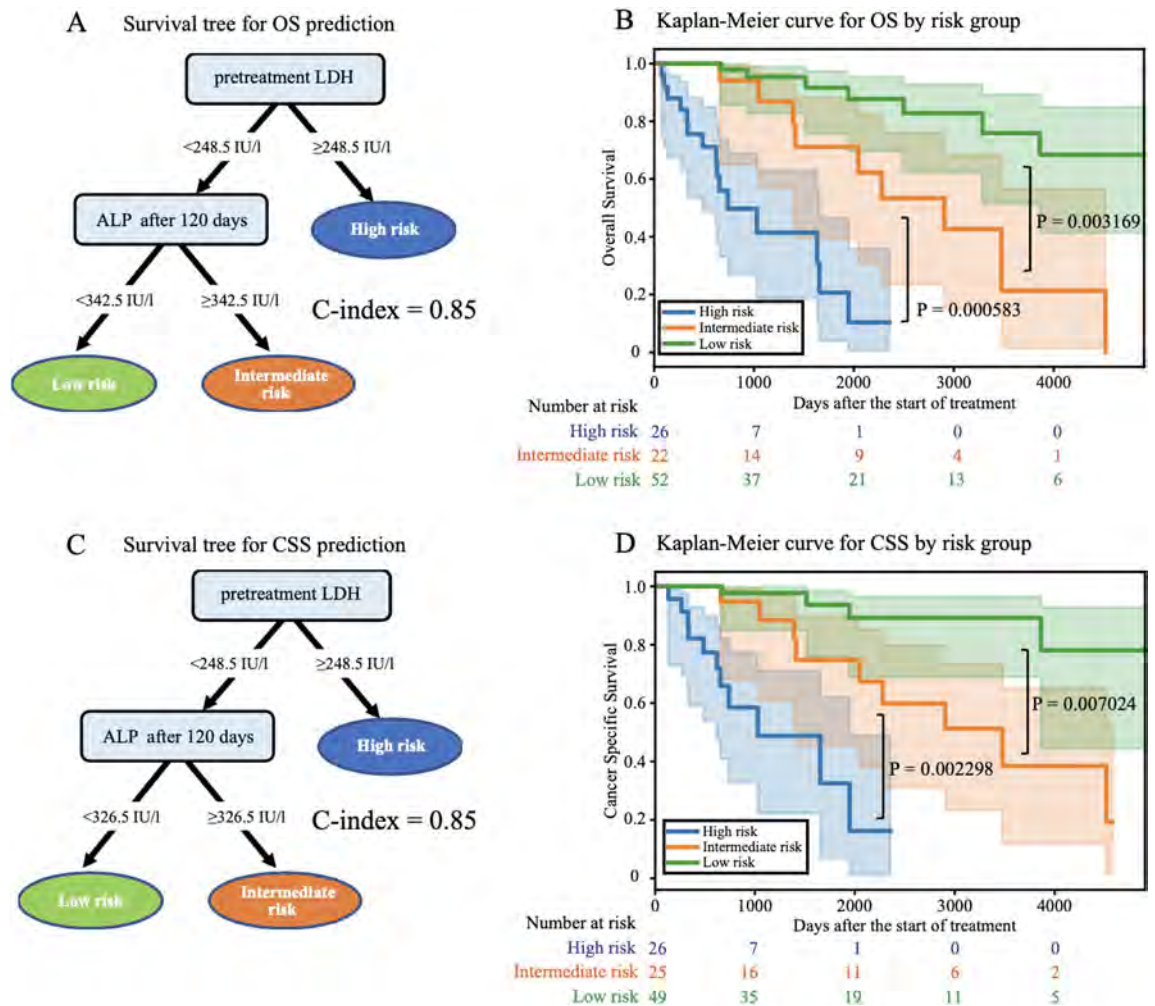


**Figure 3.** Survival tree predicting overall survival (A) and cancer-specific survival (C). Kaplan–Meier curves of survival tree prognostic classification results for overall survival prediction (B) and cancer-specific survival prediction (D). P-values were calculated by the log-rank test.

Gravis et al. reported a prediction model for NCMPC based on the prediction model proposed by Glass et al.<sup>7</sup>. They claimed that ALP levels at the start of treatment (normal vs. abnormal) were the strongest predictor of OS. This prediction model had a C-index of 0.64, was simpler than the prediction model developed by Glass et al., and exhibited comparable performance. The C-index of the model reported by Gravis et al. was 0.72 in the analysis using the data in this study. The C-index for our RSF model in this study using the data at the start of treatment was 0.74. Although our RSF model was only slightly more accurate than the previously reported model, the C-index was improved to 0.85 in this study by creating an algorithm using a survival tree with the addition of time-series data. The new algorithm for metastatic prostate cancer we have created based on the survival tree made predictions using two variables (pre-treatment LDH and post-treatment ALP) with a C-index of 0.85, which was higher than the accuracy of previous prediction models. LDH and ALP values can be obtained from routine blood tests and can be used for time-series evaluation.

Our study had several limitations. First, it was a retrospective analysis with a limited number of cases at a single institution, and there may have been a selective bias. In general, machine learning methods divide datasets into training and test data, create a prediction model with the training data, and evaluate the model using the test data. If the number of cases is small, a biased prediction model (overfitting) may be created if the training data have extreme characteristics. We used data from 129 patients with metastatic prostate cancer for the training in our analysis. To increase variation in the training data and suppress overfitting, we intend to conduct further analysis using larger-scale data from multiple institutions in the future. In this study, we performed random data splitting. Although there were no significant differences between the train cohort and the test cohort, it is necessary to consider the use of data splitting methods such as cross validation in future analyses to create a new model. Second, because we defined progression as biological progression caused by elevated PSA levels, post-treatment PSA inevitably became the most important factor for predicting progression. Future research should focus on clinical progression, such as disease worsening on imaging and the appearance of new metastases.

In conclusion, this study demonstrated that machine learning and combined assessment of pre- and post-treatment variables were useful for creating an accurate prognostic prediction model for ADT in metastatic

prostate cancer. This result may be harnessed as a new evaluation index for the treatment of metastatic prostate cancer.

## Methods

**Patient selection and analysis factors.** This retrospective study included 340 patients with prostate cancer who received ADT as an initial treatment between 1996 and 2019 at the Department of Urology, Chiba University Hospital. Of these, 30 patients who had started treatment at other hospitals were excluded. The dataset was randomly divided into training and test cohorts. In total, 207 and 103 patients were classified into the training and test cohorts, respectively. We first analysed 36 features before treatment including age at diagnosis, peripheral blood sampling, and urinalysis to examine their association with progression-free survival (PFS), overall survival (OS), and cancer-specific survival (CSS). An additional analysis focusing on patients with metastatic prostate cancer was performed, which considered data at the start of treatment as well as subsequent changes. In the analysis, 35 features after the start of treatment including peripheral blood sampling and urinalysis were combined with the 36 pretreatment features and used for prediction. This study was conducted in accordance with the ethical principles of the Declaration of Helsinki. This retrospective study of clinical information was approved by the Ethics Committee of Chiba University (Institutional Review Board (IRB) no. M10238). The IRB waived the requirement for written consent in this study due to the retrospective nature of data collection.

**Survival analysis.** We employed random survival forests (RSF) for machine-learning survival analysis. The rationale for this is as follows. First, Random forests and derivatives outperform other machine learning methods in predictions using clinical laboratory values<sup>24,25</sup>. Secondly, RSF is implemented within scikit-survival, making it easy to calculate variable importance and transfer it to the survival tree model, which is also implemented in scikit-survival. Finally, like random forests, RSFs are suitable for variable selection because they selectively use a small number of variables<sup>26</sup>. RSF is a nonlinear survival model that combines ensemble learning and decision tree<sup>27</sup>. In RSF, multiple sets of data termed bootstrap samples are created. At each node of the survival tree, feature and its threshold value were determined such that the difference in hazard function between cases separated by the nodes was maximized. The ensemble hazard function of each patient was estimated by averaging the hazard functions of multiple trees created in this manner. In this study, RSF was used to predict PFS, OS, and CSS. Analysis was performed using scikit-survival Python package. We ran `sksurv.ensemble.RandomSurvivalForest` with the default parameters, except for the following parameters; `n_estimators = 2000`, `min_samples_split = 10`, `min_samples_leaf = 15`. The reason for using nearly default parameters is that hyperparameter optimization under limited training data conditions may result in lower accuracy, and random forests are robust to hyperparameter changes<sup>28</sup>. Since RSF uses bootstrap samples, the value of the estimated survival function varies slightly with each run. Therefore, we ran the RSF 10 times independently and used the average C-index as the prognostic performance indicator. We calculated permutation importance to evaluate the contribution of explanatory variables to RSF prediction performance. The permutation importance indicates the change in predictive performance (AUC in this case) when an explanatory variable is randomly shuffled, with a positive importance indicating that the variable is necessary for prediction and a negative importance indicating that using the variable reduces predictive performance<sup>29</sup>. For example, if the AUC drops by 0.05 when a variable is randomly shuffled, the permutation importance score for that variable is 0.05. Permutation importance was calculated using `eli5` Python package.

A Cox proportional hazards model was used as the conventional statistical survival analysis for comparison. To make the conditions fair across models, the variables were selected based on the permutation importance calculated by RSF pretraining, and the same variables were used in the Cox proportional hazards model.

**Survival tree.** A survival tree represents the individual tree comprising the aforementioned RSF. This method analyses data using a tree diagram and exhibits excellent semantic interpretability in that it visualizes the classification criteria, facilitating comprehension of the results<sup>30</sup>. RSF can calculate feature importance during classification. By integrating the results of multiple survival trees, RSF allows highly accurate predictions for individual patients, but make it difficult for humans to interpret the predictive results and rationale. In this regard, survival tree may be a better solution for clinical implementation. In this study, we developed survival trees for OS and CSS using the top five important features obtained in the RSF analysis. We used the `Optuna` Python package to optimize the parameters of survival tree to achieve the highest prediction rate in training cohort<sup>31</sup>.

**Missing value imputation.** To compensate for missing values in the dataset used in this study, we used the `missForest` algorithm implemented in R<sup>32</sup>. `MissForest` is a non-parametric imputation method that uses a random forest which can learn nonlinear relationship between variables, easily handle mixed-type data, and calculate out-of-bag (OOB) errors. First, the average value was used to tentatively fill the missing values, and the random forest was then repeatedly applied to predict the missing parts. Stekhoven et al. reported that `missForest` was superior to other widely used imputation algorithms such as `KNNimpute`, `MICE`, and `MissPALasso`.

**Evaluation of survival model accuracy.** The predictive performance of the survival models, including RSF, Cox proportional hazards model, and survival tree, was evaluated using the Harrell's concordance index (C-index). The C-index is a generalization of the area under the ROC curve (AUC) that considers censored data<sup>33</sup>. This represents an assessment of the discriminatory power of the model, which is the ability of the model to correctly provide a ranking of survival times for each patient based on hazard function. Time-dependent

ROC analysis is another method of evaluating prediction accuracy in survival analysis. However, we adopted the C-index to express the transition of prediction accuracy in the time-series analysis in an easily understandable manner, given the need for analysis at multiple time points after the start of treatment.

**Statistical analysis.** The Kaplan–Meier method was used to generate survival curves to evaluate survival probability of given groups. Statistical difference in the survival probabilities between groups was assessed using log-rank test. For the analysis of the training and test cohorts, Welch's t-test and Fisher's exact test were used for continuous and categorical variables, respectively. Statistical analysis was performed using JMP<sup>®</sup> 15.2. The significance level for each test was set at  $\alpha = 0.05$ .

### Data availability

The datasets generated and analysed during the current study are not publicly available due to ethical regulations because the data contain personal information but are available from the corresponding author on reasonable request.

Received: 17 January 2023; Accepted: 5 April 2023

Published online: 18 April 2023

### References

1. Fitzmaurice, C. *et al.* Global, regional, and national cancer incidence, mortality, years of life lost, years lived with disability, and disability-adjusted life-years for 29 cancer groups, 1990 to 2016: A systematic analysis for the global burden of disease study. *JAMA Oncol.* **4**, 1553–1568. <https://doi.org/10.1001/jamaoncol.2018.2706> (2018).
2. Cancer Cancer Registry and Statistics. Cancer mortality and incidence. Cancer Information Service, National Cancer Center, Japan. [http://ganjoho.jp/reg\\_stat/statistics/dl/index.html](http://ganjoho.jp/reg_stat/statistics/dl/index.html).
3. Halabi, S. *et al.* Prognostic model for predicting survival in men with hormone-refractory metastatic prostate cancer. *J. Clin. Oncol.* **21**, 1232–1237. <https://doi.org/10.1200/jco.2003.06.100> (2003).
4. Shafiq, K. *et al.* The modified Glasgow prognostic score in prostate cancer: results from a retrospective clinical series of 744 patients. *BMC Cancer* **13**, 292. <https://doi.org/10.1186/1471-2407-13-292> (2013).
5. Matsuda, T. *et al.* Population-based survival of cancer patients diagnosed between 1993 and 1999 in Japan: A chronological and international comparative study. *Jpn. J. Clin. Oncol.* **41**, 40–51. <https://doi.org/10.1093/jco/hyq167> (2011).
6. Glass, T. R., Tangen, C. M., Crawford, E. D. & Thompson, I. Metastatic carcinoma of the prostate: Identifying prognostic groups using recursive partitioning. *J. Urol.* **169**, 164–169. <https://doi.org/10.1097/01.ju.0000042482.18153.30> (2003).
7. Gravis, G. *et al.* Prognostic factors for survival in noncastrate metastatic prostate cancer: Validation of the glass model and development of a novel simplified prognostic model. *Eur. Urol.* **68**, 196–204. <https://doi.org/10.1016/j.eururo.2014.09.022> (2015).
8. Tomašev, N. *et al.* A clinically applicable approach to continuous prediction of future acute kidney injury. *Nature* **572**, 116–119. <https://doi.org/10.1038/s41586-019-1390-1> (2019).
9. Eksi, M. *et al.* Machine learning algorithms can more efficiently predict biochemical recurrence after robot-assisted radical prostatectomy. *Prostate* **81**, 913–920. <https://doi.org/10.1002/pros.24188> (2021).
10. Ström, P. *et al.* Artificial intelligence for diagnosis and grading of prostate cancer in biopsies: A population-based, diagnostic study. *Lancet Oncol.* **21**, 222–232. [https://doi.org/10.1016/s1470-2045\(19\)30738-7](https://doi.org/10.1016/s1470-2045(19)30738-7) (2020).
11. Kourou, K., Exarchos, T. P., Exarchos, K. P., Karamouzis, M. V. & Fotiadis, D. I. Machine learning applications in cancer prognosis and prediction. *Comput. Struct. Biotechnol. J.* **13**, 8–17. <https://doi.org/10.1016/j.csbj.2014.11.005> (2015).
12. Rakha, E. A., Reis-Filho, J. S. & Ellis, I. O. Combinatorial biomarker expression in breast cancer. *Breast Cancer Res. Treat.* **120**, 293–308. <https://doi.org/10.1007/s10549-010-0746-x> (2010).
13. Zhu, W., Xie, L., Han, J. & Guo, X. The application of deep learning in cancer prognosis prediction. *Cancers* <https://doi.org/10.3390/cancers12030603> (2020).
14. Hung, T. N. K. *et al.* An AI-based prediction model for drug–drug interactions in osteoporosis and Paget's diseases from SMILES. *Mol. Inform.* **41**, e2100264. <https://doi.org/10.1002/minf.202100264> (2022).
15. Vo, T. H., Nguyen, N. T. K., Kha, Q. H. & Le, N. Q. K. On the road to explainable AI in drug–drug interactions prediction: A systematic review. *Comput. Struct. Biotechnol. J.* **20**, 2112–2123. <https://doi.org/10.1016/j.csbj.2022.04.021> (2022).
16. Breiman, L. Random forests. *Mach. Learn.* **45**, 5–32. <https://doi.org/10.1023/a:1010933404324> (2001).
17. Bulten, W. *et al.* Automated deep-learning system for Gleason grading of prostate cancer using biopsies: A diagnostic study. *Lancet Oncol.* **21**, 233–241. [https://doi.org/10.1016/s1470-2045\(19\)30739-9](https://doi.org/10.1016/s1470-2045(19)30739-9) (2020).
18. Liu, H. *et al.* Predicting prostate cancer upgrading of biopsy Gleason grade group at radical prostatectomy using machine learning-assisted decision-support models. *Cancer Manag. Res.* **12**, 13099–13110. <https://doi.org/10.2147/cmar.S286167> (2020).
19. Fendler, W. P. *et al.* Prostate-specific membrane antigen ligand positron emission tomography in men with nonmetastatic castration-resistant prostate cancer. *Clin. Cancer Res.* **25**, 7448–7454. <https://doi.org/10.1158/1078-0432.Ccr-19-1050> (2019).
20. Moreira, D. M. *et al.* Predictors of time to metastasis in castration-resistant prostate cancer. *Urology* **96**, 171–176. <https://doi.org/10.1016/j.urology.2016.06.011> (2016).
21. Smith, M. R. *et al.* Denosumab and bone metastasis-free survival in men with nonmetastatic castration-resistant prostate cancer: Exploratory analyses by baseline prostate-specific antigen doubling time. *J. Clin. Oncol.* **31**, 3800–3806. <https://doi.org/10.1200/jco.2012.44.6716> (2013).
22. Yamada, Y. *et al.* Treatment strategy for metastatic prostate cancer with extremely high PSA level: Reconsidering the value of vintage therapy. *Asian J. Androl.* **20**, 432–437. [https://doi.org/10.4103/aja.aja\\_24\\_18](https://doi.org/10.4103/aja.aja_24_18) (2018).
23. Kanesaka, M. *et al.* Revision of CHARTED and LATITUDE criteria among Japanese de novo metastatic prostate cancer patients. *Prostate Int.* **9**, 208–214. <https://doi.org/10.1016/j.prn.2021.06.001> (2021).
24. Kawakami, E. *et al.* Application of artificial intelligence for preoperative diagnostic and prognostic prediction in epithelial ovarian cancer based on blood biomarkers. *Clin. Cancer Res.* **25**, 3006–3015. <https://doi.org/10.1158/1078-0432.Ccr-18-3378> (2019).
25. Sakr, S. *et al.* Comparison of machine learning techniques to predict all-cause mortality using fitness data: The Henry ford exercise testing (FIT) project. *BMC Med. Inform. Decis. Mak.* **17**, 174. <https://doi.org/10.1186/s12911-017-0566-6> (2017).
26. Genuer, R., Poggi, J.-M. & Tuleau-Malot, C. Variable selection using random forests. *Pattern Recogn. Lett.* **31**, 2225–2236 (2010).
27. Ishwaran, H., Kogalur, U. B., Blackstone, E. H. & Lauer, M. S. Random survival forests. *Ann. Appl. Stat.* <https://doi.org/10.1214/08-aos169> (2008).
28. Liaw, A. & Wiener, M. Classification and regression by randomForest. *R News* **2**, 18–22 (2002).
29. Altmann, A., Tološi, L., Sander, O. & Lengauer, T. Permutation importance: A corrected feature importance measure. *Bioinformatics* **26**, 1340–1347. <https://doi.org/10.1093/bioinformatics/btq134> (2010).

30. Leblanc, M. & Crowley, J. Survival trees by goodness of split. *J. Am. Stat. Assoc.* **88**, 457–467. <https://doi.org/10.1080/01621459.1993.10476296> (1993).
31. Akiba, T., Sano, S., Yanase, T., Ohta, T. & Koyama, M. Oputuna: A Next-generation Hyperparameter Optimization Framework. (2019).
32. Stekhoven, D. J. & Buhlmann, P. MissForest—non-parametric missing value imputation for mixed-type data. *Bioinformatics* **28**, 112–118. <https://doi.org/10.1093/bioinformatics/btr597> (2012).
33. Heagerty, P. J. & Zheng, Y. Survival model predictive accuracy and ROC curves. *Biometrics* **61**, 92–105. <https://doi.org/10.1111/j.0006-341X.2005.030814.x> (2005).

## Acknowledgements

We thank the members of the Urology Department of Chiba University School of Medicine for their enthusiastic clinical practice and the Artificial Intelligence Medicine Department of Chiba University Graduate School of Medicine for technical assistance. This work was supported by a Grant-in-Aid for Scientific Research (C) (grant #20K09555) to S.S., Grant-in-Aid for Scientific Research (B) (grant #20H03813) to T.I., Grant-in-Aid for Scientific Research (B) (grant #21H03065) to N.A. and Japan Science and Technology Agency (JST) CREST Grant (grant #JPMJCR20H4) to E.K.

## Author contributions

S.S. participated in study design, conduct of the study, data collection, data analysis, and writing of the article; S.S. participated in study design and revision of the article; K.H. and K.S. participated in study design, data collection, and data analysis; X.Z., K.W., M.K., S.K., N.T., T.S. and Y.I. participated in data collection; N.A. and T.I. participated in the study design and revision of the article; E.K. participated in the study design, data analysis, and revision of the article.

## Competing interests

The authors declare no competing interests.

## Additional information

**Supplementary Information** The online version contains supplementary material available at <https://doi.org/10.1038/s41598-023-32987-6>.

**Correspondence** and requests for materials should be addressed to S.S.

**Reprints and permissions information** is available at [www.nature.com/reprints](http://www.nature.com/reprints).

**Publisher's note** Springer Nature remains neutral with regard to jurisdictional claims in published maps and institutional affiliations.



**Open Access** This article is licensed under a Creative Commons Attribution 4.0 International License, which permits use, sharing, adaptation, distribution and reproduction in any medium or format, as long as you give appropriate credit to the original author(s) and the source, provide a link to the Creative Commons licence, and indicate if changes were made. The images or other third party material in this article are included in the article's Creative Commons licence, unless indicated otherwise in a credit line to the material. If material is not included in the article's Creative Commons licence and your intended use is not permitted by statutory regulation or exceeds the permitted use, you will need to obtain permission directly from the copyright holder. To view a copy of this licence, visit <http://creativecommons.org/licenses/by/4.0/>.

© The Author(s) 2023

available at [www.sciencedirect.com](http://www.sciencedirect.com)journal homepage: [euoncology.europeanurology.com](http://euoncology.europeanurology.com)

European Association of Urology



# The Oncological and Functional Prognostic Value of Unconventional Histology of Prostate Cancer in Localized Disease Treated with Robotic Radical Prostatectomy: An International Multicenter 5-Year Cohort Study

David Leung<sup>a,†</sup>, Daniele Castellani<sup>b,†</sup>, Rossella Nicoletti<sup>a,c,d</sup>, Roser Vives Dilme<sup>e</sup>, Jesus Moreno Sierra<sup>e</sup>, Sergio Serni<sup>c,d</sup>, Carmine Franzese<sup>b</sup>, Giuseppe Chiacchio<sup>b</sup>, Andrea Benedetto Galosi<sup>b</sup>, Roberta Mazzucchelli<sup>f</sup>, Erika Palagonia<sup>g</sup>, Paolo Dell'Oglio<sup>g</sup>, Antonio Galfano<sup>g</sup>, Aldo Massimo Bocciardi<sup>g</sup>, Xue Zhao<sup>h</sup>, Chi Fai Ng<sup>a</sup>, Hsiang Ying Lee<sup>i</sup>, Shinichi Sakamoto<sup>h</sup>, Nikhil Vasdev<sup>j</sup>, Juan Gomez Rivas<sup>e</sup>, Riccardo Campi<sup>c,d</sup>, Jeremy Yuen-Chun Teoh<sup>a,\*</sup>

<sup>a</sup> Division of Urology, Department of Surgery, Prince of Wales Hospital, The Chinese University of Hong Kong, Hong Kong, China; <sup>b</sup> Division of Urology, Azienda Ospedaliero-Universitaria, Ospedali Riuniti di Ancona, Università Politecnica delle Marche, Ancona, Italy; <sup>c</sup> Unit of Urological Robotic Surgery and Renal Transplantation, Careggi Hospital, University of Florence, Florence, Italy; <sup>d</sup> Department of Experimental and Clinical Medicine, University of Florence, Florence, Italy; <sup>e</sup> Department of Urology, Hospital Clínico San Carlos, Madrid, Spain; <sup>f</sup> Section of Pathological Anatomy, Polytechnic University of the Marche Region, School of Medicine, Azienda Ospedaliero-Universitaria delle Marche, Ancona, Italy; <sup>g</sup> Urology Department, ASST Grande Ospedale Metropolitano Niguarda, Milan, Italy; <sup>h</sup> Department of Urology, Chiba University Graduate School of Medicine, Chiba, Japan; <sup>i</sup> Kaohsiung Medical University Hospital, Kaohsiung, Taiwan; <sup>j</sup> Department of Urology, Lister Hospital, East and North Herts NHS Trust, Stevenage, UK

## Article info

### Article history:

Received 2 October 2023  
Received in Revised form  
3 December 2023  
Accepted 11 December 2023

### Associate Editor:

Guillaume Ploussard

### Keywords:

Prostate cancer  
Cribriform pattern  
Intraductal prostate cancer  
Ductal prostate cancer  
Unusual histologies

## Abstract

**Background and objective:** The impact of prostate cancer of unconventional histology (UH) on oncological and functional outcomes after robot-assisted radical prostatectomy (RARP) and adjuvant radiotherapy (aRT) receipt is unclear. We compared the impact of cribriform pattern (CP), ductal adenocarcinoma (DAC), and intraductal carcinoma (IDC) in comparison to pure adenocarcinoma (AC) on short- to mid-term oncological and functional results and receipt of aRT after RARP.

**Methods:** We retrospectively collected data for a large international cohort of men with localized prostate cancer treated with RARP between 2016 and 2020. The primary outcomes were biochemical recurrence (BCR)-free survival, erectile and continence function. aRT receipt was a secondary outcome. Kaplan-Meier survival and Cox regression analyses were performed.

**Key findings and limitations:** A total of 3935 patients were included. At median follow-up of 2.8 yr, the rates for BCR incidence (AC 10.7% vs IDC 17%;  $p < 0.001$ ) and aRT receipt (AC 4.5% vs DAC 6.3% [ $p = 0.003$ ] vs IDC 11.2% [ $p < 0.001$ ]) were higher with UH. The 5-yr BCR-free survival rate was significantly poorer for UH groups, with hazard ratios of 1.67 (95% confidence interval [CI] 1.16–2.40;  $p = 0.005$ ) for DAC, 5.22 (95% CI 3.41–8.01;  $p < 0.001$ ) for IDC, and 3.45 (95% CI 2.29–5.20;  $p < 0.001$ ) for CP in comparison to AC. Logistic regression analysis revealed that the presence of UH doubled the risk of new-onset erectile dysfunction at 1 yr, in comparison to AC (grade group 1–3), with hazard

<sup>†</sup> These authors contributed equally to this work.

\* Corresponding author. S.H. Ho Urology Centre, Department of Surgery, The Chinese University of Hong Kong, Hong Kong, China.

E-mail address: [jeremyteoh@surgery.cuhk.edu.hk](mailto:jeremyteoh@surgery.cuhk.edu.hk) (J.Y.-C. Teoh).

<https://doi.org/10.1016/j.euo.2023.12.006>

2588-9311/© 2023 European Association of Urology. Published by Elsevier B.V. All rights reserved.

ratios of 2.13 ( $p < 0.001$ ) for DAC, 2.14 ( $p < 0.001$ ) for IDC, and 2.01 ( $p = 0.011$ ) for CP. Moreover, CP, but not IDC or DAC, was associated with a significantly higher risk of incontinence (odds ratio 1.97;  $p < 0.001$ ). The study is limited by the lack of central histopathological review and relatively short follow-up.

**Conclusions and clinical implications:** In a large cohort, UH presence was associated with worse short- to mid-term oncological outcomes after RARP. IDC independently predicted a higher rate of aRT receipt. At 1-yr follow-up after RP, patients with UH had three times higher risk of erectile dysfunction post RARP; CP was associated with a twofold higher incontinence rate.

**Patient summary:** Among patients with prostate cancer who undergo robot-assisted surgery to remove the prostate, those with less common types of prostate cancer have worse results for cancer control, erection, and urinary continence and a higher probability of receiving additional radiotherapy after surgery.

© 2023 European Association of Urology. Published by Elsevier B.V. All rights reserved.

## 1. Introduction

Prostate cancer (PCa) is the second most frequently diagnosed cancer among men worldwide [1], with a worldwide estimated incidence of 1 414 259 new cases in 2020 [2]. PCa is a urological malignancy for which the economic burden is growing, especially for the elderly population [3]. Acinar adenocarcinoma (AC) is the most prevalent PCa histology. The Gleason grade, and the International Society of Urological Pathology (ISUP) grade group (GG) derived from the Gleason system [4], is one of the most important prognostic factors and is widely used for driving disease management plans [5]. In addition to the Gleason score, a recent systematic review demonstrated that the presence of an unconventional histology (UH), in particular intraductal carcinoma (IDC), cribriform pattern (CP), or ductal adenocarcinoma (DAC), may be associated with worse oncological prognosis in comparison to conventional and mucinous or prostatic intraepithelial neoplasia (PIN)-like PCa [6]. While the histology results in the review were for prostate biopsy and radical prostatectomy (RP) specimens, recent studies have suggested that prostatectomy rather than biopsy should be the gold standard in determining Gleason scores and diagnosing IDC/CP, in light of the limited concordance rates [7,8]. Both the Genitourinary Pathology Society and the ISUP recommend reporting of the percentage of Gleason pattern 4 and the presence of CP (present in 1% of PCa cases), which is associated with higher rates of biochemical recurrence (BCR; hazard ratio [HR] 2.1) and cancer-specific mortality (HR 3.3) [9–12]. According to the literature, DAC is the second most frequent UH and its presence predicted prostate-specific antigen (PSA) recurrence in one study [13] and was associated with worse overall mortality and metastasis-free survival [14]; IDC was found to be more prevalent in metastatic PCa [15]. However, most of these data were collected in the early 2000s, details regarding the surgical approaches used were lacking, and the UH impact on functional outcomes was not explained.

RP is one of the curative treatment options for localized PCa [5]. In the past decade, the techniques for RP have evolved from open to minimally invasive surgery. And robot-assisted laparoscopic RP (RARP) has become an established and safe surgical modality [16]. Unanswered

questions remain regarding the impact of UH in PCa on functional and oncological results after RARP.

Although current guidelines support the use of adjuvant radiation therapy (aRT) in patients with pN0 status with GG 4–5 pT3 disease  $\pm$  positive margins [5], there is no clear recommendation on the need for adjuvant treatment for patients with CP, DAC, or IDC types.

The aim of this study was to provide contemporary updates on the prognostic value of PCa UH on oncological and functional outcomes, by investigating a large multicenter cohort of patients treated with RARP. The secondary aim was to evaluate potential differences in the rates of aRT receipt after RARP among the various UH groups.

## 2. Patients and methods

We retrospectively collected data for the consecutive RARP cases performed from 2016 to 2020 in seven international high-volume centers. Patients with prior PCa treatment and mixed histology subtypes were excluded. Preoperative imaging for metastatic screening was performed for patients with intermediate- or high-risk cancer according to the European Association of Urology (EAU) risk categories. Decisions on the need for lymph node dissection were made according to risk nomograms.

Baseline demographic (age, PSA, and prostate size) and pathological data (histological patterns, tumor and node stages) were retrieved and analyzed.

### 2.1. Outcomes of interest

The oncological outcomes of interest included BCR, defined according to EAU guidelines as two consecutive rising PSA values  $>0.2$  ng/ml [5] and aRT receipt, defined as RT planned after RARP on the basis of clinicopathological risk factors before the occurrence of BCR and performed within 4–22 wk after RARP [17], regardless of dose and fractionation. Data for other oncological outcomes, such as the incidence of positive surgical margins, lymph node involvement, and nodal and distant metastases, were also collected.

The functional outcomes of interest included continence, defined as no more than one protective pad per day [18], and potency, defined as the ability to obtain an erection

rigid enough for intercourse with or without the use of a phosphodiesterase type 5 inhibitor at least half of the time [19].

### 2.2. Pathological evaluation and study groups

In each centre, RARP specimens had been sampled and embedded for diagnostic purposes as previously described [20] and were assessed by dedicated uropathologists. Data on histological types, Gleason score, ISUP grade group according to the 2014 ISUP/2016 World Health Organization (WHO) guidelines [21], presence of IDC, pT and pN stage according to the 8th edition of the American Joint Committee on Cancer TNM scheme [22], and surgical margin status were retrospectively retrieved from reports for RARP specimens.

Four groups of prostate malignancy were considered: pure AC, AC with CP, DAC, and IDC (Fig. 1A). The latter three groups consisted of malignant prostatic lesions with CP and were defined according to the WHO classification [23]. In brief, DAC is composed of papillary structures and/or cribriform glands lined by tall columnar pseudostratified cells; basal cells are absent. We considered both the pure form and DAC admixed with acinar AC. IDC was defined as complex cribriform growth and lumen expansile proliferation of malignant epithelial cells within native ducts and acini with intact basal cells. We included IDC cases associated with invasive acinar AC. CP, one of the four patterns of Gleason grade 4 AC, was defined as a confluent sheet of contiguous malignant epithelial cells with multiple glandular lumina without intervening stroma or mucin separating the glandular structures [9].

### 2.3. Statistical analyses

Statistical comparisons were made among the four groups. Results for continuous variables are presented as the median and interquartile range (IQR) and were compared using a Mann-Whitney *U* test. Results for categorical variables are presented as the frequency and percentage and were compared using a  $\chi^2$  test or Fisher's exact test. Kaplan-Meier curves were used to compare outcomes, and Cox regression analysis was performed to adjust for potential confounding factors. SPSS was used for the statistical analyses. Given that DAC without an AC component is, by definition, assigned a Gleason score of 4 + 4 = 8 (ISUP GG 4), for their similar clinical behavior [24], we compared AC GG 1–3 versus GG 4 versus GG 5 versus the three UH types.

## 3. Results

Among a total of 5005 patients, 1070 had mixed or unreported histology and were therefore excluded, leaving 3935 PCa cases suitable for analysis. Among these, 3126 patients had pure AC, 174 had AC with CP, 447 had DAC, and 188 had IDC (Fig. 1A).

### 3.1. Baseline characteristics

Baseline patient and disease characteristics are listed in Table 1. Overall, the median age was 65 yr (IQR 60–70),

the median PSA was 6.8 ng/ml (IQR 5–10), and the median prostate size was 38 cm<sup>3</sup> (IQR 28–53). Regarding the ISUP grade groups in the overall cohort, 22.6% had GG 1, 38.0% had GG 2, 17.6% had GG 3, 7.4% had GG 4, and 5.6% had GG 5 disease; the ISUP grade group was not reported for 8.7% of the cohort.

The IDC and CP groups had similar median PSA and prostate size to the AC group. The DAC group had significantly lower median PSA (6.1 ng/ml) than the AC group (6.9 ng/ml) but similar median age and prostate size. In comparison to the AC group, ISUP grade groups were significantly higher for each of the UH groups ( $p < 0.001$ ). In the AC group, 77.6% of cases were GG 1–3 disease, whereas the majority of cases in the UH groups were GG 2–3 disease (DAC 66.7%, IDC 74.5%, CP 81.6%).

### 3.2. Oncological outcomes

At median follow-up of 2.8 yr, BCR was more frequent for IDC than for AC (17% vs 10.7%;  $p < 0.001$ ). The rate of positive surgical margins was significantly higher in DAC (33.6%;  $p = 0.04$ ), IDC (42.6%;  $p < 0.001$ ), and CP (43.1%;  $p < 0.001$ ) than in AC (27.3%). Lymph node involvement was also more common in DAC (6.9%;  $p < 0.001$ ) and IDC (8%;  $p < 0.001$ ) than in AC (0.5%). More nodal recurrence was observed in DAC (1.6%;  $p < 0.001$ ) and CP (2.9%;  $p = 0.049$ ) than in AC (0.4%). Distant metastases occurred more frequently in DAC (1.1%;  $p = 0.002$ ) and IDC (3.7%;  $p = 0.002$ ) than in AC (0.9%; Table 2).

Kaplan-Meier curve revealed significant differences in 5-yr BCR-free survival (Fig. 1B). In comparison to AC GG 1–3, IDC had the worst BCR rate, followed by CP, AC GG 5, DAC, and AC GG 4 ( $p < 0.001$ ).

Univariable Cox regression analysis revealed significantly poorer 5-yr BCR-free survival for the UH groups in comparison to pure AC, with HRs of 1.67 for DAC, 5.22 for IDC, and 3.45 for CP (Table 3). According to multivariable Cox regression analysis with AC GG1–3 taken as the reference, the significant predictors for BCR at 5 yr included DAC (HR 3.15;  $p < 0.001$ ), IDC (HR 5.63;  $p < 0.01$ ), CP (HR 3.94;  $p < 0.001$ ), PSA (HR 1.63;  $p = 0.001$ ), and pT3b stage (HR 2.19;  $p = 0.007$ ; Table 4). Meanwhile, GG 4 (HR 2.07;  $p = 0.096$ ), GG 5 (HR 3.15;  $p = 0.101$ ), age (HR 1.0;  $p = 0.98$ ), pT3a (HR 2.19;  $p = 0.097$ ), positive margin status (HR 1.47;  $p = 0.069$ ), and positive node status (HR 0.88;  $p = 0.724$ ) were not significant predictors for BCR.

### 3.3. Functional outcomes

In comparison to AC, a two-to-three-fold increase in the risk of de novo erectile dysfunction at 1 yr after RARP was observed for each UH subgroup. In addition, CP was associated with twofold higher risk of incontinence than AC at one yr after RARP (Table 5). Upon multivariable Cox regression analysis taking AC GG 1–3 as the reference, the presence of DAC (HR 2.13;  $p < 0.001$ ), IDC (HR 2.14;  $p < 0.001$ ), or CP (HR 2.01;  $p = 0.011$ ) doubled the risk of erectile dysfunction at one year postoperatively (Table 6). The other significant predictors for erectile dysfunction found were pT3a stage (HR 1.67;  $p < 0.001$ ) and pT3b stage (HR 1.69;  $p = 0.003$ ). GG 4 disease, GG 5 disease, and positive margin

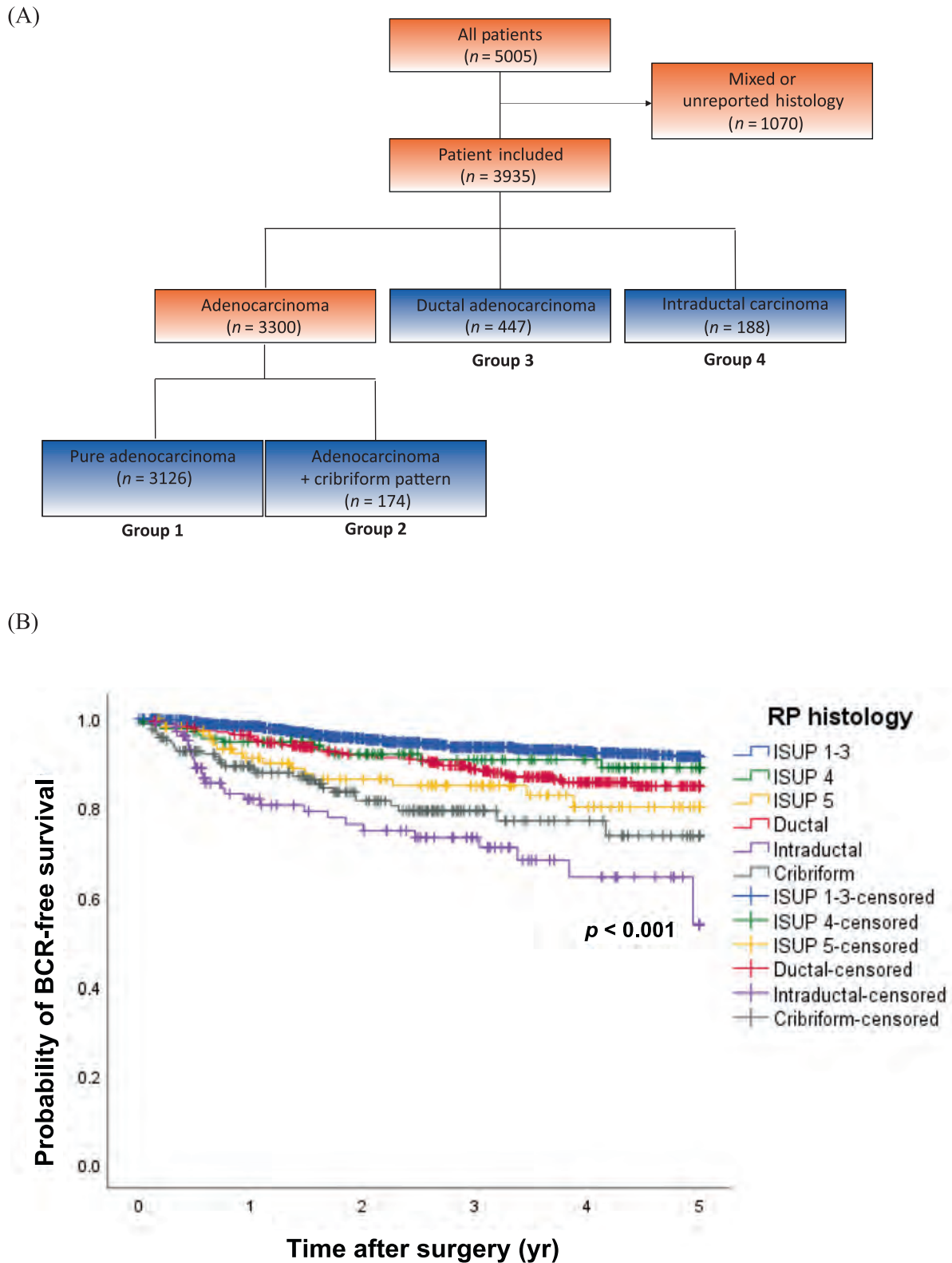


Fig. 1 – (A) Histology groups and the number of patients in each group. Four groups were compared in the analysis: group 1 = pure adenocarcinoma; group 2 = adenocarcinoma with cribriform pattern; group 3 = ductal adenocarcinoma; and group 4 = intraductal carcinoma. (B) Biochemical recurrence (BCR)-free survival after robot-assisted radical prostatectomy by International Society of Urological Pathology (ISUP) grade group and unusual histology groups.

**Table 1 – Baseline patient and disease characteristics**

Parameter	Pure AC (n = 3126)	DAC (n = 447)	p value	IDC (n = 188)	p value	CP (n = 174)	p value	Overall (n = 3935)
Age (yr) <sup>a</sup>	65 (60–70)	65 (60–70)	0.683	67 (61–71)	0.043	67 (62–70)	0.015	65 (60–70)
PSA (ng/ml) <sup>a</sup>	6.9 (5.0–10.0)	6.1 (4.3–8.5)	<0.001	7.2 (5.0–12.1)	0.365	6.5 (5.1–9.0)	0.243	6.8 (5.0–10.0)
Prostate size (cm <sup>3</sup> ) <sup>a</sup>	39 (28–54)	37 (30–52)	0.733	41 (32–59)	0.054	33 (25–50)	0.001	38 (28–53)
RP pathology, n (%)			<0.001		<0.001		<0.001	
GG 1	815 (26.1)	73 (16.3)		1 (0.5)		1 (0.6)		890 (22.6)
GG 2	1123 (35.9)	213 (47.7)		63 (33.5)		98 (56.3)		1497 (38.0)
GG 3	488 (15.6)	85 (19.0)		77 (41.0)		44 (25.3)		694 (17.6)
GG 4	240 (7.7)	21 (4.7)		14 (7.4)		17 (9.8)		292 (7.4)
GG 5	164 (5.2)	21 (4.7)		22 (11.7)		14 (8.0)		221 (5.6)
Data missing	296 (9.5)	34 (7.6)		11 (5.9)		0 (0)		341 (8.7)

AC = adenocarcinoma; CP = cribriform pattern; DAC = ductal AC; GG = International Society of Urological Pathology grade group; IDC = intraductal carcinoma; RP = radical prostatectomy.  
<sup>a</sup> Results are reported as the median (interquartile range).

**Table 2 – Oncological outcomes**

Parameter	Pure AC (n = 3126)	DAC (n = 447)	p value	IDC (n = 188)	p value	CP (n = 174)	p value	Total (N = 3935)
Surgical margin, n (%)			0.039		<0.001		<0.001	
Positive	854 (27.3)	150 (33.6)		80 (42.6)		75 (43.1)		1159 (29.5)
Negative	2009 (64.3)	282 (63.1)		95 (50.5)		96 (55.2)		2482 (63.1)
Data missing	263 (8.4)	15 (3.4)		13 (6.9)		3 (1.7)		294 (7.5)
LNI, n (%)			<0.001		<0.001		0.273	
Yes	16 (0.5)	31 (6.9)		15 (8.0)		4 (2.3)		66 (1.7)
No	781 (25.0)	236 (52.8)		51 (27.1)		99 (56.9)		1167 (29.7)
Missing	2329 (74.5)	180 (40.3)		122 (64.9)		71 (40.8)		2702 (68.7)
Adjuvant RT, n (%)			0.003		<0.001		0.902	
Yes	141 (4.5)	28 (6.3)		21 (11.2)		9 (5.2)		199 (5.1)
No	2400 (76.8)	251 (56.2)		93 (49.5)		160 (92.0)		2904 (73.8)
Data missing	585 (18.7)	168 (37.6)		74 (39.4)		5 (2.9)		832 (21.1)
Salvage RT, n (%)			<0.001		0.002		0.214	
Yes	239 (7.6)	23 (5.1)		16 (8.5)		21 (12.1)		299 (7.6)
No	2200 (70.4)	36 (8.1)		61 (32.4)		143 (82.2)		2440 (62.0)
Data missing	687 (22.0)	388 (86.8)		111 (59.0)		10 (5.7)		1196 (30.4)
BCR, n (%)			0.671		<0.001		0.078	
Yes	334 (10.7)	48 (10.7)		32 (17.0)		30 (17.2)		444 (11.3)
No	2203 (70.5)	295 (66.0)		85 (45.2)		137 (78.7)		2720 (69.1)
Data missing	589 (18.8)	104 (23.3)		71 (37.8)		7 (4.0)		771 (19.6)
Nodal recurrence, n (%)			<0.001		0.325		0.049	
Yes	11 (0.4)	7 (1.6)		1 (0.5)		5 (2.9)		24 (0.6)
No	1045 (33.4)	24 (5.4)		34 (18.1)		156 (89.7)		1259 (32.0)
Data missing	2070 (66.2)	416 (93.1)		153 (81.4)		13 (7.5)		2652 (67.4)
Metastasis, n (%)			0.002		0.002		1	
Yes	29 (0.9)	5 (1.1)		7 (3.7)		4 (2.3)		45 (1.1)
No	1181 (37.8)	28 (6.3)		57 (30.3)		160 (92.0)		1426 (36.2)
Data missing	1916 (61.3)	414 (92.6)		124 (66.0)		10 (5.7)		2464 (62.6)
Status, n (%)			0.007		1		1	
Alive	2592 (82.9)	445 (99.6)		139 (73.9)		166 (95.4)		3342 (84.9)
Dead	43 (1.4)	0 (0)		2 (1.1)		2 (1.1)		47 (1.2)
Unknown	491 (15.7)	2 (0.4)		47 (25.0)		6 (3.4)		546 (13.9)
Median follow-up, d (interquartile range)	1039 (553–1674)	1223 (803–1647)	<0.001	888 (357–1212)	<0.001	867 (480–1190)	<0.001	1045 (573–1616)

AC = adenocarcinoma; BCR = biochemical recurrence; CP = cribriform pattern; DAC = ductal AC; IDC = intraductal carcinoma; LNI = lymph node involvement; RP = radical prostatectomy; RT = radiation therapy.

**Table 3 – Univariable Cox regression results for unconventional histologies associated with 5-yr biochemical recurrence versus pure adenocarcinoma as the reference**

Histology	HR (95% CI)	p value
Ductal adenocarcinoma	1.67 (1.16–2.40)	0.005
Intraductal carcinoma	5.22 (3.41–8.01)	<0.001
Cribriform pattern	3.45 (2.29–5.20)	<0.001

CI = confidence interval; HR = hazard ratio.

status were not significant predictors. Conversely, nerve-sparing surgery (HR 0.75;  $p = 0.005$ ) and lymph node dissection (HR 0.58;  $p < 0.001$ ) were associated with lower incidence of erectile dysfunction.

### 3.4. aRT rates

The use of aRT in all the participating centers was in accordance with the EAU guidelines [5]. aRT use was more fre-

**Table 4 – Multivariable Cox regression results for factors associated with 5-yr biochemical recurrence**

Variable	HR (95% CI)	p value
RP histology		
AC GG 1–3	Reference	
AC GG 4	2.07 (0.88–4.90)	0.096
AC GG 5	2.02 (0.87–4.68)	0.101
Ductal AC	3.15 (1.72–5.78)	<0.001
Intraductal carcinoma	5.63 (2.74–11.58)	<0.001
Cribriform pattern	3.94 (2.14–7.25)	<0.001
Age	1.00 (0.97–1.03)	0.985
Log PSA	1.63 (1.21–2.19)	0.001
Nerve-sparing surgery	0.63 (0.40–0.99)	0.047
Pathological T stage		
pT2	Reference	
pT3a	1.56 (0.92–2.64)	0.097
pT3b	2.19 (1.24–3.85)	0.007
Positive surgical margin	1.47 (0.97–2.24)	0.069
Positive lymph node	0.88 (0.42–1.83)	0.724

AC = prostate adenocarcinoma; CI = confidence interval; GG = International Society of Urological Pathology grade group; HR = hazard ratio; IDC = intraductal carcinoma; PSA prostate-specific antigen; RP = radical prostatectomy.

**Table 5 – Association of unconventional histologies with functional outcomes at 1 yr postoperatively in comparison to pure adenocarcinoma**

Histology	Odds ratio (95% confidence interval)	
	Incontinence	Erectile dysfunction
Ductal adenocarcinoma	1.03 (0.77–1.39); <i>p</i> = 0.839	1.95 (1.58–2.42); <i>p</i> < 0.001
Intraductal carcinoma	1.51 (0.92–2.50); <i>p</i> = 0.104	2.63 (1.85–3.73); <i>p</i> < 0.001
Cribriform pattern	1.97 (1.33–2.92); <i>p</i> < 0.001	3.03 (1.82–5.05); <i>p</i> < 0.001

**Table 6 – Logistic regression results for the risk of erectile dysfunction at 1 yr**

Risk factor	HR (95% CI)	p value
RP histology		
AC GG 1–3	Reference	
AC GG 4	0.94 (0.67–1.31)	0.700
AC GG 5	0.76 (0.50–1.16)	0.201
Ductal AC	2.13 (1.67–2.70)	<0.001
Intraductal carcinoma	2.14 (1.45–3.17)	<0.001
Cribriform pattern	2.01 (1.18–3.45)	0.011
Age	1.00 (0.98–1.01)	0.477
Log PSA	1.14 (1.00–1.30)	0.057
Nerve-sparing surgery	0.75 (0.62–0.92)	0.005
Lymph node dissection	0.58 (0.47–0.70)	<0.001
Pathological T stage		
pT2	Reference	
pT3a	1.67 (1.38–2.02)	<0.001
pT3b	1.52 (1.15–2.00)	0.003
pT4	1.69 (0.15–19.02)	0.673
Positive surgical margin	0.99 (0.82–1.19)	0.898

AC = prostate adenocarcinoma; CI = confidence interval; GG = International Society of Urological Pathology grade group; HR = hazard ratio; IDC = intraductal carcinoma; PSA prostate-specific antigen; RP = radical prostatectomy.

quent in DAC (6.3%; *p* = 0.003) and IDC (11.2%; *p* < 0.001) than in AC (4.5%).

Logistic regression analysis with AC GG 1–3 as the reference revealed that IDC was associated with a higher likelihood of aRT receipt (odds ratio [OR] 27.3, 95% confidence

**Table 7 – Logistic regression results for the odds of receipt of adjuvant radiation therapy**

Risk factor	Odds ratio (95% CI)	p value
RP histology		
AC GG 1–3	Reference	
AC GG 4	3.41 (0.96–12.09)	0.058
AC GG 5	0.70 (0.12–3.94)	0.686
Ductal AC	3.27 (1.25–8.55)	0.015
Intraductal carcinoma	27.31 (6.79–109.74)	<0.001
Cribriform pattern	0.42 (0.08–2.27)	0.313
Log PSA	1.60 (0.91–2.80)	0.101
Positive surgical margin	1.08 (0.48–2.41)	0.856
Seminal vesicle invasion	8.13 (3.51–18.82)	<0.001
Positive lymph node	9.09 (2.49–33.24)	<0.001

AC = prostate adenocarcinoma; CI = confidence interval; GG = International Society of Urological Pathology grade group; PSA = prostate-specific antigen; RP = radical prostatectomy.

**Table 8 – Univariable logistic regression results for unconventional histologies associated with receipt of adjuvant radiation therapy versus pure adenocarcinoma as the reference**

Histology	HR (95% CI)	p value
Ductal adenocarcinoma	1.90 (1.24–2.91)	0.003
Intraductal carcinoma	3.84 (2.32–6.36)	<0.001
Cribriform pattern	0.96 (0.48–1.91)	0.902

CI = confidence interval; HR = hazard ratio.

interval [CI] 6.79–109.7; *p* < 0.001; Table 7). DAC was also associated with a higher likelihood of aRT receipt (OR 3.27, 95% CI 1.25–8.55; *p* = 0.015). Nodal metastasis (OR 9.09, 95% CI 2.49–33.24; *p* < 0.001), and seminal vesicle invasion (OR 8.13, 95% CI 3.51–18.8; *p* < 0.001) were the other significant predictors. CP (OR 4.2, 95% CI 0.08–2.27; *p* = 0.313), GG 4 and GG 5 disease, positive margin status, and PSA were not significant predictors for aRT receipt.

In addition, aRT was more likely to be required in DAC (HR 1.9) and in IDC (HR 3.84) than in AC according to univariable logistic regression analysis (Table 8).

#### 4. Discussion

In this large multicenter cohort of men with localized PCa treated with RARP, the presence of any UH (DAC, CP, or IDC) was significantly associated with three to five times higher risk of BCR at 5 years in comparison to GG 1–3 pure AC (Table 4). Moreover, logistic regression analyses revealed that the risk of aRT receipt was three times higher for DAC and 27 times higher for IDC in comparison to AC GG 1–3. Regarding functional outcomes, the risk of new-onset erectile dysfunction at one year after RARP was consistently two-fold higher for all UH subtypes in comparison to AC GG 1–3 (Table 6). In addition, CP was associated with a higher risk of urinary incontinence.

To the best of our knowledge, this is the first large multicenter study to evaluate the impact of PCa UH on functional and oncological outcomes after RARP and on the rate of aRT receipt.

UHs are not as rare as conventionally perceived, and an accurate pathological description is mandatory. A systematic review by Porter et al. [15] highlighted that IDC incidence could reach 36.7% in high-risk disease and 56% in

metastatic or recurrent disease. A review by Montironi et al. [25] showed that IDC was strongly associated with aggressive PCa with high Gleason score and large tumor volume, and usually had a deleterious impact on prognosis. The authors suggested that pathologists should report IDC in prostate specimens, especially from prostate biopsy, because its presence has a critical impact on patient management.

Ericson et al. [26] reported that prostate biopsy had sensitivity of 56.5% and specificity of 87.2% for detection of CP and/or IDC after RP, and that magnetic resonance imaging/ultrasound-guided fusion prostate biopsy did not improve UH detection. Although biopsy cannot confidently rule out UH, patients with biopsy-proven UH histology (especially IDC) should be informed of the higher risk of BCR and aRT receipt, and advised to receive active treatment. In addition, post-RARP diagnosis of UH should trigger discussion about aRT as an option, or at least stricter follow-up in order to pick up the relatively early BCR observed in our study.

Reports on adverse oncological behaviors of these UHs are by no means isolated, and therefore these PCa entities warrant more attention from urologists. Kweldam et al. [10] showed that among the different Gleason 4 grade patterns, CP was independently associated with inferior metastasis-free survival and disease-specific mortality rates after RP among patients with Gleason 7 PCa. In the 2005–2018 cohort described by Ranasinghe et al. [14], DAC treated with either RP or RT was associated with worse 5-yr metastasis-free and overall survival rates in comparison to high-risk PCa. Besides the systematic review by Russo et al. [27] showing inferior oncological outcomes for CP, a recent study found that CP cases typically had a worse response to androgen blockade, suggesting that this UH could contribute to hormonal deprivation resistance [28]. In addition, CP was associated with a higher risk of lymph node positivity at RP [29]. In our analysis, IDC was the strongest predictor of BCR on Cox regression analysis, with a 5.5-fold higher risk. This reiterates the importance for uropathologists to actively look for and report PCa UH.

Several unanswered questions remain for the management of UH PCa: whether there are differences in response to RT (especially for IDC), multimodal therapy, androgen deprivation therapy in the (neo-)adjuvant and palliative settings, novel hormonal agents, or chemotherapy, as well as optimal follow-up protocols. In addition, genomic alterations have been linked to the development of IDC and CP subtypes [30]. Future trials are therefore needed to elucidate the role of genetics and the optimal management for patients with these PCa UH types.

Functional outcomes after RARP are clearly multifactorial and affected by intraoperative (eg, nerve-sparing surgery, urethral length, and strategies for bladder neck preservation and reconstruction) and postoperative factors (eg, rehabilitation programs). Our results can be explained in part by the higher aRT rates for UH. Nevertheless, this study does shed some light on the myths of unconventional PCa histology, and help substantiate our patient counselling. Further studies are warranted to elucidate the association between UH and inferior functional outcomes.

Our study has several limitations: (1) the retrospective nature of the data collected; (2) the lack of central review of histological specimens; (3) the lack of preoperative imaging details and data for patients treated primarily with RT; (4) the omission of rarer UH entities such as mucinous/neuroendocrine disease; (5) the use of nonstandardized follow-up protocols among the participating centers; and (6) the relatively short follow-up (2.8 yr) for our series. The authors hope this cohort acts as a milestone in our pursuit for the optimal management of rarer disease, although further prospective studies are certainly needed to confirm our findings.

## 5. Conclusions

For patients with PCa treated with RARP, the presence of UH (CP, DAC, or IDC) was associated with a higher rate of early BCR in comparison to pure AC (GG 1–3). Moreover, the presence of DAC or IDC predicted a higher rate of aRT receipt. In terms of functional results, presence of any of the three UH types investigated here predicted two-fold higher risk of erectile dysfunction at 1 yr after RARP, and CP was also associated with higher risk of incontinence. Patients diagnosed with these UHs should be well counselled about such risk, followed up more stringently, and educated about the higher likelihood of multimodal treatment.

## Acknowledgement

We would like to acknowledge Dr. Kimberly Chan (Lister Hospital, UK); Dr. Chris Wong, Alex Liu, Ivan Ko, Alex Mok and Mr. Steven Leung (CUHK/ Prince of Wales Hospital, HK); and Dr. Sunny Tsang (Queen Mary Hospital, HK) for their input in data collection and analyses.

**Author contributions:** Jeremy Yuen-Chun Teoh had full access to all the data in the study and takes responsibility for the integrity of the data and the accuracy of the data analysis.

*Study concept and design:* Teoh, Leung, Castellani.

*Acquisition of data:* All authors.

*Analysis and interpretation of data:* Leung, Nicoletti.

*Drafting of the manuscript:* Leung, Nicoletti.

*Critical revision of the manuscript for important intellectual content:* Castellani, Mazzucchelli.

*Statistical analysis:* Teoh, Leung, Nicoletti.

*Obtaining funding:* None.

*Administrative, technical, or material support:* None.

*Supervision:* Castellani, Teoh.

*Other:* None.

**Financial disclosures:** Jeremy Yuen-Chun Teoh certifies that all conflicts of interest, including specific financial interests and relationships and affiliations relevant to the subject matter or materials discussed in the manuscript (eg, employment/affiliation, grants or funding, consultancies, honoraria, stock ownership or options, expert testimony, royalties, or patents filed, received, or pending), are the following: None.

**Funding/Support and role of the sponsor:** None.

**Data sharing statement:** Data are available for bona fide researchers on request from the authors.

## References

- [1] Culp MB, Soerjomataram I, Efstathiou JA, Bray F, Jemal A. Recent global patterns in prostate cancer incidence and mortality rates. *Eur Urol* 2020;77:38–52.
- [2] Sung H, Ferlay J, Siegel RL, et al. Global cancer statistics 2020: GLOBOCAN estimates of incidence and mortality worldwide for 36 cancers in 185 countries. *CA Cancer J Clin* 2021;2021(71):209–49.
- [3] Schroeck FR, Jacobs BL, Bhayani SB, Nguyen PL, Penson D, Hu J. Cost of new technologies in prostate cancer treatment: systematic review of costs and cost effectiveness of robotic-assisted laparoscopic prostatectomy, intensity-modulated radiotherapy, and proton beam therapy. *Eur Urol* 2017;72:712–35. <https://doi.org/10.1016/j.eururo.2017.03.028>.
- [4] van Leenders GJLH, van der Kwast TH, Grignon DJ, et al. The 2019 International Society of Urological Pathology (ISUP) consensus conference on grading of prostatic carcinoma. *Am J Surg Pathol* 2020;44:e87–99. <https://doi.org/10.1097/PAS.0000000000001497>.
- [5] Mottet N, van den Bergh RCN, Briers E, et al. EAU-EANM-ESTRO-ESUR-SIOG guidelines on prostate cancer—2020 update. Part 1: screening, diagnosis, and local treatment with curative intent. *Eur Urol* 2021;79:243–62. <https://doi.org/10.1016/j.eururo.2020.09.042>.
- [6] Marra G, van Leenders GJLH, Zattoni F, et al. Impact of epithelial histological types, subtypes, and growth patterns on oncological outcomes for patients with nonmetastatic prostate cancer treated with curative intent: a systematic review. *Eur Urol* 2023;84:65–85. <https://doi.org/10.1016/j.eururo.2023.03.014>.
- [7] Epstein JI, Feng Z, Trock BJ, Pierorazio PM. Upgrading and downgrading of prostate cancer from biopsy to radical prostatectomy: incidence and predictive factors using the modified Gleason grading system and factoring in tertiary grades. *Eur Urol* 2012;61:1019–24. <https://doi.org/10.1016/j.eururo.2012.01.050>.
- [8] Masoomian M, Downes MR, Sweet J, et al. Concordance of biopsy and prostatectomy diagnosis of intraductal and cribriform carcinoma in a prospectively collected data set. *Histopathology* 2019;74:474–82. <https://doi.org/10.1111/his.13747>.
- [9] Choy B, Pearce SM, Anderson BB, et al. Prognostic significance of percentage and architectural types of contemporary Gleason pattern 4 prostate cancer in radical prostatectomy. *Am J Surg Pathol* 2016;40:1400–6. <https://doi.org/10.1097/PAS.0000000000000691>.
- [10] Kweldam CF, Wildhagen MF, Steyerberg EW, Bangma CH, van der Kwast TH, van Leenders GJ. Cribriform growth is highly predictive for postoperative metastasis and disease-specific death in Gleason score 7 prostate cancer. *Mod Pathol* 2015;28:457–64. <https://doi.org/10.1038/modpathol.2014.116>.
- [11] Dong F, Yang P, Wang C, et al. Architectural heterogeneity and cribriform pattern predict adverse clinical outcome for Gleason grade 4 prostatic adenocarcinoma. *Am J Surg Pathol* 2013;37:1855–61. <https://doi.org/10.1097/PAS.0b013e3182a02169>.
- [12] Epstein JI, Amin MB, Fine SW, et al. The 2019 Genitourinary Pathology Society (GUPS) white paper on contemporary grading of prostate cancer. *Arch Pathol Lab Med* 2021;145:461–93. <https://doi.org/10.5858/arpa.2020-0015-RA>.
- [13] Jang WS, Shin SJ, Yoon CY, et al. Prognostic significance of the proportion of ductal component in ductal adenocarcinoma of the prostate. *J Urol* 2017;197:1048–53. <https://doi.org/10.1016/j.juro.2016.11.104>.
- [14] Ranasinghe W, Shapiro DD, Hwang H, et al. Ductal prostate cancers demonstrate poor outcomes with conventional therapies. *Eur Urol* 2021;79:298–306. <https://doi.org/10.1016/j.eururo.2020.11.015>.
- [15] Porter LH, Lawrence MG, Ilic D, et al. Systematic review links the prevalence of intraductal carcinoma of the prostate to prostate cancer risk categories. *Eur Urol* 2017;72:492–5. <https://doi.org/10.1016/j.eururo.2017.03.013>.
- [16] Fan S, Hao H, Chen S, et al. Robot-assisted laparoscopic radical prostatectomy using the KangDuo surgical robot system vs the da Vinci Si robotic system. *J Endourol* 2023;37:568–74. <https://doi.org/10.1089/end.2022.0739>.
- [17] Vale CL, Fisher D, Kneebone A, et al. Adjuvant or early salvage radiotherapy for the treatment of localised and locally advanced prostate cancer: a prospectively planned systematic review and meta-analysis of aggregate data. *Lancet* 2020;396:1422–31. [https://doi.org/10.1016/S0140-6736\(20\)31952-8](https://doi.org/10.1016/S0140-6736(20)31952-8).
- [18] Lepor H, Kaci L, Xue X. Continence following radical retropubic prostatectomy using self-reporting instruments. *J Urol* 2004;171:1212–5. <https://doi.org/10.1097/01.ju.0000110631.81774.9c>.
- [19] Novara G, Ficarra V, D'Elia C, Secco S, Cavalleri S, Artibani W. Trifecta outcomes after robot-assisted laparoscopic radical prostatectomy. *BJU Int* 2011;107:100–4. <https://doi.org/10.1111/j.1464-410X.2010.09505.x>.
- [20] Samaratunga H, Montironi R, True L, et al. International Society of Urological Pathology (ISUP) consensus conference on handling and staging of radical prostatectomy specimens. Working group 1: specimen handling. *Mod Pathol* 2011;24:6–15. <https://doi.org/10.1038/modpathol.2010.178>.
- [21] Epstein JI, Egevad L, Amin MB, et al. The 2014 International Society of Urological Pathology (ISUP) consensus conference on Gleason grading of prostatic carcinoma: definition of grading patterns and proposal for a new grading system. *Am J Surg Pathol* 2016;40:244–52. <https://doi.org/10.1097/PAS.0000000000000530>.
- [22] Amin MB, Greene FL, Edge SB, et al. The eighth edition AJCC cancer staging manual: continuing to build a bridge from a population-based to a more “personalized” approach to cancer staging. *CA Cancer J Clin* 2017;67:93–9. <https://doi.org/10.3322/caac.21388>.
- [23] Netto GJ, Amin MB, Berney DM, et al. The 2022 World Health Organization classification of tumors of the urinary system and male genital organs—part B: prostate and urinary tract tumors. *Eur Urol* 2022;82:469–82. <https://doi.org/10.1016/j.eururo.2022.07.002>.
- [24] Lindh C, Samaratunga H, Delahunt B, et al. Ductal and acinar components of mixed prostatic adenocarcinoma frequently have a common clonal origin. *Prostate* 2022;82:576–83. <https://doi.org/10.1002/pros.24304>.
- [25] Montironi R, Zhou M, Magi-Galluzzi C, Epstein JI. Features and prognostic significance of intraductal carcinoma of the prostate. *Eur Urol Oncol* 2018;1:21–8.
- [26] Ericson KJ, Wu SS, Lundy SD, Thomas LJ, Klein EA, McKenney JK. Diagnostic accuracy of prostate biopsy for detecting cribriform Gleason pattern 4 carcinoma and intraductal carcinoma in paired radical prostatectomy specimens: implications for active surveillance. *J Urol* 2020;203:311–9.
- [27] Russo GI, Soeterik T, Puche-Sanz I, et al. Oncological outcomes of cribriform histology pattern in prostate cancer patients: a systematic review and meta-analysis. *Prostate Cancer Prostat Dis* 2023;26:646–54. <https://doi.org/10.1038/s41391-022-00600-y>.
- [28] Wang X, Qi M, Zhang J, et al. Differential response to neoadjuvant hormonal therapy in prostate cancer: predictive morphological parameters and molecular markers. *Prostate* 2019;79:709–19. <https://doi.org/10.1002/pros.23777>.
- [29] Downes MR, Xu B, van der Kwast TH. Gleason grade patterns in nodal metastasis and corresponding prostatectomy specimens: impact on patient outcome. *Histopathology* 2019;75:715–22. <https://doi.org/10.1111/his.13938>.
- [30] Chua ML, Lo W, Pintilie M, et al. A prostate cancer “nimbusus”: genomic instability and SCHLAP1 dysregulation underpin aggression of intraductal and cribriform subpathologies. *Eur Urol* 2017;72:665–74.



## OPEN Tumor localization by Prostate Imaging and Reporting and Data System (PI-RADS) version 2.1 predicts prognosis of prostate cancer after radical prostatectomy

Ayumi Fujimoto<sup>1</sup>, Shinichi Sakamoto<sup>1</sup>✉, Takuro Horikoshi<sup>2</sup>, Xue Zhao<sup>1</sup>, Yasutaka Yamada<sup>1</sup>, Junryo Rii<sup>1</sup>, Nobuyoshi Takeuchi<sup>1</sup>, Yusuke Imamura<sup>1</sup>, Tomokazu Sazuka<sup>1</sup>, Keisuke Matsusaka<sup>3</sup>, Jun-ichiro Ikeda<sup>4</sup> & Tomohiko Ichikawa<sup>1</sup>

An improved reading agreement rate has been reported in version 2.1 (v2.1) of the Prostate Imaging and Reporting and Data System (PI-RADS) compared with earlier versions. To determine the predictive efficacy of bi-parametric MRI (bp-MRI) for biochemical recurrence (BCR), our study assessed PI-RADS v2.1 score and tumor location in Japanese prostate cancer patients who underwent radical prostatectomy. Retrospective analysis was performed on the clinical data of 299 patients who underwent radical prostatectomy at Chiba University Hospital between 2006 and 2018. The median prostate-specific antigen (PSA) level before surgery was 7.6 ng/mL. Preoperative PI-RADS v2.1 categories were 1–2, 3, 4, and 5 in 35, 56, 138, and 70 patients, respectively. Tumor location on preoperative MRI was 107 in the transition zone (TZ) and 192 in the peripheral zone (PZ). BCR-free survival was significantly shorter in the PZ group ( $p = 0.001$ ). In the total prostatectomy specimens, preoperative PI-RADS category 5, radiological tumor location, pathological seminal vesicle invasion, and Grade Group  $\geq 3$  were independent prognostic factors of BCR. These four risk factors have significant potential to stratify patients and predict prognosis. Radiological tumor location and PI-RADS v2.1 category using bp-MRI may enable prediction of BCR following radical prostatectomy.

Prostate cancer was the second most common male cancer and the fifth leading cause of cancer death worldwide in 2020 (GLOBOCAN 2020)<sup>1</sup>. More than 1.4 million new cases and 375,000 deaths due to prostate cancer are estimated to occur globally per year. Radical prostatectomy remains one of the standard treatments procedure for localized prostate cancer, whereas active surveillance enhances clinical benefits for the low-risk group of prostate cancer<sup>2</sup>. However, pathological Grade Group (GG) may occasionally be overestimated or underestimated in patients who undergo radical prostatectomy for locally advanced prostate cancer at the initial biopsy. Misclassification of tumor risk at diagnosis leads to inadequate treatment, which is associated with inferior outcomes that include BCR and worse survival. The precise staging and estimation of malignancy are essential in the treatment strategies for localized prostate cancer.

In the diagnosis of prostate cancer, detection and localization of malignant lesions are performed using MRI<sup>3</sup>. The Prostate Imaging and Reporting and Data System (PI-RADS) was issued in 2012 by the European Society of Urogenital Radiology (ESUR) as a standardized guideline for the imaging and interpretation of prostate MRI. PI-RADS is also used in evaluating and reporting of prostate cancer on multiparametric MRI (mp-MRI)<sup>4</sup>. In 2015, the ESUR published PI-RADS v2.0<sup>5</sup>, followed by the revised PI-RADS v2.1 in 2019<sup>6</sup>. In PI-RADS v2.1, some cases changed the TZ category from 2 to 1 or 3. TZ assessment for category 2 lesions requires background assessments. TZ nodules that were 2 points in PI-RADS v2 are downgraded to 1 point if the nodule is similar

<sup>1</sup>Department of Urology, Chiba University Graduate School of Medicine, 1-8-1 Inohana, Chuo-ku, Chiba, Chiba 260-8670, Japan. <sup>2</sup>Department of Radiology, Chiba University Hospital, Chiba 260-8677, Japan. <sup>3</sup>Department of Pathology, Chiba University Hospital, Chiba 260-8677, Japan. <sup>4</sup>Department of Diagnostic Pathology, Chiba University Graduate School of Medicine, Chiba 260-8670, Japan. ✉email: rbatbat1@gmail.com

to the background. For a case with T2W score of 2, if the DWI score is 4 or 5, the overall PI-RADS category is upgraded from 2 to 3.

A previous study has indicated the equivalent utility of bi-parametric MRI (bp-MRI) and multi-parametric MRI (mp-MRI)<sup>7</sup>. The clinical value of PI-RADS v2.0 with bp-MRI and pathological Grade Group to predict BCR following radical prostatectomy also has been reported<sup>8</sup>. Patients with renal dysfunction or an allergy to contrast agent are not able to undergo dynamic contrast-enhanced (DCE) MRI. Investigation of a method for detection of prostate cancer in these patients is a pressing clinical issue. In this regard, bp-MRI can be used without contrast agent for imaging prostate tumors. Although PI-RADS v2.1 based on MRI has become the standard option for evaluation of the prostate, as yet there is limited evidence regarding PI-RADS v2.1 and the prediction of BCR after prostatectomy, particularly for bp-MRI. There is also evidence that tumor location influences the prognosis of localized prostate cancer<sup>9</sup>. Based on this evidence, we hypothesize that tumor location as well as MRI findings influence the outcome of radical prostatectomy.

Therefore, the aim of the present study was to examine the prognostic significance of the bp-MRI findings of prostate cancer for BCR, including location and PI-RADS v2.1 category.

## Results

**Patient characteristics.** Table 1 lists the characteristics of the 299 patients that were analyzed in our study. Median follow-up was 49.8 months after radical prostatectomy, median PSA (ng/mL) was 7.6 ng/mL, and median age at operation was 67 years. Open radical prostatectomy (ORP), laparoscopic radical prostatectomy (LRP), and robotic-assisted radical prostatectomy (RARP) were performed in 33 (11.0%), 76 (25.4%), and 190 (63.5%) patients, respectively. Lymph node dissection was performed in 234 patients (78.3%). The PI-RADS v2.1 category of the index tumor was 1–2, 3, 4, and 5 in 35 (11.7%), 56 (18.7%), 138 (46.2%), and 70 (23.4%) patients, respectively. Of the 299 patients, 71 (23.7%) had extra-prostatic extension and 89 (29.8%) specimens had a positive resection margin. Seminal vesicle invasion was found in 28 (9.4%) of patients. Pathological Grade Groups 1, 2, 3, 4, and 5 were diagnosed in 23 (7.7%), 123 (41.1%), 93 (31.1%), 24 (8.0%), and 35 (11.7%) of patients, respectively (Table 1).

Forty-eight patients (16.1%) experienced BCR during the observation period. Baseline PSA, PI-RADS category, radiological location, Pathological Grade Group, resection margin positive (RM+), and seminal vesicle invasion positive (SV+) results were significantly different between the two groups of patients with or without biochemical failure (Table 2).

**Cox proportional hazard models for BCR.** Univariate Cox proportional hazard model identified the following as significant factors for BCR: initial PSA  $\geq 7.6$  ng/mL ( $p = 0.0319$ ), extra-prostatic extension (EPE) positive ( $p < 0.0001$ ), RM+ ( $p < 0.0001$ ), SV+ ( $p < 0.0001$ ), Pathological Grade Group  $\geq 3$  ( $p < 0.0001$ ), lymph node metastases ( $p = 0.013$ ), radiological tumor location at PZ ( $p = 0.002$ ), and PI-RADS category 5 ( $p < 0.0001$ ) (Table 3).

Characteristics	
Total patients	299
Median age at surgery (range), y	67 (46–77)
Median PSA (range), ng/mL	7.6 (2.3–87.16)
PI-RADS v2.0 score, n (%)	
1–2/3/4/5	66 (22.1%)/25 (8.4%)/138 (46.2%)/70 (23.4%)
PI-RADS v2.1 score, n (%)	
1–2/3/4/5	35 (11.7%)/56 (18.7%)/138 (46.2%)/70 (23.4%)
Radiological location (TZ/PZ)	107/192
Surgical approach n (%)	
Open/laparoscopic/robot-assisted	33 (11.0%)/76 (25.4%)/190 (63.5%)
Lymph node dissection, n (%)	234 (78.3%)
Pathological Grade Group, n (%)	
1/2/3/4/5	23 (7.7%)/123 (41.1%)/93 (31.1%)/24 (8.0%)/35 (11.7%)
Undiagnosed	1 (0.3%)
Extraprostatic extension (EPE1), n (%)	71 (23.7%)
Resection margin (RM+), n (%)	89 (29.8%)
Seminal vesicle invasion (SV+), n (%)	28 (9.4%)
Lymph node metastasis (N1), n (%)	4 (1.3%)
Median observation period (months)	49.8
Biochemical failure, n (%)	48 (16.1%)

**Table 1.** Patient characteristics. PSA prostate-specific antigen, PI-RADS Prostate Reporting and Imaging and Data System, TZ transition zone, PZ peripheral zone.

Characteristic	With BCR	Without BCR	p value
No. patients (%)	48 (16.1%)	251 (83.9%)	–
Median baseline PSA (range), ng/mL	10.61 (4.15–47.35)	7.22 (2.3–87.16)	0.0026**
PI-RADS v2.1 category, n	1 (0), 2 (1), 3 (7), 4 (15), 5 (25)	1 (19), 2 (15), 3 (49), 4 (123), 5 (45)	<0.0001**
PI-RADS v2.1 category 5, n (%)	25 (52.1%)	45 (17.9%)	<0.0001**
Radiological location, TZ/PZ	8 (16.7%)/40 (83.3%)	99 (39.4%)/152 (60.6%)	0.0075**
Pathological Grade Group 3–5, n	40 (83.3%)	112 (44.6%)	<0.0001**
Resection margin positive, n (%)	30 (62.5%)	59 (23.5%)	<0.0001**
Seminal vesicle invasion, n (%)	15 (31.3%)	13 (5.18%)	<0.0001**
Lymph node metastasis, n (%)	2 (4.2%)	2 (0.8%)	0.1763

**Table 2.** Clinical characteristics according to presence or absence of BCR. PSA prostate-specific antigen, PI-RADS Prostate Reporting and Imaging and Data System, BCR biochemical recurrence, TZ transition zone, PZ peripheral zone. \*\* $p < 0.01$ .

Variable	Univariate			Multivariate		
	HR	95%CI	p value	HR	95%CI	p value
Age at surgery > 67 y	1.02	0.57–1.81	0.9489			
Initial PSA > 7.63	1.92	1.06–3.48	<b>0.0319*</b>	1.24	0.65–2.34	0.5169
EPE positive	5.39	2.88–10.08	<b>&lt;0.0001**</b>	1.31	0.57–2.99	0.7719
RM positive	4.59	2.49–8.46	<b>&lt;0.0001**</b>	2.17	1.01–4.68	0.083
SV invasion positive	8.54	4.54–16.06	<b>&lt;0.0001**</b>	2.65	1.26–5.58	<b>0.0103*</b>
Grade Group 3–5	6.40	2.86–14.31	<b>&lt;0.0001**</b>	2.82	1.20–6.64	<b>0.0174*</b>
Lymph node metastases	6.07	1.46–25.18	<b>0.013*</b>	2.31	0.49–10.9	0.2927
tumor location (PZ)	3.56	1.59–7.97	<b>0.002**</b>	2.96	1.23–7.11	<b>0.0157*</b>
PI-RADS category 5	4.20	2.36–7.44	<b>&lt;0.0001**</b>	2.8	1.48–5.29	<b>0.0015**</b>

**Table 3.** Uni- and multivariate Cox proportional hazard models for BCR-free survival. Significant values are in bold. PSA prostate-specific antigen, EPE extraprostatic extension, RM resection margin, SV seminal vesicle, PZ peripheral zone, PI-RADS Prostate Reporting and Imaging and Data System, BCR biochemical recurrence, HR hazard ratio, CI confidence interval. \* $p < 0.05$ ; \*\* $p < 0.01$ .

Multivariate analysis identified the following as independent risk factors for BCR: Pathological Grade Group  $\geq 3$  ( $p = 0.0174$ ), radiological tumor location at PZ ( $p = 0.0157$ ), seminal vesicle invasion positive ( $p = 0.0103$ ), and PI-RADS category 5 ( $p = 0.0015$ ).

**Kaplan–Meier analysis.** We performed Kaplan–Meier analysis to analyze factors identified as significant in the multivariate Cox proportional hazard model, which were radiological location at PZ ( $p = 0.001$ ) (Fig. 1A), pathological Grade Group 3 (Fig. 1B), seminal vesicle invasion (SV+) (Fig. 1C), and PI-RADS category 5 (Fig. 1D) (all  $p < 0.0001$ ). We built our original prediction model based on these four risk factors accordingly.

**Prognostic model for BCR using v2.1.** We propose a new scoring system that classifies the risk categories by the four factors (Pathological Grade Group  $\geq 3$ , radiological location at PZ, seminal vesicle invasion, and PI-RADS category 5) predictive of BCR after radical prostatectomy (Fig. 2A). One point is assigned for each positive factor, and the points are summed to give the total score. We divided the patients into three groups according to the summed score, as follows: score 0–2, low-risk group; 3 points, intermediate-risk group; and 4 points, high-risk group. There were 248 (82.9%), 39 (13.0%), and 12 (4.0%) patients in the low-, intermediate-, and high-risk groups, respectively. The Kaplan–Meier method was used to evaluate prognosis. Prognosis for BCR was the worst in the high-risk group. This novel prognostic model for BCR, which takes into account PI-RADS v2.1 as well as clinical factors, enables differentiation of patients according to risk factors for PFS between high- and intermediate-risk ( $p = 0.0065$ ), intermediate- and low-risk ( $p < 0.0001$ ), and low- and high-risk groups ( $p < 0.0001$ ) (Fig. 2B).

**Radiological location as a preoperative predictive factor.** Radiological location in the PZ was a worse prognostic factor than in the TZ (Fig. 1A). Patients with tumors in the radiological TZ had a lower BCR rate (7.5%) compared with those in the radiological PZ (20.8%) ( $p = 0.0075$ ) (Table 2). We divided patients into two groups according to the radiological location (radiological TZ and PZ groups).

The univariate Cox proportional hazard model found no factors of significance for BCR in the TZ group, whereas the PZ group showed significant differences in terms of EPE positive ( $p < 0.0001$ ), RM positive ( $p < 0.0001$ ), SV positive ( $p < 0.0001$ ), GG  $\geq 3$  ( $p = 0.0003$ ), lymph node metastases ( $p = 0.0388$ ), and PI-RADS

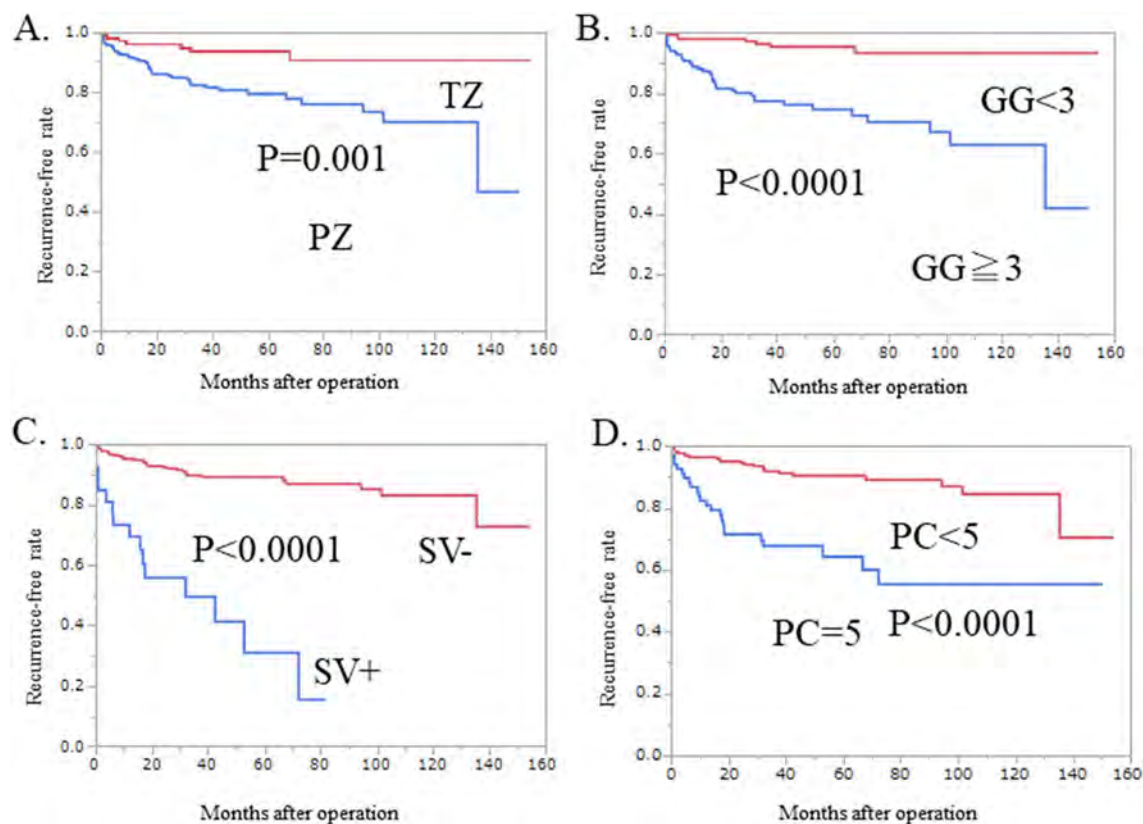


**Figure 1.** Kaplan–Meier analysis of factors identified as significant for BCR in the multivariate Cox proportional hazard model. (A) Radiological location. PFS in BCR was worse in tumors with radiological location in the PZ than in the TZ ( $p=0.001$ ). (B) Pathological Grade Group (GG). (C) Seminal vesicle invasion. (D) PI-RADS category (PC) 5. Tumors with Grade Group (3–5), seminal vesicle invasion (SV+), and PI-RADS category 5 had worse PFS in BCR ( $p < 0.0001$ ,  $p < 0.0001$ , and  $p < 0.0001$ , respectively) compared with Grade Group (1–2), SV-, and PI-RADS category (1–4).

category 5 ( $p < 0.0001$ ). Furthermore, multivariate analysis identified RM positive ( $p = 0.0219$ ), SV positive ( $p = 0.0114$ ), Grade Group  $\geq 3$  ( $p = 0.0201$ ), and PI-RADS category 5 ( $p = 0.0001$ ) as independent risk factors (Table 4).

It appears that preoperative PI-RADS location can predict the incidence of postoperative BCR. Patients with tumor in the radiological PZ region are more likely to suffer BCR if this finding is combined with the above four factors (RM positive, SV positive, Grade group  $\geq 3$ , and PI-RADS category 5) following radical prostatectomy.

**Effect of radiological localization on efficacy of predictive factors.** Tumors located in the TZ had a better prognosis for BCR (Table 4). Kaplan–Meier analysis among the radiological PZ tumors identified PI-RADS category 5 ( $p < 0.0001$ ) and Grade Group  $\geq 3$  ( $p < 0.0001$ ) as significant factors predictive of BCR. For tumors located in the TZ, neither of these factors was predictive of BCR ( $p = 0.6702$  and  $p = 0.2890$ , respectively) (Fig. 3).

These results indicate that Grade group  $\geq 3$  and PI-RADS category 5 could be used to assess the likely occurrence of BCR in PZ tumors, and show that the efficacy of the predictive factors varies according to the radiological location.

## Discussion

The present study is the first to report that BCR after radical prostatectomy can be predicted by preoperative MRI tumor location evaluated by PI-RADS v2.1. Our results showed that zonal location of the tumor on preoperative MRI was a significant predictor of BCR. Based on the factors remaining by multivariate analysis for prediction of BCR, we propose a novel risk-classification model based on the following: PZ lesion on MRI, Pathological Grade Group  $\geq 3$ , seminal vesicle invasion, and PI-RADS category 5. Classification of patients into the low-risk (0–2 points), intermediate-risk (3 points), and high-risk (4 points) groups predicted the prognosis of localized prostate cancer patients with statistically significant accuracy. The proposed risk classification system may contribute to the development of treatment strategies for localized prostate cancer.

Takahashi et al. reported that in radical prostatectomy specimens of Japanese patients, approximately 40% of prostate cancer originated in the TZ<sup>10</sup>. Compared to Caucasian men, Japanese patients had a greater incidence of TZ cancer. The pathological characteristics of TZ and PZ cancer are similar except for pathological T stage in

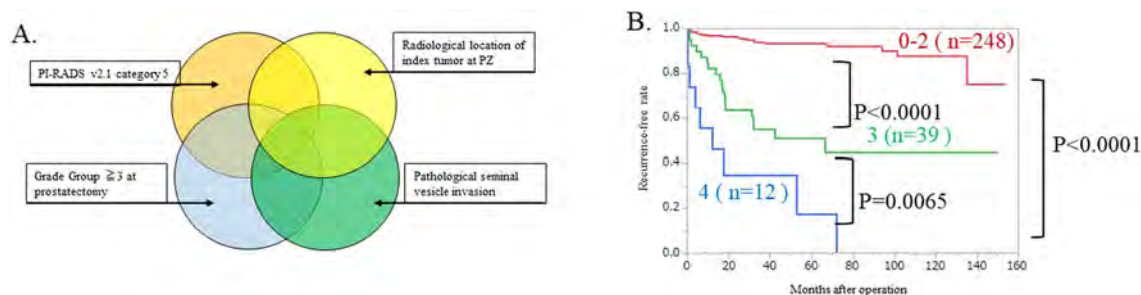


**Figure 2.** Novel prognostic model for BCR that combines PI-RADS v2.1 and clinical factors. (A) Novel prognostic model for BCR. The scoring system classifies the risk category according to the four factors predictive of BCR after radical prostatectomy. (B) Kaplan–Meier curve according to the novel prognostic model. The total score is the summed score of all positive factors (one point each). We divided the patients into three groups according to the summed score. Patients with a score of 0–2 were defined as the low-risk group ( $n = 248$ ), those with 3 points as the intermediate-risk group ( $n = 39$ ), and those with 4 points as the high-risk group ( $n = 12$ ). Risk classification significantly differentiated the PFS of BCR between the high- and intermediate-risk, between the intermediate- and low-risk, and between the low- and high-risk groups ( $p = 0.0065$ ,  $p < 0.0001$ ,  $p < 0.0001$ ).

Variable	PZ						TZ		
	Univariate			Multivariate			Univariate		
	HR	95% CI	<i>p</i> value	HR	95% CI	<i>P</i> value	HR	95% CI	<i>p</i> value
Age at surgery > 67 y	1.01	0.54–1.89	0.9653				1.03	0.23–4.65	0.9628
Initial PSA > 7.63	1.64	0.86–3.11	0.1307				3.00	0.58–15.5	0.1895
EPE positive	5.49	2.74–11.03	<b>&lt; 0.0001**</b>	1.38	0.57–3.32	0.478	2.46	0.45–13.4	0.4922
RM positive	4.97	2.46–10.04	<b>&lt; 0.0001**</b>	2.63	1.15–6.03	<b>0.0219*</b>	1.52	0.29–7.83	0.8832
SV invasion positive	7.78	3.96–15.3	<b>&lt; 0.0001**</b>	2.72	1.25–5.90	<b>0.0114*</b>	4.83	0.57–41.2	0.1501
Grade Group 3–5	6.75	2.40–19.0	<b>0.0003**</b>	3.61	1.22–10.6	<b>0.0201*</b>	2.32	0.47–11.5	0.3032
N+	4.52	1.08–18.9	<b>0.0388*</b>	2.57	0.54–12.3	0.2381	–	–	–
PI-RADS category 5	5.63	3.00–10.6	<b>&lt; 0.0001**</b>	3.85	1.93–7.70	<b>0.0001**</b>	0.63	0.76–5.27	0.6729

**Table 4.** Difference in the predictive factors between the radiological location. Significant values are in bold. PSA prostate-specific antigen, EPE extraprostatic extension, RM resection margin, SV seminal vesicle, N+: lymph-node positive, PI-RADS Prostate Reporting and Imaging and Data System, PZ peripheral zone, TZ transition zone. \* $p < 0.05$ ; \*\* $p < 0.01$ .

the case of autopsy and cystoprostatectomy for bladder cancer<sup>11</sup>. TZ cancers are associated with decreased odds of adverse pathological findings and demonstrate improved recurrence-free survival. These favorable outcomes appear to be the result of different tumor biology<sup>12</sup>. Understanding the biology of tumors originating in different prostate zones will enable zone-specific therapies<sup>13</sup>. The present study revealed that for prediction of BCR, the efficacy of Grade group  $\geq 3$  and PI-RADS category 5 differed between the radiological TZ and PZ. This risk criterion may predict BCR after radical prostatectomy and enable optimization of zone-specific therapeutic strategy. As discussed in a previous report<sup>13</sup>, zone-specific strategies may be considered when choosing between active surveillance, radical prostatectomy, and extended lymph node dissection in patients with Gleason Score and T stage in the same category but in different location. The rationale for the zone-specific strategy may be explained by the difference in the genetic background and biomarker between TZ and PZ, which will lead to the difference in the therapeutic response and prognosis<sup>13</sup>.

Previous studies have shown that seminal vesicle invasion and extraprostatic extension predict BCR after radical prostatectomy are related to predictive factors<sup>14–16</sup>. A positive surgical margin affects the incidence of BCR<sup>17,18</sup>. BCR risk is significantly higher for posterior-positive surgical margin than for other positive surgical margins<sup>19</sup>. Broad and anterior positive surgical margin has the highest risk of recurrence after radical perineal prostatectomy<sup>20</sup>. Prognosis was worse in the case of positive seminal vesicle invasion on preoperative MRI compared with negative seminal vesicle invasion<sup>21</sup>.

Several reports have evaluated oncological outcomes in patients with negative mp-MRI. Vinayak reported that patients with negative MRI findings (PI-RADS v2.0 score  $\leq 2$ ) who underwent radical prostatectomy had oncological outcomes comparable with positive MRI findings (PI-RADS v2.0 score  $\geq 3$ ) in terms of clinically significant prostate cancer rates, positive surgical margins, and BCR rates<sup>22</sup>. Shin et al. assessed patients with PI-RADS categories 4–5 on preoperative MRI who underwent prostatectomy and concluded that prognosis was predicted by the location of the lesion on preoperative MRI<sup>23</sup>.

In the present study, we analyzed patients with PI-RADS categories 1–5, not just categories 4–5. We found that prognosis was predicted by tumor location in PI-RADS v2.1 category 5 by MRI. To the best of our knowledge,

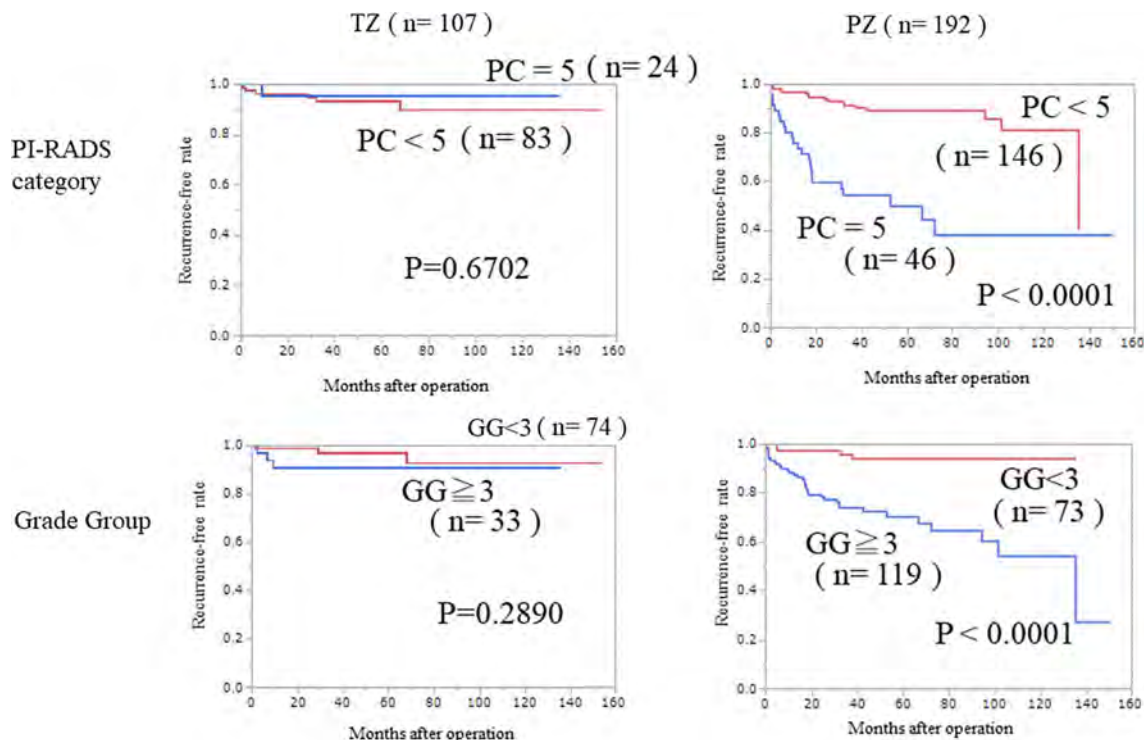


**Figure 3.** Kaplan–Meier analysis of efficacy of predictive factors according to radiological location. In PZ tumors, PI-RADS category 5 and Grade group  $\geq 3$  were significant predictive factors of BCR ( $p < 0.0001$  and  $p < 0.0001$ , respectively). In TZ tumors, PI-RADS category 5 and Grade group  $\geq 3$  were not predictive of BCR ( $p = 0.6702$  and  $p = 0.2890$ , respectively). These findings illustrate that the efficacy of  $GG \geq 3$  and PI-RADS category 5 differ according to the radiological location of the tumor.

this is the first study to report the ability of zonal location on preoperative MRI to predict post-operative BCR of prostate cancer using PI-RADS v2.1.

**Differences in evaluation between PI-RADS v2.0 and PI-RADS v2.1.** There are three significant differences between PI-RADS v2.1 and v2.0 in evaluating scoring. First, the definitions of scores 1 and 2 have been revised for TZ lesions on T2WI. Second, on evaluating the total score in TZ, a DWI score of 4 or 5 elevates the overall PI-RADS assessment category from 2 to 3 for lesions receiving a T2WI score of 2. Third, the definitions for DWI scores of 2 and 3 have been revised for lesions located in TZ/PZ. As PI-RADS v2.1 improves inter-reader reproducibility, these revisions may contribute to increased diagnostic performance<sup>6,24</sup>. We have previously reported that bp-MRI and Grade Group predict BCR after radical prostatectomy<sup>8</sup>. In the present study, we analyzed the predictive ability of location on preoperative MRI and evaluation using the new categorization in PI-RADS v2.1 in a large number of patients who underwent radical prostatectomy. In our study, changing to the PI-RADS v2.1 criteria resulted in a change in classification for 40 of the 299 patients. The data of these 40 patients are summarized in Supplementary Table 1.

**Limitations.** There are several limitations of this study. First, the number of patients analyzed was relatively limited and the evaluations were performed retrospectively. We plan to confirm our results in multi-institutional and prospective settings. Second, the median follow-up period was 49.8 months, and thus assessment related to survival was inadequate. It is necessary to assess oncological outcomes in a longer term. Third, surgery was performed mainly by three surgeons. The differences in prognosis may have been affected by the surgeons' skills. Finally, patients of a single Asian race were investigated in our study. The incidence of and deaths due to prostate cancer are lower in the Asian population than in the Western population<sup>25</sup>, which might have some impact on the generalizability of our results.

## Conclusion

To the best of our knowledge, this is the first report to evaluate the risk of BCR by radiological tumor location by PI-RADS v2.1 category on preoperative MRI and by pathological diagnosis. We propose a novel risk-classification model based on the following independent risk factors: PZ location on MRI, Pathological Grade Group  $\geq 3$ , seminal vesicle invasion, and PI-RADS category 5. This risk model could be applied to constructing and optimizing treatment strategies for patients with localized prostate cancer.

## Materials and methods

Clinical data from 299 patients who had undergone radical prostatectomy at Chiba University Hospital between 2006 to 2018 were retrospectively investigated. Ethics declaration: The study was approved by the Research ethics committee of the graduate school of medicine, Chiba University (approval number 2718). Informed consent was obtained from all participants and/or their legal guardians. The present study was conducted in accordance with ethical standards that promote and ensure respect and integrity for all human subjects and the Declaration of Helsinki. All experiments were performed in accordance with relevant named guidelines and regulations. The clinical factors of Gleason score, pathological features, and clinical tumor location were obtained from the patients' medical records. Radical prostatectomy was performed by one of three surgical approaches (open, laparoscopic, and robot-assisted). Lymph node dissection was performed in 234/299 patients (78.3%). All patients underwent preoperative MRI followed by prostate biopsy and total prostatectomy.

We compared each patient's scores for Prostate Imaging Reporting and Data System (PI-RADS) version 2.1 and version 2.0, based on bp-MRI. Overall survival and BCR-free survival were evaluated by the Kaplan–Meier method.

**Definition of PSA progression.** Using the definition of the Prostate Cancer Clinical Trial Working Group 2 (PCWG2)<sup>26</sup>, we defined BCR as an elevation in PSA of  $\geq 0.2$  ng/mL after radical prostatectomy, which was confirmed in two consecutive measurements obtained at least 2 weeks apart. We defined the operation date as the date of PSA failure if PSA was  $\geq 0.2$  ng/mL after radical prostatectomy.

**MRI protocol.** All enrolled patients underwent prostate MRI at 3 T prior to prostate biopsy. MRI was obtained with T1-weighted, T2-weighted, and diffusion-weighted imaging (DWI), and apparent diffusion coefficient maps were generated with b values of 0 and 1000 s/mm<sup>2</sup>. We used a high b-value (b = 2000) for DWI. bp-MRI comprised T2-weighted imaging and DWI. The radiologist used both bp-MRI and the apparent diffusion coefficient maps to determine the PI-RADS score.

**PI-RADS v2.1.** The PI-RADS scores were evaluated on non-contrast-enhanced bp-MRI by one radiologist (T.H.) with over 10 years of experience in diagnostic radiology. Using the scoring method of PI-RADS v2.1, each patient's score was recorded using a 5-point scale (1–5) and the zonal location. PI-RADS v2.1 was designed to improve detection, location, characterization, and risk stratification in patients with suspected cancer in treatment-naïve prostate glands, with the overall objective of improving outcomes for patients. The changes incorporated in PI-RADS v2.1 were revised scoring of DWI in all zones in categories 2–3, and scoring of the overall assessment category in TZ. In TZ, a DWI score of 4 or 5 elevates the overall PI-RADS assessment category from 2 to 3 for lesions that receive a T2W score of 2. PI-RADS v2.1 states that T2-weighted images should be evaluated in the axial plane and in at least one additional orthogonal plane<sup>27</sup>.

**Statistical analysis.** We performed univariate and multivariate Cox proportional hazard analyses to evaluate hazard ratios for BCR-free survival. Cut-offs of continuous variables were selected according to median values. Hazard ratios and 95% confidence intervals were derived. Kaplan–Meier methods were used for survival analysis. Statistical analysis was performed using JMP 14.2.0 (SAS Institute, Cary, NC, USA). Significance was considered at  $p < 0.05$ .

## Data availability

The data sets used and analyzed in the current study are available from the corresponding authors upon reasonable request.

Received: 27 January 2023; Accepted: 8 June 2023

Published online: 21 June 2023

## References

- Sung, H. *et al.* Global cancer statistics 2020: GLOBOCAN estimates of incidence and mortality worldwide for 36 cancers in 185 countries. *CA Cancer J. Clin.* **71**, 209–249. <https://doi.org/10.3322/caac.21660> (2021).
- Litwin, M. S. & Tan, H. J. The diagnosis and treatment of prostate cancer: A review. *JAMA* **317**, 2532–2542. <https://doi.org/10.1001/jama.2017.7248> (2017).
- Mohsen, N. Role of MRI, ultrasound, and computed tomography in the management of prostate cancer. *PET Clin.* **17**, 565–583. <https://doi.org/10.1016/j.cpet.2022.07.002> (2022).
- Barentsz, J. O. *et al.* ESUR prostate MR guidelines 2012. *Eur. Radiol.* **22**, 746–757. <https://doi.org/10.1007/s00330-011-2377-y> (2012).
- Weinreb, J. C. *et al.* PI-RADS prostate imaging—Reporting and data system: 2015, version 2. *Eur. Urol.* **69**, 16–40. <https://doi.org/10.1016/j.eururo.2015.08.052> (2016).
- Turkbey, B. *et al.* Prostate imaging reporting and data system version 2.1: 2019 update of prostate imaging reporting and data system version 2. *Eur. Urol.* **76**, 340–351. <https://doi.org/10.1016/j.eururo.2019.02.033> (2019).
- Thestrup, K. C. *et al.* Biparametric versus multiparametric MRI in the diagnosis of prostate cancer. *Acta Radiol. Open* **5**, 2058460116663046. <https://doi.org/10.1177/2058460116663046> (2016).
- Takeuchi, N. *et al.* Biparametric prostate imaging reporting and data system version 2 and international society of urological pathology grade predict biochemical recurrence after radical prostatectomy. *Clin. Genitourinary Cancer* **16**, e817–e829. <https://doi.org/10.1016/j.clgc.2018.02.011> (2018).
- Baba, H. *et al.* Tumor location and a tumor volume over 2.8 cc predict the prognosis for Japanese localized prostate cancer. *Cancers* <https://doi.org/10.3390/cancers14235823> (2022).

10. Takahashi, H. *et al.* Differences in prostate cancer grade, stage, and location in radical prostatectomy specimens from united states and japan. *Prostate* **74**, 321–325. <https://doi.org/10.1002/pros.22754> (2014).
11. Inaba, H. *et al.* Tumor location and pathological features of latent and incidental prostate cancer in contemporary japanese men. *J. Urol.* **204**, 267–272. <https://doi.org/10.1097/ju.0000000000000804> (2020).
12. Lee, J. J. *et al.* Biologic differences between peripheral and transition zone prostate cancer. *Prostate* **75**, 183–190. <https://doi.org/10.1002/pros.22903> (2015).
13. Ali, A. *et al.* Prostate zones and cancer: Lost in transition?. *Nat. Rev. Urol.* **19**, 101–115. <https://doi.org/10.1038/s41585-021-00524-7> (2022).
14. Epstein, J. I., Partin, A. W., Sauvageot, J. & Walsh, P. C. Prediction of progression following radical prostatectomy. A multivariate analysis of 721 men with long-term follow-up. *Am. J. Surg. Pathol.* **20**, 286–292. <https://doi.org/10.1097/00000478-199603000-00004> (1996).
15. Salomon, L. *et al.* Seminal vesicle involvement after radical prostatectomy: Predicting risk factors for progression. *Urology* **62**, 304–309. [https://doi.org/10.1016/s0090-4295\(03\)00373-x](https://doi.org/10.1016/s0090-4295(03)00373-x) (2003).
16. Matti, V. *et al.* Predictive value of pathological features for progression after radical prostatectomy. *Eur. Urol.* **26**, 197–201. <https://doi.org/10.1159/000475379> (1994).
17. Sooriakumaran, P., Dev, H. S., Skarecky, D. & Ahlering, T. The importance of surgical margins in prostate cancer. *J. Surg. Oncol.* **113**, 310–315. <https://doi.org/10.1002/jso.24109> (2016).
18. Matti, B., Reeves, F., Prouse, M. & Zargar-Shoshtari, K. The impact of the extent and location of positive surgical margins on the risk of biochemical recurrence following radical prostatectomy in men with Gleason 7 prostate cancers. *Prostate* **81**, 1428–1434. <https://doi.org/10.1002/pros.24240> (2021).
19. Iremashvili, V., Pelaez, L., Jorda, M., Parekh, D. J. & Punnen, S. A comprehensive analysis of the association between Gleason score at a positive surgical margin and the risk of biochemical recurrence after radical prostatectomy. *Am. J. Surg. Pathol.* **43**, 369–373. <https://doi.org/10.1097/pas.0000000000001204> (2019).
20. Sammon, J. D. *et al.* Risk factors for biochemical recurrence following radical perineal prostatectomy in a large contemporary series: A detailed assessment of margin extent and location. *Urol. Oncol.* **31**, 1470–1476. <https://doi.org/10.1016/j.urolonc.2012.03.013> (2013).
21. Kim, J. K., Lee, H. J., Hwang, S. I., Choe, G. & Hong, S. K. Prognostic value of seminal vesicle invasion on preoperative multiparametric magnetic resonance imaging in pathological stage T3b prostate cancer. *Sci. Rep.* **10**, 5693. <https://doi.org/10.1038/s41598-020-62808-z> (2020).
22. Wagaskar, V. G. *et al.* Clinical characteristics and oncological outcomes in negative multiparametric MRI patients undergoing robot-assisted radical prostatectomy. *Prostate* **81**, 772–777. <https://doi.org/10.1002/pros.24174> (2021).
23. Shin, N. & Park, S. Y. Postoperative biochemical failure in patients with PI-RADS category 4 or 5 prostate cancers: Risk stratification according to zonal location of an index lesion. *AJR Am. J. Roentgenol.* **215**, 913–919. <https://doi.org/10.2214/ajr.19.22653> (2020).
24. Tamada, T. *et al.* Comparison of PI-RADS version 2 and PI-RADS version 2.1 for the detection of transition zone prostate cancer. *Eur. J. Radiol.* **121**, 108704. <https://doi.org/10.1016/j.ejrad.2019.108704> (2019).
25. Akaza, H., Onozawa, M. & Hinotsu, S. Prostate cancer trends in Asia. *World J. Urol.* **35**, 859–865. <https://doi.org/10.1007/s00345-016-1939-7> (2017).
26. Scher, H. I. *et al.* Design and end points of clinical trials for patients with progressive prostate cancer and castrate levels of testosterone: Recommendations of the prostate cancer clinical trials working group. *J. Clin. Oncol.* **26**, 1148–1159. <https://doi.org/10.1200/jco.2007.12.4487> (2008).
27. Barrett, T., Rajesh, A., Rosenkrantz, A. B., Choyke, P. L. & Turkbey, B. PI-RADS version 2.1: One small step for prostate MRI. *Clin. Radiol.* **74**, 841–852. <https://doi.org/10.1016/j.crad.2019.05.019> (2019).

## Acknowledgements

The present study was supported by grants from Grant-in-Aid for Scientific Research (C) (20K09555 to S.S.), Grant-in-Aid for Scientific Research (B) (20H03813 to T.I.), and the Japan China Sasakawa Medical Fellowship (to X.Z.).

## Author contributions

A.F. contributed to collecting data, preparing figures, drawing tables, and writing; S.S. contributed to analyzing data, collecting bibliography, and writing; T.H. and Y.Y. contributed to analyzing data. X.Z., J.R., N.T., Y.I., T.S., K.M., and J.I. contributed to collecting data. S.S. and T.I. contributed to the supervision of all activities. The first draft of the manuscript was prepared by A.F., T.H.; and X.Z. performed subsequent amendments. S.S. revised the manuscript. All authors have read and agreed to the published version of the manuscript.

## Competing interests

The authors declare no competing interests.

## Additional information

**Supplementary Information** The online version contains supplementary material available at <https://doi.org/10.1038/s41598-023-36685-1>.

**Correspondence** and requests for materials should be addressed to S.S.

**Reprints and permissions information** is available at [www.nature.com/reprints](http://www.nature.com/reprints).

**Publisher's note** Springer Nature remains neutral with regard to jurisdictional claims in published maps and institutional affiliations.



**Open Access** This article is licensed under a Creative Commons Attribution 4.0 International License, which permits use, sharing, adaptation, distribution and reproduction in any medium or format, as long as you give appropriate credit to the original author(s) and the source, provide a link to the Creative Commons licence, and indicate if changes were made. The images or other third party material in this article are included in the article's Creative Commons licence, unless indicated otherwise in a credit line to the material. If material is not included in the article's Creative Commons licence and your intended use is not permitted by statutory regulation or exceeds the permitted use, you will need to obtain permission directly from the copyright holder. To view a copy of this licence, visit <http://creativecommons.org/licenses/by/4.0/>.

© The Author(s) 2023

# Preoperative PI-RADS v2.1 Scoring System Improves Risk Classification in Patients Undergoing Radical Prostatectomy

YUDAI FUKUI<sup>1+</sup>, YASUTAKA YAMADA<sup>1+</sup>, SHINICHI SAKAMOTO<sup>1</sup>, TAKURO HORIKOSHI<sup>2</sup>,  
XUE ZHAO<sup>1</sup>, KODAI SATO<sup>1</sup>, SAKIE NANBA<sup>2</sup>, YOSHIHIRO KUBOTA<sup>2</sup>,  
MANATO KANESAKA<sup>1</sup>, AYUMI FUJIMOTO<sup>1</sup>, HIROKI SHIBATA<sup>1</sup>, YUSUKE GOTO<sup>1</sup>,  
TOMOKAZU SAZUKA<sup>1</sup>, YUSUKE IMAMURA<sup>1</sup>, TAKASHI UNO<sup>2</sup> and TOMOHIKO ICHIKAWA<sup>1</sup>

<sup>1</sup>Department of Urology, Chiba University Graduate School of Medicine, Chiba, Japan;

<sup>2</sup>Department of Radiology, Chiba University Graduate School of Medicine, Chiba, Japan

**Abstract.** *Background/Aim:* The purpose of this study was to examine the prognostic value of Prostate imaging-reporting and data system (PI-RADS) v2.1 scoring system in patients who underwent radical prostatectomy (RP). *Patients and Methods:* Clinical data of 294 patients who received RP between 2006 and 2018 were reviewed and multiple parameters including PI-RADS v2.1 score were employed to identify predictive factors for biochemical recurrence (BCR). Tumor volume was calculated from prostatectomy specimens. *Results:* Median age at operation and initial PSA level were 67 years old and 7.68 ng/ml, respectively. 44.9 and 24.8% of patients were diagnosed with PI-RADS score 4 and 5 prior to biopsies, respectively. BCR was observed in 17% of patients and median observation period was 63.43 months. After multivariate analysis, PI-RADS v2.1 score 5 [hazard ratio (HR)=2.24,  $p=0.0124$ ] was an independent predictive factor of BCR in addition to clinical T stage ( $\geq 2c$ ) (HR=2.32,  $p=0.0093$ ) and biopsy Gleason score ( $\geq 8$ ) (HR=2.81,  $p=0.0007$ ). Furthermore, PI-RADS score 5 significantly stratified the prognosis in D'Amico intermediate- and high-risk groups ( $p=0.0174$  and  $p=0.0013$ , respectively). We established novel risk classifications including PI-RADS v2.1 score and found that prognostic capabilities were improved as compared to the D'Amico classification. *Conclusion:* The PI-RADS v2.1 score exhibited significant prognostic value in patients with localized prostate cancer following RP. Risk

classifications based on PI-RADS v2.1 score might provide better ability for predicting oncological outcomes as compared to the D'Amico classification system.

Prostate cancer is the most commonly diagnosed cancer among men with approximately 280,000 cases and the second leading cause of cancer death with 34,700 cases in men in the United States (1, 2). Clinically localized PCa has an extremely favorable prognosis, however, early biochemical recurrence (BCR) may occur in some cases after definitive treatment, requiring adjuvant therapy. Previous studies have attempted to develop useful models to predict prognosis after radical prostatectomy (RP). For instance, the D'Amico classification system was proposed as an optimal staging system following local treatment such as RP and radiotherapy (3). Thereafter, this classification including Gleason score sum (GS), prostate-specific antigen (PSA) level, and clinical T stage, has been widely used for risk stratification in patients with localized PCa. However, better risk-based classification systems using preoperative factors are required to enable better informed decision-making regarding treatment.

The Prostate Imaging-Reporting and Data System (PI-RADS) scoring system was first proposed to represent cancer lesion and aggression using multi-parametric magnetic resonance imaging (mp-MRI) in 2012 by the European Society of Urogenital Radiology (ESUR) (4). Thereafter, several improvements have been made, and version 2.1 is currently in clinical use (5, 6). This system assesses the detectable lesions by mp-MRI and scores the degree of clinically significant cancer lesions (4). The PI-RADS v2.1 scoring system has previously been reported to detect clinically significant prostate cancer, improve the diagnostic accuracy, and avoid unnecessary prostate biopsies (7). However, little is known about its clinical significance as a prognostic predictor after definitive treatment. Given that the PI-RADS scoring system is relevant to likelihood of prostate cancer, in other words, might be related to the size of the cancer lesions on MRI findings, it may be

+These Authors contributed equally to this study.

*Correspondence to:* Shinichi Sakamoto, Associate Professor, Chiba University Graduate School of Medicine, 1-8-1 Inohana, Chuo-ku, Chiba-city, Chiba 260-8670, Japan. Tel: +81 432262134, Fax: +81 432262136, e-mail: rbatbat1@gmail.com

*Key Words:* Prostate cancer, PI-RADS v2.1, radical prostatectomy, risk classification, tumor volume.

useful to develop a risk classification prior to local therapy for predicting oncological outcomes. The D'Amico classification system was originally developed in 1998 and has since been widely applied in approaches for assessing prostate cancer risk (8-10). This classification system was designed to evaluate the risk of recurrence following local treatment of prostate cancer and is used to make more informed decisions regarding their treatment options.

In the present study, we hypothesized that preoperative PI-RADS v2.1 scoring system would improve the accuracy of predicting postoperative BCR by modifying the existing risk classifications such as the D'Amico classification system. Herein, we explored the clinical utility of preoperative PI-RADS v2.1 score and established a novel risk classification for better prediction of clinical outcomes in patients undergoing RP.

### Patients and Methods

**Patients.** Clinical data from 294 patients who underwent RP at Chiba University Hospital and affiliated institutions between 2006 and 2018 were reviewed. Enrolled patients had undergone prostate needle biopsies and diagnosed with prostate adenocarcinoma with GS classification by the pathologists. All patients underwent RP without neoadjuvant hormone therapy using open, laparoscopic, and robot-assisted procedures. The present study was approved by all institutional review boards and informed consent was obtained from all patients.

**Data collection.** We investigated the following clinical data for each patient: age at operation, initial PSA (iPSA) level prior to biopsies, prostate volume, biopsy GS sum (bGS), clinical TNM classification, and pathological outcomes of the prostate specimen. The following method was used to measure tumor volumes of prostatectomy specimens (11). All specimens were sectioned transversely at 5-mm intervals and submitted as whole sections. If multiple tumors were present, only the index tumor was measured. All slides containing cancer lesions were imported into ImageJ (National Institutes of Health, Bethesda, MD, USA). Tumor volume was determined by scanning the specimen sections and analyzing the area of the tumor using ImageJ. The following formula was used: total tumor volume (ml)=tumor area × specimen thickness × 1.1 (shrinkage corrected) (11).

**MRI protocol and PI-RADS v2.1 scoring system.** All patients underwent MRI of the prostate at 3T prior to prostate biopsy. MRI was performed using T1-weighted, T2-weighted, and diffusion-weighted imaging (DWI) sequences to produce an apparent diffusion coefficient map. A high b value (b=2,000) was used for DWI. MRI consisted of T2-weighted images and DWI. Both the biparametric MRI (bp-MRI) comprising T2-weighted imaging and DWI, and the apparent diffusion coefficient map were employed by the radiologist to determine the PI-RADS v2.1 score.

PI-RADS v2.1 scores were assessed by the radiologist with non-contrast bp-MRI. The score for each patient was documented using the PI-RADS v2.1 scoring method (5-point scale). The modifications implemented in PI-RADS v2.1 were the scoring of DWI in all zones in categories 2-3 and the revised scoring of the overall rating category in the transition zones (TZs). A DWI score of 4 or 5 elevated the overall PI-RADS rating category from 2 to 3 for lesions with a T2W score of 2 in a TZ (12).

Table I. Patient background.

No. of patients	294
Median age at diagnosis (range), years	67 (46-77)
Median initial PSA (range), ng/ml	7.68 (0.02-87.16)
Prostate volume (range) ml	29 (10.97-112)
PI-RADS v2.1 score n (%)	
≤3	89 (30.3)
4	132 (44.9)
5	73 (24.8)
Clinical T stage, n (%)	
≤2b	213 (72.9)
≥2c	79 (27.0)
Biopsy GS, n (%)	
≤7	227 (77.2)
≥8	67 (22.8)
Surgical procedures (Open/LRP/RARP), n (%)	33 (11.2)/77 (26.2)/184 (62.6)
Pathological T stage, n (%)	
≤2b	213 (72.9)
≥2c	79 (27.0)
Pathological GS, n (%)	
≤7	231 (79.3)
≥8	60 (20.7)
RM, n (%)	88 (31.2)
Tumor volume (ml)	1.88 (0.02-25.02)
Biochemical recurrence, n (%)	50 (17)
Median observation period (range), months	63.43 (4.87-161.47)

PSA: Prostate-specific antigen; PI-RADS: prostate imaging-reporting and data system; GS: Gleason score; RM: resection margin; LRP: laparoscopic radical prostatectomy; RARP: robot-assisted radical prostatectomy.

**Definition of biochemical recurrence (BCR).** The Prostate Cancer Clinical Trial Working Group 2 (PCWG2) definition was employed to determine BCR in the present study (13). BCR was defined as a PSA concentration ≥0.2 ng/ml following RP, measured on two consecutive occasions at least 2 weeks apart. The date of surgery was defined as the date of BCR if PSA level was ≥0.2 ng/ml even postoperatively.

**Statistical analysis.** Student's *t*-test and the  $\chi^2$  test were used for comparisons between groups. Kaplan–Meier methods (log-rank test) and Cox proportional hazard models were implemented to evaluate the clinical outcomes and predictive factors. Multivariate analysis was performed with clinical parameters showing statistical significance in univariate analyses. JMP Pro 15 (SAS Institute, Tokyo, Japan) was used to for statistical analyses. Statistical significance was set at the level of  $p < 0.05$ .

### Results

**Patients background.** The study included 294 patients with localized prostate cancer. Median age and PSA level at operation were 67 years old and 7.68 ng/ml, respectively (Table I). Pre-biopsy PI-RADS v2.1 score was 44.9% for score 4 and 24.8% for score 5. Sixty-seven patients (22.8%)

Table II. Characteristics of patients classified according to the prostate imaging-reporting and data system (PI-RADS) v2.1 score.

	PI-RADS score		p-Value
	≤3 (n=89)	≥4 (n=205)	
Median age (range), years	66 (50-76)	68 (46-77)	0.0465 <sup>#</sup>
Median initial PSA (range), ng/ml	6.35 (0.02-25.31)	8.33 (2.45-87.16)	0.0006 <sup>#</sup>
Median prostate volume (range), ml	30.5 (15.95-112)	28.1 (10.97-106)	0.0004 <sup>#</sup>
Clinical T stage, n (%)			0.0002 <sup>*</sup>
≤2b	81 (94.2)	155 (77.1)	
≥2c	5 (5.8)	46 (22.8)	
Biopsy GS, n (%)			0.0006 <sup>*</sup>
≤7	78 (87.6)	149 (72.7)	
≥8	11 (12.4)	56 (27.3)	
D'Amico classification, n (%)			0.0033 <sup>*</sup>
Low	20 (22.5)	15 (7.3)	
Intermediate	55 (61.8)	125 (61)	
High	14 (15.7)	65 (31.7)	
Pathological T stage, n (%)			<0.0001 <sup>*</sup>
≤2b	42 (48.8)	45 (22.6)	
≥2c	44 (51.2)	154 (77.4)	
Pathological GS, n (%)			0.0228 <sup>*</sup>
≤7	76 (87.4)	154 (75.5)	
≥8	11 (12.6)	50 (24.5)	
RM, n (%)	11 (12.6)	77 (39.5)	<0.0001 <sup>*</sup>
Tumor volume (ml)	0.715 (0.02-8.55)	2.1655 (0.0913-25.02)	<0.0001 <sup>#</sup>
Biochemical recurrence, n (%)	9 (10.1)	41 (20)	0.0309 <sup>+</sup>

PSA: Prostate-specific antigen; GS: Gleason score; RM: resection margin; <sup>#</sup>Student's *t*-test; <sup>\*</sup> $\chi^2$  test; <sup>+</sup>Kaplan-Meier method.

were diagnosed with bGS ≥8 prior to surgery. A positive resection margin (RM) was observed in 31.2% of patients. Median tumor volume was 1.88 ml and 17% showed BCR following RP. Median observation period in this study was 63.43 months (Table I).

*The prognostic significance of PI-RADS v2.1 scoring system and its relation to patient backgrounds.* We divided patients into those with PI-RADS v2.1 score ≤3 and those with ≥4 and compared patient backgrounds between groups (Table II). Patients with a score ≥4 were more likely to be older ( $p=0.0465$ ), with a higher iPSA level ( $p=0.0006$ ), more advanced T stage ( $p=0.0002$ ) and classification as high risk by the D'Amico classification ( $p=0.0033$ ). A higher incidence of a positive RM was observed in patients with a score ≥ 4 as compared to those with a score of ≤3 (39.5 vs. 12.6%,  $p<0.0001$ ). In addition, higher PI-RADS v2.1 score was correlated positively with larger tumor volume ( $p<0.0001$ , Table II and Figure 1A). Median tumor volumes were 0.57 ml, 0.78 ml, 0.73 ml, 1.87 ml, and 4.28 ml for scores 1-5, respectively (Figure 1A). Kaplan–Meier analysis showed shorter progression-free survival (PFS) in patients with PI-RADS v2.1 score 5 than those with ≤4 ( $p<0.0001$ , Figure 1B). Furthermore, to moderate the difference in patients' backgrounds, the propensity score-matching (PSM)

method was employed for evaluating the prognostic value. After 1:1 PSM based on age at operation, initial PSA, and bGS, a total of 112 patients, 56 each, were considered. Patients with preoperative PI-RADSv2.1 score 5 had unfavorable outcomes as compared to those with ≤4 ( $p=0.0366$ , Figure 1C).

In addition, we investigated a prognostic significance of PI-RADS v2.1 score 5 using Cox proportional hazard models and found that iPSA [hazard ratio (HR)=1.88,  $p=0.0291$ ], PSA density (HR=1.09,  $p=0.0008$ ), clinical T stage (≥2c) (HR=4.16,  $p<0.0001$ ), bGS (≥8) (HR=4.37,  $p<0.0001$ ), and PI-RADS v2.1 score 5 (HR=4.12,  $p<0.0001$ ) were associated with PFS in univariate analyses (Table III). After multivariate analysis, clinical T stage [HR=2.32, 95% confidence interval (CI)=1.23-4.38,  $p=0.0093$ ], bGS (HR=2.81, 95%CI=1.55-5.1,  $p=0.0007$ ), and PI-RADS v2.1 (HR=2.24, 95%CI=1.19-4.23,  $p=0.0124$ ) were found to be independent prognostic factors for PFS (Table III).

*Prognostic value of the D'Amico classification and PI-RADS v2.1 scoring system.* Based on the prognostic importance of PI-RADS v2.1 score, we hypothesized that PI-RADS v2.1 could improve the capability to predict clinical outcomes of existing risk classifications (e.g., D'Amico classification). We confirmed that the D'Amico classification system

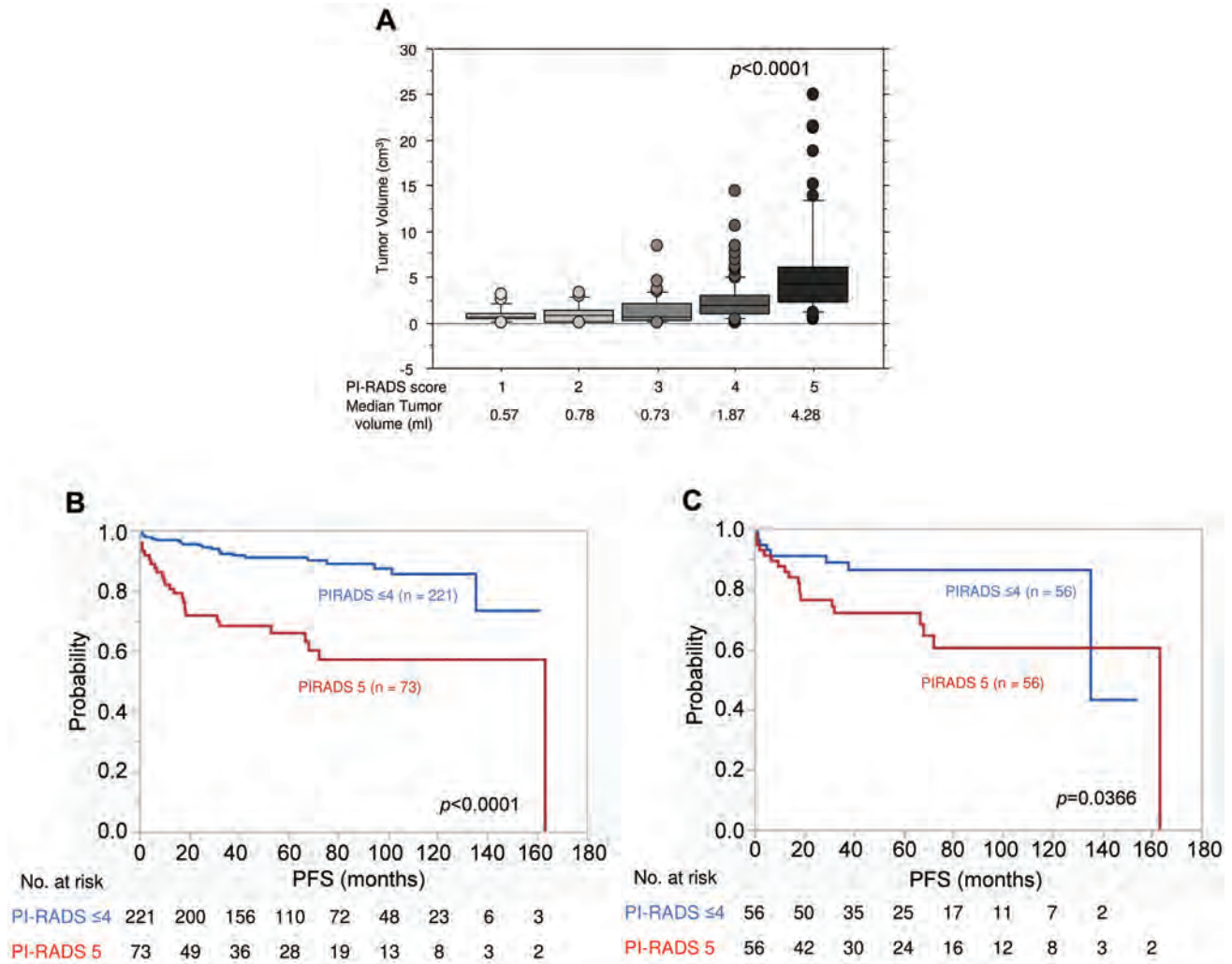


Figure 1. Prognostic significance of the PI-RADS v2.1 score in patients who underwent radical prostatectomy. (A) Tumor volumes calculated from prostatectomy specimens at each PI-RADS score. (B) Kaplan–Meier analysis classified by the PI-RADS score ≤4 vs. 5 for progression-free survival (PFS). (C) Kaplan–Meier analysis classified by the PI-RADS score ≤4 vs. 5 for PFS after propensity score-matching.

Table III. Uni- and multivariate cox proportional hazard models for progression-free survival.

	Univariate			Multivariate		
	HR	95% CI	p-Value	HR	95% CI	p-Value
Age (≥67)	1.21	0.69-2.15	0.5065	-	-	-
Initial PSA (≥7.68)	1.88	1.07-3.42	0.0291	1.11	0.56-2.21	0.7587
Prostate volume (≥29 ml)	1.09	0.61-1.92	0.7741	-	-	-
PSAD	2.79	1.51-5.51	0.0008	1.62	0.77-3.41	0.2081
Clinical T stage (≥T2c)	4.16	2.30-7.37	<0.0001	2.32	1.23-4.38	0.0093
Biopsy GS (≥8)	4.37	2.48-7.69	<0.0001	2.81	1.55-5.10	0.0007
PI-RADS v2.1 score 5	4.12	2.36-7.23	<0.0001	2.24	1.19-4.23	0.0124

HR: Hazard ratio; CI: confidence interval; PSA: prostate-specific antigen; PSAD: PSA density; GS: Gleason score; PI-RADS: prostate imaging-reporting and data system.

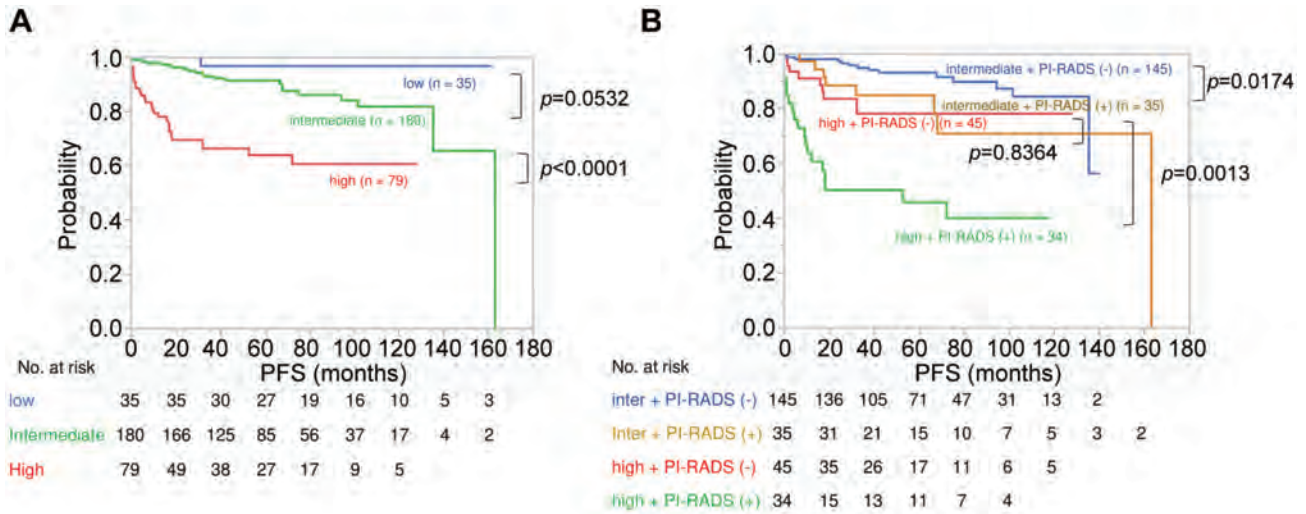


Figure 2. Validation of the risk classifications for progression-free survival following radical prostatectomy. (A) The D'Amico classification system. (B) Risk classification integrating the D'Amico classification and PI-RADS v2.1 score.

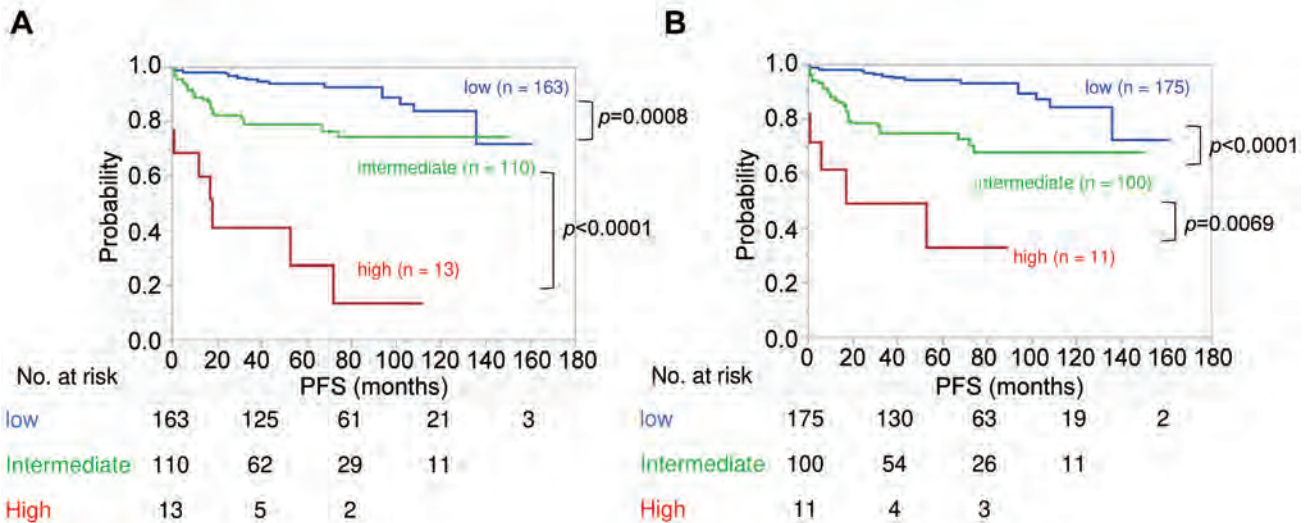


Figure 3. Prognostic significance of novel risk classifications. (A) A risk classification based on  $cT \geq 2c$ ,  $bGS \geq 8$ , and PI-RADS 5. (B) A risk classification based on  $PSA \geq 7.68$ ,  $bGS \geq 8$ , and PI-RADS 5.

including clinical T stage, PSA level, and bGS stratified patient prognosis in our cohort (Figure 2A). Patients with the D'Amico high-risk had shorter PFS than those with intermediate risk ( $p<0.0001$ , Figure 2A). Of note, PI-RADS v2.1 score 5 significantly differentiated prognosis in both intermediate- and high-risk groups in the D'Amico classification ( $p=0.0174$  and  $p=0.0013$ , respectively, Figure 2B). Moreover, patients with intermediate-risk and PI-RADS v2.1 score 5 showed comparable prognosis as compared to those with high-risk and PI-RADS v2.1 score  $\leq 4$  with 84.8%

and 78.1% in 5-year PFS rate ( $p=0.8364$ , Figure 2B). HR (high vs. others) of the risk classification was improved from 4.74 to 7.2 when combined PI-RADS v2.1 score to the D'Amico classification (Table IV). This analysis indicated the importance of PI-RADS v2.1 score in addition to the D'Amico risk classification for better risk classification when considering treatment options.

*Novel risk classification to predict BCR following RP.* We further proposed a novel risk classification comprising clinical

Table IV. Comparison of the capability of risk classifications to predict progression-free survival.

	Univariate		
	HR	95% CI	p-Value
D'Amico classification	4.74	2.68-8.49	<0.0001
D'Amico + PI-RADS v2.1 classification	7.2	3.92-12.83	<0.0001
Our risk classification (cT, bGS, PI-RADS v2.1)	9.71	4.38-19.35	<0.0001
Our risk classification (PSA, bGS, PI-RADS v2.1)	7.03	2.66-15.5	0.0004

HR: Hazard ratio; CI: confidence interval; PSA: prostate-specific antigen; GS: Gleason score; PI-RADS: prostate imaging-reporting and data system.

T stage ( $\geq 2c$ ), bGS ( $\geq 8$ ), and PI-RADS v2.1 score from multivariate analysis (Table III). This novel classification was defined as low (met 0 factors), intermediate (met 1 or 2 factors), or high (met 3 factors) and Kaplan–Meier analysis showed significant difference between these three groups (low vs. intermediate:  $p=0.0008$ ; intermediate vs. high:  $p<0.0001$ ) (Figure 3A). The HR for the high-risk group compared to others was 9.71 (95%CI=4.38-19.35) (Table IV).

In addition, we established another risk classification including PSA ( $\geq 7.68$  ng/ml), bGS ( $\geq 8$ ), and PI-RADS v2.1 score, since PI-RADS score basically reflects cancer size and might have a positive correlation with clinical T stage. Risk classification was similarly defined, and significant differences were observed between low-, intermediate-, and high-risk groups ( $p<0.0001$  and  $p=0.0069$ , respectively) (Figure 3B). The HR was 7.03 (95%CI=2.66-15.5) (Table IV). Thus, our risk classification identified a patient population with extremely poor prognosis, achieving a higher HR than the conventional classification.

## Discussion

Our study revealed the prognostic importance of the preoperative PI-RADS v2.1 scoring system in patients who had undergone RP. Higher PI-RADS score was associated with increased tumor volumes in the RP specimens. Furthermore, novel risk classifications integrating PI-RADS v2.1 score and the D'Amico classification were developed to improve prognostic capability in comparison with the D'Amico classification alone.

Previous studies have focused on how this scoring system could improve the accuracy of targeted prostate biopsy and avoid unnecessary biopsies (7, 14-16). Positive biopsy rates were significantly improved by fusion prostate biopsy using PI-RADS 4 and 5 lesions as compared to systematic biopsy (64% vs. 42.9%, respectively;  $p=0.035$ ) although inclusion of PI-RADS 3 did not improve rates, indicating that PI-RADS  $\geq 4$  lesions should be recommended for prostate biopsy (16). Wang *et al.* established a nomogram including

bpMRI PI-RADS v2.1 to minimize unnecessary biopsies (7). They found that a predictive model based on bpMRI could improve the ability of clinically significant prostate cancer detection and bpMRI score was correlated strongly with Gleason grade group (7). These findings indicated the clinical utility of PI-RADS scoring system to determine the relevance of performing prostate biopsies.

In addition, several studies have shown that pre-biopsy PI-RADS score could predict clinical outcomes following definitive local treatment (17, 18). A systematic review and meta-analysis revealed that higher PI-RADS v2 classifications were correlated with an increased risk of BCR after local treatment (18). Gandaglia *et al.* investigated 804 patients who received prostate biopsies and developed a risk classification for predicting PSA failure following RP (19). A predictive model including PI-RADS v2 score achieved the highest accuracy to predict clinically significant prostate cancer for identifying patient populations harboring a higher risk of early recurrence after operation (19). Furthermore, a recent study proposed simplified PI-RADS (S-PI-RADS) that is based on bi-parametric MRI (bpMRI) and is easier to use in clinical practice (20). S-PI-RADS has been found to enhance the detection and diagnosis of PCa as well as local recurrence following radiotherapy and RP (20). These results suggested a prognostic role for PI-RADS v2 classification in addition to diagnosis prior to prostate biopsies (18). However, few reports have examined the prognostic significance of PI-RADS v2.1 since the revision in 2019.

The D'Amico classification system has emerged in 1998 and has become one of the most widely used modalities for risk assessment of localized prostate cancer (8). The system is based on tumor stage by serum PSA level, Gleason grade, and clinical T-score, and divides patients into low-, intermediate-, and high-risk groups to evaluate the probability of recurrence (8). These risk groups have been employed in determining the duration of androgen deprivation therapy (ADT) when radiation therapy is administered (21-23). Furthermore, this risk classification has also been used to determine whether and to what extent

lymph node dissection should be performed, and to determine the course of treatment for RP (24, 25). Mandel *et al.* studied the rationale of lymph node dissection among the D'Amico intermediate-risk patients, and found that the detection rate for lymph node metastasis was low among patients with GS  $\leq$ 6, cT  $\leq$ 2b, PSA 10-20 ng/ml, indicating that lymph node dissection may not be necessary in some intermediate-risk cases (25). Thus, this classification is an indicator that serves as a basis for making treatment decisions in localized prostate cancer.

However, this classification has never been modified, and its ambiguity is sometimes noted. In particular, the clinical T stage classification has been obscure in that the diagnostic method is not defined as digital rectal examination or MRI image finding (26). In addition, there is a difference between the National Comprehensive Cancer Network (NCCN) guidelines and the D'Amico classification, *e.g.*, cT2c is classified as an intermediate risk in the NCCN guidelines, however, as high risk in the D'Amico classification system. Our findings showed that PI-RADS scoring was significantly correlated with tumor volume. Based on these results, we hypothesized that the PI-RADS scoring system might offer an alternative implement to the cT stage. Our novel risk classification including PI-RADS score, bGS, and PSA level achieved higher HRs than the D'Amico classification. Furthermore, given that the PI-RADS scoring system is an objective indicator and can be clearly scored, it might be a better clinical biomarker of tumor progression in combination with PSA level and bGS.

In conclusion, we indicated the prognostic significance of the PI-RADS v2.1 scoring system in patients who had undergone RP. The PI-RADS v2.1 scoring system can further stratify patient prognosis in the D'Amico classification and can be incorporated into risk stratification schemes to improve the precision of predicting patient prognosis. Our current exploration might help the decision-making for treatment and post-treatment follow-up in patients with localized prostate cancer who underwent definitive treatment.

### Conflicts of Interest

The Authors declare that there are no conflicts of interest in relation to this study.

### Authors' Contributions

Conceptualization: Y.F., Y.Y., S.S.; Methodology: Y.F., Y.Y., T.H., X.Z., K.S., S.N., Y.K., H.S., Y.G., T.S., Y.I.; Supervision: M.K., A.F., S.S., T.U., T.I.; Writing – original draft: Y.F.; Writing – review & editing: Y.Y., S.S.

### Acknowledgements

The present study was supported by the KAKENHI grant 23K19497 and Translational Research Grant of Urological Oncology.

### References

- 1 Yamada Y, Beltran H: The treatment landscape of metastatic prostate cancer. *Cancer Lett* 519: 20-29, 2021. DOI: 10.1016/j.canlet.2021.06.010
- 2 Siegel RL, Miller KD, Wagle NS, Jemal A: Cancer statistics, 2023. *CA Cancer J Clin* 73(1): 17-48, 2023. DOI: 10.3322/caac.21763
- 3 D'Amico AV, Whittington R, Schultz D, Malkowicz SB, Tomaszewski JE, Wein A: Outcome based staging for clinically localized adenocarcinoma of the prostate. *J Urol* 158(4): 1422-1426, 1997.
- 4 Barentsz JO, Richenberg J, Clements R, Choyke P, Verma S, Villeirs G, Rouviere O, Logager V, Fütterer JJ, European Society of Urogenital Radiology: ESUR prostate MR guidelines 2012. *Eur Radiol* 22(4): 746-757, 2012. DOI: 10.1007/s00330-011-2377-y
- 5 Weinreb JC, Barentsz JO, Choyke PL, Cornud F, Haider MA, Macura KJ, Margolis D, Schnall MD, Shtern F, Tempany CM, Thoeny HC, Verma S: PI-RADS Prostate Imaging - Reporting and Data System: 2015, Version 2. *Eur Urol* 69(1): 16-40, 2016. DOI: 10.1016/j.eururo.2015.08.052
- 6 Turkbey B, Rosenkrantz AB, Haider MA, Padhani AR, Villeirs G, Macura KJ, Tempany CM, Choyke PL, Cornud F, Margolis DJ, Thoeny HC, Verma S, Barentsz J, Weinreb JC: Prostate Imaging Reporting and Data System version 2.1: 2019 update of prostate imaging reporting and data system version 2. *Eur Urol* 76(3): 340-351, 2019. DOI: 10.1016/j.eururo.2019.02.033
- 7 Wang Y, Wang L, Tang X, Zhang Y, Zhang N, Zhi B, Niu X: Development and validation of a nomogram based on biparametric MRI PI-RADS v2.1 and clinical parameters to avoid unnecessary prostate biopsies. *BMC Med Imaging* 23(1): 106, 2023. DOI: 10.1186/s12880-023-01074-7
- 8 D'Amico AV, Whittington R, Malkowicz SB, Schultz D, Blank K, Broderick GA, Tomaszewski JE, Renshaw AA, Kaplan I, Beard CJ, Wein A: Biochemical outcome after radical prostatectomy, external beam radiation therapy, or interstitial radiation therapy for clinically localized prostate cancer. *Jama* 280(11): 969, 1998. DOI: 10.1001/jama.280.11.969
- 9 D'Amico AV, Desjardin A, Chung A, Chen MH: Assessment of outcome prediction models for localized prostate cancer in patients managed with external beam radiation therapy. *Semin Urol Oncol* 16(3): 153-159, 1998.
- 10 D'Amico AV, Desjardin A, Chung A, Chen MH, Schultz D, Whittington R, Malkowicz SB, Wein A, Tomaszewski JE, Renshaw AA, Loughlin K, Richie JP: Assessment of outcome prediction models for patients with localized prostate carcinoma managed with radical prostatectomy or external beam radiation therapy. *Cancer* 82(10): 1887-1896, 1998.
- 11 Takeshita N, Sakamoto S, Yamada Y, Sazuka T, Imamura Y, Komiya A, Akakura K, Sato N, Nakatsu H, Kato T, Sugimoto M, Tsuzuki T, Ichikawa T: Detection of intraductal carcinoma in prostate cancer patients with small tumor volume. *Prostate* 83(6): 580-589, 2023. DOI: 10.1002/pros.24492
- 12 Barrett T, Rajesh A, Rosenkrantz AB, Choyke PL, Turkbey B: PI-RADS version 2.1: one small step for prostate MRI. *Clin Radiol* 74(11): 841-852, 2019. DOI: 10.1016/j.crad.2019.05.019
- 13 Scher HI, Halabi S, Tannock I, Morris M, Sternberg CN, Carducci MA, Eisenberger MA, Higano C, Bubley GJ, Dreicer R, Petrylak D, Kantoff P, Basch E, Kelly WK, Figg WD, Small

- EJ, Beer TM, Wilding G, Martin A, Hussain M, Prostate Cancer Clinical Trials Working Group: Design and end points of clinical trials for patients with progressive prostate cancer and castrate levels of testosterone: recommendations of the Prostate Cancer Clinical Trials Working Group. *J Clin Oncol* 26(7): 1148-1159, 2008. DOI: 10.1200/JCO.2007.12.4487
- 14 Arafa MA, Farhat KH, Khan FK, Rabah DM, Elmorshedy H, Mokhtar A, Al-Taweel W: Development and internal validation of a nomogram predicting significant prostate cancer: Is it clinically applicable in low prevalent prostate cancer countries? A multicenter study. *Prostate*, 2023. DOI: 10.1002/pros.24625
- 15 Kim JY, Jeon SS, Chung JH, Lee SS, Park SW: How to avoid prostate biopsy in men with Prostate Image-Reporting and Data System 3 lesion? Development and external validation of new biopsy indication using prostate health index density. *Prostate Int* 11(3): 167-172, 2023. DOI: 10.1016/j.pnil.2023.07.001
- 16 Guerra-Lacambra M, Yañez-Castillo Y, Folgueral-Corral M, Melgarejo-Segura MT, Del Carmen Cano-García M, Sánchez-Tamayo FJ, Martín-Rodríguez JL, Arrabal-Polo MA, Arrabal-Martin M: Results of fusion prostate biopsy comparing with cognitive and systematic biopsy. *J Cancer Res Clin Oncol* 149(16): 15085-15090, 2023. DOI: 10.1007/s00432-023-05293-x
- 17 Fujimoto A, Sakamoto S, Horikoshi T, Zhao X, Yamada Y, Rii J, Takeuchi N, Imamura Y, Sazuka T, Matsusaka K, Ikeda JI, Ichikawa T: Tumor localization by Prostate Imaging and Reporting and Data System (PI-RADS) version 2.1 predicts prognosis of prostate cancer after radical prostatectomy. *Sci Rep* 13(1): 10079, 2023. DOI: 10.1038/s41598-023-36685-1
- 18 Rajwa P, Mori K, Huebner NA, Martin DT, Sprengle PC, Weinreb JC, Ploussard G, Pradere B, Shariat SF, Leapman MS: The prognostic association of prostate MRI PI-RADS™ v2 assessment category and risk of biochemical recurrence after definitive local therapy for prostate cancer: a systematic review and meta-analysis. *J Urol* 206(3): 507-516, 2021. DOI: 10.1097/JU.0000000000001821
- 19 Gandaglia G, Ploussard G, Valerio M, Marra G, Moschini M, Martini A, Roumiguié M, Fossati N, Stabile A, Beauval JB, Malavaud B, Scuderi S, Barletta F, Afferi L, Rakauskas A, Gontero P, Mattei A, Montorsi F, Briganti A: Prognostic implications of multiparametric magnetic resonance imaging and concomitant systematic biopsy in predicting biochemical recurrence after radical prostatectomy in prostate cancer patients diagnosed with magnetic resonance imaging-targeted biopsy. *Eur Urol Oncol* 3(6): 739-747, 2020. DOI: 10.1016/j.euo.2020.07.008
- 20 Scialpi M, Martorana E, Scialpi P, Scalera GB, Belatti E, Aisa MC, D'Andrea A, Mancioli FM, DI Marzo A, Trippa F, DI Blasi A: S-PI-RADS and PI-RRADS for biparametric MRI in the detection of prostate cancer and post-treatment local recurrence. *Anticancer Res* 43(1): 297-303, 2023. DOI: 10.21873/anticancer.16163
- 21 Jones CU, Hunt D, McGowan DG, Amin MB, Chetner MP, Bruner DW, Leibenhaut MH, Husain SM, Rotman M, Souhami L, Sandler HM, Shipley WU: Radiotherapy and short-term androgen deprivation for localized prostate cancer. *N Engl J Med* 365(2): 107-118, 2011. DOI: 10.1056/NEJMoa1012348
- 22 Vargas CE, Alam NB, Terk M, Niska JR, Cesaretti J, Swartz D, Vashi A, Kasraeian A, West CS, Blasser M, Moore C: Initial results of a randomized phase III trial of high dose image guided radiation with or without androgen deprivation therapy for intermediate-risk prostate cancer. *Cancer Treat Res Commun* 19: 100119, 2019. DOI: 10.1016/j.ctarc.2019.100119
- 23 Dong Y, Ruth KJ, Churilla TM, Viterbo R, Sobczak ML, Smaldone MC, Chen DY, Uzzo RG, Hallman MH, Horwitz EM: The need for androgen deprivation therapy in patients with intermediate-risk prostate cancer treated with dose-escalated external beam radiation therapy. *Can J Urol* 24(1): 8656-8662, 2017.
- 24 Preisser F, Bandini M, Marchioni M, Nazzani S, Tian Z, Pompe RS, Fossati N, Briganti A, Saad F, Shariat SF, Heinzer H, Huland H, Graefen M, Tilki D, Karakiewicz PI: Extent of lymph node dissection improves survival in prostate cancer patients treated with radical prostatectomy without lymph node invasion. *Prostate* 78(6): 469-475, 2018. DOI: 10.1002/pros.23491
- 25 Mandel P, Kriegmair MC, Veleva V, Salomon G, Graefen M, Huland H, Tilki D: The role of pelvic lymph node dissection during radical prostatectomy in patients with Gleason 6 intermediate-risk prostate cancer. *Urology* 93: 141-146, 2016. DOI: 10.1016/j.urology.2016.02.046
- 26 D'Amico AV, Whittington R, Malkowicz SB, Wu YH, Chen M, Art M, Tomaszewski JE, Wein A: Combination of the preoperative PSA level, biopsy Gleason score, percentage of positive biopsies, and MRI T-stage to predict early PSA failure in men with clinically localized prostate cancer. *Urology* 55(4): 572-577, 2000. DOI: 10.1016/s0090-4295(99)00479-3

*Received October 14, 2023*

*Revised November 10, 2023*

*Accepted November 13, 2023*



Anticancer Res. 2024 Feb;44(2):639-647. doi: 10.21873/anticanres.16853.

## Copy Number Gain in Androgen Receptors Predicts the Poor Prognosis in Japanese Castration-resistant Prostate Cancer

Shinichi Sakamoto <sup># 1</sup>, Keisuke Ando <sup># 2</sup>, Sangjon Pae <sup>2 3</sup>, Xue Zhao <sup>2</sup>, Kazuko Sakai <sup>4</sup>, Kodai Sato <sup>2</sup>, Shinpei Saito <sup>2 3</sup>, Yasutaka Yamada <sup>2</sup>, Junryo Rii <sup>2</sup>, Yusuke Goto <sup>2</sup>, Tomokazu Sazuka <sup>2</sup>, Yusuke Imamura <sup>2</sup>, Naohiko Anzai <sup>3</sup>, Koichiro Akakura <sup>5</sup>, Kazuto Nishio <sup>4</sup>, Tomohiko Ichikawa <sup>2</sup>

Affiliations

PMID: 38307556 DOI: [10.21873/anticanres.16853](https://doi.org/10.21873/anticanres.16853)

### Abstract

**Background/aim:** The prognostic significance of androgen receptor amplification (AR amp) in cell-free DNA (cfDNA) was studied in Japanese patients with castration-resistant prostate cancer (CRPC).

**Patients and methods:** A total of 120 serum samples were obtained from 38 patients with CRPC. Serum cfDNA was purified and the AR copy number was determined. Factors associated with progression-free survival (PFS) and overall survival (OS) were statistically investigated.

**Results:** The number of patients administered enzalutamide (Enza)/abiraterone (Abi)/docetaxel (DTX) was 33/25/11, respectively. The median PSA was 16.5 ng/ml. Thirty patients (79%) had bone metastases and three patients (7.9%) had lung metastases. The median follow-up was 655 days. The median initial AR copy number was 1.27 (1.10-11.50); an AR copy number of 1.27 or higher was defined as an AR-amp. Regarding PFS, the presence of AR-amp, Gleason score (GS), and ALP were significant factors in univariate analysis. In multivariate analysis, AR amplification was an independent prognostic factor (hazard ratio=7.7, p=0.0035). For OS, PSA and AR-amp were significant factors. In multivariate analysis, AR-amp (hazard ratio=4.65, p=0.0188) was the only independent prognostic factor.

**Conclusion:** AR-amp was associated with high nadir PSA and low iPSA/PSA ratio. AR-amp was significantly associated with poor prognosis in Japanese patients with CRPC.

**Keywords:** Cell-free DNA; biochemical recurrence; castration-resistant prostate cancer; liquid biopsy; prognosis.

Copyright © 2024 International Institute of Anticancer Research (Dr. George J. Delinasios), All rights reserved.

[PubMed Disclaimer](#)

### Related information

[MedGen](#)

[PubChem Compound \(MeSH Keyword\)](#)

### LinkOut - more resources

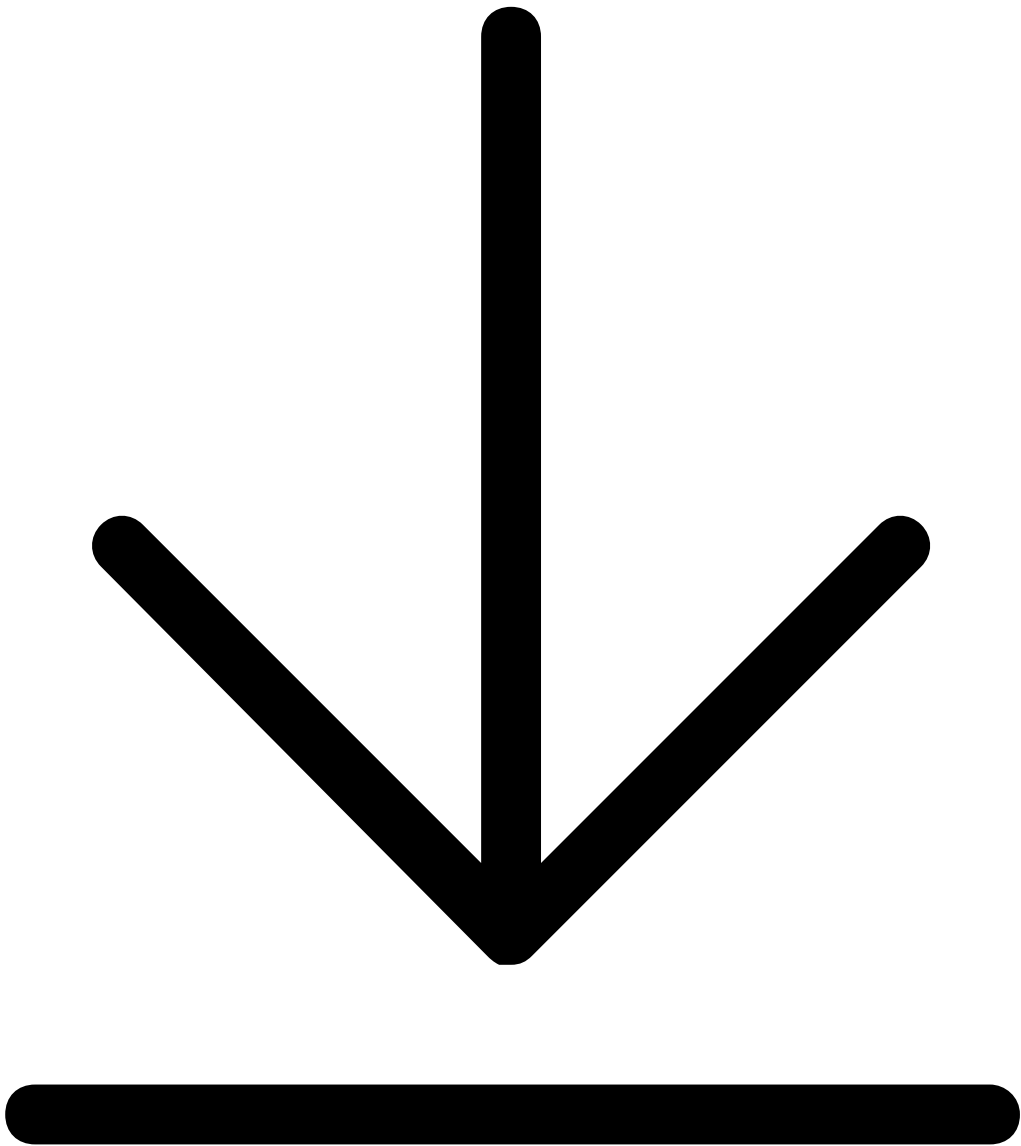
Full Text Sources

[HighWire](#)

Medical



Research Materials



拖拽到此处  
图片将完成下载

# 日中笹川医学奨学金制度(学位取得コース)評価書

## 課程博士：指導教官用



第 43 期

研究者番号： G4303

作成日： 2023 年 3 月 10 日

氏名	姚利	Yao Li	性別	F	生年月日	1990. 11. 20
所属機関(役職)	千葉大学大学院 看護学研究科看護学専攻(大学院生)					
研究先(指導教官)	千葉大学大学院 看護学研究院(正木 治恵教授)					
研究テーマ	在留中国人高齢者を介護する家族支援プログラムの開発 Development of a support program for elderly Chinese residents' family caregivers in Japan					
専攻種別	<input type="checkbox"/> 論文博士			<input checked="" type="checkbox"/> 課程博士		

### 研究者評価(指導教官記入欄)

成績状況	<input checked="" type="checkbox"/> 優 <input type="checkbox"/> 良 <input type="checkbox"/> 可 <input type="checkbox"/> 不可 学業成績係数=	取得単位数
		12/12
学生本人が行った研究の概要	姚氏は、修士論文の研究を発展させ、博士後期課程において「在留中国人高齢者の老いへの準備教育プログラムの開発ービデオカンファレンスを活用してー」と題する研究に取り組んだ。開発した教育プログラムは、在留中国人高齢者の要介護生活の送り方に関する認識の広がりや老後の生活の方向性の明確化を促すなど要介護生活に焦点を当てた老いへの準備に有用であること、また、ビデオカンファレンスを活用したプログラムは便利で参加しやすく、参加者の経験を共有しつつ多様な意見を交換できたことから、実現可能であることが確認できた。看護援助が十分に行き届かない在留中国人高齢者に対して、ビデオカンファレンスという新たな教育方法を用いた老いへの準備性を高めるプログラム開発は新規性があり、今後の普及が期待できる研究であると高く評価された。	
総合評価	<b>【良かった点】</b> 姚氏は、積極的に博士研究を遂行し、規程の3年間でやり遂げた。その過程で3本の論文を執筆・投稿している。また、研究能力向上のための研修を自ら探して受講したり、中国語と日本語に堪能であることからオリンピックの通訳なども担った。向上心を持ち、何事にも果敢にチャレンジする積極性は群を抜いている。明るい性格で、後輩育成に尽力するなど人望も厚い。	
	<b>【改善すべき点】</b> 様々なことにチャレンジするため、提出期限が定められているものに対して、ギリギリになることもある。好奇心旺盛であることは評価できるので、それを維持しつつ、期限を意識した計画的な遂行ができるとなお良いと思われる。	
	<b>【今後の展望】</b> 大学教員として必要な教育・研究能力を高め、博士課程で培った能力を人材育成と研究の発展に思う存分発揮してほしい。また、看護学分野での中国と日本の架け橋となり、両国の親交に寄与することを期待する。	
学位取得見込	2023年3月に博士(看護学)の学位を取得予定。	
評価者(正木治恵)		

# 日中笹川医学奨学金制度(学位取得コース)報告書

## 研究者用



第43期

研究者番号: G4303

作成日: 2023年3月8日

氏名	姚 利	Yao Li	性別	F	生年月日	1990. 11. 20
所属機関(役職)	千葉大学大学院看護学研究科看護学専攻(大学院生)					
研究先(指導教官)	千葉大学大学院看護学研究院(正木治恵)					
研究テーマ	在留中国人高齢者の老いへの準備教育プログラムの開発ービデオカンファレンスを活用してー Development of an education program on aging-related preparation through videoconference for old Chinese migrants in Japan					
専攻種別	論文博士	<input type="checkbox"/>	課程博士	<input checked="" type="checkbox"/>		

### 1. 研究概要 (1)

#### 1) 研究背景と目的

在留外国人高齢者の増加に伴い、要介護リスクが高い在留中国人高齢者も増えている。言語の障壁で日本の介護保険制度の認知度が低いことに加え、母国に介護保険制度はなく、高齢者の介護は外部の支援を得ず家庭内で担うといった文化の違いがある。そのため、要介護在留中国人高齢者及びその家族は、介護保険サービスの理解や利用に困難がある。老いに伴う「母国語がえり」現象(日本語の忘れが多く、母国語での会話が増えること)によって、専門職との意思疎通はさらに困難である。加えて、介護サービスの提供側も文化・言語の障壁があるため、外国人高齢者のニーズや意思の把握に困難を抱えている。そして、これから要介護生活を迎える在留中国人高齢者およびその家族が、いざとなったとき困難に陥らず自分が望んだ要介護生活や介護に関する意思を専門職に伝え、適時に専門的な支援を得るための準備が必要であると考えた。しかしながら、将来のケアニーズの予測困難、ケアに関する資源・情報の欠如、計画を組み立てる自信がないなどが将来のケアニーズの準備に影響を与えると報告されている。これらのことから、要介護生活に焦点を当てた老いへの準備教育支援が必要と考える。よって、本研究の目的は、ビデオカンファレンスを活用して要介護生活に焦点を当てた老いへの準備教育プログラムの開発とした。

#### 2) 用語の定義

##### (1) 在留中国人高齢者

本研究では、中長期在留資格を持つ日本に住んでいる65歳以上の中国国籍を持つ者、日本の国籍を取得した華僑・華人と、長年に中国で生活していた中国残留邦人とする。

##### (2) 要介護生活に焦点を当てた老いへの準備性

加齢とともに心身が衰えることに起因した要介護状態に対して、介護が必要となる心身的健康状態・生活状態への理解や態度、社会資源の知識、要介護生活の準備に関する認識および自己意思表示の能力などを指す。

#### 3) 戦略と方法

本研究は以下の2段階に構成された。

##### 【研究1】要介護生活に焦点を当てた老いへの準備教育プログラムの作成

##### (1) 研究1-1: 教育プログラム原案の設計

システマティック・レビューを通して、中国国内および海外に在住する中国人高齢者の施設及び自宅での療養生活のあり様と課題を明らかにし、プログラム原案の内容を作成した。また、ジェロゴジ理論(高齢者の学習理論)を基盤として、教育プログラムの実施形態を設計し、教育プログラム原案を作成した。

##### (2) 研究1-2: 教育プログラム原案の妥当性の検討

勤務経験5年以上の看護学研究者3名と訪問看護師1名、ケアマネジャー1名に教育プログラム原案の資料(講義の動画と冊子)及び評価アンケートを送り、アンケートに回答した結果を踏まえて専門家会議を実施し、教育プログラム原案の妥当性を検討した。

##### 【研究2】作成した教育プログラムの実現可能性と有用性の検討

この段階の研究デザインはpre-post testを用いた混合的研究法の説明的順次デザインであった。有用性は介入前後に中国語版の老いへの態度尺度(The Attitudes To Aging Questionnaire: AAQ)及び将来のケアニーズへの準備尺度(Preparation for Future Care Needs Scale-14: PFCN-14)の回答を通して検討した。実現可能性は介入中に各回授業の評価アンケートを回答した結果を踏まえて、参加経験に関するインタビューの実施を通して検討した。

研究実施にあたり、千葉大学大学院看護学研究院倫理審査委員会の承認を得ていた(承認番号: RN4-13, RN4-26)。

データ分析は単純集計と質的帰納的分析を実施した。

#### 4) 結果

##### (1) 対象者の基本属性

本研究は首都圏のA県とB県、関西のC県から7組(14名)の研究対象者を募集した。夫婦関係のペアが6組であり、母と娘の親子関係のペアが1組であった。性別について、男性が6名で、女性が8名であった。年齢は53歳から84歳であり、平均年齢は74.9歳であった。在日年数は4年から40年であり、平均在日年数は27.1年であった。

##### (2) 参加経験の全体分析結果

個々対象者が語った参加経験の個別分析で得られた79枚の最終ラベルから、4段階の集めを経て、6つのカテゴリーが生成された。これらは【支援が得られる老後の生活環境を確かめた安心感】【健康で充実した日々と不確定な将来によって抑えられた老いへの準備姿勢】【老いや老後の生活に関する認識の広がりや啓発】【授業中に起こった老後の生活を備える認識や行動の変容】【オンライン授業のアクセスしやすさ】【自立と持病状況に影響された自己健康評価】であった。

(次のページに続く)

### (3) 各回授業アンケートの分析結果

14名の対象者から6章分の授業評価アンケートを計84部（100%）回収した。アンケートは選択項目と自由記載欄を設けた。選択項目について、「4回目：今回の授業を通して、自宅や施設の介護サービスの利用を始めたい状況を述べるようになった」を「当てはまらない」と評価した対象者は1名であり、「授業中の音声の聞きやすさ」を「当てはまらない」と評価した対象者は2名があった。その他の評価項目はすべて「大体当てはまる」「かなり当てはまる」「非常に当てはまる」と評価された。自由記載欄のコメントは、質的帰納的分析を経て、次の6つのカテゴリーが生成された。これらは、「オンライン授業を参加するメリットと不便」「講義内容は実用性がある自分のニーズに満たした」「要介護生活への関心が高くなり、考えられるようになった」「将来の生活の予測困難」「講義内容と資料は多様性があり、わかりやすかった」「ビデオの活用と議論を加えることで、講義が豊かになり、講義内容をより深く理解でき、イメージしやすくなった」であった。

### (4) 介入前後のAAQ及びPFCN-14の変化

14名の対象者からAAQ尺度とPFCN-14尺度は介入前後にわたって、計28部（100%）を回収した。その結果、介入後にAAQとPFCN-14の総点数が両方とも高くなった対象者は4名（28.6%）であり、いずれが高くなった対象者は9名（64.3%）であった。つまり、13名（92.9%）の対象者に老いへの態度や将来のケアニーズへの準備性の向上にポジティブな効果があった。また、9名（62.3%）の対象者に将来のケアニーズへの準備性の向上にポジティブな効果が見られた。AAQとPFCN-14尺度の各ドメインの変化について、AAQの心理的獲得ドメイン（78.6%）とPFCN-14の意識ドメイン（85.7%）にポジティブな変化が最も多かった。しかし、1名（7.1%）の対象者は老いへの態度および将来のケアニーズへの準備性にポジティブな効果が見えなかった。

### 5) 考察

【オンライン授業のアクセスしやすさ】「オンライン授業を参加するメリットと不便」という参加者の参加経験と授業評価のコメントがあった。Chenら（2016）は、高齢者に対してICTの活用は、社会とのつながり、興味がある活動の参加、ソーシャルサポートを得ることに効果があると報告している。在留中国人高齢者は文化や言語の違いから地域で開催される支援プログラムに参加しにくい上に、地域で中国人高齢者向け講座は少なく、各地域に散住している彼らを1つの地域に集めることは困難である。そこで、中国人高齢者が社会や他者とのつながる重要な手段となっているICTの活用が有効と考え、ビデオカンファレンスを活用して教育プログラムを開催した。ビデオカンファレンスの活用は、便利かつアクセスしやすく、高齢者にとって外出疲労の軽減や地域での支援を得にくい現状の改善に貢献できるため、在留中国人高齢学習者に良い学び場の提供に新規性があると考えられる。

一方、各回授業評価アンケートでは、「ビデオの活用と議論を加えることで、講義が豊かになり、講義内容をより深く理解でき、イメージしやすくなった」というコメントが多く見られた。ジェロゴジーという高齢者学習援助理論では、ライフスパンに渡って重ねてきた経験は高齢者の学習に貢献できるため、高齢者の人生経験を活用できる学習セッションを設ける必要性が述べられている（John, 1988）。本研究はジェロゴジー理論を基盤として教育プログラムの実施形態を検討し開発した。教育プログラムの実施では、講義内容をスライドに示しながら、講義内容を伝えるビデオや写真を活用した。また、講義後に参加者間の議論も設けた。議論では老後の生活と老いの経験について多様な意見を交換でき、要介護生活の理解を深めることと認識の広がり促した。その理由は、在留中国人高齢者にとって、これから迎える要介護生活は未経験であり、周りに参考となるケースも少ない。議論では、同じ背景がある参加者が講義内容と自身の状況に合わせて個々の意見や経験を共有し、現実的な事例を提供していた。対象者は議論を通して、今経験している高齢期の生活及び将来の要介護生活の計画に参考となる新たなアイデアや情報を入手でき、講義内容を深く理解することに促しうると言える。また、講義中のビデオや写真の活用は、授業中に挙げられた事例をリアルに示され、授業内容のイメージしやすさと理解の深さにつながった。よって、本研究で開発した教育プログラムは在留中国人高齢者にとって実現可能であり、ジェロゴジー理論は中国人高齢者にとって効果的な学習援助方法であると考えられる。

毎回事業評価アンケートの回収結果では、授業内容を「実用性がある自分のニーズに満たした」「将来に役に立つ」と高く評価された。また、彼らが語った参加経験から【支援が得られる老後の生活環境を確かめた安心感】というカテゴリーが生成された。堀（2012）は、60代より70代以上の高齢者は「老後」や「老後の生き方」に関する内容の学習要求率が比較的に高いと報告している。本研究に参加した14名の対象者の平均年齢は74.9歳であり、そのうち、後期高齢者は11名であった。教育プログラムの内容は要介護生活に焦点を当てた学習であり、老いの自覚症状を経験している対象者自身の状況に強く関連し、在留中国人高齢者の学習ニーズに満たし、将来、日本での老後の生活を安心して送ることに寄与できると言える。

介入後のAAQやPFCN-14のいずれかがポジティブになった対象者は9割弱であり、老いへの準備意識が強まった対象者は8割強だった。また、彼らの参加経験では、【老いや老後の生活に関する認識の広がり】と【授業中に起こった老後の生活を備える認識や行動の変容】というカテゴリーがあった。春日（2018）は「老いの支度」を高齢期で生じる様々なリスクを最小限にとどめるために、まだ判断力や自己決定力がある元気な間に、必要な福祉や医療・介護に関する制度的知識や情報収集、対処方法を学び、暮らしのあり方や人間関係を組み替え、自分自身の将来のために自ら備える活動であると定義し、さらに、高齢者はその支度に着手する必要性を主張している。しかし、一般的な高齢者はその支度について、何をどのように備えるのかはわからないと述べられている。本研究で開発した教育プログラムの内容は老いに伴う変化、自宅及び施設での療養生活のあり様、日本における介護保険制度、老いへの準備の必要性、要介護生活の計画が含まれた。教育プログラムの参加を通して、老後の生活の変移、要介護生活のイメージ付き及びその準備の方向性が明瞭になったから、対象者の将来のケアニーズの準備性の向上に見られたと言える。これらのことから、本研究で開発した教育プログラムは一般市民向けの講座として開催し、地域に在住する元気な中国人高齢者の生涯学習に期待できる。また、保健や福祉に関する行政や医療の専門職にとって、在留中国人高齢者の老いへの準備の支援策の検討に貢献できると考えられる。

### 7) 参考文献

- Chen, Y.-R. R. (2016). The Effect of Information Communication Technology Interventions on Reducing Social Isolation in the Elderly: A Systematic Review. *Journal of medical Internet research*, 18(1), e18.  
<https://doi.org/10.2196/jmir.4596>
- John, M. T. (1988). *Geragogy: a theory for teaching the elderly*. Haworth Press.
- 堀薫夫. (2012). 教育老年学と高齢者学習. 学文社.
- 春日キスヨ. (2018). 百まで生きる覚悟：超長寿時代の「身じまい」の作法. P101, 光文社.

## 1. 研究概要 (2)

## 1) 研究題名

在留中国人高齢者の健康に関する思い -中国人が集まる地域活動に参加する対象者に焦点を当てて- (投稿論文一原著)

## 2) 目的

中国人が集まる地域活動に参加する在留中国人高齢者を対象に異国在住での健康に関わる経験の調査を通して、彼らの健康に関する思いを明らかにすることである。

## 2) 用語の定義

(1) 在留中国人高齢者: 中長期在留資格を持ち日本に住む65歳以上の中国国籍を持つ人, 日本の国籍を取得した華僑, 華人と, 中国で生まれ50年以上中国で生活していた中国残留孤児とする。

(2) 健康に関する思い: 日本に住んでいることの影響を含めた, 自分自身の身体的・精神的・社会的健康及びそれに関連する受診や健康増進について感じる事・希望すること・気にかけて考えを持つことやその内容とする。

## 3) 研究方法

## (1) 対象者および募集方法

対象者は, 本研究で定義する在留中国人高齢者とした。ただし, 認知機能障害を持つ者は除外した。首都圏都市部にある公民館およびコミュニティーセンター, 中国語対応が可能な施設で対象者を募集した。また, 対象者の多様性を確保するため, 雪だるま式募集方法を併用した。

## (2) データ収集期間

2019年3月~10月

## (3) 調査方法

調査はインタビューガイドを用いて対象者に半構造化面接を1~3回, 1回60分を目安に行った。面接内容は, 対象者の同意を得てICレコーダーに録音し, 逐語録を作成した。個別面接で使用した言語は対象者の希望に沿い, 中国語とした。

## (4) 調査内容

調査内容は対象者の基礎情報と健康に関する思いや考えとした。先行研究を参考に, インタビューガイドを作成した。基礎情報は年齢, 収入, 家族構成, 学歴, 在留年数とした。

インタビューガイドの内容は, 在留外国人の健康阻害要因と健康に関する異文化体験に関する先行研究 (Jiang, 2016; 中嶋, 2015; 平野, 2003) を参考に, 在留期間中の受診経験, 日常生活の過ごし方, 健康増進方法, 今後の生活や健康上の心配や希望, 日本語の自己評価理由についてどのような考えや思いを持っているかを含めた。

## (5) 分析手法

対象者の基礎情報と日本語能力の自己評価は記述的統計学で分析した。面接データは質的帰納的に分析した。本研究の対象者は社会的・文化的背景に強く影響を受け, 個性が高いと考え, 個々の事例が持つ個性・独自性を把握できる質的統合法 (KJ法) (山浦, 2012) を参考にした。

## 4) 倫理的配慮

本研究は, 千葉大学大学院看護学研究科倫理審査委員会の承認と対象者が活用する組織や施設の承認を得て実施した (承認番号30-97)。

## 5) 結果

## (1) 対象者の概要

本研究の対象者は男性5名, 女性8名の計13名であった。対象者全員が首都圏在住であった。在留年数は, 5年から30年以上であり, 平均22.8年であった。10名の対象者は日本の病院を受診した経験があった。対象者は生活支援金や中国あるいは日本の年金で生活を送っていた。日本語能力の自己評価について, 日常会話, 医療会話が「まあ良い」と評価した対象者はそれぞれ5名と7名であったが, 日本人の友人を持ち, 主に日本人で構成されたメンバーでの活動に定期的に参加する人は1名だけだった。対象者は全員中国人が集まる活動や中国人向け地域活動に参加していた。

## (2) 健康に関する思い

全体分析結果は, テーマを【 】, サブテーマを〈 〉で示す。全体分析結果は80枚の各個別分析の最終ラベルを素材とし, 類似性に沿って統合し, 以下の8つのテーマ, 16のサブテーマを生成した。

## 【身体機能や精神状態から主観的に健康の良し悪しを評価している】

これは健康状態の評価に関する思いであり, 〈病弱による良くない自己健康評価〉と〈老いを感じながらも良い自己健康評価〉が含まれた。

## 【安全で便利な社会に住むことを安心だと感じている】

これは自分にとって, 困難がなく医療機関を利用でき, 安全で便利な社会環境に住んでいることに安心しているという〈自分にとって安心できる住む環境〉に関する思いであった。

(次のページに続く)

- 【他者の支援を受けることで安心して生活できている】  
これは、他者の支援に関する思いであり、〈支援された生活〉、〈助けを求める生活〉と〈助けを求める対象がいない大変さ〉が含まれた。
- 【老いを受け止めて前向きに生きている】  
これは老いの受容に関する思いであり、〈余生への希望〉と〈前向きな生き方〉を含んでいた。
- 【言葉の壁で生活は制限されたが中国人との関わりや趣味を通して気楽に生活している】  
これは、言葉の壁があり日本人とのコミュニケーションが難しいことによる制限された生活の中で、中国人との関わりや趣味を通して、社会とのつながりを作り、気楽に生活しているという、〈制限された生活の中での楽しさ〉に関する思いであった。
- 【家族で互いに支える生活を継続したい】  
これは家族関係への思いであり、〈子供に迷惑をかけたくない〉と〈家族の支え〉を含んでいた。
- 【良い医療サービスをうまく利用できるので安心して】  
これは、医療サービスの利用に関する思いであり、〈心配のない医療サービス〉と〈言語の壁に影響された受診〉を含んでいた。
- 【健康を維持するため中医学に基づき自主的に健康管理をしている】  
これは、中医学に基づいた健康管理に関する思いであり、〈健康情報の入手〉〈中医学に基づく健康促進〉と〈総合的な健康管理〉を含んでいた。

## 6) 考察

本研究では、中国人が集まる地域活動に参加する在留中国人高齢者に焦点を当てた8つの健康に関する思いを明らかにした。高齢期の発達課題や、言葉による制限、中国文化に影響された思いが含まれていた。本研究は、高齢期の発達課題や、言語による制限、儒教思想や中医学の影響から対象者の特徴を考察する。

### (1) 高齢期の発達課題に影響した健康に関する思い

【身体機能や精神状態から主観的に健康の良し悪しを評価している】【安全で便利な社会に住むことを安心だと感じている】【他者の支援を受けることで安心して生活できている】【老いを受け止めて前向きに生きている】という思いは高齢期に直面する健康や生活の変化に関連していた。

対象者は健康上の変化に適応するために身体・精神面の状態をとらえると同時に、生活上の支援や居心地のよい便利な住まい環境を整えていた。対象者らは高齢期における変化への対応を踏まえて、加齢に伴う現状を受容していたと考える。健康の衰退に適応し、生活を満足におくれるように（住まいを）準備することや、自分の人生の受容は高齢期の発達課題として挙げられている。本研究の対象者は健康の衰退およびそれによって変化した現状への適応は、異国での老後の生活の中で、高齢期の発達課題に直面しつつ発達し続けていると考えられる。

### (2) 言葉による制限が影響した健康に関する思い

【言葉の壁で生活は制限されたが中国人との関わりや趣味を通して気楽に生活している】【良い医療サービスをうまく利用できるので安心して】という思いは言葉の制限が社会活動の参加と医療機関の利用に関連したことを示した。

本研究の対象者が居住する首都圏都市部では、在留中国人高齢者が多く、中国人が自発的に集まる活動や外国人向けの活動がさかんであった。そこでは交通が便利で、高齢者に対する交通費の公的な補助制度があるため、中国人が集まる活動にアクセスしやすいと考える。一方、本研究の対象者は、老いに伴う身体機能や記憶力の衰えによって外出が制限され、日本語を忘れることが増えた実感から、今後も療養生活を自宅で送ることを希望していた。今後自宅で療養生活を送る在留中国人高齢者が増えると推測されるため、医療・福祉分野における専門的通訳ボランティアの養成やICTを活用して遠方から通訳を受ける仕組みづくりなど、医療サービスにアクセスしやすい環境の整備が必要であると考える。

### (3) 儒教思想や中医学に影響される健康に関する思い

【家族で互いに支える生活を継続したい】【健康を維持するため中医学に基づき自主的に健康管理をしている】という思いは中国文化に影響していた。

本研究の対象者の健康に関する思いには、子は親の面倒を見るべきであり、できる限り健康に生きることで子供の負担を軽減しようとする親としてのあり方が反映された中国の伝統的な親子関係が継承されており、それは対象者の老後生活の希望、健康を維持する意欲につながっていたと考える。また、在留中国人高齢者では、移住後の生活においても中医学の影響が継続しており、ケアを提供する際は、健康への対処方法に中医学が根づいていることを理解する必要がある。中医学の健康促進方法の特徴や効果を考慮して食生活や運動習慣などにケアに活かすことは、彼らにとって馴染みがある継続可能な支援となると考える。

## 7) 結論

在留中国人高齢者においては、高齢期の発達課題や、中国文化、言葉の壁が彼らの健康に関する思いに影響を与えていることが明らかとなった。言葉による制限や母国文化の継承は彼らの安心感や、健康促進、老後生活の希望に強く影響を及ぼすため、言葉の壁を取り除く環境整備や彼らに馴染んだ文化や健康促進方法に基づいたケアの提供の重要性が示唆された。

## 8) 参考文献

- (1) Jiang Y, Huang CY, Yoon H, et al. (2016). Correlates of Self-Rated Health and Self-Rated Mental Health in Older Chinese Americans. Soc Work Public Health, 31(4), 309-315.
- (2) 中嶋知世, 大木秀一 (2015). 外国人住民における健康課題の文献レビュー. 石川看護雑誌, 12, 93-104.
- (3) 平野裕子 (2003). 在日外国人の身体的・精神的健康 保健学・看護学的視点から. 福岡医学雑誌, 94(8), 241-249.
- (4) 山浦晴男 (2012). 質的統合法入門 : 考え方と手順. 医学書院.

## 2. 執筆論文 Publication of thesis ※記載した論文を添付してください。Attach all of the papers listed below.

論文名 1 Title	在留中国人高齢者の健康に関する思い — 中国人が集まる地域活動に参加する対象者に焦点を当てて —					
掲載誌名 Published journal	文化看護学会誌(原著)					
	2022 年 5 月	14(1) 巻(号)	21 頁 ~ 30 頁	言語 Language	日本語	
第1著者名 First author	姚利	第2著者名 Second author	石井優香	第3著者名 Third author	山崎由利亜	
その他著者名 Other authors	石橋みゆき,正木治恵					
論文名 2 Title	日本に長期在住する中国人高齢者の健康管理—地域で自立した生活を送る1事例の語りより—					
掲載誌名 Published journal	日中医学(一般投稿)					
	2023 年 2 月	37(4) 巻(号)	26 頁 ~ 32 頁	言語 Language	日本語/中国語	
第1著者名 First author	姚利	第2著者名 Second author	石井優香	第3著者名 Third author	正木治恵	
その他著者名 Other authors	無					
論文名 3 Title	Older Chinese people's experiences of relocation to long-term care facilities: A literature review of qualitative studies					
掲載誌名 Published journal	Journal of International Nursing Research(査読中)					
	年 月	巻(号)	頁 ~ 頁	言語 Language	英語	
第1著者名 First author	Li Yao	第2著者名 Second author	Harue Masaki	第3著者名 Third author	無	
その他著者名 Other authors	無					
論文名 4 Title						
掲載誌名 Published journal						
	年 月	巻(号)	頁 ~ 頁	言語 Language		
第1著者名 First author		第2著者名 Second author		第3著者名 Third author		
その他著者名 Other authors						
論文名 5 Title						
掲載誌名 Published journal						
	年 月	巻(号)	頁 ~ 頁	言語 Language		
第1著者名 First author		第2著者名 Second author		第3著者名 Third author		
その他著者名 Other authors						

## 3. 学会発表 Conference presentation ※筆頭演者として総会・国際学会を含む主な学会で発表したものを記載してくだ

※Describe your presentation as the principal presenter in major academic meetings including general meetings or international me

学会名 Conference	World Academy of Nursing Science The 7th International Nursing Research Conference of WANS		
演題 Topic	Chinese older adults' perspective of home care: A systematic review of qualitative studies(査読あり)		
開催日 date	2022 年 10 月 18~19 日	開催地 venue	Taiwan
形式 method	<input type="checkbox"/> 口頭発表 Oral <input checked="" type="checkbox"/> ポスター発表 Poster	言語 Language	<input type="checkbox"/> 日本語 <input checked="" type="checkbox"/> 英語 <input type="checkbox"/> 中国語
共同演者名 Co-presenter	Yang Huiching; Masaki Harue; Zhou Wei		
学会名 Conference	第14回文化看護学会学術集会		
演題 Topic	中国人高齢者の施設での療養生活に関する認識 ―文献検討を通して―(査読あり)		
開催日 date	2022 年 3 月 12 日	開催地 venue	栃木県下野市
形式 method	<input checked="" type="checkbox"/> 口頭発表 Oral <input type="checkbox"/> ポスター発表 Poster	言語 Language	<input checked="" type="checkbox"/> 日本語 <input type="checkbox"/> 英語 <input type="checkbox"/> 中国語
共同演者名 Co-presenter	正木治恵		
学会名 Conference	日本老年看護学会 第28回学術集会 合同開催 第33回 日本老年学会総会		
演題 Topic	在留中国人高齢者の老いへの準備教育プログラムの有用性の検討(採択)(査読あり)		
開催日 date	2023 年 6 月 16~18 日	開催地 venue	日本・横浜
形式 method	<input checked="" type="checkbox"/> 口頭発表 Oral <input type="checkbox"/> ポスター発表 Poster	言語 Language	<input checked="" type="checkbox"/> 日本語 <input type="checkbox"/> 英語 <input type="checkbox"/> 中国語
共同演者名 Co-presenter	正木治恵、呉小玉		
学会名 Conference	International Association of Gerontology & Geriatrics(IAGG) Asia/Oceania Regional Congress 2023		
演題 Topic	Verification of the feasibility of an education program on aging-related preparation through videoconferences for old Chinese migrants in Japan(査読中)		
開催日 date	2023 年 6 月 12~15 日	開催地 venue	Japan/Yokohama
形式 method	<input checked="" type="checkbox"/> 口頭発表 Oral <input type="checkbox"/> ポスター発表 Poster	言語 Language	<input type="checkbox"/> 日本語 <input checked="" type="checkbox"/> 英語 <input type="checkbox"/> 中国語
共同演者名 Co-presenter	Masaki Harue		

## 4. 受賞(研究業績) Award (Research achievement)

名称 Award name	国名 Country	受賞年 Year of	年	月
名称 Award name	国名 Country	受賞年 Year of	年	月

## 5. 本研究テーマに関わる他の研究助成金受給 Other research grants concerned with your research theme

受給実績 Receipt record	<input checked="" type="checkbox"/> 有 <input type="checkbox"/> 無
助成機関名称 Funding agency	文化看護学会
助成金名称 Grant name	2021年度文化看護学会研究助成金
受給期間 Supported period	2022 年 1 月 ~ 2024 年 12 月
受給額 Amount received	100,000 円
受給実績 Receipt record	<input checked="" type="checkbox"/> 有 <input type="checkbox"/> 無
助成機関名称 Funding agency	公益財団法人 在宅医療助成 勇美記念財団
助成金名称 Grant name	2021年度在宅医療助成(後期)一般公募「在宅医療研究への助成」
受給期間 Supported period	2022 年 3 月 ~ 2024 年 3 月
受給額 Amount received	885,396 円

## 6. 他の奨学金受給 Another awarded scholarship

受給実績 Receipt record	<input type="checkbox"/> 有 <input checked="" type="checkbox"/> 無
助成機関名称 Funding agency	
奨学金名称 Scholarship name	
受給期間 Supported period	年 月 ~ 年 月
受給額 Amount received	円

## 7. 研究活動に関する報道発表 Press release concerned with your research activities

※記載した記事を添付してください。Attach a copy of the article described below

報道発表 Press release	<input type="checkbox"/> 有 <input checked="" type="checkbox"/> 無	発表年月日 Date of release	
発表機関 Released medium			
発表形式 Release method	・新聞 ・雑誌 ・Web site ・記者発表 ・その他( )		
発表タイトル Released title			

## 8. 本研究テーマに関する特許出願予定 Patent application concerned with your research theme

出願予定 Scheduled	<input type="checkbox"/> 有 <input checked="" type="checkbox"/> 無	出願国 Application	
出願内容(概要) Application contents			

## 9. その他 Others

--

指導責任者(記名) 正木治恵

原著論文

在留中国人高齢者の健康に関する思い  
— 中国人が集まる地域活動に参加する対象者に焦点を当てて —

Health Perspective of Elderly Chinese Migrants in Japan:  
Focus on Participants of Chinese Attracted Community Activities

姚 利<sup>1)</sup>, 石井優香<sup>1)</sup>, 山崎由利亜<sup>1)</sup>, 石橋みゆき<sup>2)</sup>, 正木治恵<sup>2)</sup>

Li Yao, Yuka Ishii, Yuria Yamasaki, Miyuki Ishibashi, Harue Masaki

キーワード：主観的健康感, 健康に関する思い, 高齢者, 在留中国人, 文化看護

Key words : self-rated health, health perspective, elderly, Chinese migrant, Transcultural Nursing

Abstract

Purpose

To investigate the health perspectives regarding to self-rated health and health experiences of elderly Chinese migrants who were involved in Chinese attracted community activities in Japan.

Method

Participants were 13 elderly Chinese residents who were recruited in the Tokyo Area; individual semi-structured interviews and qualitative and inductive analyses were performed.

Results

From the results of the overall analysis, eight health perspectives were identified: (1) subjectively examining health according to physical and mental faculties; (2) feeling secure by living in a safe and amenity social environment; (3) feeling peaceful by accepting support from others to solve daily life issues; (4) keeping a positive frame of mind by accepting the realities of aging; (5) communicating and engaging with other Chinese residents, so that daily life is not restricted by the language barriers; (6) preferring to reside with family members and support each other; (7) feeling relieved to be able to access Japanese healthcare services successfully by themselves; and (8) independently using traditional Chinese medicine to manage health and keep fit.

Conclusion

We confirmed that late adulthood developmental tasks, Chinese culture, and language barriers affected the health perspectives of elderly Chinese migrants in Japan. Because the language barriers and continuity of the native culture influenced their security, health promotion, and expectation of later life, it is important to create

受付日：2021年9月30日

採択日：2022年3月9日

1) 千葉大学大学院看護学研究科 Doctoral Program, Graduate School of Nursing; Chiba University

2) 千葉大学大学院看護学研究科 Graduate School of Nursing; Chiba University

姚 利 Li Yao

〒260-8672 千葉県千葉市中央区亥鼻1-8-1

1-8-1 Inohana, Chuo-ku, Chiba-shi, Chiba 260-8672, JAPAN

E-mail: yaoyong134193@gmail.com

an accommodating environment to resolve language barriers and provide care based on the cultural and health promotion standards that are familiar to elderly Chinese migrants.

## 要 旨

### 目 的

中国人が集まる地域活動に参加する在留中国人高齢者を対象に異国在住での主観的健康感と健康に関わる経験の調査を通して、彼らの健康に関する思いを明らかにすることである。

### 方 法

日本の首都圏に在住する中国人高齢者13名を対象に個別に半構造化面接を実施し、質的帰納的に分析した。

### 結 果

全体分析により、【身体機能や精神状態から主観的に健康の良し悪しを評価している】【安全で便利な社会に住むことを安心だと感じている】【他者の支援を受けることで安心して生活できている】【老いを受け止めて前向きに生きている】【言葉の壁で生活は制限されたが中国人との関わりや趣味を通して気楽に生活している】【家族で互いに支える生活を継続したい】【良い医療サービスをうまく利用できるので安心してしている】【健康を維持するため中医学に基づき自主的に健康管理をしている】という8つの健康に関する思いが明らかとなった。

### 結 論

在留中国人高齢者においては、高齢期の発達課題や、中国文化、言葉の壁が彼らの健康に関する思いに影響を与えていることが明らかとなった。言葉による制限や母国文化の継続は彼らの安心感や、健康促進、老後生活の希望に強く影響を及ぼすため、言葉の壁を取り除く環境整備や彼らに馴染んだ文化や健康促進方法に基づいたケアの提供の重要性が示唆された。

## I. 背 景

2020年末時点で65歳以上の在留外国人の総数は197,197人に達し、2019年より0.7%増え、日本全人口の6.7%を占めている。そのうち、中国人高齢者は23,080人(11.7%)であり、在留外国人高齢者総数の第2位である(出入国在留管理庁, 2021)。彼らは、1978年の日中国交正常化および1980年代後半の外国人労働力の受け入れ政策によって、就職するために来日し、現在、高齢期を迎えている。また、2012年には、高度外国人材の優遇措置の一つとして「親の帯同」を許可し始め(法務省入国管理局, 2012)、母国にいる高齢の親を日本に呼び寄せることが少なくない。そのため、現在の在留中国人高齢者には、中国で生まれ中国文化の中で長年過ごし、来日した人が多いと思われる。

先行研究では、外国人患者の看護提供において、言葉(近藤, 2021)、文化、病気に関する考え方の違い(久保, 2014)による困難が多く報告されている。今

後、外国人患者への看護ケア提供の機会の増加に伴い、ケア提供上の困難も増えることが推察される。一方、在日外国人にとって、保健医療機関を利用する際、言葉の壁・異なる文化や価値観の壁・異文化不適応から生じた悩みの解消の壁は、彼らの健康問題を及ぼす要因である(呉, 2016)と指摘されている。つまり、日本に移住することによる言葉や文化の壁は、在留外国人の健康に影響を及ぼしていると考えられる。

Leininger (1995) は、看護の対象となる多くの人々に健康と安寧をもたらすために文化に適したケアの提供を目標とし、多様な文化を理解することが不可欠であることを提唱している。高齢者ケアでは、高齢者を支えている内在化した「文化」を十分に理解した上で、ケアに生かすことが重要である(正木, 2004)。在留中国人高齢者が、日本で高齢期の変化を経験しつつ心身ともに健康で安寧に暮らし続けるために、看護師は彼らが持っている文化、価値観や習慣を理解し、文化を考慮したケアを提供する必要があると考えられる。しかし、異国で老いを経験している中国人高齢者

の健康に対する内在化された中国文化の影響と、移住したことの影響は明らかになっていない。

一方、個々の生活様式や価値観が多様化してきた現在、主観的健康感などの、個人レベルでみた主観的な健康指標が重視されている（小田，2007）。芳賀（1984）は主観的健康感とは身体的、精神的、社会的な統合体としての健康の主観的認識を表していると示唆している。主観的健康感を1つの指標として、中国の文化が内在化した在留中国人高齢者の健康状態及び健康に関する思いを理解できるのではないかと考える。本研究は、在留中国人高齢者の主観的健康感と日本で健康に関わる経験を明らかにすることで、より適切なケア提供への示唆が得られると考える。また、各地域に散住している在留中国人高齢者にアクセスするため、中国人が集まる地域活動に参加する対象者に焦点を当てた。

## II. 研究目的

中国人が集まる地域活動に参加する在留中国人高齢者を対象に異国在住での主観的健康感と健康に関わる経験の調査を通して、彼らの健康に関する思いを明らかにすることである。

## III. 用語の定義

**在留中国人高齢者**：中長期在留資格を持ち日本に住む65歳以上の中国国籍を持つ人、日本の国籍を取得した華僑、華人と、中国で生まれ50年以上中国で生活していた中国残留孤児とする。

**主観的健康感 (Self-Rated Health)**：生活機能の状態や疾病の有無にかかわらず、自分自身が自己の健康状態をどのようにとらえるかを評価するもの（大内，2010）とする。

**健康に関する思い**：日本に住んでいることの影響を含めた、自分自身の身体的・精神的・社会的健康及びそれに関連する受診や健康増進について感じること・希望すること・気にかけて考えを持つことやその内容とする。

## IV. 研究方法

### 1. 対象者および募集方法

対象者は、本研究で定義する在留中国人高齢者とし

た。ただし、認知機能障害を持つ者は除外した。

首都圏都市部にある公民館およびコミュニティーセンター、中国語対応が可能な施設で対象者を募集した。また、対象者の多様性を確保するため、雪だるま式募集方法を併用した。

### 2. データ収集期間

2019年3月～10月

### 3. 調査方法

調査はインタビューガイドを用いて対象者に半構造化面接を1～3回、1回60分を目安に行った。面接内容は、対象者の同意を得てICレコーダーに録音し、逐語録を作成した。個別面接で使用した言語は対象者の希望に沿い、中国語とした。

### 4. 調査内容

調査内容は対象者の基礎情報と主観的健康感、健康に関する思いや考えとした。先行研究を参考に、インタビューガイドを作成した。

基礎情報は年齢、収入、家族構成、学歴、在留年数とした。

主観的健康感とは健康に関する思いの1つの指標として調査を行い、その測定方法は杉澤ら（1995）が明らかにした測定方法を参考に、「自分の健康状態を全体的にどう評価しますか」「他の同年齢の方と比べて自分の健康をどう評価しますか」の問いに、「とても良い」から「良くない」まで4段階での回答を求めた。また、「去年の自分の状態と比較すると、現在の健康状態をどう評価しますか」の問いに対しては、「いつも通り」を含めた5段階での回答を求めた。

インタビューガイドの内容は、在留外国人の健康障害要因と健康に関する異文化体験に関する先行研究（Jiang, 2016；中嶋，2015；平野，2003）を参考に、在留期間中の受診経験、日常生活の過ごし方、健康増進方法、今後の生活や健康上の心配や希望、主観的健康感の評価理由および日本語の自己評価理由についてどのような考えや思いを持っているかを含めた。日常会話および受診時の言葉の壁は在留外国人の精神的健康・主観的健康感に影響を及ぼす（大植，2018）ため、日本語の自己評価についても「日本語の日常会話能力をどう評価しますか」と「日本語の医療会話能力をどう評価しますか」の問いに、「とても良い」から「良くない」まで4段階での回答を求めた。

### 5. 分析手法

対象者の基礎情報、主観的健康感、日本語能力の自己評価は記述的統計学で分析した。面接データは質的

帰納的に分析した。本研究の対象者は社会的・文化的背景に強く影響を受け、個性が高いと考え、個々の事例が持つ個性・独自性を把握できる質的統合法（KJ法）（山浦，2012）を参考にした。

個別分析は、面接の逐語録から一つの「健康に関する思い」が含まれるようにラベルを作成し、ラベル内容の類似性に沿ってグループを編成し表札を作成した。最終ラベルが5～7枚になるまで同じ作業を繰り返した。

全体分析は、個別分析の最終ラベルを内容の類似性に沿って集め、サブテーマをつけた。さらにサブテーマを類似性に沿って集め、テーマとした。ただし、類似する内容がないサブテーマはテーマとした。

## 6. 信憑性

研究者は質的統合法（KJ法）研修会へ参加し、分析手法の精度の向上に努めた。分析の全過程において老年看護学ならびに質的統合法（KJ法）に精通する研究者のスーパーバイズを受けた。

収集したデータはすべて中国語であった。日本語でスーパーバイズを受けて分析方法の妥当性を確保するため、最初の5名の個別分析は中国語から日本語に訳したあと行った。訳したデータの妥当性を確保するため、研究者の所属する大学の日本語支援室に添削を依頼した。言語のニュアンスを確保するために、6人目からは中国語で分析を行った。ただし、最終ラベルは日本語と中国語で作成し、指導教員のスーパーバイズを受けた。

## V. 倫理的配慮

本研究は、千葉大学大学院看護学研究科倫理審査委員会の承認と対象者が活用する組織や施設の承認を得て実施した（承認番号30-97）。

対象者に対して研究の目的と参加の自由、個人情報保護の方法、研究に参加しない場合であっても不利益を受けないこと、研究結果の公表の可能性などの倫理事項について分かりやすい言葉と文章で説明し、書面にて同意を得られた後に面接を実施した。

## VI. 結果

### 1. 対象者の概要

本研究の対象者は男性5名、女性8名の計13名であった（表1）。対象者全員が首都圏在住であった。

在留年数は、5年から30年以上であり、平均22.8年であった。10名の対象者は日本の病院を受診した経験があった。対象者は生活支援金や中国あるいは日本の年金で生活を送っていた。日本語能力の自己評価について、日常会話、医療会話が「まあ良い」と評価した対象者はそれぞれ5名と7名であったが、日本人の友人を持ち、主に日本人で構成されたメンバーでの活動に定期的に参加する人は1名だけだった。対象者は全員中国人が集まる活動や中国人向け地域活動に参加していた。

各対象者の総面接時間は30分から140分であり、平均時間は50分であった。個別分析に用いた元ラベルは40枚から80枚であった。

### 2. 研究対象者が活用する組織や施設の概要

#### 1) X県健康教室

X県健康教室は中国残留邦人と在留中国人が日本の社会に入れるように、日本文化を学び、健康知識や日本語能力を高めるため、自発的に立ち上げられた組織である。活動の頻度は週1回である。およそ35名の参加者は全員70歳以上である。

#### 2) X県日本語サークル

X県都市部の公民館で週1回、近隣に住む中国人に、日常会話能力の向上と日本の文化の学習を目的として、日本語授業を開催している。参加者12名のうち、70歳以上の中国人高齢者は4名である。

#### 3) Y県デイサービス

中国残留邦人や中国人高齢者に介護サービスを提供するデイサービスである。サービス内容は中華風の食事や入浴、健康チェック、機能訓練、中国の昔のゲームなどである。職員は看護師1名、生活相談員6名、調理人1名である。生活相談員は全員介護職経験が長く、日本語が堪能な中国人や中国残留邦人2世である。看護師は日本人で中国語を翻訳する機器を用い、コミュニケーションを取っている。

#### 4) その他

1) - 3) 以外の地域活動に参加する対象者は雪だるま式を通して募集した。これらの活動は、公園など公的な場所で近所の中国人が自発的に集まり、活動の内容・参加人数・参加時間などは明確に決められておらず自由に参加できる。

### 3. 全体分析結果

#### 1) 主観的健康感

主観的健康感の結果を表2に示す。全体的評価、同年齢者との比較に対し、「とても良い」及び「まあ良

表1 対象者概要 (n = 13)

性別	年齢	学歴	在留年数 (年)	在留 資格	世帯 状況	収入	日本語能力の 自己評価		ADL	募集 方法	
							日常会話	医療会話			
A氏	男	60代後半	高校	5-9	永住	同	年金	良くない	良くない	自立	雪
B氏	女	70代前半	小学校	30-34	永住	同	生活支援金	良くない	良くない	自立	健
C氏	女	60代後半	大学	25-29	永住	独	年金	まあ良い	まあ良い	自立	雪
D氏	男	70代後半	大学	30-34	永住	同	年金	良くない	まあ良い	自立	健
E氏	女	70代後半	中学校	20-24	定住	独	生活支援金	良くない	まあ良い	自立	日
F氏	女	70代後半	中学校	30-34	定住	同	生活支援金	良くない	まあ良い	要介護	デイ
G氏	男	60代後半	高校	5-9	特定活動	同	年金	良くない	良くない	自立	雪
H氏	女	70代後半	大学	35-39	日籍華人	同	年金	まあ良い	まあ良い	自立	健
I氏	女	70代前半	無	20-24	永住	独	年金	まあ良い	良くない	自立	健
J氏	男	60代後半	高校	5-9	特定活動	同	年金	良くない	良くない	自立	雪
K氏	女	60代後半	高校	20-24	永住	同	自営業収入	まあ良い	まあ良い	自立	雪
L氏	女	70代後半	無	25-29	永住	同	生活支援金	良くない	良くない	自立	健
M氏	男	70代後半	大学	35-39	定住	同	年金	まあ良い	まあ良い	自立	健

※特定活動：法務大臣が個々の外国人について特に指定する活動  
 ※定住者：法務大臣が特別な理由を考慮し一定の在留期間を指定して居住を認める者。残留孤児を含む  
 ※日籍華人：日本の国籍を取得した中国系住民  
 ※永住者：法務大臣が永住を認める者  
 ※同：同居  
 ※独：独居  
 ※雪：Z県雪だるま式で募集  
 ※健：X県健康教室  
 ※日：X県日本語サークル  
 ※デイ：Y県デイサービス

表2 主観的健康感 (n = 13)

	とても 良い	まあ良い	いつも 通り	あまり 良くない	良くない
全体的評価	5(39%)	6(46%)	—	2(15%)	0(0%)
同年齢者と比較	4(31%)	8(61%)	—	0(0%)	1(8%)
去年と比較	1(8%)	3(23%)	5(38%)	1(8%)	3(23%)

い」と評価したのはそれぞれ11名(85%)、12名(92%)であった。去年との比較に対し、「とても良い」及び「まあ良い」と評価したのはそれぞれ1名(8%)、3名(23%)であった。

## 2) 健康に関する思い

全体分析結果は、テーマを【】、サブテーマを〈〉、研究対象者の語りの内容を斜字で示す。全体分析結果は80枚の各個別分析の最終ラベルを素材とし、類似性に沿って統合し、以下の8つのテーマ、16のサブテーマを生成した。

### (1) 【身体機能や精神状態から主観的に健康の良し悪しを評価している】

これは健康状態の評価に関する思いであり、〈病弱による良くない自己健康評価〉と〈老いを感じながらも良い自己健康評価〉が含まれた。〈病弱による良く

ない自己健康評価〉は、重病や自立して生活できないことで健康状態が良くないと思っていることだった。〈老いを感じながらも良い自己健康評価〉は、老いを感じているが、体や精神の状態が良いから、健康状態は相対的に良いと思っていることだった。

### (2) 【安全で便利な社会に住むことを安心だと感じている】

これは自分にとって、困難がなく医療機関を利用でき、安全で便利な社会環境に住んでいることに安心しているという〈自分にとって安心できる住む環境〉に関する思いであった。

日本の食品は天然で体には無害、加えて空気はきれいだし、安心できる(A氏)。

(私は)近所に中国語が対応できる病院があり、(高齢者が)無料で乗れる電車の駅の近く、南向きで静かな部屋に引っ越した。外出と受診が便利だから(B氏)。

### (3) 【他者の支援を受けることで安心して生活できている】

これは、他者の支援に関する思いであり、〈支援された生活〉、〈助けを求める生活〉と〈助けを求める対象がいない大変さ〉が含まれた。〈支援された生活〉

は、日本の行政機関の生活支援を受けながら安心して暮らしていることだった。〈助けを求める生活〉は、困難を取り除くために周りの人や行政機関に助けを求めることだった。一方で、〈助けを求める対象がいない大変さ〉について、C氏は、自分は独身で、将来認知症や他の病気で自立して生活できなくなったら、介護保険を利用して支援を得るが、介護保険に認定されない期間に急に病気になって面倒を見てくれる人がいない状況になることを心配していると語った。

#### (4) 【老いを受け止めて前向きに生きている】

これは老いの受容に関する思いであり、〈余生への希望〉と〈前向きな生き方〉を含んでいた。

〈余生への希望〉は人生の最期は死であり、老いに伴う身体機能の衰え、社会の役割の制限等の現状を受け止めて、思うように生きたいという思いだった。

人生の最期は死なので、生活に希望や心配はないが、寝たきりや虚弱になり、不自由や苦しみを味わい、他の人に面倒をかけることが嫌なので、最期はコロリと逝きたい(D氏)。

〈前向きな生き方〉は加齢や疾病などの現状を受け止めて、前向きに生きているという思いだった。

人間の生死は運命であり、楽あれば苦ありを信じていて、毎日後悔なく楽しんで大事に過ごせば、人生は有意義になる(E氏)。

#### (5) 【言葉の壁で生活は制限されたが中国人との関わりや趣味を通して気楽に生活している】

これは、言葉の壁があり日本人とのコミュニケーションが難しいことによる制限された生活の中で、中国人との関わりや趣味を通して、社会とのつながりを作り、気楽に生活しているという、〈制限された生活の中での楽しさ〉に関する思いであった。

(中国人向けの) デイサービスでは中国語で活動に参加し友達と雑談することが楽しい(F氏)。

違う言語や文化(の影響)で日本人とのコミュニケーションができないから、朝中国人が集まる公園で太極拳を見たり、中国人の床屋さんで散髪したりして、のんびりと過ごしている(A氏)。

年をとって記憶力が衰えるため、日本語を覚えるより忘れる方が多い……楽しく、有意義な生活を過ごすため、毎日外出して(中国人の)友達と歓談したり、互いに助けあったり、優しい言葉をかけて人間関係を維持している(E氏)。

#### (6) 【家族で互いに支える生活を継続したい】

これは家族関係への思いであり、〈子供に迷惑を

かけたくない〉と〈家族の支え〉を含んでいた。

〈子供に迷惑をかけたくない〉は老後は子供に迷惑をかけないように過ごしたいということだった。

一家団欒の方が安心だと思い、将来の老後の生活は、(病気になると子供に迷惑をかけるから)子供に迷惑をかけず健康で(子供と)同居生活を送りたい(G氏)。

今後私は寝たきりになって(自分で)病院にも行けなくなり、娘も仕事があるから、迷惑をかけたくないし。もし仕方がないなら、老人ホームに行くしかない…でも私は本当に老人ホームに入りたくない、自分の家がいい(H氏)。

〈家族の支え〉は家族の支えで悩みがなく暮らしていることだった。

夫が亡くなった後、(私に)寂しさを感じさせないように孫が同居してくれて、日常生活に悩みがある時、娘が相談にのってくれるし、孝行な家族に支えられて、悩みや辛い時期を乗り越えた。日常生活に解決できないことはない(I氏)。

#### (7) 【良い医療サービスをうまく利用できるので安心している】

これは、医療サービスの利用に関する思いであり、〈心配のない医療サービス〉と〈言語の壁に影響された受診〉を含んでいた。

〈心配のない医療サービス〉は医療サービスを心配なく利用できるので安心を感じるという思いだった。

年を取ったら必ず病気をすると思うが、病気になる事を心配しながらも日本の医者は責任を持って薬を処方してくれるし、自分も中国と日本の健康保険があるから、病気になっても経済的な心配がなく、安心して速やかに受診できるので、病気になっても怖くない(J氏)。

〈言語の壁に影響された受診〉は、日本語がわからない対象者の受診の困難さであった。一方で、日本語が概ねわかる人にとって、あるいはよく受けている医療行為であれば、一人で受診する自信があること、対応できない場合でも家族や役所の通訳者に同伴してもらい、中国語が対応できる医療機関を利用することであった。

日本語は大体わかるので、いつも受診や入院している主治医や病院があり、救急車を呼んだ経験もあるし、自分一人で受診や入院することに問題はない(F氏)。

入院期間中や受診時の悩みは、子供に迷惑をかけな

いように自分で解決し……遠い病院に行くときや受診時に日本語が分からないなど自分で解決できない場合は夫と娘に同伴してもらった (H氏)。

(8) 【健康を維持するため中医学に基づき自主的に健康管理をしている】

これは、中医学に基づいた健康管理に関する思いであり、〈健康情報の入手〉〈中医学に基づく健康促進〉と〈総合的な健康管理〉を含んでいた。その中でも、老いを感じたため中医学に基づく多様な方法で健康を促進しているという〈中医学に基づく健康促進〉についての思いが多かった。

蓮の葉や枸杞を使って調理するという「求人不如求自己」の中医学の本に書かれたコレステロール値をコントロールできる料理を食べたり、毎朝ツボマッサージをして風邪を予防したりしている (I氏)。

長生きのためにカシュウを調理して白髪を予防したり、天然の蜂蜜を食べて免疫力を高めたり、辛い食べ物を減らしたりという健康な飲食習慣を守っている (A氏)。

〈健康情報の入手〉は、健康を管理するため、メディアから中国や日本の健康促進情報を入手することだった。〈総合的な健康管理〉は、健康な体を守るため、自主的に運動や飲食、外出の増加などを通して、身体的、精神的、社会的健康を総合的に管理していることだった。

自分の体を鍛えるため、毎朝公園で太極拳を実践している……毎日家にいることは良くない。家で寝るより活動に参加することが良い。活動に参加した後は、(家にいるより) 精神状態が違う (気分が晴れる) (D氏)。

## Ⅶ. 考 察

本研究では、中国人が集まる地域活動に参加する在留中国人高齢者に焦点を当てた8つの健康に関する思いを明らかにした。高齢期の発達課題や、言葉による制限、中国文化に影響された思いが含まれていた。本研究は、主観的健康感や、高齢期の発達課題、言語による制限、儒教思想や中医学の影響から対象者の特徴を考察する。

### 1) 主観的健康感

全体的および同年齢者と比較した健康感が良いと評価した対象者が8割以上を占めた。一方、先行研究(胡, 2007)では、日本に在住する中国残留孤児の主

観的健康感は低かった。この違いの要因は2つ考えられる。

1つ目は、本研究の対象者は定期的に中国人や中国残留孤児が集まる地域活動に参加していた。于ら(于, 2019)は、中国都市部に居住する高齢者は付き合い・交流の頻度が高いほど主観的健康感が高かったと明らかにしている。本研究の対象者の主観的健康感是中国人や中国残留孤児が集まる組織活動の参加の楽しさの影響を受けていたと考える。

2つ目は、本研究の対象者は身体機能や精神状態から主観的に健康の良し悪しを評価していた。13名の対象者のうち11名は、健康状態を同年齢者と比べた際、大きな持病がなく、精神状態が良く、さらに自立して生活できるので、自分の健康に自信を持っていた。先行研究では、疾病への罹患、精神的な不安定感(五十嵐, 2006; 山内, 2015)、慢性的な健康障害や機能障害(Jiang, 2016)は主観的健康感に影響を与えると報告している。本研究の対象者は、老いに伴う体力の低下などを経験していたが、重病がなくADLが高い者が多かった。そのことが、主観的健康感を良いと評価した対象者の割合が高かったことに関連していると考えられる。

### 2) 高齢期の発達課題に影響した健康に関する思い

【身体機能や精神状態から主観的に健康の良し悪しを評価している】【安全で便利な社会に住むことを安心だと感じている】【他者の支援を受けることで安心して生活できている】【老いを受け止めて前向きに生活している】という思いは高齢期に直面する健康や生活の変化に関連していた。

対象者は健康上の変化に適応するために身体・精神面の状態をとらえると同時に、生活上の支援や居心地のよい便利な住まい環境を整えていた。対象者らは高齢期における変化への対応を踏まえて、加齢に伴う現状を受容していたと考える。健康の衰退に適応し、生活を満足におくれるように(住まいを)準備すること(Havighurst, 1995)や、自分の人生の受容(Newman, 1988)は高齢期の発達課題として挙げられている。本研究の対象者は健康の衰退およびそれによって変化した現状への適応は、異国での老後の生活の中で、高齢期の発達課題に直面しつつ発達し続けていると考えられる。

### 3) 言葉による制限が影響した健康に関する思い

【言葉の壁で生活は制限されたが中国人との関わりや趣味を通して気楽に生活している】【良い医療サー

ビスをうまく利用できるので安心している】という思いは言葉の制限が社会活動の参加と医療機関の利用に関連したことを示した。

社会活動の参加について、現在、日本では、在留外国人が日本社会で孤立しないようにするために、多文化共生の地域づくり活動を通して、地域社会へ参画できる仕組みを整備している（総務省、2020）。本研究の対象者が居住する首都圏都市部では、在留中国人高齢者が多く、中国人が自発的に集まる活動や外国人向けの活動がさかんであった。そこでは交通が便利で、高齢者に対する交通費の公的な補助制度があるため、中国人が集まる活動にアクセスしやすいと考える。彼らは日本人とのコミュニケーションが難しい中で、中国人との関わりや趣味を通して社会とのつながりを持っていた。Maoら（2020）が行った中国系アメリカ人高齢者を対象にした健康行為と文化変容に関する研究では、中国の文化背景を有する海外移住高齢者は、中国の生活行動パターンを保つことや言葉の障壁で、中国人との関わりを好み、地元の人との関わりが乏しく、移住社会に入りにくいことが多いことが示唆された。つまり、同じ文化背景を有する在留中国人同士の交流にアクセスしやすくするため、交通や地域活動の開催・情報の提供を含む環境の整備が必要であると考える。

医療機関の利用について、本研究の対象者は、在日してすぐの頃は医療サービスを利用する際に困難があったと語ったが、現在、受診の困難があると語ったのは13人の対象者のうち1人だけだった。また、在留年数が10年未満の対象者の方が、医療会話と日常会話能力の自己評価について、両方とも良くない傾向があった。対象者からは在留年数が長いほど受診の経験は多いため、よく受けている医療行為は1人で対応できると語られた。そして、健康教室や日本語サークルに参加している対象者は、日常会話や医療会話能力のいずれかを「まあ良い」と自己評価する人が多かった。対象者の日本での在留期間が長いこと、日本語を学ぶことができる地域活動に参加していることは、日本語での受診時の自信につながると考えられる。

一方、本研究の対象者は、老いに伴う身体機能や記憶力の衰えによって外出が制限され、日本語を忘れることが増えた実感から、今後も療養生活を自宅で送ることを希望していた。自分で対応できない場合は、家族や行政機関の通訳者に同伴してもらい、中国語が対応できる医療機関を利用し、家族の手助けを受けら

れ、公的医療通訳者や中国語が対応できる医療機関にアクセスしやすい地域に在住していることが受診時の言語の障壁を取り除いていた。Luiら（2017）は、イギリスに在住する中国系移民高齢者は言語の障壁で医療サービスの利用に困難はあるが、家族や、慈善組織、公的通訳者はこの困難を乗り越えるための橋わたしの役割をもつことを報告している。今後自宅で療養生活を送る在留中国人高齢者が増えると推測されるため、医療・福祉分野における専門的通訳ボランティアの養成やICTを活用して遠方から通訳を受ける仕組みづくりなど、医療サービスにアクセスしやすい環境の整備が必要であると考えられる。

#### 4) 儒教思想や中医学に影響される健康に関する思い

【家族で互いに支える生活を継続したい】【健康を維持するため中医学に基づき自主的に健康管理をしている】という思いは中国文化に影響していた。

本研究の対象者は、〈家族の支え〉を受けながら異国で生活し、今後も家族に〈迷惑をかけたくない望み〉を抱いており、健康に老後生活を送りたいという思いがあった。黄ら（2010）は中国系移民高齢者は、青年期までに中国で経験した文化や価値観が移住生活の中でも主導的な価値観となり、老いへの態度・経験に影響を与えていると明らかにしている。これは、本結果と一致する。「中華人民共和国の婚姻法」（1985）では、親に孝行することは法的な義務である。中国の伝統的な文化の主流である儒教思想によると、子供は親孝行すべきであり、親の老後生活は自宅で子供が身体的な介助を担うべきで、家族で全員を支え合いながら老後の生活を送るべきと考えられている。対象者の健康に関する思いには、子は親の面倒を見るべきであり、できる限り健康に生きることで子供の負担を軽減しようとする親としてのあり方が反映された中国の伝統的な親子関係が継承されており、それは対象者の老後生活の希望、健康を維持する意欲につながっていたと考える。

健康の維持について、本研究の対象者からは、生理的老化を予防するため、カシユウ（生薬の一つ）を調理して食べたり、ツボマッサージや太極拳をするなど中医学の健康促進方法について多く語られた。中医学は中国の春秋時期から記載が始まり、1991年には、「中医学と西洋医学を同等に重視する」方針が中国の憲法に記された。中医学の「医食同源」（薬膳）の基本的な考え方によると、食事は薬であり、薬としての効能が働く食べ物を食べて健康を促進する。また、太

極拳は中医学の陰陽概念を取り入れた武道や護身術の一つとして、古代中国で始まった。中華人民共和国が誕生した後、国民の健康促進方法として採用され大衆化した。太極拳はゆったりとした動きが筋力の向上や身体バランスの改善に効果的で(胡, 2007)、転倒リスクの低下や身体機能改善に有用であると示唆されている(Yu, 2012)。つまり、在留中国人高齢者では、移住後の生活においても中医学の影響が継続しており、ケアを提供する際は、健康への対処方法に中医学が根づいていることを理解する必要がある。中医学の健康促進方法の特徴や効果を考慮して食生活や運動習慣などにケアに活かすことは、彼らにとって馴染みがある継続可能な支援となると考える。

## VIII. 研究の限界と課題

本研究は、活動の参加中や終了直後にデータ収集を実施したため、結果に影響を与えた可能性がある。また、本研究の対象者は中国人が集まる地域活動へ参加する者を対象者とした。今後は、中国人同士での活動に参加していない対象者を調査する必要があると考える。さらに、在留中国人高齢者に対する内在化した文化を考慮した健康促進方法を検討する必要があると考える。

## IX. 結 論

本研究は、在留中国人高齢者の健康に関する思いを明らかにすることを目的に調査を行い、8つの健康に関する思いを明らかにした。その結果、在留中国人高齢者の健康に関する思いは高齢期の発達課題に影響を受けた一方で、言葉の壁および中国文化に強く影響されており、中国人同士の関わりの中での楽しさや医療サービスをうまく利用できる安心感は言葉の壁を乗り越えることに関連していた。儒教思想や中医学の健康促進方法という母国文化の継続は彼らの老後生活の希望、健康促進に影響を及ぼしていた。そして、言葉の壁を取り除く環境整備や在留中国人高齢者が馴染んだ文化や健康促進方法に基づいたケアの提供の重要性が示唆された。文化に配慮したケアは在留中国人高齢者の生活の効果的な支援につながると考えられる。

## 謝 辞

本研究にご理解とご協力をいただいた研究参加者の皆様に謹んで御礼申し上げます。本研究は、2019年度千葉看護学会研究支援金支給事業と日中笹川医学奨学金より助成を受け実施し、2020年度千葉大学大学院修士論文を加筆・修正したもので、要旨は2020TWINC台湾国際看護学会学術集會にて発表した。本研究において利益相反は存在しない。

## 引用文献

- 出入国在留管理庁 (2021). 在留外国人統計 (旧登録外国人統計) 統計表. [http://www.moj.go.jp/isa/policies/statistics/toukei\\_ichiran\\_touroku.html](http://www.moj.go.jp/isa/policies/statistics/toukei_ichiran_touroku.html) (2021.9.5 閲覧)
- 芳賀博 (1984). 健康度自己評価と社会・心理・身体的要因. 社会老年学 (20), 15-23.
- 平野裕子 (2003). 在日外国人の身体的・精神的健康 保健学・看護学的視点から. 福岡医学雑誌, 94(8), 241-249.
- Havighurst, R.J (著), 莊司雅子 (監訳) (1995). 人間の発達課題と教育. 玉川大学出版部. 278-284.
- 法務省入国管理局 (2012). 高度人材に対するポイント制による出入国管理上の優遇制度. [https://www.bunka.go.jp/seisaku/bunkashingikai/kondankaito/nihongo\\_suishin/03/pdf/siryou\\_8\\_1.pdf](https://www.bunka.go.jp/seisaku/bunkashingikai/kondankaito/nihongo_suishin/03/pdf/siryou_8_1.pdf) (2021.12.20 閲覧)
- 黄一帆, 王大華, 刘永广ほか (2010). 老化態度問卷 (AAQ) 中文版的初步試用. 中国臨床心理學雜誌18(04), 447-450.
- 胡秀英 (2007). 中国帰国高齢者の身体機能および主観的健康感に及ぼす太極拳の効果: 無作為割付け比較試験. 体力科学, 56(4), 409-418.
- 胡秀英, 石垣和子, 山本則子 (2007). 帰国10年以上の中国帰国者1世およびその中国人配偶者の精神的健康とその関連要因. 日本公衆衛生雑誌, 54(7), 454-464.
- 五十嵐久人 (2006). 主観的健康感に影響を及ぼす生活習慣と健康関連要因. 山梨大学看護学会誌, 4(2), 19-24.
- Jiang Y, Huang CY, Yoon H, et al. (2016). Correlates of Self-Rated Health and Self-Rated Mental Health in Older Chinese Americans. Soc Work Public Health, 31(4), 309-315.
- 近藤暁子, 上林千佳, 小泉麻美ほか (2021). 日本の看護師が外国人患者をケアするときの困難感に関連する要因. 国際保健医療, 36(2), 39-47.
- 久保陽子, 高木幸子, 野元由美 (2014). 日本の病院における救急外来での外国人患者への看護の現状に関する調査. 厚生指針, 61(1), 17-25.
- Leininger, M (著), 稲岡文昭 (監訳) (1995). レイニンガー看護論: 文化ケアの多様性と普遍性. 医学書院. 36-48.
- Liu, X (2017). Support networks for Chinese older immigrants accessing English health and social care services: the concept of Bridge People. Health, 25(2), 667-677.

- Mao, W (2020). Acculturation and health behaviors among older Chinese immigrants in the United States: A qualitative descriptive study. *Nursing & health sciences*, 22(3), 714-722.
- 正木治恵 (2004). 老年看護における文化と家族看護. *家族看護学研*, 10(1), 57-61.
- 中嶋知世, 大木秀一 (2015). 外国人住民における健康課題の文献レビュー. *石川看護雑誌*, 12, 93-104.
- Newman, B. M, Newman, P. R (著), 福富護 (訳) (1988). *生涯発達心理学：エリクソンによる人間の一生とその可能性*. 川島書店. 452-464.
- 小田利勝, 宮原洋八 (2007). 地域高齢者の主観的健康感と運動能力, 生活機能, ライフスタイル, 社会的属性間との関連. *理学療法科学*, 22(3), 397-342.
- 大植崇 (2018). 地域に住む在留外国人の健康に影響する諸要因の検討. *兵庫大学論集* (23), 35-43.
- 大内尉義, 秋山弘子, 折茂肇 (2010). *新老年学* (第3版). 東京大学出版会. 1651-1655.
- 杉澤秀博, 杉澤あつ子 (1995). 健康度自己評価に関する研究の展開：米国での研究を中心に. *日本公衆衛生雑誌*, 42(6), 366-378.
- 総務省 (2020). 「地域における多文化共生推進プラン」の改訂. [https://www.soumu.go.jp/menu\\_news/s-news/01gyosei05\\_02000138.html](https://www.soumu.go.jp/menu_news/s-news/01gyosei05_02000138.html) (2021.12.20 閲覧)
- 呉小玉, 佐藤文子, 中田涼子ほか (2016). 在日外国人住民の健康を支援するための「国際まちの保健室」に関する実践報告. *兵庫県立大学地域ケア開発研究所活動報告集*, 1, 19-27.
- 山内加奈子, 齊藤功, 加藤匡宏ほか (2015). 地域高齢者の主観的健康感の変化に影響を及ぼす心理・社会活動要因5年間の追跡研究. *日本公衆衛生雑誌*, 62(9), 537-547.
- 山浦晴男 (2012). *質的統合法入門：考え方と手順*. 医学書院.
- Yu D.H, Yang H. X (2012). The effect of Tai Chi intervention on balance in older males. *Journal of Sport and Health Science*, 1(1), 57-60.
- 于進, 小林恵子, 成田太一ほか (2019). 中国都市部における高齢者の主観的健康感と健康習慣, ソーシャル・キャピタルとの関連. *新潟大学保健学雑誌*, 16(1), 23-31.
- 中华人民共和国婚姻法 (1981). [http://www.gov.cn/banshi/2005-08/21/content\\_25037.htm](http://www.gov.cn/banshi/2005-08/21/content_25037.htm) (2021.9.5 閲覧)

## 日本に長期在住する中国人高齢者の健康管理 —地域で自立した生活を送る1事例の語りより—

### Health Promotion Narratives of an Older Chinese Migrant Living Independently in a Community in Japan

千葉大学大学院看護学研究院看護学研究科  
博士後期課程

姚 利

東京情報大学看護学部看護学科  
助教

石井優香

千葉大学大学院看護学研究院看護学研究科  
教授

正木治恵

#### 【Abstract】

In this case study, we used a semi-structured interview to clarify the health promotion and perspectives of an older Chinese migrant living independently in a community in Japan. The KJ method, a qualitative data synthesis method was used to analyze the data. We found that based on the life attitude of actively problem-solving, Mr. A visited physicians without language barriers, felt comfortable managing his health, and accepted the realities of aging. As a result, he was satisfied with his health and hoped to spend the rest of his life pain-free.

#### 【Key words】

Aged, Case reports, Chinese, Migrant, Health promotion

#### はじめに

在日中国人永住者は296,600人(2021年末時点)であり、そのうち65歳以上の高齢者は22,885人に達し、今後も増加していくと予想される<sup>[1]</sup>。法務省は、外国人との共生社会のビジョン実現に向けて、中長期的課題及び具体的施策を公表しており、高齢の外国人を取り巻く実態・課題把握の不十分さとそれらを踏まえた支援策の検討の必要性を主張している<sup>[2]</sup>。

高齢者は、加齢に伴い身体機能の低下など老いの自覚症状が増えるため、健康管理への関心が高くな

る。また、健康管理の方法は長年の生活体験とともに築かれるものであり、その人の文化背景や生活環境から影響を受けている<sup>[3]</sup>。移住期間<sup>[4]</sup>、移住した国の文化や言葉、医療システムの違いなどは、外国からの移住者の健康管理行動において困難が生じる要因であり、これらの要因は心身の健康に影響を及ぼす<sup>[5,6]</sup>。以上のことから、日本に長期在住する中国人高齢者が直面した健康管理上の課題と対応方法を明らかにすることは重要であり、在日中国人高齢者の健康促進のための支援策検討に寄与することができる。

家高<sup>[7]</sup>は1事例の特殊性と複雑さの解明は重要な諸状況における活動の理解を通して、様々な類似

事例の理解を促すと述べている。また、石川ら<sup>[8]</sup>は、高齢者が語るライフストーリー中で一般的には健康づくりとして認識されない内容や本人が健康づくりとしてこれまで意識していなかった内容についても、健康づくりとして意味付けられたと述べている。したがって、本研究の目的を日本に長期在住する中国人高齢者1事例の健康管理に関する語りを通して、地域で自立した生活を送る在日中国人高齢者の健康管理と健康管理に関連する考えを明らかにすることとした。

## 方法

### 1. 研究デザイン

本研究は事例研究である。

### 2. 対象者募集

本研究は地域のコミュニティーセンターで開催されている外国人向けの活動を通して対象者を募集した。

### 3. データ収集方法

研究者はインタビューガイドを用いた半構造化インタビューを行い、データを収集した。インタビューガイドは日本における医療機関の受診経験、日常生活の過ごし方、健康増進の方法、今後の生活を含めた健康上の不安や望み、主観的健康感の評価理由などで構成されている。なお、インタビューガイドは外国人住民の健康問題に関する先行研究<sup>[5]</sup>をもとに作成した。インタビューは対象者居住地域のコミュニティーセンター内にあるプライバシーが確保された静かな個室で行われた。全てのインタビューは研究者によって録音された。

### 4. データ収集期日

2019年4月X日に行った。

### 5. データ分析方法

研究者はインタビューの逐語録をデータ源とし、質的統合法（KJ法）<sup>[9]</sup>を用いた質的分析を行った。まず、研究者は“日常生活の中でどのように健康管理を行っているか”を分析テーマとしてインタビュー逐語録を単位化し、元ラベルを作成した。次に、類似したラベルを集めてグループ化し、集めたラベル群に対してその内容を最もよく表す一文をラベルとして作成した。同じ作業を類似性がなくなるまで繰り返し、最終的に残ったラベルを最終ラベルとした。その後、最終ラベル同士の相互関係を表す空間配置図を作成し、分析テーマに基づいて空間配置図の構造が直観的にわかるシンボルマークをつけ、関係性を叙述化した。シンボルマークは【健康管理に関する要因：その方法】と示した。分析過程において、老年看護学ならびに質的統合法（KJ法）に精通する研究者のスーパーバイズを受けた。

### 6. 倫理的配慮

本研究は千葉大学大学院看護学研究科倫理審査委員会の承認を得た（承認番号30-97）。対象者に対して研究の目的、個人情報保護、インタビューを録音すること、研究結果の公表などの倫理事項について中国語で分かりやすい言葉と文章で説明し、書面にて同意を得た後にインタビューを実施した。

## 結果

### 1. 事例の概要

A氏はB県に在住する70代後半の永住在留資格を持つ男性である。A氏はデータ収集時点から32

年前に妻と息子2人と共に家族4人で日本に移住した。中国では大学卒業後に研究者として働き、来日後は技術者として定年まで働いた。現在は、妻の介護をしながら夫婦2人で生活している。A氏は骨折によって日本の病院を受診した経験はあったが、インタビュー時点では持病はなかった。A氏は主観的健康感を去年と比べて“悪くなった”が、同年齢者と比べると“とてもいい”と評価した。また、A氏は中国人向け健康増進教室に1回/週の頻度で参加し、地域の日本人及び中国人に対して、中国語と日本語の授業を行っていた。毎朝、公園で太極拳やラジオ体操を行い、毎日、約8,000歩以上を歩いていた。

## 2. 分析結果

インタビュー逐語録から65枚の元ラベルが作成され、5段階のグループ化を経て、6つの最終ラベルとシンボルマークが生成された。以下本文において、シンボルマークを【 】, 最終ラベルを〈 〉、シンボルマークの内容を表している元ラベルを斜字にて示した上で、シンボルマークの内容及びそれらの関係性が反映された空間配置図(図1)について説明している。

### (1) A氏の健康管理のシンボルマークの内容

【人生の基本姿勢: 入手できるところから適切な解決方法を探し困難を取り除く】

この最終ラベルは〈研究者として、日常生活や健康に問題があった時、メディアや社会資源など手の届く範囲で解決方法を探求し、自分に合う物を判断し、手に入れて困難を取り除く〉であった。

もし(健康情報が)欲しいなら、情報を入手するためにその情報を探す方法を自分で考えるはず。解決方法を自分で考える。…研究に関する仕事をする人(自分)は、分からないままにはしない。分から

ないなら、自分で解決方法を探す。

【受診への自信: 言葉の壁がなく受診できている】

この最終ラベルは〈言葉の壁により日本の病院の受診が難しい人と違い、自分は必要な時に医療用語を自分で調べることができるので言葉の問題はなく、日本での病院受診に自信がある〉であった。

(医師の話は)全部わかったよ。…私は通訳者は1回も呼ばなかった。…他の人は言葉(日本語)の問題がある。(彼らは)病気になった時、日本で治療を受けたが、なかなか(病気が)治らなかった。結局中国の病院に行った(中国に戻って受診した)。彼らは言葉(の意味)も通じないし、通訳者も彼らの考えを医師にうまく伝えられなかったからだ。

【健康管理による心地よさ: 運動や団体活動の参加が楽しい】

この最終ラベルは〈運動で健康を維持することが当然だと思ったり、授業の準備や団体活動への参加を楽しんだり、自らの健康をきちんと管理している〉であった。

他の人に太極拳を教えるのが私の目的ではない。お金ももらっていない。毎朝、自分ひとりでやる。一緒にやりたい人(日本人)がいたらやるし、誰もいなくても大丈夫。(その理由は)自分の体を鍛えるのが目的だから。…(授業を準備する事は)楽しい。暇を潰せるから。朝から晩まで寝るより良い。

【現実の受容: 自分でコントロールできない現実を素直に受け入れる】

この最終ラベルは〈老いに伴う体の衰え、社会役割の喪失、受診の待ち時間が長いことなどに対しては対処方法を探し、どうしても対処出来ない場合、現実を受け入れる〉であった。

今、歯が19本しか残ってない。元々は24本ある

はず、5本なくなってしまった。…日本の“8020(運動)”によると、私は今1本足りない。…しょうがない、このままでいい。

【健康への自負：老いなどの現実を含め自分の健康には相対的に満足している】

この最終ラベルは〈人生の終点は死である事や老い、自分の経済状況などの現実を受け止めた上で、今の健康状態は、相対的にいいと思っている〉であった。

同年齢の人と比べ(自分の健康状態は)、私のほうがいい。日本人でも、中国人でも、私より健康な人はいない。…身体、心理状態、知識も。私の知識は広い。

【最期に対する希望：不自由や苦しみをなく逝きたい】

この最終ラベルは〈人生の終点は死なので、将来の生活に心配はないが、最期は不自由や苦しみをなく、他者に迷惑をかけずに逝きたい〉であった。

(将来の生活に)心配はない。人間はどうせ死ぬから。心配してもしなくても、変わらない。体が不自由になってから死ぬより、自由に動ける間に死んだほうがいい。他の人に迷惑をかけるより、今死んだほうがいい。社会に負担をかけないし、自分も苦しくない。

## (2) A氏の健康管理の空間配置図(図1)

空間配置図(図1)に含まれた6つのシンボルマーク【健康管理に関する要因：その方法】の関係

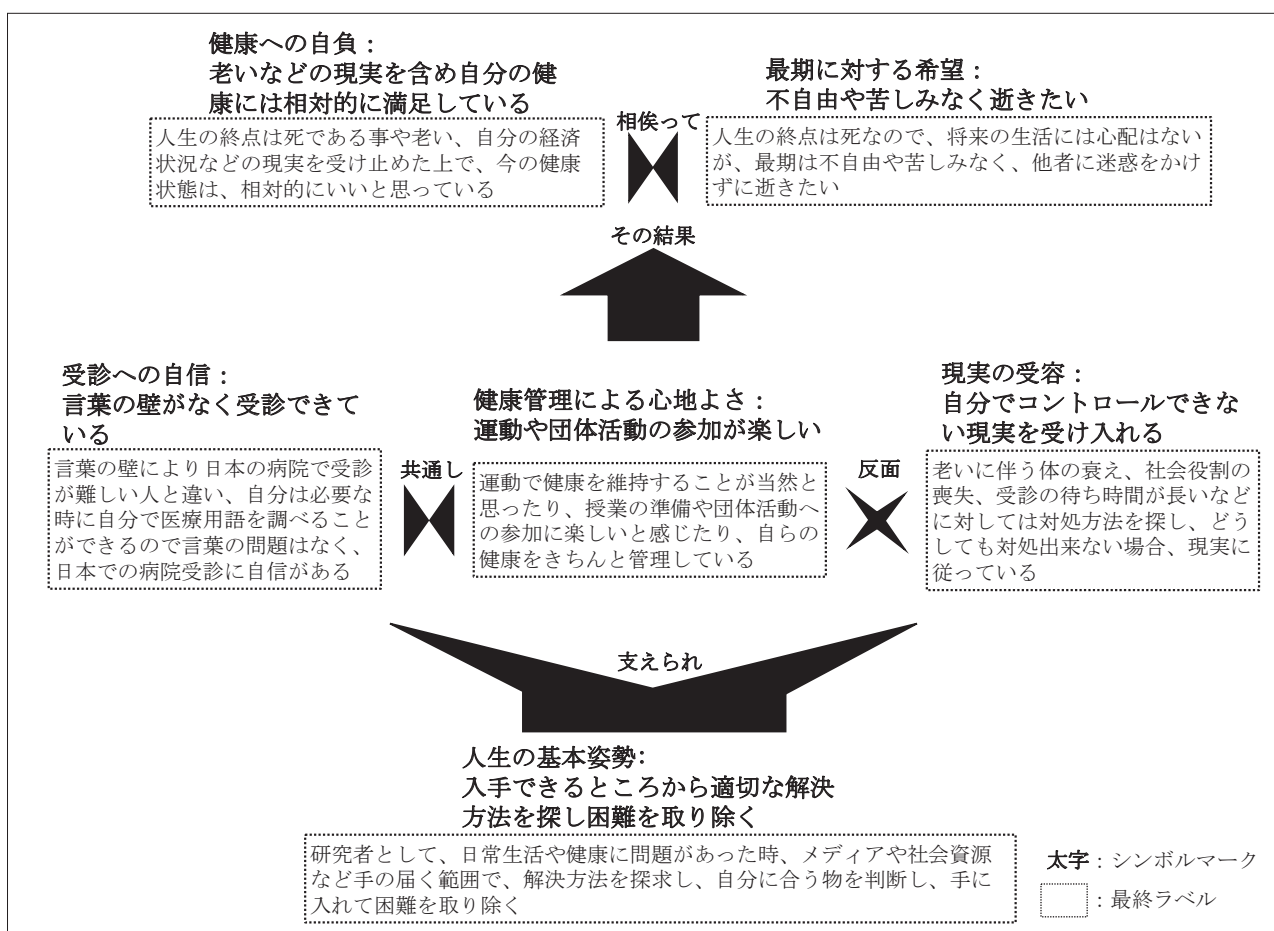


図1 A氏の健康管理の空間配置図

性を以下のように叙述化した。[ ]はシンボルマークにおける「健康管理に関する要因」、「」はシンボルマークにおける「その方法」を示している。

A氏は「言葉の壁がなく受診できている」という「受診への自信」と「運動や団体活動の参加が楽しい」という「健康管理による心地よさ」を共通して感じている。一方、「自分でコントロールできない現実を素直に受け入れる」という「現実の受容」をしている。

そして、これらの健康管理の結果、「老いなどの現実を含め自分の健康には相対的に満足している」という「健康への自負」と「不自由や苦しみなく逝きたい」という「最期に対する希望」を持っている。

これらの健康管理は「入手できるところから適切な解決方法を探し、困難を取り除く」という「人生の基本姿勢」に支えられている。

## 考 察

A氏の健康管理に関する語りの分析から得られた6つのシンボルマークについて考察する。

A氏は必要時にわからない言葉を調べることで「言葉の壁がなく受診できている」という「受診への自信」を持っていた。世界保健機関はヘルスリテラシーを自身と周囲の人々の健康と幸福を促進し維持するために、情報やサービスへアクセスし、それを理解し利用するための個人的な知識とコンピテンシーと定義している<sup>[10]</sup>。これは健康に関する情報の理解や医療従事者に自分の心配を伝えるなどのヘルスケアに関するスキルに影響を及ぼす<sup>[11]</sup>。A氏のように受診時に医療用語を調べるといった言葉の不安に対する事前の対応策を講じることは、在日中国人高齢者のヘルスリテラシーの発揮を促すと考え

られる。

A氏は太極拳やラジオ体操をきっかけにした地域の人との関わりなど「運動や団体活動の参加が楽しい」という「健康管理による心地よさ」を感じていた。移住者は文化や言葉の違いで移住した社会において、つながりを持つことに困難を感じる<sup>[5]</sup>。一方で、高齢者は社会参加機会の増加によって、地域における社会的ネットワークやサポートが充実し、社会的孤独やメンタルヘルスの改善、より良い身体的活動に繋がる<sup>[12]</sup>ことが報告されている。つまり、太極拳など中国文化にある健康管理方法は移住した社会における社会的つながりを促し、社会的サポートの充実とさらなる健康増進が期待できると言える。

A氏は積極的な健康管理を行う一方で、歯の喪失や定年による引退などの「自分でコントロールできない現実を素直に受け入れる」という「現実の受容」をしていた。高齢期における生涯発達の課題には身体的健康の危機と引退の危機が含まれている<sup>[13]</sup>。守屋<sup>[14]</sup>は、高齢者は身体的機能の低下ならびに社会の役割などの喪失に直面せざるを得ないが、これらの事実を受け止めることは高齢期の自我発達につながると述べている。つまり、老いに伴う自分でコントロールできない「現実の受容」は、高齢者の心理社会的健康管理において重要であると考ええる。

これらの健康管理の結果として、A氏は「老いなどの現実を含め自分の健康については相対的に満足している」という「健康への自負」と同時に、「不自由や苦しみなく逝きたい」という「最期に対する希望」を持っていた。そして、A氏が実施した健康管理は「入手できるところから適切な解決方法を探し、困難を取り除く」という「人生の基本姿勢」に支えられていた。地域で暮らす高齢者は「自分の理想とする逝き方」、「いずれ訪れる死への準

備”に取り組んでおり、理想の最期を実現するために生前から死への準備を行うという特徴がある<sup>[15]</sup>。また、遠藤ら<sup>[16]</sup>は日常的に生じる困難や問題の解決策を見つけることができるという対処可能感は、直接男性高齢者の健康行動につながる促進要因であると報告している。A氏が実施している健康管理は健康への自負を生み出すとともに、最期の迎え方の希望につながっており、A氏の研究者としての経験が健康管理の行動を支えていた。医療従事者が在日外国人高齢者に対する健康促進策を検討する際、彼/彼女らの健康管理方法を理解することが重要であり、そのためには、彼/彼女らがそれまでの経験を通して構築してきた人生に対する姿勢を理解することの必要性が示唆された。

## 研究の限界

本研究は事例研究であるため、結果における個人的な傾向が強く、結果の一般化には限界がある。一方で、長期在日中国人高齢者であるA氏が日常生活の中で実施した健康管理およびそれに関する考えを深く探究できたことは、今後の在日中国人高齢者の健康促進の方策を検討するための一助となると考える。今後、在日中国人高齢者を対象とした研究成果を蓄積する必要がある。

## 結論

本研究は地域で自立した生活を送る長期在日中国人高齢者A氏が行っている健康管理およびそれに関連する考えを明らかにした。A氏は「人生の基本姿勢」に支えられた「受診への自信」を持ち、「健康管理による心地よさ」を感じている。一方

「現実の受容」をしており、これらの健康管理の行動の結果、「健康への自負」と「最期に対する希望」を持っていた。

## 謝辞

本研究にご理解とご協力をいただいたA氏に謹んで御礼申し上げます。本研究は日中笹川医学奨学金より助成を受けて実施し、研究者の千葉大学大学院修士論文の一部を加筆・修正したものであり、The 9th Hong Kong International Nursing Forum cum 1st Greater Bay Area Nursing Conferenceにてポスター発表した。本研究における利益相反は存在しない。

引用文献：

- [1] 出入国在留管理庁：在留外国人統計（旧登録外国人統計）統計表. [http://www.moj.go.jp/isa/policies/statistics/toukei\\_ichiran\\_touroku.html](http://www.moj.go.jp/isa/policies/statistics/toukei_ichiran_touroku.html)（最終閲覧2022年11月20日）
- [2] 法務省：外国人との共生社会の実現に向けたロードマップ. [https://www.moj.go.jp/isa/policies/coexistence/04\\_00033.html](https://www.moj.go.jp/isa/policies/coexistence/04_00033.html)（最終閲覧2022年11月20日）
- [3] 橘里佳子、畠中香織、河井伸子ほか：外来通院中の中長期在留者が日本で2型糖尿病と共に生きる生活体験のあり様. 日本看護科学会誌、40(0)、661-671、2020.
- [4] 高久道子、市川誠一、金子典代：愛知県に在住するスペイン語圏の南米地域出身者におけるスペイン語対応の医療機関に関する情報行動と関連する要因. 日本公衆衛生雑誌、62(11)、684-693、2015.
- [5] 中嶋知世、大木秀一：外国人住民における健康課題の文献レビュー. 石川看護雑誌、1293-104、2015.
- [6] 大植崇：地域に住む在留外国人の健康に影響する諸要因の検討. 兵庫大学論集、(23)、35-43、2018.
- [7] 家高洋：看護実践の事例研究の学術性. 家族看護学研究、27(1-2)、191-196、2022.
- [8] 石川麻衣、宮崎美砂子：高齢者のライフストーリーから捉えた健康づくりの構造—独居女性高齢者の健康づくりの意味付けを通して—. 千葉看護学会誌、14(2)、10-19、2008.
- [9] 山浦晴男：質的統合法入門：考え方と手順. 医学書院、2012.

- [10] Nutbeam Don, Muscat Danielle M.: Health Promotion Glossary 2021. Health Promotion International, 36(6), 1578-1598, 2021.
- [11] Berkman Nancy D.: Low health literacy and health outcomes: an updated systematic review. Annals of internal medicine, 155 (2), 97-107, 2011.
- [12] Hashidate Hiroyuki, Shimada Hiroyuki, Fujisawa Yuhki.et al: An Overview of Social Participation in Older Adults: Concepts and Assessments. Physical Therapy Research, 24(2), 85-97, 2021.
- [13] 下仲順子: 老人と人格: 自己概念の生涯発達プロセス. p.32-35, 川島書店、1988.
- [14] 守屋国光: 老年期の自我発達心理学的研究. p.1, 風間書房、1994.
- [15] 大崎涼菜、岡林真、谷口桃花ほか: 地域で暮らす高齢者の死生観—“いきいき百歳体操”に参加する高齢者に焦点を当てて—. 高知女子大学看護学会誌、46(1)、75-84、2020.
- [16] 遠藤寛子、中山和久、鈴木はる江: 首都圏在住中高年者における健康行動を促進する心理社会的要因の研究 共分散構造分析を用いた因果関係モデルの検討. 心身健康科学、14(1)、2-16、2018.

◆ 著者連絡先 ◆

姚 利

千葉大学大学院看護学研究科 博士後期課程

E-mail : yaoyong134193@gmail.com



**糖尿病患者さんの日々を、  
よりよいものにするために。**

「糖尿病患者さんにとって、  
制限のない世界を創造する」それが私たちのビジョン。  
LifeScan, Inc.は世界中で2,000万人以上の  
糖尿病患者の方々に製品をご利用いただいている、  
血糖測定器のリーディングカンパニーです。  
糖尿病患者さんが使用される測定器をはじめ、  
センサーや穿刺針、また医療機関で使用される  
院内専用測定器など、様々な製品をご提供して35年。  
糖尿病患者さんの日々を、  
よりよいものにするために、  
これからも変わることなく貢献してまいります。

**LifeScan** 

LifeScan Japan株式会社  
東京都中央区日本橋室町3-4-4 OVOL 日本橋ビル

©LifeScan Japan K.K. 2022

# 日中笹川医学奨学金制度(学位取得コース)評価書

## 課程博士：指導教官用



第 43 期

研究者番号： G4304

作成日： 2023 年 3 月 10 日

氏名	張 茂芮	Zhang Maorui	性別	F	生年月日	1993.06.23
所属機関(役職)	西南医科大学附属口腔医院インプラント科(医師)					
研究先(指導教官)	東京医科歯科大学大学院医歯学総合研究科口腔機能再構築学講座生体補綴歯科学分野(若林 則幸教授)					
研究テーマ	歯科疾患に対する mRNA を用いた治療戦略の確立 Establishment of mRNA therapy for dental disease					
専攻種別	<input type="checkbox"/> 論文博士			<input checked="" type="checkbox"/> 課程博士		

### 研究者評価(指導教官記入欄)

成績状況	優 学業成績係数=3.75	取得単位数
		30/30
学生本人が行った研究の概要	<p>本研究は、歯科口腔外科・歯周外科分野において、大規模に骨欠損を生じた症例における効率的な骨再生を促進する治療方法を提案するために、①mRNA を用いて投与する骨誘導治療因子の選定および最適化、②ラットを用いた動物モデルにおける骨再生治療効果を明らかにすることを目的としている。</p> <p>本年度は、ラット顎骨にクリティカルサイズの骨欠損を作製し、前年度に最適化した 2 種の骨誘導治療因子を投与し、骨再生の促進を検討した。初めに投与するキャリアの部位および経時的代謝を評価するために、Gluc mRNA を内包するキャリアを投与したところ、投与した骨欠損部に一致した発光を認め、96 時間まで持続した発現を認めた。次に 2 種の治療因子を投与し骨形成量をマイクロ CT により評価を行った。投与 1 週間後では骨増生は認められなかったが、投与 2 週間後より母床骨より骨再生が生じた。また、単一因子の投与と比較して、2 種の因子を同時に投与した際に有意に骨再生の促進が認められた。このことは、複数の治療因子を同時投与することにより治療の短期間化が望めることを示唆している。</p>	
総合評価	<p><b>【良かった点】</b> 本年度は、昨年度行った in vitro の実験を発展させ、臨床応用に向けた in vivo の実験を行った。動物事件に関わる研究スキルの習得と実験データの解析を行い、十分な研究活動を行ったと評価できる。また、論文作成にあたり、十分な過去の知見を引用しながら自分の考えと新たな知見を記載できたことは特筆すべき点であると考えられる。また、研究室の移動に伴い、新たなチームとも協調性をもって活動することができ、十分な議論も行っている。</p> <p><b>【改善すべき点】</b> 今後、自立した研究者として活躍するためには、後輩への教育も必要と考えられる。現在の所、直接指導する後輩がいないため難しいが、次年度以降に学生が配属されるため、教育係としても活躍を期待している。</p> <p><b>【今後の展望】</b> 治療因子の投与による骨再生の促進が達成されたが、他の手法による骨再生速度と比較すると、未だ十分でない事が問題とされる。治療因子の生体内での拡散が原因の一つとして考えられるため、新たなキャリアや東洋方法の検討など、次年度より新たな実験を開始する予定である。</p>	
学位取得見込	<p>研究は順調に進捗しており、本学が定める学位取得の単位も到達している。論文執筆が完了し、本年度中に学術雑誌への投稿を予定しており、十分に学位取得の要件を満たすと考える。</p>	
評価者 若林 則幸		

# 日中笹川医学奨学金制度(学位取得コース)報告書

## 研究者用



第43期

研究者番号: G4304

作成日: 2023年 2 月 28 日

氏名	張 茂芮	ZHANG Maorui	性別	F	生年月日	1993. 06. 23
所属機関(役職)	西南医科大学附属口腔医院インプラント科(医師)					
研究先(指導教官)	東京医科歯科大学 大学院医歯学総合研究科 口腔機能再構築学講座 生体補綴歯科学分野(若林 則幸 教授)					
研究テーマ	骨誘導因子Runx2 mRNAとVEGF mRNA医薬を用いた顎骨再生 Co-delivery of VEGF and RUNX2 Messenger RNA by Polyplex Nanomicelles improves the process of mandibular bone regeneration					
専攻種別	論文博士		<input type="checkbox"/>	課程博士		<input checked="" type="checkbox"/>

### 1. 研究概要(1)

#### 1) 目的 (Goal)

The combine use of different kinds of osteogenic proteins (Runx2 and VEGF) may have some positive implications on the treatment of bone regeneration who suffers from bone fractures and bone defects. Using Runx2 and VEGF for bone repair and regeneration is feasible for mRNA delivery treatment strategies in future. The objective of this study is to explore whether local delivering of Runx2 and VEGF mRNA would enhance mandibular defects repair of rat by in vivo and in vitro study. From this study, I hope to find evidence that Runx2 and VEGF mRNA promote bone repair and provide reliable experimental results for mRNA treatment in the field of bone regeneration.

#### 2) 戦略 (Approach)

From the literature reviews, there are a lot of evidences that Runx2 and VEGF are important promoters of osteogenic differentiation[1,2]. But the intrinsic interactions among Runx2 and VEGF in bone regeneration still needs to be well documented. In this study, I plan to use mRNA encoding Runx2 and VEGF sequences as the method of osteogenic factor transmission, establish an mandibular defect model of SD rat, and explore the effect of Runx2 and VEGF mRNA on bone repair. By comparing the different effects of two factors and their combination of mRNA on mandibular bone defect using histological and molecular biological analysis, I want to find one candidate one mRNA or one mRNA pair which has the most effective osteo-induction effect.

#### 3) 材料と方法 (Materials and methods)

Materials: VEGFa165 mRNA, Runx2 mRNA, Gluc mRNA, Luc2 mRNA, pladmid, Lipofectamin MessengerMAX, Renilla-Glo™ Luciferase Assay System, NIPPON GENETICS mRNA extraction, TOYOBO Reverse transcription kit, GeneAce SYBR® qPCR Mix α, PEG-PAspDET(43-63) polymer, Hepes aqueous solution, Masson golden staining, CD-31 antibody, ALP antibody, OCN antibody, 8-week-old male SD rat, low speed minimotor and handpiece, 4-mm circle drill, micro-CT, in vivo imaging system(IVIS).

#### Methods:

a) mRNA transfection Lipofectamin MessengerMAX: Seeding primary-osteoblasts(POBs) to be 70% confluent at transfection at day0. 24 hours later, dilute MessengerMAX Reagent(5μl) in Opti-MEM Medium(175μl) and prepare diluted mRNA master mix by adding mRNA(2μg) to OptiMEM Medium(175μl). Then mixing diluted mRNA to each tube of Diluted MessengerMAX Reagent(1:1 ratio). Finally, change the medium 24 hours later.

b) Gluc expression analyze: Add 100μl of Renilla Luciferase Assay Reagent to the luminometer tube. Add 20μl of cell lysate. Mix quickly by flicking the tube or vortexing for 1-2 seconds. Place the tube in a luminometer and initiate measurement. Luminescence should be integrated over 10 seconds with a 2-second delay. Other integration times may be used. If the luminometer is not connected to a printer or computer, record the Renilla luciferase activity measurement.

c) Runx2 and VEGF mRNA transfection: P4-primary cells are seeding into 6-well-plate( $1 \times 10^5$  cells/well), group setting: A-only medium, B-Lipofectamine+Luc2, C-Lipofectamine+RUNX2, D-Lipofectamine+VEGF, E-Lipofectamine +RUNX2 (1 μg/well)+VEGF(1 μg/well), F-Lipofectamine+osteogenic medium.

d) Realtime PCR: mRNA extraction by fastGene™ RNA Basic Kit. Reverse transfection the RNA by ReverTra Ace™ qPCR RT Master Mix kit. Target gene(ocn and opn) are analyzed by real-time qPCR using SYBR Green I dye method. All the data are calculated by  $2^{-\Delta\Delta CT}$  method.

e) Mandibular defect: 8-week-old male rats are conducted mandibular defect surgery(4mm defect hole) under anesthesia.

f) IVIS: Luc2 mRNA(10μg)+PEG-PAspDET(43-63) polymer with total 50μl volume is injected into mandibular defect area. 4h, 24h, 48h, 72, 96h, 1week after injection, Luciferase expression is imaged by IVIS.

g) Runx2 and VEGF mRNA in vivo treatment: group: A-Hepes solution, B-Runx2(10μg), C-VEGF(10μg), E-RUNX2 (10μg)+VEGF(10μg), from post-surgery 1week, conduct mRNA injection treatment every week.

h) micro-CT: post-surgery 4week, conduct microCT to analyze the bone mineral density and bone volume for new bone formation.

i) Immunofluorescence staining: 8week mandibular samples are collected to making frozen slides, then using CD-31 antibody to mark the angiogenesis and ALP and OCN antibody to mark the osteogenesis of the bone defect area by immunofluorescence staining.

## 1. 研究概要(2)

## 4) 実験結果 (Results)

- a) mRNA synthesis and validity verification: western blot image showed that Runx2 and Vegf mRNA made in our lab successfully produced protein in Hela cells (Figure1a). successful Gluc mRNA transfection: Gluc expression curve demonstrated that the mRNA expression peaked at 24 hours post-transfection and gradually decrease with time.
- b) Runx2 mRNA and VEGF mRNA promoted the osteogenic markers in vitro: After transfected with mRNA in different groups, the RT-PCR results showed that expression of osteopontin and osteocalcin were relatively highest in RUNX2+VEGF group, while using RUNX2 or VEGF mRNA alone weakly stimulates osteogenic differentiation compared with blank group and Luc2 group (Figure 1d-f). The  $\beta$ -catenin, Lef1, and Osterix mRNA expression at 7 days also showed a slight increase in Runx2 mRNA/VEGF mRNA transfection group than the Blank and Luc2 group. These in vitro data revealed that the use of Runx2 mRNA or VEGF mRNA alone only upregulated the expression of OCN at 11 days.
- d) PEG-PAsp(DET)-nanomicelles successfully delivered Luc2 mRNA into target area: IVIS observed the luciferase signal 4 hours after Luc2 mRNA injection. The images demonstrated the luciferase expression peaked at 24 h then decreased with time. The distribution of ZsGreen1 from microscopic images verified that ZsGreen1 mRNA-loaded by polyplex nanomicelles was nonspecifically delivered into multiple cells in vivo. And the ZsGreen1 signal was dispersed in the mandibular defect area.
- e) mandibular defect model identification and mRNA treatment by microCT: 3D construction image showed a clear  $\varnothing$ 4mm-circle bone defect was established. The results showed local co-administration of Runx2/VEGF mRNA accelerated the new bone regeneration and bone mineralization in the early phase of mandible bone healing. After the first mRNA injection, the new bone tissue was observed in the Runx2 mRNA group, VEGF mRNA, and Runx2/VEGF mRNA group, and the process of bone regeneration continued after weekly administration. The ROI of mandible defect showed a large amount of new bone tissue was produced in the Runx2/VEGF mRNA group, followed by VEGF mRNA group.

## 5) 考察 (Discussion)

The combination of Runx2 and VEGF mRNA treatment in bone tissue regeneration is an exploration of an mRNA-based therapeutic strategy. In this study, Runx2 and VEGF mRNA transfection enhanced the expression of osteogenic differentiation genes in osteoblasts, which was confirmed by in vitro experiments. The subsequent in vivo animal experiments provided strong evidence that co-delivery of Runx2 and VEGF mRNA by polyplex nanomicelles accelerated mandibular defect healing and enhanced new bone formation over the Runx2 or VEGF mRNA single-administration groups. The morpho-histological analyses of ALP, OCN, and CD31 proteins expression revealed that osteogenesis and angiogenesis coupling was activated by co-administration in the early phase of bone repair. Our in vitro and in vivo results substantiated that the co-administration of Runx2 and VEGF mRNA has the advantage of synergistic effect on bone tissue regeneration and osteogenesis and angiogenesis coupling compared with the single factor administration within a mandibular defect model. In the complicated bone healing period, not only bone mesenchymal progenitors and osteoblasts lineages but also endothelial progenitors are recruited into the bone defect area, and the cellular interactions between different types of cells participate in the process of osteogenesis and angiogenesis[3]. Based on this concept of co-administration therapy, our study provides a feasible approach to add more candidates of osteogenic factors for combination therapy in bone regeneration medicine.

The mRNA delivery achieves the combined administration of Runx2 and VEGF in the mandible defect area based on its characteristics of efficiently, low cost, and safely stimulating cells to produce activity proteins. As a protein-replacement therapy, IVT mRNA is designed to be structurally similar to those that occur naturally in eukaryotic cells and stimulates cells to produce the target bioactive protein, which overcomes the difficulties such as the high cost of artificial recombinant protein synthesis and strict manufacturing conditions[4]. And it is also easy to evaluate the optimal dose by adjusting different mRNA doses and dosage ratios, hence achieving better efficacy in bone regeneration treatment.[5].

mRNA therapeutics have made rapid progress in the fields of cancer immunotherapies and infectious disease vaccines in recent years, but their application in bone tissue regeneration is still in its infancy. In our study, the dose ratio and administration time of Runx2 and VEGF mRNA in the treatment of mandibular defects need to be further optimized. And the mechanism of synergistic effect between RUNX2 and VEGF mRNA in osteogenesis and angiogenesis coupling also requires our in-depth exploration. Although this study has some limitations, the successful application of co-delivery Runx2 and VEGF mRNA for early bone healing in our research has expanded the idea of mRNA medicine. Our results provide a reliable experimental basis for the treatment of bone regeneration based on mRNA administration and support the feasibility of mRNA-loaded polyplex nanomicelles drugs for bone regeneration.

## 6) 参考文献 (References)

- [1] Komori T. R. International journal of molecular sciences. 2019;20
- [2] Hu K, Olsen BR. Bone. 2016;91:30-38.
- [3] Liu WC CS, Zheng L, et al. Adv Healthc Mater. 2017;6(5):1600434.
- [4] Sahin U, Karikó K, Türeci Ö. Nature Reviews Drug Discovery 2014; 13:759-780.
- [5] Lee E KJ, Kim J, et al. Biomater Sci. 2019;7(11):4588-602.

## 2. 執筆論文 Publication of thesis ※記載した論文を添付してください。Attach all of the papers listed below.

論文名 1 Title	Metformin Rescues the Impaired Osteogenesis Differentiation Ability of Rat Adipose-Derived Stem Cells in High Glucose by Activating Autophagy					
掲載誌名 Published journal	Stem Cells and Development					
	2021 年 9 月	30 巻(号)	1017 頁 ~ 1027 頁	言語 Language	English	
第1著者名 First author	Maorui ZHANG	第2著者名 Second author	Bo YANG	第3著者名 Third author	Shuanglin PENG	
その他著者名 Other authors	Jingang XIAO					
論文名 2 Title	Downregulation of DNA methyltransferase-3a ameliorates the osteogenic differentiation ability of adipose-derived stem cells in diabetic osteoporosis via Wnt/ $\beta$ -catenin signaling pathway					
掲載誌名 Published journal	Stem Cell Research & Therapy					
	2022 年 8 月	13 巻(号)	397 頁 ~ 414 頁	言語 Language	English	
第1著者名 First author	Maorui ZHANG	第2著者名 Second author	Yujin GAO	第3著者名 Third author	Qing LI	
その他著者名 Other authors	Huayue CAO, Jianghua YANG, Xiaoxiao CAI, Jingang XIAO					
論文名 3 Title						
掲載誌名 Published journal						
	年 月	巻(号)	頁 ~ 頁	言語 Language		
第1著者名 First author		第2著者名 Second author		第3著者名 Third author		
その他著者名 Other authors						
論文名 4 Title						
掲載誌名 Published journal						
	年 月	巻(号)	頁 ~ 頁	言語 Language		
第1著者名 First author		第2著者名 Second author		第3著者名 Third author		
その他著者名 Other authors						
論文名 5 Title						
掲載誌名 Published journal						
	年 月	巻(号)	頁 ~ 頁	言語 Language		
第1著者名 First author		第2著者名 Second author		第3著者名 Third author		
その他著者名 Other authors						

## 3. 学会発表 Conference presentation ※筆頭演者として総会・国際学会を含む主な学会で発表したものを記載してください

※Describe your presentation as the principal presenter in major academic meetings including general meetings or international meetings

学会名 Conference	第22回日本再生医療学会総会			
演題 Topic	mRNA Therapeutics for the Treatment of Mandibular Bone Defect: Co-administration of Runx2/VEGF mRNA			
開催日 date	2023 年 3 月 24 日	開催地 venue	京都 国立京都国際会館1階(Event Hall)	
形式 method	<input type="checkbox"/> 口頭発表 Oral <input checked="" type="checkbox"/> ポスター発表 Poster	言語 Language	<input type="checkbox"/> 日本語 <input checked="" type="checkbox"/> 英語 <input type="checkbox"/> 中国語	
共同演者名 Co-presenter				
学会名 Conference				
演題 Topic				
開催日 date	年 月 日	開催地 venue		
形式 method	<input type="checkbox"/> 口頭発表 Oral <input type="checkbox"/> ポスター発表 Poster	言語 Language	<input type="checkbox"/> 日本語 <input type="checkbox"/> 英語 <input type="checkbox"/> 中国語	
共同演者名 Co-presenter				
学会名 Conference				
演題 Topic				
開催日 date	年 月 日	開催地 venue		
形式 method	<input type="checkbox"/> 口頭発表 Oral <input type="checkbox"/> ポスター発表 Poster	言語 Language	<input type="checkbox"/> 日本語 <input type="checkbox"/> 英語 <input type="checkbox"/> 中国語	
共同演者名 Co-presenter				
学会名 Conference				
演題 Topic				
開催日 date	年 月 日	開催地 venue		
形式 method	<input type="checkbox"/> 口頭発表 Oral <input type="checkbox"/> ポスター発表 Poster	言語 Language	<input type="checkbox"/> 日本語 <input type="checkbox"/> 英語 <input type="checkbox"/> 中国語	
共同演者名 Co-presenter				

## 4. 受賞(研究業績) Award (Research achievement)

名称 Award name	国名 Country	受賞年 Year of award	年 月
名称 Award name	国名 Country	受賞年 Year of award	年 月

## 5. 本研究テーマに関わる他の研究助成金受給 Other research grants concerned with your research theme

受給実績 Receipt record	<input checked="" type="checkbox"/> 有 <input type="checkbox"/> 無
助成機関名称 Funding agency	国立研究開発法人科学技術振興機構
助成金名称 Grant name	次世代研究者挑戦的研究プログラム[東京医科歯科大学卓越大学院生制度(Ⅱ)]
受給期間 Supported period	2021 年 10 月 ~ 2024 年 3 月
受給額 Amount received	月額16万円
受給実績 Receipt record	<input type="checkbox"/> 有 <input type="checkbox"/> 無
助成機関名称 Funding agency	
助成金名称 Grant name	
受給期間 Supported period	年 月 ~ 年 月
受給額 Amount received	円

## 6. 他の奨学金受給 Another awarded scholarship

受給実績 Receipt record	<input type="checkbox"/> 有 <input type="checkbox"/> 無
助成機関名称 Funding agency	
奨学金名称 Scholarship name	
受給期間 Supported period	年 月 ~ 年 月
受給額 Amount received	円

## 7. 研究活動に関する報道発表 Press release concerned with your research activities

※記載した記事を添付してください。Attach a copy of the article described below

報道発表 Press release	<input type="checkbox"/> 有 <input type="checkbox"/> 無	発表年月日 Date of release	
発表機関 Released medium			
発表形式 Release method	・新聞 ・雑誌 ・Web site ・記者発表 ・その他( )		
発表タイトル Released title			

## 8. 本研究テーマに関する特許出願予定 Patent application concerned with your research theme

出願予定 Scheduled	<input type="checkbox"/> 有 <input type="checkbox"/> 無	出願国 Application	
出願内容(概要) Application contents			

## 9. その他 Others

--

指導責任者(記名) 若林 則幸

# Metformin Rescues the Impaired Osteogenesis Differentiation Ability of Rat Adipose-Derived Stem Cells in High Glucose by Activating Autophagy

Maorui Zhang,<sup>1-3,i</sup> Bo Yang,<sup>4</sup> Shuanglin Peng,<sup>1,2</sup> and Jingang Xiao<sup>1,2</sup>

The incidence and morbidity of diabetes osteoporosis (DOP) are increasing with each passing year. Patients with DOP have a higher risk of bone fracture and poor healing of bone defects, which make a poor quality of their life. Bone tissue engineering based on autologous adipose-derived stem cells (ASCs) transplantation develops as an effective technique to achieve tissue regeneration for patients with bone defects. With the purpose of promoting auto-ASCs transplantation, this research project explored the effect of metformin on the osteogenic differentiation of ASCs under a high-glucose culture environment. In this study, we found that 40 mM high glucose inhibited the physiological function of ASCs, including cell proliferation, migration, and osteogenic differentiation. Indicators of osteogenic differentiation were all downregulated by 40 mM high glucose, including alkaline phosphatase activity, runt-related transcription factor 2, and osteopontin gene expression, and Wnt signaling pathway. At the same time, the cell autophagy makers BECLIN1 and microtubule-associated protein 1 light chain 3 (LC3 I/II) were decreased. While 0.1 mM metformin upregulated the expression of BECLIN1 and LC3 I/II gene and inhibited the expression of mammalian target of rapamycin (mTOR) and GSK3 $\beta$ , it contributed to reverse the osteogenesis inhibition of ASCs caused by high glucose. When 3-methyladenine was used to block the activity of metformin, metformin could not exert its protective effect on ASCs. All the findings elaborated the regulatory mechanism of metformin in the high-glucose microenvironment to protect the osteogenic differentiation ability of ASCs. Metformin plays an active role in promoting the osteogenic differentiation of ASCs with DOP, and it may contribute to the application of ASCs transplantation for bone regeneration in DOP.

**Keywords:** metformin, adipose-derived stem cells, autophagy, Wnt signaling pathway, GSK3 $\beta$ , osteogenic differentiation

## Introduction

THE BONE TISSUE complication caused by a persistent high blood glucose of diabetes mellitus (DM) is called diabetic osteoporosis (DOP), which is characterized by bone loss, destruction of the bone microstructure, increased bone fragility, and high fracture risk [1]. Hyperglycemia is one of the main manifestations of DM patients, and the abnormal glucose metabolism in the internal environment leads to osteogenesis disorder in bone tissue. Literature showed that the number of mesenchymal stem cells and osteoblasts decreased, and the synthesis and secretion of regulatory factors of osteogenic differentiation were also impeded in DM [1,2]. The insufficient osteogenic differentiation and bone formation in DM made it difficult to repair and regenerate bone tissue. The poor bone healing and remaining bone defects in

DOP patients after the bone defect or fracture leading to a decline in the quality of life of patients. So it is of great significance and urgent necessity to explore the treatment to improve the osteogenesis differentiation process in DOP.

In recent years, the induction of autologous mesenchymal stem cells for tissue regeneration and cell-based tissue-engineered bone provides a new therapy for promoting DOP bone defect repair. Adipose-derived stem cells (ASCs) are a type of adult mesenchymal stem cells from fat tissue that have a capacity for self-renewal [3]. ASCs can be directionally differentiated into osteogenesis, adipogenesis, and chondrogenesis, which have a wide application prospect in the research fields of bone regeneration, bone healing, and bone integration. Under somatic osteogenic induction conditions, ASCs differentiate into osteogenic precursors expressing genes and proteins related to osteogenic differentiation such

<sup>1</sup>Department of Oral Implantology and <sup>2</sup>Oral & Maxillofacial Reconstruction and Regeneration Laboratory, The Affiliated Stomatology Hospital of Southwest Medical University, Luzhou, People's Republic of China.

<sup>3</sup>Division of Oral Health Sciences, Department of Fixed Prosthodontics, Graduate School of Medical and Dental Sciences, Tokyo Medical and Dental University, Tokyo, Japan.

<sup>4</sup>Department of Anesthesiology, The Affiliated Hospital of Southwest Medical University, Luzhou, People's Republic of China.

<sup>i</sup>ORCID ID (<https://orcid.org/0000-0002-1420-6515>).

as runt-related transcription factor 2 (Runx2), osteopontin (Opn), DLX5, and Osterix. However, studies have proved that the internal environment disturbance caused by diabetic hyperglycemia had an impact on the metabolism of ASCs, leading to significantly impaired ASCs bone-orientation differentiation ability under the DOP microenvironment. However, the reasons for the osteogenic differentiation injury of ASCs in the diabetes microenvironment are not fully understood, and the treatment of bone repair and regeneration using autologous ASCs from DOP still needs further exploration.

Metformin (MF) is one of the first-line drugs for type 2 diabetes treatment. Recent studies presented that metformin maintained the stability of cell metabolism, activate autophagy, and also had a relieving effect on osteoporosis [4–6]. Autophagy is a process in which cells self-regulate and degrade intracellular macromolecules and damaged organelles. The cell degradation products are recycled by cell autophagy, which maintains the homeostasis of the intracellular environment [7]. Researchers found an increasing number of autophagic vesicles in femur tissue during postnatal development, while the femur and tibia were underdeveloped in *Fgf18<sup>+/-</sup>* transgenic mice [8]. Gao et al. demonstrated that metformin regulated the development of bone marrow cells and promoted the differentiation of bone marrow mesenchymal stem cells to osteogenesis by regulating the expression of *Cbfa1*, *LRP5*, and *COL1* genes [9]. Although studies have shown that metformin promoted the osteogenic differentiation of mesenchymal stem cell lines, the regulatory mechanism of metformin on ASCs osteogenic differentiation under the high-glucose environment is still not clear, and the relationship between autophagy and ASCs osteogenic differentiation needs to be clarified.

Our previous study found that the DOP microenvironment significantly inhibited the osteogenic differentiation of ASCs; then, we want to further study the effect of metformin in the osteogenic differentiation process of ASCs. Therefore, in this project, rat ASCs from fat tissue were cultured in vitro and treated with high glucose, metformin, and 3-methyladenine (3-MA) to explore whether metformin can activate cell autophagy level to promote the process of bone orientation differentiation of ASCs, as well as the molecular mechanism and signaling pathway involved.

## Materials and Methods

### Isolation of ASCs

This animal research was approved by the Animal Ethics Committee of Southwest Medical University, Luzhou, China. All the procedures, including anesthesia, surgery, nursing, and euthanasia, were conducted according to the guidelines of the National Institutes of Health of China.

The Sprague-Dawley male rats were given general anesthesia. After removing the inguinal adipose tissue, the skin wound was sutured and resuscitated. The tissue sample was cultured by the tissue block culture method under aseptic conditions. First, adipose tissue was washed by phosphate-buffered solution (PBS; HyClone) containing 1% penicillin–streptomycin solution (FBS; HyClone). Then, it was carefully cut into mince and laid on the bottom of the culture flask. Next, we gently added alpha-modified eagle's medium ( $\alpha$ -MEM; HyClone) medium containing 10% fetal bovine serum (FBS; HyClone), and cultured in an incubator in 5% CO<sub>2</sub> at 37°C for primary cell culture.

The culture medium was changed every 3 days. The multilineage differentiation capacity of ASCs was proved by our previous article [10]. The cells were passed to third-generation for the following experiments.

### Cell proliferation analysis after reagents treatment

Cell Counting Kit-8 (CCK-8; Dojindo, China) was used to detect the toxicity of different glucose concentration of ASCs. The third-passage ASCs ( $5 \times 10^4$  cells/mL, 100  $\mu$ L/well) were cultured in 96-well plates with  $\alpha$ -MEM for 24 h. Then, ASCs were treated with different concentrations of glucose (10, 25, 50, 75, and 100 mM; MedChemExpress). After 48 and 96 h, we added a reagent of the CCK-8 into medium and incubated for 2–3 h. The optical densities of the incubated medium in different groups were measured at 450 nm by an automatic microplate reader (Spectra Thermo, Switzerland).

### Cell wound healing assay

The third-passage ASCs ( $5 \times 10^4$  cells/well) were seeded into 6-well plates, and then, ASCs were treated with 40 mM glucose and 0.1 mM metformin (MedChemExpress) [11,12]. When the cell density reached 95%–100%, a 100  $\mu$ L pipette tip (Thermo Scientific) was used to make a straight scratch in the center of each plate. Images were collected at 6-h intervals to observe the wound healing ability of ASCs.

### Alizarin red-S staining

ASCs ( $5 \times 10^4$  cells/well) were seeded into 6-well plates and cultured in an osteogenic medium (Cyagen Biosciences, Inc.) with high glucose, metformin, and 3-MA. The components of osteogenic medium were as follows: basal medium (175 mL), FBS (20 mL), glutamine (2 mL), penicillin–streptomycin (2 mL), ascorbate (400  $\mu$ L),  $\beta$ -glycerophosphate (2 mL), and dexamethasone (20  $\mu$ L). After 21 days, the number of mineralized nodes with alizarin red stain was used to demonstrate the osteogenic differentiation ability of ASCs. After 21 days, PBS was used to wash cells thrice, and 4% paraformaldehyde was used to fix ASCs for 30 min. Then ASCs with mineralized matrix was stained with Alizarin red-S dye for 1 h and the images were collected by inverted light microscope (Olympus, Japan).

### Alkaline phosphatase staining

After drug treatment cultured with osteogenic induction medium in 7 days, ASCs were fixed by 4% paraformaldehyde and washed by PBS thrice. The activity of alkaline phosphatase (ALP) was examined by 5-bromo-4-chloro-3-indolyl phosphate/Nitro Blue Tetrazolium Color Development Kit (Beyotime, China) overnight. Also, the stained cells were observed by an inverted light microscope.

### Western blot assay

Total protein of ASCs was lysed using the Total Protein Extraction Kit (Keygen Biotech, China) after drug treatment. Then, we detected the concentration of total protein by Bicinchoninic Acid Protein Assay Kit (Thermo Scientific). Then, different proteins among each group were divided by 8% or 10% or 12% (v/v) sodium dodecyl sulfate–polyacrylamide gel electrophoresis (SDS-PAGE) gel

(Beyotime) with 90 V for 1 h and 120 V for 1 h. Also, the SDS-PAGE gel was transferred to polyvinylidene difluoride (PVDF) membranes (Bio-Rad) at a constant current of 100 mA for 1 h. All PVDF strips were blocked with 5% skim milk (Bio-Rad), which was diluted in 0.05% (v/v) Tween-20 Tris-buffer saline (TBST) and incubated with target primary antibodies (1:1,000) overnight at 4°C, including glyceraldehyde 3-phosphate dehydrogenase (GAPDH; ab181602), OPN (ab91655), GSK3β (ab32391), mammalian target of rapamycin (mTOR) (ab32028) and BECLIN1 (ab62557; Abcam, United Kingdom), and RUNX2 (12556s), LEF1 (2230p), β-catenin (D10A8), and light chain 3 (LC3) I/II (12741T; Cell Signaling Technology). Membranes were washed with TBST thoroughly for 30 min and immersed in goat-anti-rabbit secondary antibodies (Beyotime) for 1 h. The image results were visualized using an Enhanced Chemiluminescence Detection System (Bio-Rad).

**Immunofluorescence staining and confocal laser scanning**

ASCs (1 × 10<sup>4</sup> cells) were inoculated on confocal dishes (Corning) and treated as previously described with high glucose and metformin for 4 days. Cells were gently washed with PBS and fixed with 4% paraformaldehyde for 15 min. Permeabilized the cytomembrane of ASCs by 0.5% Triton X-100 and immersed them in 5% goat serum (Beyotime) for 1 h. Next, rabbit primary antibodies of BECLIN1 and GSK3β (1:200) were used to incubate ASC samples overnight at 4°C, and a fluorescence-conjugated goat-anti-rabbit secondary antibody (Beyotime) was used to combine the primary antibody for 1 h. Finally, the nucleus of ASCs was stained by 4',6-diamidino-2-phenylindole (Beyotime). The fluorescence images were captured by the inverted fluorescence microscope (Olympus).

**RNA extraction and real-time fluorescent polymerase chain reaction**

Total RNA of ASCs in each group was extracted by Total RNA Extraction Kit (BioFlux, China). The mRNAs were

reverse transcribed into cDNA by PrimeScript RT Reagent Kit (Takara Bio, Japan). Then real-time polymerase chain reaction (RT-PCR) was conducted by SYBR Premix ExTaq kit (Takara Bio) with ABI 7900 system machine (Applied Biosystems) as follows: 95°C for 45 s; then 40 cycles of 95°C for 5 s; and finally 60°C for 30 s. All the primer sequences details are shown in Table 1. The quality of the PCR product was examined by melting curve, while the gene cycle threshold (CT) values from all groups were calibrated with Gapdh CT values and calculated by the 2<sup>-ΔΔCt</sup> method.

**Statistical analysis**

Experimental results were repeated over three times independently, and the data were calculated by SPSS 19.0 software (SPSS, Inc.) with Student's *t*-test or one-way ANOVA. Differences were marked as statistically significant if *P* < 0.05.

**Results**

**High glucose restrained cell proliferation and cell migration**

Cultured with different differentiation induction mediums, ASCs derived from adipose tissue were induced into osteoblasts, adipocytes, and chondrocytes, which demonstrated the multidirectional differentiation ability of ASCs (Fig. 1A). After osteogenic induction, ASCs changed their morphology from spindle shape of fibroblasts to typical polygon shape of osteoblast, and mineralized matrix accumulates around the cells. While in the adipogenic medium, the shape of ASCs became ovoid and filled with lipid, which was dyed orange by Oil Red O. When ASCs differentiate into chondroblasts, they secreted proteoglycan, collagen, and other extracellular matrices to make the cells stick together.

Excessive glucose concentrations are toxic to the proliferation, migration, and differentiation of ASCs. The CCK-8 results showed that the cell proliferation ability of ASCs was gradually

TABLE 1. PRIMER SEQUENCES INFORMATION FOR AMPLIFICATION OF GENES

Gene name	RefSeq transcripts	Sequence (5' → 3')
Gapdh	NM_017008.4	Forward: ACAGCAACAGGGTGGTGGAC Reverse: TTTGAGGGTGCAGCGAACTT
Runx2	NM_001278483.1	Forward: AGGACTATGGCGTCAAACA Reverse: GGCTCACGTCGCTCATCTT
Opn	NM_012881.2	Forward: CACTCCAATCGTCCCTACA Reverse: CTTAGACTCACCGCTCTTCAT
β-Catenin	NM_053357.2	Forward: AAGTTCTTGGCTATTACGACA Reverse: ACAGCACCTTCAGCACTCT
Gsk3β	NM_019827.7	Forward: AACTCCACCCAGAGGCAATCG Reverse: CGTTGCACTCTTAGCCCTGT
Lef1	NM_130429.1	Forward: CAGACCTGTCACCCTTCAGC Reverse: GTGAGACGGATTGCCAAACG
mTOR	NM_019906.2	Forward: AGTGGGAAGATCCTGCACATT Reverse: TGGAAACTTCTCTCGGGTCAT
Beclin1	NM_053739.2	Forward: AGCACGCCATGTATAGCAAAGA Reverse: GGAAGAGGGAAAGGACAGCAT
LC3 II	NM_022867.2	Forward: GAGTGGAAAGATGTCCGGCTC Reverse: CCAGGAGGAAGAAGGCTTGG

Gapdh, glyceraldehyde 3-phosphate dehydrogenase; LC3, light chain 3; mTOR, mammalian target of rapamycin; Opn, osteopontin; Runx2, runt-related transcription factor 2.

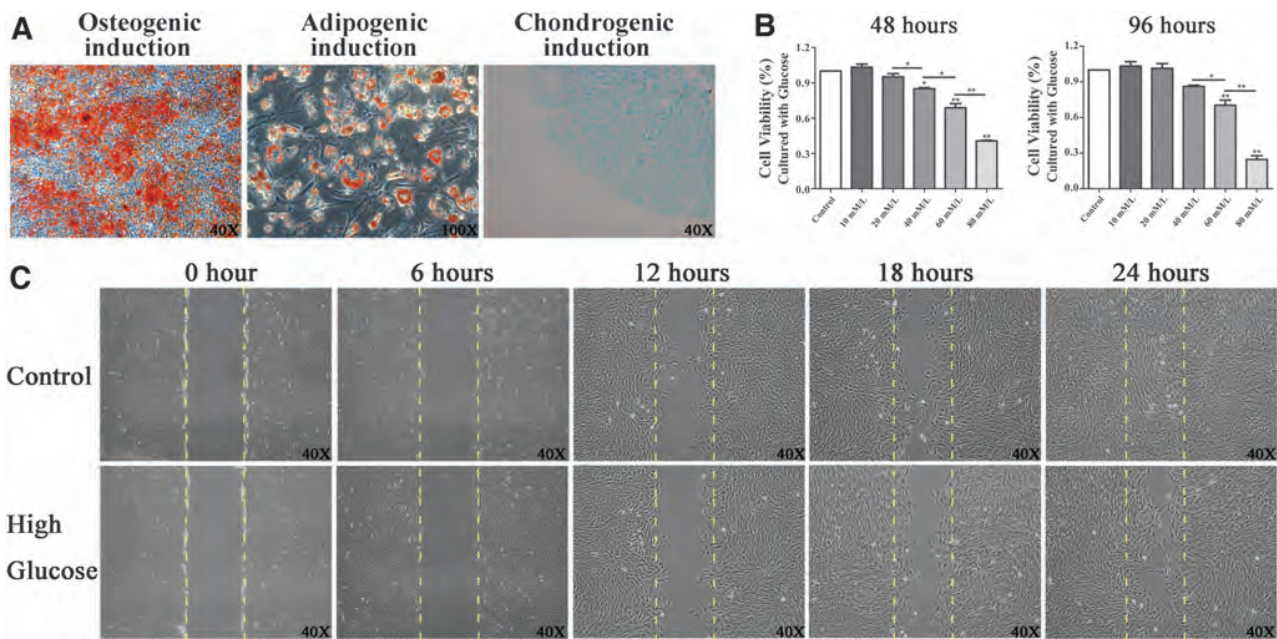


**FIG. 1.** ASCs had multidirectional differentiation ability, but high-glucose inhibited the cell proliferation and migration of ASCs. (A) ASCs multidirectional differentiation was analyzed by Alizarin red-S staining (in red), Oil Red O staining (in orange), and Alcian blue assay (in blue) after induction culture; (B) CCK-8 assay data showed that the high-glucose concentration inhibited the cell proliferation activity at 48 and 96 h. At 40 mM high glucose, the cell proliferation activity was reduced to 80% which was statistically different from the control group; (C) cell wound healing progress was detected every 6 h with an inverted light microscope, the images showed that the cell migration ability was suppressed in the high-glucose group and its scratch was not healed within 24 h. The yellow dotted line shows the initial boundary of the scratch. \* $P < 0.05$ , \*\* $P < 0.01$ . ASC, adipose-derived stem cell; CCK-8, Cell Counting Kit-8. Color images are available online.

declined with the increase of glucose concentration in 48 and 96 h (Fig. 1B). Also, the cell migration ability of ASCs was depressed under 40 mM glucose treatment compared with the control group at different time points (Fig. 1C). Then, we studied the inhibiting effect of high glucose on osteogenic differentiation of ASCs in the following part of our research.

#### High glucose inhibited osteogenic differentiation capacity and Wnt signaling pathway in ASCs

To explore the relationship between high glucose and ASCs osteogenic differentiation, we treated ASCs with 40 mM glucose and 0.1 mM metformin and detected the changes of cell mineralization, ALP activity, osteogenic factors, and Wnt signaling pathway. After osteogenic differentiation induction for 21 days, the mineralized external matrix produced by ASCs was stained by Alizarin red-S staining. The staining results demonstrated that high-glucose treatment caused the lower formation of mineralized nodules in the high-glucose group, while the addition of metformin in high glucose promoted the formation of mineralized nodules to a certain extent (Fig. 2A). The ALP staining results of ASCs after osteogenic differentiation for 7 days also proved that a high-glucose environment inhibited ALP activity, while metformin upregulated its expression (Fig. 2C). RUNX2 and OPN were the represent proteins for osteogenic differentiation,  $\beta$ -CATENIN and LEF1 represented the activity of the Wnt signaling pathway. After 4 days of ASCs osteogenic differentiation, the western blot and RT-PCR results were consistent with the results of Alizarin red-S staining and ALP staining (Fig. 2B, D).

#### High glucose suppressed the autophagy level and metformin modulated autophagy inhibition induced by high glucose

Our results showed a correlation between osteogenic differentiation potential damage of ASCs and the inhibition of autophagy level by high glucose. After being cultured under high glucose and metformin condition, the protein and mRNA of ASCs in different groups were analyzed. The western blot images showed that high glucose inhibited the expression of two key proteins in autophagy: BECLIN1 and LC3 I/II, while they were upregulated by metformin (Fig. 3A, B). However, the expression of mTOR and GSK3 $\beta$ , which negatively regulated the autophagy signaling pathway, was increased in the high-glucose group. The gene expression results detected by RT-PCR were consistent with western blot results (Fig. 3D). Then, the fluorescence signal images showed that the expression of Beclin1 was the weakest in the high glucose group, while metformin activated the expression of Beclin1 and showed the strongest fluorescence (Fig. 3C).

#### 3-MA antagonized the effect of metformin on osteogenic differentiation and cell autophagy in ASCs

To further prove the important role of autophagy in promoting osteogenic differentiation of ASCs, we added 3-MA, an inhibitor of metformin, to verify that once inhibited by 3-MA, metformin was not able to recover the damaged osteogenic differentiation potential of ASCs by high

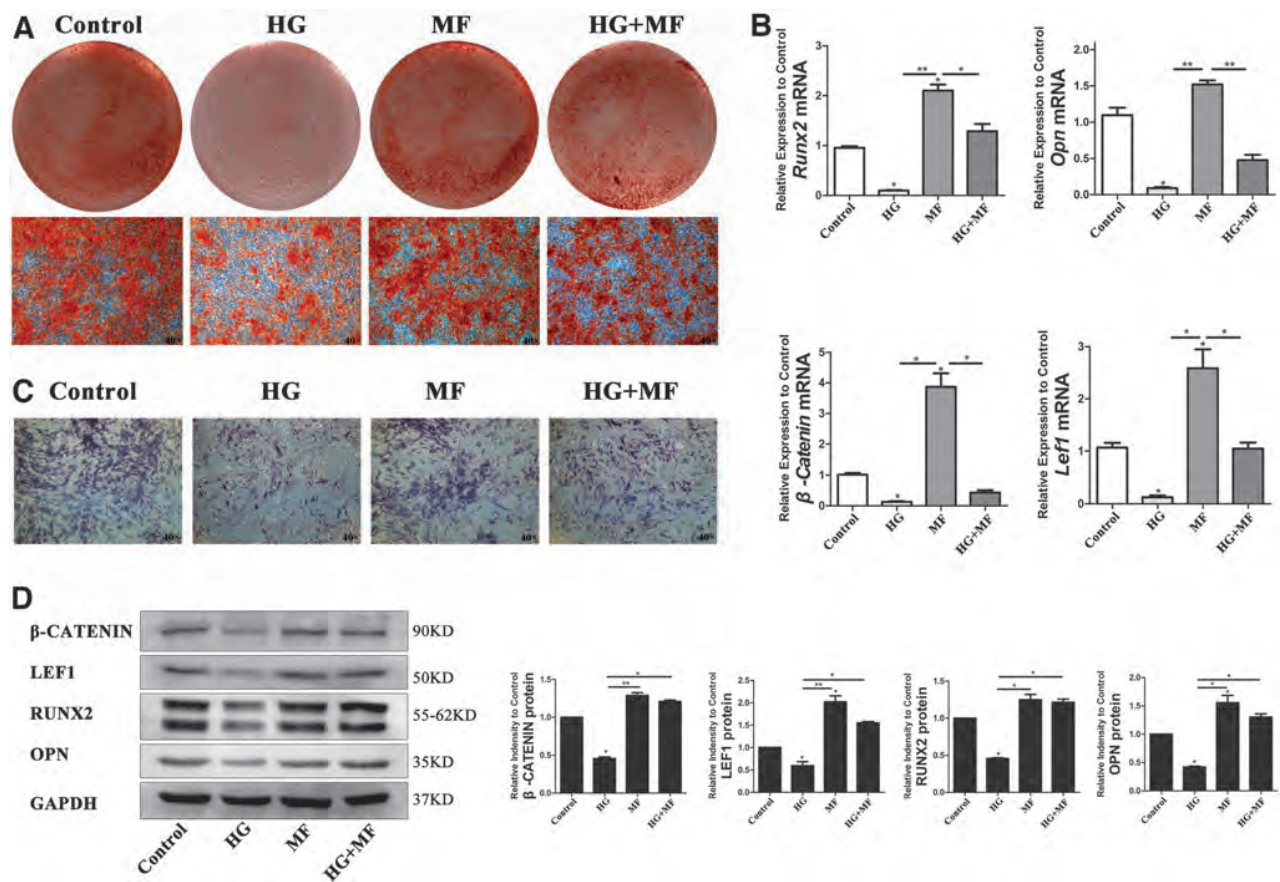


**FIG. 2.** The osteogenic differentiation capacity of ASCs and the Wnt signaling pathway were detected after glucose and metformin treatment. (A) Osteogenesis cultured for 21 days, mineralized nodules were stained by Alizarin red-S; (C) osteogenesis cultured for 7 days, and the active ALP in ASCs was dyed purple. Metformin group had the highest of mineralized nodules formation and ALP activity; (B, D) RT-PCR and western blot data showed that the expression of typical osteogenic genes *Runx2* and *Opn* and Wnt signaling pathway genes *β-catenin* and *Lef1* was higher in the metformin group than that of the high-glucose group. Although the expression level of the HG+MF group was not as good as that of the metformin group, it was also higher than that of the HG group. The difference was statistically significant. All the results showed that metformin resisted the negative effect of high glucose and promoted bone formation. \* $P < 0.05$ , \*\* $P < 0.01$ . ALP, alkaline phosphatase; MF, metformin; Opn, osteopontin; RT-PCR, real-time polymerase chain reaction; Runx2, runt-related transcription factor 2. Color images are available online.

glucose. The Alizarin red-S staining images demonstrated that after the addition of 3-MA, the ability of metformin to promote osteogenic differentiation was offset by 3-MA (Fig. 4A). The results of western blot and RT-PCR demonstrated that the expression of Beclin1 and LC3 I/II was successfully inhibited by 3-MA, and metformin could not upregulate their expression (Fig. 4B, C). The expression of RUNX2 and OPN was higher in the HG+MF group than in the HG group. When 3-MA inhibited the effect of metformin, the expression of RUNX2 and OPN was downregulated in the 3-MA+MF+HG group compared with the MF+HG group (Fig. 4B, C). The results meant that the positive effect of metformin on ASCs osteogenesis was inhibited by 3-MA.

*Metformin-modulated autophagy activated Wnt signaling pathway in the process of osteogenic differentiation*

So far, we have proved that high glucose inhibited the osteogenic differentiation potential of ASCs through auto-

phagy, while metformin reversed this negative effect. However, we still need to find the clues behind the osteogenesis damage of ASCs and autophagy. The literature review found that GSK3β could not only negatively regulate the level of autophagy but also targeted to bind the β-CATENIN to inhibit the Wnt signaling pathway [13,14]. Therefore, we were committed to exploring whether GSK3β is a link between the Wnt signaling pathway and cell autophagy. After treatment with high glucose, metformin, and 3-MA, we detected the expression activity of mTOR, GSK3β, β-CATENIN, and LEF1 among each group (Fig. 5A, C). The protein expression of mTOR and GSK3β was upregulated in the high-glucose group, and metformin could not depress them in the HG +3-MA+MF group. The expression of β-CATENIN and LEF1 was higher in the HG+MF group than that in the HG group and the HG +3-MA+MF group. The results demonstrated that the Wnt signaling was activated when the cell autophagy level was upregulated by metformin, which promoted the progress of osteogenic differentiation. The fluorescence staining of GSK3β showed that it was highly

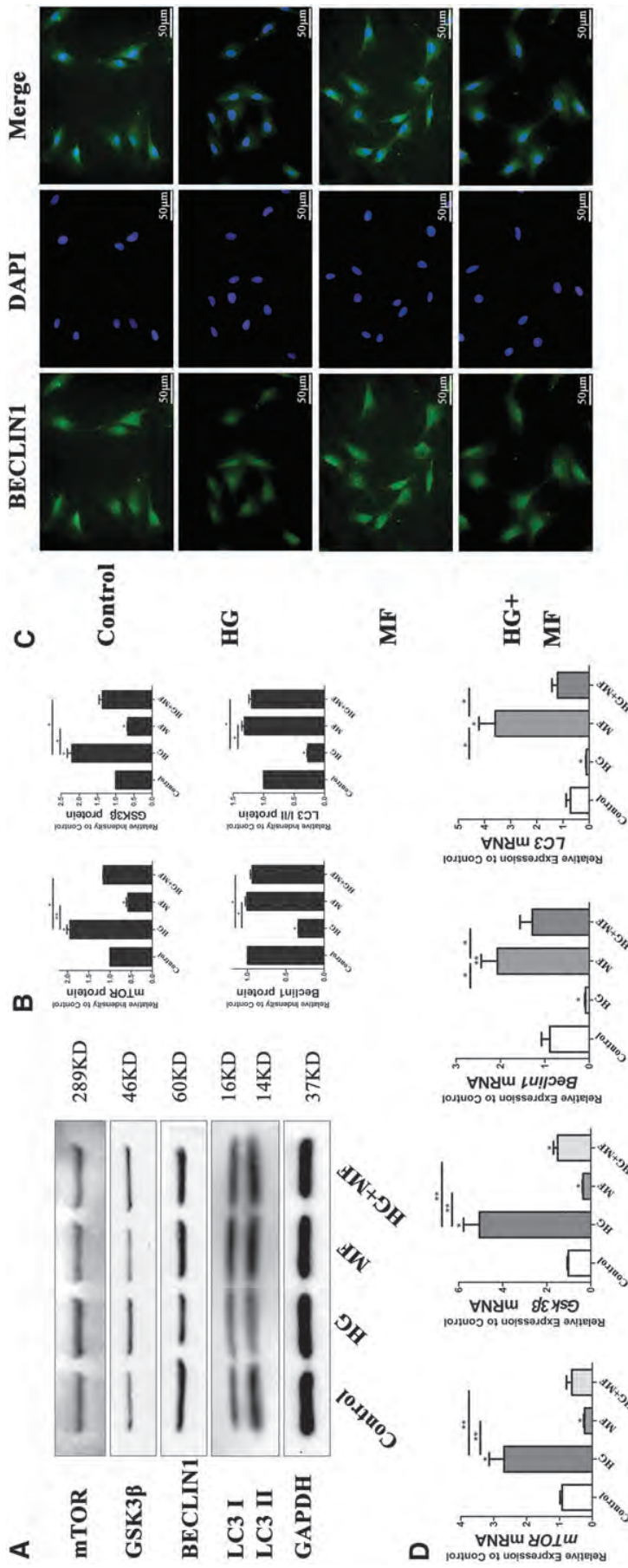


**FIG. 3.** Metformin upregulated the expression level of autophagy protein BECLIN1 and LC3 I/II was significantly less at 0.5 times in the high-glucose group than that of the control group, while metformin was able to upregulate them in the HG+MF group. The expression of mTOR and GSK3β was suppressed in the metformin group compared with the high-glucose group, which was the opposite results of BECLIN1 and LC3 I/II; (C) fluorescence staining image of BECLIN1 showed the weakest expression in the high-glucose group, while it was strongest in the HG+MF group; (D) the gene expression trend of *Beclin1*, *LC3 II*, *mTOR*, and *Gsk3β* in each group was consistent with that of western blot. \* $P < 0.05$ , \*\* $P < 0.01$ . LC3, light chain 3; mTOR, mammalian target of rapamycin. Color images are available online.

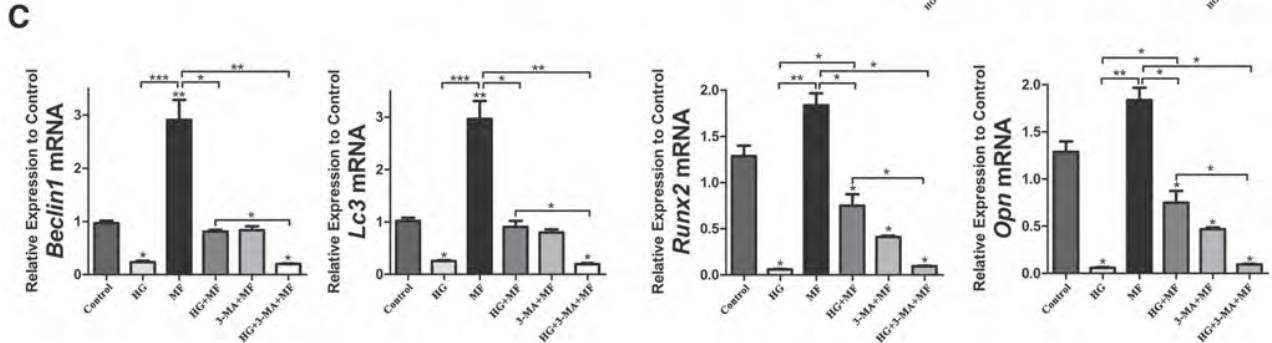
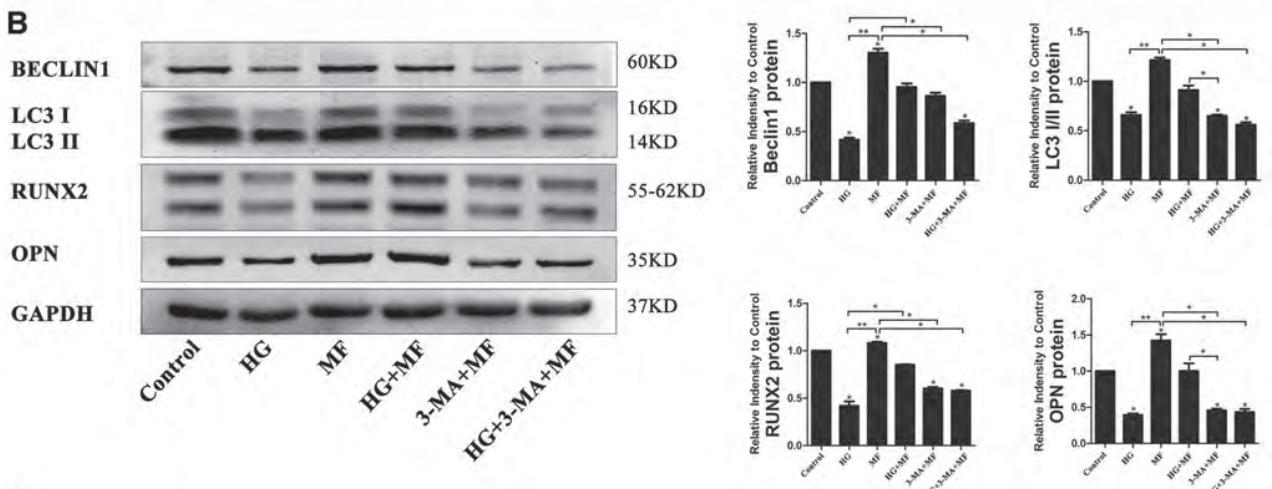
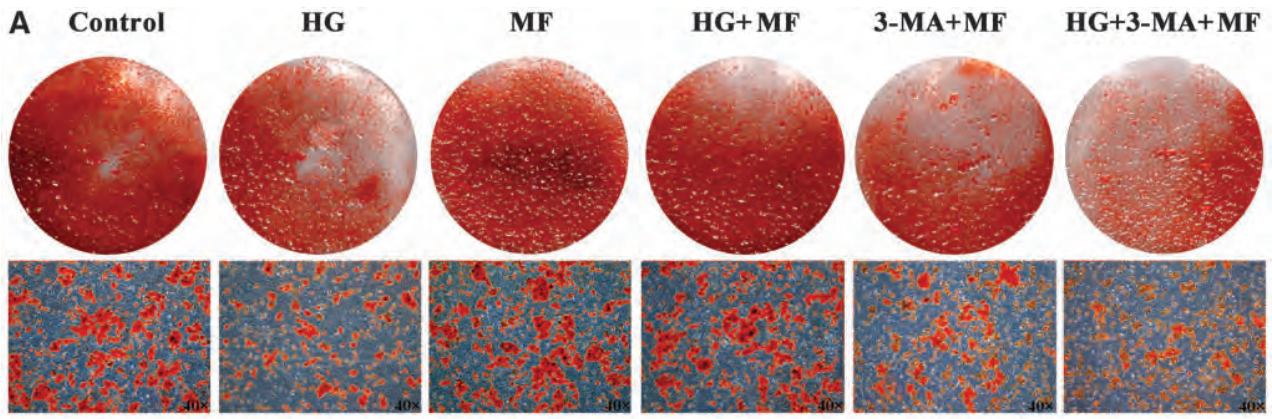
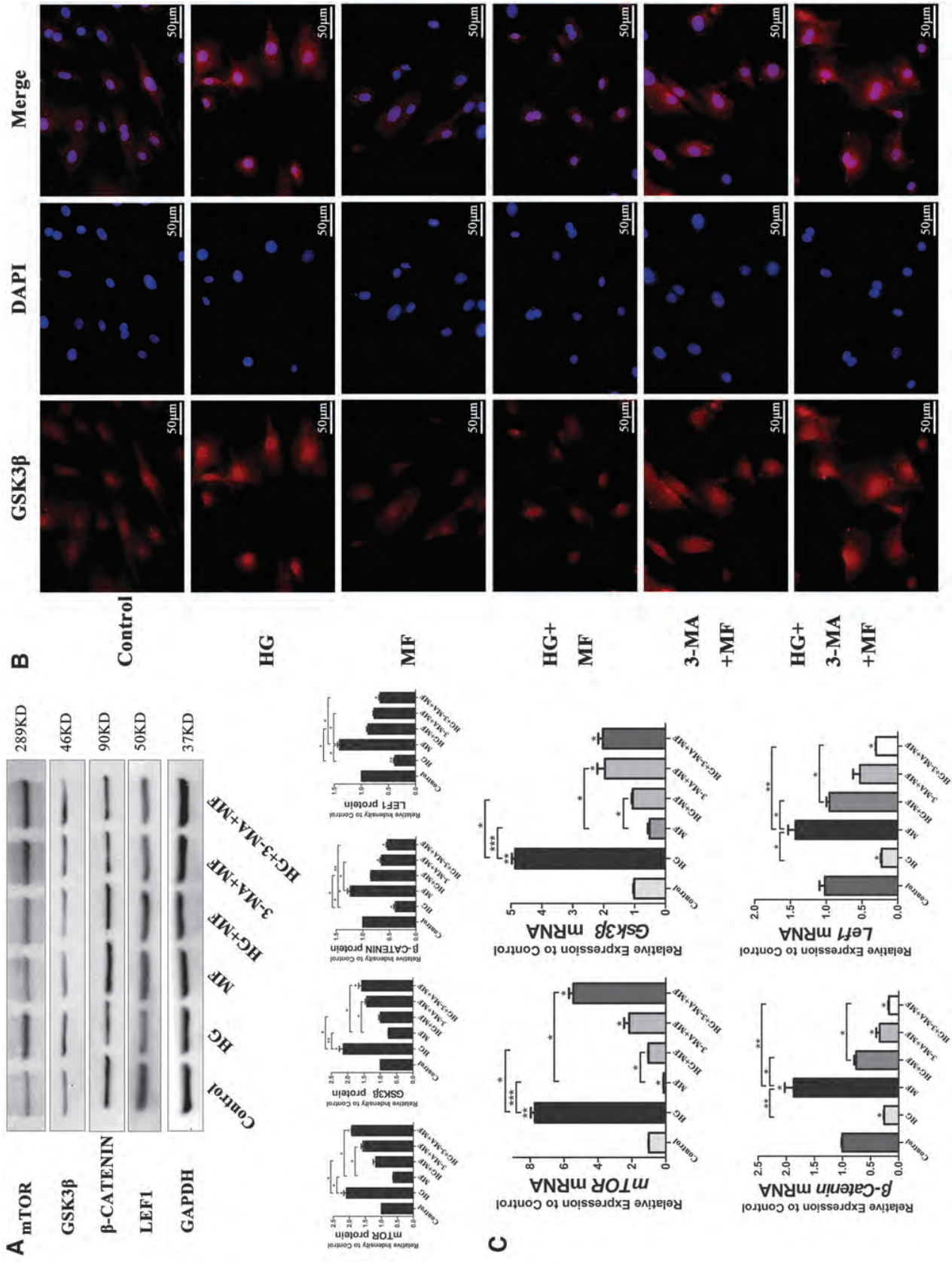


**FIG. 4.** Metformin alleviated the high glucose-induced damage to the osteogenic capacity of ASCs by activating autophagy. (A) The Alizarin red-S staining images showed that metformin was helpful for osteogenesis and promoted the production of mineralized nodules even in the HG+MF group. But after adding 3-MA, the size and the number of mineralized nodules were reduced, especially in the HG +3-MA+MF group; (B, C) the protein and gene expression of Beclin1 and LC3 I/II was downregulated in the 3-MA+MF group and the HG +3-MA+MF group. The expression of Runx2 and Opn was also decreased and could not recover in the HG +3-MA+MF group. \* $P < 0.05$ , \*\* $P < 0.01$ , \*\*\* $P < 0.001$ . 3-MA, 3-methyladenine. Color images are available online.

**FIG. 5.** Metformin regulated Wnt signaling pathway. (A) Western blot image and bar graph showed that the expression of mTOR and GSK3 $\beta$  was the lowest in the MF group, but was increased under the treatment of 3-MA. Because of the inhibitory effect of 3-MA on metformin, the expression of  $\beta$ -CATENIN and LEF1 was suppressed in the HG +3-MA+MF group. The activation effect of metformin on the expression of  $\beta$ -CATENIN and LEF1 was negatively influenced by 3-MA. (B) The red fluorescence showed the expression of GSK3 $\beta$  of ASCs. It was obvious that the fluorescence signal of GSK3 $\beta$  was weakest in the MF group, and it was weaker in the HG+MF group than the HG group and HG +3-MA+MF group. These images showed that GSK3 $\beta$  was significantly inhibited by metformin. (C) The mRNA expression results of  $\beta$ -Catenin, LEF1, mTOR, and GSK3 $\beta$  were consistent with western blot analysis, which demonstrated that the depress effect of metformin on GSK3 $\beta$  activated the Wnt signaling pathway. \* $P < 0.05$ , \*\* $P < 0.01$ , \*\*\* $P < 0.001$ . Color images are available online.



expressed in the HG group and downregulated by metformin in the HG+MF group. But metformin failed to work on GSK3 $\beta$  in the presence of 3MA in the 3-MA+MF group and HG +3-MA+MF group (Fig. 5B).

## Discussion

Although studies have reported that the risk of bone metabolic disease due to diabetes is not consistent across ethnic groups, it has become a global public health issue affecting over 422 million individuals all over the world [15–19]. It was found that skeletal fragility in diabetes caused an increased incidence of osteoporosis, a higher risk of fracture and poor bone healing [20]. Rodent models of diabetes proved that obesity, insulin resistance, and hyperglycemia of the T2D diabetes model caused skeletal abnormalities, including lower femoral cortical thickness, decreased stiffness, and abnormalities of multiple trabecular and cortical microarchitectural [21]. Studies of osteoblast cell lines based on diabetes and hyperglycemia environment also showed that diabetes has a significant negative effect on cell physiological function. Previous studies in my research group showed that the osteogenic differentiation ability of ASCs was significantly suppressed by advanced glycation end products, which is a kind of glucose and protein metabolites due to hyperglycemia [10,22]. In this study, we used high-dose glucose to simulate a hyperglycemia environment, and the results showed that the proliferation, migration, and osteogenic differentiation of ASCs are significantly inhibited, which is consistent with the published literature.

To solve the problem of osteogenic differentiation inhibition of ASCs with high glucose, we set our sights on the first-line hypoglycemic drugs, trying to find the positive effect of metformin on osteogenic differentiation of ASCs. Numerous researches give experimental evidence for a promising benefit of metformin for skeletal metabolism [23,24]. *In vitro* studies (Wang P et al.) found that metformin contributed to the differentiation of human-induced pluripotent stem cell-derived mesenchymal stem cell to osteoblast cell line by mediating the LKB1/AMPK pathway [25]. Agnieszka S et al. proposed that low concentration metformin promoted the metabolic activity of ASCs, while high-concentration metformin inhibited it [26]. On the flip side, high-concentration metformin had a stronger effect on osteogenesis, while low-concentration metformin appeared to have a weak effect. According to existing literatures, 0.1 mM metformin is a nontoxic concentration for different types of cells and showed good effects on osteogenic differentiation [11,12]. Therefore, the 0.1 mM metformin was used in our study as the treatment concentration. Our research data based on ASCs proved a positive effect of 0.1 mM metformin in expediting the osteogenic differentiation of ASCs. Most intuitively, there is a significant increase in the production of mineralized nodules visible to the naked eye after 0.1 mM metformin treatment. In addition, the expression of osteogenic markers and the Wnt signaling pathway was upregulated by metformin.

In recent years, the role of metformin as an autophagy activator has been gradually discovered. Our study analyzed the expression of autophagy key proteins Beclin1 and LC3 I/II, which was significantly inhibited under high-glucose conditions while was rescued by metformin. At the same time,

metformin decreased the expression of the negative regulatory factors of autophagy, mTOR, and p-GSK3 $\beta$  (Fig. 3). Some research work has demonstrated that the disturbance of physiological activity of cells in a high-glucose environment is closely related to the change of autophagy level [27,28]. Metformin prominently regulates the osteoprotegerin-mediated inhibition of osteoclasts differentiation by upregulating the level of autophagy [29]. Another study on metformin showed that the autophagic capacity, antiaging ability, and osteogenic differentiation were positively improved after being treated with metformin every day [6]. In this study, we demonstrated that the high expression of autophagy-related genes and proteins altered by adding metformin, and their changes are positively correlated with osteogenic differentiation of ASCs. Therefore, the activating effect of metformin on autophagy maybe its key mechanism to promote osteogenesis.

With the development of autophagy study, researchers revealed that the negative regulator of autophagy is also an important factor affecting autophagy. A close relationship between autophagy level and cell osteogenesis was found not only in osteoblasts and osteoclasts but also in hematopoietic progenitors and macrophagocyte [30,31]. GSK3 $\beta$  was reported to have negative regulatory effects on the autophagy pathway in cancer cells but also in other diseases [32,33]. Azoulay-Alfaguter et al. reported that a high level of GSK3 $\alpha$  and GSK3 $\beta$  activated mTORC1 and suppressed Beclin1 expression in MCF-7 human breast cancer cells, contributing to cancer therapy [34]. It was also showed a negative correlation between Akt/GSK3 $\beta$ / $\beta$ -catenin signaling and autophagy in atrial fibrosis of human atrial fibroblasts [32]. Our data found that the inhibition of high glucose on the autophagy pathway was related to the over-expression of GSK3 $\beta$  and mTOR1 in ASCs. Metformin appeared to inhibit the expression of GSK3 $\beta$  while activating autophagy.

As we know, GSK3 $\beta$  is also an important protein that inhibited the key factor,  $\beta$ -Catenin, in the Wnt signaling pathway [10,14,22,35]. Glucagon-like peptide-1 improved the glucose tolerance and insulin tolerance in a diabetic mouse model and promoted the expression of osteogenic markers via the Wnt/GSK3 $\beta$ / $\beta$ -catenin pathway [14]. The osteogenic differentiation ability of human BMSCs was activated by Ginsenoside Rg1 because of its inhibitory effect on GSK3 $\beta$  [35]. What's more, it is worth noting that direct evidence showed that GSK3 $\beta$  is a link factor between the autophagy pathway and the Wnt signaling pathway [36]. The authors proved that electroacupuncture pretreatment provided neuroprotective effects and ischemic stroke prevention by up-regulating autophagy and  $\beta$ -catenin through the inhibition of GSK3 $\beta$  in the cerebral ischemia injury model. Therefore, based on the literature and our research, we believe GSK3 $\beta$  might be an important connection point on the impetus of metformin on osteogenic differentiation of ASCs. When metformin activated the cell autophagy of ASCs, it also gave a negative feedback effect on GSK3 $\beta$ . The expression suppression of GSK3 $\beta$  by metformin relieved its inhibiting effect on the cell autophagy and Wnt signaling pathway ultimately promoted the recovery of osteogenic differentiation ability of ASCs. In our next stage, we will continue to in-depth study about the molecular mechanisms of metformin and GSK3 $\beta$  regulating the osteogenic

differentiation of ASCs in the diabetic microenvironment and provide more experimental evidence to promote the application of metformin in bone repair and regeneration with diabetic osteoporosis.

## Conclusion

Current results demonstrated that the expression of autophagy and the Wnt signaling pathway was significantly inhibited under the high-glucose culture environment, resulting in the damage of the osteogenic differentiation ability of ASCs. As an autophagy agonist, metformin resisted the negative effects of high glucose and restored the activity of autophagy and the Wnt signaling pathway, playing a positive role in the osteogenic differentiation process of ASCs. This study elaborated a mechanism of metformin reducing the inhibitory effect of high glucose on the osteogenic differentiation of ASCs by activating cellular autophagy and the Wnt signaling pathway, which provided a possibility for the application of metformin in transplantation of ASCs for bone repair under diabetes osteoporosis conditions.

## Acknowledgments

The authors thank Oral & maxillofacial Reconstruction and Regeneration Laboratory, The Affiliated Stomatology Hospital of Southwest Medical University for experimental equipments in this research.

## Author Disclosure Statement

No competing financial interests exist.

## Funding Information

This work was funded by National Natural Science Foundation of China (81870746), Program of Southwest Medical University (2019ZQN167, 2019ZQN143), Program of The Affiliated Stomatology Hospital of Southwest Medical University (202017), Climb Plan Project of The Affiliated Stomatology Hospital of Southwest Medical University (2020QY04), and Open Project of the State Key Laboratory of Oral Disease Research (SKLOD2021OF08).

## References

- Hofbauer LC, CC Brueck, SK Singh and H Dobnig. (2007). Osteoporosis in patients with diabetes mellitus. *J Bone Miner Res* 22:1317–1328.
- Tan J, L Zhou, Y Zhou, P Xue, G Wu, G Dong, H Guo and Q Wang. (2017). The influence of diabetes mellitus on proliferation and osteoblastic differentiation of MSCs. *Curr Stem Cell Res Ther* 12:388–400.
- Wallner C, S Abraham, JM Wagner, K Harati, B Ismer, L Kessler, H Zöllner, M Lehnhardt and B Behr. (2016). Local application of isogenic adipose-derived stem cells restores bone healing capacity in a type 2 diabetes model. *Stem Cells Transl Med* 5:836–844.
- Aung M, S Amin, A Gulraiz, FR Gandhi, JA Pena Escobar and BH Malik. (2020). The future of metformin in the prevention of diabetes-related osteoporosis. *Cureus* 12:e10412–e10418.
- Bahrambeigi S, B Yousefi, M Rahimi and V Shafiei-Irannejad. (2019). Metformin; an old antidiabetic drug with new potentials in bone disorders. *Biomed Pharmacother* 109:1593–1601.
- Lin J, R Xu, X Shen, H Jiang and S Du. (2020). Metformin promotes the osseointegration of titanium implants under osteoporotic conditions by regulating BMSCs autophagy, and osteogenic differentiation. *Biochem Biophys Res Commun* 531:228–235.
- Djajadikerta A, S Keshri, M Pavel, R Prestil, L Ryan and DC Rubinsztein. (2020). Autophagy induction as a therapeutic strategy for neurodegenerative diseases. *J Mol Biol* 432:2799–2821.
- Greenhill C. (2016). Bone: autophagy regulates bone growth in mice. *Nat Rev Endocrinol* 12:4.
- Gao Y, Y Li, J Xue, Y Jia and J Hu. (2010). Effect of the anti-diabetic drug metformin on bone mass in ovariectomized rats. *Eur J Pharmacol* 635:231–236.
- Zhang M, Y Li, P Rao, K Huang, D Luo, X Cai and J Xiao. (2018). Blockade of receptors of advanced glycation end products ameliorates diabetic osteogenesis of adipose-derived stem cells through DNA methylation and Wnt signaling pathway. *Cell Prolif* 51:e12471–e12482.
- Ma J, Z-L Zhang, X-T Hu, X-T Wang and AM Chen. (2018). Metformin promotes differentiation of human bone marrow derived mesenchymal stem cells into osteoblast via GSK3 $\beta$  inhibition. *Eur Rev Med Pharmacol Sci* 22: 7962–7968.
- Jia L, Y Xiong, W Zhang, X Ma and X Xu. (2020). Metformin promotes osteogenic differentiation and protects against oxidative stress-induced damage in periodontal ligament stem cells via activation of the Akt/Nrf2 signaling pathway. *Exp Cell Res* 386:111717.
- Ren J, T Liu, Y Han, Q Wang, Y Chen, G Li and L Jiang. (2018). GSK-3 $\beta$  inhibits autophagy and enhances radiosensitivity in non-small cell lung cancer. *Diagn Pathol* 13:33–43.
- Li Y, H Fu, H Wang, S Luo, L Wang, J Chen and H Lu. (2020). GLP-1 promotes osteogenic differentiation of human ADSCs via the Wnt/GSK-3 $\beta$ /beta-catenin pathway. *Mol Cell Endocrinol* 515:110921.
- Koromani F, L Oei, E Shevroja, K Trajanoska, J Schoufour, T Muka, OH Franco, MA Ikram, MC Zillikens, et al. (2020). Vertebral fractures in individuals with type 2 diabetes: more than skeletal complications alone. *Diabetes Care* 43:137–144.
- Moayeri A, M Mohamadpour, SF Mousavi, E Shirzadpour, S Mohamadpour and M Amraei. (2017). Fracture risk in patients with type 2 diabetes mellitus and possible risk factors: a systematic review and meta-analysis. *Ther Clin Risk Manag* 13:455–468.
- Looker AC, MS Eberhardt and SH Saydah. (2016). Diabetes and fracture risk in older U.S. adults. *Bone* 82:9–15.
- Hothersall EJ, SJ Livingstone, HC Looker, SF Ahmed, S Cleland, GP Leese, RS Lindsay, J McKnight, D Pearson, et al. (2014). Contemporary risk of hip fracture in type 1 and type 2 diabetes: a national registry study from Scotland. *J Bone Miner Res* 29:1054–1060.
- World Health Organization. (2016). *World Health Organization: Global Report on Diabetes*. World Health Organization, Geneva, Switzerland.
- Rubin MR. (2017). Skeletal fragility in diabetes. *Ann N Y Acad Sci* 1402:18–30.
- Gimble JM. (2011). Leptin's balancing act between bone and fat. *J Bone Miner Res* 26:1694–1697.

22. Li Y, L Wang, M Zhang, K Huang, Z Yao, P Rao, X Cai and J Xiao. (2020). Advanced glycation end products inhibit the osteogenic differentiation potential of adipose-derived stem cells by modulating Wnt/beta-catenin signalling pathway via DNA methylation. *Cell Prolif* 53: e12834-e12847.
23. Hampp C, V Borders-Hemphill, DG Moeny and DK Wysowski. (2014). Use of antidiabetic drugs in the U.S., 2003-2012. *Diabetes Care* 37:1367-1374.
24. Jang WG, EJ Kim, IH Bae, KN Lee, YD Kim, DK Kim, SH Kim, CH Lee, RT Franceschi, HS Choi and JT Koh. (2011). Metformin induces osteoblast differentiation via orphan nuclear receptor SHP-mediated transactivation of Runx2. *Bone* 48:885-893.
25. Wang P, T Ma, D Guo, K Hu, Y Shu, HHK Xu and A Schneider. (2017). Metformin induces osteoblastic differentiation of human induced pluripotent stem cell-derived mesenchymal stem cells. *J Tissue Eng Regen Med* 12:437-446.
26. Agnieszka S, AT Krzysztof, K Katarzyna and M Krzysztof. (2018). Metformin promotes osteogenic differentiation of adipose-derived stromal cells and exerts pro-osteogenic effect stimulating bone regeneration. *J Clin Med* 7:482-507.
27. Zhou DM, F Reng, HZ Ni, LL Sun, LXiao, XQ Li, WD Li. (2020). Metformin inhibits high glucose-induced smooth muscle cell proliferation and migration. *Aging* 12:5352-5361.
28. Zhao K, H Hao, J Liu, C Tong, Y Cheng, Z Xie, L Zang, Y Mu and W Han. (2015). Bone marrow-derived mesenchymal stem cells ameliorate chronic high glucose-induced beta-cell injury through modulation of autophagy. *Cell Death Dis* 6:e1885-e1898.
29. Tong X, C Zhang, D Wang, R Song, Y Ma, Y Cao, H Zhao, J Bian, J Gu and Z Liu. (2020). Suppression of AMP-activated protein kinase reverses osteoprotegerin-induced inhibition of osteoclast differentiation by reducing autophagy. *Cell Prolif* 53:e12714-e12730.
30. Li Z, X Liu, Y Zhu, Y Du, X Liu, L Lv, X Zhang, Y Liu, P Zhang and Y Zhou. (2019). Mitochondrial phosphoenolpyruvate carboxykinase regulates osteogenic differentiation by modulating AMPK/ULK1-dependent autophagy. *Stem Cells* 37:1542-1555.
31. Chen Z, S Ni, S Han, R Crawford, S Lu, F Wei, J Chang, C Wu and Y Xiao. (2017). Nanoporous microstructures mediate osteogenesis by modulating the osteo-immune response of macrophages. *Nanoscale* 9:706-718.
32. Lin R, S Wu, D Zhu, M Qin and X Liu. (2020). Osteopontin induces atrial fibrosis by activating Akt/GSK-3beta/beta-catenin pathway and suppressing autophagy. *Life Sci* 245:117328.
33. Mancinelli R, G Carpino, S Petrunaro, CL Mammola, L Tomaipitca, A Filippini, A Facchiano, E Ziparo and C Giampietri. (2017). Multifaceted roles of GSK-3 in cancer and autophagy-related diseases. *Oxid Med Cell Longev* 2017:4629495.
34. Azoulay-Alfaguter I, R Elya, L Avrahami, A Katz and H Eldar-Finkelman. (2015). Combined regulation of mTORC1 and lysosomal acidification by GSK-3 suppresses autophagy and contributes to cancer cell growth. *Oncogene* 34: 4613-23.
35. Peng S, S Shi, G Tao, Y Li, D Xiao, L Wang, Q He, X Cai and J Xiao. (2021). JKAMP inhibits the osteogenic capacity of adipose-derived stem cells in diabetic osteoporosis by modulating the Wnt signaling pathway through intragenic DNA methylation. *Stem Cell Res Ther* 12:120-135.
36. Chen C, Q Yu, K Xu, L Cai, BM Felicia, L Wang, A Zhang, Q Dai, W Geng, J Wang and Y Mo. (2020). Electroacupuncture pretreatment prevents ischemic stroke and inhibits Wnt signaling-mediated autophagy through the regulation of GSK-3beta phosphorylation. *Brain Res Bull* 158:90-98.

Address correspondence to:

*Dr. Jingang Xiao*  
*Department of Oral Implantology*  
*The Affiliated Stomatology Hospital*  
*of Southwest Medical University*  
*No. 2 Jiangyang South Road*  
*Luzhou 646000*  
*People's Republic of China*

*E-mail: drxiaojingang@163.com*

Received for publication July 23, 2021

Accepted after revision August 30, 2021

Prepublished on Liebert Instant Online September 5, 2021

RESEARCH

Open Access



# Downregulation of DNA methyltransferase-3a ameliorates the osteogenic differentiation ability of adipose-derived stem cells in diabetic osteoporosis via Wnt/ $\beta$ -catenin signaling pathway

Maorui Zhang<sup>1,2†</sup>, Yujin Gao<sup>1,3†</sup>, Qing Li<sup>4</sup>, Huayue Cao<sup>1</sup>, Jianghua Yang<sup>4</sup>, Xiaoxiao Cai<sup>2\*</sup> and Jingang Xiao<sup>1,3,4\*</sup> 

## Abstract

**Background:** Diabetes-related osteoporosis (DOP) is a chronic disease caused by the high glucose environment that induces a metabolic disorder of osteocytes and osteoblast-associated mesenchymal stem cells. The processes of bone defect repair and regeneration become extremely difficult with DOP. Adipose-derived stem cells (ASCs), as seed cells in bone tissue engineering technology, provide a promising therapeutic approach for bone regeneration in DOP patients. The osteogenic ability of ASCs is lower in a DOP model than that of control ASCs. DNA methylation, as a mechanism of epigenetic regulation, may be involved in DNA methylation of various genes, thereby participating in biological behaviors of various cells. Emerging evidence suggests that increased DNA methylation levels are associated with activation of Wnt/ $\beta$ -catenin signaling pathway. The purpose of this study was to investigate the influence of the diabetic environment on the osteogenic potential of ASCs, to explore the role of DNA methylation on osteogenic differentiation of DOP-ASCs via Wnt/ $\beta$ -catenin signaling pathway, and to improve the osteogenic differentiation ability of ASCs with DOP.

**Methods:** DOP-ASCs and control ASCs were isolated from DOP C57BL/6 and control mice, respectively. The multipotency of DOP-ASCs was confirmed by Alizarin Red-S, Oil Red-O, and Alcian blue staining. Real-time polymerase chain reaction (RT-PCR), immunofluorescence, and western blotting were used to analyze changes in markers of osteogenic differentiation, DNA methylation, and Wnt/ $\beta$ -catenin signaling. Alizarin Red-S staining was also used to confirm changes in the osteogenic ability. DNMT small interfering RNA (siRNA), shRNA-Dnmt3a, and LVRNA-Dnmt3a were used to assess the role of Dnmt3a in osteogenic differentiation of control ASCs and DOP-ASCs. Micro-computed

<sup>†</sup>Maorui Zhang and Yujin Gao contributed equally to this work

\*Correspondence: xcai@scu.edu.cn; drxiaojingang@163.com

<sup>1</sup> Department of Oral Implantology, The Affiliated Stomatological Hospital of Southwest Medical University, Luzhou 646000, China

<sup>2</sup> State Key Laboratory of Oral Diseases, West China Hospital of Stomatology, Sichuan University, Chengdu 610041, China

Full list of author information is available at the end of the article



© The Author(s) 2022. **Open Access** This article is licensed under a Creative Commons Attribution 4.0 International License, which permits use, sharing, adaptation, distribution and reproduction in any medium or format, as long as you give appropriate credit to the original author(s) and the source, provide a link to the Creative Commons licence, and indicate if changes were made. The images or other third party material in this article are included in the article's Creative Commons licence, unless indicated otherwise in a credit line to the material. If material is not included in the article's Creative Commons licence and your intended use is not permitted by statutory regulation or exceeds the permitted use, you will need to obtain permission directly from the copyright holder. To view a copy of this licence, visit <http://creativecommons.org/licenses/by/4.0/>. The Creative Commons Public Domain Dedication waiver (<http://creativecommons.org/publicdomain/zero/1.0/>) applies to the data made available in this article, unless otherwise stated in a credit line to the data.

tomography, hematoxylin and eosin staining, and Masson staining were used to analyze changes in the osteogenic capability while downregulating Dnmt3a with lentivirus in DOP mice *in vivo*.

**Results:** The proliferative ability of DOP-ASCs was lower than that of control ASCs. DOP-ASCs showed a decrease in osteogenic differentiation capacity, lower Wnt/ $\beta$ -catenin signaling pathway activity, and a higher level of Dnmt3a than control ASCs. When Dnmt3a was downregulated by siRNA and shRNA, osteogenic-related factors Runt-related transcription factor 2 and osteopontin, and activity of Wnt/ $\beta$ -catenin signaling pathway were increased, which rescued the poor osteogenic potential of DOP-ASCs. When Dnmt3a was upregulated by LVRNA-Dnmt3a, the osteogenic ability was inhibited. The same results were obtained *in vivo*.

**Conclusions:** Dnmt3a silencing rescues the negative effects of DOP on ASCs and provides a possible approach for bone tissue regeneration in patients with diabetic osteoporosis.

**Keywords:** DNA methyltransferase-3a, Diabetic osteoporosis, Adipose-derived stem cells, Osteogenic differentiation, Wnt/ $\beta$ -catenin signaling pathway

## Background

Diabetic osteoporosis (DOP) is a systemic metabolic bone disease that involves bone mass reduction, destruction of the bone tissue microstructure, and prone fractures [1, 2]. The high glucose environment and metabolic disorders caused by diabetes disrupt physiological activities such as cell growth, proliferation, and differentiation [3]. Glucose metabolism disorders break the balance between osteogenesis and osteoclast processes, which reduces the numbers of osteoblasts and mesenchymal stem cells (MSCs), and activation of osteoclasts [4, 5]. The imbalance of bone metabolism also reduces the bone differentiation ability and makes it difficult to repair bone tissue and regenerate bone [6].

In recent years, bone tissue engineering technology has provided a new approach for regeneration of bone defects. Adult stem cells are a major element of bone regeneration and have become a major research topic [7–9]. Adipose-derived mesenchymal stem cells (ASCs), as a type of MSC, have a multi-directional differentiation potential for osteogenic, cartilage, and adipose cell lineages [10–12]. They are widely used in studies of bone defect repair and regeneration, and have positive application prospects. However, the proliferation and differentiation of ASCs may be affected in the diabetic environment. Therefore, it is worth exploring whether DOP-ASCs have a normal osteogenic differentiation ability.

DNA methylation is a mechanism of epigenetic regulation. It is generally believed that the hypermethylation status of DNA sequences is related to inhibition of gene expression [13, 14]. There are three kinds of DNA methyltransferases (DNMTs) in animals, namely DNMT1, DNMT3a, and DNMT3b [15–17]. Studies have shown that DNMT3a is essential for establishment of mammalian DNA methylation during development [18, 19]. Scholars believe that the increased expression of DNMT3a regulates the increased DNA methylation

level [19, 20]. Under catalysis mediated by DNMTs, the cytosines of two nucleotides of CG in DNA are selectively conjugated with methyl groups to form 5-methylcytosine (5-MC). The occurrence of various skeletal diseases, which include osteoporosis and osteoarthritis, is closely related to impaired DNA methylation in stem cells [10, 13, 21].

The canonical Wnt pathway is activated when  $\beta$ -catenin transfers to the nucleus and binds to TCF/LEF in the nucleus to regulate target genes [22].  $\beta$ -catenin and LEF1 may reflect the status of Wnt/ $\beta$ -catenin pathway [23, 24]. Emerging evidence indicates that increased DNA methylation levels are associated with activation of Wnt/ $\beta$ -catenin pathway [25–28]. Liu T et al. [26] reported that miR708-5p inhibits the expression of Dnmt3a, resulting in the reduced global DNA methylation and, preventing  $\beta$ -catenin nuclear transport, thereby inhibiting Wnt/ $\beta$ -catenin signaling pathway. Exploring the role of DNA methylation in osteogenic differentiation of DOP-ASCs via Wnt/ $\beta$ -catenin signaling is not only conducive to elucidate the mechanism of DOP, but also to develop bone tissue engineering.

In our previous study, we found that advanced glycation end products inhibit the osteogenic differentiation ability of normal ASCs with a high level of DNA methylation [5]. This suggested that DNA methylation is a cause of the decline in the osteogenic differentiation ability of DOP-ASCs in the diabetic environment. In this study, we isolated ASCs from control and DOP C57BL/6 mice and compared their osteogenic differentiation potentials. Moreover, we investigated whether DNA methylation inhibits the osteogenic differentiation potential of DOP-ASCs by modulating Wnt/ $\beta$ -catenin signaling pathways.

## Methods

### Isolation and culture of ASCs and DOP-ASCs

All procedures that involved animals were reviewed and approved by the Southwest Medical University

Ethical Committee. Anesthesia and animal care were implemented by following the guidelines for the Care and Use of Laboratory Animals (Ministry of Science and Technology of China, 2006). Adipose tissue in the inguinal region was collected from C57BL/6 DOP and control mice under sterile conditions. The adipose tissue was cut finely and fragments were seeded in 25-cm<sup>2</sup> culture flasks (Corning Inc., NY) and cultured in alpha-modified Eagle's medium ( $\alpha$ -MEM, Hyclone, USA) supplemented with 10% fetal bovine serum (FBS, Hyclone) and 1% penicillin/streptomycin (Hyclone) at 37 °C with 5% CO<sub>2</sub>. The medium was changed every 3 days. Adherent cells were cultured and non-adherent cells were removed.

DOP-ASCs were passaged three times to obtain relatively pure ASCs. Osteogenic, adipogenic, and cartilage media (Cyagen, USA) were used to define the multipotential differentiation capacity of DOP-ASCs. DOP-ASCs ( $5 \times 10^4$  cells) were seeded in a 6-well plate for osteogenic induction. DOP-ASCs ( $1 \times 10^5$  cells) were also seeded for adipogenic induction. All cells were cultured for 21 days. Then, the cells were washed three times with PBS and fixed with 4% paraformaldehyde for 1 h. Alizarin Red-S (osteogenic dye) and 0.3% Oil Red-O (adipogenic dye) were used to stain mineralized nodules and lipid droplets, respectively, for 30 min. The stained cells were imaged under an inverted phase contrast microscope (Nikon, Japan). For cartilage induction, DOP-ASCs ( $2.5 \times 10^5$  cells) were centrifuged and cell aggregates were cultured in cartilage medium. After 21 days, the cell aggregates were washed three times with PBS and fixed with 4% paraformaldehyde. The cartilage pellets were imaged under a stereo fluorescence microscope (Carl Zeiss Microscopy, Germany). Then, they were embedded in paraffin and sections were stained with Alcian blue. Cartilage matrix was imaged under an optical microscope (Nikon).

#### Proliferation assay

A Cell Counting Kit-8 (CCK-8) assay (Sigma-Aldrich, St Louis, Missouri, USA) and xCelligence system for real-time cellular analysis (RTCA) (Roche Diagnostics GmbH, Basel, Switzerland) were used to assess cell proliferation. For the CCK-8 assay, cells were seeded in 96-well plates (Corning Inc.) at a density of  $3 \times 10^3$  cells per well and cultured in  $\alpha$ -MEM with 10% FBS for 5 days. A BioTek ELX800 (Bio-Tek, USA) was used to measure absorbance at 450 nm. For RTCA, cells were seeded in 96-well E-plates (Roche Diagnostics GmbH) at  $3 \times 10^3$  cells per well. Cell proliferation in the RTCA SP xCelligence system was monitored in real-time as the impedance value over 5 days. Data were analyzed by the provided RTCA software.

#### Alizarin red-S staining

Mineralized nodule formation in ASCs was stained by Alizarin Red-S (Cyagen). DOP-ASCs and control ASCs ( $5 \times 10^4$  cells) in 6-well plates were treated with osteogenic medium for 21 days. Cells were then washed with PBS three times, fixed in 4% paraformaldehyde for 1 h, and stained with Alizarin Red-S for 30 min.

#### Real-time polymerase chain reaction (RT-PCR)

Total RNA was extracted using a Total mRNA Extraction Kit (Takara Bio, Japan). cDNA was synthesized by reverse transcription using a Prime Script Reverse Transcription Reagent Kit (Takara Bio). Then, RT-PCR was conducted to measure the gene expression of Runt-related transcription factor 2 (*Runx2*), osteopontin (*Opn*), DNA methyltransferase 1/3a/3b (*Dnmt1/3a/3b*),  $\beta$ -catenin, and lymphoid enhancer-binding factor-1 (*Lef1*). Primer sequences are shown in Table 1. Samples were analyzed using a SYBR Premix ExTaq kit (Takara Bio), following the standard procedure, in an ABI 7900 system (Applied Biosystems, USA), which included melting curve analysis and obtaining CT values. The results were normalized to *Gapdh* CT values and the  $2^{-\Delta\Delta Ct}$  method was used to calculate gene expression.

#### Western blot assay

A Total Protein Extraction Kit (Keygen Biotech, China) was used to extract total cellular proteins. A bicinchoninic acid protein assay kit (Thermo Fisher Scientific, MA, USA) was used to measure the protein concentration. Proteins were separated by 10% (v/v) sodium dodecyl sulfate–polyacrylamide gel electrophoresis and then

**Table 1** Primer sequences for RT-PCR

Genes		Sequence (5' → 3')
<i>Gapdh</i>	Forward	GGTGAAGGTCGGTGTGAACG
	Reverse	CTCGCTCCTGGAAGATGGTG
<i>Runx2</i>	Forward	CCGAAGTGGTCCGCACCGAC
	Reverse	CTTGAAGGCCACGGGCAGGG
<i>Opn</i>	Forward	GGATTCTGTGGACTCGGATG
	Reverse	CGACTGTAGGGACGATTGGA
<i>Dnmt1</i>	Forward	CCGAAGTGGTCCGCACCGAC
	Reverse	CTTGAAGGCCACGGGCAGGG
<i>Dnmt3a</i>	Forward	GAGGGAAGTGGAGACCCAC
	Reverse	CTGGAAGGTGAGTCTTGGCA
<i>Dnmt3b</i>	Forward	AGCGGGTATGAGGAGTGCAT
	Reverse	GGGAGCATCTTCGTGTCTG
$\beta$ -Catenin	Forward	AAGTCTTGGCTATTACGACA
	Reverse	ACAGCACCTTCAGCACTCT
<i>Lef1</i>	Forward	ACAGATCACCCACCTTCTTG
	Reverse	TGATGGGAAAACCTGGACAT

transferred onto a polyvinylidene difluoride membrane at 200 mA for 1 h. Tris-buffered saline with 0.05% (v/v) Tween-20 (TBST) was used to dissolve dry skimmed milk (Keygen Biotech). PVDF membranes were blocked with 5% dry skimmed milk for 1 h and then incubated with antibodies against GAPDH (ab181602), DNMT3a (ab188470), DNMT3b (ab79822), and OPN (ab91655) (Abcam, UK), RUNX2 (12556 s), DNMT1 (5032S),  $\beta$ -catenin (D10A8), or LEF1 (2230p) (Cell Signaling Technology, USA) for 1 day at 4 °C. Then, PVDF membranes were washed three times with TBST and incubated with a goat anti-rabbit secondary antibody (Beyotime, Shanghai, China) for 1 h. They were then washed again with TBST and developed with an enhanced chemiluminescence detection system (Bio-Rad, USA).

#### Immunofluorescence staining

Cells were seeded on round coverslips (Corning Inc.) and cultured for 4 days. After various treatments, the cells were carefully washed three times with PBS, fixed with 4% paraformaldehyde for 1 h, and permeabilized with 0.5% Triton X-100 for 10 min. Then, they were blocked with 5% goat serum (Beyotime) for 1 h and incubated for 1 day at 4 °C with antibodies against RUNX2, OPN, DNMT1, DNMT3a, DNMT3b, 5-MC (28692S),  $\beta$ -catenin, or LEF1. The next day, the samples were incubated with a fluorescent dye-conjugated secondary antibody (Beyotime) for 1 h. Nuclei were counterstained with 4'-diamidino-2-phenylindole (Beyotime) for 10 min and phalloidin (Beyotime) was used to stain microfilaments

for 10 min. Cells were imaged under a laser scanning confocal microscope (Olympus, Japan).

#### Transfection of small interfering RNA (siRNA)

Small interfering RNA (siRNA) that targeted *Dnmt1*, *Dnmt3a*, and *Dnmt3b* was designed and provided by GenePharma Co., Ltd (Shanghai, China). siRNA sequences are shown in Table 2. DOP-ASCs ( $5 \times 10^4$  cells) were seeded in a 12-well plate before siRNA transfection. The transfection reagent (Lipofectamine 2000; Thermo Fisher Scientific) was diluted with Opti-MEM I Reduced Serum Medium (Hyclone) and incubated at room temperature for 5 min. The siRNA was added to the diluted Lipofectamine 2000 and gently mixed to form the siRNA-lipofectamine-Opti-MEM complex. Then, the mixture was added to cells at 1 ml per well and incubated at 37 °C with 5% CO<sub>2</sub>.

#### Transduction of shRNA-*Dnmt3a* and LVRNA-*Dnmt3a*

The *Dnmt3a* overexpression lentiviral vector (pLenti-EF1a-EGFP-P2A-Puro-CMV-*Dnmt3a*-3Flag) and *Dnmt3a*-silencing lentiviral vector (pLDK-CMV-EGFP-P2A-Puro-U6-shRNAD*Dnmt3a*) were designed and manufactured by OBiO Technology Corp., Ltd. (Shanghai, China). The oligonucleotide sequences of shRNA with *Dnmt3a* RNA interference targets are shown in Table 3. Various virus concentrations were used to determine the multiplicity of infection (MOI). The transduction efficiency was evaluated by analyzing the percentage of green fluorescent protein (GFP)-positive cells under a fluorescence microscope. ASCs at a density of  $5 \times 10^4$ /ml were seeded in a 6-well plate at 2 ml per well. After 12 h of culture, the medium was replaced with a lentivirus suspension medium (MOI:80; 0.6  $\mu$ g/ml puromycin; 5  $\mu$ g/ml polybrene). The gene and protein expression were analyzed by RT-PCR and western blotting, respectively, after 4 days of osteogenic induction and their osteogenic ability was assessed by Alizarin Red-S staining after induction for 21 days.

#### Analysis of DOP-ASCs seeded on BCP by scanning electron microscopy (SEM)

Before seeding DOP-ASCs, scaffolds sterilized by ultraviolet light were placed in 12-well plates. Then, 1 ml of

**Table 2** siRNA sequences for gene silencing

siRNA		Sequence (5' → 3')
<i>Dnmt1</i>	Sense	CCGAAGAUAACAUCACCAATT
	Antisense	UUGGUGAGUUGAUCUUCGGTT
<i>Dnmt3a</i>	Sense	CCAUGUACCGCAAAGCCAUTT
	Antisense	AUGGCUUUGCGGUACAUGGTT
<i>Dnmt3b</i>	Sense	CCUCAAGACAAAUAGCUAUTT
	Antisense	AUAGCUAUUUGUCUUGAGGTT
Negative control	Sense	UUCUUCGAACGUGUCACGUTT
	Antisense	ACGUGACACGUUCGGAGAATT

**Table 3** Dnmt3a shRNA sequences

5'		STEM	Loop	STEM	3'
sh-Dnmt3a-F	Ccgg	CCACCAGGTCAAACCTCTAT	TTCAAGAGA	ATAGAGTTTGACCTGGTGG	TTTTTTg
sh-Dnmt3a-R	aattcaaaaa	CCACCAGGTCAAACCTCTAT	TCTCTTGAA	ATAGAGTTTGACCTGGTGG	
sh-NC-F	CCGG	TTCTCCGAACGTGTCACGT	TTCAAGAGA	ACGTGACACGTTCCGGAGAA	TTTTTTg
sh-NC-R	AATCAAAAAA	TTCTCCGAACGTGTCACGT	TCTCTTGAA	ACGTGACACGTTCCGGAGAA	

passage 2 DOP-ASCs at a density of  $5 \times 10^4$ /ml was seeded on the surface of BCP in each well. After culture at 37 °C with 5% CO<sub>2</sub> for 3 days, samples were fixed with paraformaldehyde. After alcohol gradient dehydration, critical point drying, and spraying the cells with gold, scaffolds were observed by SEM.

#### **Implantation of BCP seeded with DOP-ASCs transduced with shRNA into a DOP mouse model with critically sized calvarial defects**

DOP-ASCs were divided into DOP-blank, negative control, and Dnmt3a shRNA groups. DOP-ASCs infected with the silence-Dnmt3a lentivirus were cultured in osteogenic induction medium. A 1-ml cell suspension ( $5 \times 10^4$  cells/ml) was added to the surface of BCP in a 12-well plate and cultured for 48 h. Nine DOP mice received calvarial surgery to establish critically sized calvarial defect models. After anaesthetization, the DOP mice were subjected to prone fixation, skin preparation, and disinfection at the top of the skull. An incision was made along the median of the calvarium and the periosteum was bluntly separated to expose the calvarial bone surface. Then, a 4-mm diameter trephine bur was applied to drill a standardized round defect on the side of the sagittal suture. A 0.9% saline solution was used to irrigate the skull surface during drilling. Subsequently, the BCP seeded with DOP-ASCs was implanted into the skull defect area and the periosteum and dermis were sutured in position. After 8 weeks, mice were euthanized and skull specimens were obtained.

#### **Micro-computed tomography (Micro-CT), hematoxylin and eosin staining (HE) staining, and Masson staining**

At 8 weeks, the calvarium was removed intact and fixed in freshly prepared 4% formaldehyde for 24 h at 4 °C. Micro-CT scans of skull defects were performed to observe new bone formation. Then, three-dimensional reconstructed images were analyzed. The ratio of the bone volume to total volume available in the scaffold (BV/TV) was calculated. A high ratio indicated that more bone had grown into the scaffolds. Then, tissue samples of the mouse skull defect were decalcified for HE and Masson staining. Next, the samples were dehydrated in an alcohol gradient, clarified, and embedded in paraffin for sectioning. Lastly, the sections were stained with hematoxylin and eosin and Masson trichrome.

#### **Statistical analysis**

All experiments were repeated at least three times independently. Two group comparisons were made by the independent-samples t-test and multiple comparisons were made by one-way ANOVA with SPSS 18.0 software

(SPSS Inc., Chicago, USA).  $P < 0.05$  was regarded to be statistically significant.

## **Results**

### **Cell proliferation and multipotent differentiation of DOP-ASCs**

ASCs from inguinal adipose tissue were isolated and passaged three times (Fig. 1A). RTCA (Fig. 1B) and CCK-8 assays (Fig. 1D) showed that the proliferation rate of the DOP group was relatively lower than that of the control group. After culture in osteogenic and adipogenic media, the morphology of DOP-ASCs had distinctly changed to osteogenic-like in osteogenic medium and adipose-like in adipogenic medium (Fig. 1C). In cartilage medium, ASCs were aggregated to culture for 21 days and then stained with Alcian blue to indicate cartilage-like cells. The findings demonstrated the multipotency of DOP-ASCs (Fig. 1C).

### **Osteogenic differentiation capacity decreases in DOP-ASCs**

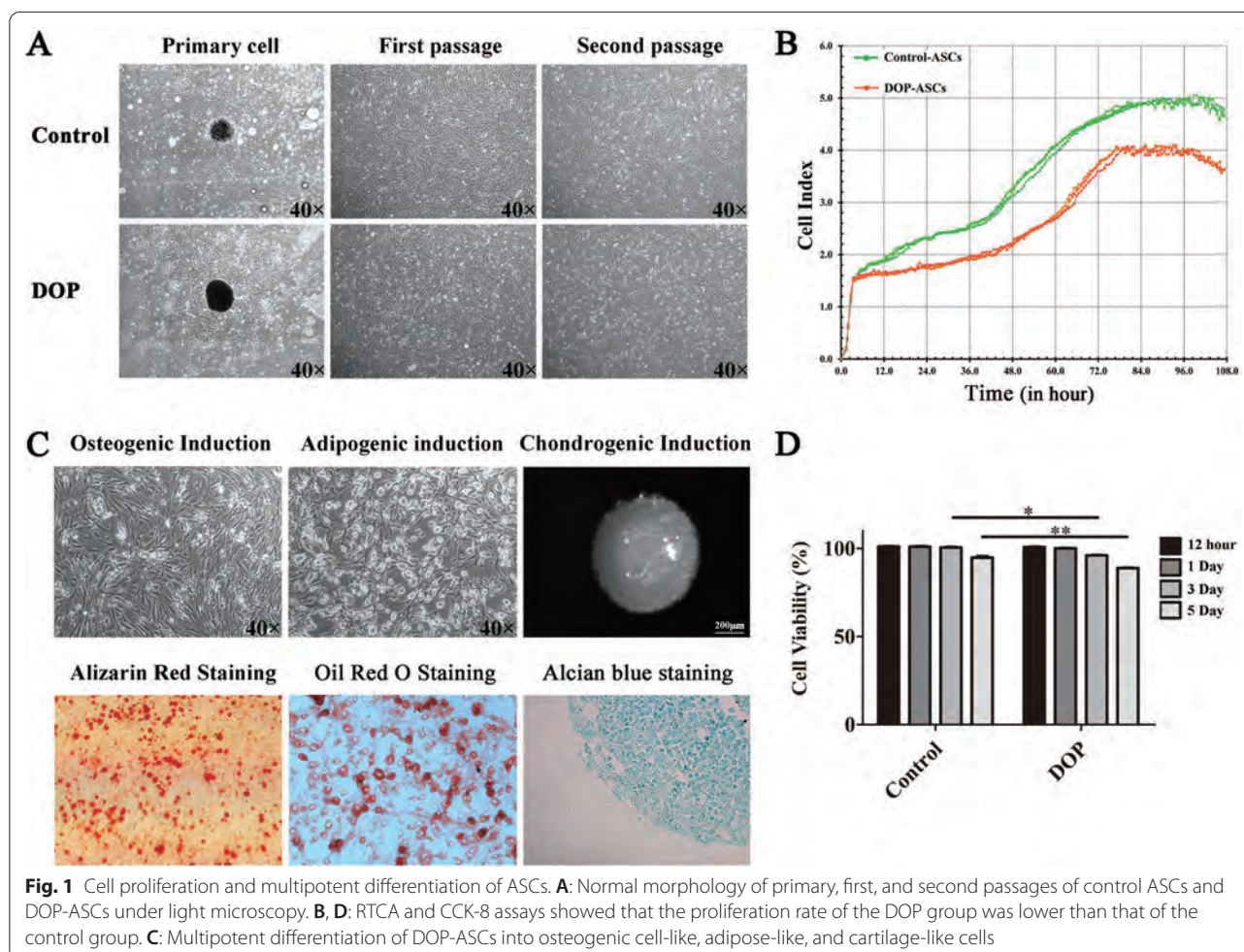
To investigate the osteogenic differentiation capacity, we cultured control ASCs and DOP-ASCs to analyze mineralized nodule formation as well as gene and protein expression of OPN and RUNX2. Alizarin Red-S staining showed that the degree of mineralized nodule formation was reduced in DOP-ASCs compared with control ASCs (Fig. 2A). RT-PCR showed that the mRNA levels of *Runx2* and *Opn* in DOP-ASCs were significantly lower than those in control ASCs at 3 and 7 days (Fig. 2B). The protein levels of OPN and RUNX2 were analyzed by immunofluorescence and western blotting, which showed that the fluorescence signals (Fig. 2C) and band intensities (Fig. 2D) at 4 days in DOP-ASCs were weaker compared with those in control ASCs.

### **DNA methylation increases in DOP-ASCs**

DNMT1, DNMT3a, and DNMT3b are major enzymes in DNA methylation and 5-MC is the product of this process. We analyzed the expression of these factors by RT-PCR, western blotting, and immunofluorescence. The expression of *Dnmt1*, *Dnmt3a*, and *Dnmt3b* in DOP-ASCs increased compared with that in control ASCs (Fig. 3A, B). Immunofluorescence confirmed the increases in 5-MC, DNMT1, DNMT3a, and DNMT3b at 4 days (Fig. 3C–F).

### **Wnt/ $\beta$ -Catenin signaling pathway is suppressed in DOP-ASCs**

The Wnt/ $\beta$ -Catenin signaling pathway is a major regulatory pathway in the process of osteogenic differentiation [29, 30]. Therefore, the main factors, which included  *$\beta$ -catenin* and *Lef1*, were detected to demonstrate the activation level of Wnt/ $\beta$ -Catenin signaling pathway.



RT-PCR showed that the expression of  $\beta$ -catenin and *Lef1* decreased in DOP-ASCs compared with that in CON-ASCs, and the results of western blotting were consistent with those of RT-PCR (Fig. 4A, B). Immunofluorescence confirmed that the expression of  $\beta$ -catenin and LEF1 was low in DOP-ASCs (Fig. 4C, D).

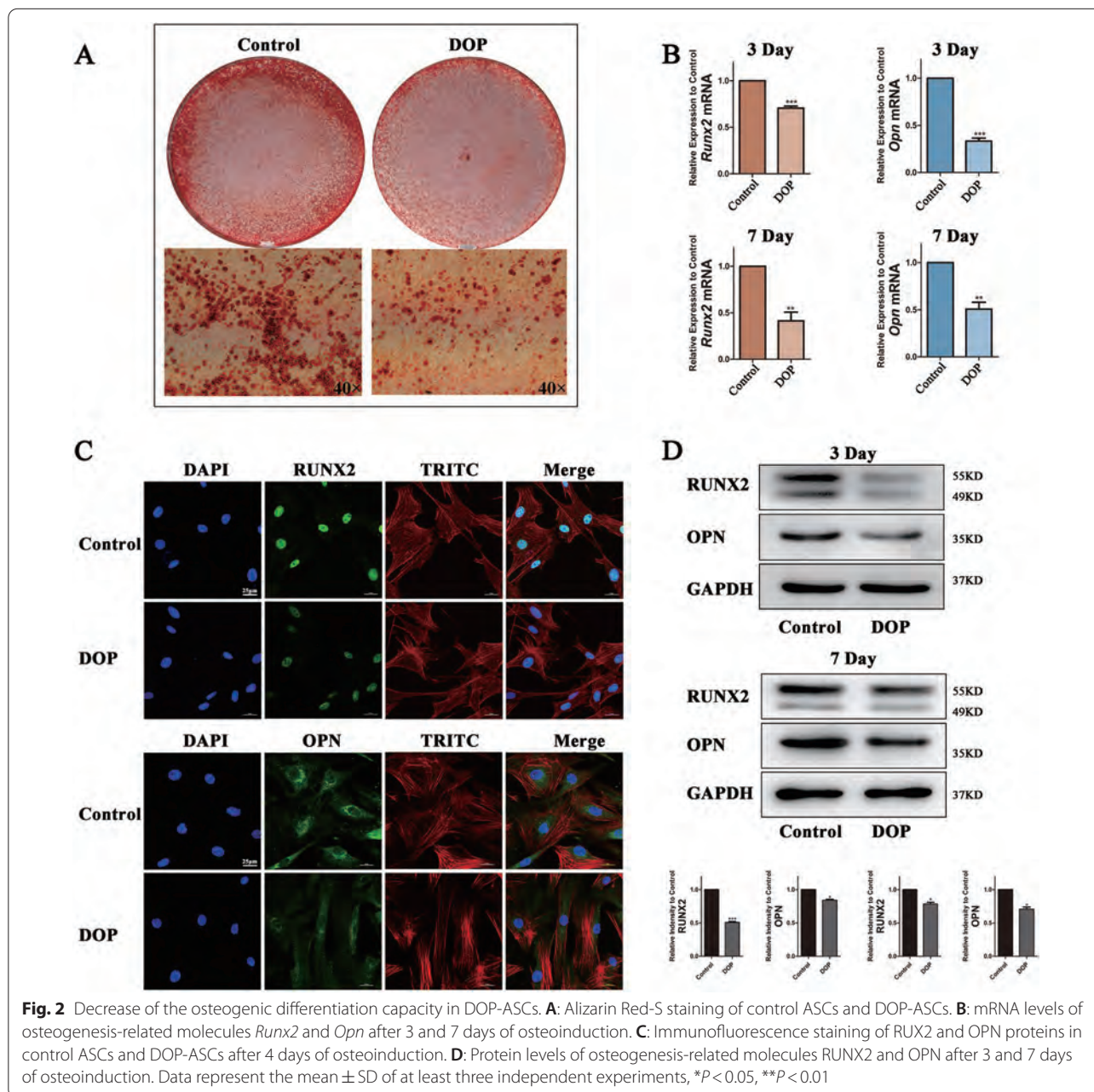
**Inhibiting DNA methyltransferases rescues loss of the osteogenic potential in DOP-ASCs**

The results showed that the reduced osteogenic differentiation capacity of DOP-ASCs was related to increases in DNA methylation levels and suppression of Wnt/ $\beta$ -Catenin signaling pathway. Next, we used siRNA to inhibit the expression of DNA methylation enzymes and explored the relationship between DNA methylation and the osteogenic differentiation ability of DOP-ASCs. After siRNA treatment, the formation of mineralized nodules was increased when the DNA methylation level was downregulated (Fig. 5A). RT-PCR and western blotting showed that RUNX2 was increased in Dnmt1-siRNA, Dnmt3a-siRNA, and Dnmt3b-siRNA groups, and OPN

was particularly increased in the Dnmt3a-siRNA group (Fig. 5B, C). In terms of Wnt/ $\beta$ -Catenin signaling pathway,  $\beta$ -catenin and LEF1 were upregulated after siRNA treatment and their expression was the highest in the Dnmt3a-siRNA group compared with the other groups (Fig. 5D, E). These data suggested that downregulation of Dnmt3a inhibited osteogenic differentiation and activity of Wnt/ $\beta$ -Catenin signaling pathway.

**Knockdown of Dnmt3a promotes osteogenic differentiation of DOP-ASCs**

To further demonstrate the effect of Dnmt3a on osteogenic differentiation of DOP-ASCs, we used lentiviruses to knockdown or overexpress Dnmt3a in DOP-ASCs. The cells were successfully infected by the lentiviruses and showed green fluorescence at an MOI of 80 (Fig. 6A). RT-PCR and western blotting showed that Dnmt3a was successfully knocked down by Dnmt3a shRNA and overexpressed by Dnmt3a LVRNA. 3-Flag was a marker of positive overexpression (Fig. 6B, D). Immunofluorescence confirmed the differences in expression of



DNMT3a among the DOP-blank group, Negative Control, Dnmt3a shRNA and Dnmt3a LVRNA. (Fig. 6C).

Next, we found that the formation of mineralized nodules was the highest in the Dnmt3a shRNA group and the lowest in the Dnmt3a LVRNA group (Fig. 7A). Expression of *Opn* and *Runx2* was upregulated in the Dnmt3a shRNA group compared with the other three groups and the results of western blot assays were consistent with those of RT-PCR (Fig. 7B–D). Detection of osteogenic differentiation by Alizarin Red-S staining, RT-PCR, and western blotting showed that knockdown

of Dnmt3a rescued the osteogenic differentiation capacity of DOP-ASCs. Although Dnmt3a LVRNA treatment decreased the expression of  $\beta$ -catenin and *Lef1* compared with DOP-ASC and negative control groups, the expression of these factors was recovered by Dnmt3a shRNA treatment. This suggested that the low activity of the Wnt signaling pathway in DOP-ASCs was recovered by knocking down Dnmt3a (Fig. 7E–G). Taken together, these results suggested that knock-down of Dnmt3a decreased the DNA methylation level, alleviated inhibition of Wnt by DNA methylation,

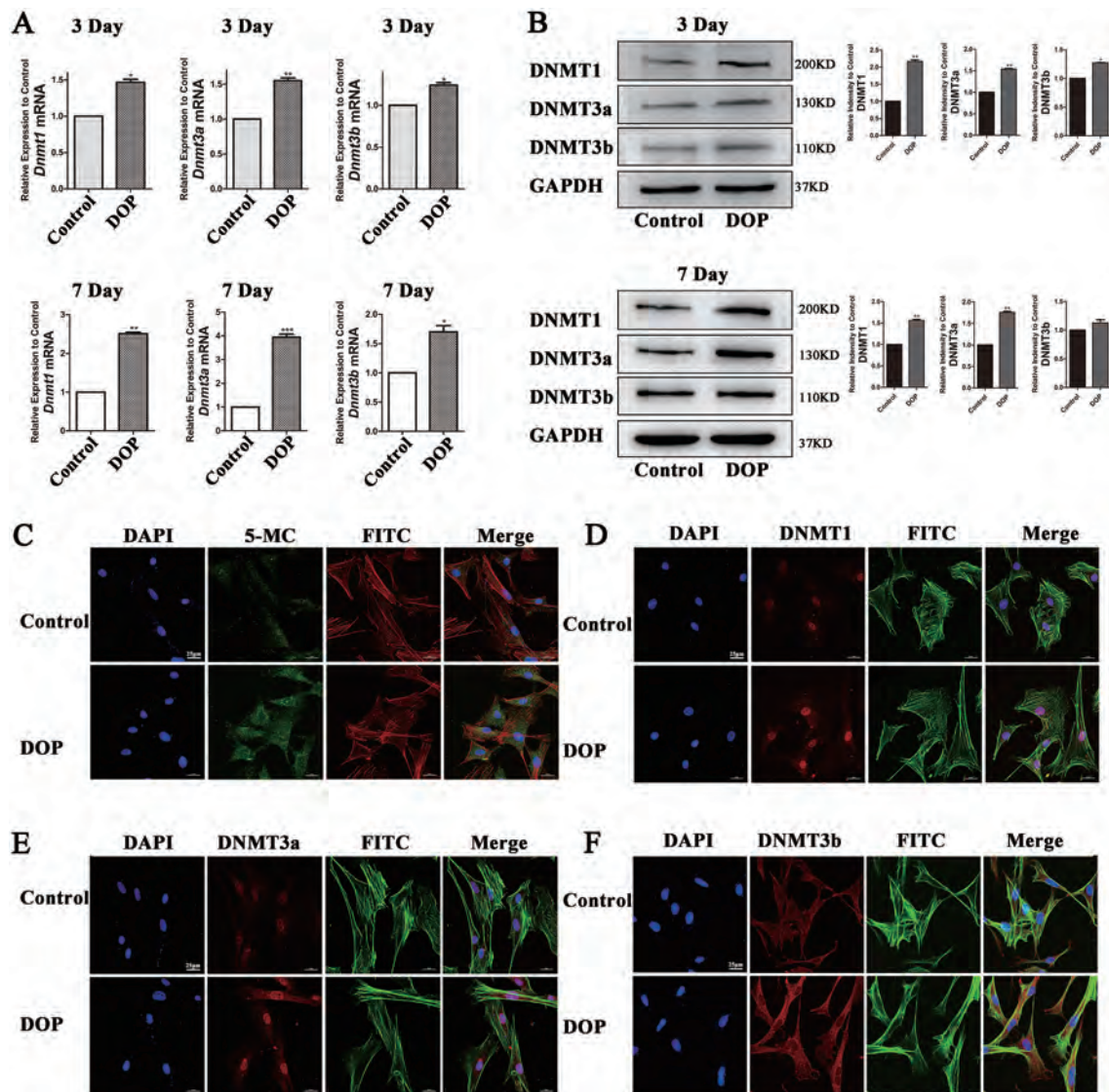


**Fig. 3** Increase of the DNA methylation level in DOP-ASCs. **A, B:** RT-PCR and western blot analyses showing that the expression of Dnmt1, Dnmt3a, and Dnmt3b in DOP-ASCs was increased compared with that in control ASCs. **C, D:** Immunofluorescence showing increases in 5-MC, DNMT1, DNMT3a, and DNMT3b after 4 days of osteoinduction. Data represent the mean  $\pm$  SD of at least three independent experiments, \* $P < 0.05$ , \*\* $P < 0.01$

and rescued the loss of the osteogenic capacity of DOP-ASCs.

**Downregulation of Dnmt3a promotes the osteogenic capacity of DOP-ASCs in vivo**

RT-PCR and western blotting showed that Dnmt3a was successfully knocked down by Dnmt3a shRNA (Fig. 8A, B). SEM and fluorescence microscopy showed that DOP-ASCs grew adherently on the surface and pores of BCP (Fig. 8C). The DOP mouse model with critically sized calvarial defects was successfully established and BCP seeded with transfected DOP-ASCs were implanted into

the defect area (Fig. 8D). Eight weeks later, Micro-CT showed new bone matrix on BCP at sagittal and coronal levels. Three-dimensional reconstruction showed that the amount of new bone matrix in the Dnmt3a shRNA group was significantly larger than that in DOP-ASC and negative control groups. BV/TV, BS/BV, and TbTh analyses further demonstrated that the osteogenic capacity was greatly increased when Dnmt3a was downregulated by shRNA in vivo (Fig. 9A, B). HE and Masson staining were also used to observe the osteogenic capacity of DOP-ASCs in vivo. HE staining showed new bone matrix as red and Masson staining showed new bone matrix as

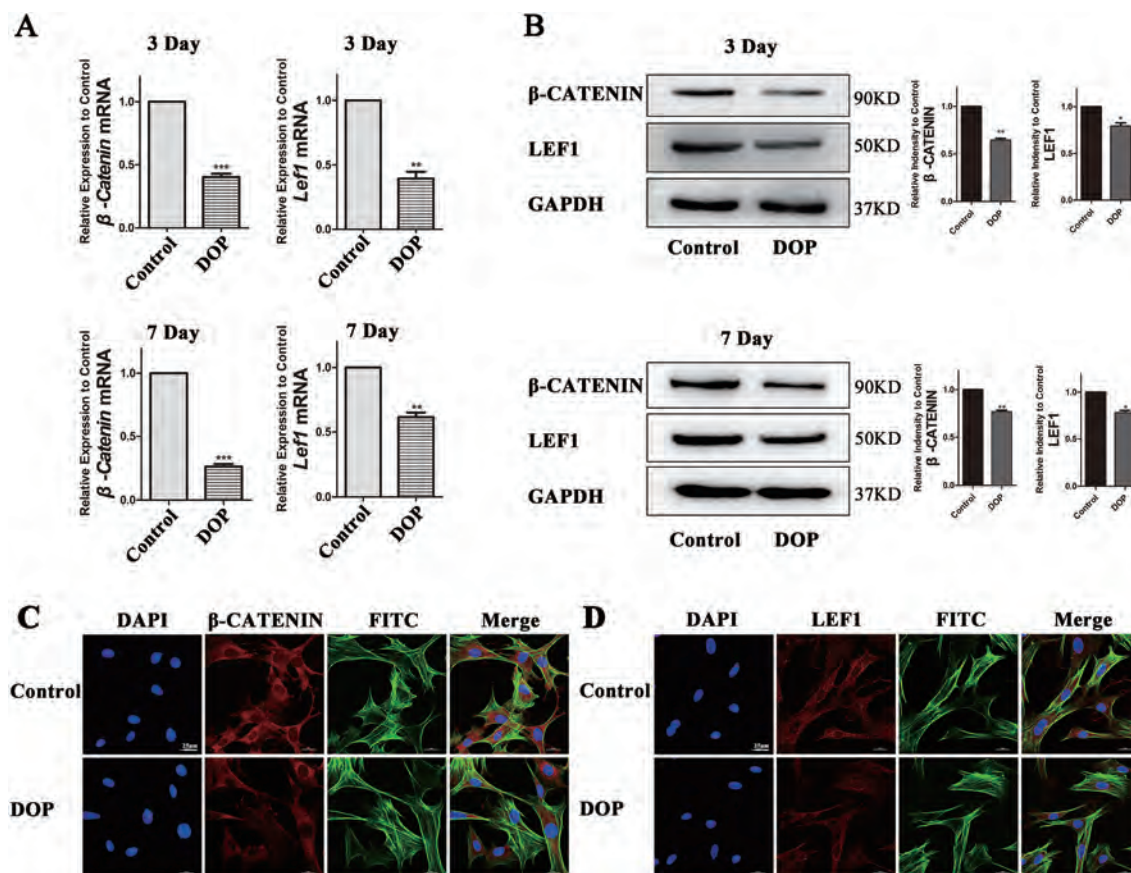


**Fig. 4** Wnt/ $\beta$ -Catenin signaling pathway is suppressed in DOP-ASCs. **A, B**: RT-PCR and western blot analyses showing that the expression of  $\beta$ -catenin and LEF1 was decreased compared with that in CON-ASCs. **C, D**: Immunofluorescence staining of  $\beta$ -catenin and LEF1. Data represent the mean  $\pm$  SD of at least three independent experiments, \* $P < 0.05$ , \*\* $P < 0.01$

blue. Both staining showed that the staining degree in the Dnmt3a shRNA group was stronger than that in DOP-ASC and negative control groups (Fig. 9C). These results suggested that knockdown of Dnmt3a rescued the loss of the osteogenic capacity of DOP-ASCs.

## Discussion

Many studies have shown that hyperglycemia and the glycolytic metabolites of diabetes decrease cell viability and proliferation, and even promote apoptosis of MSCs, which impairs osteogenic differentiation [29–33]. Heilmeyer et al. found that serum miR-550a-5p inhibited the osteogenic differentiation of ASCs in postmenopausal women with type 2 diabetes [34]. Liu et al. reported that osteogenic differentiation of hPDLSCs was significantly inhibited in a high glucose environment and the levels of osteoblast-related factors expressed by cells were reduced significantly [35]. In this study, DOP-ASCs were isolated from DOP mice by the tissue block method, which had osteogenic, adipogenic, and chondrogenic differentiation

abilities. However, the expression of osteogenic-related genes *Runx2* and *Opn* was downregulated in DOP-ASCs compared with control ASCs, which demonstrated inhibition of the differentiation process of DOP-ASCs to osteoblasts.

The differentiation of MSCs into osteogenic progenitor cells is regulated by various growth factors and signaling pathways [36, 37]. The Wnt/ $\beta$ -Catenin signaling pathway plays a major role in regulating the proliferation and differentiation of MSCs. Activation of Wnt/ $\beta$ -Catenin signaling pathway promotes osteogenic differentiation of ASCs [38, 39]. Moldes et al. reported that  $\beta$ -catenin expression was higher in 3T3-L1 precursor adipocytes and the expression level of  $\beta$ -catenin was significantly reduced during adipogenesis [40]. In our previous studies, after activation of Wnt/ $\beta$ -Catenin signaling pathway, the expression of Wnt-related signaling molecules, such as  $\beta$ -catenin and LEF1, was upregulated in normal ASCs, which promoted the expression of osteogenic differentiation factors such as *Opn* and *Runx2* [5, 41]. In this

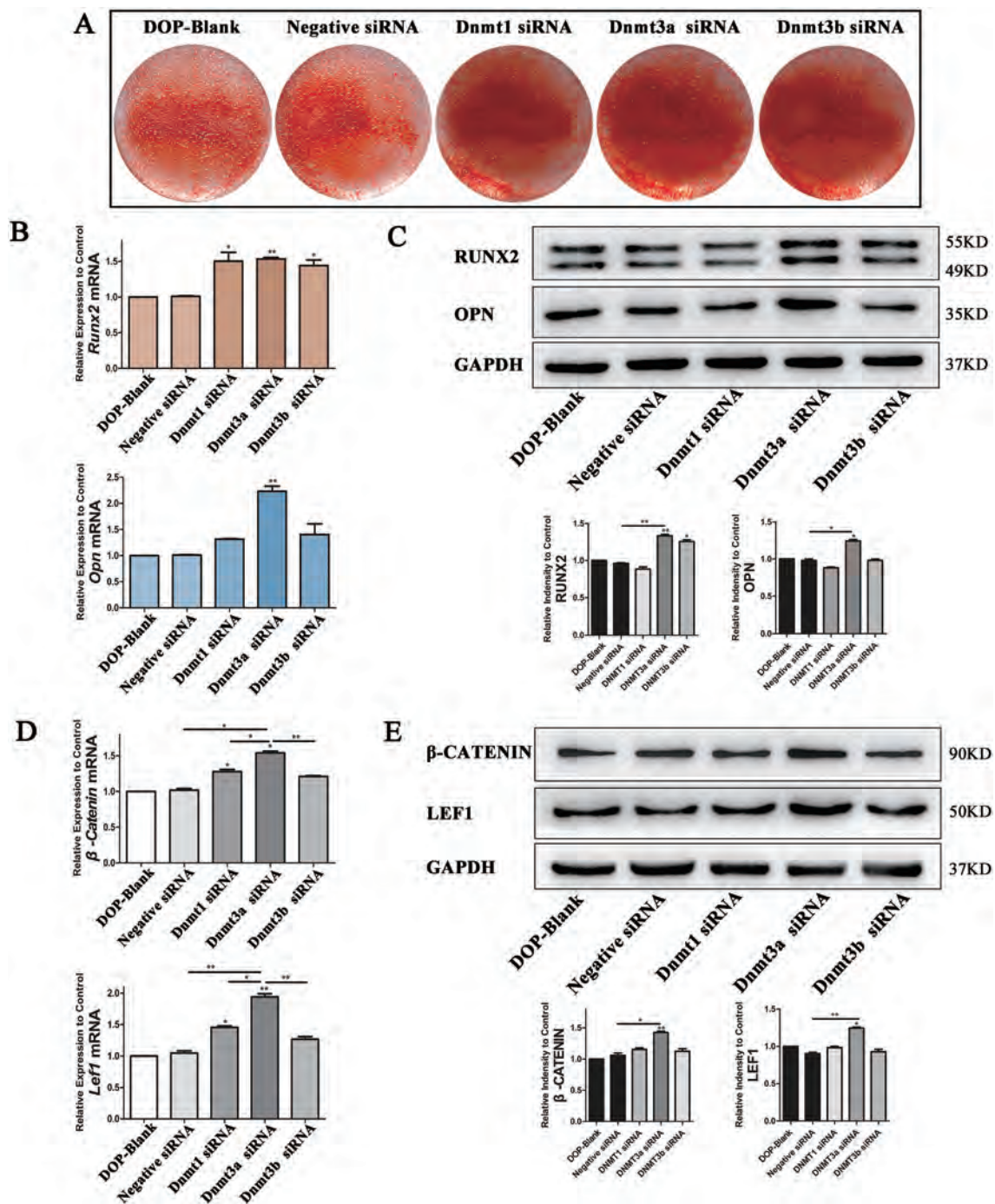
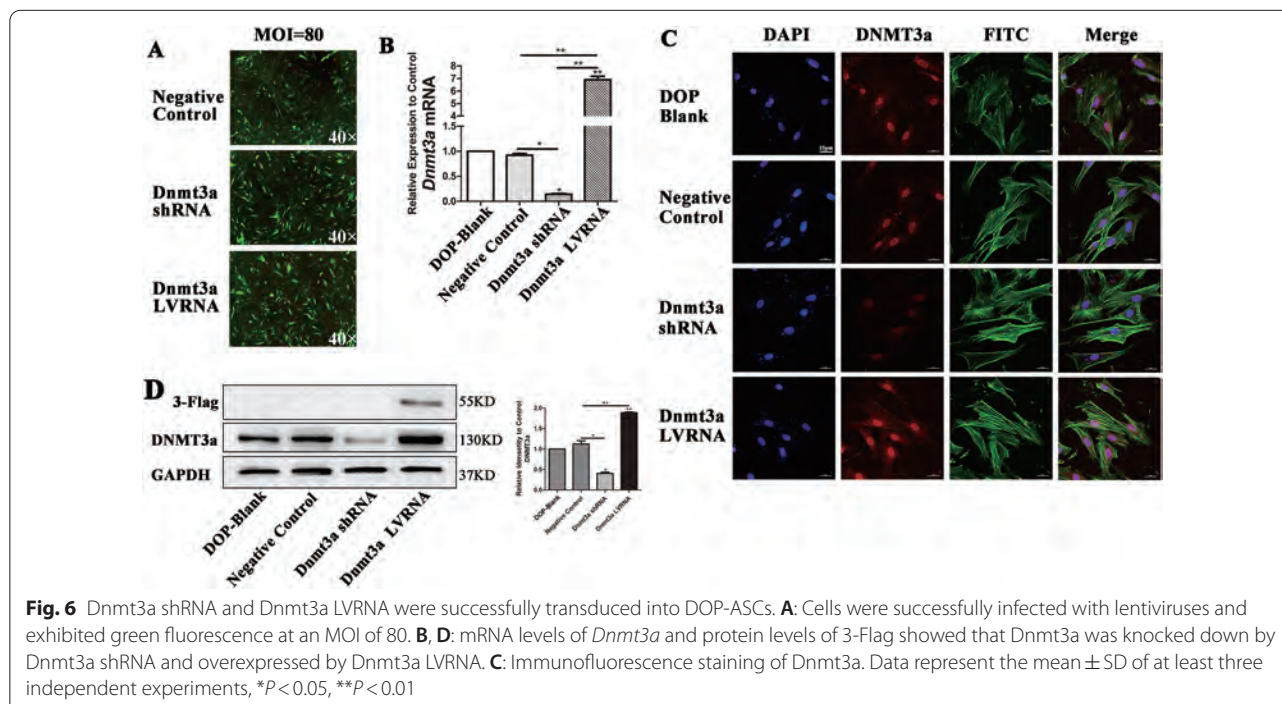


**Fig. 5** *Dnmt* siRNAs increase the osteogenic potential of DOP-ASCs. **A:** Alizarin Red-S staining showing that the formation of mineralized nodules in *Dnmt3a* shRNA was increased compared with that in Negative Control after *Dnmt* siRNA treatment of DOP-ASCs (osteoinduction for 21 days). **B–E:** mRNA and protein levels of Wnt/ $\beta$ -Catenin signaling pathway markers and osteogenesis-related molecules were upregulated after *Dnmt* siRNA transfection into DOP-ASCs (osteoinduction for 4 days). Data represent the mean  $\pm$  SD of at least three independent experiments, \* $P < 0.05$ , \*\* $P < 0.01$



study, we compared DOP-ASCs and control ASCs and demonstrated that osteogenic differentiation and Wnt/ $\beta$ -Catenin signaling pathway were suppressed in ASCs of DOP mice.

The high glucose environment caused by diabetes increases DNA methylation in cells, which affects their differentiation processes [42, 43]. Many studies have suggested that DNA methylation is involved in the osteogenic differentiation of stem cells [44–48]. Wang et al. reported that KDM6A promoted chondrogenic differentiation of periodontal ligament stem cells by demethylation of SOX9 [49]. Zhang et al. reported that a demethylated Runx2 gene in bone marrow mesenchymal stem cells promoted their differentiation into osteoblasts [47]. These studies showed that, during the process of osteogenic differentiation of ASCs, the DNA methylation levels of osteogenesis-specific genes *Dlx5* and *Runx2*, and the CpG island region of the Osterix promoter were downregulated significantly, and the expression of these genes was upregulated. Seman et al. found that the DNA methylation level of the promoter region of the *SLC30A8* gene in a diabetic population was higher than that in non-diabetic patients, which suggested that high DNA methylation of the *SLC30A8* gene affects the occurrence of diabetes [50]. We observed that the DNA methylation levels and expression of DNMT genes in DOP-ASCs were upregulated significantly. After decreasing DNMTs by siRNA, we found that the expression of osteogenic differentiation factors *RUNX2* and *OPN* was relatively

increased, which indicated that DNA methylation had a close relationship with the osteogenic differentiation process of ASCs.

DNA methylation at specific sites is catalyzed by DNMTs, which might play various roles in cell differentiation. Dnmt3a, as the main methyltransferase in embryonic development and differentiation, is mainly located in the chromatin region and is highly expressed in oocytes, spermatogonia, and stem cells [51, 52]. Mark A. Casillas Jr NL et al. found that the expression of Dnmt3a was highly abundant in oocytes, but gradually decreased during maturation [53]. They observed that the overall methylation level of genomic DNA in senescent cells was reduced, which corresponded to the decrease in expression of Dnmt1, while some genes were hypermethylated with high expression of Dnmt3a and Dnmt3b [53]. Disturbances in epigenetic regulation may be a factor that contributes to diseases [54, 55]. In our study, RNA interference was used to silence the expression of Dnmt1, Dnmt3a, and Dnmt3b. Silencing of Dnmt3a promoted the expression of bone-related genes and Wnt/ $\beta$ -Catenin signaling pathway-related genes were induced, thereby promoting the osteogenic differentiation of DOP-ASCs. Overexpression of Dnmt3a by lentivirus infection confirmed that Dnmt3a significantly inhibited the expression of osteogenic-related genes and Wnt/ $\beta$ -Catenin signaling pathway in DOP-ASCs and the osteogenic differentiation ability of DOP-ASCs was restored after inhibition of Dnmt3a.

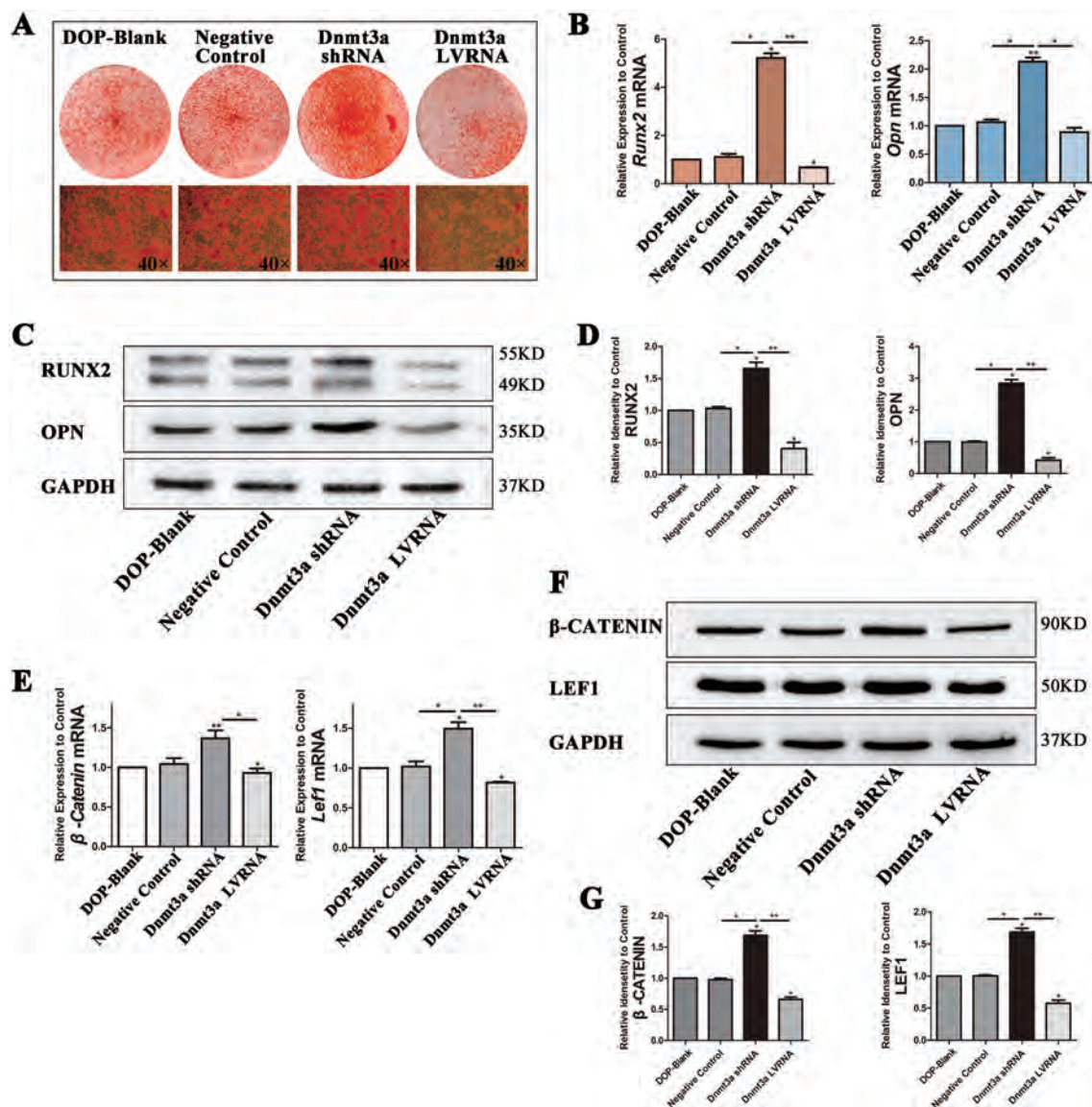


**Fig. 7** Knockdown of Dnmt3a promotes osteogenic differentiation of DOP-ASCs. **A:** Alizarin Red-S staining showing that the formation of mineralized nodules was the highest in the Dnmt3a shRNA group and the lowest in the Dnmt3a LVRNA group (osteinduction for 21 days). **B–D:** mRNA and protein levels of osteogenesis-related molecules were upregulated in the Dnmt3a shRNA group compared with the other three groups (osteinduction for 4 days). **E–G:** mRNA and protein levels of Wnt signaling pathway markers were recovered by knockdown of Dnmt3a. Data represent the mean ± SD of at least three independent experiments, \* $P < 0.05$ , \*\* $P < 0.01$

We also confirmed the osteogenic effects of Dnmt3a in DOP mice in vivo. BCP is considered to be a biomaterial with high porosity and penetration, which creates a favorable microenvironment for bone regeneration [56, 57]. Tang et al. implanted various BCP scaffolds into a critically sized bone defect model in OVX rats and applied Micro-CT to analyze new bone formation [58–60]. In our study, we seeded DOP-ASCs on BCP and implanted the scaffold into a mouse critically sized

skull defect to assess the osteogenic capacity in vivo. Three-dimensional reconstruction of Micro-CT images showed that new bone formation in the Dnmt3a shRNA group had obviously increased compared with that in DOP-ASC and negative control groups. Furthermore, histology of the corresponding tissue samples was consistent with the results of Micro-CT, i.e., the amount of new bone formation in the Dnmt3a shRNA group was more obvious than that in DOP-blank and Negative Control.

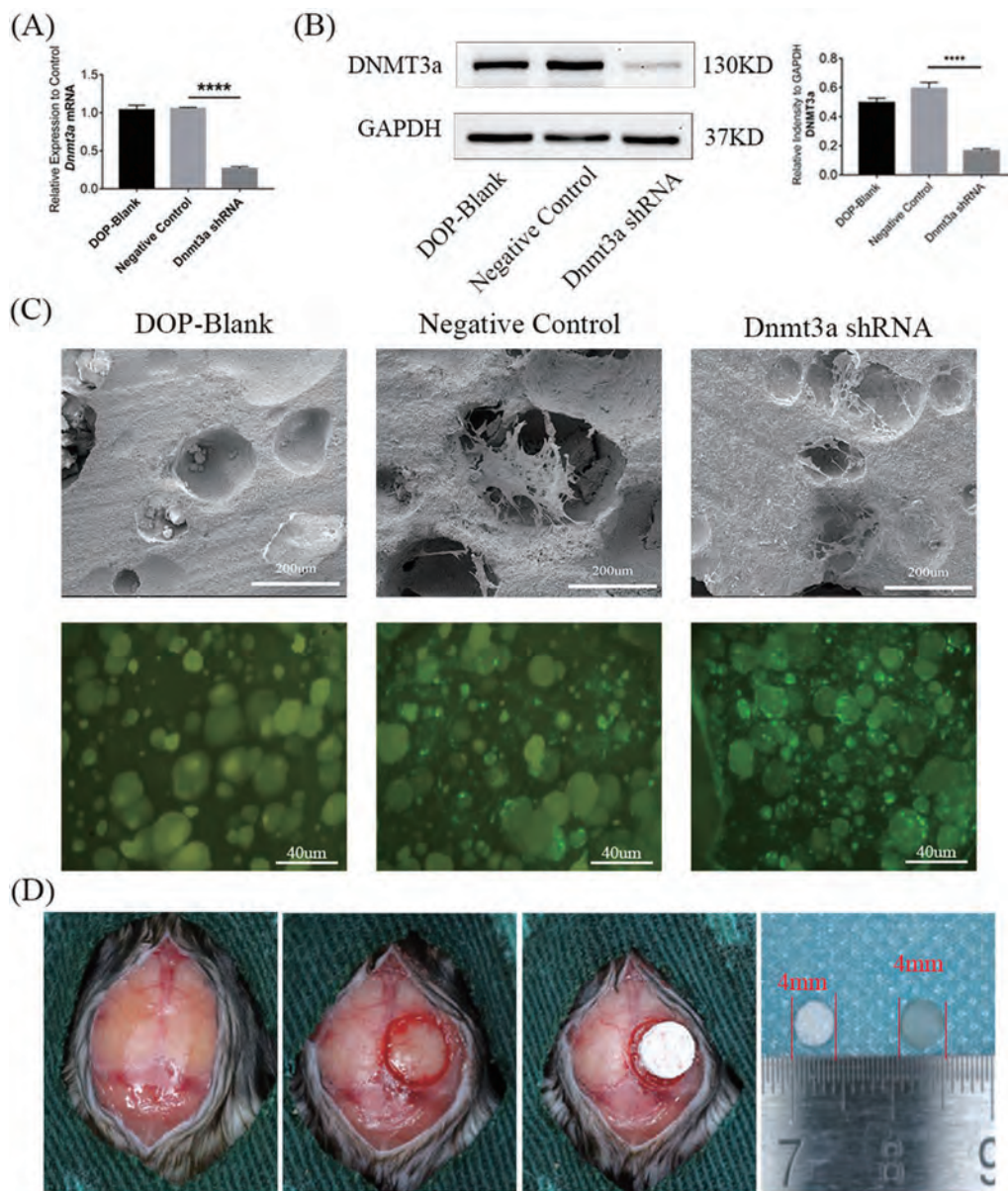


**Fig. 8** BCP was successfully implanted into the skull defect of mice. BCP seeded with transfected DOP-ASCs were implanted into critically sized calvarial defects in DOP mouse models. **A, B:** mRNA and protein levels of Dnmt3a were successfully knocked down by Dnmt3a shRNA (osteoinduction for 3 days). **C:** SEM and fluorescence microscopy showing that DOP-ASCs grew adherently on the surface and pores of BCP. **D:** The DOP mouse model with critically sized calvarial defects was successfully established and BCP seeded with transfected DOP-ASCs were implanted into the defect area

DOP has become a severe public health problem. DNA methylation as a kind of stable epigenetic alteration is involved in bone formation and resorption [61]. Epigenetic modifications play an important role in cell differentiation and development [62]. Many studies have demonstrated that DNA methylation is a therapeutic target for bone diseases [61]. Our study

demonstrated that a high level of Dnmt3a may impair the osteogenic ability of ASCs, and the osteogenic differentiation ability of DOP-ASCs was restored after inhibition of Dnmt3a. Therefore, this study explains the decrease in the osteogenic capacity of DOP-ASCs from the viewpoint of epigenetics and provides a potential therapeutic target for the prevention and treatment of DOP.

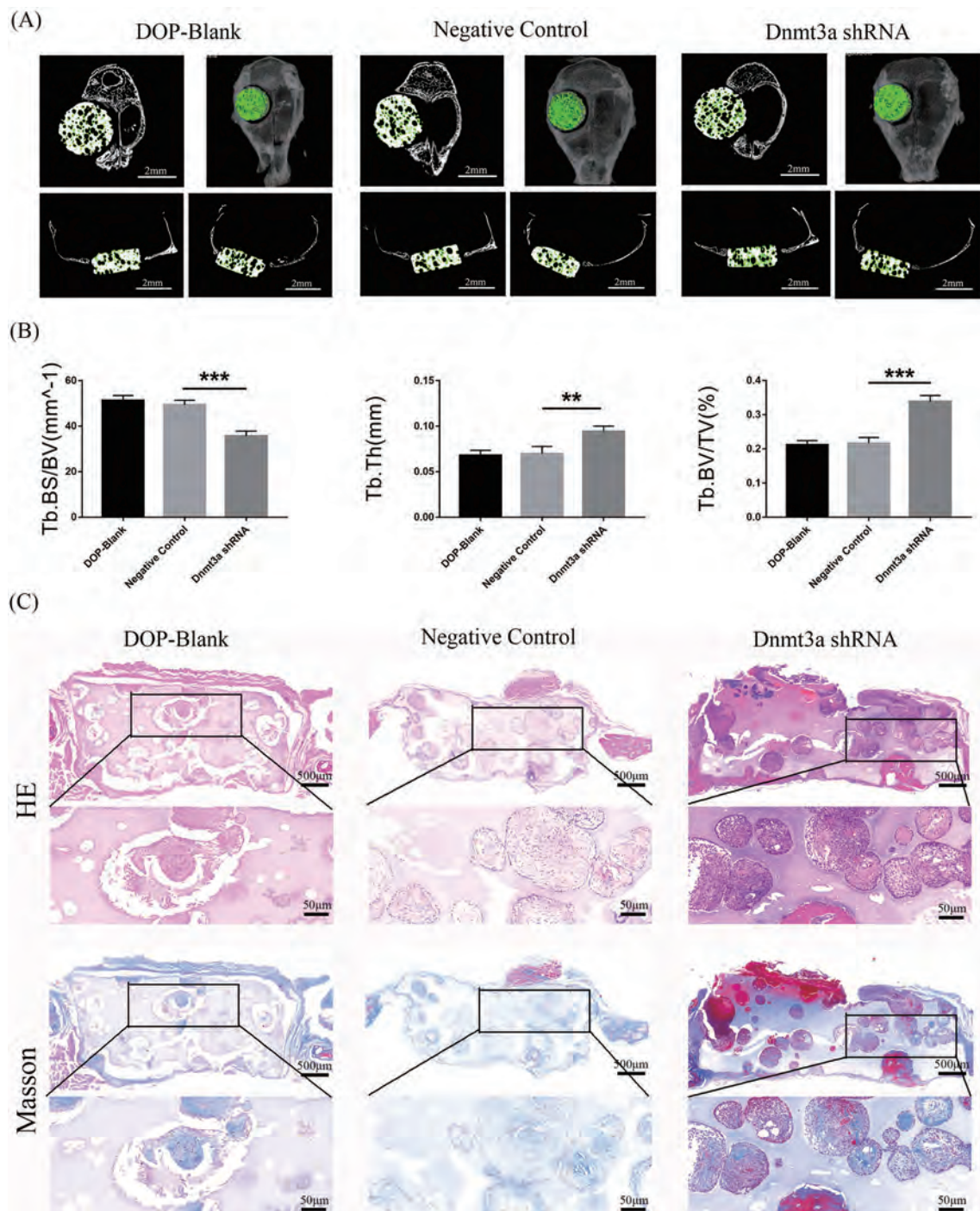


**Fig. 9** Downregulation of Dnmt3a promotes the osteogenic capacity of DOP-ASCs in vivo. **A** Micro-CT showed that the amount of new bone matrix (green) in the Dnmt3a shRNA group was significantly higher than that in DOP-ASC and negative control groups. **B** BV/TV, BS/BV, and TbTh analysis demonstrated that the osteogenic capacity was greatly increased when Dnmt3a was downregulated by shRNA in vivo. Data represent the mean  $\pm$  SD of at least three independent experiments, \* $P < 0.05$ , \*\*\* $P < 0.01$ . **C**: HE and Masson staining of BCP showed that the staining degree in the Dnmt3a shRNA group was stronger than that in DOP-ASC and negative control groups

## Conclusions

Our study showed that Wnt/ $\beta$ -catenin signaling pathway is a major player in the process of osteogenic differentiation of DOP-ASCs and DNA methylation is an important factor that affects the osteogenic differentiation of DOP-ASCs, which has significance for bone regeneration in DOP. Downregulation of Dnmt3a activated Wnt/ $\beta$ -catenin pathway, and promoted the osteogenic differentiation of DOP-ASCs. These findings indicate that Dnmt3a knockdown rescues the impaired osteogenic ability of DOP-ASCs *in vitro* and *in vivo*, thereby providing a possible approach for bone regeneration using DOP-ASCs in DOP patients.

## Abbreviations

DOP: Diabetic osteoporosis; DM: Diabetes mellitus; ASCs: Adipose-derived stem cells; PCR: Quantitative real-time polymerase chain reaction; ALP: Alkaline phosphatase;  $\beta$ -Catenin: Cadherin associated protein; Runx2: Runt-related transcription factor 2; Opn: Osteopontin; GAPDH: Glyceraldehyde phosphate dehydrogenase; DNMT1: DNA methyltransferases 1; DNMT3a: DNA methyltransferases 3a; DNMT3b: DNA methyltransferases 3b; BV/TV: Ratio of bone volume to tissue volume; BS/BV: The area of bone tissue per unit volume; TbTh: Trabecular thickness.

## Acknowledgements

Not applicable.

## Author contributions

All authors have made important contributions to this research. MZ conducted *in vitro* experiments, executed the analysis of the data, and wrote the main manuscript. YG conducted *in vivo* experiments and wrote the main manuscript. QL reviewed and revised the manuscript. HC collected the data. JY established the animal model of diabetic osteoporosis. XC designed the experimental project, analyzed data, and revised the manuscript. JX conceived and designed the experiment, analyzed data, revised the manuscript, and provided funding. All authors have read and approved the final manuscript.

## Funding

This work was funded by National Natural Science Foundation of China (81870746, 81970986, 81771125), Open Project of the State Key Laboratory of Oral Disease Research (SKLOD2021OF08), Joint project of Luzhou Municipal People's Government and Southwest Medical University (2020LZXNYDZ09), Program of Southwest Medical University (2019ZQN167), Program of The Affiliated Stomatological Hospital of Southwest Medical University (202017), Climb Plan Project of The Affiliated Stomatological Hospital of Southwest Medical University (2020QY04), Key Program of Southwest Medical University (2021ZKZD009), and Project of Stomatological Institute of Southwest Medical University (2021XJYS01).

## Availability of data and materials

The datasets generated or analyzed during the current study can be obtained from the corresponding author in accordance with reasonable requirements.

## Declarations

### Ethics approval and consent to participate

The Ethics Committee of Southwest Medical University reviewed and approved the experimental animal procedures, and we conducted animal care and anesthesia in accordance with the guidelines of the Care and Use of Laboratory Animals (Ministry of Science and Technology of China, 2006).

### Consent for publication

Not applicable.

## Competing interests

The authors declare that there is no conflict of interests regarding the publication of this paper.

## Author details

<sup>1</sup>Department of Oral Implantology, The Affiliated Stomatological Hospital of Southwest Medical University, Luzhou 646000, China. <sup>2</sup>State Key Laboratory of Oral Diseases, West China Hospital of Stomatology, Sichuan University, Chengdu 610041, China. <sup>3</sup>Department of Oral and Maxillofacial Surgery, The Affiliated Hospital of Southwest Medical University, Luzhou 646000, China. <sup>4</sup>Luzhou Key Laboratory of Oral & Maxillofacial Reconstruction and Regeneration, The Affiliated Stomatological Hospital of Southwest Medical University, Luzhou 646000, China.

Received: 20 March 2022 Accepted: 23 July 2022

Published online: 04 August 2022

## References

- Motyl KJ, Mccauley LK, McCabe LR. Amelioration of type I diabetes-induced osteoporosis by parathyroid hormone is associated with improved osteoblast survival. *J Cell Physiol.* 2012;227(4):1326–34.
- Zheng HX, Chen J, Zu YX, Wang EZ, Qi SS. Chondroitin sulfate prevents STZ induced diabetic osteoporosis through decreasing blood glucose, antioxidative stress, anti-inflammation and OPG/RANKL expression regulation. *Int J Mol Sci.* 2020;21(15):5303.
- Wang N, Xu P, Wang X, Yao W, Wang B, Wu Y, Shou D. Timosaponin AIII attenuates inflammatory injury in AGEs-induced osteoblast and alloxan-induced diabetic osteoporosis zebrafish by modulating the RAGE/MAPK signaling pathways. *Phytomedicine.* 2020;75: 153247.
- Chen S, Du K, Zou C. Current progress in stem cell therapy for type 1 diabetes mellitus. *Stem Cell Res Ther.* 2020;11(1):275.
- Zhang M, Li Y, Rao P, Huang K, Luo D, Cai X, Xiao J. Blockade of receptors of advanced glycation end products ameliorates diabetic osteogenesis of adipose-derived stem cells through DNA methylation and Wnt signalling pathway. *Cell Prolif.* 2018;51(5): e12471.
- Oliveira PAD, Oliveira AMSD, Pablos AB, Costa FO, Silva GA, Santos JN, Cury PR. Influence of hyperbaric oxygen therapy on peri-implant bone healing in rats with alloxan-induced diabetes. *J Clin Periodontol.* 2012;39(9):879–86.
- Wallner C, Abraham S, Wagner JM, Harati K, Ismer B, Kessler L, Zöllner H, Lehnhardt M, Behr B. Local application of isogenic adipose-derived stem cells restores bone healing capacity in a type 2 diabetes model. *Stem Cells Transl Med.* 2016;5(6):836–44.
- Wu R, Ruan J, Sun Y, Liu M, Sha Z, Fan C, Wu Q. Long non-coding RNA HIF1A-AS2 facilitates adipose-derived stem cells (ASCs) osteogenic differentiation through miR-665/IL6 axis via PI3K/Akt signaling pathway. *Stem Cell Res Ther.* 2018;9(1):348.
- Li S, Liu Y, Tian T, Zhang T, Lin S, Zhou M, Zhang X, Lin Y, Cai X. Bioswitchable delivery of microRNA by framework nucleic acids: application to bone regeneration. *Small.* 2021;17(47): e2104359.
- Vanhatupa S, Ojansivu M, Autio R, Juntunen M, Miettinen S. Bone Morphogenetic protein-2 induces donor-dependent osteogenic and adipogenic differentiation in human adipose stem cells. *Stem Cells Transl Med.* 2015;4(12):1391–402.
- Zhou N, Li Q, Lin X, Hu N, Liao JY, Lin LB, Zhao C, Hu ZM, Liang X, Xu W, Chen H, Huang W. BMP2 induces chondrogenic differentiation, osteogenic differentiation and endochondral ossification in stem cells. *Cell Tissue Res.* 2016;366(1):101–11.
- Uccelli A, Moretta L, Pistoia V. Mesenchymal stem cells in health and disease. *Nat Rev Immunol.* 2008;8(9):726–36.
- Vrtacnik P, Marc J, Ostanek B. Hypoxia mimetic deferoxamine influences the expression of histone acetylation- and DNA methylation-associated genes in osteoblasts. *Connect Tissue Res.* 2015;56(3):228–35.
- Chen Q, Yan W, Duan E. Epigenetic inheritance of acquired traits through sperm RNAs and sperm RNA modifications. *Nat Rev Genet.* 2016;17(12):733–43.
- Portela A, Esteller M. Epigenetic modifications and human disease. *Nat Biotechnol.* 2010;28(10):1057–68.

16. Moore LD, Le T, Fan G. DNA methylation and its basic function. *Neuropsychopharmacology*. 2013;38(1):23–38.
17. Law PP, Holland ML. DNA methylation at the crossroads of gene and environment interactions. *Essays Biochem*. 2019;63(6):717–26.
18. Deplus R, Denis H, Putmans P, Calonne E, Fourrez M, Yamamoto K, Suzuki A, Fuks F. Citrullination of DNMT3A by PAD14 regulates its stability and controls DNA methylation. *Nucleic Acids Res*. 2014;42(13):8285–96.
19. Veland N, Lu Y, Hardikar S, Gaddis S, Zeng Y, Liu B, Estecio MR, Takata Y, Lin K, Tomida MW, Shen J, Saha D, Gowher H, Zhao H, Chen T. DNMT3L facilitates DNA methylation partly by maintaining DNMT3A stability in mouse embryonic stem cells. *Nucleic Acids Res*. 2019;47(1):152–67.
20. Antehh H, Fang J, Song J. Structural basis for impairment of DNA methylation by the DNMT3A R882H mutation. *Nat Commun*. 2020;11(1):2294.
21. Ghayor C, Weber FE. Epigenetic regulation of bone remodeling and its impacts in osteoporosis. *Int J Mol Sci*. 2016;17(9):1446.
22. Liu J, Xiao Q, Xiao J, Niu C, Li Y, Zhang X, Zhou Z, Shu G, Yin G. Wnt/ $\beta$ -catenin signalling: function, biological mechanisms, and therapeutic opportunities. *Signal Transduct Target Ther*. 2022;7(1):3.
23. Peng S, Gao Y, Shi S, Zhao D, Cao H, Fu T, Cai X, Xiao J. LncRNA-AK137033 inhibits the osteogenic potential of adipose-derived stem cells in diabetic osteoporosis by regulating Wnt signaling pathway via DNA methylation. *Cell Prolif*. 2022;55(1): e13174.
24. Yu AX, Xu ML, Yao P, Kwan KK, Liu YX, Duan R, Dong TT, Ko RK, Tsim KW. Corylin, a flavonoid derived from *Psoralea Fructus*, induces osteoblastic differentiation via estrogen and Wnt/ $\beta$ -catenin signaling pathways. *FASEB J*. 2020;34(3):4311–28.
25. Svedlund J, Aurén M, Sundström M, Dralle H, Akerström G, Björklund P, Westin G. Aberrant Wnt/ $\beta$ -catenin signaling in parathyroid carcinoma. *Mol Cancer*. 2010;9:294.
26. Liu T, Wu X, Chen T, Luo Z, Hu X. Downregulation of DNMT3A by miR-708-5p inhibits lung cancer stem cell-like phenotypes through repressing Wnt/ $\beta$ -catenin signaling. *Clin Cancer Res*. 2018;24(7):1748–60.
27. Wong CC, Xu J, Bian X, Wu JL, Kang W, Qian Y, Li W, Chen H, Gou H, Liu D, Yat Luk ST, Zhou Q, Ji F, Chan LS, Shirasawa S, Sung JJ, Yu J. In colorectal cancer cells with mutant KRAS, SLC25A22-mediated glutaminolysis reduces DNA demethylation to increase WNT signaling, stemness, and drug resistance. *Gastroenterology*. 2020;159(6):2163–2180.e6.
28. Wu B, Li Y, Li B, Zhang B, Wang Y, Li L, Gao J, Fu Y, Li S, Chen C, Surani MA, Tang F, Li X, Bao S. DNMTs play an important role in maintaining the pluripotency of leukemia inhibitory factor-dependent embryonic stem cells. *Stem Cell Rep*. 2021;16(3):582–96.
29. Luo W, Zhang L, Huang B, Zhang H, Zhang Y, Zhang F, Liang P, Chen Q, Cheng Q, Tan D, Tan Y, Song J, Zhao T, Haydon RC, Reid RR, Luu HH, Lee MJ, El Dafrawy M, Ji P, He TC, Gou L. BMP9-initiated osteogenic/odontogenic differentiation of mouse tooth germ mesenchymal cells (TGMCS) requires Wnt/ $\beta$ -catenin signalling activity. *J Cell Mol Med*. 2021;25(5):2666–78.
30. Kim JH, Liu X, Wang J, Chen X, Zhang H, Kim SH, Cui J, Li R, Zhang W, Kong Y, Zhang J, Shui W, Lamplot J, Rogers MR, Zhao C, Wang N, Rajan P, Tomal J, Statz J, Wu N, Luu HH, Haydon RC, He TC. Wnt signaling in bone formation and its therapeutic potential for bone diseases. *Ther Adv Musculoskelet Dis*. 2013;5(1):13–31.
31. Wang C, Wang M, Xu T, Zhang X, Lin C, Gao W, Xu H, Lei B, Mao C. Engineering bioactive self-healing antibacterial exosomes hydrogel for promoting chronic diabetic wound healing and complete skin regeneration. *Theranostics*. 2019;9(1):65–76.
32. Abdulameer SA, Sulaiman SA, Hassali MA, Subramaniam K, Sahib MN. Osteoporosis and type 2 diabetes mellitus: what do we know, and what we can do? *Patient Prefer Adherence*. 2012;6:435–48.
33. Heilmeyer U, Hackl M, Skalicky S, Weilner S, Schroeder F, Vierlinger K, Patsch JM, Baum T, Oberbauer E, Lobach I, Burghardt AJ, Schwartz AV, Grillari J, Link TM. Serum miRNA signatures are indicative of skeletal fractures in postmenopausal women with and without type 2 diabetes and influence osteogenic and adipogenic differentiation of adipose tissue-derived mesenchymal stem cells in vitro. *J Bone Miner Res*. 2016;31(12):2173–92.
34. Tencerova M, Figeac F, Ditzel N, Taipaleenmäki H, Nielsen TK, Kassem M. High-fat diet-induced obesity promotes expansion of bone marrow adipose tissue and impairs skeletal stem cell functions in mice. *J Bone Miner Res*. 2018;33:1154–65.
35. Liu Z, Chen T, Sun W, Yuan Z, Yu M, Chen G, Guo W, Xiao J, Tian W. DNA demethylation rescues the impaired osteogenic differentiation ability of human periodontal ligament stem cells in high glucose. *Sci Rep*. 2016;6:27447.
36. Fan T, Qu R, Yu Q, Sun B, Jiang X, Yang Y, Huang X, Zhou Z, Ouyang J, Zhong S, Dai J. Bioinformatics analysis of the biological changes involved in the osteogenic differentiation of human mesenchymal stem cells. *J Cell Mol Med*. 2020;24(14):7968–78.
37. Saidova AA, Vorobjev IA. Lineage commitment, signaling pathways, and the cytoskeleton systems in mesenchymal stem cells. *Tissue Eng Part B Rev*. 2020;26(1):13–25.
38. Wang CG, Hu YH, Su SL, Zhong D. LncRNA DANCER and miR-320a suppressed osteogenic differentiation in osteoporosis by directly inhibiting the Wnt/ $\beta$ -catenin signaling pathway. *Exp Mol Med*. 2020;52(8):1310–25.
39. Hang K, Ying L, Bai J, Wang Y, Kuang Z, Xue D, Pan Z. Knockdown of SERPINE2 enhances the osteogenic differentiation of human bone marrow mesenchymal stem cells via activation of the Wnt/ $\beta$ -catenin signalling pathway. *Stem Cell Res Ther*. 2021;12(1):525.
40. Moldes M, Zuo Y, Morrison RF, Silva D, Park BH, Liu J, Farmer SR. Peroxisome-proliferator-activated receptor  $\gamma$  suppresses Wnt/ $\beta$ -catenin signalling during adipogenesis. *Biochem J*. 2003;376:607–13.
41. Li Y, Wang L, Zhang M, Huang K, Yao Z, Rao P, Cai X, Xiao J. Advanced glycation end products inhibit the osteogenic differentiation potential of adipose-derived stem cells by modulating Wnt/ $\beta$ -catenin signalling pathway via DNA methylation. *Cell Prolif*. 2020;53(6): e12834.
42. Davegårdh C, García-Calzón S, Bacos K, Ling C. DNA methylation in the pathogenesis of type 2 diabetes in humans. *Mol Metab*. 2018;14:12–25.
43. Ling C, Rönn T. Epigenetics in human obesity and type 2 diabetes. *Cell Metab*. 2019;29(5):1028–44.
44. An Y, Zhang H, Wang C, Jiao F, Xu H, Wang X, Luan W, Ma F, Ni L, Tang X, Liu M, Guo W, Yu L. Activation of ROS/MAPKs/NF- $\kappa$ B/NLRP3 and inhibition of efferocytosis in osteoclast-mediated diabetic osteoporosis. *FASEB J*. 2019;33(11):12515–27.
45. Sun B, Shi Y, Yang X, Zhao T, Duan J, Sun Z. DNA methylation: a critical epigenetic mechanism underlying the detrimental effects of airborne particulate matter. *Ecotoxicol Environ Saf*. 2018;161:173–83.
46. Kornicka K, Szlapka-Kosarzewska J, Śmieszek A, Marycz K. 5-Azacytidine and resveratrol reverse senescence and ageing of adipose stem cells via modulation of mitochondrial dynamics and autophagy. *J Cell Mol Med*. 2019;23:237–59.
47. Zhang RP, Shao JZ, Xiang LX. GADD45A protein plays an essential role in active DNA demethylation during terminal osteogenic differentiation of adipose-derived mesenchymal stem cells. *J Biol Chem*. 2011;286:41083–94.
48. Ma W, Zhan Y, Zhang Y, Mao C, Xie X, Lin Y. The biological applications of DNA nanomaterials: current challenges and future directions. *Signal Transduct Target Ther*. 2021;6(1):351.
49. Li ZF, Meng DD, Liu YY, Bi FG, Tian K, Xu JZ, Sun JG, Gu CX, Li Y. Hypoxia inducible factor-3 $\alpha$  promotes osteosarcoma progression by activating KDM3A-mediated demethylation of SOX9. *Chem Biol Interact*. 2021;351: 109759.
50. Seman NA, Mohamud WN, Östenson CG, Brismar K, Gu HF. Increased DNA methylation of the SLC30A8 gene promoter is associated with type 2 diabetes in a Malay population. *Clin Epigenetics*. 2015;7(1):30.
51. Ko YG, Nishino K, Hattori N, Arai Y, Tanaka S, Shiota K. Stage-by-stage change in DNA methylation status of Dnmt1 locus during mouse early development. *J Biol Chem*. 2005;280(10):9627–34.
52. Zhang ZM, Lu R, Wang P, Yu Y, Chen D, Gao L, Liu S, Ji D, Rothbart SB, Wang Y, Wang GG, Song J. Structural basis for DNMT3A-mediated de novo DNA methylation. *Nature*. 2018;554(7692):387–91.
53. Casillas MA Jr, Lopatina N, Andrews LG, Tollefsbol TO. Transcriptional control of the DNA methyl-transferases is altered in aging and neoplastically-transformed human fibroblasts. *Mol Cell Biochem*. 2003;252(1–2):33–43.
54. Lyko F. The DNA methyltransferase family: a versatile toolkit for epigenetic regulation. *Nat Rev Genet*. 2018;19(2):81–92.
55. Jung YD, Park SK, Kang D, Hwang S, Kang MH, Hong SW, Moon JH, Shin JS, Jin DH, You D, Lee JY, Park YY, Hwang JJ, Kim CS, Suh N. Epigenetic regulation of miR-29a/miR-30c/DNMT3A axis controls SOD2 and mitochondrial oxidative stress in human mesenchymal stem cells. *Redox Biol*. 2020;37: 101716.

56. Mofakhami S, Salahinejad E. Biphasic calcium phosphate microspheres in biomedical applications. *J Control Release*. 2021;338:527–36.
57. Liao J, Cai X, Tian T, Shi S, Xie X, Ma Q, Li G, Lin Y. The fabrication of biomimetic biphasic CAN-PAC hydrogel with a seamless interfacial layer applied in osteochondral defect repair. *Bone Res*. 2017;5:17018.
58. Wu T, Yao Z, Tao G, et al. Role of Fzd6 in regulating the osteogenic differentiation of adipose-derived stem cells in osteoporotic mice. *Stem Cell Rev Rep*. 2021;17(5):1889–904.
59. Tang Q, Hu Z, Jin H, Zheng G, Yu X, Wu G, Liu H, Zhu Z, Xu H, Zhang C, Shen L. Erratum: Microporous polysaccharide multilayer coated BCP composite scaffolds with immobilised calcitriol promote osteoporotic bone regeneration both *in vitro* and *in vivo*: Erratum. *Theranostics*. 2021;11(13):6524–5.
60. Wu J, Chen T, Wang Z, Chen X, Qu S, Weng J, Zhi W, Wang J. Joint construction of micro-vibration stimulation and BCP scaffolds for enhanced bioactivity and self-adaptability tissue engineered bone grafts. *J Mater Chem B*. 2020;8(19):4278–88.
61. Yu L, Xia K, Cen X, Huang X, Sun W, Zhao Z, Liu J. DNA methylation of noncoding RNAs: new insights into osteogenesis and common bone diseases. *Stem Cell Res Ther*. 2020;11(1):109.
62. Qi Q, Wang Y, Wang X, Yang J, Xie Y, Zhou J, Li X, Wang B. Histone demethylase KDM4A regulates adipogenic and osteogenic differentiation via epigenetic regulation of C/EBP $\alpha$  and canonical Wnt signaling. *Cell Mol Life Sci*. 2020;77(12):2407–21.

### Publisher's Note

Springer Nature remains neutral with regard to jurisdictional claims in published maps and institutional affiliations.

Ready to submit your research? Choose BMC and benefit from:

- fast, convenient online submission
- thorough peer review by experienced researchers in your field
- rapid publication on acceptance
- support for research data, including large and complex data types
- gold Open Access which fosters wider collaboration and increased citations
- maximum visibility for your research: over 100M website views per year

At BMC, research is always in progress.

Learn more [biomedcentral.com/submissions](https://biomedcentral.com/submissions)



日中笹川医学奨学金制度<学位取得コース>評価書

論文博士：指導教官用



第 43 期

研究者番号：G4305

作成日：2024年3月10日

氏名	江傑	JIANG JIE	性別	M	生年月日	1982/05/15
所属機関（役職）	東莞市人民医院腎内科（副主任醫師）					
研究先（指導教官）	日本医科大学医学部解析人体病理学（清水 章 教授）					
研究テーマ	腎疾患の進展機序の解明とその制御 The elucidation of the mechanism of the development of renal disease, and its control					
専攻種別	<input checked="" type="checkbox"/> 論文博士			<input type="checkbox"/> 課程博士		

研究者評価（指導教官記入欄）

成績状況	優 (良) 可 不可	取得単位数
		取得単位数 / 取得すべき単位数総数
学生本人が行った研究の概要	IgA 腎症自然発症モデルマウスとして知られている HIGA マウスに Lipopolysaccharides (LPS) や Zymosan を投与して炎症反応を増強し、糸球体腎炎の進展や糸球体障害の機序や様式を検討している。その過程で、Gasdermin D (GSDMD) の免疫染色から highly inflammatory form of lytic programmed cell death として知られているパイロトーシス(Pyroptosis)が誘導されていることを示した。炎症反応の増強で糸球体内への浸潤マクロファージに接着した係蹄内皮細胞にパイロトーシスが誘導され、浸潤炎症細胞による係蹄傷害が糸球体腎炎の進展に関わっていることを示した。係蹄内皮細胞障害からの係蹄上皮細胞障害や係蹄基底膜障害への進展について検討を進めている。	
総合評価	【良かった点】 糸球体腎炎の進展過程で壊死やアポトーシスの細胞死は知られているが、新たに炎症性に誘導されるパイロトーシス細胞死が糸球体腎炎の過程で誘導されていることを示すことができた。パイロトーシスの制御により糸球体腎炎の進展を抑制することができ、新規治療戦略につながることを期待している。パイロトーシス細胞死は広く炎症性疾患に関わっている可能性もあり、多くの炎症性疾患に応用が可能で、今後の展開に期待が持てる。	
	【改善すべき点】 得られた結果の考察が不十分で、得られた結果の積み重ねからの次の研究への発展が十分に導かれていない。自身の研究結果を大切に、その考察から連続する研究の大切さを実感され、継続的な研究に進める必要がある。	
	【今後の展望】 IgA 腎症のモデルマウスへの炎症反応増強による糸球体腎炎の進展過程でパイロトーシス細胞死が誘導されている結果が得られた。このモデルマウスでのパイロトーシス誘導機序を明らかにするとともに、臨床腎生検検体で IgA 腎症を含む多くの糸球体腎炎での、炎症性パイロトーシスの誘導を検討し、さらにその細胞死と糸球体腎炎の進展との関連を明らかにする必要がある。	
学位取得見込	現在の研究結果、および今後の展望の研究を丁寧に進めることにより、十分に学位論文の作成は可能であり、かつ、学位の取得は可能であると考え。日本医科大学での論文博士の取得には、研究歴が5年必要であり、中国に帰国後も研究を継続しながら、論文の作成を行うが、研究から得られた結果に基づき、学位論文の作成は可能で、学位の取得は可能であると考え。	
		評価者（指導教官名） 清水 章

# 日中笹川医学奨学金制度<学位取得コース>報告書 研究者用



第43期

研究者番号: G4305

作成日: 2024年3月10日

氏名	江 杰	JIANG JIE	性別	M	生年月日 1982/05/15
所属機関(役職)	東莞市人民医院腎内科(副主任醫師)				
研究先(指導教官)	日本医科大学医学部解析人体病理学(清水 章 教授)				
研究テーマ	腎疾患の進展機序の解明とその制御 The elucidation of the mechanism of the development of renal disease, and its control				
専攻種別	論文博士	<input checked="" type="checkbox"/>	課程博士	<input type="checkbox"/>	

1. 研究概要(1)

1) 目的(Goal)  
Hematuria and proteinuria after infection is the most common clinical manifestation of IgA nephropathy (IgAN). However, the pathophysiological mechanisms is not fully studied because lacking of animal models similar to the patient. Although inflammasome are reported to contribute to immunomodulation following injury, proinflammatory cytokine manufacturing and microvascular barrier dysfunction are unclear, we hypothesized that innate immune-induced HIGA mice will set one active and progressive IgAN model.

2) 戦略(Approach):  
Immunoglobulin A nephropathy (IgAN) is the most common form of primary glomerulonephritis worldwide among patients undergoing renal biopsy, especially in the Asian Pacific region. It's recognized that 20-50% of affected patients progress to kidney failure over 10 to 20 years.(1,2) The most characteristic clinical feature of this disease is hematuria and proteinuria coinciding with or immediately following an upper respiratory or gastrointestinal tract infection. Thus, a dysregulation of innate immunity has been extensively postulated in IgAN.(3) Recent progress in understanding of how metabolic regulation relates to type 2 immunity firstly by considering specifics of metabolism within type 2 immune cells and type 2 immune cells are integrated more broadly into the metabolism of the organism as a whole.(4) Here, recent reports have both confirmed and analyzed in more detail the importance of glycolysis and fatty acid metabolism for the development and airway inflammation initiated by epithelial cells.(5) Glucose metabolism was shown to be essential for the function, proliferation, and differentiation capacity of airway progenitor cells.(6) In contrast, complete inhibition of glycolysis inhibited both the differentiation and proliferation of the progenitor cells.(7) Type 2 immunity has been noticed by researchers in the field of IgAN. Chintalacharuvu S. reported that the glycosylation of IgA produced by murine B cells is altered by Th2 cytokines.(8) Yamada K also find that down-regulation of core 1  $\beta$  1,3-galactosyltransferase and Cosmc by Th2 cytokine alters O-glycosylation of IgA1.(9) However, the effects of type 2 immune-related glycolysis metabolic reprogramming on renal epithelial cells have not been studied in IgAN. Podocytes and proximal tubular epithelial cells (PTECs) is important in the pathogenesis of IgAN.(10) Segmental sclerotic lesions are commonly seen in glomeruli in IgAN, which regarded as a form of podocyte dysregulation and transdifferentiation. In the Oxford Classification, the presence of segmental sclerosis was found to predict an adverse outcome.(11,12) However, evidence has shown that in many cases the sclerotic lesions in IgAN are more like those found in primary focal segmental glomerulosclerosis (FSGS).(13) Detailed biopsy examinations from a homogeneous group of IgAN patients has shown that it was very common to find capsular adhesion without any inflammation in the underlying glomerular tuft. This was present in 41% of cases of IgAN studied, compared with only 8% of cases of lupus glomerulonephritis. In primary FSGS, this figure was 69%.(14) Therefore, in terms of adhesions and segmental sclerosis, IgAN behaves more like primary FSGS than like an immune complex glomerulonephritis. Shimizu's study demonstrated that there was an association between severity of glomerular endothelial cells (GEC) damage and FSGS activity. GEC injury contributes to the process of sclerosis and may be a potential therapeutic target in the future. And GEC injury is associated with the formation of necrotizing and crescentic lesions in crescentic glomerulonephritis.(15,16) They also proved that the severity of GEC injury is associated with infiltrating macrophage heterogeneity in endocapillary proliferative glomerulonephritis.(17) Shimizu's found that GEC injury in acute and chronic glomerular lesions in patients with IgA nephropathy.(18) Hou Fanfan discovered glomerular macrophage can predict IgAN patients' response to subsequent immunosuppression.(19) But the relationship and mechanism of macrophage and GEC injure in IgAN still unknown. Therefore, it's important to focus on type 2 immunity mediates innate immune and develops inflammation in glomeruli and renal tubules in IgAN. A high IgA strain (HIGA) of ddY mice have been reported to constantly increase serum levels of IgA and IL-4 from the age of 10-60 weeks.(20,21) We hypothesis that the innate immune responses of LPS-induced play an important role in activate and progressive pathophysiology due to their metabolism change respond to type 2 cytokines in this inbred murine model of IgAN.

3) 材料と方法 (Materials and methods)

- 3.1. Experimental animals and in vivo mouse models.
- 3.2. Histopathological examination, Light microscopy.
- 3.3. Electron microscopy.
- 3.4. Immunohistochemistry and OPAL IHC, imaging and quantifications.
- 3.5. RNA sequencing, library construction and analysis.
- 3.6. Enzyme-linked immunosorbent assays.
- 3.7. Low vacuum scanning electron microscopy.
- 3.8. Statistical analysis.

## 1. 研究概要(2)

## 4) 実験結果 (Results)

4.1. A model of IgA nephropathy similar to human phenotype was successfully established. During day3–35, proteinuria increased significantly in 36w LPS-induced HIGA mice and part of them accompanied by hematuria. Compared to age matching HIGA mice, under light microscopy, IgA deposition in mesangial region increased significantly, complement activate and mesangial cells proliferated. Under electron microscope, foot process effacement with focal detaching from glomerular basement membrane (GBM).

4.2. Immunohistochemistry showed that CD68+WT1+ cells pyroptosis mediated inflammation and injury with much higher iNOS express in HIGA mice after LPS stimulation at 36w old. But only co-deposition with Arg1 in hematuric HIGA mice.

4.3. CD68+WT1+ cells is aerobic glycolysis metabolic and epigenetic reprogramming after type 2 inflammatory primer.

4.4. After the intervention of LPS in vivo, mitochondrial ROS mediated the pyroptosis of CD68+WT1+ cells, showing significantly enhanced glycolytic and oxidative phosphorylation metabolism, and expressing obvious pro-inflammatory phenotypes of H3K4me3 and H3K27ac. By electron microscopy abnormal mitochondria and lysosome swelling were observed in both podocytes and tubular epithelial cells, and endoplasmic reticulum meshing in endothelial cells.

4.5. NT-GSDMD mediated GBM holes caused hematuria and tubular injury significantly aggravated after GBM broken.

4.6. Blocking GSDMD by disulfiram significantly aggravate proteinuria, activation of the inflammasome promotes CASP8(C362S)-mediated apoptosis and tissue pathology in LPS-HIGA mice.

4.7. CD68+WT1+ cells is distinguished to be yolk sac macrophage of kidney resident macrophages based on their expression of Lyve1 but not MHC-II.

4.8. Zymosan induced monocytes transformed into F4/80 macrophages in the glomeruli in C57B/6 and 36w HIGA mice, but not BALAB/C and 12w HIGA mice.

4.9. F4/80 macrophage expressing iNOS triggered pyroptosis in GEC of zym-primed 36w HIGA mice with high serum IFN- $\gamma$ .

4.10. To further verify which subtypes of human IgAN have the pyroptosis phenotype. And macrophage infiltration predicted the progressive histological change in human kidney biopsy specimen.

## 5) 考察 (Discussion)

In this work, we find that a hallmark of pro-inflammatory CD68+WT1+ cells is the upregulation of aerobic glycolysis in 36w HIGA mice. Type 2 inflammatory induce this kind of cells proliferation and transdifferentiation by increasing glycolytic metabolism and epigenetic reprogramming. LPS stimulates macrophage-like responses by enhancing the state of aerobic glycolysis and oxidative phosphorylation in CD68+WT1+ cells. CD68+WT1+ cells in tubular area is distinguished to be yolk sac macrophage of kidney resident macrophages based on their expression of Lyve1. Pyroptosis is induced CD68+WT1+ cells when ROS levels rise beyond the cellular lysosomal processing capacity, mediate inflammation and podocyte damage. Progressive histological change of segmental sclerosis related to IFN  $\gamma$  and CD68+iNOS+ macrophage induced TNF- $\alpha$  mediated impaired angiogenesis and GEC pyroptosis. The epigenetic state of IL-4-polarized macrophages enables inflammatory cistronic expansion and extended synergistic response to TLR ligands.<sup>22</sup>The glycolysis/HIF-1 $\alpha$  axis defines the inflammatory role of IL-4-primed macrophages.<sup>23</sup>Glycolysis-dependent phagocytic activity of LPS/IL-4-induced macrophages was strongly enhanced as was that of M1 macrophages; however, the energy metabolism of LPS/IL-4-induced macrophages, such as activation state of glycolytic and oxidative phosphorylation, was quite different from that of M1 or M2 macrophages.<sup>24</sup>We found the resident macrophage CD68+WT1+LYVE1+ show proinflammatory phenotype upon LPS stimulation in the HIGA mice with high IL-4. LPS/IL-4-induced CD68+WT1+LYVE1+ cell have a higher ROS production capacity induced pyroptosis. Glycolytic ATP serving as a rheostat to gauge PI3K-Akt-Foxo1 signaling in T cell immunity control CD8+ T cell expansion and differentiation.<sup>25</sup>Aerobic glycolysis promotes T helper 1 cell differentiation through an epigenetic mechanism.<sup>26</sup> IFN- $\gamma$  and IL-4 gene polymorphisms could influence disease susceptibility and disease progression in IgA nephropathy in Japanese patients.<sup>27</sup>IFN- $\gamma$  exposure inhibited basal glycolysis of quiescent primary human coronary artery endothelial cells by 20% through the global transcriptional suppression of glycolytic enzymes resulting from decreased basal HIF1  $\alpha$ .<sup>28</sup>TNF and IFN  $\gamma$  synergistically inhibited endothelial-cell proliferation by up to 80%.<sup>29</sup>When we induced M1 macrophage in the glomeruli, causing GFB barrier both in C57BL/6 and HIGA mice. However, vascular repair and angiogenesis were impaired only in HGA mice with high IFN  $\gamma$ . It shows TNF- $\alpha$  and IFN  $\gamma$  synergistically inhibits angiogenesis following vascular injury induced progressive IgAN tissue change.

In conclusion, CD68+WT1+ cell is progenitor pro-inflammation cell of IgA nephropathy, by which LPS-induced pyroptosis mediates innate immune and develops inflammation state in glomeruli and renal tubules, and the inhibition of its activation is not a safe therapeutic method. F4/80 macrophage induced pyroptosis in GEC relate to progressive histological change in IgAN.

## 6) 参考文献 (References)

- Manno C, et al. *Am J Kidney Dis* 2007; 49: 763–775.
- McGrogan A, et al. *Nephrol Dial Transplant* 2011;26(2):414–30.
- Coppo R, et al. *J Nephrol* 2010; 23: 626–632.
- Agnieszka M, et al. *Immunity* 2023 ;56(4):723–741.
- Lin Y, et al. *Curr Allergy Asthma Rep* 2023;23(1):41–52.
- Li K, et al. *Cell Death Dis* 2019;10:875.
- Hammad H, et al. *Immunity* 2015;43:29–40.
- Chintalacharuvu S. *J Immunol* 1997;159(5):2327–33.
- Yamada K, et al. *Nephrol Dial Transplant* 2010;25: 3890–3897.
- Joseph CKL, et al. *Semin Nephrol* 2018;38(5):485–495.
- Menon MC, et al. *Contribute Nephrol* 2013;181:41–51.
- Cook HT. *Kidney Int* 2011;79:581–3.
- El Karoui K, et al. *Kidney Int* 2011;79:643–54.
- Hill GS, et al. *Kidney Int* 2011;79:635–42.
- Morita M, et al. *Kidney Int Rep* 2022;7(6):1229–1240.
- Fujita E, et al. *J Nippon Med Sch* 2015;82(1):27–35.
- Arai M, et al. *Sci Rep* 2021;11(1):13339.
- Kusano T. *Hum Pathol* 2016;49:135–44.
- Xie D, et al. *J Am Soc Nephrol* 2021;32(12):3187–3196.
- Imai H, et al. *Kidney Int* 1985; 27: 756–761.
- Nogaki F, et al. *Nephrol Dial Transplant* 2000 ;15(8):1146–54.
- Czimmerer Z, et al. *Immunity* 2022;55(11):2006–2026.e6.
- Dang B, et al. *Cell Rep* 2023;42(5):112471.
- Ishida K, et al. *Front Immunol.* 2023 ;14:1111729.
- Xu K, et al. *Science* 2021;371(6527):405–410.
- Peng M. *Science* 2016 ;354(6311):481–484.
- Masutani K, et al. *Am J Kidney Dis* 2003 ;41(2):371–9.
- Lee LYH, et al. *Circulation* 2021;144(20):1612–1628.

## 2. 執筆論文 Publication of thesis ※記載した論文を添付してください。Attach all of the papers listed below.

論文名 1 Title						
掲載誌名 Published journal						
	年	月	巻(号)	頁 ~	頁	言語 Language
第1著者名 First author			第2著者名 Second author			第3著者名 Third author
その他著者名 Other authors						
論文名 2 Title						
掲載誌名 Published journal						
	年	月	巻(号)	頁 ~	頁	言語 Language
第1著者名 First author			第2著者名 Second author			第3著者名 Third author
その他著者名 Other authors						
論文名 3 Title						
掲載誌名 Published journal						
	年	月	巻(号)	頁 ~	頁	言語 Language
第1著者名 First author			第2著者名 Second author			第3著者名 Third author
その他著者名 Other authors						
論文名 4 Title						
掲載誌名 Published journal						
	年	月	巻(号)	頁 ~	頁	言語 Language
第1著者名 First author			第2著者名 Second author			第3著者名 Third author
その他著者名 Other authors						
論文名 5 Title						
掲載誌名 Published journal						
	年	月	巻(号)	頁 ~	頁	言語 Language
第1著者名 First author			第2著者名 Second author			第3著者名 Third author
その他著者名 Other authors						

3. 学会発表 Conference presentation ※筆頭演者として総会・国際学会を含む主な学会で発表したものを記載してくだ

※Describe your presentation as the principal presenter in major academic meetings including general meetings or international me

学会名 Conference					
演題 Topic					
開催日 date	年	月	日	開催地 venue	
形式 method	<input type="checkbox"/> 口頭発表 Oral	<input type="checkbox"/> ポスター発表 Poster	言語 Language	<input type="checkbox"/> 日本語	<input type="checkbox"/> 英語 <input type="checkbox"/> 中国語
共同演者名 Co-presenter					
学会名 Conference					
演題 Topic					
開催日 date	年	月	日	開催地 venue	
形式 method	<input type="checkbox"/> 口頭発表 Oral	<input type="checkbox"/> ポスター発表 Poster	言語 Language	<input type="checkbox"/> 日本語	<input type="checkbox"/> 英語 <input type="checkbox"/> 中国語
共同演者名 Co-presenter					
学会名 Conference					
演題 Topic					
開催日 date	年	月	日	開催地 venue	
形式 method	<input type="checkbox"/> 口頭発表 Oral	<input type="checkbox"/> ポスター発表 Poster	言語 Language	<input type="checkbox"/> 日本語	<input type="checkbox"/> 英語 <input type="checkbox"/> 中国語
共同演者名 Co-presenter					
学会名 Conference					
演題 Topic					
開催日 date	年	月	日	開催地 venue	
形式 method	<input type="checkbox"/> 口頭発表 Oral	<input type="checkbox"/> ポスター発表 Poster	言語 Language	<input type="checkbox"/> 日本語	<input type="checkbox"/> 英語 <input type="checkbox"/> 中国語
共同演者名 Co-presenter					

4. 受賞(研究業績) Award (Research achievement)

名称 Award name	国名 Country		受賞年 Year of	年	月
	国名 Country		受賞年 Year of	年	月

## 5. 本研究テーマに関わる他の研究助成金受給 Other research grants concerned with your research theme

受給実績 Receipt record	<input type="checkbox"/> 有 <input checked="" type="checkbox"/> 無
助成機関名称 Funding agency	
助成金名称 Grant name	
受給期間 Supported period	年 月 ~ 年 月
受給額 Amount received	円
受給実績 Receipt record	<input type="checkbox"/> 有 <input checked="" type="checkbox"/> 無
助成機関名称 Funding agency	
助成金名称 Grant name	
受給期間 Supported period	年 月 ~ 年 月
受給額 Amount received	円

## 6. 他の奨学金受給 Another awarded scholarship

受給実績 Receipt record	<input type="checkbox"/> 有 <input checked="" type="checkbox"/> 無
助成機関名称 Funding agency	
奨学金名称 Scholarship name	
受給期間 Supported period	年 月 ~ 年 月
受給額 Amount received	円

## 7. 研究活動に関する報道発表 Press release concerned with your research activities

※記載した記事を添付してください。Attach a copy of the article described below

報道発表 Press release	<input type="checkbox"/> 有 <input checked="" type="checkbox"/> 無	発表年月日 Date of release	
発表機関 Released medium			
発表形式 Release method	・新聞 ・雑誌 ・Web site ・記者発表 ・その他( )		
発表タイトル Released title			

## 8. 本研究テーマに関する特許出願予定 Patent application concerned with your research theme

出願予定 Scheduled	<input type="checkbox"/> 有 <input checked="" type="checkbox"/> 無	出願国 Application	
出願内容(概要) Application contents			

## 9. その他 Others

--

指導責任者(記名) 清水 章

日中笹川医学奨学金制度＜学位取得コース＞中間評価書

論文博士：指導教官用



第 43 期

研究者番号：G4306

作成日：2024年3月10日

氏名	王 晴	WANG QING	性別	F	生年月日	1985/12/20
所属機関（役職）	中国医科大学附属第四医院胸部外科(主治医師)					
研究先（指導教官）	順天堂大学医学部消化器外科講座上部消化管外科学(峯 真司 教授)					
研究テーマ	食道癌に対する基礎的臨床的研究 Basic and clinical researches of esophageal cancer					
専攻種別	<input checked="" type="checkbox"/> 論文博士			<input type="checkbox"/> 課程博士		

研究者評価（指導教官記入欄）

成績状況	優 良 可 不可	取得単位数
		取得単位数 / 取得すべき単位数総数
学生本人が行った研究の概要	<p>1 食道癌に対する食道切除術において High volume center は low volume center と比べて全生存期間に差があるということは知られているが症例数の適切な cutoff 値は知られていない。この件について Meta-analysis を行った。Cutoff 値は示せなかったが、症例数が増えると一貫して生存期間が改善するというを示し論文化した。</p> <p>2 食道癌手術においてリンパ節郭清個数と予後が関連することは知られているが、この事実はある程度のリンパ節郭清が必要であることを示していると考えられている。しかし、同程度の手術でもリンパ節個数に個人差があることも多く、同じ手術を行った場合の個人差が予後と関連するかということについて検討し、同程度の郭清を行った場合にはリンパ節個数と予後に関連はないことを示した（論文作成中）</p> <p>3 食道癌検体を用いてオルガノイドを作成し、cancer-associated fibroblast の機能解析を行った</p>	
総合評価	<p>【良かった点】 毎日熱心に基礎的研究を行った。 臨床研究においても論文作成も早く、論文や研究の改善点を指摘した場合も Response も早く修正できた。</p> <p>【改善すべき点】 Covid 19 感染症流行期に来日したためであるが、研究以外ではあまり交流が持てなかった。基礎研究についてはやや時間が短く十分な成果が出なかった。</p> <p>【今後の展望】 中国に戻られたあとに食道癌手術や研究について中国を引っ張って行っていただきたいし、我々とも keep in touch できればと思う。</p>	
学位取得見込	博士審査も終了し、取得予定である	
評価者（指導教官名） 峯 真司		

# 日中笹川医学奨学金制度<学位取得コース>報告書 研究者用



第43期

研究者番号: G4306

作成日: 2024年3月10日

氏名	王 晴	WANG QING	性別	F	生年月日	1985/12/20
所属機関(役職)	中国医科大学附属第四医院胸部外科(主治医師)					
研究先(指導教官)	順天堂大学医学部消化器外科講座上部消化管外科学(峯 真司 教授)					
研究テーマ	食道癌に対する基礎的臨床的研究 Basic and clinical researches of esophageal cancer					
専攻種別	論文博士	<input checked="" type="checkbox"/>	課程博士	<input type="checkbox"/>		

## 1. 研究概要(1)

### 1) 目的(Goal)

Esophageal cancer is the eighth most commonly diagnosed cancer and the sixth most common cause of cancer death in the world [1]. In addition to esophagectomy, there are neoadjuvant chemotherapy, chemoradiotherapy molecular targeted therapy, immunotherapy, or a combination of modalities, but the prognosis for esophageal cancer is extremely poor, with a 5-year survival rate of less than 30% [2, 3]. Therefore, it is urgent to identify biomarkers that can predict treatment effects and to find new molecular targets.

Fibroblasts present in tumors are called cancer-associated fibroblasts (CAFs), which have been shown to promote cancer cell proliferation and malignant transformation [4]. Research on CAFs' function has been active in breast cancer, pancreatic cancer, and other areas, and some reports suggest that they contribute to tumor growth, metastasis, and treatment resistance in esophageal cancer [5].

In this study, we used immortalized fibroblasts to create CAFs using semi-artificial methods. CAFs produced by this method are called experimental CAFs, which have long-term stability and can be cultured on a large scale. They can also be used in in vitro co-culture experiments of cancer cells and CAFs, as well as in in vivo co-implantation experiments of cancer cells and CAFs. By creating these experimental CAFs and using them in various experiments, we will elucidate the characteristics and functions of CAFs in esophageal cancer. In addition to cancer cell lines, we also aim to create experimental CAFs that are more similar to in vivo CAFs by using cancer organoids in this study.

### 2) 戦略(Approach)

To create experimental CAF and analyze it, two different types of cells (immortalized normal esophageal fibroblasts and patient-derived esophageal cancer organoids) were co-transplanted into immunodeficient mice.

### 3) 材料と方法(Materials and methods)

#### ①Immortalization of normal esophageal fibroblasts:

Immortalized fibroblasts are obtained by introducing the hTERT (telomerase) gene into fibroblasts derived from human esophagus. The fibroblasts are obtained from Cell Biologics and normal human esophagus specimens.

#### ②Establishing patient-derived esophageal cancer organoids

Organoids derived from human esophageal cancer samples provide a novel and unique platform to model esophageal development, homeostatic regenerative differentiation, and benign and malignant esophageal diseases.

#### ③Creation of experimental CAFs using esophageal cancer cells (cell lines/organoids):

CAF can be obtained by primary culture from surgical samples, but there are reports that their properties change after several passages and they become unstable, and it is difficult to use them as stable experimental materials due to cell aging. The method for creating experimental CAFs was developed in this course. This cell can be massively propagated and its properties are stable.

Immortalized fibroblasts with antibiotic resistance are mixed with cancer cells and co-transplanted into immunodeficient mice to convert fibroblasts into CAFs within the tumor.

#### ④Analysis using established experimental CAFs:

By comparing the gene expression of normal fibroblasts and established experimental CAFs, signal pathways that are upregulated in CAFs are identified, and the mechanism of CAF formation is predicted. In addition, functional evaluation is performed by mixing experimental CAFs with cancer cells and transplanting them into mice (to investigate tumor growth and cancer malignancy function).

### 4) 実験結果(Results)

#### ①Immortalization of normal esophageal fibroblasts:

By detecting the population doubling level (PDL) of the cells, it was determined that the normal esophageal fibroblasts had become immortalized normal esophageal fibroblasts (by introduction of hTERT gene (hygromycin resistance)).

#### ②Establishing patient-derived esophageal cancer organoids

Esophageal cancer organoids have been established using patient-derived esophageal cancer tissue. These are three-dimensional culture systems that can be grown in vitro to form miniaturized, self-organizing structures that mimic the architecture and function of the original tumor. These organoids are composed of different types of cells, including cancer cells, stromal cells, and immune cells, and can recapitulate the heterogeneity and complexity of the original tumor.

#### ③Establishing an esophageal cancer patient-derived xenograft (PDX) model by co-transplanting esophageal cancer

## 1. 研究概要(2)

organoids or esophageal cancer cell lines with immortalized esophageal fibroblast. Inject subcutaneous injections into both sides of the mice, and tumor were resected 2 weeks, 1 month, 2 month, and 3 months after co-transplantation, respectively. Then culture the cells in medium containing hygromycin. Only hygromycin-resistance fibroblast can survive and proliferate.

④Performing Immunohistochemistry on the resected tumor, we found that the expression of human vimentin 9 was very little.

⑤Immunofluorescent staining revealed that human vimentin 9 was expressed in counterpart fibroblasts, and exp-CAFs.  $\alpha$ -SMA was expressed in counterpart fibroblasts, exp-CAFs and 10T1/2.

⑥Examining marker expression of CAF subtypes mCAF and iCAF by RT-qPCR.

KYSE150 esophageal cancer+ Normal hTERT fibroblast cells tend to express SDF1 (CXCL12). ): KYSE270 esophageal cancer + Normal hTERT fibroblast cells can be seen upregulation of inflammatory cytokines.

## 5) 考察(Discussion)

This study represents the first establishment of experimental cancer-associated fibroblasts (CAFs) related to esophageal cancer. Experimental CAFs can be used to simulate the microenvironment surrounding esophageal cancer cells, providing researchers with a more physiologically relevant experimental platform.

CAFs are stromal cells that are mainly induced in tumor microenvironment, and are involved in cancer cell proliferation and invasion, angiogenesis, inflammation, immunosuppress, and extracellular matrix remodeling [6]. There are 2 main subtypes of CAFs: myofibroblastic CAFs (mCAFs), which is a subtype that expresses  $\alpha$ -SMA and exhibits myofibroblast phenotype, and inflammatory CAFs (iCAFs), which is a subtype that produces inflammatory cytokines [7]. In our study, we successfully established two subtypes of CAFs respectively.

CAFs can be used to simulate the microenvironment surrounding cancer cells, providing researchers with a more physiologically relevant experimental platform. CAFs can also be utilized for screening potential drugs targeting the cancer microenvironment, as well as assessing the effects of these drugs on the microenvironment. Research on CAFs can aid in the development of therapeutic strategies targeting the cancer microenvironment to improve cancer treatment outcomes [6, 8].

Experimental cancer-associated fibroblasts (CAFs) are CAFs created using immortalized fibroblasts through semi-artificial methods. CAFs produced using this method have long-term stability and can be cultivated on a large scale. They can also be used in in vitro co-culture experiments of cancer cells and CAFs, as well as in in vivo co-implantation experiments of cancer cells and CAFs. By creating these experimental CAFs and using them in various experiments, we will elucidate the characteristics and functions of CAFs in esophageal cancer.

In our study, we also use establish patient-derived esophageal cancer organoids. Organoid technology can cultivate gastrointestinal tumors in a way that preserves their genetic, phenotypic, and behavioral characteristics, which is far superior to traditional tumor cell cultures [9].

In subsequent experiments, we need to conduct another round of animal transplant experiments to ensure that the performance of experimental CAF is more stable. Then study the mechanism of CAF's influence on esophageal cancer tumorigenesis.

## 6) 参考文献(References)

1. Sung H, Ferlay J, Siegel RL, Laversanne M, Soerjomataram I, Jemal A, Bray F. Global Cancer Statistics 2020: GLOBOCAN Estimates of Incidence and Mortality Worldwide for 36 Cancers in 185 Countries. *CA Cancer J Clin.* 2021;71(3):209-249.
2. Allemani C, Matsuda T, Di Carlo V, Harewood R, Matz M, Nikšić M, Bonaventure A, Valkov M, Johnson CJ, Estève J, Ogundiyi OJ, Azevedo E Silva G, Chen WQ, Eser S, Engholm G, Stiller CA, Monnereau A, Woods RR, Visser O, Lim GH, Aitken J, Weir HK, Coleman MP; CONCORD Working Group. Global surveillance of trends in cancer survival 2000-14 (CONCORD-3): analysis of individual records for 37 513 025 patients diagnosed with one of 18 cancers from 322 population-based registries in 71 countries. *Lancet.* 2018;391(10125):1023-1075.
3. Siegel RL, Miller KD, Fuchs HE, Jemal A. Cancer statistics, 2022. *CA Cancer J Clin.* 2022;72(1):7-33.
4. Orimo A, Gupta PB, Sgroi DC, Arenzana-Seisdedos F, Delaunay T, Naeem R, Carey VJ, Richardson AL, Weinberg RA. Stromal fibroblasts present in invasive human breast carcinomas promote tumor growth and angiogenesis through elevated SDF-1/CXCL12 secretion. *Cell.* 2005;121(3):335-348.
5. Qiao Y, Zhang C, Li A, Wang D, Luo Z, Ping Y, Zhou B, Liu S, Li H, Yue D, Zhang Z, Chen X, Shen Z, Lian J, Li Y, Wang S, Li F, Huang L, Wang L, Zhang B, Yu J, Qin Z, Zhang Y. IL6 derived from cancer-associated fibroblasts promotes chemoresistance via CXCR7 in esophageal squamous cell carcinoma. *Oncogene.* 2018;37(7):873-883.
6. Biffi G, Tuveson DA. Diversity and Biology of Cancer-Associated Fibroblasts. *Physiol Rev.* 2021;101(1):147-176.
7. Lavie D, Ben-Shmuel A, Erez N, Scherz-Shouval R. Cancer-associated fibroblasts in the single-cell era. *Nat Cancer.* 2022;3(7):793-807.
8. Chen X, Song E. Turning foes to friends: targeting cancer-associated fibroblasts. *Nat Rev Drug Discov.* 2019;18(2):99-115.
9. Lau HCH, Kranenburg O, Xiao H, Yu J. Organoid models of gastrointestinal cancers in basic and translational research. *Nat Rev Gastroenterol Hepatol.* 2020;17(4):203-222.

## 2. 執筆論文 Publication of thesis ※記載した論文を添付してください。Attach all of the papers listed below.

論文名 1 Title	Association of Hospital Volume and Long-term Survival After Esophagectomy: A Systematic Review and Meta-Analysis					
掲載誌名 Published journal	Front Surg					
	2023 年 4 月	10 巻(号)	1E+06 頁 ~	頁	言語 Language	English
第1著者名 First author	Qing Wang	第2著者名 Second author	Shinji Mine	第3著者名 Third author	Motomi Nasu	
その他著者名 Other authors	Tetsu Fukunaga , Shuko Nojiri, Chun-Dong Zhang					
論文名 2 Title	Effect of the number of dissected lymph nodes on the survival of patients who underwent the same extent of lymphadenectomy for esophageal cancer					
掲載誌名 Published journal	The article is being submitted.					
	年 月	巻(号)	頁 ~	頁	言語 Language	
第1著者名 First author	Qing Wang	第2著者名 Second author	Shinji Mine	第3著者名 Third author	Takashi Hashimoto	
その他著者名 Other authors	Hajime Orita, Motomi Nasu, Tadasuke Hashiguchi, Sanae Kaji, Daisuke Fujiwara, Yukinori Yube, Asako Ozaki, Kohei Yoshino, Yuki Sugahara, Akira Kubota, Hiroki Egawa, Tetsu Fukunaga, Yoshiaki Kajiyama, Masahiko Tsurumaru					
論文名 3 Title						
掲載誌名 Published journal						
	年 月	巻(号)	頁 ~	頁	言語 Language	
第1著者名 First author		第2著者名 Second author		第3著者名 Third author		
その他著者名 Other authors						
論文名 4 Title						
掲載誌名 Published journal						
	年 月	巻(号)	頁 ~	頁	言語 Language	
第1著者名 First author		第2著者名 Second author		第3著者名 Third author		
その他著者名 Other authors						
論文名 5 Title						
掲載誌名 Published journal						
	年 月	巻(号)	頁 ~	頁	言語 Language	
第1著者名 First author		第2著者名 Second author		第3著者名 Third author		
その他著者名 Other authors						

## 3. 学会発表 Conference presentation ※筆頭演者として総会・国際学会を含む主な学会で発表したものを記載してください

※Describe your presentation as the principal presenter in major academic meetings including general meetings or international meetings

学会名 Conference	No			
演題 Topic				
開催日 date	年	月	日	開催地 venue
形式 method	<input type="checkbox"/> 口頭発表 Oral	<input type="checkbox"/> ポスター発表 Poster	言語 Language	<input type="checkbox"/> 日本語 <input type="checkbox"/> 英語 <input type="checkbox"/> 中国語
共同演者名 Co-presenter				
学会名 Conference				
演題 Topic				
開催日 date	年	月	日	開催地 venue
形式 method	<input type="checkbox"/> 口頭発表 Oral	<input type="checkbox"/> ポスター発表 Poster	言語 Language	<input type="checkbox"/> 日本語 <input type="checkbox"/> 英語 <input type="checkbox"/> 中国語
共同演者名 Co-presenter				
学会名 Conference				
演題 Topic				
開催日 date	年	月	日	開催地 venue
形式 method	<input type="checkbox"/> 口頭発表 Oral	<input type="checkbox"/> ポスター発表 Poster	言語 Language	<input type="checkbox"/> 日本語 <input type="checkbox"/> 英語 <input type="checkbox"/> 中国語
共同演者名 Co-presenter				
学会名 Conference				
演題 Topic				
開催日 date	年	月	日	開催地 venue
形式 method	<input type="checkbox"/> 口頭発表 Oral	<input type="checkbox"/> ポスター発表 Poster	言語 Language	<input type="checkbox"/> 日本語 <input type="checkbox"/> 英語 <input type="checkbox"/> 中国語
共同演者名 Co-presenter				

## 4. 受賞(研究業績) Award (Research achievement)

名称 Award name	No			
	国名 Country		受賞年 Year of award	年 月
名称 Award name				
	国名 Country		受賞年 Year of award	年 月

## 5. 本研究テーマに関わる他の研究助成金受給 Other research grants concerned with your research theme

受給実績 Receipt record	<input type="checkbox"/> 有 <input checked="" type="checkbox"/> 無
助成機関名称 Funding agency	
助成金名称 Grant name	
受給期間 Supported period	年 月 ~ 年 月
受給額 Amount received	円
受給実績 Receipt record	<input type="checkbox"/> 有 <input checked="" type="checkbox"/> 無
助成機関名称 Funding agency	
助成金名称 Grant name	
受給期間 Supported period	年 月 ~ 年 月
受給額 Amount received	円

## 6. 他の奨学金受給 Another awarded scholarship

受給実績 Receipt record	<input type="checkbox"/> 有 <input checked="" type="checkbox"/> 無
助成機関名称 Funding agency	
奨学金名称 Scholarship name	
受給期間 Supported period	年 月 ~ 年 月
受給額 Amount received	円

## 7. 研究活動に関する報道発表 Press release concerned with your research activities

※記載した記事を添付してください。Attach a copy of the article described below

報道発表 Press release	<input type="checkbox"/> 有 <input checked="" type="checkbox"/> 無	発表年月日 Date of release	
発表機関 Released medium			
発表形式 Release method	・新聞 ・雑誌 ・Web site ・記者発表 ・その他( )		
発表タイトル Released title			

## 8. 本研究テーマに関する特許出願予定 Patent application concerned with your research theme

出願予定 Scheduled	<input type="checkbox"/> 有 <input checked="" type="checkbox"/> 無	出願国 Application	
出願内容(概要) Application contents			

## 9. その他 Others

--

指導責任者(記名) 峯 真司



## OPEN ACCESS

## EDITED BY

Atalel Fentahun Awedew,  
Addis Ababa University, Ethiopia

## REVIEWED BY

François Dépret,  
Assistance Publique Hopitaux De Paris, France  
Yasuhiro Tsubosa,  
Shizuoka Cancer Center, Japan

## \*CORRESPONDENCE

Shinji Mine  
✉ s.mine.gv@juntendo.ac.jp

## SPECIALTY SECTION

This article was submitted to Visceral Surgery, a section of the journal Frontiers in Surgery

RECEIVED 13 February 2023

ACCEPTED 27 March 2023

PUBLISHED 21 April 2023

## CITATION

Wang Q, Mine S, Nasu M, Fukunaga T, Nojiri S and Zhang C-D (2023) Association of hospital volume and long-term survival after esophagectomy: A systematic review and meta-analysis.  
Front. Surg. 10:1161938.  
doi: 10.3389/fsurg.2023.1161938

## COPYRIGHT

© 2023 Wang, Mine, Nasu, Fukunaga, Nojiri and Zhang. This is an open-access article distributed under the terms of the [Creative Commons Attribution License \(CC BY\)](https://creativecommons.org/licenses/by/4.0/). The use, distribution or reproduction in other forums is permitted, provided the original author(s) and the copyright owner(s) are credited and that the original publication in this journal is cited, in accordance with accepted academic practice. No use, distribution or reproduction is permitted which does not comply with these terms.

# Association of hospital volume and long-term survival after esophagectomy: A systematic review and meta-analysis

Qing Wang<sup>1,2</sup>, Shinji Mine<sup>1\*</sup>, Motomi Nasu<sup>1</sup>, Tetsu Fukunaga<sup>1</sup>, Shuko Nojiri<sup>3</sup> and Chun-Dong Zhang<sup>4</sup>

<sup>1</sup>Department of Esophageal and Gastroenterological Surgery, Juntendo University Graduate School of Medicine, Tokyo, Japan, <sup>2</sup>Department of Thoracic Surgery, The Fourth Affiliated Hospital of China Medical University, Shenyang, China, <sup>3</sup>Medical Technology Innovation Center, Juntendo University, Tokyo, Japan, <sup>4</sup>Department of Gastrointestinal Surgery, Graduate School of Medicine, The University of Tokyo, Tokyo, Japan

**Background:** It remains controversial whether esophageal cancer patients may benefit from esophagectomy in specialized high-volume hospitals. Here, the effect of hospital volume on overall survival (OS) of esophageal cancer patients post esophagectomy was assessed.

**Methods:** PubMed, Embase, and Cochrane Library were systematically searched for relevant published articles between January 1990 and May 2022. The primary outcome was OS after esophagectomy in high- vs. low-volume hospitals. Random effect models were applied for all meta-analyses. Subgroup analysis were performed based on volume grouping, sample size, study country, year of publication, follow-up or study quality. Sensitivity analyses were conducted using the leave-one-out method. The Newcastle-Ottawa Scale was used to assess the study quality. This study followed the Preferred Reporting Items for Systematic Reviews and Meta-analysis guidance, and was registered (identifier: INPLASY202270023).

**Results:** A total of twenty-four studies with 113,014 patients were finally included in the meta-analysis. A significant improvement in OS after esophagectomy was observed in high-volume hospitals as compared to that in their low-volume counterparts (HR: 0.77; 95% CI: 0.71–0.84,  $P < 0.01$ ). Next, we conducted subgroup analysis based on volume grouping category, consistent results were found that high-volume hospitals significantly improved OS after esophagectomy than their low-volume counterparts. Subgroup analysis and sensitivity analyses further confirmed that all the results were robust.

**Conclusions:** Esophageal cancer should be centralized in high-volume hospitals.

## KEYWORDS

esophageal carcinoma, esophagectomy, hospital volume, overall survival, centralization

## 1. Introduction

Centralization of demanding cancer surgeries to improve the safety and effectiveness of cancer treatment is a topic of ongoing concern in many countries around the world (1–4). Esophagectomy is one of the most complex surgery with high morbidity and mortality, and whether it should be centralized in high-volume hospitals remains controversial (5–9).

## Abbreviations

CI, confidence interval; HR, hazard ratio; HV, hospital volume; HVH, high-volume hospital; LVH, low-volume hospital; No., number; NR, not reported; ref, reference; USA, United States of America.

Clinical long-term outcomes of esophageal cancer after surgery are usually affected by standardization of surgical procedures, chemotherapy, radiation therapy, molecular targeted therapy and immunotherapy (10–12); moreover, hospital volume also influences mortality after esophagectomy (13). Some previous studies have been reported that esophagectomy for cancer centralized in high-volume hospitals benefited long-term prognosis outcomes (6, 7, 14, 15), whereas, there are also some reports showing inconsistent results (5, 8, 9, 16). Therefore, whether a better long-term overall survival after esophagectomy showing high-volume hospitals remains to be established.

In the present study, we evaluated the influence of high- vs. low-volume hospitals on the long-term OS of patients with esophageal cancer after esophagectomy.

## 2. Materials and methods

### 2.1. Literature search strategy

This systematic review was registered in <https://doi.org/10.37766/inplasy2022.7.0023> (identifier: INPLASY202270023) (17). We conducted a systematic search for all relevant articles on the relationship between hospital volume of esophagectomies and long-term OS (17). The search was performed in PubMed, Embase, and Cochrane Library. For example, we combined Medical Subject Headings (MeSH) terms and text terms for the search in PubMed. The following search terms were used: (“esophagectomy” OR “esophageal surgery “ OR “esophageal cancer surgery” OR “esophageal resection” OR “esophageal cancer resection”) AND (“hospital volume” OR “high volume” OR “low volume” OR “healthcare institution size” OR “surgical volume”). We also searched the references of the included studies to search for potentially eligible articles. The last search was completed on May 30, 2022. This study followed the Preferred Reporting Items for Systematic Reviews and Meta-analysis guidance (PRISMA) (17, 18).

### 2.2. Study selection and eligibility criteria

As we previously described, after the retrieval of the relevant articles, they were screened to remove the duplicates (17). All studies were published in English. Search results were screened by two authors (Q.W. and C.D.Z.) independently according to the titles and abstracts. To better reflect modern surgical practices and perioperative management, this study focuses only on articles published after 2002. Next, the retained studies were searched for their full text and further were screened according to the following eligibility criteria: publication in English language; surgery for esophageal carcinoma as the theme; primary outcomes included hospital volume and long-term OS; comparison of OS between high- and low-volume hospitals; original articles with informative data; articles reporting adjusted hazard ratios (HRs) in multivariate analysis; publication before 2002; and articles in which procedural volume was an exact

cutoff. Any disagreements were resolved through consultation with the third author (17).

### 2.3. Data extraction

Two authors (QW and CDZ) independently extracted data from the included studies and collated the following information: author, published year, country, study period, population, the unit of exposure (hospital volume), volume classification for hospitals, volume grouping (dichotomies, tertiles, quartiles, quintiles or others) and the longest follow-up and clinical outcomes (OS) (17). Any disagreements were resolved by discussion with the third author. We further assessed the extent of risk adjustment (17).

### 2.4. Study quality evaluation

All included studies were rigorously assessed for methodological quality and risk of bias by two authors (QW and CDZ) by using the Newcastle-Ottawa Scale (17, 19). This scale assesses the quality of studies from three aspects: selection of study population (0–4 points), comparability between groups (0–2 points), and outcome measurement (0–3 points) (17). The total score is 9 points.

### 2.5. Data integration

High-volume hospitals or low-volume hospitals were defined by the authors of the included studies. We used hazard ratios (HRs) in low-volume groups as the reference. If an included study reported more than two surgical volume groups, only the lowest and highest volume groups were compared in the analysis. The primary outcome was OS at the last follow-up, excluding 30-day mortality, 90-day mortality, in-hospital mortality, and postoperative mortality (17).

### 2.6. Statistical analyses

The results were calculated by HRs with 95% confidence intervals (CIs) for long-term outcomes. Heterogeneity among the studies was quantified by the  $I^2$  test, and studies with a statistic of 25%–50% of  $I^2$  were regarded as low heterogeneous, 51%–75% as moderate, and more than 75% as highly heterogeneous (20). Regarding the clinical heterogeneity (inconsistency in pathological staging, therapeutic regimens, and other confounding factors among the studies), we applied random-effect models for all the analyses. To obtain adequate statistical power, subgroup analysis was conducted based on volume grouping category. Then meta-analyses of at least five included studies were performed for different cutoff values (high-volume hospital vs. low-volume hospital). In addition, subgroup analyses in relation to volume group, sample size, study country, year of

publication, follow-up or study quality and sensitivity analyses of a leave-one-out method were conducted to verify the results. Funnel plots were used to evaluate potential publication bias.  $P < 0.05$  was considered to be statistically significant. All statistical analyses were performed by Review Manager 5.4.1 and Stata 13.1.

## 3. Results

### 3.1. Study selection and characteristics

This systematic review was registered in <https://doi.org/10.37766/inplasy2022.7.0023> (identifier: INPLASY202270023). **Figure 1** shows the process of literature selection. We retrieved 115 articles from PubMed and 66 from Embase; of these, 136 studies were retained for primary selection after 59 duplicate

studies were excluded. After screening of titles and abstracts, 30 studies were excluded. Among the remaining 106 articles, which were related to the volume-outcome relationship in esophageal cancer surgery, we further excluded 24 reviews without primary data, three articles not related to esophagectomy, 23 articles without data of long-term survival, 10 articles without data of hospital volume, three articles without data of low-volume hospitals, four articles published before 2002. Finally, 24 studies published from 2002 to May 2022 with 113,014 participants were included in the meta-analysis.

Among the 24 included studies, six were from the United States (6–8, 21–23), four from Sweden (9, 15, 24, 25), three each from Australia (26–28) and Netherlands (29–31), two each from Japan (32, 33) and England (14, 34), and one each from China (35), Korea (36), Brazil (37), and Canada (38) (**Table 1**). The longest follow-up period was 24 years.

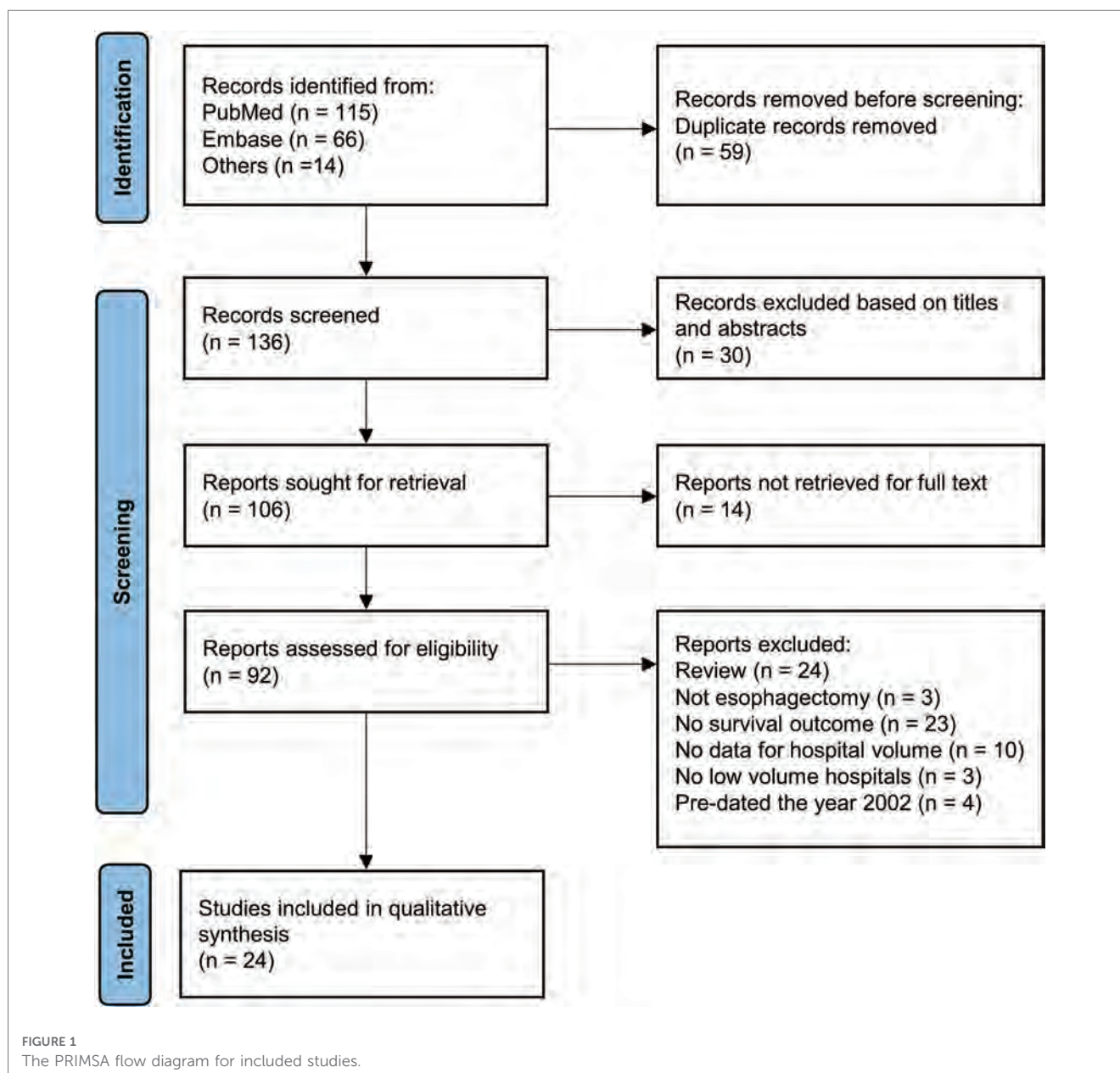


TABLE 1. Basic characteristics of all included studies for meta-analysis on the relation between hospital volume and outcome of esophagectomies for cancer.

Author, year	Year	Country	Study	Population	Age, years	Male (%)	Exposure	Hospital volume		Volume grouping	The longest Follow-up, year	Survival	Hospital
								High	Low				
[Ref]			Period							Category		After	Number
Dikken (4)	2012	Netherlands	1989–2009	10,025	NR	76.0%	HV	≥21	≤5	Quartiles	3 years	Surgery	44
Van de Poll-Fansse (5)	2011	Netherlands	1995–2006	638	66.0	76.5%	HV	15–20	<4	Tertiles	3 years	Surgery	NR
Yang (10)	2018	USA	2004–2013	2445	62.0	90.6%	HV	3.1–15.8	0.1–1.0	Tertiles	11 years	Surgery	450
Coupland (11)	2013	England	2004–2008	5403	NR	71.9%	HV	≥80	<20	Quintiles	6 years	Surgery	NR
Derogar (13)	2013	Sweden	1987–2005	1335	66.0	74.0%	HV	≥17	≤8	Tertiles	24 years	Surgery	NR
Patel (26)	2021	USA	2006–2013	11,739	62.0–63.0	85.1%	HV	>6	≤6	Dichotomies	5 years	Surgery	1018
Han (27)	2020	USA	2004–2016	37,695	NR	NR	HV	≥25	<5	Quintiles	5 years	Surgery	NR
Gasper (28)	2009	USA	1995–2004	2404	NR	75.9%	HV	>6	<2	Quintiles	5 years	Surgery	NR
Bilimoria (29)	2008	USA	1994–1999	12,246	64.0–65.0	NR	HV	>15	<3	Quintiles	6 years	Surgery	1154
Birkmeyer (30)	2007	USA	1992–2002	822	NR	79.6%	HV	>14	<4	Tertiles	5 years	Surgery	206
Sundelof (31)	2008	Sweden	1994–1997	232	67.0	83.2%	HV	≥10	6–9	Dichotomies	10 years	Surgery	33
Rouvelas (32)	2007	Sweden	1987–2000	1199	65.0–66.0	71.9%	HV	≥10	<10	Dichotomies	17 years	Surgery	53
Wenner (33)	2005	Sweden	1987–1996	1429	66.0–67.0	72.8%	HV	>15	<5	Tertiles	13 years	Surgery	74
Narendra (34)	2021	Australia	2001–2015	11167	NR	NR	HV	≥6	NR	Dichotomies	5 years	Surgery	24
Smith (35)	2014	Australia	2001–2008	908	NR	80.5%	HV	>6	≤6	Dichotomies	9 years	Surgery	42
Stavrou (36)	2010	Australia	2000–2005	321	NR	74.0%	HV	>20	≤10	Tertiles	3 years	Surgery	NR
Verhoef (37)	2007	Netherlands	1994–2002	213	NR	69.1%	HV	≥20	<20	Dichotomies	10 years	Surgery	18
Taniyama (38)	2021	Japan	2006–2013	3578	NR	83.5%	HV	54–70	≤10	Tertiles	10 years	Surgery	96
Ioka (39)	2007	Japan	1994–1998	2961	NR	NR	HV	>43	<8	Quartiles	5 years	Surgery	143
Bachmann (40)	2002	England	1996–1997	781	NR	NR	HV	60–83	7–32	Tertiles	3 years	Surgery	23
Hsu (41)	2014	China	2008–2011	2151	55.2	94.1%	HV	>22	≤22	Dichotomies	3 years	Surgery	58
Kim (42)	2021	Korea	2004–2017	11,346	64.2	92.6%	HV	≥48	<12	Tertiles	5 years	Surgery	122
Duarte (43)	2020	Brazil	2000–2013	1347	NR	84.9%	HV	>8	<5	Dichotomies	5 years	Surgery	NR
Simunovic (44)	2006	Canada	1990–2000	629	63.0–65.0	NR	HV	≥44	≤7	Quartiles	10 years	Surgery	68

Ref. reference.

### 3.2. Quality assessment

The quality of the included studies was assessed using the Newcastle-Ottawa Scale. The median Newcastle-Ottawa Scale score of the included studies was 7, with a range of 6–9 (Table 2).

### 3.3. Long-term OS in relation to hospital volume

A total of 24 studies was included to assess the impact of high-volume vs. low-volume hospitals on long-term overall survival after esophagectomy. Regarding to the longest period of follow-ups, high-volume hospitals showed significantly better overall survival than low-volume hospitals (HR: 0.77; 95% CI: 0.71–0.84,  $P < 0.01$ ) (Figure 2).

Next, we analyzed the pooled HRs of OS (high-volume hospital vs. low-volume hospital) for multiple cutoff values (Table 3). Consistent results were found that high-volume hospitals showed a significant improvement in OS after esophagectomy than their low-volume counterparts (all  $P \leq 0.05$ ).

### 3.4. Subgroup analysis

Subgroup analysis was conducted based on volume grouping category in Figure 2. A significant improvement in OS after

esophagectomy was observed in high-volume hospitals as compared to that in their low-volume counterparts in each volume grouping category. The pooled HRs were 0.76 (95% CI: 0.71–0.81) for quintiles, 0.72 (95% CI: 0.61–0.85) for quartiles, 0.77 (95% CI: 0.62–0.96) for tertiles, and 0.82 (95% CI: 0.78–0.87) for dichotomies, respectively (Figure 2, Table 4).

In addition, we carried out subgroup analyses in relation to sample size, study country, year of publication, follow-up or study quality. Overall, the results were robust and that patients with esophagectomy significantly benefited from high-volume hospitals than from low-volume hospitals (Table 3).

### 3.5. Sensitivity analyses

Sensitivity analyses with the leave-one-out method further revealed the consistent results, which were observed a significant improvement in OS after esophagectomy in high-volume hospitals as compared to that in their low-volume counterparts, with HRs ranging from 0.75 (95% CI: 0.68–0.83) to 0.79 (95% CI: 0.73–0.85) (Table 5).

### 3.6. Publication bias

We further assessed the publication bias (Figure 3). Because of the relatively small number of included studies in some volume

TABLE 2 Quality assessment of all included studies by Newcastle-Ottawa scale.

Study	Selection				Comparability	Outcome			Total score
	I	II	III	IV	V	VI	VII	VIII	
Dikken 2012 (29)		★	★	★	★★	★	★	★	8
Van de Poll-Fansse 2011 (30)	★	★	★		★★	★	★	★	8
Yang 2019 (21)	★	★	★		★	★	★	★	7
Coupland 2013 (14)	★	★	★	★	★★	★	★	★	9
Derogar 2013 (15)	★	★	★	★	★★	★	★	★	9
Patel 2022 (6)	★	★	★		★★	★	★	★	8
Han 2021 (7)	★	★	★	★	★★	★	★	★	9
Gaspar 2009 (8)	★	★	★	★	★★	★	★	★	9
Bilimoria 2008 (22)	★	★	★	★	★★	★	★	★	9
Birkmeyer 2007 (23)	★	★	★	★	★★	★	★	★	9
Sundelof 2008 (24)			★	★	★★	★	★	★	7
Rouvelas 2007 (9)			★	★	★★	★	★		6
Wenner 2005 (25)		★	★	★	★★		★		6
Narendra 2021 (26)		★	★	★	★	★	★		6
Smith 2014 (27)		★	★	★	★★	★	★	★	8
Stavrou 2010 (28)			★	★	★★	★	★	★	7
Verhoef 2007 (31)	★	★	★	★	★★	★	★		8
Taniyama 2021 (32)	★	★		★	★★	★	★		7
Ioka 2007 (33)			★	★	★★		★	★	6
Bachmann 2002 (34)	★	★	★	★	★	★	★	★	8
Hsu 2014 (35)			★	★	★★	★	★	★	7
Kim 2021 (36)	★	★	★	★	★	★	★		7
Duarte 2020 (37)		★	★	★	★	★	★		6
Simunovic 2006 (38)		★	★	★	★	★	★		6

\*One score. I, representativeness of the exposed cohorts; II, selection of the non-exposed cohorts; III, ascertainment of exposure; IV, demonstration that outcome of interest was not present at start of study of interest; V, comparability of cohorts on the basis of the design or analysis; VI, assessment of outcomes; VII, was follow-up long enough for outcomes to occur; VIII, adequacy of follow-up of cohorts.

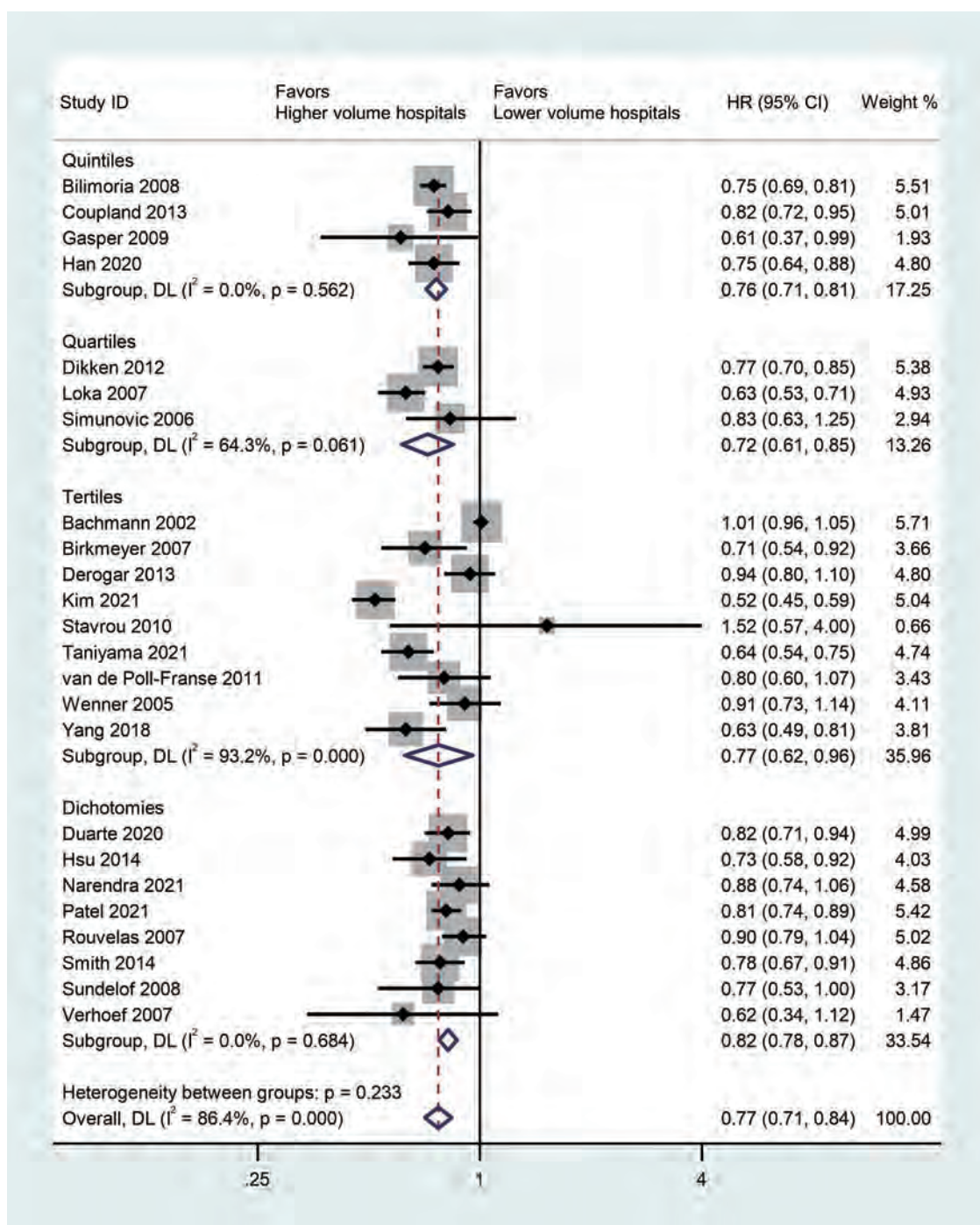


FIGURE 2 Forest plot of long-term survivals following esophagectomy comparing high- with low-volume hospitals (reference) according to volume grouping.

grouping category meta-analyses, we consider that publication bias should exist.

### 4. Discussion

This meta-analysis outlined the most up-to-date evidence on the relationship between hospital volume and long-term survival outcomes in esophagectomy. We found for the first time that

centralization of esophagectomy in high-volume hospitals improved OS as compared to that in low-volume hospitals and patients with esophageal cancer will benefit from an esophagectomy conducted in a higher volume hospital than in a lower one, whether in total or in volume grouping category. However, we were still unable to decide the optimal cutoff value of dividing high- and low-volume hospitals in current study.

Centralization of esophageal cancer surgery has been common in the Netherlands, England, and Canada (18, 39, 40), Comparing a

**TABLE 3** Comparisons of the overall survivals between high- and low-volume hospitals by different cutoff values of hospital volume.

Cutoff values of hospital volume (CV) HVH ( $\geq$ CV) vs. LVH ( $<$ CV)	No. of studies	No. of patients	Effect estimate		
			HR	(95% CI)	P value
5	6	55,152	0.76	0.71–0.80	<0.001
6	11	80,408	0.79	0.75–0.84	<0.001
7	8	66,606	0.79	0.73–0.85	<0.001
8	9	67,261	0.79	0.74–0.84	<0.001
9	10	68,596	0.78	0.74–0.83	<0.001
10	12	74,347	0.77	0.72–0.83	<0.001
11	11	73,148	0.77	0.72–0.83	<0.001
12–14	12	84,494	0.75	0.68–0.83	<0.001
15	11	83,672	0.75	0.68–0.84	<0.001
16	9	80,741	0.72	0.65–0.80	<0.001
17	8	68,494	0.72	0.63–0.81	<0.001
18–19	7	67,159	0.71	0.61–0.82	<0.001
20	9	77,976	0.71	0.63–0.81	<0.001
21	8	71,427	0.72	0.63–0.82	<0.001
22	7	63,232	0.64	0.56–0.73	<0.001
23–25	6	61,081	0.70	0.60–0.82	<0.001
26–32	5	23,386	0.69	0.57–0.84	<0.001
33–43	6	24,167	0.75	0.59–0.95	0.02
44	5	21,737	0.74	0.55–1.00	0.05

CI, confidence interval; HR, hazard ratio; HVH, high-volume hospital; LVH, low-volume hospital; No., number.

**TABLE 4** Subgroup analyses of comparisons of the overall survivals between high- and low-volume hospitals.

Subgroup HVH vs. LVH	No. of studies	No. of patients	Effect estimate	
			HR (95% CI)	P value
Total	24	113,014	0.77 (0.71–0.84)	<0.001
<b>Volume group</b>				
Dichotomies	8	18,956	0.82 (0.78–0.87)	<0.001
Tertiles	9	22,695	0.77 (0.62–0.96)	0.02
Quartiles	3	13,615	0.72 (0.61–0.85)	<0.001
Quintiles	4	57,748	0.76 (0.71–0.81)	<0.001
<b>Sample size</b>				
>5,000	6	88,454	0.73 (0.65–0.82)	<0.001
<5,000	18	24,560	0.79 (0.72–0.87)	<0.001
<b>Study country</b>				
Western countries	20	98,381	0.82 (0.76–0.88)	<0.001
Eastern countries	4	20,036	0.61 (0.53–0.70)	<0.001
<b>Year of publication</b>				
2002–2012	13	33,900	0.80 (0.70–0.90)	<0.001
2013–2022	11	79,114	0.75 (0.67–0.83)	<0.001
<b>Follow-up</b>				
Longest follow-up $\geq$ 10 years	8	11,060	0.79 (0.69–0.91)	<0.001
Longest follow-up <10 years	16	101,954	0.76 (0.69–0.85)	<0.001
<b>Study quality</b>				
High	19	107,243	0.74 (0.67–0.83)	<0.001
Moderate	5	5771	0.87 (0.80–0.94)	<0.001

CI, confidence interval; HR, hazard ratio; HVH, high-volume hospital; LVH, low-volume hospital; No., number.

centralized country (England) with a non-centralized country (U.S.), a previous study of 13,291 patients illustrated a lower in-hospital mortality in England hospitals than those in the U.S. (4.2% vs. 5.5%) (41). Regarding this, centralization is urgently

**TABLE 5** Sensitivity analysis using leave-one-out method for overall survival of high-volume hospitals vs. low-volume hospitals.

Given named study is omitted	Hazard ratio	95% CI	P value
Dikken (29)	0.77	0.70–0.84	<0.001
Van de Poll-Fansee (30)	0.77	0.71–0.84	<0.001
Yang (21)	0.78	0.71–0.85	<0.001
Coupland (14)	0.77	0.70–0.84	<0.001
Derogar (15)	0.76	0.70–0.83	<0.001
Patel (6)	0.77	0.70–0.84	<0.001
Han (7)	0.77	0.71–0.84	<0.001
Gasper (8)	0.75	0.68–0.83	<0.001
Bilimoria (22)	0.77	0.70–0.85	<0.001
Birkmeyer (23)	0.77	0.71–0.84	<0.001
Sundelof (24)	0.77	0.70–0.84	<0.001
Rouvelas (9)	0.76	0.70–0.84	<0.001
Wenner (25)	0.77	0.70–0.84	<0.001
Narendra (26)	0.77	0.70–0.84	<0.001
Smith (27)	0.77	0.70–0.84	<0.001
Stavrou (28)	0.77	0.70–0.84	<0.001
Verhoef (31)	0.77	0.71–0.84	<0.001
Taniyama (32)	0.78	0.71–0.85	0.02
Ioka (33)	0.78	0.72–0.85	0.05
Bachmann (34)	0.76	0.71–0.81	<0.001
Hsu (35)	0.77	0.71–0.84	<0.001
Kim (36)	0.79	0.73–0.85	<0.001
Duarte (37)	0.77	0.70–0.84	<0.001
Simunovic (38)	0.77	0.70–0.84	<0.001

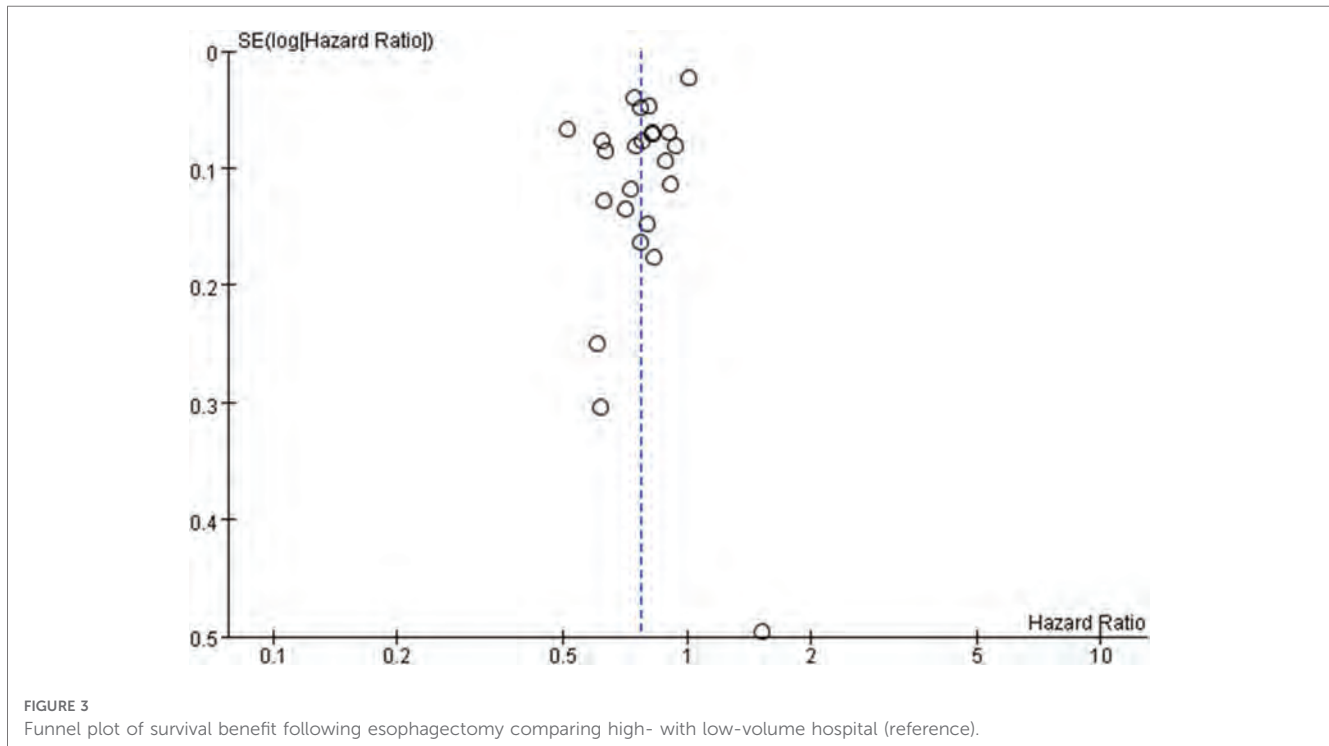
CI, confidence interval.

required, in terms of high-volume hospitals with sufficient surgical volumes, skillful interdisciplinary teams, to provide the optimal treatment for patients with esophageal cancer.

Although the reasons why high-volume hospitals are associated with better long-term survival are still not fully understood, high-volume hospitals may provide patients with better multidisciplinary teams, more comprehensive preoperative examinations, more accurate preoperative diagnosis, perioperative management, and high-quality surgical care, more specialized surgeons who have more consistent skills of performing curable operations for esophageal cancer patients (42–45). Compared with low-volume hospitals, high-volume hospitals not only have a lower complication rate after esophagectomies, but also the ability of managing complications (46). In addition, the applications of neoadjuvant chemoradiation, perioperative chemotherapy, and postoperatively follow-up can improve long-term outcomes after esophagectomies; therefore, high-volume hospitals are more likely to provide a better overall cancer therapy and care, and the size of hospital volume may serve as a significant indicator of the overall medical quality and health care (47).

Unfortunately, it is difficult for patients to know the overall quality of nearby hospitals. Based on the main findings of current study, patients can select relatively higher volume hospitals nearby. Considering the importance of such knowledges, policy makers should make efforts to educate people for selecting the optimal hospitals for the treatments of specific diseases (e.g., esophagectomy for esophageal cancer), through public reporting systems.

Our study still has limitations. First, this study has the potential for selection bias of individual studies because of



the original data, even with case mix adjustment. Second, all the included studies were observational and retrospective. Third, some of the included studies used the same database (e.g., Sweden), and some participants might be overlapped, even though the study period were different; however, sensitivity analyses of a leave-one-out method confirmed that all the current results were robust. Fourth, as some of the data in the included studies were obtained from the National Cancer Registry, some details of the surgery, such as surgical approach and the extent of lymph nodes dissection, were unknown. Fifth, the volume grouping categories of the annual hospital volumes across the included studies varied greatly, and there was still no optimal threshold, and the main findings of current study thus need to be verified in further studies.

## 5. Conclusion

In summary, high-volume hospitals significantly improved long-term OS of patients with esophageal cancer after esophagectomy as compared to their low-volume counterparts. Esophagectomy should be centralized in high-volume hospitals.

## Data availability statement

The original contributions presented in the study are included in the article, further inquiries can be directed to the corresponding author.

## Author contributions

Conceptualization: QW, CDZ. Methodology: QW, SN. Software: QW. Validation: QW, MN, TF, SN, CDZ, SM. Formal analysis: QW, CDZ. Investigation: QW, MN, TF, SN, CDZ, SM. Resources: QW, CDZ. Data curation: QW, CDZ. Writing—original draft preparation: QW. Writing—review and editing: MN, SM. Visualization: QW. Supervision: SM. Reading and approving the final manuscript: QW, MN, TF, SN, CDZ, SM. All authors contributed to the article and approved the submitted version.

## Acknowledgments

The authors thank the members of the Department of Esophageal and Gastroenterological Surgery, Juntendo University Graduate School of Medicine, for their thoughtful discussion and helpful advice. The authors also thank all participants and study authors in this study. QW was partly supported by the Japan China Sasakawa Medical Fellowship. CDZ was partly supported by the China Scholarship Council (201908050148).

## Conflict of interest

The authors declare that the research was conducted in the absence of any commercial or financial relationships that could be construed as a potential conflict of interest.

## Publisher's note

All claims expressed in this article are solely those of the authors and do not necessarily represent those of their affiliated

organizations, or those of the publisher, the editors and the reviewers. Any product that may be evaluated in this article, or claim that may be made by its manufacturer, is not guaranteed or endorsed by the publisher.

## References

- Sheetz KH, Dimick JB, Nathan H. Centralization of high-risk cancer surgery within existing hospital systems. *J Clin Oncol.* (2019) 37(34):3234–42. doi: 10.1200/JCO.18.02035
- Balzano G, Guarneri G, Pecorelli N, Paiella S, Rancoita PMV, Bassi C, et al. Modelling centralization of pancreatic surgery in a nationwide analysis. *Br J Surg.* (2020) 107(11):1510–9. doi: 10.1002/bjs.11716
- van Putten M, Nelen SD, Lemmens VEPP, Stoot JHMB, Hartgrink HH, Gisbertz SS, et al. Overall survival before and after centralization of gastric cancer surgery in The Netherlands. *Br J Surg.* (2018) 105(13):1807–15. doi: 10.1002/bjs.10931
- Asplund J, Mattsson F, Plecka-Ostlund M, Markar SR, Lagergren J. Annual surgeon and hospital volume of gastrectomy and gastric adenocarcinoma survival in a population-based cohort study. *Acta Oncol.* (2022) 61(4):425–32. doi: 10.1080/0284186X.2022.2025612
- Lagergren J, Lagergren P. Recent developments in esophageal adenocarcinoma. *CA Cancer J Clin.* (2013) 63(4):232–48. doi: 10.3322/caac.21185
- Patel DC, Jeffrey Yang CF, He H, Liou DZ, Backhus LM, Lui NS, et al. Influence of facility volume on long-term survival of patients undergoing esophagectomy for esophageal cancer. *J Thorac Cardiovasc Surg.* (2022) 163(4):1536–1546 e1533. doi: 10.1016/j.jtcvs.2021.05.048
- Han S, Kolb JM, Hosokawa P, Friedman C, Fox C, Scott FI, et al. The volume-outcome effect calls for centralization of care in esophageal adenocarcinoma: results from a large national cancer registry. *Am J Gastroenterol.* (2021) 116(4):811–5. doi: 10.14309/ajg.0000000000001046
- Gasper WJ, Glidden DV, Jin C, Way LW, Patti MG. Has recognition of the relationship between mortality rates and hospital volume for major cancer surgery in California made a difference?: a follow-up analysis of another decade. *Ann Surg.* (2009) 250(3):472–83. doi: 10.1097/SLA.0b013e3181b47c79
- Rouvelas I, Lindblad M, Zeng W, Viklund P, Ye W, Lagergren J. Impact of hospital volume on long-term survival after esophageal cancer surgery. *Arch Surg.* (2007) 142(2):113–7; discussion 118. doi: 10.1001/archsurg.142.2.113
- Yang H, Liu H, Chen Y, Zhu C, Fang W, Yu Z, et al. Long-term efficacy of neoadjuvant chemoradiotherapy plus surgery for the treatment of locally advanced esophageal squamous cell carcinoma: the NEOCRTEC5010 randomized clinical trial. *JAMA Surg.* (2021) 156(8):721–9. doi: 10.1001/jamasurg.2021.2373
- Yu S, Zhang W, Ni W, Xiao Z, Wang Q, Zhou Z, et al. A propensity-score matching analysis comparing long-term survival of surgery alone and postoperative treatment for patients in node positive or stage III esophageal squamous cell carcinoma after R0 esophagectomy. *Radiother Oncol.* (2019) 140:159–66. doi: 10.1016/j.radonc.2019.06.020
- He S, Xu J, Liu X, Zhen Y. Advances and challenges in the treatment of esophageal cancer. *Acta Pharm Sin B.* (2021) 11(11):3379–92. doi: 10.1016/j.apsb.2021.03.008
- Lagergren J, Smyth E, Cunningham D, Lagergren P. Oesophageal cancer. *Lancet.* (2017) 390(10110):2383–96. doi: 10.1016/S0140-6736(17)31462-9
- Coupland VH, Lagergren J, Luchtenborg M, Jack RH, Allum W, Holmberg L, et al. Hospital volume, proportion resected and mortality from oesophageal and gastric cancer: a population-based study in England, 2004–2008. *Gut.* (2013) 62(7):961–6. doi: 10.1136/gutjnl-2012-303008
- Derogar M, Sadr-Azodi O, Johar A, Lagergren P, Lagergren J. Hospital and surgeon volume in relation to survival after esophageal cancer surgery in a population-based study. *J Clin Oncol.* (2013) 31(5):551–7. doi: 10.1200/JCO.2012.46.1517
- Gillison E. W., Powell J., McConkey C. C., Spychal R. T. Surgical workload and outcome after resection for carcinoma of the oesophagus and cardia. *Br J Surg.* (2002) 89(3):344–8. doi: 10.1046/j.0007-1323.2001.02015.x
- Wang Q, Nasu M, Fukunaga T, Nojiri S, Zhang C-D, Mine S. Association of hospital volume and long-term survival after esophagectomy: a systematic review and meta-analysis. *INPLASY.* (2022). doi: 10.37766/inplasy2022.7.0023
- Page MJ, McKenzie JE, Bossuyt PM, Boutron I, Hoffmann TC, Mulrow CD, et al. The PRISMA 2020 statement: an updated guideline for reporting systematic reviews. *Br Med J.* (2021) 372:n71. doi: 10.1136/bmj.n71
- Stang A. Critical evaluation of the Newcastle-Ottawa scale for the assessment of the quality of nonrandomized studies in meta-analyses. *Eur J Epidemiol.* (2010) 25(9):603–5. doi: 10.1007/s10654-010-9491-z
- Higgins J, Thompson S, Deeks J, Altman D. Measuring inconsistency in meta-analyses. *Br Med J.* (2003) 327(7414):557–60. doi: 10.1136/bmj.327.7414.557
- Yang GQ, Mhaskar R, Rishi A, Naghavi AO, Frakes JM, Almhanna K, et al. Intensity-modulated radiotherapy at high-volume centers improves survival in patients with esophageal adenocarcinoma receiving trimodality therapy. *Dis Esophagus.* (2019) 32(8):doy124. doi: 10.1093/dote/doy124
- Bilimoria KY, Bentrem DJ, Feinglass JM, Stewart AK, Winchester DP, Talamonti MS, et al. Directing surgical quality improvement initiatives: comparison of perioperative mortality and long-term survival for cancer surgery. *J Clin Oncol.* (2008) 26(28):4626–33. doi: 10.1200/JCO.2007.15.6356
- Birkmeyer JD, Sun Y, Wong SL, Stukel TA. Hospital volume and late survival after cancer surgery. *Ann Surg.* (2007) 245(5):777–83. doi: 10.1097/01.sla.0000252402.33814.dd
- Sundelof M, Lagergren J, Ye W. Surgical factors influencing outcomes in patients resected for cancer of the esophagus or gastric cardia. *World J Surg.* (2008) 32(11):2357–65. doi: 10.1007/s00268-008-9698-2
- Wenner J, Zilling T, Bladström A, Alvegård T. The influence of surgical volume on hospital mortality and 5-year survival for carcinoma of the oesophagus and gastric cardia. *Anticancer Res.* (2005) 25(1B):419–24.
- Narendra A, Baade PD, Aitken JF, Fawcett J, Leggett B, Leggett C, et al. Hospital characteristics associated with better “quality of surgery” and survival following oesophagogastric cancer surgery in Queensland: a population-level study. *ANZ J Surg.* (2021) 91(3):323–8. doi: 10.1111/ans.16397
- Smith RC, Creighton N, Lord RV, Merrett ND, Keogh GW, Liauw WS, et al. Survival, mortality and morbidity outcomes after oesophagogastric cancer surgery in New South Wales, 2001–2008. *Med J Aust.* (2014) 200(7):408–13. doi: 10.5694/mja13.11182
- Stavrou EP, Smith GS, Baker DF. Surgical outcomes associated with oesophagectomy in New South Wales: an investigation of hospital volume. *J Gastrointest Surg.* (2010) 14(6):951–7. doi: 10.1007/s11605-010-1198-7
- Dikken JL, Dassen AE, Lemmens VE, Putter H, Krijnen P, van der Geest L, et al. Effect of hospital volume on postoperative mortality and survival after oesophageal and gastric cancer surgery in The Netherlands between 1989 and 2009. *Eur J Cancer.* (2012) 48(7):1004–13. doi: 10.1016/j.ejca.2012.02.064
- van de Poll-Franse LV, Lemmens VE, Roukema JA, Coebergh JW, Nieuwenhuijzen GA. Impact of concentration of oesophageal and gastric cardia cancer surgery on long-term population-based survival. *Br J Surg.* (2011) 98(7):956–63. doi: 10.1002/bjs.7493
- Verhoef C, van de Weyer R, Schaapveld M, Bastiaannet E, Plukker JT. Better survival in patients with esophageal cancer after surgical treatment in university hospitals: a plea for performance by surgical oncologists. *Ann Surg Oncol.* (2007) 14(5):1678–87. doi: 10.1245/s10434-006-9333-0
- Taniyama Y, Tabuchi T, Ohno Y, Morishima T, Okawa S, Koyama S, et al. Hospital surgical volume and 3-year mortality in severe prognosis cancers: a population-based study using cancer registry data. *J Epidemiol.* (2021) 31(1):52–8. doi: 10.2188/jea.EJ20190242
- Ioka A, Tsukuma H, Ajiki W, Oshima A. Hospital procedure volume and survival of cancer patients in Osaka, Japan: a population-based study with latest cases. *Jpn J Clin Oncol.* (2007) 37(7):544–53. doi: 10.1093/jjco/hym052
- Bachmann M, Alderson D, Edwards D, Wotton S, Bedford C, Peters T, et al. Cohort study in south and west England of the influence of specialization on the management and outcome of patients with oesophageal and gastric cancers. *Br J Surg.* (2002) 89(7):914–22. doi: 10.1046/j.1365-2168.2002.02135.x
- Hsu PK, Chen HS, Wu SC, Wang BY, Liu CY, Shih CH, et al. Impact of hospital volume on long-term survival after resection for oesophageal cancer: a population-based study in taiwandagger. *Eur J Cardiothorac Surg.* (2014) 46(6):e127–135; discussion e135. doi: 10.1093/ejcts/ezu377
- Kim BR, Jang EJ, Jo J, Lee H, Jang DY, Ryu HG. The association between hospital case-volume and postoperative outcomes after esophageal cancer surgery: a population-based retrospective cohort study. *Thorac Cancer.* (2021) 12(18):2487–93. doi: 10.1111/1759-7714.14096
- Duarte MBO, Pereira EB, Lopes LR, Andreollo NA, Carvalheira JBC. Chemoradiotherapy with or without surgery for esophageal squamous cancer according to hospital volume. *JCO Glob Oncol.* (2020) 6:828–36. doi: 10.1200/JGO.19.00360

38. Simunovic M, Rempel E, Thériault M, Coates A, Whelan T, Holowaty E, et al. Influence of hospital characteristics on operative death and survival of patients after major cancer surgery in Ontario. *Can J Surg.* (2006) 49(4):251–8.
39. Varghese TK Jr., Wood DE, Farjah F, Oelschlager BK, Symons RG, MacLeod KE, et al. Variation in esophagectomy outcomes in hospitals meeting leapfrog volume outcome standards. *Ann Thorac Surg.* (2011) 91(4):1003–9; discussion 1009–1010. doi: 10.1016/j.athoracsur.2010.11.006
40. Chang AC. Centralizing esophagectomy to improve outcomes and enhance clinical research: invited expert review. *Ann Thorac Surg.* (2018) 106(3):916–23. doi: 10.1016/j.athoracsur.2018.04.004
41. Munasinghe A, Markar SR, Mamidanna R, Darzi AW, Faiz OD, Hanna GB, et al. Is it time to centralize high-risk cancer care in the United States? Comparison of outcomes of esophagectomy between England and the United States. *Ann Surg.* (2015) 262(1):79–85. doi: 10.1097/SLA.0000000000000805
42. Van den Broeck T, Oprea-Lager D, Moris L, Kailavasan M, Briers E, Cornford P, et al. A systematic review of the impact of surgeon and hospital caseload volume on oncological and nononcological outcomes after radical prostatectomy for nonmetastatic prostate cancer. *Eur Urol.* (2021) 80(5):531–45. doi: 10.1016/j.eururo.2021.04.028
43. Khanna A, Saarela O, Lawson K, Finelli A, Haber GP, Lee B, et al. Hospital quality metrics for radical cystectomy: disease specific and correlated to mortality outcomes. *J Urol.* (2019) 202(3):490–7. doi: 10.1097/JU.0000000000000282
44. Wright JD, Chen L, Hou JY, Burke WM, Tergas AI, Ananth CV, et al. Association of hospital volume and quality of care with survival for ovarian cancer. *Obstet Gynecol.* (2017) 130(3):545–53. doi: 10.1097/AOG.0000000000002164
45. Ghaferi AA, Birkmeyer JD, Dimick JB. Complications, failure to rescue, and mortality with major inpatient surgery in medicare patients. *Ann Surg.* (2009) 250(6):1029–34. doi: 10.1097/SLA.0b013e3181bef697
46. Ghaferi A, Birkmeyer J, Dimick J. Hospital volume and failure to rescue with high-risk surgery. *Med Care.* (2011) 49(12):1076–81. doi: 10.1097/MLR.0b013e3182329b97
47. Eskander A, Irish J, Groome PA, Freeman J, Gullane P, Gilbert R, et al. Volume-outcome relationships for head and neck cancer surgery in a universal health care system. *Laryngoscope.* (2014) 124(9):2081–8. doi: 10.1002/lary.24704

日中笹川医学奨学金制度<学位取得コース>評価書

課程博士：指導教官用



第 43 期

研究者番号：G4307

作成日：2024年3月10日

氏名	張 瑛	ZHANG YING	性別	F	生年月日	1985/08/14
所属機関（役職）	寧波市医療中心李惠利医院超音波科（主治医師）					
研究先（指導教官）	横浜市立大学大学院 医学研究科消化器内科学（前田 慎 主任教授）					
研究テーマ	肝胆膵疾患・炎症性腸疾患における超音波を主体とした画像診断と治療 Ultrasound-based multi-modality imaging and therapy for hepatobiliary and pancreatic oncology and inflammatory bowel disease					
専攻種別	<input type="checkbox"/> 論文博士			<input checked="" type="checkbox"/> 課程博士		

研究者評価（指導教官記入欄）

成績状況	優 (良) 可 不可	取得単位数
	学業成績係数=	取得単位数 40 / 取得すべき単位数総数 60
学生本人が行った研究の概要	1. 超音波造影剤と CT/MRI 造影剤についての総説を記載し、受理された (Frontiers in Oncology 2022 Jun 2;12:921667). 2. 多施設で後ろ向き検討ではあるが、Intermediate stage の切除不能肝癌に対して肝癌の抗がん剤である Lenvatinib 投与後にラジオ波を実施し腫瘍量を減らし、さらに再度 Lenvatinib を投与する群と Lenvatinib 群の baseline を matching させて全生存期間を比較した。Lenvatinib とラジオ波逐次治療群は有意に全生存期間を延長した。Hepatology research に投稿した。 3. Sonazoid 造影超音波後血管相でクッパー細胞がない中分化・低分化肝癌は低エコー病変として検出される。従来の低音圧造影では超音波の減衰のため十分に評価できないが、高音圧に切り替えることで有意には低エコー病変として検出できることを統計学的に証明し、その論文をアメリカの超音波学会雑誌 (Journal of Ultrasound in Medicine) に投稿した。	
総合評価	【良かった点】 超音波造影剤と CT/MRI 造影剤についての総説を最初に記載したので、造影超音波に関する知見が深まったと考える。 肝細胞癌の対する診断と治療についての論文を、統計を含め、真摯な態度で詳細に記載しましたので、今後の診療に役立つと思われる。 【改善すべき点】 コロナの時期も重なっていたが、対面で、もっと一緒に造影超音波やラジオ波治療を体験してもらいたかった。 【今後の展望】 原著論文が revise になれば、accept するために修正していく予定。	
学位取得見込	原著論文を 2 つ投稿しており、いずれも質が高い内容なので、accept されると期待している。Accept されれば、残りの 20 単位が加算され、学位は取得されると考える。その阿知はずでに中間審査は済み、最終審査に進む予定。	
評価者（指導教官名）		前田 慎

# 日中笹川医学奨学金制度<学位取得コース>報告書 研究者用



第43期

研究者番号: G4307

作成日: 2024年3月6日

氏名	张 瑛	ZHANG YING	性別	F	生年月日	1985/08/14
所属機関(役職)	寧波市医療中心李惠利医院超音波科(主治医師)					
研究先(指導教官)	横浜市立大学大学院 医学研究科消化器内科学(前田 慎 主任教授)					
研究テーマ	肝胆膵疾患・炎症性腸疾患における超音波を主体とした画像診断と治療 Ultrasound-based multi-modality imaging and therapy for hepatobiliary and pancreatic oncology and inflammatory bowel disease					
専攻種別	論文博士		<input type="checkbox"/>	課程博士		<input checked="" type="checkbox"/>
<p>1. 研究概要(1) Lenvatinib radiofrequency ablation sequential therapy offers survival benefits for patients with unresectable hepatocellular carcinoma at intermediate stage and the liver reserve of Child-Pugh A category: A Multicenter Study</p> <p>1) 目的(Goal) This study aims to evaluate the efficacy and safety of lenvatinib radiofrequency ablation (RFA) sequential therapy for certain hepatocellular carcinoma (HCC) patients.</p> <p>2) 戦略(Approach) As a multi-targeted TKI for systemic pharmacotherapy, lenvatinib acts as an antiangiogenic treatment to slow tumor growth, demonstrating non-inferiority in OS but superiority in PFS, time to progression, and ORR compared to sorafenib1, 2. The combined effect of lenvatinib-induced reduction in tumor blood flow and tumor growth, along with additional RFA, was observed to effectively reduce viable tumor volume3. With the reduction in tumor volume achieved through additional local therapy, the resumption of lenvatinib at a reduced dose was contemplated to mitigate AEs and extend the duration of administration, rendering patients apt for prolonged lenvatinib treatment4.</p> <p>3) 材料と方法(Materials and methods) Unresectable HCC patients in the intermediate stage with a liver reserve of Child-Pugh A were retrospectively recruited in a multicenter setting. Those in the lenvatinib RFA sequential therapy group received lenvatinib initially, followed by RFA and the re-administration of lenvatinib. The study compared overall survival (OS), progression-free survival (PFS), tumor response, and adverse events (AEs) between patients undergoing sequential therapy and lenvatinib monotherapy.</p> <p>4) 実験結果(Results) A total of 119 patients from nine institutions were included. After propensity score matching, independent factors influencing OS were identified as sequential therapy and modified Albumin-Bilirubin (mALBI) grade with hazard ratios (HR) of 0.426 (95% confidence intervals, CI: 0.221-0.824) and 1.672 (95% CI: 1.158-2.414), respectively. Stratified analysis based on mALBI grades confirmed the independent influence of treatment strategy across all mALBI grades for OS (HR: 0.443, 95% CI: 0.226-0.869). Furthermore, sequential therapy was identified as an independent factor of PFS (HR: 0.363, 95% CI: 0.212-0.621). Sequential therapy significantly outperformed monotherapy on survival benefits (OS: 38.27 vs. 19.38 months for sequential therapy and monotherapy, respectively, p=0.012; PFS: 13.80 vs. 5.32 months for sequential therapy and monotherapy, respectively, p&lt;0.001). The sequential therapy significantly associated with objective response by modified Response Evaluation Criteria in Solid Tumors (mRECIST) (odds ratio: 10.060). Regarding safety, ten out of 119 experienced grade 3 AEs, with no AE beyond grade 3 observed.</p> <p>5) 考察(Discussion) The findings in the current research affirmed that the lenvatinib RFA sequential therapy serves as a protective measure for uHCC patients' survival benefits. The effectiveness of lenvatinib RFA sequential therapy appears to be primarily attributed to volume reduction induced by both lenvatinib and RFA, and the sustained administration of lenvatinib with tolerable dose adjustments. Meanwhile, as a strong inhibitor of vascular endothelial growth factor receptor and fibroblast growth factor receptor, lenvatinib has also been reported being involved in the cancer immune cycle5, 6. The demonstrated superior antitumor efficacy of lenvatinib, attributable to its underlying immunomodulatory activity, surpasses that of sorafenib7. Additionally, anti-angiogenic therapies may normalize tumor blood vessels8-10, potentially enhancing drug delivery9-13 and immune infiltration and interferon response through reconstructing the TME6, 14, 15. Hence, the reintroduction of lenvatinib at a dose that is well-tolerated post-RFA is helpful at averting potential relapse, ultimately contributing to extended OS and PFS. RFA, in addition to its primary role in volume reduction for HCC, may also exert a mild influence on the immune system to avert potential relapse. Through the release of tumor-specific antigens and the induction of proinflammatory cytokines, these immunomodulatory effects bring about changes in the TME, thereby activating immune responses16. The synergy between TKI and RFA, as observed by Qi et al., enhances anti-tumor immune responses, suppressing certain signaling pathways17. Activation of the immune system post-RFA extends beyond the primary tumor site, suppressing distant tumor growth in rodent models18, 19. RFA has also been reported to reinforces host adaptive immunity through various pathways, such as up-regulating CD8+ T cells and dendritic cells while down-regulating regulatory T cells20. However, the potency of RFA-induced immune activation alone may not be sufficient for fully recurrent tumor elimination21, necessitating exploration of synergistic mechanisms involved the anti-angiogenic benefits of lenvatinib and the changeable TME associated with RFA. Wang F et al. firstly validated the efficacy of lenvatinib RFA sequential therapy for intermediate-stage HCC patients that exceeded the up-to-seven criterion, demonstrating improved OS (median: 21.3 months, 95% CI:14.0-28.0) and PFS (median: 12.5 months, 95% CI: 9.3-20.7) over a median follow-up period of 17.2 (6.7-38.5) months22. With an extended follow-up duration</p>						

## 1. 研究概要(2)

(median: 18.42 months, range: 1.81–61.38 months) and an expanded cohort that includes patients beyond the up-to-seven criteria in the present study, the lenvatinib RFA sequential treatment group exhibited relatively longer median OS (38.27, 95%CI, 21.62–54.92 months) and PFS (13.80 ± 3.67 months), further emphasizing the promising survival outcomes associated with lenvatinib RFA sequential therapy.

## 6)参考文献(References)

- 1Kudo M, Finn RS, Qin S, et al. Lenvatinib versus sorafenib in first-line treatment of patients with unresectable hepatocellular carcinoma: a randomised phase 3 non-inferiority trial. *Lancet*. 2018 Mar 24;391: 1163–73.
- 2Eso Y, Marusawa H. Novel approaches for molecular targeted therapy against hepatocellular carcinoma. *Hepatol Res*. 2018 Jul;48: 597–607.
- 3Numata K, Wang F. New developments in ablation therapy for hepatocellular carcinoma: combination with systemic therapy and radiotherapy. *Hepatobiliary Surg Nutr*. 2022 Oct;11: 766–9.
- 4Mawatari S, Tamai T, Kumagai K, et al. Clinical Effect of Lenvatinib Re-Administration after Transcatheter Arterial Chemoembolization in Patients with Intermediate Stage Hepatocellular Carcinoma. *Cancers (Basel)*. 2022 Dec 13;14.
- 5Hoshi T, Watanabe Miyano S, Watanabe H, et al. Lenvatinib induces death of human hepatocellular carcinoma cells harboring an activated FGF signaling pathway through inhibition of FGFR-MAPK cascades. *Biochem Biophys Res Commun*. 2019 May 21;513: 1–7.
- 6Kato Y, Tabata K, Kimura T, et al. Lenvatinib plus anti-PD-1 antibody combination treatment activates CD8+ T cells through reduction of tumor-associated macrophage and activation of the interferon pathway. *PLoS One*. 2019;14: e0212513.
- 7Kimura T, Kato Y, Ozawa Y, et al. Immunomodulatory activity of lenvatinib contributes to antitumor activity in the Hepa1-6 hepatocellular carcinoma model. *Cancer Sci*. 2018 Dec;109: 3993–4002.
- 8Goel S, Wong AH, Jain RK. Vascular normalization as a therapeutic strategy for malignant and nonmalignant disease. *Cold Spring Harb Perspect Med*. 2012 Mar;2: a006486.
- 9Goel S, Duda DG, Xu L, et al. Normalization of the vasculature for treatment of cancer and other diseases. *Physiol Rev*. 2011 Jul;91: 1071–121.
- 10Liu Z-L, Chen H-H, Zheng L-L, Sun L-P, Shi L. Angiogenic signaling pathways and anti-angiogenic therapy for cancer. *Signal Transduction and Targeted Therapy*. 2023 2023/05/11;8: 198.
- 11Jain RK. Normalizing tumor microenvironment to treat cancer: bench to bedside to biomarkers. *J Clin Oncol*. 2013 Jun 10;31: 2205–18.
- 12Fu Z, Li X, Zhong J, et al. Lenvatinib in combination with transarterial chemoembolization for treatment of unresectable hepatocellular carcinoma (uHCC): a retrospective controlled study. *Hepatol Int*. 2021 Jun;15: 663–75.
- 13Ikeda M, Yamashita T, Ogasawara S, et al. Multicenter Phase II Trial of Lenvatinib plus Hepatic Intra-Arterial Infusion Chemotherapy with Cisplatin for Advanced Hepatocellular Carcinoma: LEOPARD. *Liver Cancer*. 2023: 1–10.
- 14Deng H, Kan A, Lyu N, et al. Dual Vascular Endothelial Growth Factor Receptor and Fibroblast Growth Factor Receptor Inhibition Elicits Antitumor Immunity and Enhances Programmed Cell Death-1 Checkpoint Blockade in Hepatocellular Carcinoma. *Liver Cancer*. 2020 Jun;9: 338–57.
- 15Choi Y, Jung K. Normalization of the tumor microenvironment by harnessing vascular and immune modulation to achieve enhanced cancer therapy. *Experimental & Molecular Medicine*. 2023 2023/11/01.
- 16Napoletano C, Taurino F, Biffoni M, et al. RFA strongly modulates the immune system and anti-tumor immune responses in metastatic liver patients. *Int J Oncol*. 2008 Feb;32: 481–90.
- 17Qi X, Yang M, Ma L, et al. Synergizing sunitinib and radiofrequency ablation to treat hepatocellular cancer by triggering the antitumor immune response. *J Immunother Cancer*. 2020 Oct;8.
- 18Dromi SA, Walsh MP, Herby S, et al. Radiofrequency ablation induces antigen-presenting cell infiltration and amplification of weak tumor-induced immunity. *Radiology*. 2009 Apr;251: 58–66.
- 19Erös de Bethlenfalva-Hora C, Mertens JC, Piguat AC, et al. Radiofrequency ablation suppresses distant tumour growth in a novel rat model of multifocal hepatocellular carcinoma. *Clin Sci (Lond)*. 2014 Feb;126: 243–52.
- 20Ahmed M, Kumar G, Moussa M, et al. Hepatic Radiofrequency Ablation-induced Stimulation of Distant Tumor Growth Is Suppressed by c-Met Inhibition. *Radiology*. 2016 Apr;279: 103–17.
- 21Löffler MW, Nussbaum B, Jäger G, et al. A Non-interventional Clinical Trial Assessing Immune Responses After Radiofrequency Ablation of Liver Metastases From Colorectal Cancer. *Front Immunol*. 2019;10: 2526.
- 22Wang F, Numata K, Komiyama S, et al. Combination Therapy With Lenvatinib and Radiofrequency Ablation for Patients With Intermediate-Stage Hepatocellular Carcinoma Beyond Up-To-Seven Criteria and Child-Pugh Class A Liver function: A Pilot Study. *Front Oncol*. 2022;12: 843680.

## 2. 執筆論文 Publication of thesis ※記載した論文を添付してください。Attach all of the papers listed below.

論文名 1 Title	Lenvatinib radiofrequency ablation sequential therapy offers survival benefits for patients with unresectable hepatocellular carcinoma at intermediate stage and the liver reserve of Child-Pugh A category: A Multicenter Study					
掲載誌名 Published journal	Hepatology Research (under review)					
	年	月	巻(号)	頁 ~	頁	言語 Language
第1著者名 First author	Ying Zhang		第2著者名 Second author	Kazushi Numata		第3著者名 Third author
その他著者名 Other authors	Haruki Uojima, Akihiro Funaoka, Satoshi Komiyama, Katsuaki Ogushi, Makoto Chuma, Kuniyasu Irie, Shigehiro Kokubu, Masato Yoneda, Takashi Kobayashi, Hisashi Hidaka, Taito Fukushima, Satoshi Kobayashi, Manabu Morimoto.					
論文名 2 Title	Enhancing Deep-Seated Hepatocellular Carcinoma Detection: Assessing the Added Value of Additional High Mechanical Index Setting in Sonazoid-based Contrast-Enhanced Ultrasound during Post-Vascular Phase					
掲載誌名 Published journal	Journal of Ultrasound in Medicine (under review)					
	年	月	巻(号)	頁 ~	頁	言語 Language
第1著者名 First author	Ying Zhang		第2著者名 Second author	Kazushi Numata		第3著者名 Third author
その他著者名 Other authors	Akihiro Funaoka, Haruo Miwa, Ritsuko Oishi, Akito Nozaki, Shin Maeda					
論文名 3 Title	Contrast Agents for Hepatocellular Carcinoma Imaging: Value and Progression					
掲載誌名 Published journal	Frontiers in Oncology					
	2022	年	6	月	12	巻(号)
				頁 ~	頁	言語 Language
第1著者名 First author	Ying Zhang		第2著者名 Second author	Kazushi Numata		第3著者名 Third author
その他著者名 Other authors	Shin Maeda					
論文名 4 Title						
掲載誌名 Published journal						
	年	月	巻(号)	頁 ~	頁	言語 Language
第1著者名 First author			第2著者名 Second author			第3著者名 Third author
その他著者名 Other authors						
論文名 5 Title						
掲載誌名 Published journal						
	年	月	巻(号)	頁 ~	頁	言語 Language
第1著者名 First author			第2著者名 Second author			第3著者名 Third author
その他著者名 Other authors						

## 3. 学会発表 Conference presentation ※筆頭演者として総会・国際学会を含む主な学会で発表したものを記載してください

※Describe your presentation as the principal presenter in major academic meetings including general meetings or international meetin

学会名 Conference					
演題 Topic					
開催日 date	年	月	日	開催地 venue	
形式 method	<input type="checkbox"/> 口頭発表 Oral	<input type="checkbox"/> ポスター発表 Poster	言語 Language	<input type="checkbox"/> 日本語	<input type="checkbox"/> 英語 <input type="checkbox"/> 中国語
共同演者名 Co-presenter					
学会名 Conference					
演題 Topic					
開催日 date	年	月	日	開催地 venue	
形式 method	<input type="checkbox"/> 口頭発表 Oral	<input type="checkbox"/> ポスター発表 Poster	言語 Language	<input type="checkbox"/> 日本語	<input type="checkbox"/> 英語 <input type="checkbox"/> 中国語
共同演者名 Co-presenter					
学会名 Conference					
演題 Topic					
開催日 date	年	月	日	開催地 venue	
形式 method	<input type="checkbox"/> 口頭発表 Oral	<input type="checkbox"/> ポスター発表 Poster	言語 Language	<input type="checkbox"/> 日本語	<input type="checkbox"/> 英語 <input type="checkbox"/> 中国語
共同演者名 Co-presenter					
学会名 Conference					
演題 Topic					
開催日 date	年	月	日	開催地 venue	
形式 method	<input type="checkbox"/> 口頭発表 Oral	<input type="checkbox"/> ポスター発表 Poster	言語 Language	<input type="checkbox"/> 日本語	<input type="checkbox"/> 英語 <input type="checkbox"/> 中国語
共同演者名 Co-presenter					

## 4. 受賞(研究業績) Award (Research achievement)

名称 Award name	国名 Country		受賞年 Year of award	年	月
	国名 Country		受賞年 Year of award	年	月

## 5. 本研究テーマに関わる他の研究助成金受給 Other research grants concerned with your research theme

受給実績 Receipt record	<input type="checkbox"/> 有 <input checked="" type="checkbox"/> 無
助成機関名称 Funding agency	
助成金名称 Grant name	
受給期間 Supported period	年 4 月 ~ 2024 年 3 月
受給額 Amount received	円
受給実績 Receipt record	<input type="checkbox"/> 有 <input checked="" type="checkbox"/> 無
助成機関名称 Funding agency	
助成金名称 Grant name	
受給期間 Supported period	年 月 ~ 年 月
受給額 Amount received	円

## 6. 他の奨学金受給 Another awarded scholarship

受給実績 Receipt record	<input checked="" type="checkbox"/> 有 <input type="checkbox"/> 無
助成機関名称 Funding agency	公益財団法人首藤奨学財団
奨学金名称 Scholarship name	首藤奨学財団奨学金
受給期間 Supported period	2023 年 4 月 ~ 2024 年 3 月
受給額 Amount received	600,000 円

## 7. 研究活動に関する報道発表 Press release concerned with your research activities

※記載した記事を添付してください。Attach a copy of the article described below

報道発表 Press release	<input type="checkbox"/> 有 <input checked="" type="checkbox"/> 無	発表年月日 Date of release	
発表機関 Released medium			
発表形式 Release method	・新聞 ・雑誌 ・Web site ・記者発表 ・その他( )		
発表タイトル Released title			

## 8. 本研究テーマに関する特許出願予定 Patent application concerned with your research theme

出願予定 Scheduled	<input type="checkbox"/> 有 <input checked="" type="checkbox"/> 無	出願国 Application	
出願内容(概要) Application contents			

## 9. その他 Others

--



# Contrast Agents for Hepatocellular Carcinoma Imaging: Value and Progression

Ying Zhang<sup>1,2,3</sup>, Kazushi Numata<sup>2\*</sup>, Yuewu Du<sup>1</sup> and Shin Maeda<sup>3</sup>

<sup>1</sup> Department of Medical Ultrasound, Ningbo Medical Centre Li Hui Hospital, Ningbo, China, <sup>2</sup> Gastroenterological Center, Yokohama City University Medical Center, Yokohama, Japan, <sup>3</sup> Department of Gastroenterology, Graduate School of Medicine, Yokohama City University, Yokohama, Japan

Hepatocellular carcinoma (HCC) has the third-highest incidence in cancers and has become one of the leading threats to cancer death. With the research on the etiological reasons for cirrhosis and HCC, early diagnosis has been placed great hope to form a favorable prognosis. Non-invasive medical imaging, including the associated contrast media (CM)-based enhancement scan, is taking charge of early diagnosis as mainstream. Meanwhile, it is notable that various CM with different advantages are playing an important role in the different imaging modalities, or even combined modalities. For both physicians and radiologists, it is necessary to know more about the proper imaging approach, along with the characteristic CM, for HCC diagnosis and treatment. Therefore, a summarized navigating map of CM commonly used in the clinic, along with ongoing work of agent research and potential seeded agents in the future, could be a needed practicable aid for HCC diagnosis and prognosis.

**Keywords:** ultrasound, MRI, CECT, hepatocellular carcinoma (HCC), contrast media (CM)

## OPEN ACCESS

### Edited by:

Kun Zhang,  
Tongji University, China

### Reviewed by:

Dan Zhao,  
Hangzhou Red Cross Hospital, China  
Chengcheng Niu,  
Central South University, China

### \*Correspondence:

Kazushi Numata  
kz\_numa@yokohama-cu.ac.jp

### Specialty section:

This article was submitted to  
Radiation Oncology,  
a section of the journal  
Frontiers in Oncology

**Received:** 16 April 2022

**Accepted:** 02 May 2022

**Published:** 02 June 2022

### Citation:

Zhang Y, Numata K, Du Y  
and Maeda S (2022) Contrast  
Agents for Hepatocellular Carcinoma  
Imaging: Value and Progression.  
Front. Oncol. 12:921667.  
doi: 10.3389/fonc.2022.921667

## INTRODUCTION

Hepatocellular carcinoma (HCC) has the third-highest incidence in cancers, along with the fourth leading cause of cancer death in 2020 globally. Moreover, cirrhosis, a major source of HCC, composed 2.4% of death with all causes in 2019 according to the WHO. Meanwhile, hepatitis B virus (HBV) and hepatitis C virus (HCV) infection, alcohol abuse, and non-alcoholic steatohepatitis (NASH) are dominating etiological reasons for cirrhosis and HCC. Modern medicine believes the small HCC is preventable and curable through early diagnosis and timely etiological treatment if screening and surveillance could be well conducted for cirrhosis (1). Therefore, non-invasive medical imaging techniques, such as MRI, ultrasound (US), and CT, have contributed to HCC patients' management (2–6).

For early diagnosis, treatment assessment, and follow-up, multiple medical imaging modalities were improved and adapted in every corner of HCC prevention and supervision. In the past decades, the diagnostic efficacy of medical imaging has been elevated through the improvement of imaging resolution and associated intravenous contrast agents. US elastography and MR elastography are recommended to supervise and assess hepatic fibrosis, which may gradually progress to cirrhosis without medical intervention (7). On the other hand, taking characteristic advantage of the dual blood supply of the liver, transvenous contrast agents depict the liver lesion by illustrating the tumorous

blood supply with characteristics of arterial enhancement (wash-in) and portal hypodensity or hyposignal (wash-out). The classical imaging findings of wash-in and wash-out were believed to have a sensitivity of approximately 60% and a specificity of 96%–100% for small HCCs with a size of 10–20 mm. Still, a biopsy is needed in 40% of these lesions. Along with a deeper investigation of clinical research, an experienced radiologist can achieve a much more satisfying diagnostic efficacy through guidelines like the American College of Radiology Liver Imaging Reporting and Data System (ACR LIRADS) (8, 9). As a result, contrast enhancement imaging, like dynamic MRI and contrast-enhanced CT (CECT), is recommended in mainstream guidelines for preoperative HCC diagnosis with certainty. Screening using the non-enhanced US is also recommended for patients at a higher risk of HCC every 6 months. When it comes to contrast-enhanced US (CEUS), though it is not recommended by the World Federation for Ultrasound in Medicine and Biology (WFUMB) guidelines for liver lesion detection due to the narrow window for arterial phase observation (10), some meta-analyses indicated it to be a promising diagnostic approach for HCC with a sensitivity of 93% (95% CI: 91%–95%) and a specificity of 90% (95% CI: 88%–92%) (11), as well as the diagnostic efficacy of 93% in small HCCs ( $\leq 2$  cm) (12).

Contrast-enhanced imaging for the tumor is a tracer technique of contrast media (CM) in essence. The distribution and dynamic phases of the agent are analyzed for lesion detection and characterization for early diagnosis and possible prognosis prediction. Therefore, a summarized navigating map of CM commonly used in the clinic, along with ongoing work of agent research and potential seeded agents in the future, could be a needed reference work for both physicians and radiologists.

## BLOOD POOL CONTRAST AGENTS

### Ultrasound Contrast Agents

As early as the late 1960s, people found that the microbubbles (MBs) that provide many reflecting interfaces for echo are a good intravascular flow tracer for US imaging (13), and the hydrogen peroxide solution was launched for echocardiography thereafter. According to the inner gas of the MB, US contrast agent (UCA) could be classified into two generations. Air core with the polymeric coat is the so-called first-generation UCA, such as Levovist (Schering, Berlin-Wedding, Germany). The first-generation UCA is a milestone in the history of medical US imaging development, though it comes with defects like unstableness and unsafety (13). Thereafter, inert gas that is enveloped with a lipid shell at a diameter of approximately several micrometers is developed as the second-generation UCA, which is slightly smaller than that of the red blood cell. Taking advantage of materials science and technology development, the second-generation UCA with greater stability and biosafety can achieve a promising diagnostic efficacy for HCC (11, 12), along with the negligible report of anaphylaxis compared with CT and MRI, which means that UCA can be employed for the patients having iodine allergy, chronic kidney

disease, hepatic function failure, asthma, and so on. Moreover, the bedside operation with a portable US machine could be performed in the emergency department (ED) and intensive care unit (ICU) as needed. However, concerning clinical practice, CEUS is not good at imaging the hepatic lesion located near the lung and behind the costal bone, due to the so-called shadow zone caused by the costal bone and lung. The other weakness is US attenuation in far-field of a fatty liver can lead to the indefinable hepatic situation.

Currently, sulfur hexafluoride (i.e., SonoVue, Bracco Imaging, Milan, Italy) is the most consumed in the global UCA market, followed by perfluorinated butane (i.e., Sonazoid, GE Healthcare, Oslo, Norway). The former is a pure blood pool agent, while the latter behaves similarly at the beginning but permeates into extravascular space soon after administration, which will be discussed in Section 3.

### Iodinated Agents for Contrast-Enhanced CT

Many iodinated agents are pure blood pool agents, which are the widest and longest used CM for X-ray-based enhancement scans (i.e., CECT) (**Figure 1**). To date, the effort of optimizing small-molecule iodinated agents for contrast enhancement could be mainly classified into three eras, including four categories of compounds, from ionic to non-ionic, from monomers to dimers, from high-osmolality to iso-/low-osmolality, associating with decreasing toxicity and increasing bio-tolerability. Commercially available agents are abundant in the clinic, such as iohexol (Omnipaque, GE Healthcare), iopromide (Ultravist, Bayer Healthcare, Leverkusen, Germany), iodixanol (Visipaque, GE Healthcare), iopamidol (Isovue, Bracco Imaging, Milan, Italy), and iothalamate (Cysto-Conray II, Mallinckrodt Imaging, St. Louis, MO, USA). Moreover, novel agents, like iosimenol and GE-145, are on the way to commercialization with the improvements made on an existing basis. The diagnostic efficacy of CECT for HCC in terms of area under the receiver operating characteristic (ROC) curve (AUC), sensitivity, and specificity were reported to be 0.93, 93%, and 82%, respectively (14). For HCC patients, the most distinctive role that CT perfusion imaging has played is the transarterial chemoembolization (TACE) assessment (15). However, despite great improvements that have been made in the bone and cartilage tissue, iodinated contrast agents employed in parenchymal organs, like the liver, have not yet been largely renovated (16, 17).

The blood pool agent applied to MRI is mainly established for MR angiography rather than the liver tumor, which is beyond the scope of the present review article and will not be discussed herein.

## EXTRACELLULAR CONTRAST AGENTS

### Non-Specific Agents

For MRI, gadolinium-based micromolecule agents that have five or seven unpaired electrons could be stimulated to be paramagnetic under an external magnetic field. Those so-called paramagnetic contrast agents for dynamic MRI are developed

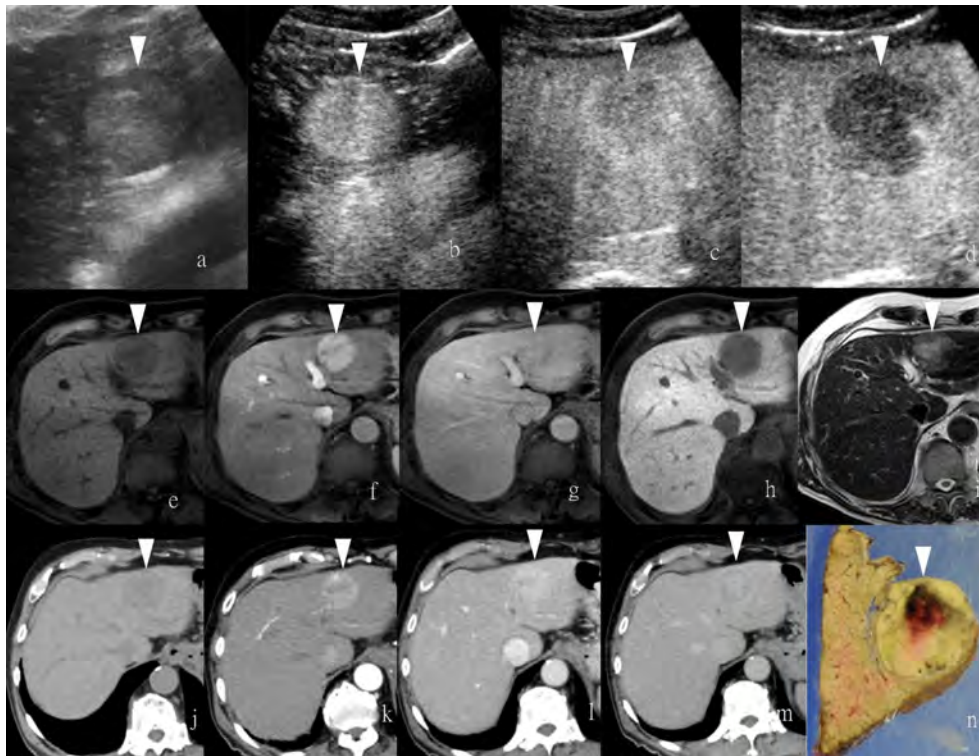


**FIGURE 1** | Images of a man in his eighties with a pathological diagnosis of moderately differentiated hepatocellular carcinoma (HCC) and had a history of hepatitis (C). At the Sonazoid-enhanced ultrasound (US), the liver lesion at a size of 43 mm with a thin halo located at segment III was observed on B-mode US (A). It was rapidly enhanced in the arterial phase (wash-in) (B), started to fade (wash-out) in portal phase (C), and was totally exhausted in the post-vascular phase (D). At Gd-EOB-DTPA-enhanced MRI, the lesion was hypointense on T1-weighted image (E), with the typical characteristics of wash-in and wash-out from arterial phase, portal phase, to delayed phase (F–H). It showed hyperintensity on T2-weighted image (I). At iodine agent-enhanced CT, it has low-density before enhancement (J). It also showed wash-in and wash-out from arterial phase, portal phase, to delayed phase (K–M). Finally, the gross specimen vividly reflected the morphological information of tumor (N). Arrowheads indicate the margin of the HCC lesion.

and enriched (18). Gadolinium chelates (Gd-chelates) are clinically available mainstream for dynamic MRI on T1-weighted images, including Gd-DTPA (gadopentetic acid, Magnevist, Berlex, Berlin, Germany), Gd-DTPA-BMA (gadodiamide, Omniscan, Nycomed Amersham, Amersham, UK), Gd-HP-DO3A (gadoteridol, ProHance, Bracco Diagnostics, Milan, Italy), Gd-DTPA-BMEA (gadoversetamide, Optimark, Mallinckrodt, Staines-upon-Thames, UK), Gd-DOTA (gadoterate, meglumine, Dotarem Guerbet, Princeton, NJ, USA), and Gd-BT-DO3A (gadobutrol Gadovist, Schering Diagnostics, Berlin, Germany). These extracellular agents for non-specific liver MRI are commonly used worldwide because of the good patient tolerance and satisfying diagnostic efficacy (19). Thus, clinical recommendations from guidelines are almost based on the Gd-chelates (8, 9). Moreover, the informative images provided by contrast-enhanced MRI (CEMRI) also contribute to the therapy assessment (Table 1).

### Reticuloendothelial System Endocytosis

Ferumoxytol, a kind of iron oxide nanoparticles (IONPs) approved by the Food and Drug Administration (FDA) as medicine for iron deficiency in adults, was recently reported to

be feasible for MR angiography thanks to the characteristic of longer half-life in circulation and the advantage of superparamagnetism (20–23). The so-called negative contrast agents, containing iron oxide particles, darken the normal liver background on T2-weighted images to negatively enhance the target issue, in contrast with the so-called positive agents that brighten the target tissue on T1-weighted images, like Gd-chelates. The first commercially available reticuloendothelial system (RES)-specific contrast agent is ferumoxides (Feridex) (24), which makes lesions that contain negligible RES cells conspicuous on T2-weighted images since the normal liver background containing many RES cells can selectively take up iron oxide particulates to lower the T2 signal intensity (25). Iron oxide crystals coated with dextran or carboxydextran are named superparamagnetic iron oxide (SPIO), which is normally employed as T2 MR CM. With a sufficient infusion of SPIO, normal hepatocytes containing many Kupffer cells are supposed to catch most SPIO particles, leading to a dark area on T2-weighted images. By contrast, tumors, whether benign or malignant, primary or metastatic, that are deficient in Kupffer cells cannot exhibit SPIO uptake, shaping a relatively hyperintense area. However, focal nodular hyperplasia (FNH)

**TABLE 1** | The categories of extracellular contrast agents in clinical practice.

Category	Specificity	Class	Classical agents	Featured purposes	Modality
Extracellular agent	Non-specific	Gadolinium chelates	Gadopentetic acid (Gd-DTPA)	Tumor imaging; blood pool imaging	T1 agent for MRI
Reticuloendothelial system (RES) agent (Kupffer cells included)	RES specific	Iron oxide	Ferucarbotran (Feridex)	Liver tumor imaging	T2 agent for MRI
		Microbubbles	Perfluorinated butane (Sonazoid)	Liver tumor imaging; blood pool imaging	Ultrasound contrast agent
Hepatobiliary agent	Hepatobiliary specific	Manganese-based compound	Mangafodipir (Mn-DPDP)	MR cholangiography; liver function indicator	T1 agent for MRI
			Gadobenate dimeglumine (Gd-BOPTA); gadoxetic acid (Gd-EOB-DTPA)	Liver tumor imaging	T1 agent for MRI

seems to be an exception, since SPIO particles may accumulate there and lead to a resultant isointense or even hypointense appearance (26, 27). Following SPIO, the derivative in terms of ultrasmall particulate iron oxides (USPIO) with advantages of convenient administration and striking prolonged plasma half-life that enables it also as a blood pool agent was developed thereafter (28, 29) (**Table 1**).

Regarding UCA, Sonazoid is an MB of perfluorobutane core wrapped by the shell of hydrogenated egg phosphatidylserine. At first, Sonazoid MBs were used as the blood pool contrast agent. As early as 1 min after the intravenous administration, the MBs start to diffuse into extravascular and intercellular space where they will be phagocytosed by the Kupffer cells in the normal liver sinusoids. Approximately 10 min later, once intravascular MBs are mostly eliminated, the remaining stable MBs endocytosed by resident macrophages in liver parenchyma will shape the so-called additional Kupffer phase or post-vascular phase, which can last to 2 h after injection (30–32) (**Table 1**). Moreover, in the classical enhancement features of wash-in and wash-out, HCC theoretically appears to be perfusion defects in the Kupffer phase

or post-vascular phase because of Kupffer cell shortage (**Figures 1, 2**). The characteristics of the additional post-vascular phase aid much in HCC detection and diagnosis. Recently, Sonazoid has been proven to be non-inferior to SonoVue in a retrospective clinical study for focal liver lesion (FLL) (33). However, if the lesion is isoechoic in the post-vascular phase, misdiagnosis can happen at a rate of approximately 17% (34). Worse still, owing to histological reasons of some well-differentiated HCC, the sign of perfusion defect in the Kupffer phase could be observed at a rate of only 69% among HCC patients (35). Also, some benign lesions that lack Kupffer cells have a chance to be misdiagnosed as a false-positive sign in the Kupffer phase (36). Therefore, the expected additional clinical benefit on diagnosis gained from the Kupffer phase has not yet been confirmed (37). As for HCC intervention, after US brings real-time monitoring for minimally invasive operations like lesion biopsy and regional ablation, CEUS is employed for more accurate guidance and unique immediate evaluation during therapy (38–43). Vascular-sensitive assessment makes CEUS an indispensable aid for effective

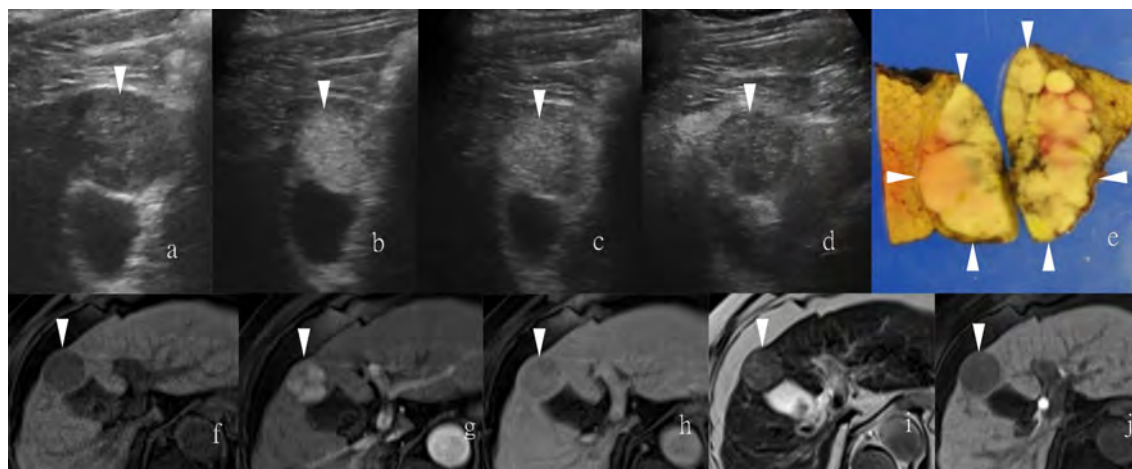


**FIGURE 2** | Images of a man in his sixties with a pathological diagnosis of poorly to moderately differentiated hepatocellular carcinoma (HCC) and had a history of cirrhosis. At the Sonazoid-enhanced ultrasound (US), the liver lesion was heterogeneous hyperechoic with the indistinct margin on B-mode US (**A**). It was rapidly enhanced in the arterial phase (wash-in) (**B**), still iso-echoic in portal phase (**C**), and was totally exhausted in the post-vascular phase (**D**). At Gd-EOB-DTPA-enhanced MRI, the lesion was hypointense on T1-weighted image (**F**), with uncharacteristic wash-in and delayed wash-out from arterial phase to delayed phase (**G, H**). It showed hyperintensity on T2-weighted image (**I**). The contrast media (CM) were totally exhausted till the hepatobiliary phase (**J**). The gross specimen indicated the heterogeneous pathological differentiation of HCC (**E**). Arrowheads indicate the margin of the HCC lesion.

radiofrequency (RF)/microwave (MV) ablation (44, 45). On the other hand, three-dimensional (3D) US can provide additional lateral and other viewing angles, and morphological information offers UCA another usable imaging modality (i.e., contrast-enhanced 3D US, CE 3D US) (46, 47) (**Figure 3**). Moreover, contrast enhancement is also employed in fusion imaging to reveal extra small liver lesions and biopsy navigation (48) (**Figure 4**).

### Hepatocyte-Specific Uptake

Mangafodipir trisodium (Mn-DPDP) used to be a classical hepatocyte-selective contrast agent that was developed in the last century and has favorable contrast-to-noise measurements and lesion detection rate as compared to non-enhanced MRI (49, 50). It was high-profile at the beginning for the prolonged enhancement relative to the traditional T1 contrast agents (51). The uptake of Mn-DPDP occurs in hepatocytes, and its elimination is in the biliary tree. Thus, the metabolism process of Mn-DPDP can indicate hepatobiliary function (52, 53). Moreover, it is reported that the hepatocyte-selective contrast agent is correlative with the pathological differentiation degree of HCC (54). Since the uptake of Mn-DPDP strictly occurs in hepatocytes, the extrahepatic originated metastases can be negatively illustrated (55). However, in contrast to the question of how many normal hepatocytes are contained in a lesion, the question of whether a liver lesion is malignant or not will be the highest concern for patients.

By integrating the mechanisms of both hepatocyte-selective contrast agents and non-specific extracellular Gd-chelates, gadolinium-based hepatobiliary-specific agents were thereby developed, such as gadobenate dimeglumine (Gd-BOPTA) and gadoxetic acid (Gd-EOB-DTPA), which are worldwide commercially available and have become a promising MRI contrast agent for FLL (56–58). For HCC diagnostic imaging, the so-called hepatobiliary contrast agents achieve further detection in the early stage for primary, recurrent, and metastatic HCCs through usual dynamic imaging and additional hepatobiliary delayed phase (59–62) (**Figures 1, 2**). Beyond diagnosis, uptake of Gd-EOB-DTPA of HCC lesions is reported to be a biomarker for prognosis (63), as well as the estimation of liver function (64). Concerning patients' tolerance, Gd-EOB-DTPA only requires a minimum injection dose to present a satisfying enhancement in the liver and smaller branch of the biliary tree relative to Gd-BOPTA (55) (**Table 1**).

### MOLECULAR IMAGING AGENTS

For the diagnostic and therapeutic purpose of molecular imaging, by means of conjugating some antibody, peptide, or ligand, molecular imaging agents are artificially designed to anchor the targeted cellular and molecular hallmarks pathologically (65).

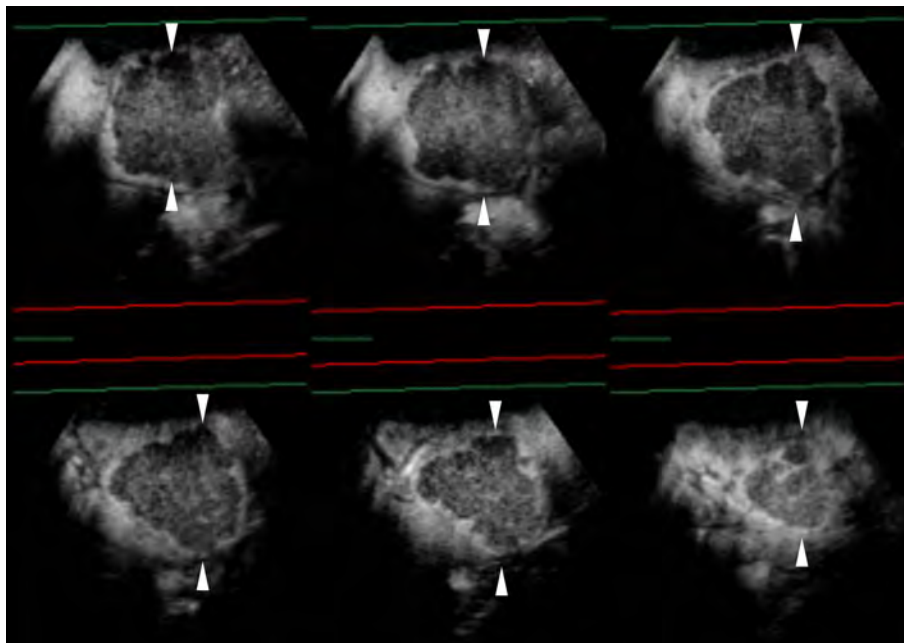


**FIGURE 3** | Sonazoid-enhanced ultrasound (US) images of a man in his seventies with a pathological diagnosis of moderately differentiated hepatocellular carcinoma (HCC), who had a history of hepatitis C. The tumor was 70mm. Consecutive lateral images of the tumor remarkably illumed the irregular margin on the three-dimensional (3D) US, which was obtained by auto-sweep 3D scanning in the post-vascular phase. Tomographic ultrasound images in plane A, which can be translated from front to rear, with a slice distance of 4.8 mm. Arrowheads indicate the margin of the HCC lesion.

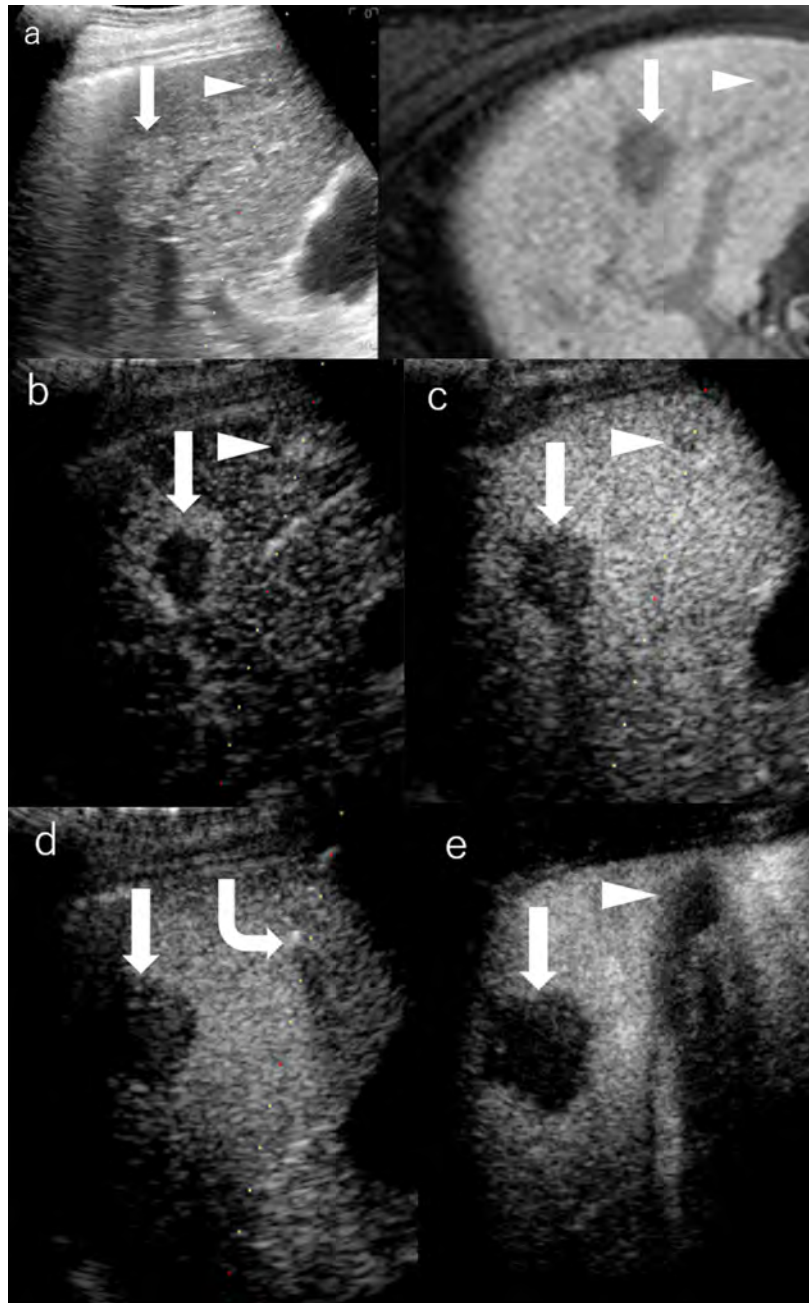


**FIGURE 4** | Images of a man in his seventies with a pathological diagnosis of moderately differentiated hepatocellular carcinoma (HCC) and had a history of cirrhosis and HCC. The hepatobiliary phase of EOBMRI (right side), as the reference, was combined with conventional grayscale US (left side), displayed an 8-mm indistinctive hypointense area (the triangular arrow) in segment V on the same screen for the fusion imaging (A). The extrasmall lesion was hypervascular in the arterial phase of Sonazoid-enhanced ultrasound (US) (B), while the post-vascular phase indicated it to be a slightly hypoechoic area (C). Pathway guidance was ready for radiofrequency ablation (RFA) needle manipulation on real-time US (B–D), along with tracking for the metallic needle tip (the curved arrow) (D). The contrast-enhanced US (CEUS) evaluated the target ablation area to be non-enhanced after RFA (E). Arrows indicate the margin of the bigger HCC lesion, which was previously treated by RFA. And Arrowheads indicate the margin of the extrasmall HCC lesion.

### Immune Molecular Anchoring

By means of immunoreaction, gadolinium-labeled reagents for liver tumor marking and monitoring of the MR modality are commonly employed in a tumor-bearing animal model for cancer research (66,

67). The molecular weight of reagents mainly ranges from dozens to hundreds of kDa. Likewise, the MBs or nanobubbles binding compounds marked with the tumor-specific immune molecule are also available for cancer research in the CEUS modality (66).

## Stimulus-Responsive/Microenvironment-Dependent Contrast Agents

A T1/T2 switchable MR contrast agent was recently validated on a mouse model for HCC early diagnosis (68, 69). Previously, the diagnostic efficacy of IONP-based MRI was not as high as expected when it was simply employed as a liver-specific T2 agent (70). However, researchers recently found that IONP clusters could be accordingly disaggregated thanks to the acidic tumor microenvironment, which can generate a downstream tumor-specific T1 contrast agent. As a result, the IONP agents can additionally be employed to delineate HCC on T1-weighted images after switching to a downstream tumor-specific contrast agent. Based on IONP, agents decorated with functional small-molecular ligands through surface engineering are thereafter designed to be stimulus-responsive agents, pH-sensitive, and nanoscale distance-dependent (68, 71–75). Furthermore, concerning the aggregation phenomenon that commonly happened in nanoparticles with a large surface area/volume ratio, ultrafine nanoparticles could facilitate intratumoral homogeneous distribution of contrast agents (76). IONP at a diameter of 3.6 nm is supposed to be an optimal T1 agent *in vivo* (77). Moreover, core engineering of various designs of size, shape, composition, surface coating, molecular weight, and drug delivery has indicated IONP to be a hopeful T1 contrast agent (78–85). Beyond imaging, Yang et al. developed a novel nanoparticle that releases Fe<sup>2+</sup> for the treatment of folic acid (FA) receptor-positive solid tumors through the ferroptosis pathway while being supervised through the Mn agent-enhanced imaging (86, 87). Also, Song et al. developed an assay of therapeutic natural killer cells (NK cells) conjugated with Sonazoid MB to make the antitumor process visible in real-time CEUS (88).

## Scale-Dependent Particles

As nanomedicine was developed recently, emerging nanomaterials have been studied for contrast enhancement imaging. Some nanoscaled CM can permeate into tumor stroma through weak tumor vessels to depict the tumor with or without the assistance from functional parts equipped in advance (89). Moreover, sonoporation induced by external stimulation of focused US can reversibly increase the permeabilization of the cell membrane, leading to the potential visualization of HCC intracellular therapy in the future (90).

## CLINICAL CHALLENGES AND PROSPECTS

As for the clinically commonly used contrast agents, Guang et al. performed a meta-analysis to compare the diagnostic value of CEUS, CT, and MRI in FLL. To rule out HCC from FLL, CECT has the highest sensitivity of 90% (95% CI: 88%–92%), followed by CEUS (88%) and CEMRI (86%). Both CEUS and CEMRI have a higher sensitivity of 81% than CECT (77%). However, all results have no statistical significance (16, 91). Moreover, Westwood et al.

found that CEUS could be a cost-effective alternative for HCC diagnosis relative to CECT or CEMRI with similar diagnostic performance (92). Research about combined multimodal medical imaging (including Sonazoid-enhanced US, Gd-EOB-DTPA-enhanced MRI, and CECT) conducted by Masatoshi Kudo figured out that the sensitivity for HCC diagnosis is 72%, 74%, and 86% for CEUS, CECT, and Gd-EOB-DTPA-enhanced MRI, respectively, with no significance among the three imaging modalities. When combining US with MRI, the sensitivity soared as high as 90% (93).

Meanwhile, controversies still remain regarding the diagnostic efficacy of HCC. Despite that the hepatobiliary agent-enhanced MRI is believed to reach an early diagnosis for HCC that is still in the hypovascular stage (94), researchers analyzed the clinical trials that use different contrast agents for HCC diagnosis and found no significant difference in the diagnostic efficacy in terms of sensitivity and specificity between the MRI using extracellular agents and hepatobiliary agents (95, 96). Imbriaco et al. claimed that Gd-EOB-DTPA-enhanced MRI has a better diagnostic performance than CECT only for lesions that are smaller than 20 mm and patients with Child-Pugh class A (97). Moreover, for patients with cirrhosis, Kim et al. demonstrated better performance of hepatobiliary agent-enhanced MRI relative to routine US screening for surveillance of people at a higher risk of HCC (2). In addition, molecular imaging agents, like IONP-based MR agents, are still on the way to fulfilling the various clinical needs (98). On the other hand, although current CM has been deeply improved through materials science, biosafety is still the most crucial factor for patients having various allergies and metabolism troubles. Necessary reinjection of contrast agents for CT and MRI may come with a potential risk of side effects. Minimized dose of contrast agent that meets all clinical needs will be a future trend for CM research.

To sum up, the CM brings out the best diagnostic performance for suitable patients under appropriate conditions. Although Gd-DTPA-enhanced MRI and non-ionic iodinated agents-enhanced CT are usually recommended for HCC diagnosis by mainstream guidelines, liver-specific CM, like Gd-EOB-DTPA and Sonazoid, have already played an anticipated role in HCC diagnosis and prognosis prediction. Furthermore, the amelioration of molecular imaging agents has drawn a blueprint for future medical imaging.

## AUTHOR CONTRIBUTIONS

Concept and design: KN and YZ. Manuscript writing: YZ. Figure presentation: KN. Reviewed the manuscript: all authors. All authors contributed to the article and approved the submitted version.

## FUNDING

This work was partially supported by grants from the Natural Science Foundation of Ningbo (No. 2019A610313), Medical

Science and Technology Project of Zhejiang Province (No. 2021KY312), Ningbo Medical Science and Technology Project (No. 2019Y05), Ningbo Clinical Medicine Research Center

Project (No. 2019A21003), Japan-China Sasakawa Medical Scholarship, and Young Talents Training Program of Ningbo Municipal Health Commission.

## REFERENCES

- Ferlay J, Colombet M, Soerjomataram I, Parkin DM, Piñeros M, Znaor A, et al. Cancer Statistics for the Year 2020: An Overview. *Int J Cancer* (2021).
- Kim SY, An J, Lim YS, Han S, Lee JY, Byun JH, et al. MRI With Liver-Specific Contrast for Surveillance of Patients With Cirrhosis at High Risk of Hepatocellular Carcinoma. *JAMA Oncol* (2017) 3(4):456–63. doi: 10.1001/jamaoncol.2016.3147
- Elsayes KM, Hooker JC, Agrons MM, Kielar AZ, Tang A, Fowler KJ, et al. Version of LI-RADS for CT and MR Imaging: An Update. *Radiographics* (2017) 37(7):1994–2017. doi: 10.1148/rg.2017170098
- Marrero JA, Ahn J, Rajender Reddy K. ACG Clinical Guideline: The Diagnosis and Management of Focal Liver Lesions. *Am J Gastroenterol* (2014) 109(9):1328–47. doi: 10.1038/ajg.2014.213
- Kudo M, Matsui O, Izumi N, Iijima H, Kadoya M, Imai Y, et al. JSH Consensus-Based Clinical Practice Guidelines for the Management of Hepatocellular Carcinoma: 2014 Update by the Liver Cancer Study Group of Japan. *Liver Cancer* (2014) 3(3–4):458–68. doi: 10.1159/000343875
- Park J-W, Hyeok LJ, Lee JS, Tak TY, Bae SH, Yeon JE, et al. 2014 Korean Liver Cancer Study Group-National Cancer Center Korea Practice Guideline for the Management of Hepatocellular Carcinoma. *Korean J Radiol* (2015) 16(3):465–522. doi: 10.3348/kjr.2015.16.3.465
- Horowitz JM, Kamel IR, Arif-Tiwari H, Asrani SK, Hindman NM, Kaur H, et al. ACR Appropriateness Criteria® Chronic Liver Disease. *J Am Coll Radiol* (2017) 14(11s):S391–s405. doi: 10.1016/j.jacr.2017.08.045
- American College of Radiology. *Liver Reporting and Data Systems (LI-RADS)* Available at: <https://www.acr.org/Clinical-Resources/Reporting-and-Data-Systems/LI-RADS> (Accessed June 4, 2019).
- Marks RM, Masch WR, Chernyak V. LI-RADS: Past, Present, and Future, From the AJR Special Series on Radiology Reporting and Data Systems. *AJR Am J Roentgenol* (2021) 216(2):295–304. doi: 10.2214/AJR.20.24272
- Dietrich CF, Nolsoe CP, Barr RG, Berzigotti A, Burns PN, Cantisani V, et al. Guidelines and Good Clinical Practice Recommendations for Contrast-Enhanced Ultrasound (CEUS) in the Liver-Update 2020 WFUMB in Cooperation With EFSUMB, AFSUMB, AIUM, and FLAUS. *Ultrasound Med Biol* (2020) 46(10):2579–604. doi: 10.1016/j.ultrasmedbio.2020.04.030
- Friedrich-Rust M, Klopffleisch T, Nierhoff J, Herrmann E, Vermehren J, Schneider MD, et al. Contrast-Enhanced Ultrasound for the Differentiation of Benign and Malignant Focal Liver Lesions: A Meta-Analysis. *Liver Int* (2013) 33(5):739–55. doi: 10.1111/liv.12115
- Niu Y, Huang T, Lian F, Li F. Contrast-Enhanced Ultrasonography for the Diagnosis of Small Hepatocellular Carcinoma: A Meta-Analysis and Meta-Regression Analysis. *Tumour Biol* (2013) 34(6):3667–74. doi: 10.1007/s13277-013-0948-z
- Gramiak R, Shah PM. Echocardiography of the Aortic Root. *Invest Radiol* (1968) 3(5):356–66. doi: 10.1097/00004424-196809000-00011
- Jia GS, Feng GL, Li JP, Xu HL, Wang H, Cheng YP, et al. Using Receiver Operating Characteristic Curves to Evaluate the Diagnostic Value of the Combination of Multislice Spiral CT and Alpha-Fetoprotein Levels for Small Hepatocellular Carcinoma in Cirrhotic Patients. *Hepatobiliary Pancreat Dis Int* (2017) 16(3):303–9. doi: 10.1016/S1499-3872(17)60018-3
- Saake M, Lell MM, Eller A, Wuest W, Heinz M, Uder M, et al. Imaging Hepatocellular Carcinoma With Dynamic CT Before and After Transarterial Chemoembolization: Optimal Scan Timing of Arterial Phase. *Acad Radiol* (2015) 22(12):1516–21. doi: 10.1016/j.acra.2015.08.021
- Kim KA, Kim MJ, Choi JY, Park MS, Lim JS, Chung YE, et al. Detection of Recurrent Hepatocellular Carcinoma on Post-Operative Surveillance: Comparison of MDCT and Gadoxetic Acid-Enhanced MRI. *Abdom Imaging* (2014) 39(2):291–9. doi: 10.1007/s00261-013-0064-y
- Matoba M, Kitadate M, Kondou T, Yokota H, Tonami H. Depiction of Hypervascular Hepatocellular Carcinoma With 64-MDCT: Comparison of Moderate- and High-Concentration Contrast Material With and Without Saline Flush. *AJR Am J Roentgenol* (2009) 193(3):738–44. doi: 10.2214/AJR.08.2028
- Gandhi SN, Brown MA, Wong JG, Aguirre DA, Sirlin CB. MR Contrast Agents for Liver Imaging: What, When, How. *Radiographics* (2006) 26(6):1621–36. doi: 10.1148/rg.266065014
- Bellin MF, Vasile M, Morel-Precetti S. Currently Used non-Specific Extracellular MR Contrast Media. *Eur Radiol* (2003) 13(12):2688–98. doi: 10.1007/s00330-003-1912-x
- Bashir MR, Bhatti L, Marin D, Nelson RC. Emerging Applications for Ferumoxytol as a Contrast Agent in MRI. *J Magn Reson Imaging* (2015) 41(4):884–98. doi: 10.1002/jmri.24691
- Ersoy H, Jacobs P, Kent CK, Prince MR. Blood Pool MR Angiography of Aortic Stent-Graft Endoleak. *AJR Am J Roentgenol* (2004) 182(5):1181–6. doi: 10.2214/ajr.182.5.1821181
- Hope MD, Hope TA, Zhu C, Faraji F, Haraldsson H, Ordoas KG, et al. Vascular Imaging With Ferumoxytol as a Contrast Agent. *AJR Am J Roentgenol* (2015) 205(3):W366–73. doi: 10.2214/AJR.15.14534
- Huang Y, Hsu JC, Koo H, Cormode DP. Repurposing Ferumoxytol: Diagnostic and Therapeutic Applications of an FDA-Approved Nanoparticle. *Theranostics* (2022) 12(2):796–816. doi: 10.7150/thno.67375
- Ros PR, Freeny PC, Harms SE, Seltzer SE, Davis PL, Chan TW, et al. Hepatic MR Imaging With Ferumoxides: A Multicenter Clinical Trial of the Safety and Efficacy in the Detection of Focal Hepatic Lesions. *Radiol* (1995) 196(2):481–8. doi: 10.1148/radiology.196.2.7617864
- Tanimoto A, Kuribayashi S. Application of Superparamagnetic Iron Oxide to Imaging of Hepatocellular Carcinoma. *Eur J Radiol* (2006) 58(2):200–16. doi: 10.1016/j.ejrad.2005.11.040
- Grazioli L, Morana G, Kirchin MA, Caccia P, Romanini L, Bondioni MP, et al. MRI of Focal Nodular Hyperplasia (FNH) With Gadobenate Dimeglumine (Gd-BOPTA) and SPIO (Ferumoxides): An Intra-Individual Comparison. *J Magn Reson Imaging* (2003) 17(5):593–602. doi: 10.1002/jmri.10289
- Terkivatan T, van den Bos IC, Hussain SM, Wielopolski PA, de Man RA, IJzermans JNM. Focal Nodular Hyperplasia: Lesion Characteristics on State-of-the-Art MRI Including Dynamic Gadolinium-Enhanced and Superparamagnetic Iron-Oxide-Uptake Sequences in a Prospective Study. *J Magn Reson Imaging* (2006) 24(4):864–72. doi: 10.1002/jmri.20705
- Zhao M, Liu Z, Dong L, Zhou H, Yang S, Wu W, et al. A GPC3-Specific Aptamer-Mediated Magnetic Resonance Probe for Hepatocellular Carcinoma. *Int J Nanomed* (2018) 13:4433–43. doi: 10.2147/IJN.S168268
- Shan L. Superparamagnetic Iron Oxide Nanoparticles (SPIO) Stabilized by Alginate. In: *Molecular Imaging and Contrast Agent Database (MICAD)*. Bethesda (MD: National Center for Biotechnology Information (US) (2004).
- Li P, Hoppmann S, Du P, Li H, Evans PM, Moestue SA, et al. Pharmacokinetics of Perfluorobutane After Intra-Venous Bolus Injection of Sonazoid in Healthy Chinese Volunteers. *Ultrasound Med Biol* (2017) 43(5):1031–9. doi: 10.1016/j.ultrasmedbio.2017.01.003
- Yanagisawa K, Moriyasu F, Miyahara T, Yuki M, Iijima H. Phagocytosis of Ultrasound Contrast Agent Microbubbles by Kupffer Cells. *Ultrasound Med Biol* (2007) 33(2):318–25. doi: 10.1016/j.ultrasmedbio.2006.08.008
- Shunichi S, Hiroko I, Fuminori M, Waki H. Definition of Contrast Enhancement Phases of the Liver Using a Perfluoro-Based Microbubble Agent, Perflubutane Microbubbles. *Ultrasound Med Biol* (2009) 35(11):1819–27. doi: 10.1016/j.ultrasmedbio.2009.05.013
- Zhai HY, Liang P, Yu J, Cao F, Kuang M, Liu FY, et al. Comparison of Sonazoid and SonoVue in the Diagnosis of Focal Liver Lesions: A Preliminary Study. *J Ultrasound Med* (2019) 38(9):2417–25. doi: 10.1002/jum.14940
- Kunishi Y, Numata K, Morimoto M, Okada M, Kaneko T, Maeda S, et al. Efficacy of Fusion Imaging Combining Sonography and Hepatobiliary Phase MRI With Gd-EOB-DTPA to Detect Small Hepatocellular Carcinoma. *AJR Am J Roentgenol* (2012) 198(1):106–14. doi: 10.2214/AJR.10.6039

35. Duisyenbi Z, Numata K, Nihonmatsu H, Fukuda H, Chuma M, Kondo M, et al. Comparison Between Low Mechanical Index and High Mechanical Index Contrast Modes of Contrast-Enhanced Ultrasonography: Evaluation of Perfusion Defects of Hypervascular Hepatocellular Carcinomas During the Post-Vascular Phase. *J Ultrasound Med* (2019) 38(9):2329–38. doi: 10.1002/jum.14926
36. Ishibashi H, Maruyama H, Takahashi M, Shimada T, Kamesaki H, Fujiwara K, et al. Demonstration of Intrahepatic Accumulated Microbubble on Ultrasound Represents the Grade of Hepatic Fibrosis. *Eur Radiol* (2012) 22(5):1083–90. doi: 10.1007/s00330-011-2346-5
37. Barr RG, Huang P, Luo Y, Xie X, Zheng R, Yan K, et al. Contrast-Enhanced Ultrasound Imaging of the Liver: A Review of the Clinical Evidence for SonoVue and Sonazoid. *Abdom Radiol (NY)* (2020) 45(11):3779–88. doi: 10.1007/s00261-020-02573-9
38. Spârchez Z, Radu P, Kacso G, Spârchez M, Zaharia T, Al Hajjar N. Prospective Comparison Between Real Time Contrast Enhanced and Conventional Ultrasound Guidance in Percutaneous Biopsies of Liver Tumors. *Med Ultrason* (2015) 17(4):456–63. doi: 10.11152/mu.2013.2066.174.deu
39. Park HS, Kim YJ, Yu MH, Jung SI, Jeon HJ. Real-Time Contrast-Enhanced Sonographically Guided Biopsy or Radiofrequency Ablation of Focal Liver Lesions Using Perflubutane Microbubbles (Sonazoid): Value of Kupffer-Phase Imaging. *J Ultrasound Med* (2015) 34(3):411–21. doi: 10.7863/ultra.34.3.411
40. Liu F, Yu X, Liang P, Cheng Z, Han Z, Dong B. Contrast-Enhanced Ultrasound-Guided Microwave Ablation for Hepatocellular Carcinoma Inconspicuous on Conventional Ultrasound. *Int J Hyperthermia* (2011) 27(6):555–62. doi: 10.3109/02656736.2011.564262
41. Yan SY, Zhang Y, Sun C, Cao HX, Li GM, Wang YQ, et al. Comparison of Real-Time Contrast-Enhanced Ultrasonography and Standard Ultrasonography in Liver Cancer Microwave Ablation. *Exp Ther Med* (2016) 12(3):1345–8. doi: 10.3892/etm.2016.3448
42. Miyamoto N, Hiramatsu K, Tsuchiya K, Sato Y, Terae S, Shirato H. Sonazoid-Enhanced Sonography for Guiding Radiofrequency Ablation for Hepatocellular Carcinoma: Better Tumor Visualization by Kupffer-Phase Imaging and Vascular-Phase Imaging After Reinjection. *Jpn J Radiol* (2009) 27(4):185–93. doi: 10.1007/s11604-009-0317-4
43. Numata K, Morimoto M, Ogura T, Sugimori K, Takebayashi S, Okada M, et al. Ablation Therapy Guided by Contrast-Enhanced Sonography With Sonazoid for Hepatocellular Carcinoma Lesions Not Detected by Conventional Sonography. *J Ultrasound Med* (2008) 27(3):395–406. doi: 10.7863/jum.2008.27.3.395
44. Wiggermann P, Zuber-Jerger I, Zausig Y, Loss M, Scherer MN, Schreyer AG, et al. Contrast-Enhanced Ultrasound Improves Real-Time Imaging of Ablation Region During Radiofrequency Ablation: Preliminary Results. *Clin Hemorheol Microcirc* (2011) 49(1-4):43–54. doi: 10.3233/CH-2011-1456
45. Mauri G, Porazzi E, Cova L, Restelli U, Tondolo T, Bonfanti M, et al. Intraoperative Contrast-Enhanced Ultrasound (CEUS) in Liver Percutaneous Radiofrequency Ablation: Clinical Impact and Health Technology Assessment. *Insights Imaging* (2014) 5(2):209–16. doi: 10.1007/s13244-014-0315-7
46. Luo W, Numata K, Morimoto M, Oshima T, Ueda M, Okada M, et al. Role of Sonazoid-Enhanced Three-Dimensional Ultrasonography in the Evaluation of Percutaneous Radiofrequency Ablation of Hepatocellular Carcinoma. *Eur J Radiol* (2010) 75(1):91–7. doi: 10.1016/j.ejrad.2009.03.021
47. Numata K, Luo W, Morimoto M, Kondo M, Kunishi Y, Sasaki T, et al. Contrast Enhanced Ultrasound of Hepatocellular Carcinoma. *World J Radiol* (2010) 2(2):68–82. doi: 10.4329/wjr.v2.i2.68
48. Kang TW, Lee MW, Song KD, Kim M, Kim SS, Kim SH, et al. Added Value of Contrast-Enhanced Ultrasound on Biopsies of Focal Hepatic Lesions Invisible on Fusion Imaging Guidance. *Korean J Radiol* (2017) 18(1):152–61. doi: 10.3348/kjr.2017.18.1.152
49. Bernardino ME, Young SW, Lee JK, Weinreb JC. Hepatic MR Imaging With Mn-DPDP: Safety, Image Quality, and Sensitivity. *Radiol* (1992) 183(1):53–8. doi: 10.1148/radiology.183.1.1549694
50. Young SW, Bradley B, Muller HH, Rubin DL. Detection of Hepatic Malignancies Using Mn-DPDP (Manganese Dipyridoxal Diphosphate) Hepatobiliary MRI Contrast Agent. *Magn Reson Imaging* (1990) 8(3):267–76. doi: 10.1016/0730-725X(90)90099-N
51. Rofsky NM, Earls JP. Mangafodipir Trisodium Injection (Mn-DPDP). A Contrast Agent for Abdominal MR Imaging. *Magn Reson Imaging Clin N Am* (1996) 4(1):73–85. doi: 10.1016/S1064-9689(21)00555-9
52. Mitchell DG, Alam F. Mangafodipir Trisodium: Effects on T2- and T1-Weighted MR Cholangiography. *J Magn Reson Imaging* (1999) 9(2):366–8. doi: 10.1002/(SICI)1522-2586(199902)9:2<366::AID-JMRI33>3.0.CO;2-E
53. Seale MK, Catalano OA, Saini S, Hahn PF, Sahani DV. Hepatobiliary-Specific MR Contrast Agents: Role in Imaging the Liver and Biliary Tree. *Radiographics* (2009) 29(6):1725–48. doi: 10.1148/rg.296095515
54. Murakami T, Baron RL, Peterson MS, Oliver JH3rd, Davis PL, Confer SR, et al. Hepatocellular Carcinoma: MR Imaging With Mangafodipir Trisodium (Mn-DPDP). *Radiol* (1996) 200(1):69–77. doi: 10.1148/radiology.200.1.8657947
55. Reimer P, Schneider G, Schima W. Hepatobiliary Contrast Agents for Contrast-Enhanced MRI of the Liver: Properties, Clinical Development and Applications. *Eur Radiol* (2004) 14(4):559–78. doi: 10.1007/s00330-004-2236-1
56. Vogl TJ, Kümmel S, Hammerstingl R, Schellenbeck M, Schumacher G, Balzer T, et al. Liver Tumors: Comparison of MR Imaging With Gd-EOB-DTPA and Gd-DTPA. *Radiol* (1996) 200(1):59–67. doi: 10.1148/radiology.200.1.8657946
57. Huppertz A, Balzer T, Blakeborough A, Breuer J, Giovagnoni A, Heinz-Peer G, et al. Improved Detection of Focal Liver Lesions at MR Imaging: Multicenter Comparison of Gadoteric Acid-Enhanced MR Images With Intraoperative Findings. *Radiol* (2004) 230(1):266–75. doi: 10.1148/radiol.2301020269
58. Neri E, Bali MA, Ba-Ssalamah A, Boraschi P, Brancatelli G, Alves FC, et al. ESGAR Consensus Statement on Liver MR Imaging and Clinical Use of Liver-Specific Contrast Agents. *Eur Radiol* (2016) 26(4):921–31. doi: 10.1007/s00330-015-3900-3
59. Li XQ, Wang X, Zhao DW, Sun J, Liu JJ, Lin DD, et al. Application of Gd-EOB-DTPA-Enhanced Magnetic Resonance Imaging (MRI) in Hepatocellular Carcinoma. *World J Surg Oncol* (2020) 18(1):219. doi: 10.1186/s12957-020-01996-4
60. Yoo SH, Choi JY, Jang JW, Bae SH, Yoon SK, Kim DG, et al. Gd-EOB-DTPA-Enhanced MRI is Better Than MDCT in Decision Making of Curative Treatment for Hepatocellular Carcinoma. *Ann Surg Oncol* (2013) 20(9):2893–900. doi: 10.1245/s10434-013-3001-y
61. Rimola J, Forner A, Sapena V, Llarch N, Darnell A, Díaz A, et al. Performance of Gadoteric Acid MRI and Diffusion-Weighted Imaging for the Diagnosis of Early Recurrence of Hepatocellular Carcinoma. *Eur Radiol* (2020) 30(1):186–94. doi: 10.1007/s00330-019-06351-0
62. Kuwatsuru R, Kadoya M, Ohtomo K, Tanimoto A, Hirohashi S, Murakami T, et al. Comparison of Gadobenate Dimeglumine With Gadopentetate Dimeglumine for Magnetic Resonance Imaging of Liver Tumors. *Invest Radiol* (2001) 36(11):632–41. doi: 10.1097/00004424-200111000-00002
63. Yamashita T, Kitao A, Matsui O, Hayashi T, Nio K, Kondo M, et al. Gd-EOB-DTPA-Enhanced Magnetic Resonance Imaging and Alpha-Fetoprotein Predict Prognosis of Early-Stage Hepatocellular Carcinoma. *Hepatology* (2014) 60(5):1674–85. doi: 10.1002/hep.27093
64. Katsube T, Okada M, Kumano S, Hori M, Imaoka I, Ishii K, et al. Estimation of Liver Function Using T1 Mapping on Gd-EOB-DTPA-Enhanced Magnetic Resonance Imaging. *Invest Radiol* (2011) 46(4):277–83. doi: 10.1097/RLI.0b013e318200f67d
65. Burtea C, Laurent S, Vander Elst L, Muller RN. Contrast Agents: Magnetic Resonance. *Handb Exp Pharmacol* (2008) (185 Pt 1):135–65. doi: 10.1007/978-3-540-72718-7\_7
66. Serkova NJ, Glunde K, Haney CR, Farhoud M, De Lille A, Redente EF, et al. Preclinical Applications of Multi-Platform Imaging in Animal Models of Cancer. *Cancer Res* (2021) 81(5):1189–200. doi: 10.1158/0008-5472.CAN-20-0373
67. Anani T, Rahmati S, Sultana N, David AE. MRI-Traceable Theranostic Nanoparticles for Targeted Cancer Treatment. *Theranostics* (2021) 11(2):579–601. doi: 10.7150/thno.48811
68. Lu J, Sun J, Li F, Wang J, Liu J, Kim D, et al. Highly Sensitive Diagnosis of Small Hepatocellular Carcinoma Using pH-Responsive Iron Oxide Nanocluster Assemblies. *J Am Chem Soc* (2018) 140(32):10071–4. doi: 10.1021/jacs.8b04169
69. Lin J, Xin P, An L, Xu Y, Tao C, Tian Q, et al. Fe(3)O(4)-ZIF-8 Assemblies as pH and Glutathione Responsive T(2)-T(1) Switching Magnetic Resonance Imaging Contrast Agent for Sensitive Tumor Imaging *In Vivo*. *Chem Commun (Camb)* (2019) 55(4):478–81. doi: 10.1039/C8CC08943D

70. Yu MH, Kim JH, Yoon JH, Kim HC, Chung JW, Han JK, et al. Small ( $\leq 1$ -Cm) Hepatocellular Carcinoma: Diagnostic Performance and Imaging Features at Gadoteric Acid-Enhanced MR Imaging. *Radiol* (2014) 271(3):748–60. doi: 10.1148/radiol.14131996
71. Choi JS, Kim S, Yoo D, Shin TH, Kim H, Gomes MD, et al. Distance-Dependent Magnetic Resonance Tuning as a Versatile MRI Sensing Platform for Biological Targets. *Nat Mater* (2017) 16(5):537–42. doi: 10.1038/nmat4846
72. Ling D, Park W, Park SJ, Lu Y, Kim KS, Hackett MJ, et al. Multifunctional Tumor pH-Sensitive Self-Assembled Nanoparticles for Bimodal Imaging and Treatment of Resistant Heterogeneous Tumors. *J Am Chem Soc* (2014) 136(15):5647–55. doi: 10.1021/ja4108287
73. Kievit FM, Zhang M. Surface Engineering of Iron Oxide Nanoparticles for Targeted Cancer Therapy. *Acc Chem Res* (2011) 44(10):853–62. doi: 10.1021/ar2000277
74. Li F, Liang Z, Liu J, Sun J, Hu X, Zhao M, et al. Dynamically Reversible Iron Oxide Nanoparticle Assemblies for Targeted Amplification of T1-Weighted Magnetic Resonance Imaging of Tumors. *Nano Lett* (2019) 19(7):4213–20. doi: 10.1021/acs.nanolett.8b04411
75. Xiao S, Yu X, Zhang L, Zhang Y, Fan W, Sun T, et al. Synthesis Of PEG-Coated, Ultrasmall, Manganese-Doped Iron Oxide Nanoparticles With High Relaxivity For T(1)/T(2) Dual-Contrast Magnetic Resonance Imaging. *Int J Nanomed* (2019) 14:8499–507. doi: 10.2147/IJN.S219749
76. Wang L, Huang J, Chen H, Wu H, Xu Y, Li Y, et al. Exerting Enhanced Permeability and Retention Effect Driven Delivery by Ultrafine Iron Oxide Nanoparticles With T(1)-T(2) Switchable Magnetic Resonance Imaging Contrast. *ACS Nano* (2017) 11(5):4582–92. doi: 10.1021/acsnano.7b00038
77. Shen Z, Chen T, Ma X, Ren W, Zhou Z, Zhu G, et al. Multifunctional Theranostic Nanoparticles Based on Exceedingly Small Magnetic Iron Oxide Nanoparticles for T(1)-Weighted Magnetic Resonance Imaging and Chemotherapy. *ACS Nano* (2017) 11(11):10992–1004. doi: 10.1021/acsnano.7b04924
78. Khandhar AP, Wilson GJ, Kaul MG, Salamon J, Jung C, Krishnan KM. Evaluating Size-Dependent Relaxivity of PEGylated-USPIOs to Develop Gadolinium-Free T1 Contrast Agents for Vascular Imaging. *J BioMed Mater Res A* (2018) 106(9):2440–7. doi: 10.1002/jbma.a.36438
79. Tao C, Chen Y, Wang D, Cai Y, Zheng Q, An L, et al. Macromolecules With Different Charges, Lengths, and Coordination Groups for the Coprecipitation Synthesis of Magnetic Iron Oxide Nanoparticles as T(1) MRI Contrast Agents. *Nanomater (Basel)* (2019) 9(5). doi: 10.3390/nano9050699
80. Sherwood J, Rich M, Lovas K, Warram J, Bolding MS, Bao Y. T(1)-Enhanced MRI-Visible Nanoclusters for Imaging-Guided Drug Delivery. *Nanoscale* (2017) 9(32):11785–92. doi: 10.1039/C7NR04181K
81. Vangjizegem T, Stanicki D, Boutry S, Paternoster Q, Vander Elst L, Muller RN, et al. VSION as High Field MRI T(1) Contrast Agent: Evidence of Their Potential as Positive Contrast Agent for Magnetic Resonance Angiography. *Nanotechnology* (2018) 29(26):265103. doi: 10.1088/1361-6528/aabdb0
82. Yang L, Wang Z, Ma L, Li A, Xin J, Wei R, et al. The Roles of Morphology on the Relaxation Rates of Magnetic Nanoparticles. *ACS Nano* (2018) 12(5):4605–14. doi: 10.1021/acsnano.8b01048
83. Tran HV, Ngo NM, Medhi R, Srinoi P, Liu T, Rittikulsittichai S, et al. Multifunctional Iron Oxide Magnetic Nanoparticles for Biomedical Applications: A Review. *Mater (Basel)* (2022) 15(2). doi: 10.3390/ma15020503
84. Reynders H, Van Zundert I, Silva R, Carlier B, Deschaume O, Bartic C, et al. Label-Free Iron Oxide Nanoparticles as Multimodal Contrast Agents in Cells Using Multi-Photon and Magnetic Resonance Imaging. *Int J Nanomed* (2021) 16:8375–89. doi: 10.2147/IJN.S334482
85. Zhang W, Liu L, Chen H, Hu K, Delahunty I, Gao S, et al. Surface Impact on Nanoparticle-Based Magnetic Resonance Imaging Contrast Agents. *Theranostics* (2018) 8(9):2521–48. doi: 10.7150/thno.23789
86. Yang B, Liu Q, Yao X, Zhang D, Dai Z, Cui P, et al. FePt@MnO-Based Nanotheranostic Platform With Acidity-Triggered Dual-Ions Release for Enhanced MR Imaging-Guided Ferroptosis Chemodynamic Therapy. *ACS Appl Mater Interfaces* (2019) 11(42):38395–404. doi: 10.1021/acsnano.9b11353
87. Yang B, Dai Z, Zhang G, Hu Z, Yao X, Wang S, et al. Ultrasmall Ternary FePtMn Nanocrystals With Acidity-Triggered Dual-Ions Release and Hypoxia Relief for Multimodal Synergistic Chemodynamic/Photodynamic/Photothermal Cancer Therapy. *Adv Healthc Mater* (2020) 9(21):e1901634. doi: 10.1002/adhm.201901634
88. Song HW, Lee HS, Kim SJ, Kim HY, Choi YH, Kang B, et al. Sonazoid-Conjugated Natural Killer Cells for Tumor Therapy and Real-Time Visualization by Ultrasound Imaging. *Pharmaceutics* (2021) 13(10). doi: 10.3390/pharmaceutics13101689
89. Goertz DE, Todorova M, Mortazavi O, Agache V, Chen B, Karshafian R, et al. Antitumor Effects of Combining Docetaxel (Taxotere) With the Antivascular Action of Ultrasound Stimulated Microbubbles. *PLoS One* (2012) 7(12):e52307. doi: 10.1371/journal.pone.0052307
90. Yin H, Sun L, Pu Y, Yu J, Feng W, Dong C, et al. Ultrasound-Controlled CRISPR/Cas9 System Augments Sonodynamic Therapy of Hepatocellular Carcinoma. *ACS Cent Sci* (2021) 7(12):2049–62. doi: 10.1021/acscentsci.1c01143
91. Guang Y, Xie L, Ding H, Cai A, Huang Y. Diagnosis Value of Focal Liver Lesions With SonoVue®-Enhanced Ultrasound Compared With Contrast-Enhanced Computed Tomography and Contrast-Enhanced MRI: A Meta-Analysis. *J Cancer Res Clin Oncol* (2011) 137(11):1595–605. doi: 10.1007/s00432-011-1035-8
92. Westwood M, Joore M, Grutters J, Redekop K, Armstrong N, Lee K, et al. Contrast-Enhanced Ultrasound Using SonoVue® (Sulphur Hexafluoride Microbubbles) Compared With Contrast-Enhanced Computed Tomography and Contrast-Enhanced Magnetic Resonance Imaging for the Characterisation of Focal Liver Lesions and Detection of Liver Metastases: A Systematic Review and Cost-Effectiveness Analysis. *Health Technol Assess* (2013) 17(16):1–243. doi: 10.3310/hta17160
93. Alaboudy A, Inoue T, Hatanaka K, Chung H, Hyodo T, Kumano S, et al. Usefulness of Combination of Imaging Modalities in the Diagnosis of Hepatocellular Carcinoma Using Sonazoid®-Enhanced Ultrasound, Gadolinium Diethylene-Triamine-Pentaacetic Acid-Enhanced Magnetic Resonance Imaging, and Contrast-Enhanced Computed Tomography. *Oncol* (2011) 81 Suppl 1:66–72. doi: 10.1159/000333264
94. Motosugi U, Bannas P, Sano K, Reeder SB. Hepatobiliary MR Contrast Agents in Hypovascular Hepatocellular Carcinoma. *J Magn Reson Imaging* (2015) 41(2):251–65. doi: 10.1002/jmri.24712
95. Kim DW, Choi SH, Kim SY, Byun JH, Lee SS, Park SH, et al. Diagnostic Performance of MRI for HCC According to Contrast Agent Type: A Systematic Review and Meta-Analysis. *Hepatol Int* (2020) 14(6):1009–22. doi: 10.1007/s12072-020-10100-7
96. Zhao C, Dai H, Shao J, He Q, Su W, Wang P, et al. Accuracy of Various Forms of Contrast-Enhanced MRI for Diagnosing Hepatocellular Carcinoma: A Systematic Review and Meta-Analysis. *Front Oncol* (2021) 11. doi: 10.3389/fonc.2021.680691
97. Imbriaco M, De Luca S, Coppola M, Fusari M, Klain M, Puglia M, et al. Diagnostic Accuracy of Gd-EOB-DTPA for Detection Hepatocellular Carcinoma (HCC): A Comparative Study With Dynamic Contrast Enhanced Magnetic Resonance Imaging (MRI) and Dynamic Contrast Enhanced Computed Tomography (Ct). *Pol J Radiol* (2017) 82:50–7. doi: 10.12659/PJR.899239
98. Frtús A, Smolková B, Uzhytchak M, Lunova M, Jirsa M, Kubinová Š, et al. Analyzing the mechanisms of iron oxide nanoparticles interactions with cells: A road from failure to success in clinical applications. *J Control Release* (2020) 328:59–77. doi: 10.1016/j.jconrel.2020.08.036

**Conflict of Interest:** The authors declare that the research was conducted in the absence of any commercial or financial relationships that could be construed as a potential conflict of interest.

**Publisher's Note:** All claims expressed in this article are solely those of the authors and do not necessarily represent those of their affiliated organizations, or those of the publisher, the editors and the reviewers. Any product that may be evaluated in this article, or claim that may be made by its manufacturer, is not guaranteed or endorsed by the publisher.

Copyright © 2022 Zhang, Numata, Du and Maeda. This is an open-access article distributed under the terms of the Creative Commons Attribution License (CC BY). The use, distribution or reproduction in other forums is permitted, provided the original author(s) and the copyright owner(s) are credited and that the original publication in this journal is cited, in accordance with accepted academic practice. No use, distribution or reproduction is permitted which does not comply with these terms.

日中笹川医学奨学金制度<学位取得コース>評価書

課程博士：指導教官用



第 43 期

研究者番号：G4308

作成日：2024年3月8日

氏名	葉盛	YE SHENG	性別	M	生年月日	1982/03/19
所属機関（役職）	南京紅十字血液中心成分採血科（副主任医師）					
研究先（指導教官）	奈良県立医科大学大学院医学研究科 循環器システム医科学 （中川修教授、小亀浩市教授）					
研究テーマ	ADAMTS13 による VON WILLEBRAND 因子制御破綻がもたらす疾患の病態解析 Pathological analysis of diseases caused by the regulation failure of ADAMTS13 to von Willebrand factor					
専攻種別	<input type="checkbox"/> 論文博士			<input checked="" type="checkbox"/> 課程博士		

研究者評価（指導教官記入欄）

成績状況	(優) 良 可 不可 学業成績係数=	取得単位数
		4 / 4
学生本人が行った研究の概要	von Willebrand 因子（VWF）は止血を担う血漿タンパク質であり、ADAMTS13 は VWF を切断して止血機能を抑制する。VWF と ADAMTS13 の機能的バランスが崩れると出血性あるいは血栓性の疾患につながる。von Willebrand 病は VWF の遺伝子異常に伴う出血性疾患であり、その診断や病型分類のためには遺伝子解析が重要であるが、VWF 遺伝子の特徴から、従来の解析方法では実施のハードルが高い。そこで、新しいロングリードシーケンシング法を工夫して VWF 遺伝子を効率よくかつ正確に解析することを目標とした。2022 年度は、遺伝子異常を正確に同定するためのワークフローを構築した。2023 年度は、患者 DNA 試料を解析して VWF 遺伝子のバリエントを同定し、その機能解析を進めた。	
総合評価	<b>【良かった点】</b> 研究に対する熱意はきわめて高く、常に向上心を持って取り組んだ。VWF 遺伝子全長の PCR とロングリードシーケンシングの実験条件検討にはかなりの労力を要したが、日々の計画をしっかりと立て、アドバイスを活かして着々と研究を進めた。当初の目的であった遺伝子解析方法の確立は達成したため、解析手法を広げ、多くの知識と技術を習得した。	
	<b>【改善すべき点】</b> 2022 年度には「新しい技術を習得する際、ミスを避けたい気持ちが強いと過度に慎重になることがある。ポイントを正確に把握することで、もう少し気持ちに余裕を持って実験を行うことができると研究能力が伸びると思われる。」と評価したが、2023 年度にはこれを理解し克服した。現在の意欲を維持し続けることが重要である。	
	<b>【今後の展望】</b> この2年間で、新しい VWF 遺伝子解析方法の確立を達成し、さらに VWF タンパク質機能解析を開始するところまで進んだ。今後、病態との関連を明確にし、近いうちに原著論文として投稿する。	
学位取得見込	2年間の研究計画は順調に進んだ。論文投稿に向けた最終実験も進んでいるため、目標期間内（1年以内）に学位を取得できる見込みは大きい。	
評価者（指導教官名） 小亀浩市		

# 日中笹川医学奨学金制度<学位取得コース>報告書

## 研究者用



第43期

研究者番号: G4308

作成日: 2024年3月1日

氏名	叶 盛	YE SHENG	性別	M	生年月日	1982/03/19
所属機関(役職)	南京紅十字血液中心成分採血科(副主任医師)					
研究先(指導教官)	奈良県立医科大学大学院医学研究科循環器システム医科学(中川修教授、小亀浩市教授)					
研究テーマ	ADAMTS13によるVON WILLEBRAND因子制御破綻がもたらす疾患の病態解析 Pathological analysis of diseases caused by the regulation failure of ADAMTS13 to von Willebrand factor					
専攻種別	論文博士	<input type="checkbox"/>	課程博士	<input checked="" type="checkbox"/>		

### 1. 研究概要 (1)

#### 1) 目的 (Goal)

To establish a long-read sequencing method using Oxford Nanopore Technology (ONT) to overcome the difficulties in von Willebrand factor (VWF) gene analysis.

#### 2) 戦略 (Approach)

The identification of causative variants in VWF is important for the diagnosis, classification, and clinical management of von Willebrand disease (VWD) and acquired von Willebrand syndrome (AVWS)[1]. In this study, we demonstrated an optimal solution by using long-range PCR and ONT sequencing[2]. Specific primers were designed and optimized to amplify ~15-kb PCR amplicons covering the entire VWF (175 kb), avoiding unwanted amplification due to repetitive sequences or pseudogene VWFP1[3]. All amplicons were subjected to DNA library preparation. ONT data were analyzed using dedicated software and identified candidate variants were verified by Sanger sequencing and expressed on HEK293 cells to investigate its impact on secretion and multimer distribution of VWF by multimer analysis and western blotting.

#### 3) 材料と方法 (Materials and methods)

##### *Patients and samples*

One VWD patient and two AVWS patients registered in the NCVC Biobank were enrolled in this study[4], their genomic DNA (gDNA) samples were diluted to 50 ng/μL concentration for long-range PCR.

##### *Mammalian cell cultures*

HEK293 cells were cultured in D-MEM high glucose medium with 10% fetal bovine serum at 37°C in 5% CO<sub>2</sub>.

##### *Long-range PCR*

PCR primer pairs were basically designed by Primer-Blast on NIH with SNP handling, repeat and low complexity filters on. For 21~29 kb pseudogene-homology region, four verified primers were used[5]. All PCR amplicons subjected to library preparation were verified by 1.2% agarose gel electrophoresis then purified and quantified accordingly.

##### *ONT sequencing and data analysis*

The final 20 fmol DNA library was prepared using the ligation kit (SQK-LSK114). ONT sequencing performed on GridION sequencer were run for 5-12 hrs using R10.4 flow-cell. Variants were called using the Clair3 and Longshot. All identified candidate variants were verified by Sanger sequencing.

##### *Expression of VWF mutant*

Wild-type (wt) and mutant VWF were expressed on HEK293 cells using vector pcDNA3.1 and Avalanche Transfection Reagent (EZ Biosystems, Maryland, USA) according to the manufacturer's instructions. Forty-eight or seventy-two hours after the transfection, medium was collected and the expression level of recombinant VWF (rVWF) protein was measured by western blotting.

##### *Multimers analysis*

1.2% SDS-agarose gels were used, and the multimers were visualized by fluorescence luminescent-based imaging using HRP-polyclonal rabbit anti-human VWF antibody P0226 (Dako, Jena, Germany) and secondary goat anti-rabbit 800CW antibody (LI-COR Biosciences, Nebraska, USA).

##### *Generation of high shear stress*

Given enzyme called a disintegrin-like and metalloproteinase with thrombospondin type 1 motif 13 (ADAMTS13) can specially cleave VWF under shear, to examine the rVWF cleavage by ADAMTS13 at high shear stress, we created an original instrument with two syringes and one injection needle to generate high shear stress[6].

#### 4) 実験結果 (Results)

##### *Amplification of VWF gene using long-range PCR*

According to the agarose check following the PCR, some primer pairs with low efficiency were redesigned to generate favorable DNA products for ONT sequencing. After several optimizations, forty-two primers were determined, and twenty-one 12~15 kb PCR amplicons covering entire VWF were produced despite yielding some minor nonspecific products.

##### *ONT sequencing and variants calling*

Total reads of 95.38k, 128.13k, and 114.55k were generated from three samples by ONT sequencing, respectively. Using selected reads by quality score and size, over 200 variants (SNV and INDEL) were identified per sample. Although no candidate variant was found in VWD, among two AVWS, p.Gln2442His and g.6087520\_6090118del were identified respectively.

## 1. 研究概要 (2)

## 4) 実験結果 (Results)

*Variants validation using Sanger sequencing*

p.Gln2442His was validated, however, g.6087520\_6090118del was confirmed as an artifact derived from long-range PCR due to a special sequence called “direct repeats”[7]. Although this kind of sequence also exists in reference sequence of VWF gene, it only generated <1% deletion-amplicons. Nevertheless, eight heterozygous SNPs possessed by the third patient in the region of g.6087416-6087659 made it easily generate more deletion-amplicons than reference sequence (50% vs <1%).

*Functional analysis of VWF SNV mutant identified in AVWS*

Expression analysis showed that the level of rVWF-mutant protein is identical to rVWF-WT, suggesting this mutation may less disturb the synthesise and secretion of rVWF in HEK293 cell. Multimers patterns of secreted rVWF-mutant exhibited a similar profile to rVWF-WT, even with ADAMTS13 under high shear stress, that implied this mutation may not induce alterations in the VWF structure or domains related to ADAMTS13 cleavage.

## 5) 考察 (Discussion)

Here, we present a genetic analysis method to identify causative variants in VWF gene to overcome the difficulties usually faced by Sanger or short-read next-generation sequencing (NGS). ONT can measure the changes in electrical charges while DNA passing through biological nanopores, which offers exceptionally long reads that allows direct sequencing through regions like long repetitive sequences, pseudogene-homology regions, and complex gene loci[2]. We used long-range PCR to amplify the whole VWF gene sequence for subsequent library preparation and long-read sequencing, and the optimization of long-range PCR was mainly focused on DNA polymerase, primer design, template volume, and PCR microtubes.

For DNA polymerase, we used TaKaRa PrimeSTAR GXL DNA Polymerase, which performed superbly in our study. For primer design, it is necessary to exclude all primers that may contain known SNPs or be located in repetitive or low complexity regions. In addition to that, especially in VWFP1-homology region, we used four VWF-selective primers already verified and designed the corresponding reverse or forward primers outside the VWFP1-homology region[5]. The amount of gDNA template used in our PCR was determined as 100~200 ng after several attempts. Surprisingly, we noticed even PCR microtube can greatly influence the long-range PCR results. It seemed PCRs using microtubes with thinner plastic wall have superior performance. This emphasized the importance of selection of PCR microtubes for long-range PCR, which is in consistent of the implication showed by Chua et al.[8].

Direct repeats is one kind of non-B DNA motifs consisting of two copies of the repeated unit separated by a nonrepetitive spacer, which can lead to a slipped strand structure with looped out bases, just like we discovered in the third patient with AVWS[7]. This indicated that amplification of regions containing multiple repetitive sequences using long-range PCR remains a challenge. Therefore, more careful validation and confirmation of variants identified by this method is needed to avoid any associated misleading results. A research group investigated the molecular mechanisms behind the generation of PCR artifacts caused by repetitive sequences. They proposed using primers that anneal to locations far from the repeats to decrease artifact products and alleviate this issue[9]. Similarly, we also noticed that PCR using primer near these repetitive sequences produced fewer no-deletion reads, which may coincide with their findings.

Genetic defects in type 1 VWD have been reported to be located throughout the whole VWF gene, but new variants still may not necessarily cause disease due to the highly polymorphic nature of VWF gene[10]. Moreover, many studies revealed that not all patients of this type have a VWF genetic defect, the rate of genetic variants ranged from 45% to 68%, which may explain our result of the VWD patient[11, 12].

We identified p.Gln2442His, a C3 domain coding region SNV in a left ventricular assist device (LVAD)-associated AVWS patient. It was predicted be a deleterious mutation in Asian population[13]. This is the first report of it in clinical case, which may indicate some potential association with the onset risk of AVWS. Thus, we conducted a thorough investigation of its impact on VWF structure and functions. Although no significant correlation was found to the synthesise, secretion or ADAMTS13 cleavage yet, as a mutation near the binding site of platelet receptor glycoprotein (GP)IIb/IIIa, further work needs to be done to look into its impact on the binding of GPIIb/IIIa with appropriate approaches.

In general, we reported a novel VWF gene analysis method combining with ONT technology and long-range PCR which could be a powerful tool to investigate the pathogenetic mechanisms of VWF disorders.

## 6) 参考文献 (Reference)

1. James PD, Connell NT, Ameer B, et al. ASH ISTH NHF WFH 2021 guidelines on the diagnosis of von Willebrand disease. *Blood Adv.* 2021;5(1):280-300.
2. Lin B, Hui J, and Mao H. Nanopore Technology and Its Applications in Gene Sequencing. *Biosensors (Basel)*. 2021;11(7).
3. Matsushita T. [The management strategy for von Willebrand disease]. *Rinsho Ketsueki*. 2021;62(5):435-444.
4. Guidelines for the Management of von Willebrand Disease 2021. *Japanese Journal of Thrombosis and Hemostasis*. 2021;32(4):413-481.
5. Mancuso DJ, Tuley EA, Westfield LA, et al. Human von Willebrand factor gene and pseudogene: structural analysis and differentiation by polymerase chain reaction. *Biochemistry*. 1991;30(1):253-69.
6. Hayakawa M, Kato S, Matsui T, et al. Blood group antigen A on von Willebrand factor is more protective against ADAMTS13 cleavage than antigens B and H. *J Thromb Haemost.* 2019;17(6):975-983.
7. Weissensteiner MH, Cremona MA, Guiblet WM, et al. Accurate sequencing of DNA motifs able to form alternative (non-B) structures. *Genome Res.* 2023;33(6):907-922.
8. Chua EW, Miller AL, and Kennedy MA. Choice of PCR microtube can impact on the success of long-range PCRs. *Anal Biochem.* 2015;477:115-7.
9. Hommelsheim CM, Frantzeskakis L, Huang M, and Ülker B. PCR amplification of repetitive DNA: a limitation to genome editing technologies and many other applications. *Sci Rep.* 2014;4:5052.
10. Flood VH, Garcia J, and Haberichter SL. The role of genetics in the pathogenesis and diagnosis of type 1 Von Willebrand disease. *Curr Opin Hematol.* 2019;26(5):331-5.
11. Yadegari H, Driesen J, Pavlova A, et al. Mutation distribution in the von Willebrand factor gene related to the different von Willebrand disease (VWD) types in a cohort of VWD patients. *Thromb Haemost.* 2012;108(4):662-71.
12. Flood VH, Christopherson PA, Gill JC, et al. Clinical and laboratory variability in a cohort of patients diagnosed with type 1 VWD in the United States. *Blood.* 2016;127(20):2481-8.
13. Wang QY, Song J, Gibbs RA, et al. Characterizing polymorphisms and allelic diversity of von Willebrand factor gene in the 1000 Genomes. *J Thromb Haemost.* 2013;11(2):261-9.

2. 執筆論文 Publication of thesis ※記載した論文を添付してください。Attach all of the papers listed below.

論文名 1 Title						
掲載誌名 Published journal						
	年	月	巻(号)	頁 ~	頁	言語 Language
第1著者名 First author			第2著者名 Second author			第3著者名 Third author
その他著者名 Other authors						
論文名 2 Title						
掲載誌名 Published journal						
	年	月	巻(号)	頁 ~	頁	言語 Language
第1著者名 First author			第2著者名 Second author			第3著者名 Third author
その他著者名 Other authors						
論文名 3 Title						
掲載誌名 Published journal						
	年	月	巻(号)	頁 ~	頁	言語 Language
第1著者名 First author			第2著者名 Second author			第3著者名 Third author
その他著者名 Other authors						
論文名 4 Title						
掲載誌名 Published journal						
	年	月	巻(号)	頁 ~	頁	言語 Language
第1著者名 First author			第2著者名 Second author			第3著者名 Third author
その他著者名 Other authors						
論文名 5 Title						
掲載誌名 Published journal						
	年	月	巻(号)	頁 ~	頁	言語 Language
第1著者名 First author			第2著者名 Second author			第3著者名 Third author
その他著者名 Other authors						

## 3. 学会発表 Conference presentation ※筆頭演者として総会・国際学会を含む主な学会で発表したものを記載してください。

※Describe your presentation as the principal presenter in major academic meetings including general meetings or international meetings.

学会名 Conference	第45回日本血栓止血学会学術集会		
演題 Topic	VWF遺伝子解析の困難性を克服するロングリードシーケンシング法の構築		
開催日 date	2023 年 6 月 15 日	開催地 venue	福岡県北九州市
形式 method	<input checked="" type="checkbox"/> 口頭発表 Oral	<input checked="" type="checkbox"/> ポスター発表 Poster	言語 Language: <input checked="" type="checkbox"/> 日本語 <input type="checkbox"/> 英語 <input type="checkbox"/> 中国語
共同演者名 Co-presenter	樋口(江浦)由佳、松本雅則、小亀浩市		
学会名 Conference	1st National Cerebral and Cardiovascular Center Annual Symposium		
演題 Topic	Genetic analysis using long-read sequencing to overcome the difficulties in VWF gene		
開催日 date	2023 年 7 月 21 日	開催地 venue	大阪府吹田市
形式 method	<input type="checkbox"/> 口頭発表 Oral	<input checked="" type="checkbox"/> ポスター発表 Poster	言語 Language: <input type="checkbox"/> 日本語 <input checked="" type="checkbox"/> 英語 <input type="checkbox"/> 中国語
共同演者名 Co-presenter	Yuka Eura, Masanori Matsumoto, Koichi Kokame		
学会名 Conference	第46回日本血栓止血学会学術集会		
演題 Topic	ロングリードシーケンシングでVWF遺伝子に同定したバリエーションの検証と機能解析		
開催日 date	2024 年 6 月 13 日	開催地 venue	石川県金沢市
形式 method	<input checked="" type="checkbox"/> 口頭発表 Oral	<input type="checkbox"/> ポスター発表 Poster	言語 Language: <input checked="" type="checkbox"/> 日本語 <input type="checkbox"/> 英語 <input type="checkbox"/> 中国語
共同演者名 Co-presenter	樋口(江浦)由佳、松本雅則、小亀浩市		
学会名 Conference	The 32nd Congress of the International Society on Thrombosis and Haemostasis		
演題 Topic	Genetic analysis using long-read sequencing to overcome the difficulties in VWF gene		
開催日 date	2024 年 6 月 22-26 日	開催地 venue	Bangkok, Thailand
形式 method	<input type="checkbox"/> 口頭発表 Oral	<input checked="" type="checkbox"/> ポスター発表 Poster	言語 Language: <input type="checkbox"/> 日本語 <input checked="" type="checkbox"/> 英語 <input type="checkbox"/> 中国語
共同演者名 Co-presenter	Yuka Eura, Masanori Matsumoto, Koichi Kokame		

## 4. 受賞(研究業績) Award (Research achievement)

名称 Award name	第45回日本血栓止血学会学術集会優秀ポスター賞		
国名 Country name	日本	受賞年 Year of award	2023 年 6 月
名称 Award name	国名 Country name	受賞年 Year of award	年 月

5. 本研究テーマに関わる他の研究助成金受給 Other research grants concerned with your research theme

受給実績 Receipt record	<input type="checkbox"/> 有 <input type="checkbox"/> 無
助成機関名称 Funding agency	
助成金名称 Grant name	
受給期間 Supported period	年 月 ~ 年 月
受給額 Amount received	円
受給実績 Receipt record	<input type="checkbox"/> 有 <input type="checkbox"/> 無
助成機関名称 Funding agency	
助成金名称 Grant name	
受給期間 Supported period	年 月 ~ 年 月
受給額 Amount received	円

6. 他の奨学金受給 Another awarded scholarship

受給実績 Receipt record	<input type="checkbox"/> 有 <input type="checkbox"/> 無
助成機関名称 Funding agency	
奨学金名称 Scholarship name	
受給期間 Supported period	年 月 ~ 年 月
受給額 Amount received	円

7. 研究活動に関する報道発表 Press release concerned with your research activities

※記載した記事を添付してください。Attach a copy of the article described below

報道発表 Press release	<input type="checkbox"/> 有 <input type="checkbox"/> 無	発表年月日 Date of release	
発表機関 Released medium			
発表形式 Release method	・新聞 ・雑誌 ・Web site ・記者発表 ・その他( )		
発表タイトル Released title			

8. 本研究テーマに関する特許出願予定 Patent application concerned with your research theme

出願予定 Scheduled application	<input type="checkbox"/> 有 <input type="checkbox"/> 無	出願国 Application country	
出願内容(概要) Application contents			

9. その他 Others

--

指導責任者(記名)

小、亀 浩市

# 日中笹川医学奨学金制度(学位取得コース)評価書

## 課程博士：指導教官用



第 43 期

研究者番号： G4309

作成日： 2023 年 3 月 8 日

氏名	王 喻	Wang Yu	性別	F	生年月日	1989. 12. 18
所属機関 (役職)	京都大学大学院医学研究科医学専攻免疫ゲノム医学 (大学院生)					
研究先 (指導教官)	京都大学大学院医学研究科附属がん免疫総合研究センター (本庶 佑センター長)					
研究テーマ	PD-1 阻害による免疫賦活化異常疾患の研究 Studies on diseases caused by hyperimmune activities due to PD-1 blockade					
専攻種別	<input type="checkbox"/> 論文博士			<input checked="" type="checkbox"/> 課程博士		

### 研究者評価 (指導教官記入欄)

成績状況	優 学業成績係数=	取得単位数
		26/30
学生本人が行った研究の概要	PD-1 阻害抗体治療を受けた 200-300 人のがん患者 (複数のがん種) から収集した plasma を用いて、約 300 種類のメタボライトを測定した。臨床データから統計解析を行い、irAE (自己免疫様副作用) を予測できる複数のメタボライト A を同定した。そのうちの一つはマウス自己免疫疾患モデルにおいても高値であることを発見した。さらにそのメタボライト A が結合するリガンドタンパクを同定した。	
総合評価	<p>【良かった点】まさに寝食を忘れて実験に没頭できる優秀な学生である。コロナにより入国が遅れ 1 年少ないにもかかわらず確実に成果を出し、大きな論文として完成間近である。また礼儀正しく、正直で素直なため、新しい技術や知識に対する吸収力が非常に高い。それらを用いたアウトプットも正確に出すことができるため、データに対する信用性も高い。Discussion も活発に行い、好奇心旺盛な学生である。新しい技術を他人教えることもでき、既にリーダー的存在である。</p> <p>【改善すべき点】大変よく働く反面、体を壊さないか多少心配になることもある。ただその時は無理せず休むように勧めている。自分でよく考えよく実験を行うが、それらを他人にアピールする方法はまだ改善の余地がある。2 年の経験を経て、英語で理論的に論文作成する能力は確実に伸びたが、プレゼンテーションスライドを用いた発表技術等についてはまだ改善余地がある。</p> <p>【今後の展望】王さんは、飲み込みが早く手技も正確なため、研究の方は予想以上に順調に進んでいる。また行っている研究はがん免疫治療分野においても非常に注目されつつあるテーマであり、早期に完成させることで世界に大きなインパクトを与えることができると確信している。</p>	
学位取得見込	本奨学金終了後、おそらく 2 年以内に論文発表できると思われる。行っている研究内容も次の課題を生み出す末広がりなテーマであり、生理学の根源を開拓する良いテーマである。予測不能なことが起こらない限り、予定通り学位を取得できる見込みである。	
		評価者 (指導教官名) 本庶佑

# 日中笹川医学奨学金制度(学位取得コース)報告書 研究者用



第43期                      研究者番号: G4309                      作成日: 2023年3月 3 日

氏名	王 喻	Wang Yu	性別	F	生年月日 1989. 12. 18
所属機関(役職)	京都大学大学院医学研究科医学専攻免疫ゲノム医学(大学院生)				
研究先(指導教官)	京都大学大学院 医学研究科附属がん免疫総合研究センター(本庶 佑センター長)				
研究テーマ	PD-1阻害による免疫賦活化異常疾患の研究 Studies on diseases caused by hyperimmune activities due to PD-1 blockade				
専攻種別	論文博士	<input type="checkbox"/>	課程博士	<input checked="" type="checkbox"/>	

## 1. 研究概要(1)

### 1) 目的(Goal)

Cancer immunotherapy with immune checkpoint inhibitors (ICIs) represented by PD-1 blockade antibodies has prevailed in the world as the first line therapy these days. However, since the PD-1 molecule on lymphocytes serves as an immune brake, the administration of PD-1 blockade antibody sometimes induces adverse events called Immune-Related Adverse Events (irAEs), which resemble autoimmune diseases in cancer patients (Figure 1). IrAE is generated by the over-activation of T cell immunity, which is kind of off-target of ICI therapy (Ye, W. et al. Br J Cancer 124, 1661-1669 (2021)(1). The incidence of clinical irAEs is around 10 % among the ICI-treated patients, and 30-40% are severe (more than grade 3) among those who experienced irAEs at any level (Golnaz Moradet al. cell 184, October 14, 2021)(2). Mechanism investigation and biomarkers identification of irAEs is therefore important for better-personalized medicine, and prevention or earlier intervention of irAEs. (Jing, Y. Nat Commun 11, 4946 (2020)(3). Our laboratory has studied responsive and unresponsive mechanisms to PD-1 blockade cancer immunotherapy from the view of immune metabolism in order to develop combination therapy and biomarkers (Al-Hansi et al. Science, 378:eabj3510, 2022)(4). However, solid metabolite biomarkers for irAE prediction have not been reported. In this project we explored the candidate of irAE biomarkers and the mechanisms involved in the found biomarker.

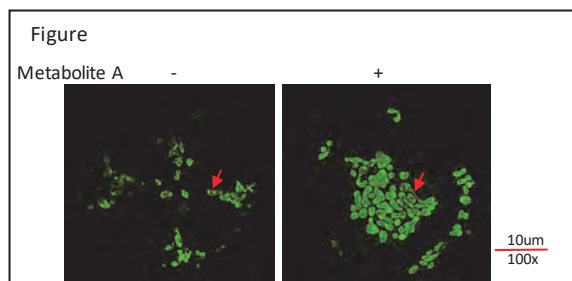
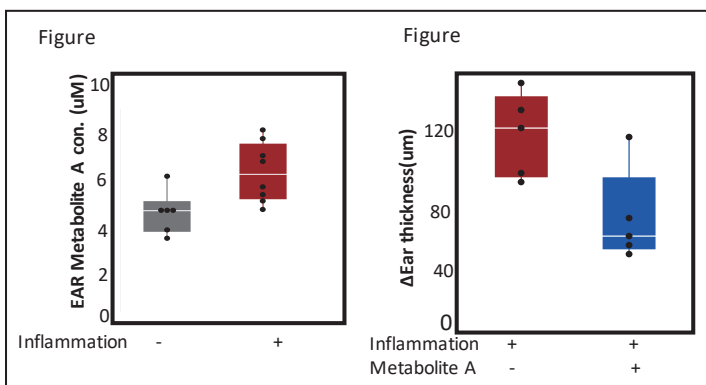
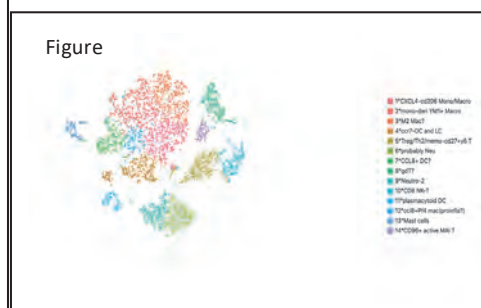
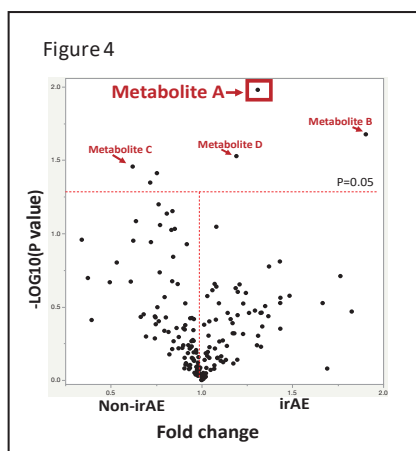
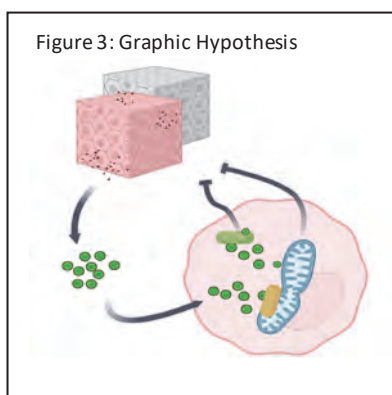
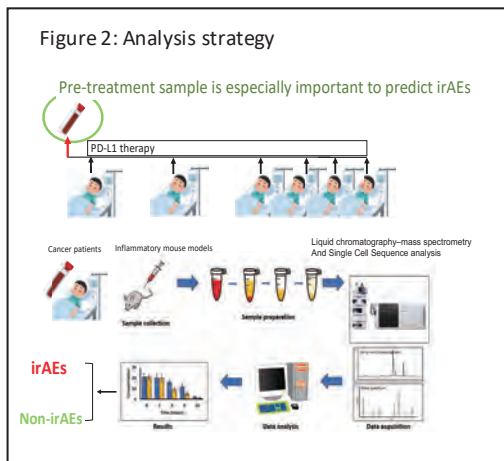
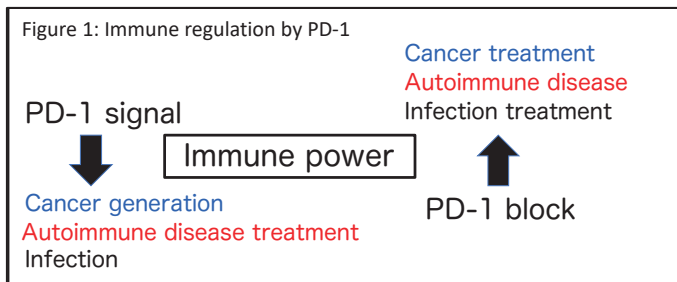
2) 戦略(Approach) Our laboratory has studied immune metabolism in the field of cancer immunotherapy. Our group already published the prediction biomarker of ICI responsiveness using plasma metabolites which are related to microbiota (Hatae et al, JCI insight 5:e133501, 2020)(5). We will use similar methods to identify the prediction biomarkers of irAEs. Note that as plasma metabolites were identified using the patients' blood before the first ICI treatment, these metabolite markers could be predictive. After the identification of metabolite biomarkers, we investigated the physiological meaning and mechanism of the metabolite biomarkers using cross-disciplinary methods and technologies.

3) 材料と方法 (Materials and methods) Collaborated with Kyoto University hospital, we collected the plasma from 200-300 patients who suffered non-small cell lung cancer, renal cell carcinoma, and urothelial carcinoma. Around 200-300 metabolites were measured from the patient's plasma by liquid chromatography-mass spectrometry before the 1st injection of PD-1 blockade therapy. In order to identify the metabolites which discriminate between the patients with irAE and without irAE group, we compared each metabolite level between the patients with irAE and without irAE. To understand the physiological meaning of the identified metabolite markers, we tested the target metabolite in the autoimmune disease mouse models including NOD diabetes models and contact hypersensitivity models (CHS: skin inflammation model) which is one of the most frequent symptoms of irAE. To understand the function of the candidate metabolite biomarkers, we analyzed the inflamed tissues and the infiltrated immune cells, by integrating the latest technologies such as metabolomics, single-cell sequencing analysis. We collaborated with Tohoku University and further examined the regulation function and molecular mechanisms of the metabolite by Seahorse, confocal microscopy and super resolution microscopy, and molecular biology methods (Fig. 2 and 3).

4) 実験結果 (Results) By comparison of the plasma metabolites between patients with irAE and without irAE, we detected several metabolites which could predict irAE patients before starting the treatments. Among the candidates, metabolite A is prominently high in the irAE patients (Fig. 4). We found this metabolite was also upregulated in inflammatory ears in the CHS model (Fig. 5). Interestingly, when we intravenously injected the metabolite A, the skin inflammation of CHS was attenuated (Fig.6), indicating that metabolite A serves as an immune modulator and this might be evolved in a negative feedback system of inflammation. Single cell analysis demonstrated that the metabolite A modulated the immune cells populations (Fig.7), which is now under the detail analysis. Molecular biology analysis revealed that metabolite A could bind to a mitochondrial protein and promote the mitochondria respiration accompanying with the mitochondria fusion (Fig.8).

5) 考察(Discussion) We successfully identified the candidate of metabolite biomarker for irAE patients before the treatment. This discovery should improve the diagnosis of cancer immunotherapy and personalized medicine. Molecular biology methods and single-cell sequencing analysis uncovered its molecular mechanism and functions which are very novel among previous studies of metabolite A. Based on these findings, we have hypothesized the mechanism as follows. 1) The patients who might develop irAE by the treatment have preexisting inflammatory diseases or microinflammation niches. 2) The systemic circulation of metabolite was upregulated to reduce these inflammatory niches but insufficient. 3) The exogenous metabolite A supplement can help to reduce the inflammation sufficiently. We will search more and complete this project in the next year utilizing the conditional KO mouse and transgenic mouse of the related genes to investigate the detail mechanisms in vivo. Thank you very much for the support of my scientific life. 日中笹川医学奨学金.

1. 研究概要(2)



6) 参考文献 (References)

1. Ye, W., Olsson-Brown, A., Watson, R.A. et al. Checkpoint-blocker-induced autoimmunity is associated with favourable outcome in metastatic melanoma and distinct T-cell expression profiles. *Br J Cancer* 124, 1661–1669 (2021).
2. Golnaz Morad, Beth A. Helmink, Padmanee Sharma. et al. Hallmarks of response, resistance, and toxicity to immune checkpoint blockade. *Cell* 184, October 14, 2021 a 2021 Elsevier Inc.
3. Jing, Y., Liu, J., Ye, Y. et al. Multi-omics prediction of immune-related adverse events during checkpoint immunotherapy. *Nat Commun* 11, 4946 (2020).
4. Muna Al-Habsi, Kenji Chamoto, Tasuku Honjo, et al. Spermidine activates mitochondrial trifunctional protein and improves antitumor immunity in mice. *Science*. abj3510. Epub 2022 Oct 28.
5. Ryusuke Hatae, Toyohiro Hirai, Tasuku Honjo. et al. Combination of host immune metabolic biomarkers for the PD-1 blockade cancer immunotherapy. *JCI Insight*. 2020;5(2):e133501.

2. 執筆論文 Publication of thesis ※記載した論文を添付してください。Attach all of the papers listed below.

論文名 1 Title					
掲載誌名 Published journal					
	年	月	巻(号)	頁 ~	頁
					言語 Language
第1著者名 First author	第2著者名 Second author		第3著者名 Third author		
その他著者名 Other authors					
論文名 2 Title					
掲載誌名 Published journal					
	年	月	巻(号)	頁 ~	頁
					言語 Language
第1著者名 First author	第2著者名 Second author		第3著者名 Third author		
その他著者名 Other authors					
論文名 3 Title					
掲載誌名 Published journal					
	年	月	巻(号)	頁 ~	頁
					言語 Language
第1著者名 First author	第2著者名 Second author		第3著者名 Third author		
その他著者名 Other authors					
論文名 4 Title					
掲載誌名 Published journal					
	年	月	巻(号)	頁 ~	頁
					言語 Language
第1著者名 First author	第2著者名 Second author		第3著者名 Third author		
その他著者名 Other authors					
論文名 5 Title					
掲載誌名 Published journal					
	年	月	巻(号)	頁 ~	頁
					言語 Language
第1著者名 First author	第2著者名 Second author		第3著者名 Third author		
その他著者名 Other authors					

3. 学会発表 Conference presentation ※筆頭演者として総会・国際学会を含む主な学会で発表したものを記載してください。

※Describe your presentation as the principal presenter in major academic meetings including general meetings or international meetings.

学会名 Conference					
演題 Topic					
開催日 date	年	月	日	開催地 venue	
形式 method	<input type="checkbox"/> 口頭発表 Oral	<input type="checkbox"/> ポスター発表 Poster	言語 Language	<input type="checkbox"/> 日本語	<input type="checkbox"/> 英語 <input type="checkbox"/> 中国語
共同演者名 Co-presenter					
学会名 Conference					
演題 Topic					
開催日 date	年	月	日	開催地 venue	
形式 method	<input type="checkbox"/> 口頭発表 Oral	<input type="checkbox"/> ポスター発表 Poster	言語 Language	<input type="checkbox"/> 日本語	<input type="checkbox"/> 英語 <input type="checkbox"/> 中国語
共同演者名 Co-presenter					
学会名 Conference					
演題 Topic					
開催日 date	年	月	日	開催地 venue	
形式 method	<input type="checkbox"/> 口頭発表 Oral	<input type="checkbox"/> ポスター発表 Poster	言語 Language	<input type="checkbox"/> 日本語	<input type="checkbox"/> 英語 <input type="checkbox"/> 中国語
共同演者名 Co-presenter					
学会名 Conference					
演題 Topic					
開催日 date	年	月	日	開催地 venue	
形式 method	<input type="checkbox"/> 口頭発表 Oral	<input type="checkbox"/> ポスター発表 Poster	言語 Language	<input type="checkbox"/> 日本語	<input type="checkbox"/> 英語 <input type="checkbox"/> 中国語
共同演者名 Co-presenter					

4. 受賞(研究業績) Award (Research achievement)

名称 Award name	国名	受賞年	年	月
	Country name	Year of award		
名称 Award name	国名	受賞年	年	月
	Country name	Year of award		

5. 本研究テーマに関わる他の研究助成金受給 Other research grants concerned with your research theme

受給実績 Receipt record	<input type="checkbox"/> 有 <input checked="" type="checkbox"/> 無
助成機関名称 Funding agency	
助成金名称 Grant name	
受給期間 Supported period	年 月 ~ 年 月
受給額 Amount received	円
受給実績 Receipt record	<input type="checkbox"/> 有 <input checked="" type="checkbox"/> 無
助成機関名称 Funding agency	
助成金名称 Grant name	
受給期間 Supported period	年 月 ~ 年 月
受給額 Amount received	円

6. 他の奨学金受給 Another awarded scholarship

受給実績 Receipt record	<input type="checkbox"/> 有 <input checked="" type="checkbox"/> 無
助成機関名称 Funding agency	
奨学金名称 Scholarship name	
受給期間 Supported period	年 月 ~ 年 月
受給額 Amount received	円

7. 研究活動に関する報道発表 Press release concerned with your research activities

※記載した記事を添付してください。Attach a copy of the article described below

報道発表 Press release	<input type="checkbox"/> 有 <input checked="" type="checkbox"/> 無	発表年月日 Date of release	
発表機関 Released medium			
発表形式 Release method	・新聞 ・雑誌 ・Web site ・記者発表 ・その他( )		
発表タイトル Released title			

8. 本研究テーマに関する特許出願予定 Patent application concerned with your research theme

出願予定 Scheduled application	<input type="checkbox"/> 有 <input checked="" type="checkbox"/> 無	出願国 Application country	
出願内容(概要) Application contents			

9. その他 Others

--

指導責任者(記名) 本庶 佑

日中笹川医学奨学金制度<学位取得コース>評価書

課程博士：指導教官用



第 43 期

研究者番号：G4310

作成日：2024年3月8日

氏名	孔 徳川	KONG DECHUAN	性別	M	生年月日	1987/09/13
所属機関（役職）	上海市疾病预防控制中心伝染病防治所急性伝染病防治科（医師）					
研究先（指導教官）	熊本大学大学院 医学教育部ヒトレトロウイルス学共同研究センター 感染免疫学分野（上野 貴将 教授、徳永 研三 客員教授）					
研究テーマ	新型コロナウイルスの複製を制御する宿主因子の同定と機能解析 — Identification and functional analysis of host factors that regulate SARS-CoV-2 replication					
専攻種別	<input type="checkbox"/> 論文博士			<input checked="" type="checkbox"/> 課程博士		

研究者評価（指導教官記入欄）

成績状況	(優) 良 可 不可 学業成績係数= 90		取得単位数
			取得単位数/取得すべき単位数総数
学生本人が行った 研究の概要	<p>ウイルスの複製に関わる宿主因子の研究は特にレトロウイルス学において最先端で進んでいることから、まず HIV の複製を阻害する抗ウイルス宿主因子 MARCH8 の分子ウイルス学的研究に着手した。</p> <p>HIV-1 エンベロープ糖タンパク質 (HIV-1 Env) および水胞性口炎ウイルス G タンパク質 (VSV-G) に対する動物種別 MARCH8 の抑制効果について検討した。サル、マウス、ウシの MARCH8 野生型および 2 種類の変異体を作製した。これらの抗ウイルス活性を検討するため、各 MARCH8 を HIV-1 Env 欠損型ルシフェラーゼレポーターウイルス DNA、HIV-1 Env 発現プラスミドまたは VSV-G 発現プラスミドと共にヒト胎児腎細胞株 293T にコトランスフェクションして、産生されたウイルスの感染性を検討した。その結果、ヒト MARCH8 と同様、サル、マウス、ウシ MARCH8 の野生型は HIV-1 Env と VSV-G に対する抑制能を保持し、一方で 2 種類の変異体はどちらも抑制活性を失っていた。このことから MARCH8 の抗ウイルスエンベロープ活性およびその機能領域は動物種間で高度に保存されていることが明らかになった。</p> <p>次に、HIV-1 潜伏機構に関与する宿主側要因を探るべく潜伏感染細胞モデルの樹立を試みた。まず蛍光強度および光安定性において GFP より優れた新規蛍光タンパク質 StayGold およびルシフェラーゼの二つのレポーター遺伝子を挿入した HIV-1 ミニジーン (gag-pol、vif、vpr 遺伝子を欠損) を構築した。この HIV-1 ミニジーンのコトランスフェクションで得られたウイルスを用いて感染実験を行った。その結果、感染後 4 週以内で StayGold および Luc2 の活性が徐々に低下したことから、最終的に潜伏感染細胞が樹立できることが確認できた。また一部の持続感染状態の細胞に Gag-Pol 発現プラスミドを再導入した後に産生されたウイルスが感染性を保持することも証明した。HIV-1 制御遺伝子 tat を標的とした CRISPR ノックアウトにより、潜伏感染細胞のプロウイルス DNA を効率よく破壊することができた。</p>		
総合評価	<p><b>【良かった点】</b></p> <ul style="list-style-type: none"> <li>ウイルス学研究に対するモチベーションが高い。</li> <li>真摯に実験に取り組み、失敗しても諦めずに何度もやり直す姿勢を持っている。</li> <li>関連研究に関する情報を収集するべく、最新論文のチェックを細目に行っている。</li> </ul> <p><b>【改善すべき点】</b></p> <ul style="list-style-type: none"> <li>最初に研究指導を受ける際にメモを取りノートにまとめる習慣をつける。</li> <li>試薬/消耗品を使い切って初めて発注要求したりせず、事前に誰かに伝える。</li> <li>トラブルシューティングを全て自分で行おうとせず、悩む前に指導教官に相談する。</li> </ul> <p><b>【今後の展望】</b></p> <p>日常的に十分な実験量をこなしており、徐々に良質なデータが増えてきているので、更なる伸びしろは感じられる。</p>		
学位取得見込	equal first author (3 <sup>rd</sup> author) としての論文を現在投稿中である。それに加えて first author 論文用別の研究プロジェクトも進行中であり期限内の学位取得は可能である。		
		評価者（指導教官名）	徳永 研三

# 日中笹川医学奨学金制度<学位取得コース>報告書

## 研究者用



第43期

研究者番号: G4310

作成日: 2024年3月 8日

氏名	孔 徳川	KONG DECHUAN	性別	M	生年月日	1987/09/13
所属機関(役職)	上海市疾病予防控制中心伝染病防治所急性伝染病防治科(医師)					
研究先(指導教官)	熊本大学大学院 医学教育部ヒトレトロウイルス学共同研究センター 感染免疫学分野(上野 貴将 教授、徳永 研三 客員教授)					
研究テーマ	新型コロナウイルスの複製を制御する宿主因子の同定と機能解析 Identification and functional analysis of host factors that regulate SARS-CoV-2 replication					
専攻種別	論文博士	<input type="checkbox"/>	課程博士	<input checked="" type="checkbox"/>		

### 1. 研究概要(1)

**1) 目的(Goal):** 過去4年間に渡り、全世界を席卷した新型コロナウイルス(SARS-CoV-2)はようやく世界各地で収束しつつある。現在のオミクロン変異株JN.1の場合でも、mRNAワクチンの繰返し接種のおかげで、たとえ感染はしても重症化することはなくなり、インフルエンザと変わらぬ風邪ウイルスの一種と見なせるほど制御可能となってきた。こうした感染防御の役割を担うのは、ワクチン接種や感染後に得られる獲得免疫やそれらに即座に反応する自然免疫だけでなく、第三の免疫と呼ばれる「内因性免疫」が挙げられる。この働きを担うタンパク質としてヒト細胞が有する抗ウイルス宿主因子のいくつか、SARS-CoV-2やHIV-1を始めとする種々の病原性ウイルスに対しても有効であることがこれまで数多く報告されている。こうした宿主因子によるウイルス感染防御に関する知見を得るとともに、将来的な感染再拡大に対する予防戦略を構築することを目的とする。

**2) 戦略(Approach):** ウイルスの複製に関わる宿主因子の研究が最先端レベルで進んでいるレトロウイルス学に着手して、分子ウイルス学的研究手法および宿主因子に関する知見について学ぶ。指導教官である徳永研三先生のチームが2015年に発見してNature Medicine誌(1)に報告した後に関連研究(2-5)を次々と展開してきた「(A)抗ウイルス宿主因子MARCH8」について、さらなる機能解析に取り組んだ。また同時にウイルス複製に関わる宿主因子研究の一環として、HIV-1潜伏感染の制御機構を探るべく「(B)潜伏感染細胞モデルの樹立」を試みた。

### 3) 材料と方法(Materials and methods)

#### i) 細胞:

(A) ヒト胎児腎細胞293T(6)をトランスフェクション用に、MAGIC5細胞(7)をウイルス感染用に使用した。サル(Rhesus macaque)、マウス、ウシMARCH8発現プラスミド作製用にRT-PCRの鋳型として必要な細胞RNAの抽出のために、それぞれアカゲザル網膜内皮細胞RF/6A(8)、マウス繊維芽細胞NIH3T3(9)、ウシ腎臓細胞MDBK(10)を用いた。

(B) トランスフェクション用に293Tを、ウイルス感染用に293T細胞、MAGIC5細胞およびMOLT-4細胞(11)を使用した。

#### ii) プラスミドDNA:

(A) シュードウイルス作製用にHIV-1エンベロープ糖タンパク質(Env)発現プラスミドpC-NLenv(1)、水胞性口炎ウイルスGタンパク質(VSV-G)発現プラスミドpC-VSVg(1)、HIV-1 Env欠損型シフェラーゼレポーターウイルスDNA pNL-Luc2-IN/HiBiT-E(-)Fin(12)を用いた。またヒトMARCH8発現プラスミドとしてpC-MARCH8(1)、RING-CH変異型MARCH8発現プラスミドpC-MARCH8-W114A(1)、チロシンモチーフ変異型MARCH8発現プラスミドpC-MARCH8-222AxxL225(2)を用いた。

(B) シュードウイルス作製用に水胞性口炎ウイルスGタンパク質(VSV-G)発現プラスミドpC-VSVg(4)、Gag-Pol発現HiBiT-tagプラスミドpsPAX2-IN/HiBiT(5)を、HIV-1ミニジーン作製用にHIV-1 Env欠損型シフェラーゼレポーターウイルスDNA pNL-Luc2-IN/HiBiT-E(-)Fin(5)を用いた。CRISPR/Cas9によるノックアウトにはTat標的型pLentiCRISPRv2-tat3(6)を用いた。

#### iii) プラスミド構築:

(A) RF/6A、NIH3T3、およびMDBK細胞からReliaprep RNA Cell Miniprep system (Promega; Z6010)を用いて細胞RNAを抽出し、PrimeScript One Step RT-PCR Kit Ver. 2(Takara; RR057A)によりRT-PCR増幅を行った。得られたDNA断片を電気泳動後にアガロースゲルから切り出してQIAquick PCR Purification Kit(QIAGEN; 28104)を用いて精製した。さらに制限酵素KpnI/XhoIで処理した最終断片を同じくKpnI/XhoIで処理した哺乳類細胞発現プラスミドpCAGGSに挿入した。各々のRING-CH変異体およびチロシンモチーフ変異体を作製するため、3種類の動物由来の野生型MARCH8を鋳型に乗換えPCRを行い、増幅したKpnI/XhoI断片をpCAGGSに挿入した。またこれら全てのN末HA-tag版も作製した。作製した全ての発現プラスミドはGenewiz遺伝子解析サービスにより遺伝子配列の確認を行った。

(B) StayGold(SG)発現プラスミドまたはEGFP発現プラスミドを鋳型に、それぞれSG遺伝子またはEGFP遺伝子のPCR増幅を行った。得られたDNA断片を電気泳動後にアガロースゲルから切り出してQIAquick PCR Purification Kit(QIAGEN; 28104)を用いて精製した。さらに制限酵素NotI/XhoIで処理した最終断片を、同じくNotI/XhoIで処理したHiBiTタグ付全長HIV-1プロウイルスLuc2レポーターDNA pNL-Luc2-IN/HiBiT-E(-)Fin(12)のLuc2遺伝子と置換した。また前者からgag-pol-vif-vpr領域を一挙に欠損させVpu遺伝子開始コドンで潰すことにより構造遺伝子envと制御遺伝子tat-revのみ発現するHIV-1遺伝子を作製し初代HIV-1ミニジーンとした。それを基にSG遺伝子下流にIRES-Luc2遺伝子を挿入したプラスミドを第2世代HIV-1ミニジーンとし、さらにCD4陽性細胞で感染させる場合のCD4によるEnv発現抑制を回避するためにnef/vpuを復活させたプラスミドを第3世代HIV-1ミニジーンとした。また第3世代は元のNL-Env型(CXCR4指向性[X4])に加えADA-ENV型(CCR5指向性[R5])も作製した。構築した全ての発現プラスミドの遺伝子配列の確認はGenewiz遺伝子解析サービスにより行った。

#### iv) トランスフェクション:

(A) pC-NLenvまたはpC-VSVg(20 ng)をpNL-Luc2-IN/HiBiT-E(-)Fin(500 ng)と各動物由来の野生型または変異型MARCH8発現プラスミド(0、60、120 ng)、さらに空プラスミドpCAGGS(480、420、360 ng)と共に、FuGENE6 Transfection Reagent(Promega; E2691)を用いて $2.5 \times 10^5$ 個の293T細胞にコトランスフェクションした。

(B) SGレポーター-HIV-1プラスミドまたはレポーター-HIV-1プラスミド(500 ng)をpC-VSVg(20 ng)と空プラスミド(480 ng)と共に、第1世代ミニジーンpNL-TatRevEnv-SG、または第2世代(450 ng)をGag-Pol発現HiBiT-tagプラスミドpsPAX2-IN/HiBiT(450 ng)とpC-VSVg(20 ng)と空プラスミドpCAGGS(80 ng)と共に、FuGENE6 Transfection Reagent(Promega; E2691)を用いて $2.5 \times 10^5$ 個の293T細胞にコトランスフェクションした。または第3世代HIV-1-X4ミニジーンあるいはHIV-1-R5ミニジーン(500 ng)をpsPAX2-IN/HiBiT(450 ng)と共に、同細胞数の293T細胞にFuGENE6でコトランスフェクションした。CRISPR/ノックアウト用にpLentiCRISPRv2-tat3またはコントロール(450 ng)、psPAX2-IN/HiBiT(450 ng)、pC-VSVg(20 ng)と空プラスミドpCAGGS(80 ng)を同細胞数の293T細胞にFuGENE6でコトランスフェクションした。

**1. 研究概要(2)****3) 材料と方法 (Materials and methods) つづき****v) ウイルス定量:**

(A, B) トランスフェクションの16時間後に293T細胞をPBSで洗浄して、更に24時間後に7.5 U/ml DNase I (Roche Applied Science; 11284932001)で処理した培養上清またはp24量が既知の標準ウイルス25  $\mu$ Lを、等量のHiBiT Lytic Substrate (1:50) in Nano-Glo HiBiT Lytic Buffer (Nano-Glo HiBiT Lytic Detection System; Promega; N3030)と混合して、10分間室温静置した後、Centro LB960 luminometer (Berthold)を用いてHiBiTルシフェラーゼ活性を測定した。

**vi) 感染性アッセイ:**

(A, B) 各培養上清のHiBiTルシフェラーゼ活性をp24量に換算した後、1ng p24相当のウイルスを、(A)の実験または第2世代HIV-1ミニジーン由来VSVシュードウイルスまでは $1.2 \times 10^4$ 個の293T細胞に、第3世代ADA-Envウイルスは $1 \times 10^4$ 個のMAGIC5細胞に、また第3世代NL-Envウイルスでは $1 \times 10^4$ 個のMAGIC5細胞およびCD4陽性T細胞株MOLT-4 ( $2 \times 10^4$ 個)に感染させた。それぞれのウイルスを各細胞に感染させた後、第1世代HIV-1ミニジーン由来ウイルスまでは蛍光顕微鏡Fluoview FV1000-IX81 (Olympus)により経時的(2, 24, 26, 36日)に蛍光観察のみを行った。第2世代以降は、蛍光顕微鏡観察に加えて、経時的に感染細胞を100  $\mu$ Lの One-Glo Luciferase Assay Reagent (Promega; E6110)で溶解してホタルルシフェラーゼ活性を Centro LB960ルミノメーター(Berthold)によって測定した。

**vii) ウェスタンブロットング:**

(Aのみ) 各N末HA-tag付加MARCH8発現プラスミド(500 ng)と空プラスミドpCAGGS(500 ng)を、FuGENE6を用いて $2.5 \times 10^5$ 個の293T細胞にトランスフェクションした。48時間後に200  $\mu$ Lの細胞溶解液を加えてSDS-PAGEを行った後、PVDF膜に転写した。抗HA単クローン抗体 (Sigma; H9658) または抗 $\beta$ -actin単クローン抗体 (Sigma; A5316)を反応させ、Western ECL Substrate (Biorad; 1705061)で可視化した後、LAS-3000 imaging system (FujiFilm)で検出した。

**vii) インテグレーション確認のためのDNA PCR:**

(Bのみ) 経時的に感染細胞を回収し、DNeasy Blood & Tissue Kit (QIAGEN; 69504)により抽出した細胞DNAを鋳型に、StayGold遺伝子を標的としたPCRをPrimeSTAR Max Premix (Takara; R045Q)を用いて行い、アガロースの電気泳動によりHIV-1プロウイルスDNAの有無を確認した。

**viii) CRISPRノックアウト:**

(Bのみ) 第3世代HIV-1ミニジーン由来ウイルスを感染させたMAGIC5に対し、Tatを標的とするTat3-CRISPRレンチウイルスベクターまたはコントロールのCRISPRレンチウイルスベクターを用いてトランスダクションを行った。ノックアウト効率を検証するため、蛍光顕微鏡観察およびルシフェラーゼアッセイを実施した。

**4) 実験結果 (Results)**

(A) トランスフェクションおよびウェスタンブロットング実験により、今回新たに作製したMARCH8発現プラスミドは全て同レベルで正常に発現していることが確認できた。動物種別MARCH8のHIV-1 EnvおよびVSV-Gに対する抑制効果について、感染性アッセイにより検討した結果、ヒトMARCH8と同様、サル、マウス、およびウシMARCH8の野生型はHIV-1 EnvとVSV-Gに対する量依存的な抑制能を保持していた。その一方でRING-CH変異型およびチロシンモチーフ変異型MARCH8はどちらも抑制活性を失っていた。

(B) SG発現ウイルスとEGFP発現ウイルスのMAGIC5細胞への感染後の蛍光比較において、SG発現ウイルスの方がEGFP発現ウイルスよりも圧倒的な蛍光強度と光安定性を示すことが明らかになった。次にHIV-1から全てのアクセサリ遺伝子とgag-pol領域を取り除いた第1世代HIV-1ミニジーン由来ウイルスの感染実験において、蛍光顕微鏡観察を行った結果、感染後4週間程度かけて徐々に蛍光レベルが低下していくことが分かった。また簡易に感染後の遺伝子発現を定量化できるようにLuc2遺伝子を導入した第2世代ウイルス、およびCD4陽性細胞株に対する感染を行った第3世代ウイルスでは、蛍光レベルに加えてルシフェラーゼ活性の経時的低下も確認できた。また細胞DNAのPCRにより、蛍光及びルシフェラーゼ活性が消失した後も、HIV-1プロウイルスDNAが確かに存在することを明らかにした。また持続感染細胞に対するTatを標的としたCRISPRノックアウトは非常に効率よくHIV-1プロウイルスDNAを破壊できることが明らかになった。

**5) 考察 (Discussion)**

(A) MARCH8の抗ウイルスエンベロープ活性およびその機能領域は、異なる動物種間(ヒト、サル、マウス、およびウシ)で高度に保存されていることが明らかになった。

(B) 本研究において、完全長のHIV-1ではなく、HIV-1ミニジーンを利用した潜伏感染実験系を組むことにより、よりHIV-1の潜伏状態をsimplifyするとともに、新規蛍光タンパク質SGを用いることで更に潜伏状態を容易に可視化することが可能となった。この潜伏状態を制御する宿主側の要因を探るために、今後CRISPRライブラリーを用いたスクリーニングによって関連因子の同定を試みたい。またCRISPRノックアウトによるHIV-1破壊効率は良いものの、完全ではないことから、挿入箇所特異的なノックアウト効率の違いが認められるか否かについて今後検討する。さらに今後、HIV-1 LTRを標的とした活性化型CRISPRにより潜伏感染細胞を再活性化させ、それによって発現するEnvを認識して排除するシステムの構築に取り組みたい。

**6) 参考文献 (References)**

- Tada, T., Zhang, Y., Koyama, T., Tobiume, M., Tsunetsugu-Yokota, Y., Yamaoka, S. et al. (2015) MARCH8 inhibits HIV-1 infection by reducing virion incorporation of envelope glycoproteins *Nat Med* 21:1502-1507.
- Zhang, Y., Tada, T., Ozono, S., Kishigami, S., Fujita, H., and Tokunaga, K. (2020) MARCH8 inhibits viral infection by two different mechanisms *Elife* 9:e57763.
- Tada, T., Zhang, Y., Fujita, H., and Tokunaga, K. (2022) MARCH8: the tie that binds to viruses *FEBS J* 289:3642-3654.
- Zhang, Y., Ozono, S., Tada, T., Tobiume, M., Kameoka, M., Kishigami, S. et al. (2022) MARCH8 Targets Cytoplasmic Lysine Residues of Various Viral Envelope Glycoproteins *Microbiol Spectr* 10:e0061821.
- Zhang, Y., Tada, T., Ozono, S., Yao, W., Tanaka, M., Yamaoka, S. et al. (2019) Membrane-associated RING-CH (MARCH) 1 and 2 are MARCH family members that inhibit HIV-1 infection *J Biol Chem* 294:3397-3405.
- Pear, W. S., Nolan, G. P., Scott, M. L., and Baltimore, D. (1993) Production of high-titer helper-free retroviruses by transient transfection *Proc Natl Acad Sci U S A* 90:8392-8396.
- Hachiya, A., Aizawa-Matsuoka, S., Tanaka, M., Takahashi, Y., Ida, S., Gatanaga, H. et al. (2001) Rapid and simple phenotypic assay for drug susceptibility of HIV-1 using CCR5-expressing HeLa/CD4(+) cell clone 1-10 (MAGIC-5) *Antimicrob Agents Chemother* 45:495-501.
- Hu, F., Mah, K., and Teramura, D. J. (1986) Gossypol effects on cultured normal and malignant melanocytes *In Vitro Cell Dev Biol* 22:583-588.
- Todaro, G. J., and Green, H. (1963) Quantitative studies of the growth of mouse embryo cells in culture and their development into established lines *J Cell Biol* 17:299-313.
- Madin, S. H., and Darby, N. B., Jr. (1958) Established kidney cell lines of normal adult bovine and ovine origin *Proc Soc Exp Biol Med* 98:574-576.
- Minowada, J., Onuma, T., and Moore, G. E. (1972) Rosette-forming human lymphoid cell lines. I. Establishment and evidence for origin of thymus-derived lymphocytes *J Natl Cancer Inst* 49:891-895.
- Ozono, S., Zhang, Y., Tobiume, M., Kishigami, S., and Tokunaga, K. (2020) Super-rapid quantitation of the production of HIV-1 harboring a uminescent peptide tag *J Biol Chem* 295:13023-13030.

## 2. 執筆論文 Publication of thesis ※記載した論文を添付してください。Attach all of the papers listed below.

論文名 1 Title	Repetitive mRNA vaccination is required to improve the quality of broad-spectrum anti-SARS-CoV-2 antibodies in the absence of CXCL13. Sci. Adv. 9:eadg2122. 2023.					
掲載誌名 Published journal	Science Advances					
	2023 年 8 月	9 巻(号)	eadg2122頁 ~	頁	言語 Language	English
第1著者名 First author	Azarias Da Silva, M.	第2著者名 Second author	Nioche, P.	第3著者名 Third author	Soudaramourty, C.	
その他著者名 Other authors	Bull-Maurer, A., Tiouajni, M., <u>Kong, D.</u> , Zghidi-Abouzid, O., Picard, M., Mendes-Frias, A., Santa-Cruz, A., Carvalho, A., Capela, C., Pedrosa, J., Castro A.G., Loubet, P., Sotto, A., Muller, L., Lefrant, J.Y., Roger, C., Claret, P.G., Duvnjak, S., Tran, T.A., <u>Tokunaga, K.</u> , Silvestre, R., Corbeau, P., Mammano, F., Estaquier, J.					
論文名 2 Title						
掲載誌名 Published journal						
	年 月	巻(号)	頁 ~	頁	言語 Language	
第1著者名 First author		第2著者名 Second author		第3著者名 Third author		
その他著者名 Other authors						
論文名 3 Title						
掲載誌名 Published journal						
	年 月	巻(号)	頁 ~	頁	言語 Language	
第1著者名 First author		第2著者名 Second author		第3著者名 Third author		
その他著者名 Other authors						
論文名 4 Title						
掲載誌名 Published journal						
	年 月	巻(号)	頁 ~	頁	言語 Language	
第1著者名 First author		第2著者名 Second author		第3著者名 Third author		
その他著者名 Other authors						
論文名 5 Title						
掲載誌名 Published journal						
	年 月	巻(号)	頁 ~	頁	言語 Language	
第1著者名 First author		第2著者名 Second author		第3著者名 Third author		
その他著者名 Other authors						

## 3. 学会発表 Conference presentation ※筆頭演者として総会・国際学会を含む主な学会で発表したものを記載してください

※Describe your presentation as the principal presenter in major academic meetings including general meetings or international meetings

学会名 Conference	第70回日本ウイルス学会			
演題 Topic	The development of in vitro HIV-1 latency models using a viral minigene system.			
開催日 date	2023 年 9 月 27 日	開催地 venue	仙台	
形式 method	<input type="checkbox"/> 口頭発表 Oral <input checked="" type="checkbox"/> ポスター発表 Poster	言語 Language	<input type="checkbox"/> 日本語 <input checked="" type="checkbox"/> 英語 <input type="checkbox"/> 中国語	
共同演者名 Co-presenter	Seiya Ozono, Masanori Kameoka, Takamasa Ueno, and Kenzo Tokunaga			
学会名 Conference	24th Kumamoto AIDS Seminar			
演題 Topic	HIV-1 minigene system to establish an in vitro latency model.			
開催日 date	2023 年 11 月 6 日	開催地 venue	熊本	
形式 method	<input type="checkbox"/> 口頭発表 Oral <input checked="" type="checkbox"/> ポスター発表 Poster	言語 Language	<input type="checkbox"/> 日本語 <input checked="" type="checkbox"/> 英語 <input type="checkbox"/> 中国語	
共同演者名 Co-presenter	Seiya Ozono, Masanori Kameoka, Takamasa Ueno, and Kenzo Tokunaga			
学会名 Conference				
演題 Topic				
開催日 date	年 月 日	開催地 venue		
形式 method	<input type="checkbox"/> 口頭発表 Oral <input type="checkbox"/> ポスター発表 Poster	言語 Language	<input type="checkbox"/> 日本語 <input type="checkbox"/> 英語 <input type="checkbox"/> 中国語	
共同演者名 Co-presenter				
学会名 Conference				
演題 Topic				
開催日 date	年 月 日	開催地 venue		
形式 method	<input type="checkbox"/> 口頭発表 Oral <input type="checkbox"/> ポスター発表 Poster	言語 Language	<input type="checkbox"/> 日本語 <input type="checkbox"/> 英語 <input type="checkbox"/> 中国語	
共同演者名 Co-presenter				

## 4. 受賞(研究業績) Award (Research achievement)

名称 Award name	国名 Country		受賞年 Year of award	年 月
	国名 Country		受賞年 Year of award	年 月

## 5. 本研究テーマに関わる他の研究助成金受給 Other research grants concerned with your research theme

受給実績 Receipt record	<input type="checkbox"/> 有 <input type="checkbox"/> 無
助成機関名称 Funding agency	
助成金名称 Grant name	
受給期間 Supported period	年 月 ~ 年 月
受給額 Amount received	円
受給実績 Receipt record	<input type="checkbox"/> 有 <input type="checkbox"/> 無
助成機関名称 Funding agency	
助成金名称 Grant name	
受給期間 Supported period	年 月 ~ 年 月
受給額 Amount received	円

## 6. 他の奨学金受給 Another awarded scholarship

受給実績 Receipt record	<input checked="" type="checkbox"/> 有 <input type="checkbox"/> 無
助成機関名称 Funding agency	熊本大学
奨学金名称 Scholarship name	熊本大学大学院博士課程奨学金給付制度(KDS)(私費留学生枠)
受給期間 Supported period	2021 年 4 月 ~ 2022 年 4 月
受給額 Amount received	1,054,600 円

## 7. 研究活動に関する報道発表 Press release concerned with your research activities

※記載した記事を添付してください。Attach a copy of the article described below

報道発表 Press release	<input type="checkbox"/> 有 <input type="checkbox"/> 無	発表年月日 Date of release	
発表機関 Released medium			
発表形式 Release method	・新聞 ・雑誌 ・Web site ・記者発表 ・その他( )		
発表タイトル Released title			

## 8. 本研究テーマに関する特許出願予定 Patent application concerned with your research theme

出願予定 Scheduled	<input type="checkbox"/> 有 <input type="checkbox"/> 無	出願国 Application	
出願内容(概要) Application contents			

## 9. その他 Others

JSTさくらサイエンスオンラインプログラム(2022年11月29日~12月3日)におけるZoom講演 「Exchange and share experiences in daily life as a doctoral course student in Tokyo, Japan.」
--

指導責任者(記名)

徳永 研三



## CORONAVIRUS

# Repetitive mRNA vaccination is required to improve the quality of broad-spectrum anti-SARS-CoV-2 antibodies in the absence of CXCL13

Marne Azarias Da Silva<sup>1</sup>, Pierre Nioche<sup>1,2</sup>, Calaiselvy Soudaramoury<sup>1</sup>, Anne Bull-Maurer<sup>3</sup>, Mounira Tiouajni<sup>1,2</sup>, Dechuan Kong<sup>4,5</sup>, Ouafa Zghidi-Abouzid<sup>6</sup>, Morgane Picard<sup>1</sup>, Ana Mendes-Frias<sup>7,8</sup>, André Santa-Cruz<sup>7,8,9</sup>, Alexandre Carvalho<sup>7,8,9</sup>, Carlos Capela<sup>7,8,9</sup>, Jorge Pedrosa<sup>7,8</sup>, António Gil Castro<sup>7,8</sup>, Paul Loubet<sup>10</sup>, Albert Sotto<sup>10</sup>, Laurent Muller<sup>11</sup>, Jean-Yves Lefrant<sup>11</sup>, Claire Roger<sup>11</sup>, Pierre-Géraud Claret<sup>12</sup>, Sandra Duvnjak<sup>13</sup>, Tu-Anh Tran<sup>14</sup>, Kenzo Tokunaga<sup>5</sup>, Ricardo Silvestre<sup>7,8</sup>, Pierre Corbeau<sup>15,16</sup>, Fabrizio Mammano<sup>1,3†</sup>, Jérôme Estaquier<sup>1,6+\*</sup>

Copyright © 2023 The Authors, some rights reserved; exclusive licensee American Association for the Advancement of Science. No claim to original U.S. Government Works. Distributed under a Creative Commons Attribution License 4.0 (CC BY).

Since the initial spread of severe acute respiratory syndrome coronavirus 2 infection, several viral variants have emerged and represent a major challenge for immune control, particularly in the context of vaccination. We evaluated the quantity, quality, and persistence of immunoglobulin G (IgG) and IgA in individuals who received two or three doses of messenger RNA (mRNA) vaccines, compared with previously infected vaccinated individuals. We show that three doses of mRNA vaccine were required to match the humoral responses of preinfected vaccinees. Given the importance of antibody-dependent cell-mediated immunity against viral infections, we also measured the capacity of IgG to recognize spike variants expressed on the cell surface and found that cross-reactivity was also strongly improved by repeated vaccination. Last, we report low levels of CXCL13, a surrogate marker of germinal center activation and formation, in vaccinees both after two and three doses compared with preinfected individuals, providing a potential explanation for the short duration and low quality of Ig induced.

## INTRODUCTION

Since the initial SARS-CoV-2 (severe acute respiratory syndrome coronavirus 2) pandemic related to the Wuhan strain (1), several viral variants have emerged. These variants, particularly Beta (B.1.351), Delta (B.1.617.2), and, more recently, diverse Omicron subtypes, represent a major challenge for immune control, especially in the context of vaccination. Most of the mutations that differentiate these strains from the original isolate are localized in the two domains of the spike (S) protein shown to be targeted by neutralizing antibodies (2–4): the receptor binding domain (RBD) that interacts with the angiotensin II (ACE2) receptor and the N-terminal domain (NTD).

Current vaccines, such as those manufactured by Pfizer/BioNTech (BNT162b2) and by Moderna/National Institute of Allergy and Infectious Diseases (mRNA-1273), encode for an S protein whose sequence is similar to the early Wuhan-Hu viral isolate. The emergence of viral variants has consequently challenged vaccine effectiveness. Initial reports have shown lower levels of recognition of Beta and Delta variants, even after the second dose of vaccine (5–8). The recently emerged Omicron variants were reported to be less efficiently neutralized than the Wuhan-Hu strain by immunoglobulin G (IgG) from vaccinated individuals even after a third dose (9–15) and by therapeutic neutralizing antibodies (16–18).

Beyond neutralizing antibody, it has been shown that Fc effector mechanisms including antibody-dependent complement deposition, antibody-dependent neutrophil phagocytosis, and antibody-dependent cellular cytotoxicity responses may contribute in the control of viral dissemination by clearing viral-infected cells and limiting disease severity (19, 20). We recently demonstrated that the amount of IgG capable to recognize the Wuhan-Hu S-protein on cell surface of transfected cells are lower in patients with severe coronavirus 2019 (COVID-19), and this was associated with frequent CD4 T cell apoptosis (21, 22). Furthermore, it has been suggested that antibody cellular effector functions induced by mRNA vaccine are preserved despite the loss of Omicron neutralization, indicating a disconnection between the requirements for quantity and quality of antibodies for the two functions (23). An incomplete natural immunity against variants has been also reported in convalescent individuals (24), who displayed lower quality of Fc-mediated antibody responses compared to individuals vaccinated with two

<sup>1</sup>INSERM-U1124, Université Paris Cité, Paris, France. <sup>2</sup>Structural and Molecular Analysis Platform, BioMedTech Facilities INSERM US36-CNRS UMS2009, Université Paris Cité, Paris, France. <sup>3</sup>Université de Tours, INSERM, UMR1259 MAVIVH, Tours, France. <sup>4</sup>Joint Research Center for Human Retrovirus Infection, Kumamoto University, Kumamoto, Japan. <sup>5</sup>Department of Pathology, National Institute of Infectious Diseases, Tokyo, Japan. <sup>6</sup>CHU de Québec-Université Laval Research Center, Québec City, Québec, Canada. <sup>7</sup>Life and Health Sciences Research Institute (ICVS), School of Health Sciences, University of Minho, Braga, Portugal. <sup>8</sup>ICVS/3B's-PT Government Associate Laboratory, Braga/Guimarães, Portugal. <sup>9</sup>Department of Internal Medicine, Hospital of Braga, Braga, Portugal. <sup>10</sup>Service des Maladies Infectieuses et Tropicales, CHU de Nîmes, Nîmes, France. <sup>11</sup>Service de Réanimation Chirurgicale, CHU de Nîmes, Nîmes, France. <sup>12</sup>Urgences Médico-Chirurgicales Hospitalisation, CHU de Nîmes, Nîmes, France. <sup>13</sup>Service de Gériatrie et Prévention du Vieillessement, CHU de Nîmes, Nîmes, France. <sup>14</sup>Service de Pédiatrie, CHU de Nîmes, Nîmes, France. <sup>15</sup>Institut de Génétique Humaine, UMR9002 CNRS-Université de Montpellier, Montpellier, France. <sup>16</sup>Laboratoire d'Immunologie, CHU de Nîmes, Nîmes, France.

\*Corresponding author. Email: jerome.estaquier@crchudequebec.ulaval.ca  
†These authors contributed equally to this work.

doses of mRNA-1273 (25). Nevertheless, convalescent individuals boosted with vaccine are better protected against reinfection than vaccinated alone with two doses of vaccine (26–28).

While most of the studies have assessed the role of neutralizing IgG, little is known about mucosal humoral response induced by vaccines. Studies including ours have shown that, early after SARS-CoV-2 infection, a dominant IgA humoral response is induced against the nucleocapsid (N) and S proteins (29, 30). The presence of IgA in vaccinated individuals would be extremely important in the event of further contact with the virus, particularly during the first days of infection. The IgA in the mucosal tissue could limit viral dissemination and disease outcome, but little is known on the delay and durability of this response in individuals, with or without previous infection, who have received a vaccine boost.

Although the beneficial effect of vaccination is well established (31, 32) and vaccinees mount a competent humoral response against SARS-CoV-2 (33–37), repetitive vaccination campaigns have been necessary to maintain an efficient humoral response capable of preventing severe forms and hospitalization. The requirement for repetitive doses to improve humoral response and cross-reactivity suggests a short half-life of the antibodies induced in the absence of boost and probably a low avidity response. Paradoxically, few studies have determined the avidity of Ig in vaccinated individuals, which reflect antibody maturation following germinal center (GC) formation (38, 39). In this context, measuring the level of chemokine (C-X-C motif) ligand 13 (CXCL13) in the blood may represent an interesting biomarker of GC activation in humans associated with protective humoral response following vaccination (40–42).

In this study, we evaluated the humoral response of vaccinated individuals, some of whom had also been infected during the first wave of SARS-CoV-2 in 2020, before vaccines became available. By analyzing both the quantity and quality of IgG and IgA, our results demonstrated that the amount and persistence of Ig were higher in individuals previously exposed to the virus and boosted with vaccine compared to vaccinated-only individuals. Three doses of mRNA vaccine were required to improve the quantity, quality, and cross-reactivity against Beta and Omicron variants. We found difference in recognition among Omicron subtypes, between vaccinees only and preinfected individuals. Thus, mRNA vaccine induced Ig capable to recognize variant S proteins expressed on cell surface that is of major importance for Fc-mediated function by vaccines. While CXCL13 levels are high during the acute phase of SARS-CoV-2 infection, vaccine administration, even after the

third dose, has no impact on the levels of CXCL13 detected in the plasma. This result may help to explain why booster vaccination induces a potent humoral response in previously infected patients compared with vaccinated-only individuals who require at least three doses of vaccine to reach similar levels of humoral response. Thus, our work provides a framework to explain the need for repeated immunizations to provide stronger and longer-lasting humoral responses, which might contribute to controlling viral dissemination even against variants of concern.

## RESULTS

### Three mRNA vaccinations are required for IgG and IgA responses similar to those of convalescent and boosted individuals

To determine the impact of mRNA vaccination boosts, we analyzed humoral responses in different groups of donors (Fig. 1A). Individuals included (i) nonvaccinated convalescent individuals, from whom samples were collected 6 months after SARS-CoV-2 infection (Pre;  $n = 17$ ); (ii) convalescent individuals vaccinated with BNT162b2 (1 to 3 months after vaccination, Pre + V;  $n = 15$ ), so called hybrid immune responders; and (iii) individuals only vaccinated with two doses ( $n = 9$ , samples collected at two time points: V2,1-3M, 1 to 3 months after vaccination and V2,4-6M, 4 to 6 months after vaccination) or (iv) with three doses of mRNA vaccines (1 to 2 months after vaccination, V3,1-2M;  $n = 13$ ) and a group of naïve individuals as a negative control (naïve,  $n = 31$ ). All convalescent individuals were infected between March and December 2020, when only the original strain and the Alpha variant were circulating in Europe. As indicated in Table 1, five individuals received the Moderna vaccine for their third dose, whereas all the others only received the Pfizer formulation. We first assessed the levels of specific antibodies against the S1 and N antigens by ELISA (enzyme-linked immunosorbent assay) as previously described (16). This latter antigen was used as a marker to follow individuals that may have been infected with SARS-CoV-2. The optical density (OD) values of the ELISA performed with patients' plasma are shown in Fig. 1 (B to E). As expected, anti-N IgG were detected in convalescent individuals irrespective of their vaccination status but not in vaccinated-only individuals (Fig. 1B) nor in the naïve group. Although the OD values of anti-N IgG antibodies were significantly different ( $P = 0.048$ ), the levels of anti-S1 IgG were clearly higher in convalescents boosted with a vaccine dose (hybrid immunity, Pre + V:  $3.37 \pm 0.22$ ) compared with nonvaccinated convalescent individuals (Pre:  $1.57 \pm 0.43$ ,  $P < 0.0001$ ) both at

**Table 1. Characteristics of individuals included in this study.** M, male; F, female.

Groups/vaccine	N	Pfizer (BNT162b2)	Moderna (mRNA-1273)	Age, years Median [Range]	Gender	
					M	F
Pre: Convalescents 6 months after infection	17			67 [52–87]	11	6
Pre + V: Convalescents + vaccine (1 to 3 months after vaccination)	15	15		56 [25–81]	5	10
V2,1-3M: Vaccinated two doses (1 to 3 months after vaccination)	9	9		46 [12–85]	5	4
V2,4-6M: Vaccinated two doses (4 to 6 months after the vaccination)	9	9		57 [28–85]	4	5
V3,1-2M: Vaccinated three doses (1 to 2 months after the vaccination)	13	8	5	54 [12–85]	7	6

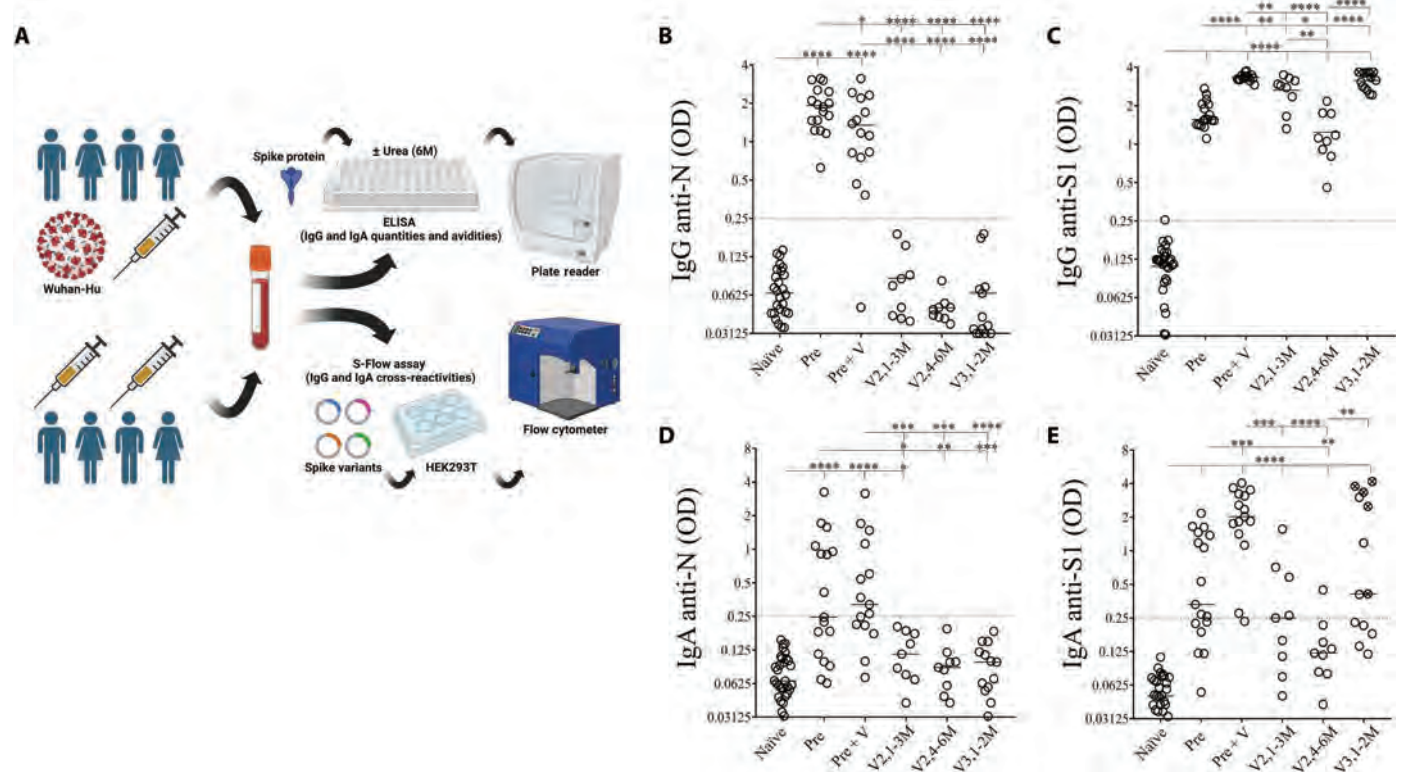


**Fig. 1. IgG response against the N and spike proteins in convalescents and vaccinated individuals.** (A) Plasma from healthy donors (naïve) convalescent individuals (Pre), convalescent individuals boosted with vaccine (Pre + V), vaccinees after two doses either at months 1 to 3 (V2,1-3M) or months 4 to 6 (V2,4-6M), and after three doses at months 1 to 2 (V3,1-2M) were diluted to 1/400. (B to E) Plasma from healthy donors (naïve) convalescent individuals (Pre), convalescent individuals boosted with vaccine (Pre + V), vaccinees after two doses either at months 1 to 3 (V2,1-3M) or months 4 to 6 (V2,4-6M), and after three doses at months 1 to 2 (V3,1-2M) were diluted to 1/400. (B) and (C) Specific immunoglobulin G (IgG) and (D) and (E) IgA were tested against the nucleocapsid (N) and spike (S1) proteins. Optical density (OD) is shown. Each circle represents one individual. Lines represent median values. Dashed lines represent antibody specificity (OD = 0.25) in comparison with IgG and IgA from healthy donors. Statistical analysis was performed using a Mann-Whitney *U* test (\**P* < 0.05; \*\**P* < 0.01; \*\*\**P* < 0.001; \*\*\*\**P* < 0.0001). (C) and (E) Symbols with a cross represent individuals who received at least one dose of mRNA-1273, whereas open symbols represent individuals who only received BNT162b2 in the vaccination scheme.

1/400 (Fig. 1C) and 1/800 dilutions (fig. S1). This difference may in part be due to the longer time after exposure of the convalescent individuals (6 months) as compared to convalescent and vaccinated individuals (1 to 3 months). Only one individual had anti-N IgG antibodies below the positive threshold. Notably, the levels of specific anti-S1 IgG, 1 to 3 months after the second dose, remained lower (V2,1-3M:  $2.88 \pm 0.73$ ) than those observed in convalescents receiving one dose of vaccine (Pre + V:  $3.37 \pm 0.22$ , *P* = 0.0035; Fig. 1C). The OD values of anti-S1 IgG were lower 4 to 6 months after the second dose (V2,4-6M:  $1.12 \pm 0.54$ ) and increased again, boosted by the third dose (V3,1-2M:  $3.24 \pm 0.48$ ).

Having observed differences in the IgG response between vaccinated individuals and those previously infected with SARS-CoV-2, we then compared their IgA responses. We and others have shown that humoral response against the S protein also includes IgA (21, 43–45). Furthermore, IgA were reported to dominate the early antibody response to SARS-CoV-2 (21, 29). The presence of IgA, boosted by the mRNA vaccine, could be of importance, since IgA is the most abundant antibody isotype in the mucosa, where these antibodies provide the first line of immune defense against pulmonary viral infections (46). Like IgG, specific IgA were assessed by ELISA at the same dilution in plasma (1/400). In convalescent individuals (Pre), we found specific IgA against the N (8 of 17) and S1

(10 of 17) proteins (Fig. 1, D and E, respectively). The OD values of IgA (Fig. 1, D and E) were significantly lower than those observed for the IgG (Fig. 1, B and C). This was observed both for Ig anti-N (Pre, *P* < 0.0001 and Pre + V, *P* = 0.0209) and for anti-S (Pre, *P* = 0.0002 and Pre + V, *P* = 0.0027). IgA response against S was improved by mRNA boost (hybrid patients, Pre + V:  $1.93 \pm 1.20$ ) compared to convalescent individuals without vaccination (Pre,  $0.33 \pm 0.69$ ; Fig. 1E). Our results highlighted that two doses of mRNA induce low levels of IgA against S1 (V2,1-3M: 4 of 10 individuals were responders), which declined after 4 to 6 months (V2,4-6M: 1 of 10 individuals were responders). After the third dose, more than half of vaccinated individuals (8 of 13) developed high level IgA responses (Fig. 1E). Of interest, IgA levels were higher in individuals who received one dose of mRNA-1273 compared to individuals who received only BNT162b2 (OD,  $3.35 \pm 1.5$  and  $0.22 \pm 1.1$ , respectively, *P* = 0.01), whereas this difference was lower for IgG response (OD: mRNA-1273,  $3.63 \pm 0.14$  and BNT162b2,  $2.8 \pm 0.41$ , *P* = 0.01). Together, our results confirm the need for repeated administration of mRNA vaccines, with at least three doses to induce a humoral response against S like that seen in individuals previously infected by SARS-CoV-2 and boosted with mRNA vaccine.

### Repeated mRNA vaccinations improve IgG and IgA responses to recognize viral variants although Beta and Omicron BA.1 remain of concern

In addition to neutralization, antibodies contribute to clearing viral-infected cells through different mechanisms limiting viral dissemination and have recently been described as participating in immune defense against SARS-CoV-2 (19). To assess the recognition of viral proteins by antibodies present in patients' plasma, the S-Flow assay relies on transfected cells expressing the S protein on the cell surface using flow cytometry (16, 47). Transfection of plasmids encoding the S protein does not require biosafety level 3 confinement and allows to test recent isolates without the need for replication-competent virus isolation. Before using transfected cells, we assessed whether antibodies present in the plasma of vaccinees and convalescent individuals were capable to recognize viral antigens on the surface of Wuhan-Hu infected cells (fig. S2). Whereas we clearly detected infected cells compared to uninfected cells, one cannot formally assume that S was the sole antigen present on cell surface.

We then analyzed the ability of IgG to cross-recognize viral variants by expressing S proteins on the cell surface upon transfection. To normalize the data for each variant, the results were expressed as the percentages of cells recognized by the patient's plasma, while a specific monoclonal antibody recognizing transfected cells against S2 was used as a positive control and attributed a value of 100% (fig. S3). Figure 2 shows the specific detection of S proteins by flow cytometry. Plasma from a healthy donor (Fig. 2A) did not recognize transfected cells, whereas plasma from a vaccinated convalescent individual recognized the S proteins of four viral variants, expressed on the cell surface (Fig. 2B). As expected, plasma from all convalescent individuals recognized the Wuhan-Hu strain (Pre:  $75.5 \pm 12.3\%$ ; Fig. 2C), whereas the percentages of S-Flow decreased for Delta (Pre:  $68 \pm 21\%$ ; Fig. 2D) and were extremely low for Beta and Omicron BA.1 (Pre:  $7.6 \pm 13.1$  and  $21 \pm 18.2\%$ , respectively; Fig. 2, E and F). Thus, convalescent individuals displayed low cross-reactivity. In contrast, convalescent individuals boosted with the mRNA vaccine (Pre + V) developed IgG that recognized all variants including Beta and Omicron. Vaccinated-only individuals demonstrated specific IgGs against the Wuhan-Hu ( $84.5 \pm 19.5\%$ ) and Delta ( $65 \pm 17.3\%$ ) after the second dose (V2,1-3M; Fig. 2, C and D). The percentages of S-Flow were lower for Beta ( $15 \pm 20.1\%$ ) and BA.1 ( $37 \pm 27.3\%$ ) compared to convalescent vaccinated individuals (Fig. 2, E and F). However, IgG reactivity markedly decreased at months 4 to 6 (V2,4-6M), including for the Wuhan-Hu strain, and was particularly low for Beta and BA.1 ( $17.5 \pm 9.3$  and  $13 \pm 7.9\%$ , respectively; Fig. 2, E and F). Boosting humoral response with a third dose not only increased the levels of specific IgG against Wuhan-Hu and Delta (Fig. 2, C and D) but also induced significantly higher humoral responses against Beta and BA.1 (Fig. 2, E and F). Patients having received a dose of mRNA-1273 vaccine were better responders against BA.1 than those who received only three doses of BTN162b2 vaccine (S-Flow,  $96 \pm 5.3$  versus  $52.7 \pm 18.6\%$ , respectively,  $P = 0.004$ ).

We had the opportunity to obtain sequential samples over more than 1 year after vaccination from three individuals (Fig. 3) including one convalescent individual who had been vaccinated (panel A), one vaccinated individual who was infected after the third dose (panel B), and a third one who had received four doses of the mRNA vaccine (panel C). For the three individuals, we found

high levels of IgG after two exposures (natural or vaccine). After the third exposure, the levels of specific IgG antibodies plateaued for at least 6 months and were boosted in the third individual after an additional dose.

Assessing variant recognition, we found that, in the individual preinfected with SARS-CoV-2 and boosted with one dose of vaccine, IgGs were capable of recognizing all four viral strains (Fig. 3D). However, the levels of antibodies capable of recognizing Beta and BA.1 markedly decreased in comparison to Wuhan-Hu and Delta until the booster (Fig. 3D). The second dose improved humoral response against the four strains, although IgGs recognizing Beta remained lower. Likewise, in the second individual (Fig. 3E), IgG induced by vaccination recognized Wuhan-Hu and Delta strains, whereas the cross-reactivity of IgG against Beta and BA.1 rapidly declined. The third dose improved cross-reactivity against all four strains, although recognition of Beta was lower compared to the other strains. In this individual, who was infected after vaccination, recognition of the BA.1 variant rose markedly and reached the same level as for the Delta variant, which had been predominant before (Fig. 3E). Last, in the third individual (Fig. 3F), two doses of vaccine were not enough to generate IgG capable of recognizing the Beta strain (Fig. 3F). After the third dose, an increase was observed but Beta and BA.1 recognition declined over the 6-month interval (Fig. 3F). Despite an additional dose (Fig. 3F), IgG did not reach higher levels against Beta, and the percentages of cross-reactivity against Beta, Delta, and BA.1 remained lower compared to Wuhan-Hu and did not exceed 50% (Fig. 3F).

We then assessed IgA cross-reactivity (Fig. 4). In some convalescent individuals and in most of those who received a boost (10 of 14), IgA recognized the Wuhan-Hu (Fig. 4A). However, while individuals with two doses of mRNA vaccine had low levels of IgA, half of the vaccinees who had received a third dose (V3,1-2M) developed specific IgA (Fig. 4A). We then assessed variant cross-reactivities in this subgroup of IgA responders. Overall, we observed a low cross-reactivity with some individuals, either convalescents boosted with the vaccine (Pre + V) or vaccinees who had received three doses (V3,1-2M), maintained a cross-reactivity against Delta (Fig. 4B), but very few recognized Beta and BA.1 (Fig. 4, C and D). IgA from convalescents (Pre) were unable to recognize Delta, Beta, or BA.1.

Thus, these results demonstrated the efficacy that can be reached by repeated administrations of mRNA vaccine to induce IgG and IgA that may contribute to the elimination of infected cells. However, without natural infection, specific IgG do not persist for long time, low levels of IgA are produced, and one of the main concerns is the low recognition of Beta and BA.1 variants.

### Structural analysis of RBD and NTD reveals potential regions in variants that may impact antibody recognition

Several studies have previously described the impact of mutations on viral infectivity and escape from recognition by monoclonal antibodies (mAbs) used in therapy, suggesting the importance of the RBD as well as the NTD (Fig. 5A) (2–4). Delta RBD mutations, which do not include N501Y, are L452R and T478K, and Omicron (BA.1) has seven mutations that map to the ACE2 binding footprint (K417N, S477N, Q493R, G496S, Q498R, N501Y, and Y505H; Fig. 5B, amino acids are indicated by an “\*”). These mutations are mainly conserved in the other BA.2 variants of concern. Beta has only three mutations in the RBD compared to

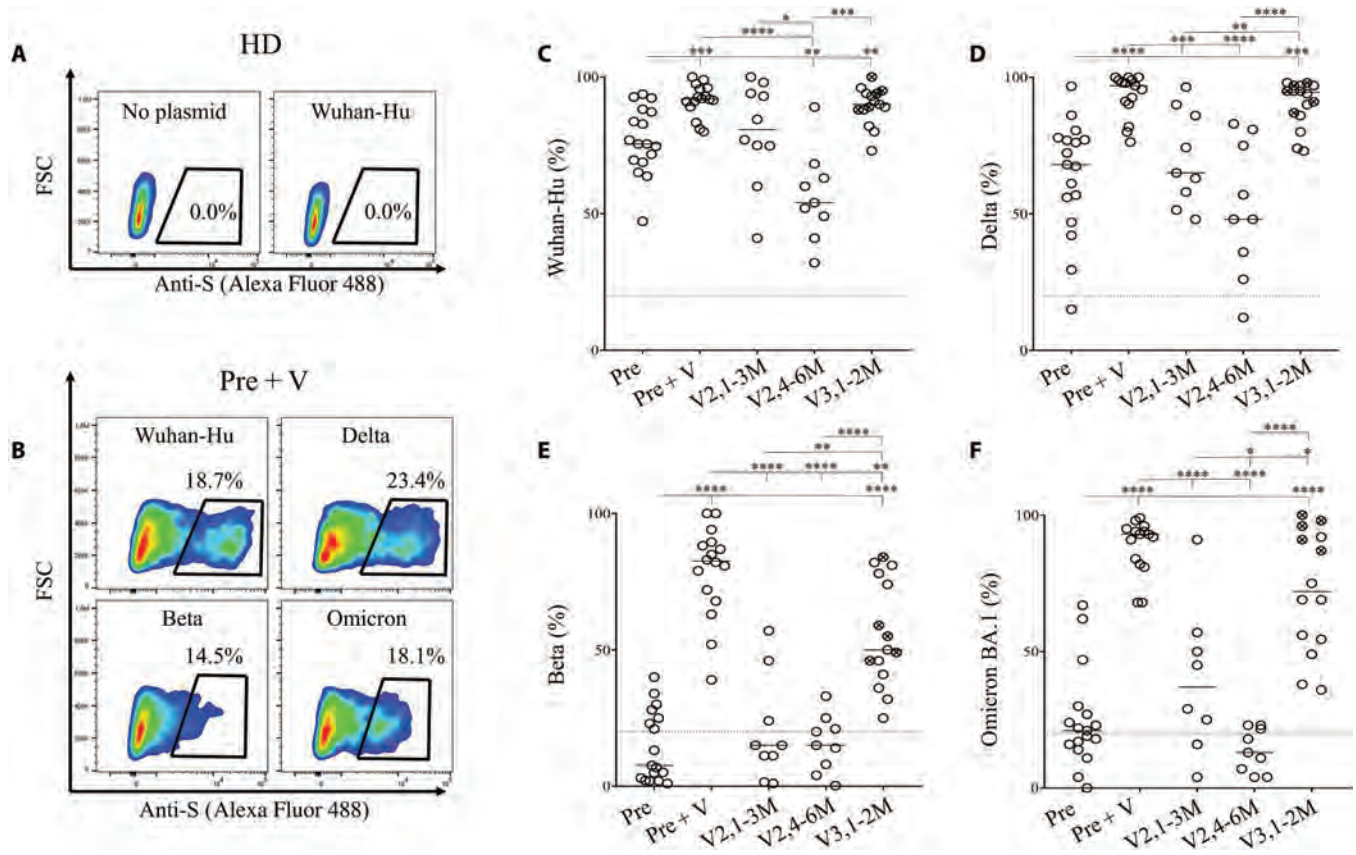


**Fig. 2. IgG cross-reactivity against viral variants in convalescents and vaccinees.** (A and B) Representative S-Flow assay. HEK293T cells either nontransfected or transfected with a plasmid encoding for the S protein were either labeled with (A) plasma from a healthy donor (HD) or (B) with plasma from a convalescent individual boosted with a vaccine dose (Pre + V). The percentages of cells recognized by specific IgG were detected by flow cytometry are shown for each variant. (C to F) Plasma from individuals, assessed in Fig. 1, were monitored for their capacity to recognize the different S variants including (C) Wuhan-Hu, (D) Delta, (E) Beta, and (F) Omicron. Relative percentages were calculated as follows: (% of IgG from plasma individuals – % of secondary IgG alone) / (% of anti-S2 mAbs – % of secondary IgG alone) \* 100. Each circle represents one individual. Lines represent median values. Statistical analysis was performed using a Mann-Whitney U test (\**P* < 0.05; \*\**P* < 0.01; \*\*\**P* < 0.001; \*\*\*\**P* < 0.0001). Symbols with a cross represent individuals who received at least one dose of mRNA-1273, whereas open symbols represent individuals who only received BNT162b2 in the vaccination scheme. Dot plots show forward size scatter (FSC) against anti-S detection.

Wuhan-Hu (K417N, E484K, and N501Y; Fig. 5B), which are also present in the Omicron subtypes. These minimal differences in the Beta RBD have been previously reported to substantially decrease neutralization by class I and class II monoclonal antibodies (16, 48, 49). By superimposing the variant structures onto the Wuhan-Hu RBD structure in the down state (not interacting with ACE2), the structural differences are centered around amino acids 365 and 380 (Fig. 5, C and D). These variations almost disappear entirely when the RBD is in the “up” conformation and interacting with the ACE2 receptor (fig. S4, A and B). The lower capacity of IgG to recognize Beta in comparison to Wuhan-Hu spike proteins in transfected cells is unlikely to be due to the differences in the RBD alone. The NTD region is the second most variable domain in which a supersite was reported flanked by glycans that also contribute in neutralizing SARS-CoV-2 infection (6, 50–53). Whereas no insertion or deletion of amino acids have been observed within RBD in any variants so far, they have been observed in the NTD (Fig. 5E). These deletions affect the main solvent-exposed loops in the Beta (due to a deletion localized inside the structure affecting the five external loops) and in the Omicron variants (Fig. 5F)

compared to the Wuhan-Hu and Delta strains (Fig. 5F). All the BA.2 variants compared to BA.1 contained a deletion in the N1 loop as well the absence of a glycan (NxT/S sequence is replaced by NxI) (Fig. 5E). The variation in the Delta structure was only observed around the single insertion at amino acids E156 and F157. This was further confirmed by plotting the root mean square (RMS) deviation of those six superimpositions compared to the insertion/deletion positions (fig. S4, C to F). On the other hand, insertion and/or deletion in the Beta and Omicron variants that induced large structural variations on external loops (Fig. 5F) could alter IgG recognition of the S protein expressed on cell surface.

We assessed in the S-Flow assay (21) the impact of such conformational changes using a mAb that recognizes the NTD domain. This mAb recognized cells expressing the Wuhan-Hu strain (fig. S5A). On the other hand, cells expressing Delta were not recognized by this clone (4A8) due to the deletion in the mAb binding site. Consistent with the notion that mutations/deletions in the NTD affect cross-reactivity, neither Beta- nor BA.1-expressing cells were recognized by this mAb (fig. S5). Therefore, considering that

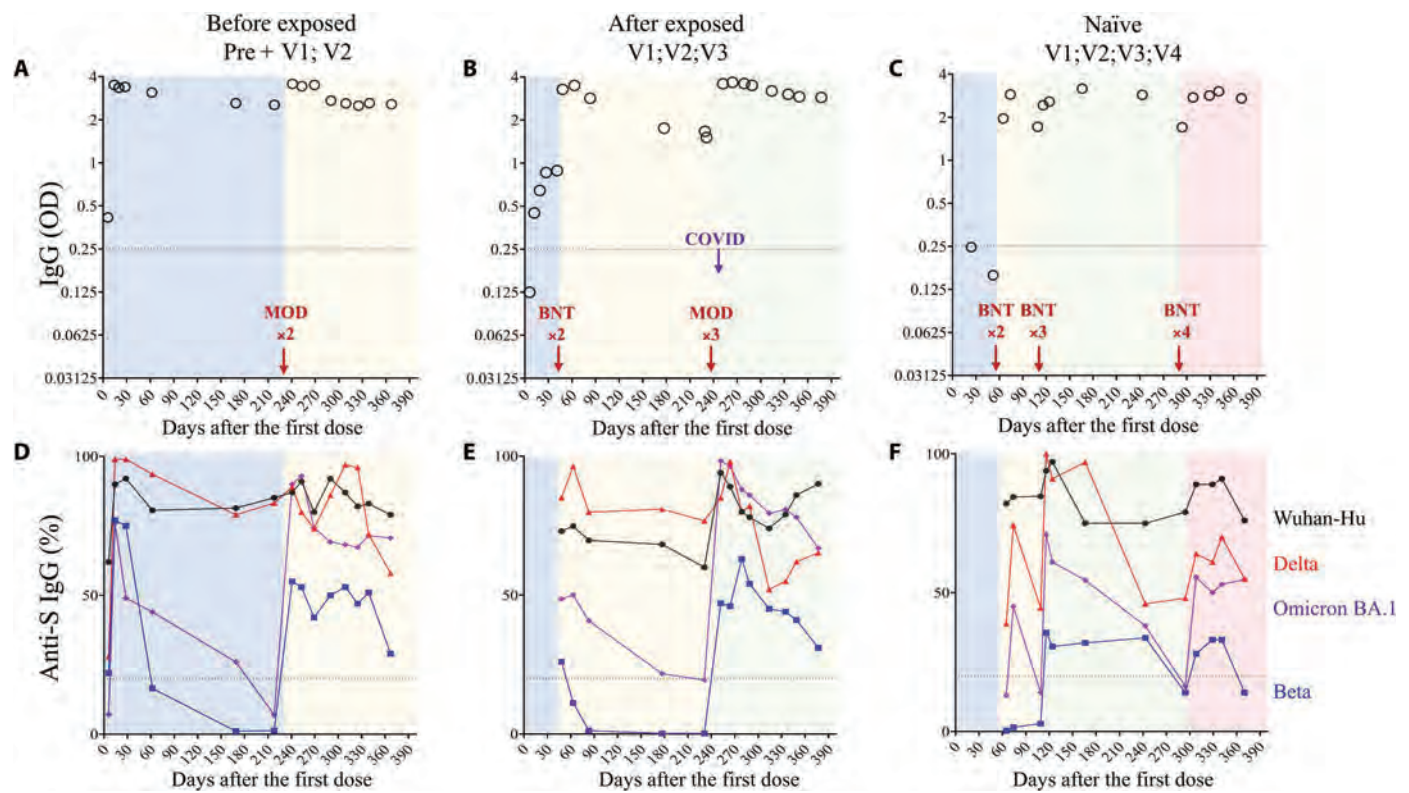


**Fig. 3. Longitudinal analysis of IgG response either in convalescents boosted with mRNA vaccine or vaccinees.** (A to C) ELISA was used to assess specific IgG response against S protein. Plasma were diluted to 1/400. Circles represent blood samplings at different time points after vaccination (first dose). Red arrows represent dates of vaccine boosts [BioNTech (BNT): BNT162b2 or Moderna (MOD): mRNA-1273]. In (B), the date of severe acute respiratory syndrome coronavirus 2 (SARS-CoV-2) infection is indicated. In (C), uninfected SARS-CoV-2 individual (naïve) is shown. OD is shown. Dashed lines represent antibody specificity (0.25). COVID, coronavirus disease. (D to F) S-Flow assay was used to detect specific IgG cross-reactivity against viral variants. Thus, plasma from the same individuals at the same time points were tested against transfected cells expressing either the Wuhan-Hu spike strain (black circles), Delta variant (red triangles), Beta variant (blue squares), or Omicron variant (violet diamonds). Results are expressed as the percentages of specific IgG recognizing transfected cells by flow cytometry.

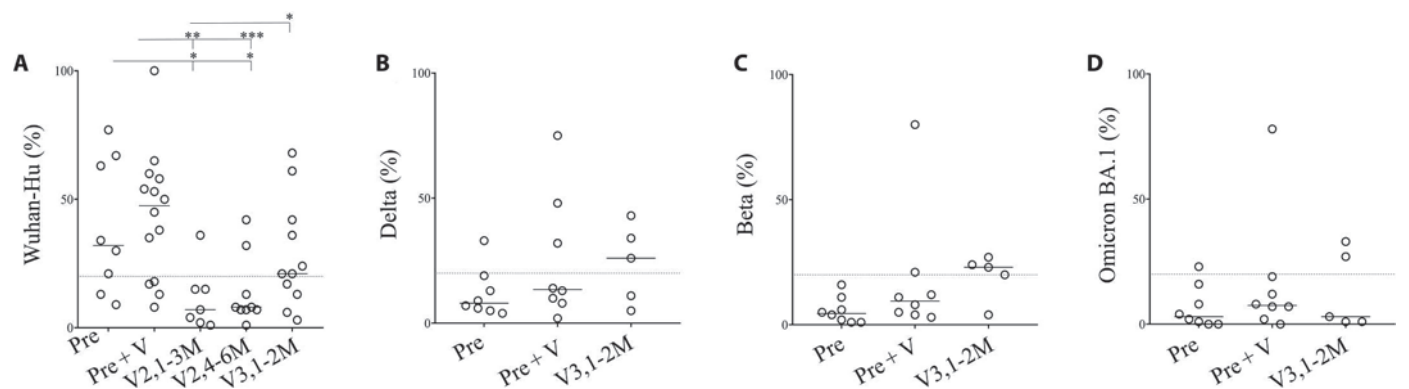


**Fig. 4. IgA cross-reactivity against viral variants in convalescents and vaccinees.** (A) Wuhan-Hu, (B) Delta, (C) Beta and (D) Omicron. Percentages of specific IgA detecting variants by flow cytometry (S-Flow assay) are shown. Plasma from V2 were not tested against Delta, Beta, and Omicron due the low levels of IgA detected by ELISA. In (B) to (D), only IgA responders against Wuhan-Hu were tested. Relative percentages were calculated as follows: (% of IgA from plasma individuals – % of secondary IgA alone) / (% of anti-S2 mAbs – % of secondary IgA alone) \* 100. Each circle represents one individual. Lines represent median values. Statistical analysis was performed using a Mann-Whitney U test (\* $P < 0.05$ ; \*\* $P < 0.01$ ; \*\*\* $P < 0.001$ ).

the main differences of BA.2 subtypes compared to BA.1 are related to the N1, N2, and N3 loops of the NTD (Fig. 5F), we hypothesized that such differences may provide a support for immune escape.

Analyses of humoral response against BA.2 sublineages (BA.4/5, BA.2.12.1, and BA.2.75) revealed that IgG from vaccinees (V3,1-2M) were less capable to recognize BA.2 than BA.1 variant

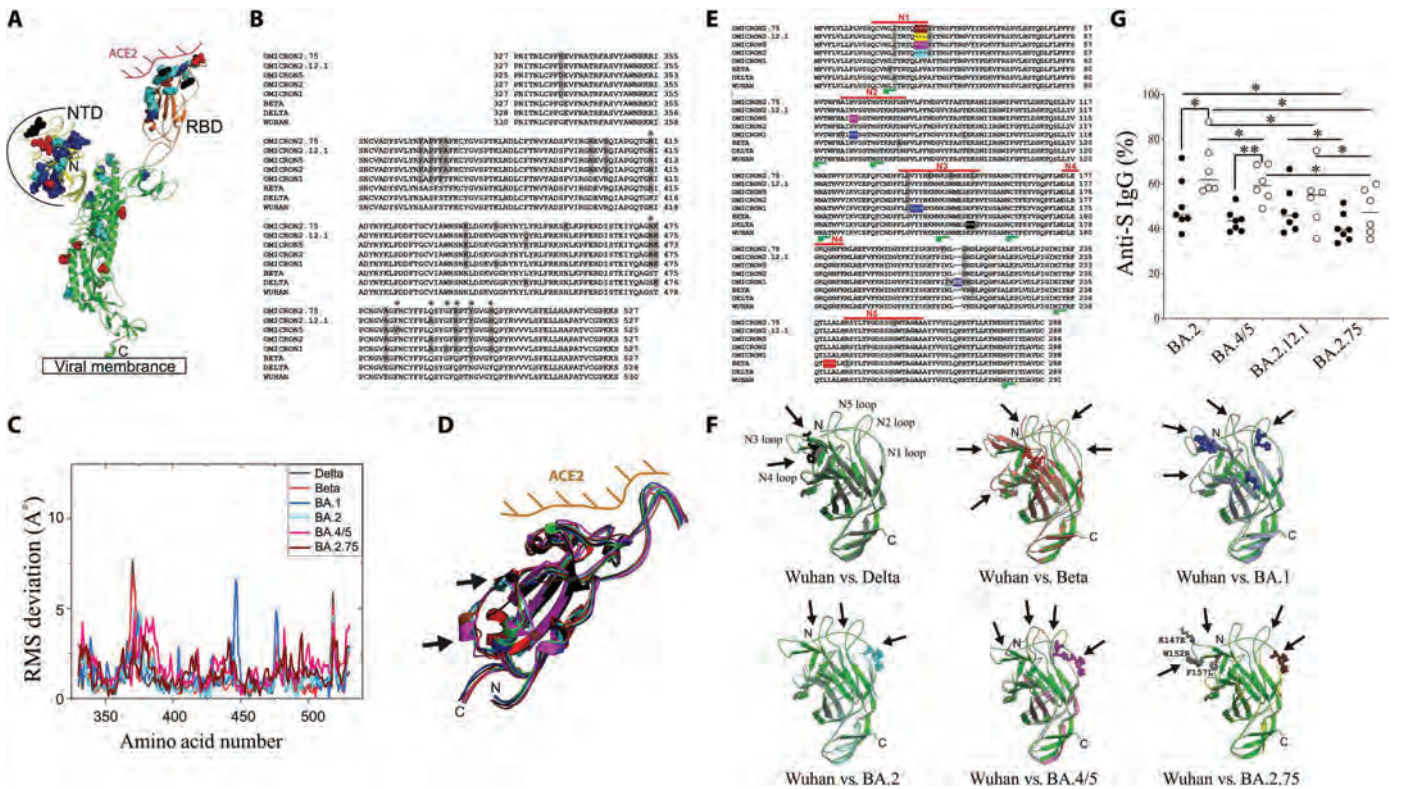


**Fig. 5. Structural comparison of SARS-CoV-2 variants and Omicron BA.2 subtype IgG cross reactivities.** (A) One monomer of S protein where the angiotensin II (ACE2) interaction with the receptor binding domain (RBD) is indicated in pink and N-terminal domain (NTD) area exposed to the solvent is indicated by a black line. (B) Sequence alignment of the RBD domains where mutations in viral variants are indicated in gray in comparison to the Wuhan sequence. (C) Root mean square (RMS) deviation from the RBD structural alignment against the Wuhan-Hu structure [Protein Data Bank identifier (PDB ID): 7L2E]. All RBD structures are in the down state (PDB ID used: 7Q9I, Beta; 7S09, Delta; 7TM0, Omicron BA.1; 7UB0, Omicron BA.2; 7XNS Omicron BA.4/5; and 7YR1, Omicron BA.2.75). The structure from Omicron BA.2.12.2 was not yet validated. (D) Structural superimposition of the Wuhan RBD with the different variants. The main differences are indicated by arrows. (E) Sequence alignment of the NTD where insertion/deletion in the Omicron variants are in color. The other mutations are indicated in gray. (F) Superimposition of the Wuhan-Hu NTD with Delta, Beta, Omicron BA.1, Omicron BA.2, Omicron BA.4/5, or Omicron BA.2.75 NTDs. Arrows indicate large structural variations of solvent exposed loops. (G) IgG cross-reactivity against Omicron BA.2 subtypes. Plasma from either preexposed vaccinated individuals (Pre + V; open circles) or individuals vaccinated either with three doses of vaccine (V3,1-2M; black circles) were monitored for their capacity to recognize the Omicron BA.2 variants. The relative percentages were calculated as described in Fig. 2. Each circle represents one individual. Statistical analysis was performed using a Mann-Whitney U test (\* $P < 0.05$ ; \*\* $P < 0.01$ ).

expressed on the cell surface of transfected cells (BA.2,  $50.8 \pm 11\%$  and BA.1,  $71.6 \pm 23\%$ ,  $P = 0.03$ , respectively; Figs. 2F and 5G). We also observed that IgG from convalescents boosted with the vaccine (Pre + V) recognized less efficiently BA.2 than BA.1 ( $66.8 \pm 12$  and  $88.5 \pm 10\%$ ,  $P = 0.007$ , respectively; Figs. 2F and 5G). Recent works suggest that Omicron BA.2 variants are more resistant to neutralization than BA.2 (54, 55). Comparing BA.2 subtypes, BA.4/5 are less recognized than BA.2 by IgG from vaccinees than individuals preinfected and vaccinated (BA.2: V3,1-2M,  $50.8 \pm 11\%$  versus Pre + V,  $66.8 \pm 12\%$ ,  $P = 0.02$  and BA.4/5: V3,1-2M,  $43.7 \pm 5\%$  versus Pre + V,  $60 \pm 8\%$ ,  $P = 0.001$ , respectively; Fig. 5G). However, BA.2.12.1 and BA.2.75 sublineages are the main variants of concern even for preinfected vaccinees (Pre + V). Thus, these percentages decreased to  $53.9 \pm 13$  and  $47.8 \pm 10\%$  in this group and were not significantly different from those observed in vaccinees (V3,1-2M,  $48.2 \pm 10$  and  $40.7 \pm 6\%$ ; Fig. 5G).

Our results support the idea that mRNA vaccines induce IgG whose recognition is also affected by the structural modifications in the NTD region, which, in addition to the RBD, is the most variable regions in SARS-CoV-2. Note that BA.2.75, which displays

three additional mutations in the third loop of the supersite (51), is the least recognized BA.2 sublineage. This may be indicative of immune pressure and represent one possible mechanism of immune escape. The lower recognition of the S proteins expressed on cell surface would limit cellular effector functions mediated by antibodies and reduce the control of SARS-CoV-2 variants, particularly in the context of BA.2.12.2 and BA.2.75 variants that recently emerged worldwide.

**Three mRNA vaccinations allow to produce antibodies with similar affinities as those from convalescent and boosted individuals**

The progressive loss in the levels and cross-reactivities of specific IgG and IgA requiring repeat vaccinations to maintain their efficacy prompted us to explore the avidity of Ig induced by the mRNA vaccine. The avidity of antibodies reflects the quality and strength of the antibody-antigen complex resulting from the Ig maturation process (38, 56). However, little attention has been paid to the avidity of anti-S antibodies during COVID-19 vaccination. Figure 6A shows the avidity index (AI) of IgG against the

Downloaded from https://www.science.org at National Institute of Infectious Disease on March 05, 2024

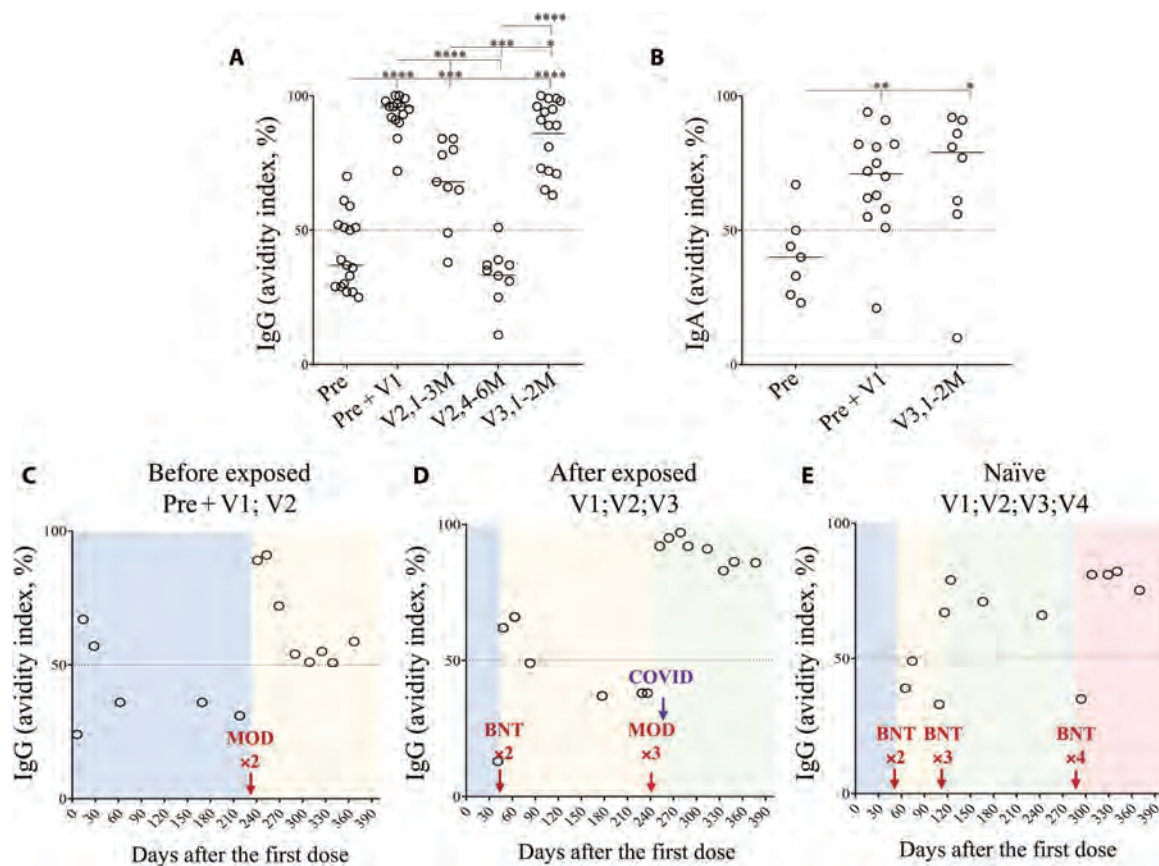


**Fig. 6. Avidity of IgG and IgA against the spike protein in convalescents and vaccinated individuals.** The avidity index (AI; OD with 6M urea/OD without urea  $\times$  100) was assessed by ELISA from plasma of individuals as described in Fig. 1. Plasma are diluted to 1/400. Thus, the AIs of (A) specific IgG and (B) IgA are shown. Dashed lines represent high avidity levels (indexes with a value above 50% are considered to be high, those between 31 and 49% was considered as intermediate, and values below 30% are considered to be low). Lines represent median values. (C to E). AIs of IgG from plasma of individuals described in Fig. 3 were measured longitudinally. Statistical analysis was performed using a Mann-Whitney *U* test (\* $P < 0.05$ ; \*\* $P < 0.01$ ; \*\*\* $P < 0.001$ ; \*\*\*\* $P < 0.0001$ ).

Wuhan-Hu S1 protein using a denaturing urea treatment (6M). The AIs of antibodies with values more than 50% are considered as high (56). Our results highlighted that a vaccine boost markedly improves the AI of IgG (Pre + V,  $95.4 \pm 7.1\%$ ) compared to IgG from convalescent individuals (Pre,  $37 \pm 13.9\%$ ; Fig. 6A). In vaccinees, the AI of IgG from individuals receiving three doses of vaccine (V3,1-2M:  $90 \pm 13\%$ ) was very high, reaching the same level of convalescent and boosted individuals. This index was higher compared to IgG from individuals receiving only two doses of vaccine either early after vaccination (V2,1-3M:  $68 \pm 16\%$ ) or later (V2,4-6M:  $35 \pm 10.8\%$ ; Fig. 6A).

By plotting the AIs against the percentages of S-Flow recognition, we found a strong association in individuals previously infected and boosted with vaccine (Pre + V; fig. S6). Only a subgroup of individuals demonstrated, despite high AIs, lower level of Beta detection ( $<70\%$  of S-Flow; fig. S6). In individuals vaccinated with three doses (V3,1-2M), the ones who displayed greater IgG cross-reactivity against variants were those with the higher AIs (fig. S7). Of interest, vaccinees who received one dose of mRNA-1273 developed IgG with stronger avidity capable to recognize better Omicron than those who received only three doses of BNT162b2 (fig. S7).

For IgA, individuals with two doses were not tested due to the low levels of IgA (Fig. 1D). We found that the IgA AI was high in

convalescent individuals boosted with the vaccine (Pre + V:  $71 \pm 18.9\%$ ) compared to convalescents (Pre:  $40 \pm 15.2\%$ ; Fig. 6B). The AIs of vaccinees with three doses are high ( $79 \pm 27.3\%$ ) and similar to those observed in convalescents with a boost (Fig. 6B).

Our results from the longitudinal follow-up of the three individuals indicated that IgG avidity declined soon after vaccination, even in individuals who had been previously infected or after two doses (Fig. 6, C to E). Thus, an additional boost was required to improve the avidity. The avidity was similar after three or four doses (Fig. 6E). Thus, these data indicated that the AI decreases rapidly despite repeated vaccinations.

Ig affinity maturation depends on the formation of GC and requires the interaction of B and T cells in B cell follicles (57). CXCL13 represents in humans a surrogate marker of GC activation and is associated with neutralizing antibodies with high avidity (40–42), while humoral response occurring in the extrafollicular zones generates short-lived B cells and Ig with low avidity (58, 59). Furthermore, type I interferon (IFN) may also contribute to the induction of CXCL13 (60). Thus, we assessed the levels of CXCL13 in vaccinees from whom samples were obtained within 2 weeks after vaccination including preexposed individuals (Pre + V) and in individuals acutely infected (SARS-CoV-2), compared to healthy individuals (naïve; Fig. 7A). In the analysis of individuals receiving

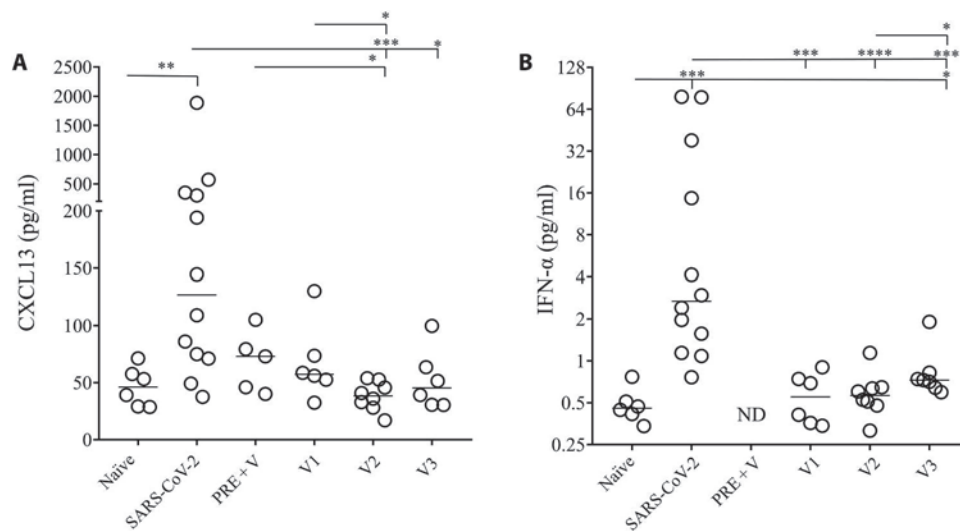


**Fig. 7. Plasma levels of CXCL13 and type I IFN measurement in healthy donors, acute SARS-CoV-2-infected individuals, and vaccinees.** (A) CXCL13 and (B) interferon- $\alpha$  (IFN- $\alpha$ ) levels in the plasma of either healthy donors (naïve), acutely infected individuals (SARS-CoV-2), preexposed vaccinated individuals (Pre + V) and individuals vaccinated with one dose (V1), two doses (V2), or three doses (V3) of vaccine. Blood was collected 15 days after vaccination or infection. Each dot represents one individual. Lines represent median values. Statistical analysis was performed using a Mann-Whitney  $U$  test (\* $P$  < 0.05; \*\* $P$  < 0.01; \*\*\* $P$  < 0.001; \*\*\*\* $P$  < 0.0001). ND, not done.

one (V1,  $57.3 \pm 13.7$  pg/ml), two (V2,  $38.5 \pm 4.4$  pg/ml), or three doses (V3,  $51.5 \pm 10.8$  pg/ml), the levels of CXCL13 were similar to those of healthy donors, whereas their levels were higher in acutely infected patients (Fig. 7A). Although not significantly different, the levels of CXCL13 were lower in healthy individuals ( $46.1 \pm 6.9$  pg/ml) compared to preexposed individuals boosted by mRNA vaccine (Pre + V,  $73.02 \pm 11.8$  pg/ml). However, because of the limited number of individuals tested, this difference deserves to be further addressed. Similarly, we found that IFN- $\alpha$  levels were low in vaccinees compared to those of acutely infected individuals (Fig. 7B). Therefore, the low levels of CXCL13 are associated with the low avidity observed in vaccinees, suggesting suboptimal GC induction.

Together, these results indicate that boosts are required to improve the avidity of specific IgG, in particular, in individuals whose immunity is only due on vaccination and is associated with low CXCL13 levels. They also suggest that loss of avidity may contribute to the loss of cross-reactivity against the different variants that we observed in vaccinees compared to previously infected individuals and boosted with the vaccine.

## DISCUSSION

Overall, our results indicate that individuals previously infected with SARS-CoV-2 and boosted with mRNA vaccines developed a strong humoral response, whereas multiple doses of vaccines are required to induce similar responses in nonexposed individuals. The immune response induced by the mRNA vaccine has valuable cross-reactivity against the different viral variants, although Beta and the more recent Omicron BA.2 sublineages are of major concern in this perspective, since their lower recognition on the cell surface will also reduce Fc effector functions. Therefore, in the absence of previous infection, repeated administrations of mRNA vaccine are required and can be boosted by a fourth dose, providing a possible

explanation for their increased preventive effect on the development of severe disease by different variants (61). Unlike IgG, the presence of IgA may also be beneficial in providing protection at the mucosal viral entry (62). IgA antibodies were induced only after the third dose. However, unfortunately, because of their short half-life and their low avidity, IgA may confer a protection of limited duration, especially regarding SARS-CoV-2 variants.

Considering the half-life and low avidity of antibodies and the requirement for repeated vaccinations, the low levels of CXCL13 probably indicate suboptimal GC activations and extrafollicular B cells maturation in vaccinated individuals. B cell maturation and Ig avidity leading to high neutralizing antibodies depend on B and T cell interaction, and CXCL13 in the plasma is a surrogate marker of GC activation (40–42). It has been shown by Samanovic *et al.* (63) that the levels of CXCL13 remain low after two doses of vaccine. We confirm this finding and show that, even after three doses of vaccine, they remain similar to those of healthy donors and lower than the levels observed in individuals infected by SARS-CoV-2. This is also consistent with the general absence of hyperplasia of draining lymph nodes following mRNA vaccination (less than 0.3% of the recipients) (32). Of interest, other vaccines have been reported to increase the levels of CXCL13 in individuals having received either yellow fever vaccine or Ad5/HIV vaccine (40). The absence of type I IFN after BNT162b2 vaccination is consistent with vaccine manufacturing in which RNA has been modified to markedly reduced innate immune sensing and inflammation (64) Thus, consistent with the earlier theory of P. Matzinger in 90s as “the danger theory of immunity” (65), the absence of innate sensing may require repetitive vaccination for maintaining high levels of antibody. A previous report, using fine needle aspirates of draining axillary lymph nodes, has indicated the presence of GC B cells in vaccinees for 2 months after the boost (66); however, this cannot exclude the detection of extrafollicular B cells. Our follow-up study showed that the avidity decreases after

2 months. Kim *et al.* (67), performing bone marrow aspirates in individuals vaccinated 6 months earlier with two doses of BNT162b2, have observed that the frequency of bone marrow plasma cells against the S protein was at least 20-fold lower compared to those induced by the 2019–2020 influenza virus vaccine. One limitation of our study is the absence of draining lymph nodes data from vaccinees that may help to elucidate lymphoid organization and GC development, as we previously described for other infectious diseases (68, 69).

In the past, the level and persistence of antibodies were demonstrated as being low, even with repeated immunizations, in the absence of T cell help and associated with extrafollicular B cells (70–72). Thus, short-lived B cell immunity was counteracted by associating a “carrier,” as a T cell dominant epitope to improve B cell immunity. Moreover, one possibility of improving mRNA vaccines could be to use cytokines such as interleukin-12 that boosts GC formation and could be considered for longer-lasting immune response (73). Of interest, in individuals previously infected and boosted with vaccine, the humoral response was extremely rapid and stronger in quantity and quality compared to individuals having received two doses of vaccine. This indicates an imprinting of SARS-CoV-2 immunity in hybrid responders. These results are consistent with the presence of activated memory B cells described by Rodda *et al.* (74) in hybrid immunity. This persistence of memory B cells could reflect larger amounts of antigen present after infection and longer ongoing B cell follicle activation contributing to the imprinting, which is consistent with the levels of CXCL13 detected in the plasma of SARS-CoV-2–infected individuals during the acute phase.

We also demonstrated that the avidity of Ig decreased rapidly even after repetitive boosts. This is of importance, because, generally, avidity is associated with the neutralizing capacity of antibodies (75). Furthermore, the lower ability of plasma from vaccines to recognize Beta and Omicron variants might also be related to the lower avidity of antibodies induced by vaccination alone. Our results, using the S-Flow assay, are indicative of a lower capacity to recognize the variants, which may also have consequences for humoral response related to cell-mediated cytotoxicity. The ability to eliminate infected cells might contribute to limiting the duration of infection and/or viral dissemination (76). In this context, it cannot be excluded that viral spread through cell-to-cell transmission can evade neutralizing antibodies. This is well known in HIV infections (77, 78) and was recently demonstrated in SARS-CoV-2 (79). Consistent with a previous report (25), we found that convalescent individuals in the absence of a vaccine boost displayed low quality of antibodies capable to recognize the S protein on the surface of cells, as compared to vaccinated individuals. However, our results highlighted that once vaccinated, convalescent individuals develop a strong humoral response with broader IgG cross-reactivities against SARS-CoV-2 variants. Nevertheless, of particular concern is the low recognition of the S protein from Beta and BA.2 Omicron sublineages (BA.2.12.1 and BA.2.75) by vaccinees' plasma. Previous reports, on the basis of neutralizing assay using both pseudoviruses and viruses, showed that BA.1 (certainly related to the higher number of mutations in the RBD) was more resistant compared to Beta (80, 81). In contrast, the S-Flow assay indicated that Beta is less recognized than BA.1 Omicron. Our longitudinal analysis also suggests that the quality of antibody is declining after the third dose, over the 6 months of follow-up, particularly

regarding the Beta and Omicron variants. Although limited to one individual, we have observed that despite a fourth dose, Beta recognition declined again. Therefore, additional studies deserve to be conducted analyzing the effect of an additional boost or even after viral exposure on the duration of the humoral response. A fourth dose was described to improve protection as compared to three doses of vaccine (61). Thus, our results suggest the importance to also assess the capacity of Ig to recognize SARS-CoV-2 variants on cell surface highlighting the role of deletions in the NTD region of new Omicron variants as a virus strategy to escape from the immune response.

There are some additional limitations in our study. Whereas we have observed that if the third vaccination was performed with mRNA-1271, then it induced IgA and improved the quality of IgG recognizing Omicron as compared with BNT162b2 vaccinees only; this was performed on a limited number of individuals. A recent report, however, also suggested a beneficial effect of mRNA-1273 to induce IgA compared to BNT162b2 (82). Given the role of mucosal immunity against such viral infection, future studies in larger cohorts are needed.

Despite these limitations, our data provided evidence for potential differences in the quantity and quality of the humoral responses in hybrid immune responders compared to individuals having received three doses of mRNA vaccine and highlighted the interest for analyzing immune response directed against S variant proteins expressed on the cell surface. In conclusion, in the context of the generalized third dose of vaccination, our study provides novel findings regarding the levels of protection and the impact of vaccine strategy to control the dynamics of COVID variants.

## MATERIALS AND METHODS

### Study design and participants

The bioclinical features of patients recruited are given in Table 1. This study was approved by the Ethics Committee of the Île-de-France (EudraCT/IDRCB 2020-A00875-34 and Clinical Trials: NCT04351711, Nîmes University Hospital) and from the Clinical Board and Ethics Committee (ref 69/2020, Hospital de Braga, Portugal). All patients had provided written informed consent. We also analyzed samples obtained longitudinally at different time points after vaccination. Blood was collected, and plasma was obtained after centrifugation was frozen to  $-80^{\circ}\text{C}$ .

### IgA and IgG humoral responses

Antibody production was monitored by measuring specific Igs via ELISA against N and S1 proteins as previously described (16). Briefly, NUNC MaxiSorp well plates were coated with antigens (0.5  $\mu\text{g}/\text{ml}$  in tris-HCl, pH 9.6) overnight. After saturation with bovine serum albumin (BSA), plasmas were diluted to 1:400 and 1:800 and incubated for 90 min. Plates were then washed and incubated with goat anti-human IgG (Fc-specific) peroxidase (A0170, MilliporeSigma) and goat anti-human IgA (Fc-specific) peroxidase (SAB3701229, MilliporeSigma) for 45 min. These antibodies were highly specific to the Fc fragments not recognizing the kappa and lambda chains of the Ig. After several washings, substrate reagent solution (R&D Systems) was added and incubated for 30 min. The reactions were stopped using sulfuric acid (1 N). The plate was read on a Thermo Scientific Varioskan reader at wavelengths of 450 and 540 nm.

**SARS-COV-2 spike avidity assay**

Like for ELISA, NUNC MaxiSorp ELISA plates were coated with S1 antigen to monitor the avidity of IgA and IgG. Once incubated in the presence of 1:400 dilution of plasma, plates were washed with phosphate-buffered saline (PBS) and then incubated for 30 min at 37°C in the absence (PBS) or presence of 6M urea. Thereafter, similarly specific IgA and IgG were detected with secondary antibodies and revealed with substrate reagent solution (R&D Systems). The AI was calculated as follows: AI% = (OD value of urea-treated sample/OD of untreated sample)\*100. Indexes with values more than 50% were considered as high IgG avidity, 31 to 49% was considered as intermediate IgG avidity, and values below 30% were considered as low IgG avidity.

**S-Flow assay**

The assay was conducted in two settings, using SARS-CoV-2-infected or SARS-CoV-2-transfected cells. The day before infection,  $4 \times 10^6$  Vero-E6 cells were seeded in 75-cm<sup>2</sup> cell culture flasks in Dulbecco's minimum essential medium (DMEM) supplemented with 10% heat-inactivated fetal bovine serum (FBS) and penicillin and streptomycin solution (100 µg/ml) and incubated at 37°C and 5% CO<sub>2</sub>. On the day of infection, the cell monolayer was 90% confluent. Medium was removed, cells were washed once with medium, and different flasks were inoculated with: SARS-CoV-2 Wuhan-Hu strain (Global Initiative on Sharing All Influenza Data accession no. EPI\_ISL\_16833248) at a multiplicity of infection of 0.01. Cells were incubated for 1 hour at 37°C with shaking. The inoculum was then replaced with DMEM containing 2% FBS. Two days after inoculation, cells were harvested with trypsin (Gibco) and centrifuged for 3 min at 900g. In the other setting, 293T cells were transfected using Lipofectamine 2000 (Life Technologies) and plasmids encoding the full length of the SARS-CoV-2 S variants (47). The Wuhan-Hu S-expressing plasmid was provided by O. Schwartz, whereas Beta and Delta were purchased from InvivoGen (Spike pseudotyping plasmid, plv-spike-v3 and plv-spike-v8, respectively), and the Omicron S protein (BA.1 and BA.2 sublineages) plasmids were produced in-house. After transfection and overnight culture, the cells were detached using PBS-EDTA and transferred into U-bottom 96-well culture plates (200,000 cells per well). For both infected and transfected cells, the cellular pellets were saturated with 10% FBS at 4°C for 10 min and incubated with the patients' plasma (1:300 dilution) in PBS containing 0.5% BSA for 30 min at 4°C. Cells were then washed and stained for 30 min at 4°C using the same antibodies as described for ELISA but labeled with fluorescein isothiocyanate (Sigma-Aldrich). After washing, cells were fixed with 2% paraformaldehyde. Furthermore, we used two mAbs as controls in this study: anti-spike (S2) (GeneTex, clone 1A9) and anti-NTD mAb (ProteoGenix, clone 4A8). The mAbs were diluted to 1:1000 and revealed using specific Alexa Fluor 488-labeled secondary antibodies. Cells were analyzed on an Attune NxT flow cytometer using FlowJo software (Tree Star Inc.).

**Quantification of CXCL13 and IFN-α**

The amounts of CXCL13 and IFN-α in the plasma were quantified by ELISA (R&D Systems). Plates were read at a reference wavelength of 490 nm.

**Statistical analyses**

Statistics were calculated using GraphPad Prism software. A non-parametric Mann-Whitney *U* test and Student's *t* test were used for comparison. *P* values indicate significant differences (\**P* < 0.05; \*\**P* < 0.01; \*\*\**P* < 0.001; \*\*\*\**P* < 0.0001). Correlations were assessed using the Spearman test. A chi-square test was used to compare frequency.

**Supplementary Materials**

This PDF file includes:

Figs. S1 to S7

**REFERENCES AND NOTES**

1. P. Zhou, X. L. Yang, X. G. Wang, B. Hu, L. Zhang, W. Zhang, H. R. Si, Y. Zhu, B. Li, C. L. Huang, H. D. Chen, J. Chen, Y. Luo, H. Guo, R. D. Jiang, M. Q. Liu, Y. Chen, X. R. Shen, X. Wang, X. S. Zheng, K. Zhao, Q. J. Chen, F. Deng, L. L. Liu, B. Yan, F. X. Zhan, Y. Y. Wang, G. F. Xiao, Z. L. Shi, A pneumonia outbreak associated with a new coronavirus of probable bat origin. *Nature* **579**, 270–273 (2020).
2. L. Piccoli, Y. J. Park, M. A. Tortorici, N. Czudnochowski, A. C. Walls, M. Beltramello, C. Silacci-Fregni, D. Pinto, L. E. Rosen, J. E. Bowen, O. J. Acton, S. Jaconi, B. Guarino, A. Minola, F. Zatta, N. Sprugasci, J. Bassi, A. Peter, A. De Marco, J. C. Nix, F. Mele, S. Jovic, B. F. Rodriguez, S. V. Gupta, F. Jin, G. Piumatti, G. Lo Presti, A. F. Pellanda, M. Biggiogero, M. Tarkowski, M. S. Pizzuto, E. Cameroni, C. Havenar-Daughton, M. Smithey, D. Hong, V. Lepori, E. Albanese, A. Ceschi, E. Bernasconi, L. Elzi, P. Ferrari, C. Garzoni, A. Riva, G. Snell, F. Sallusto, K. Fink, H. W. Virgin, A. Lanzavecchia, D. Corti, D. Veessler, Mapping neutralizing and immunodominant sites on the SARS-CoV-2 spike receptor-binding domain by structure-guided high-resolution serology. *Cell* **183**, 1024–1042.e21 (2020).
3. A. J. Greaney, A. N. Loes, K. H. D. Crawford, T. N. Starr, K. D. Malone, H. Y. Chu, J. D. Bloom, Comprehensive mapping of mutations in the SARS-CoV-2 receptor-binding domain that affect recognition by polyclonal human plasma antibodies. *Cell Host Microbe* **29**, 463–476.e6 (2021).
4. Z. Wang, F. Muecksch, A. Cho, C. Gaebler, H.-H. Hoffmann, V. Ramos, S. Zong, M. Cipolla, B. Johnson, F. Schmidt, J. DaSilva, E. Bednarski, T. Ben Tanfous, R. Raspe, K. Yao, Y. E. Lee, T. Chen, M. Turroja, K. G. Milard, J. Dizon, A. Kaczynska, A. Gazumyan, T. Y. Oliveira, C. M. Rice, M. Caskey, P. D. Bieniasz, T. Hatziioannou, C. O. Barnes, M. C. Nussenzweig, Analysis of memory B cells identifies conserved neutralizing epitopes on the N-terminal domain of variant SARS-CoV-2 spike proteins. *Immunity* **55**, 998–1012.e8 (2022).
5. W. Dejnirattisai, J. Huo, D. Zhou, J. Zahradnik, P. Supasa, C. Liu, H. M. E. Duyvesteyn, H. M. Ginn, A. J. Mentzer, A. Tuekprakhon, R. Nutalai, B. Wang, A. Djokaitte, S. Khan, O. Avinoam, M. Bahar, D. Skelly, S. Adele, S. A. Johnson, A. Amini, T. G. Ritter, C. Mason, C. Dold, D. Pan, S. Assadi, A. Bellas, N. Omo-Dare, D. Koeckerling, A. Flaxman, D. Jenkin, P. K. Aley, M. Voysey, S. A. C. Clemens, F. G. Naveca, V. Nascimento, F. Nascimento, C. F. da Costa, P. C. Resende, A. Pauvolid-Correa, M. M. Siqueira, V. Baillie, N. Serafin, G. Kwatra, K. Da Silva, S. A. Madhi, M. C. Nunes, T. Malik, P. J. M. Openshaw, J. K. Baillie, M. G. Semple, A. R. Townsend, K. A. Huang, T. K. Tan, M. W. Carroll, P. Klenerman, E. Barnes, S. J. Dunachie, B. Constantinides, H. Webster, D. Crook, A. J. Pollard, T. Lambe, N. G. Paterson, M. A. Williams, D. R. Hall, E. E. Fry, J. Mongkolsapaya, J. Ren, G. Schreiber, D. I. Stuart, G. R. Screaton, SARS-CoV-2 Omicron-B.1.1.529 leads to widespread escape from neutralizing antibody responses. *Cell* **185**, 467–484.e15 (2022).
6. M. McCallum, A. De Marco, F. A. Lempp, M. A. Tortorici, D. Pinto, A. C. Walls, M. Beltramello, A. Chen, Z. Liu, F. Zatta, S. Zepeda, J. di Iulio, J. E. Bowen, M. Montiel-Ruiz, J. Zhou, L. E. Rosen, S. Bianchi, B. Guarino, C. S. Fregni, R. Abdelnabi, S. C. Foo, P. W. Rothlauf, L. M. Bloyet, F. Benigni, E. Cameroni, J. Neyts, A. Riva, G. Snell, A. Telenti, S. P. J. Whelan, H. W. Virgin, D. Corti, M. S. Pizzuto, D. Veessler, N-terminal domain antigenic mapping reveals a site of vulnerability for SARS-CoV-2. *Cell* **184**, 2332–2347.e16 (2021).
7. C. Davis, N. Logan, G. Tyson, R. Orton, W. T. Harvey, J. S. Perkins, G. Mollett, R. M. Blacow; COVID-19 Genomics UK (COG-UK) Consortium, T. P. Peacock, W. S. Barclay, P. Cherepanov, M. Palmrini, P. R. Murcia, A. H. Patel, D. L. Robertson, J. Haughney, E. C. Thomson, B. J. Willett; COVID-19 Deployed Vaccine (DOVE) Cohort Study investigators, Reduced neutralisation of the Delta (B.1.617.2) SARS-CoV-2 variant of concern following vaccination. *PLoS Pathog.* **17**, e1010022 (2021).
8. V.-V. Edara, B. A. Pinsky, M. S. Suthar, L. Lai, M. E. Davis-Gardner, K. Floyd, M. W. Flowers, J. Wrammert, L. Hussaini, C. R. Ciric, S. Bechnak, K. Stephens, B. S. Graham, E. Bayat Mokhtari, P. Mudvari, E. Boritz, A. Creanga, A. Pegu, A. Derrien-Coleman, A. R. Henry, M. Gagne, D. C. Douek, M. K. Sahoo, M. Sibai, D. Solis, R. J. Webby, T. Jeevan, T. P. Fabrizio, Infection

- and vaccine-induced neutralizing-antibody responses to the SARS-CoV-2 B.1.617 variants. *N. Engl. J. Med.* **385**, 664–666 (2021).
9. I. Nemet, L. Kliker, Y. Lustig, N. Zuckerman, O. Erster, C. Cohen, Y. Kreiss, S. Alroy-Preis, G. Regev-Yochay, E. Mendelson, M. Mandelboim, Third bnt162b2 vaccination neutralization of SARS-CoV-2 omicron infection. *N. Engl. J. Med.* **386**, 492–494 (2022).
  10. W. F. Garcia-Beltran, K. J. St Denis, A. Hoelzemer, E. C. Lam, A. D. Nitido, M. L. Sheehan, C. Berrios, O. Ofoman, C. C. Chang, B. M. Hauser, J. Feldman, A. L. Roederer, D. J. Gregory, M. C. Poznansky, A. G. Schmidt, A. J. Iafraite, V. Naranbhai, A. B. Balazs, mRNA-based COVID-19 vaccine boosters induce neutralizing immunity against SARS-CoV-2 Omicron variant. *Cell* **185**, 457–466.e4 (2022).
  11. A. Muik, B. G. Lui, A. K. Wallisch, M. Bacher, J. Mühl, J. Reinholz, O. Ozhelvaci, N. Beckmann, R. C. Güimil Garcia, A. Poran, S. Shpyro, A. Finlayson, H. Cai, Q. Yang, K. A. Swanson, Ö. Türeci, U. Şahin, Neutralization of SARS-CoV-2 Omicron by BNT162b2 mRNA vaccine-elicited human sera. *Science* **375**, 678–680 (2022).
  12. J. M. Carreño, H. Alshammari, J. Tcheou, G. Singh, A. J. Raskin, H. Kawabata, L. A. Sominsky, J. J. Clark, D. C. Adelsberg, D. A. Bielak, A. S. Gonzalez-Reiche, N. Dambrauskas, V. Vigdorovich, K. Srivastava, D. N. Sather, E. M. Sordillo, G. Bajic, H. van Bakel, V. Simon, F. Krammer, Activity of convalescent and vaccine serum against SARS-CoV-2 Omicron. *Nature* **602**, 682–688 (2022).
  13. S. Miyamoto, T. Arashiro, Y. Adachi, S. Moriyama, H. Kinoshita, T. Kanno, S. Saito, H. Katano, S. Iida, A. Ainai, R. Kotaki, S. Yamada, Y. Kuroda, T. Yamamoto, K. Ishijima, E. S. Park, Y. Inoue, Y. Kaku, M. Tobiume, N. Iwata-Yoshikawa, N. Shiwa-Sudo, K. Tokunaga, S. Ozono, T. Hemmi, A. Ueno, N. Kishida, S. Watanabe, K. Nojima, Y. Seki, T. Mizukami, H. Hasegawa, H. Ebihara, K. Maeda, S. Fukushi, Y. Takahashi, T. Suzuki, Vaccination-infection interval determines cross-neutralization potency to SARS-CoV-2 Omicron after breakthrough infection by other variants. *Med* **3**, 249–261.e4 (2022).
  14. L. Liu, S. Iketani, Y. Guo, J. F. W. Chan, M. Wang, L. Liu, Y. Luo, H. Chu, Y. Huang, M. S. Nair, J. Yu, K. K. H. Chik, T. T. T. Yuen, C. Yoon, K. K. W. To, H. Chen, M. T. Yin, M. E. Sobieszczyk, Y. Huang, H. H. Wang, Z. Sheng, K.-Y. Yuen, D. D. Ho, Striking antibody evasion manifested by the Omicron variant of SARS-CoV-2. *Nature* **602**, 676–681 (2022).
  15. E. Cameroni, J. E. Bowen, L. E. Rosen, C. Saliba, S. K. Zepeda, K. Culp, D. Pinto, L. A. VanBlargan, A. De Marco, J. di Iulio, F. Zatta, H. Kaiser, J. Noack, N. Farhat, N. Czudnochowski, C. Havenar-Daughton, K. R. Sprouse, J. R. Dillen, A. E. Powell, A. Chen, C. Maher, L. Yin, D. Sun, L. Soriaga, J. Bassi, C. Silacci-Fregni, C. Gustafsson, N. M. Franko, J. Logue, N. T. Iqbal, I. Mazzitelli, J. Geffner, R. Grifantini, H. Chu, A. Gori, A. Riva, O. Giannini, A. Ceschi, P. Ferrari, P. E. Cippà, A. Franzetti-Pellanda, C. Garzoni, P. J. Halfmann, Y. Kawaoka, C. Hebner, L. A. Purcell, L. Piccoli, M. S. Pizzuto, A. C. Walls, M. S. Diamond, A. Telenti, H. W. Virgin, A. Lanzavecchia, G. Snell, D. Velesler, D. Corti, Broadly neutralizing antibodies overcome SARS-CoV-2 Omicron antigenic shift. *Nature* **602**, 664–670 (2022).
  16. D. Planas, N. Saunders, P. Maes, F. Guivel-Benhassine, C. Planchais, J. Buchrieser, W.-H. Bolland, F. Porrot, I. Staropoli, F. Lemoine, H. Péré, D. Veyer, J. Puech, J. Rodary, G. Baele, S. Dellicour, J. Raymenants, S. Gorissen, C. Geenen, B. Vanmechelen, T. Wawina-Bokalanga, J. Marti-Carreras, L. Cuyppers, A. Séve, L. Hocquembourg, T. Prazuck, F. A. Rey, E. Simon-Lorière, T. Bruel, H. Mouquet, E. André, O. Schwartz, Considerable escape of SARS-CoV-2 Omicron to antibody neutralization. *Nature* **602**, 671–675 (2022).
  17. M. Hoffmann, N. Krüger, S. Schulz, A. Cossmann, C. Rocha, A. Kempf, I. Nehlmeier, L. Graichen, A. S. Moldenhauer, M. S. Winkler, M. Lier, A. Dopfer-Jablonka, H. M. Jäck, G. M. N. Behrens, S. Pöhlmann, The Omicron variant is highly resistant against antibody-mediated neutralization: Implications for control of the COVID-19 pandemic. *Cell* **185**, 447–456.e11 (2022).
  18. Y. Cao, J. Wang, F. Jian, T. Xiao, W. Song, A. Yisimayi, W. Huang, Q. Li, P. Wang, R. An, J. Wang, Y. Wang, X. Niu, S. Yang, H. Liang, H. Sun, T. Li, Y. Yu, Q. Cui, S. Liu, X. Yang, S. Du, Z. Zhang, X. Hao, F. Shao, R. Jin, X. Wang, J. Xiao, Y. Wang, X. S. Xie, Omicron escapes the majority of existing SARS-CoV-2 neutralizing antibodies. *Nature* **602**, 657–663 (2022).
  19. E. S. Winkler, P. Gilchuk, J. Yu, A. L. Bailey, R. E. Chen, Z. Chong, S. J. Zost, H. Jang, Y. Huang, J. D. Allen, J. B. Case, R. E. Sutton, R. H. Carnahan, T. L. Darling, A. C. M. Boon, M. Mack, R. D. Head, T. M. Ross, J. E. Crowe Jr., M. S. Diamond, Human neutralizing antibodies against SARS-CoV-2 require intact Fc effector functions for optimal therapeutic protection. *Cell* **184**, 1804–1820.e16 (2021).
  20. Y. C. Bartsch, S. Fischinger, S. M. Siddiqui, Z. Chen, J. Yu, M. Gebre, C. Atyeo, M. J. Gorman, A. L. Zhu, J. Kang, J. S. Burke, M. Slein, M. J. Gluck, S. Beger, Y. Hu, J. Rhee, E. Petersen, B. Mormann, M. de St Aubin, M. A. Hasdianda, G. Jambaulikar, E. W. Boyer, P. C. Sabeti, D. H. Brouch, B. D. Julg, E. R. Musk, A. S. Menon, D. A. Lauffenburger, E. J. Nilles, G. Alter, Discrete SARS-CoV-2 antibody titers track with functional humoral stability. *Nat. Commun.* **12**, 1018 (2021).
  21. S. André, M. Azarias da Silva, M. Picard, A. Alleaume-Buteau, L. Kundura, R. Cezar, C. Soudaramoury, S. C. André, A. Mendes-Frias, A. Carvalho, C. Capela, J. Pedrosa, A. Gil Castro, P. Loubet, A. Sotto, L. Muller, J.-Y. Lefrant, C. Roger, P.-G. Claret, S. Duvnjak, T.-A. Tran, O. Zghidi-Abouzid, P. Nioche, R. Silvestre, P. Corbeau, F. Mammano, J. Estaquier, Low quantity and quality of anti-spike humoral response is linked to CD4 T-cell apoptosis in COVID-19 patients. *Cell Death Dis.* **13**, 741 (2022).
  22. S. André, M. Picard, R. Cezar, F. Roux-Dalvai, A. Alleaume-Butaux, C. Soudaramoury, A. S. Cruz, A. Mendes-Frias, C. Gotti, M. Leclercq, A. Nicolas, A. Tazuin, A. Carvalho, C. Capela, J. Pedrosa, A. G. Castro, L. Kundura, P. Loubet, A. Sotto, L. Muller, J. Y. Lefrant, C. Roger, P. G. Claret, S. Duvnjak, T. A. Tran, G. Racine, O. Zghidi-Abouzid, P. Nioche, R. Silvestre, A. Droit, F. Mammano, P. Corbeau, J. Estaquier, T cell apoptosis characterizes severe Covid-19 disease. *Cell Death Differ.* **29**, 1486–1499 (2022).
  23. Y. C. Bartsch, X. Tong, J. Kang, M. J. Avendaño, E. F. Serrano, T. García-Salum, C. Pardo-Roa, A. Riquelme, Y. Cai, I. Renzi, G. Stewart-Jones, B. Chen, R. A. Medina, G. Alter, Omicron variant Spike-specific antibody binding and Fc activity are preserved in recipients of mRNA or inactivated COVID-19 vaccines. *Sci. Transl. Med.* **14**, eabn9243 (2022).
  24. E. C. Sabino, L. F. Buss, M. P. S. Carvalho, C. A. Prete Jr., M. A. E. Crispim, N. A. Fraiji, R. H. M. Pereira, K. V. Parag, P. da Silva Peixoto, M. U. G. Kraemer, M. K. Oikawa, T. Salomon, Z. M. Cucunuba, M. C. Castro, A. A. de Souza Santos, V. H. Nascimento, H. S. Pereira, N. M. Ferguson, O. G. Pybus, A. Kucharski, M. P. Busch, C. Dye, N. R. Faria, Resurgence of COVID-19 in Manaus, Brazil, despite high seroprevalence. *Lancet* **397**, 452–455 (2021).
  25. P. Kaplonek, S. Fischinger, D. Cizmezi, Y. C. Bartsch, J. Kang, J. S. Burke, S. A. Shin, D. Dayal, P. Martin, C. Mann, F. Amanat, B. Julg, E. J. Nilles, E. R. Musk, A. S. Menon, F. Krammer, E. O. Saphire, C. Andrea, G. Alter, mRNA-1273 vaccine-induced antibodies maintain Fc effector functions across SARS-CoV-2 variants of concern. *Immunity* **55**, 355–365.e4 (2022).
  26. L. J. Abu-Raddad, H. Chemaitelly, H. H. Ayoub, H. M. Yassine, F. M. Benslimane, H. A. Al Khatib, P. Tang, M. R. Hasan, P. Coyle, Z. Al Kanaani, E. Al Kuwari, A. Jeremijenko, A. H. Kaleeckal, A. N. Latif, R. M. Shaik, H. F. Abdul Rahim, G. K. Nasrallah, M. G. Al Kuwari, A. A. Butt, H. E. Al Romaihi, M. H. Al-Thani, A. Al Khal, R. Bertollini, Association of prior SARS-CoV-2 infection with risk of breakthrough infection following mRNA vaccination in Qatar. *JAMA* **326**, 1930–1939 (2021).
  27. S. Gazit, R. Shlezinger, G. Perez, R. Lotan, A. Peretz, A. Ben-Tov, E. Herzal, H. Alapi, D. Cohen, K. Muhsen, G. Chodick, T. Patalon, Severe Acute Respiratory Syndrome Coronavirus 2 (SARS-CoV-2) Naturally acquired immunity versus vaccine-induced immunity, reinfections versus breakthrough infections: A retrospective cohort study. *Clin. Infect. Dis.* **75**, e545–e551 (2022).
  28. Y. Goldberg, M. Mandel, Y. M. Bar-On, O. Bodenheimer, L. S. Freedman, N. Ash, S. Alroy-Preis, A. Huppert, R. Milo, Protection and waning of natural and hybrid immunity to SARS-CoV-2. *N. Engl. J. Med.* **386**, 2201–2212 (2022).
  29. D. Sterlin, A. Mathian, M. Miyara, A. Mohr, F. Anna, L. Claër, P. Quentric, J. Fadlallah, H. Devilliers, P. Ghillani, C. Gunn, R. Hockett, S. Mudumba, A. Guihot, C. E. Luyt, J. Mayaux, A. Beurton, S. Fourati, T. Bruel, O. Schwartz, J. M. Lacorte, H. Yssel, C. Parizot, K. Dorgham, P. Charneau, Z. Amoura, G. Gorochov, IgA dominates the early neutralizing antibody response to SARS-CoV-2. *Sci. Transl. Med.* **13**, eabd2223 (2021).
  30. F. N. Zervou, P. Louie, A. Stachel, I. M. Zacharioudakis, Y. Ortiz-Mendez, K. Thomas, M. E. Aguerro-Rosenfeld, SARS-CoV-2 antibodies: IgA correlates with severity of disease in early COVID-19 infection. *J. Med. Virol.* **93**, 5409–5415 (2021).
  31. L. R. Baden, H. M. El Sahly, B. Essink, K. Kotloff, S. Frey, R. Novak, D. Diemert, S. A. Spector, M. R. Roupheal, C. B. Creech, J. McGettigan, S. Khetan, N. Segall, J. Solis, A. Brosz, C. Fierro, H. Schwartz, K. Neuzil, L. Corey, P. Gilbert, H. Janes, D. Follmann, M. Marovich, J. Mascola, L. Polakowski, J. Ledgerwood, B. S. Graham, H. Bennett, R. Pajon, C. Knightly, B. Leav, W. Deng, H. Zhou, S. Han, M. Ivarsson, J. Miller, T. Zaks, Efficacy and safety of the mRNA-1273 SARS-CoV-2 vaccine. *N. Engl. J. Med.* **384**, 403–416 (2020).
  32. F. P. Polack, S. J. Thomas, N. Kitchin, J. Absalon, A. Gurtman, S. Lockhart, J. L. Perez, G. Pérez Marc, E. D. Moreira, C. Zerbini, R. Bailey, K. A. Swanson, S. Roychoudhury, K. Koury, P. Li, W. V. Kalina, D. Cooper, R. W. Frenck, L. L. Hammit, Ö. Türeci, H. Nell, A. Schaefer, S. Ünal, D. B. Tresnan, S. Mather, P. R. Dormitzer, U. Şahin, K. U. Jansen, W. C. Gruber, Safety and efficacy of the BNT162b2 mRNA covid-19 vaccine. *N. Engl. J. Med.* **383**, 2603–2615 (2020).
  33. D. Steensels, N. Pierlet, J. Penders, D. Mesotten, L. Heylen, Comparison of SARS-CoV-2 antibody response following vaccination with BNT162b2 and mRNA-1273. *JAMA* **326**, 1533–1535 (2021).
  34. P. Naaber, L. Tserel, K. Kangro, E. Sepp, V. Jürjenson, A. Adamson, L. Haljasmägi, A. P. Rumm, R. Maruste, J. Kärner, J. M. Gerhold, A. Planken, M. Ustav, K. Kisand, P. Peterson, Dynamics of antibody response to BNT162b2 vaccine after six months: A longitudinal prospective study. *Lancet Reg. Health Eur.* **10**, 100208 (2021).
  35. J. Wei, N. Stoesser, P. C. Matthews, D. Ayoubkhani, R. Studley, I. Bell, J. I. Bell, J. N. Newton, J. Farrar, I. Diamond, E. Rourke, A. Howarth, B. D. Marsden, S. Hoosdally, E. Y. Jones, D. I. Stuart, D. W. Crook, T. E. A. Peto, K. B. Pouwels, D. W. Eyre, A. S. Walker, COVID-19 Infection Survey team, Antibody responses to SARS-CoV-2 vaccines in 45,965 adults from the general population of the United Kingdom. *Nat. Microbiol.* **6**, 1140–1149 (2021).
  36. P. B. Gilbert, D. C. Montefiori, A. B. McDermott, Y. Fong, D. Benkeser, W. Deng, H. Zhou, C. R. Houchens, K. Martins, L. Jayashankar, F. Castellino, B. Flach, B. C. Lin, S. O'Connell, C. McDanal, A. Eaton, M. Sarzotti-Kelsoe, Y. Lu, C. Yu, B. Borate, L. W. P. van der Laan,

- N. S. Hejazi, C. Huynh, J. Miller, H. M. El Sahly, L. R. Baden, M. Baron, L. De La Cruz, C. Gay, S. Kalams, C. F. Kelley, M. P. Andrasik, J. G. Kublin, L. Corey, K. M. Neuzil, L. N. Carpp, R. Pajon, D. Follmann, R. O. Donis, R. A. Koup, Immune correlates analysis of the mRNA-1273 COVID-19 vaccine efficacy clinical trial. *Science* **375**, 43–50 (2022).
37. D. S. Khoury, D. Cromer, A. Reynaldi, T. E. Schlub, A. K. Wheatley, J. A. Juno, K. Subbarao, S. J. Kent, J. A. Triccas, M. P. Davenport, Neutralizing antibody levels are highly predictive of immune protection from symptomatic SARS-CoV-2 infection. *Nat. Med.* **27**, 1205–1211 (2021).
38. M. H. Korhonen, J. Brunstein, H. Haario, A. Katnikov, R. Rescaldani, K. Hedman, A new method with general diagnostic utility for the calculation of immunoglobulin G avidity. *Clin. Diagn. Lab. Immunol.* **6**, 725–728 (1999).
39. G. J. Thorbecke, A. R. Amin, V. K. Tsiagbe, Biology of germinal centers in lymphoid tissue. *FASEB J.* **8**, 832–840 (1994).
40. C. Havenar-Daughton, M. Lindqvist, A. Heit, J. E. Wu, S. M. Reiss, K. Kendric, S. Bélanger, S. P. Kasturi, E. Landais, R. S. Akondy, H. M. McGuire, M. Bothwell, P. A. Vagefi, E. Scully, G. D. Tomaras, M. M. Davis, P. Poignard, R. Ahmed, B. D. Walker, B. Pulendran, M. J. McElrath, D. E. Kaufmann, S. Crotty, M. A. Price, J. Gilmour, P. Fast, A. Kamali, E. J. Sanders, O. Onzala, S. Allen, E. Hunter, E. Karita, W. Kilembe, S. Lakhi, M. Inambao, CXCL13 is a plasma biomarker of germinal center activity. *Proc. Natl. Acad. Sci. U.S.A.* **113**, 2702–2707 (2016).
41. J. M. Mabuka, A.-S. Dugast, D. M. Muema, T. Reddy, Y. Ramlakhan, Z. Euler, N. Ismail, A. Moodley, K. L. Dong, L. Morris, B. D. Walker, G. Alter, T. Ndung'u, Plasma CXCL13 but Not B cell frequencies in acute HIV infection predicts emergence of cross-neutralizing antibodies. *Front. Immunol.* **8**, 1104 (2017).
42. F. Moukambi, H. Rabezanahary, Y. Fortier, V. Rodrigues, J. Clain, G. Benmadid-Laktout, O. Zghidi-Abouzid, C. Soundaramourty, M. Laforge, J. Estaquier, Mucosal T follicular helper cells in SIV-infected rhesus macaques: Contributing role of IL-27. *Mucosal Immunol.* **12**, 1038–1054 (2019).
43. Q. X. Long, B. Z. Liu, H. J. Deng, G. C. Wu, K. Deng, Y. K. Chen, P. Liao, J. F. Qiu, Y. Lin, X. F. Cai, D. Q. Wang, Y. Hu, J. H. Ren, N. Tang, Y. Y. Xu, L. H. Yu, Z. Mo, F. Gong, X. L. Zhang, W. G. Tian, L. Hu, X. X. Zhang, J. L. Xiang, H. X. Du, H. W. Liu, C. H. Lang, X. H. Luo, S. B. Wu, X. P. Cui, Z. Zhou, M. M. Zhu, J. Wang, C. J. Xue, X. F. Li, L. Wang, Z. J. Li, K. Wang, C. C. Niu, Q. J. Yang, X. J. Tang, Y. Zhang, X. M. Liu, J. J. Li, D. C. Zhang, F. Zhang, P. Liu, J. Yuan, Q. Li, J. L. Hu, J. Chen, A. L. Huang, Antibody responses to SARS-CoV-2 in patients with COVID-19. *Nat. Med.* **26**, 845–848 (2020).
44. K. Röltgen, A. E. Powell, O. F. Wirz, B. A. Stevens, C. A. Hogan, J. Najeeb, M. Hunter, H. Wang, M. K. Sahoo, C. Huang, F. Yamamoto, M. Manohar, J. Manalac, A. R. Otrelo-Cardoso, T. D. Pham, A. Rustagi, A. J. Rogers, N. H. Shah, C. A. Blish, J. R. Cochran, T. S. Jardetzky, J. L. Zehnder, T. T. Wang, B. Narasimhan, S. Gombar, R. Tibshirani, K. C. Nadeau, P. S. Kim, B. A. Pinsky, S. D. Boyd, Defining the features and duration of antibody responses to SARS-CoV-2 infection associated with disease severity and outcome. *Sci. Immunol.* **5**, eabe0240 (2020).
45. C. A. Pierce, P. Preston-Hurlburt, Y. Dai, C. B. Aschner, N. Cheshenko, B. Galen, S. J. Garforth, N. G. Herrera, R. K. Jangra, N. C. Morano, E. Orner, S. Sy, K. Chandran, J. Dziura, S. C. Almo, A. Ring, M. J. Keller, K. C. Herold, B. C. Herold, Immune responses to SARS-CoV-2 infection in hospitalized pediatric and adult patients. *Sci. Transl. Med.* **12**, eabd5487 (2020).
46. P. Brandtzaeg, F.-E. Johansen, Mucosal B cells: Phenotypic characteristics, transcriptional regulation, and homing properties. *Immunol. Rev.* **206**, 32–63 (2005).
47. L. Grzelak, S. Temmam, C. Planchais, C. Demeret, L. Tondeur, C. Huon, F. Guivel-Benhassine, I. Staropoli, M. Chazal, J. Dufloo, D. Planas, J. Buchrieser, M. M. Rajah, R. Robinot, F. Porrot, M. Albert, K. Y. Chen, B. Crescenzo-Chaigne, F. Donati, F. Anna, P. Souque, M. Gransagne, J. Bellalou, M. Nowakowski, M. Backovic, L. Bouadma, L. Le Fevre, Q. Le Hingrat, D. Descamps, A. Pourbaix, C. Laouénan, J. Ghosn, Y. Yazdanpanah, C. Besombes, N. Jolly, S. Pellerin-Fernandes, O. Cheny, M. N. Ungeheuer, G. Mellon, P. Morel, S. Rolland, F. A. Rey, S. Behillil, V. Enouf, A. Lemaître, M. A. Créach, S. Petres, N. Escriou, P. Charneau, A. Fontanet, B. Hoen, T. Bruel, M. Eloit, H. Mouquet, O. Schwartz, S. van der Werf, A comparison of four serological assays for detecting anti-SARS-CoV-2 antibodies in human serum samples from different populations. *Sci. Transl. Med.* **12**, eabc3103 (2020).
48. P. Wang, M. S. Nair, L. Liu, S. Iketani, Y. Luo, Y. Guo, M. Wang, J. Yu, B. Zhang, P. D. Kwong, B. S. Graham, J. R. Mascola, J. Y. Chang, M. T. Yin, M. Sobieszczyk, C. A. Kyratsous, L. Shapiro, Z. Sheng, Y. Huang, D. D. Ho, Antibody resistance of SARS-CoV-2 variants B.1.351 and B.1.1.7. *Nature* **593**, 130–135 (2021).
49. T. Zhou, L. Wang, J. Misasi, A. Pegu, Y. Zhang, D. R. Harris, A. S. Olin, C. A. Talana, E. S. Yang, M. Chen, M. Choe, W. Shi, I. T. Teng, A. Creanga, C. Jenkins, K. Leung, T. Liu, E. D. Stancofski, T. Stephens, B. Zhang, Y. Tsybovsky, B. S. Graham, J. R. Mascola, N. J. Sullivan, P. D. Kwong, Structural basis for potent antibody neutralization of SARS-CoV-2 variants including B.1.1.529. *Science* **376**, eabn8897 (2022).
50. F. Amanat, M. Thapa, T. Lei, S. M. S. Ahmed, D. C. Adelsberg, J. M. Carreño, S. Strohmaier, A. J. Schmitz, S. Zafar, J. Q. Zhou, W. Rijnink, H. Alshammari, N. Borchering, A. G. Reiche, K. Srivastava, E. M. Sordillo, H. van Bakel, J. S. Turner, G. Bajic, V. Simon, A. H. Ellebedy, F. Krammer, SARS-CoV-2 mRNA vaccination induces functionally diverse antibodies to NTD, RBD, and S2. *Cell* **184**, 3936–3948.e10 (2021).
51. G. Cerutti, Y. Guo, T. Zhou, J. Gorman, M. Lee, M. Rapp, E. R. Reddem, J. Yu, F. Bahna, J. Bimela, Y. Huang, P. S. Katsamba, L. Liu, M. S. Nair, R. Rawi, A. S. Olin, P. Wang, B. Zhang, G. Y. Chuang, D. D. Ho, Z. Sheng, P. D. Kwong, L. Shapiro, Potent SARS-CoV-2 neutralizing antibodies directed against spike N-terminal domain target a single supersite. *Cell Host Microbe* **29**, 819–833.e7 (2021).
52. N. Suryadevara, S. Shrihari, P. Gilchuk, L. A. VanBlargan, E. Binshtein, S. J. Zost, R. S. Nargi, R. E. Sutton, E. S. Winkler, E. C. Chen, M. E. Fouch, E. Davidson, B. J. Doranz, R. E. Chen, P. Y. Shi, R. H. Carnahan, L. B. Thackray, M. S. Diamond, J. E. Crowe Jr., Neutralizing and protective human monoclonal antibodies recognizing the N-terminal domain of the SARS-CoV-2 spike protein. *Cell* **184**, 2316–2331.e15 (2021).
53. W. N. Voss, Y. J. Hou, N. V. Johnson, G. Delidakis, J. E. Kim, K. Javanmardi, A. P. Horton, F. Bartzoka, C. J. Paresi, Y. Tanno, C.-W. Chou, S. A. Abbasi, W. Pickens, K. George, D. R. Boutz, D. M. Towers, J. R. McDaniel, D. Billick, J. Goike, L. Rowe, D. Batra, J. Pohl, J. Lee, S. Gangappa, S. Sambhara, M. Gadush, N. Wang, M. D. Person, B. L. Iverson, J. D. Gollihar, J. M. Dye, A. S. Herbert, I. J. Finkelstein, R. S. Baric, J. S. McLellan, G. Georgiou, J. J. Lavinder, G. C. Ippolito, Prevalent, protective, and convergent IgG recognition of SARS-CoV-2 non-RBD spike epitopes. *Science* **372**, 1108–1112 (2021).
54. Q. Wang, Y. Guo, S. Iketani, M. S. Nair, Z. Li, H. Mohri, M. Wang, J. Yu, A. D. Bowen, J. Y. Chang, J. G. Shah, N. Nguyen, Z. Chen, K. Meyers, M. T. Yin, M. E. Sobieszczyk, Z. Sheng, Y. Huang, L. Liu, D. D. Ho, Antibody evasion by SARS-CoV-2 Omicron subvariants BA.2.12.1, BA.4 and BA.5. *Nature* **608**, 603–608 (2022).
55. E. Takashita, S. Yamayoshi, V. Simon, H. van Bakel, E. M. Sordillo, A. Pekosz, S. Fukushi, T. Suzuki, K. Maeda, P. Halfmann, Y. Sakai-Tagawa, M. Ito, S. Watanabe, M. Imai, H. Hasegawa, C. J. Kawaoka, Efficacy of antibodies and antiviral drugs against omicron BA.2.12.1, BA.4, and BA.5 subvariants. *N. Engl. J. Med.* **387**, 468–470 (2022).
56. J. Gutiérrez, C. Maroto, Are IgG antibody avidity assays useful in the diagnosis of infectious diseases? A review. *Microbios* **87**, 113–121 (1996).
57. I. C. MacLennan, A. Gulbranson-Judge, K. M. Toellner, M. Casamayor-Palleja, E. Chan, D. M. Sze, S. A. Luther, H. A. Orbea, The changing preference of T and B cells for partners as T-dependent antibody responses develop. *Immunol. Rev.* **156**, 53–66 (1997).
58. T. Defrance, M. Taillardet, L. Genestier, T cell-independent B cell memory. *Curr. Opin. Immunol.* **23**, 330–336 (2011).
59. S. Fagarasan, T. Honjo, T-Independent immune response: New aspects of B cell biology. *Science* **290**, 89–92 (2000).
60. A. E. Denton, S. Innocent, E. J. Carr, B. M. Bradford, F. Lafouresse, N. A. Mabbott, U. Mörbke, B. Ludewig, J. R. Groom, K. L. Good-Jacobson, M. A. Linterman, Type I interferon induces CXCL13 to support ectopic germinal center formation. *J. Exp. Med.* **216**, 621–637 (2019).
61. Y. M. Bar-On, Y. Goldberg, M. Mandel, O. Bodenheimer, O. Amir, L. Freedman, S. Alroy-Preis, N. Ash, A. Huppert, R. Milo, Protection by a fourth dose of BNT162b2 against Omicron in Israel. *N. Engl. J. Med.* **386**, 1712–1720 (2022).
62. M. Bemark, D. Angeletti, Know your enemy or find your friend?—Induction of IgA at mucosal surfaces. *Immunol. Rev.* **303**, 83–102 (2021).
63. M. I. Samanovic, A. R. Cornelius, S. L. Gray-Gaillard, J. R. Allen, T. Karmacharya, J. P. Wilson, S. W. Hyman, M. Tuen, S. B. Koralov, M. J. Mulligan, R. S. Herati, Robust immune responses are observed after one dose of BNT162b2 mRNA vaccine dose in SARS-CoV-2-experienced individuals. *Sci. Transl. Med.* **14**, eabi8961 (2022).
64. K. Karikó, H. Muramatsu, F. A. Welsh, J. Ludwig, H. Kato, S. Akira, D. Weissman, Incorporation of pseudouridine into mrna yields superior nonimmunogenic vector with increased translational capacity and biological stability. *Mol. Ther.* **16**, 1833–1840 (2008).
65. P. Matzinger, Tolerance, danger, and the extended family. *Annu. Rev. Immunol.* **12**, 991–1045 (1994).
66. J. S. Turner, J. A. O'Halloran, E. Kalaidina, W. Kim, A. J. Schmitz, J. Q. Zhou, T. Lei, M. Thapa, R. E. Chen, J. B. Case, F. Amanat, A. M. Rauseo, A. Haile, X. Xie, M. K. Klebert, T. Suessen, W. D. Middleton, P.-Y. Shi, F. Krammer, S. A. Teeffey, M. S. Diamond, R. M. Presti, A. H. Ellebedy, SARS-CoV-2 mRNA vaccines induce persistent human germinal centre responses. *Nature* **596**, 109–113 (2021).
67. W. Kim, J. Q. Zhou, S. C. Horvath, A. J. Schmitz, A. J. Sturtz, T. Lei, Z. Liu, E. Kalaidina, M. Thapa, W. B. Alsoussi, A. Haile, M. K. Klebert, T. Suessen, L. Parra-Rodriguez, P. A. Mudd, S. P. J. Whelan, W. D. Middleton, S. A. Teeffey, I. Pusic, J. A. O'Halloran, R. M. Presti, J. S. Turner, A. H. Ellebedy, Germinal centre-driven maturation of B cell response to mRNA vaccination. *Nature* **604**, 141–145 (2022).
68. V. Rodrigues, M. Laforge, L. Campillo-Gimenez, C. Soundaramourty, A. Correia-de-Oliveira, R. J. Dinis-Oliveira, A. Ouaissi, A. Cordeiro-da-Silva, R. Silvestre, J. Estaquier, Abortive T follicular helper development is associated with a defective humoral response in Leishmania infantum-infected macaques. *PLOS Pathog.* **10**, e1004096 (2014).
69. F. Moukambi, H. Rabezanahary, V. Rodrigues, G. Racine, L. Robitaille, B. Krust, G. Andreani, C. Soundaramourty, R. Silvestre, M. Laforge, J. Estaquier, Correction: Early loss of splenic Tfh cells in SIV-infected rhesus macaques. *PLOS Pathog.* **12**, e1005393 (2016).

70. D. H. Katz, B. Benacerraf, in *Advances in Immunology*, F. J. Dixon, H. G. Kunkel, Eds. (Academic Press, 1972), vol. 15, pp. 1–94.
71. N. A. Mitchison, The carrier effect in the secondary response to hapten-protein conjugates. II. Cellular cooperation. *Eur. J. Immunol.* **1**, 18–27 (1971).
72. N. W. Palm, R. Medzhitov, Immunostimulatory activity of haptenated proteins. *Proc. Natl. Acad. Sci. U.S.A.* **106**, 4782–4787 (2009).
73. N. Schmitt, R. Morita, L. Bourdery, S. E. Bentebibel, S. M. Zurawski, J. Banchereau, H. Ueno, Human dendritic cells induce the differentiation of interleukin-21-producing T follicular helper-like cells through interleukin-12. *Immunity* **31**, 158–169 (2009).
74. L. B. Rodda, P. A. Morawski, K. B. Pruner, M. L. Fahning, C. A. Howard, N. Franko, J. Logue, J. Eggenberger, C. Stokes, I. Golez, M. Hale, M. Gale Jr., H. Y. Chu, D. J. Campbell, M. Pepper, Imprinted SARS-CoV-2-specific memory lymphocytes define hybrid immunity. *Cell* **185**, 1588–1601.e14 (2022).
75. D. Pichler, M. Baumgartner, J. Kimpel, A. Rössler, L. Riepler, K. Bates, V. Fleischer, D. von Laer, W. Borena, R. Würzner, Marked increase in avidity of SARS-CoV-2 antibodies 7–8 months after infection is not diminished in old age. *J Infect Dis* **224**, 764–770 (2021).
76. A. T. Tan, M. Linster, C. W. Tan, N. Le Bert, W. N. Chia, K. Kunasegaran, Y. Zhuang, C. Y. L. Tham, A. Chia, G. J. D. Smith, B. Young, S. Kalimuddin, J. G. H. Low, D. Lye, L. F. Wang, A. Bertoletti, Early induction of functional SARS-CoV-2-specific T cells associates with rapid viral clearance and mild disease in COVID-19 patients. *Cell Rep.* **34**, 108728 (2021).
77. M. Malbec, F. Porrot, R. Rua, J. Horwitz, F. Klein, A. Halper-Stromberg, J. F. Scheid, C. Eden, H. Mouquet, M. C. Nussenzweig, O. Schwartz, Broadly neutralizing antibodies that inhibit HIV-1 cell to cell transmission. *J. Exp. Med.* **210**, 2813–2821 (2013).
78. I. A. Abela, L. Berlinger, M. Schanz, L. Reynell, H. F. Günthard, P. Rusert, A. Trkola, Cell-cell transmission enables HIV-1 to evade inhibition by potent CD4bs directed antibodies. *PLOS Pathog.* **8**, e1002634 (2012).
79. C. Zeng, J. P. Evans, T. King, Y.-M. Zheng, E. M. Oltz, S. P. J. Whelan, L. J. Saif, M. E. Peeples, S.-L. Liu, SARS-CoV-2 spreads through cell-to-cell transmission. *Proc. Natl. Acad. Sci. U.S.A.* **119**, e2111400119 (2022).
80. R. Kotaki, Y. Adachi, S. Moriyama, T. Onodera, S. Fukushi, T. Nagakura, K. Tonouchi, K. Terahara, L. Sun, T. Takano, A. Nishiyama, M. Shinkai, K. Oba, F. Nakamura-Uchiyama, H. Shimizu, T. Suzuki, T. Matsumura, M. Isogawa, Y. Takahashi, SARS-CoV-2 Omicron-neutralizing memory B cells are elicited by two doses of BNT162b2 mRNA vaccine. *Sci. Immunol.* **7**, eabn8590 (2022).
81. B. L. Sievers, S. Chakraborty, Y. Xue, T. Gelbart, J. C. Gonzalez, A. G. Cassidy, Y. Golan, M. Prah, S. L. Gaw, P. S. Arunachalam, C. A. Blish, S. D. Boyd, M. M. Davis, P. Jagannathan, K. C. Nadeau, B. Pulendran, U. Singh, R. H. Scheuermann, M. B. Frieman, S. Vashee, T. T. Wang, G. S. Tan, Antibodies elicited by SARS-CoV-2 infection or mRNA vaccines have reduced neutralizing activity against Beta and Omicron pseudoviruses. *Sci. Transl. Med.* **14**, eabn7842 (2022).
82. P. Kaplonek, D. Cizmeci, S. Fischinger, A. R. Collier, T. Suscovich, C. Linde, T. Broge, C. Mann, F. Amanat, D. Dayal, J. Rhee, M. de St Aubin, E. J. Nilles, E. R. Musk, A. S. Menon, E. O. Saphire, F. Krammer, D. A. Lauffenburger, D. H. Barouch, G. Alter, mRNA-1273 and BNT162b2 COVID-19 vaccines elicit antibodies with differences in Fc-mediated effector functions. *Sci. Transl. Med.* **14**, eabm2311 (2022).

**Acknowledgments:** K.T. thanks the Japan Society for the Promotion of Science (KAKENHI, 21K07060) and J.E. thanks the Canada Research Chair program for their financial support. J.E. and P.C. also thank AbbVie France and AbbVie Canada for supporting this COVID-19 study. We are grateful to T. Sawyers, Medical Writer at the BESPIM, Nîmes University Hospital, France, for critical reading of the manuscript. **Funding:** This work was supported by a grant to J.E. from the Fondation pour la Recherche Médicale and the Agence nationale de la recherche (COVID-1<sup>2</sup>A) as well as by a grant to P.C. from Nîmes University Hospital (NIMAO/2020/COVID/PC-01). This work was also funded by a grant to R.S. from the Foundation for Science and Technology (FCT), project UIDB/50026/2020 and UIDP/50026/2020; and by the NORTE-01-0145-FEDER-000013 and NORTE-01-0145-FEDER-000023 projects, supported by North Portugal Regional Operational Programme (NORTE 2020), under the PORTUGAL 2020 Partnership Agreement, through the European Regional Development Fund (ERDF) and FCT contracts 2021.07836.BD to A.M.-F. and CEECIND/00185/2020 to R.S. M.A. thanks the ANRS | Maladies infectieuses émergentes for his fellowship. This work was also supported by the Clinical Academic Centers (2CA-Braga) through the grant 2017 2CACOVID-AIR. **Author contributions:** Conceived and designed the experiments: M.A.D.S., P.N., K.T., R.S., P.C., F.M., and J.E. Performed the experiments: M.A.D.S., P.N., C.S., A.B.-M., M.T., D.K., O.Z.-A., and M.P. Patients' recruitment and clinics: A.M.-F., A.S.-C., A.C., C.C., J.P., A.G.C., P.L., A.S., L.M., J.-Y.L., C.R., P.-G.C., S.D., T.-A.T., and P.C. Analyzed the data: M.A.D.S., P.N., K.T., R.S., P.C., F.M., and J.E. Wrote the paper: M.A.D.S., P.N., K.T., R.S., P.C., F.M., and J.E. **Competing interests:** The authors declare that they have no competing interests. **Data and materials availability:** All data needed to evaluate the conclusions in the paper are present in the paper and/or the Supplementary Materials.

Submitted 9 December 2022

Accepted 5 July 2023

Published 4 August 2023

10.1126/sciadv.adg2122



公益財団法人日中医学協会  
T E L 03-5829-9123  
F A X 03-3866-9080  
E-MAIL iryo@jpcnma.or.jp  
〒101-0032 東京都千代田区岩本町 1-4-3  
住 泉 K M ビル 6 階  
URL : <https://www.jpcnma.or.jp/>